

Emerging frontiers in developmental biology in latin america

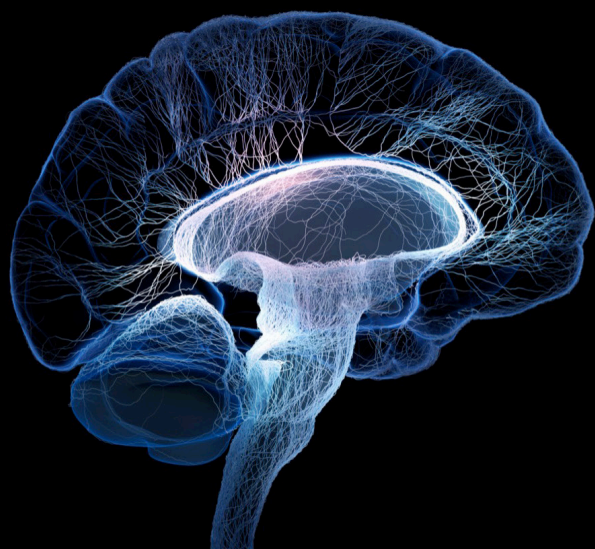
Edited by

Daniel Ortuño-Sahagún and Juan Rafael Riesgo-Escovar

Published in

Frontiers in Neuroscience

Frontiers in Cell and Developmental Biology



FRONTIERS EBOOK COPYRIGHT STATEMENT

The copyright in the text of individual articles in this ebook is the property of their respective authors or their respective institutions or funders. The copyright in graphics and images within each article may be subject to copyright of other parties. In both cases this is subject to a license granted to Frontiers.

The compilation of articles constituting this ebook is the property of Frontiers.

Each article within this ebook, and the ebook itself, are published under the most recent version of the Creative Commons CC-BY licence. The version current at the date of publication of this ebook is CC-BY 4.0. If the CC-BY licence is updated, the licence granted by Frontiers is automatically updated to the new version.

When exercising any right under the CC-BY licence, Frontiers must be attributed as the original publisher of the article or ebook, as applicable.

Authors have the responsibility of ensuring that any graphics or other materials which are the property of others may be included in the CC-BY licence, but this should be checked before relying on the CC-BY licence to reproduce those materials. Any copyright notices relating to those materials must be complied with.

Copyright and source acknowledgement notices may not be removed and must be displayed in any copy, derivative work or partial copy which includes the elements in question.

All copyright, and all rights therein, are protected by national and international copyright laws. The above represents a summary only. For further information please read Frontiers' Conditions for Website Use and Copyright Statement, and the applicable CC-BY licence.

ISSN 1664-8714
ISBN 978-2-8325-2357-5
DOI 10.3389/978-2-8325-2357-5

About Frontiers

Frontiers is more than just an open access publisher of scholarly articles: it is a pioneering approach to the world of academia, radically improving the way scholarly research is managed. The grand vision of Frontiers is a world where all people have an equal opportunity to seek, share and generate knowledge. Frontiers provides immediate and permanent online open access to all its publications, but this alone is not enough to realize our grand goals.

Frontiers journal series

The Frontiers journal series is a multi-tier and interdisciplinary set of open-access, online journals, promising a paradigm shift from the current review, selection and dissemination processes in academic publishing. All Frontiers journals are driven by researchers for researchers; therefore, they constitute a service to the scholarly community. At the same time, the *Frontiers journal series* operates on a revolutionary invention, the tiered publishing system, initially addressing specific communities of scholars, and gradually climbing up to broader public understanding, thus serving the interests of the lay society, too.

Dedication to quality

Each Frontiers article is a landmark of the highest quality, thanks to genuinely collaborative interactions between authors and review editors, who include some of the world's best academicians. Research must be certified by peers before entering a stream of knowledge that may eventually reach the public - and shape society; therefore, Frontiers only applies the most rigorous and unbiased reviews. Frontiers revolutionizes research publishing by freely delivering the most outstanding research, evaluated with no bias from both the academic and social point of view. By applying the most advanced information technologies, Frontiers is catapulting scholarly publishing into a new generation.

What are Frontiers Research Topics?

Frontiers Research Topics are very popular trademarks of the *Frontiers journals series*: they are collections of at least ten articles, all centered on a particular subject. With their unique mix of varied contributions from Original Research to Review Articles, Frontiers Research Topics unify the most influential researchers, the latest key findings and historical advances in a hot research area.

Find out more on how to host your own Frontiers Research Topic or contribute to one as an author by contacting the Frontiers editorial office: frontiersin.org/about/contact

Emerging frontiers in developmental biology in latin america

Topic editors

Daniel Ortuño-Sahagún — University of Guadalajara, Mexico

Juan Rafael Riesgo-Escovar — National Autonomous University of Mexico, Mexico

Citation

Ortuño-Sahagún, D., Riesgo-Escovar, J. R., eds. (2023). *Emerging frontiers in developmental biology in latin america*. Lausanne: Frontiers Media SA.
doi: 10.3389/978-2-8325-2357-5

Table of contents

- 05 **Editorial: Emerging frontiers in developmental biology in Latin America**
Daniel Ortuño-Sahagún and Juan Rafael Riesgo-Escovar
- 08 **Recombinant Limb Assay as *in Vivo* Organoid Model**
Roberto Damián García-García, Estefanía Garay-Pacheco, Jessica Cristina Marín-Llera and Jesús Chimal-Monroy
- 16 **The organizing role of Wnt signaling pathway during arthropod posterior growth**
Marco Mundaca-Escobar, Rodrigo E. Cepeda and Andres F. Sarrazin
- 30 **Patched-Related Is Required for Proper Development of Embryonic *Drosophila* Nervous System**
Carmen Bolatto, Sofía Nieves, Agustina Reyes, Silvia Olivera-Bravo and Verónica Cambiazo
- 46 **It takes two to tango: Widening our understanding of the onset of schizophrenia from a neuro-angiogenic perspective**
Bárbara S. Casas, David Arancibia-Altamirano, Franco Acevedo-La Rosa, Delia Garrido-Jara, Vera Maksae, Dan Pérez-Monje and Verónica Palma
- 63 **Post-amputation reactive oxygen species production is necessary for axolotls limb regeneration**
Belfran Carbonell-M, Juliana Zapata Cardona and Jean Paul Delgado
- 90 **Transcriptional expression of m⁶A and m⁵C RNA methyltransferase genes in the brain and fat body of honey bee adult workers**
Luana Bataglia, Zilá Luz Paulino Simões and Francis Morais Franco Nunes
- 99 **Recent advances in the use of CRISPR/Cas for understanding the early development of molecular gaps in glial cells**
Carla Patricia Barragán-Álvarez, José Miguel Flores-Fernandez, Oscar R. Hernández-Pérez, Daniela Ávila-Gonzalez, Nestor Fabian Díaz, Eduardo Padilla-Camberos, Octavio Dublan-García, Leobardo Manuel Gómez-Oliván and Nestor Emmanuel Diaz-Martinez
- 114 **Glycine neurotransmission: Its role in development**
Rocío Salceda
- 123 **Light-induced shifts in opsin gene expression in the four-eyed fish *Anableps anableps***
Daniele Salgado, Bertha R. Mariluz, Maysa Araujo, Jamily Lorena, Louise N. Perez, Rafaela de L. Ribeiro, Josane de F. Sousa and Patricia N. Schneider

- 131 **Radial glia and radial glia-like cells: Their role in neurogenesis and regeneration**
Yamil Miranda-Negrón and José E. García-Arrarás
- 149 ***Dll1* haploinsufficiency causes brain abnormalities with functional relevance**
Dulce-María Arzate, Concepción Valencia, Marco-Antonio Dimas, Edwards Antonio-Cabrera, Emilio Domínguez-Salazar, Gilda Guerrero-Flores, Mariana Gutiérrez-Mariscal and Luis Covarrubias



OPEN ACCESS

EDITED AND REVIEWED BY

Ariel Ávila,
Universidad Católica de la Santísima
Concepción, Chile

*CORRESPONDENCE

Daniel Ortuño-Sahagún
✉ daniel.ortuno@academicos.udg.mx
Juan Rafael Riesgo-Escovar
✉ riesgo@unam.mx

RECEIVED 21 December 2022

ACCEPTED 03 April 2023

PUBLISHED 20 April 2023

CITATION

Ortuño-Sahagún D and Riesgo-Escovar JR
(2023) Editorial: Emerging frontiers in
developmental biology in Latin America.
Front. Neurosci. 17:1129291.
doi: 10.3389/fnins.2023.1129291

COPYRIGHT

© 2023 Ortuño-Sahagún and Riesgo-Escovar.
This is an open-access article distributed under
the terms of the [Creative Commons Attribution
License \(CC BY\)](#). The use, distribution or
reproduction in other forums is permitted,
provided the original author(s) and the
copyright owner(s) are credited and that the
original publication in this journal is cited, in
accordance with accepted academic practice.
No use, distribution or reproduction is
permitted which does not comply with these
terms.

Editorial: Emerging frontiers in developmental biology in Latin America

Daniel Ortuño-Sahagún^{1*} and Juan Rafael Riesgo-Escovar^{2*}

¹Laboratorio de Neuroinmunobiología Molecular, Instituto de Investigación en Ciencias Biomédicas, Centro Universitario de Ciencias de la Salud, Universidad de Guadalajara, Jalisco, Mexico,

²Developmental Neurobiology and Neurophysiology, Instituto de Neurobiología, Campus UNAM Juriquilla, Universidad Nacional Autónoma de México, Santiago de Querétaro, Mexico

KEYWORDS

developmental biology, Latin America, neuroscience, model organisms, model system

Editorial on the Research Topic

Emerging frontiers in developmental biology in Latin America

These past couple of years have been a trying experience for us all; and we are dealing still with the aftermath of the pandemic and the lingering sequelae. That has caused numerous academic activities to be postponed, and the Latin American Society of Developmental Biology, as well as the Mexican Society of Developmental Biology meetings were not immune. Nevertheless, we have gone ahead and organized this Research Topic, and have had an enthusiastic response, in many ways a testament to the vigor and resilience in these difficult times of our members and research groups, and the excitement that permeates developmental biology in Latin America. Eleven papers constitute this Research Topic, ranging from single molecules to whole organisms, exploiting classical developmental biology models such as flies (*Drosophila melanogaster*), bees (*Apis mellifera*), and axolotls (*Ambystoma mexicanus*), to recent additions like echinoderms (*Holothuria glaberrima*), four-eyed fish (*Anableps anableps*), and organoids, enriching the developmental biology models' cornucopia, in what will hopefully be a first installment for envisioned future submissions and discoveries. We have no qualms that you, our readers, will find them interesting and motivating.

Most of the papers of the Research Topic deal with aspects of the developing nervous system. The central nervous system (CNS) has always generated great interest, an interest that is both historical and current (Pellet et al., 2022), going through topics such as embryonic development (Elshazzly et al., 2022), aging (Wolkow et al., 2010), and its regenerative capacity after injury (Buga et al., 2011).

Bolatto et al. examine *Patched-related (Ptr)* null mutant embryos in *Drosophila*. As a neuroectodermal gene, *Ptr* encodes for a protein with a *Patched (Ptc)*-like organization and domain structure, which is a canonical receptor of the *Hedgehog (Hh)* signaling pathway, and demonstrate that *Ptr* is required for proper CNS development. CRISPR/Cas editing has been widely employed in recent years for the understanding of CNS function (Cota-Coronado et al., 2019; Sandoval et al., 2020). Barragán-Álvarez et al., focusing on emerging methods, such as GESTALT and LINNAEUS, review recent advances in the application of the CRISPR/Cas system for the study of glial cell-associated neurological disorders and their potential applications in regenerative medicine.

CNS cells communicate mainly through specialized contact sites called synapses that use neurotransmitters to modulate neuronal activity (Andreae and Burrone, 2014) and

circuit development (Andreae and Burrone, 2018). Among these neurotransmitters, Salceda reviews the functions of glycine and its receptors, present from early CNS development to adulthood, focusing on glycinergic activity in the balance of excitatory and inhibitory signals during development, cell proliferation, and specification.

With the neurosciences, neurogenesis is a very attractive topic. It occurs during both embryonic and postnatal development (reviewed in Bartkowska et al., 2022), where Notch signaling plays an important role (reviewed in Engler et al., 2018). Arzate et al. document the involvement of the delta-like 1 (Dll1) gene as a transmembrane ligand that activates the Notch receptor in the developing brain. By analyzing Dll1 haploinsufficiency in adult mice, they found brain abnormalities derived from reductions in neurogenesis, that may cause slight brain disfunction and mild behavioral alterations. In addition to genetics, studies of epigenetic mechanisms regulating neural plasticity have increased recently (Ortuño-Sahagún et al., 2019). Bataglia et al. describe how dietary changes influence CNS functioning by presenting tissue-specific signatures of RNA methyltransferases expression in adult honeybee workers.

Sensory stimulation can modulate CNS function, one of which is the visual system (Kovács-Öller et al., 2022). The four-eyed fish *Anableps anableps* possesses duplicate corneas and pupils, as well as specialized retinal regions associated with aerial or aquatic vision (Perez et al., 2017). Salgado et al. analyze the expression profile of several opsin genes in dorsal and ventral retinas. Asymmetry is established after birth and different light conditions can shift opsin expression, potentially contributing to changes in spectral sensitivity in this four eyed fish.

In addition to neurons, glial cells are fundamental for CNS proper functioning (Nampoothiri et al., 2022), as well as in neural pathologies (Mata-Martínez et al., 2022). Miranda-Negrón and García-Arrarás review how radial glia and radial glia-like cells participate in neurogenesis and regeneration during homeostasis and in response to injury, using the echinoderm *Holothuria glaberrima*.

Finally, Palma's review focuses on understanding the onset of schizophrenia from a neuro-angiogenic perspective. She emphasizes the role of the cerebral vasculature, during angiogenesis and during the establishment and functioning of the neurovascular niche, in relation to the onset of schizophrenia, considered a chronic mental disorder. It offers a perspective on distinctive angiogenic and neurogenic signaling pathways that might be involved in schizophrenia.

Moving outside the CNS, other areas of developmental biology are covered in this Research Topic: body patterning, limb regeneration, and *in vitro* organoid models. Through a detailed review, Mundaca-Escobar et al. discuss how Wnt signaling could regulate segmentation to establish a repetitive pattern, suggesting that this pathway plays an organizing role in the formation of body segments, regulating the expression of segmentation

genes in most arthropods. Carbonell-M et al. show how reactive oxygen species generated after amputation are necessary for limb regeneration in the axolotl, showing that ROS/H₂O₂ are necessary for correct morphogenesis and size of skeletal structures, as well as proper integration between regenerated structures and remaining tissues. Finally, technical advances lead to the development of specialized *in vitro* culture techniques and organoid formation. The recombinant limb assay, developed by Zwilling (1964), is reviewed by García-García et al., proposing that the formation of skeletal elements induced through this system, when occurring from precursor cells, may resemble *in vivo* morphogenic properties of skeletal cells.

Overall, this Research Topic constitutes a sample of the areas of developmental biology cultivated in the region, and may serve as a kernel to detonate future collaborations and interactions, and to foster the rekindling of developmental biology studies throughout the region and elsewhere, especially at this trying post-pandemic times. It may also, hopefully, play its part in exciting and motivating a new generation of developmental biology students and scientists.

Author contributions

DO-S and JR-E wrote the manuscript, designed the Research Topic, and reviewed the manuscript. Both authors contributed to the article and approved the submitted version.

Acknowledgments

We would like to thank the authors for trusting us with this initiative and for their commitment to this proposal, by sending their manuscripts and sharing their research data and stimulating ideas. We are also in debt and grateful to all of the reviewers for their generously devoted time and highly valuable insights.

Conflict of interest

The authors declare that the research was conducted in the absence of any commercial or financial relationships that could be construed as a potential conflict of interest.

Publisher's note

All claims expressed in this article are solely those of the authors and do not necessarily represent those of their affiliated organizations, or those of the publisher, the editors and the reviewers. Any product that may be evaluated in this article, or claim that may be made by its manufacturer, is not guaranteed or endorsed by the publisher.

References

- Andreae, L. C., and Burrone, J. (2014). The role of neuronal activity and transmitter release on synapse formation. *Curr Opin. Neurobiol.* 27, 47–52. doi: 10.1016/j.conb.2014.02.008
- Andreae, L. C., and Burrone, J. (2018). The role of spontaneous neurotransmission in synapse and circuit development. *J. Neurosci. Res.* 96, 354–359. doi: 10.1002/jnr.24154
- Bartkowska, K., Tepper, B., Turlejski, K., and Djavadian, R. (2022). Postnatal and adult neurogenesis in mammals, including marsupials. *Cells* 11, 2735. doi: 10.3390/cells11172735
- Buga, A. M., Vintilescu, R., Pop, O. T., and Popa-Wagner, A. (2011). Brain aging and regeneration after injuries: an organismal approach. *Aging Dis.* 2, 64–79.
- Cota-Coronado, A., Díaz-Martínez, N. F., Padilla-Camberos, E., and Díaz-Martínez, N. E. (2019). Editing the central nervous system through CRISPR/Cas9 systems. *Front. Mol. Neurosci.* 12, 110. doi: 10.3389/fnmol.2019.00110
- Elshazzly, M., Lopez, M. J., Reddy, V., and Caban, O. (2022). “Embryology, central nervous system,” in *StatPearls* (Treasure Island, FL: StatPearls Publishing LLC).
- Engler, A., Zhang, R., and Taylor, V. (2018). Notch and neurogenesis. *Adv. Exp. Med. Biol.* 1066, 223–234. doi: 10.1007/978-3-319-89512-3_11
- Kovács-Öller, T., Dedek, K., and Hillier, D. (2022). Editorial: visual code: from the retina to the brain. *Front. Cell. Neurosci.* 16, 1018229. doi: 10.3389/fncel.2022.1018229
- Mata-Martínez, E., Díaz-Muñoz, M., Vázquez-Cuevas, F. G. (2022). Glial cells and brain diseases: inflammasomes as relevant pathological entities. *Front. Cell. Neurosci.* (2022) 16, 929529. doi: 10.3389/fncel.2022.929529
- Nampoothiri, S., Nogueiras, R., Schwaninger, M., Prevot, V. (2022). Glial cells as integrators of peripheral and central signals in the regulation of energy homeostasis. *Nat. Metab.* (2022) 4, 813–825. doi: 10.1038/s42255-022-00610-z
- Ortuño-Sahagún, D., Schliebs, R., Pallàs, M. (2019). Editorial: epigenetic mechanisms regulating neural plasticity. *Front. Cell. Neurosci.* (2019) 13, 118. doi: 10.3389/fncel.2019.00118
- Pellet, E. M., Helsdingen, A. S., and Teles-Grivo Ruivo, L. M. (2022). Editorial: fundamentals of 21st century neuroscience. *Front. Mol. Neurosci.* 14, 835419. doi: 10.3389/fnmol.2021.835419
- Perez, L. N., Lorena, J., Costa, C. M., Araujo, M. S., Frota-Lima, G. N., Matos-Rodrigues, G. E., et al. (2017). Eye development in the four-eyed fish *Anableps anableps*: cranial and retinal adaptations to simultaneous aerial and aquatic vision. *Proc. Biol. Sci.* 284, 20170157. doi: 10.1098/rspb.2017.0157
- Sandoval, A. Jr., Elahi, H., and Ploski, J. E. (2020). Genetically engineering the nervous system with CRISPR-Cas. *eNeuro.* 7, ENEURO.0419-19.2020. doi: 10.1523/ENEURO.0419-19.2020
- Wolkow, C. A., Zou, S., and Mattson, M. P. (2010). “Aging of the nervous system,” in *The Comparative Biology of Aging*, ed Wolf, N. (Dordrecht: Springer).
- Zwilling, E. (1964). Development of fragmented and of dissociated limb bud mesoderm. *Dev. Biol.* 9, 20–37. doi: 10.1016/0012-1606(64)90012-0



Recombinant Limb Assay as *in Vivo* Organoid Model

Roberto Damián García-García[†], Estefanía Garay-Pacheco[†], Jessica Cristina Marín-Llera^{†*} and Jesús Chimal-Monroy^{*}

Departamento de Medicina Genómica y Toxicología Ambiental, Instituto de Investigaciones Biomédicas, Universidad Nacional Autónoma de México, Ciudad Universitaria, Ciudad de México, México

OPEN ACCESS

Edited by:

Juan Rafael Riesgo-Escovar,
Universidad Nacional Autónoma de
México, Mexico

Reviewed by:

Jose Francisco Islas,
Autonomous University of Nuevo
León, Mexico

*Correspondence:

Jessica Cristina Marín-Llera
jmarinllera@iibimedicas.unam.mx
Jesús Chimal-Monroy
jchimal@unam.mx

[†]These authors share first authorship

Specialty section:

This article was submitted to
Morphogenesis and Patterning,
a section of the journal
Frontiers in Cell and Developmental
Biology

Received: 26 January 2022

Accepted: 04 April 2022

Published: 26 April 2022

Citation:

García-García RD, Garay-Pacheco E,
Marín-Llera JC and Chimal-Monroy J
(2022) Recombinant Limb Assay as *in Vivo*
Organoid Model.
Front. Cell Dev. Biol. 10:863140.
doi: 10.3389/fcell.2022.863140

Organ formation initiates once cells become committed to one of the three embryonic germ layers. In the early stages of embryogenesis, different gene transcription networks regulate cell fate after each germ layer is established, thereby directing the formation of complex tissues and functional organs. These events can be modeled *in vitro* by creating organoids from induced pluripotent, embryonic, or adult stem cells to study organ formation. Under these conditions, the induced cells are guided down the developmental pathways as in embryonic development, resulting in an organ of a smaller size that possesses the essential functions of the organ of interest. Although organoids are widely studied, the formation of skeletal elements in an organoid model has not yet been possible. Therefore, we suggest that the formation of skeletal elements using the recombinant limb (RL) assay system can serve as an *in vivo* organoid model. RLs are formed from undissociated or dissociated-reaggregated undifferentiated mesodermal cells introduced into an ectodermal cover obtained from an early limb bud. Next, this filled ectoderm is grafted into the back of a donor chick embryo. Under these conditions, the cells can receive the nascent embryonic signals and develop complex skeletal elements. We propose that the formation of skeletal elements induced through the RL system may occur from stem cells or other types of progenitors, thus enabling the study of morphogenetic properties *in vivo* from these cells for the first time.

Keywords: organoid, cell differentiation, patterning, recombinant limbs, limb development, limb organoid

INTRODUCTION

During embryonic development, many developmental pathways orchestrate the formation of organs in time and space. In the early stages of embryogenesis, the cell differentiation potential restricts as the pluripotent embryonic cells give rise to three germ layers: ectoderm, mesoderm, and endoderm (Chan et al., 2017; Kumar et al., 2021). Lineage-specific gene regulatory programs within each germ layer activate and coordinate the steps needed for that group of cells to develop into the cell fates required to form tissues and, finally, functional organs. Concomitant with organogenesis is the appearance of stem cells involved in the homeostasis, repair, and regeneration of adult tissues *in vivo* (Slack, 2008). Stem cells are undifferentiated cells with the ability to reproduce themselves (i.e., self-renew to maintain their cell population) and also to give rise to a range of distinct, specialized cells (i.e., differentiate into multiple cell types as needed) (Slack, 2008; Huang et al., 2021; Shu et al., 2021). Stem and progenitor cell

research has led to breakthrough developments in regenerative medicine, including stem cell-based therapies for various diseases (e.g., leukemia, aplastic anemia, osteopetrosis) (Río et al., 2018; Almohsen and Al-Mudallal, 2020; Capo et al., 2020). Likewise, this knowledge has created new research fields, such as the generation of organoids. These three-dimensional (3D) structures can be derived from induced pluripotent stem cells (iPSCs), embryonic stem cells (ESCs), or adult stem cells (ASCs). These cells self-organize following the developmental pathways of embryonic development, giving rise to an organ of a smaller size capable of performing its essential functions (Rossi et al., 2018).

Therefore, understanding developmental pathways during embryonic development enables extrapolating those into protocols to induce stem or progenitor cells toward forming an organoid. For many years, the disaggregate-reaggregates of organs or cultures from organ rudiments were used to understand cell differentiation and organogenesis involving soluble factors, cell-cell, and cell-extracellular matrix (ECM) interactions. However, these culture models originated from embryonic or fetal cells from the proper organ in formation or already established (Taketo and Koide, 1981; Escalante-Alcalde and Merchant-Larios, 1992; Saxén and Thesleff, 2007). In recent years, various protocols have been developed to direct stem or progenitor cells to develop into intestine, brain, liver, kidney organoids, among others (Lancaster et al., 2013; McCracken et al., 2014; Dye et al., 2015; Huch et al., 2015; Zhou et al., 2021). However, how to properly create complex structures formed by different cell types from distinct embryonic germ layers (e.g., limbs) has not been determined.

To study cell interactions between mesenchymal cells and the ectodermal cover of developing limb buds, E. Zwilling designed the recombinant limb (RL) assay system (Zwilling, 1964). The RL technique assembles the dissociated-reaggregated or undissociated mesoderm of a limb into an embryonic ectoderm cover and then grafting it into the back of a donor embryo. Notably, the embryonic signals provided by the ectoderm induce gene expression in a spatiotemporal manner driving the 3D organization of a limb-like structure by recapitulating the developmental programs that occur during limb development. Although this model has been mainly used to understand chicken limb development, different approaches have also been reported, including interspecies grafting (Fernandez-Teran et al., 1999), the use of different combinations of mutant and wild-type mesoderm or ectoderm (Kuhlman and Niswander, 1997), or limb mesodermal cells modified by electroporation (Marín-Llera et al., 2021). From these, it is evident that the RL experimental model is adaptable to diverse scenarios. This experimental system has enormous potential to explore the ability of different sources of stem or progenitor cells to generate a limb-like structure.

In this perspective, we discuss the potential of the RL system to generate limbs by recapitulating limb development initiated by embryonic ectodermal signals. We propose that the formation of

RLs from iPSCs, ESCs, ASCs, and other progenitor cells can result in a robust *in vivo* organoid model.

MODELING ORGANOID TO UNDERSTAND ORGAN FORMATION

Organs originate during embryonic development from different tissues to form a specialized unit that performs a particular function (Montell, 2008). An organoid is a small, 3D mass that arises by the self-organization and differentiation of stem or progenitor cells generating the substructures and functions characteristic of the organ of interest. Organoids are generated *in vitro* by inducing the differentiation of stem or progenitor cells as it occurs *in vivo* during embryonic development. Organoid models provide a greater understanding of the cellular and molecular basis of organ development, such as cell differentiation, tissue patterning, developmental timing, regulatory gene expression, and size control.

The potential use of organoid generation lies in exploring tissue repair and disease mechanisms, drug testing, tissue homeostasis, regenerative medicine, and developmental biology at the organ level in a scaled model.

While Hans Clever originally coined the concept of “organoid” (Sato et al., 2009), Yoshiki Sasai and his group were the first to demonstrate that, after the induction of developmental programs, mouse and human ESCs generate 3D complexes composed of organized substructures. They first constructed 3D forebrain models followed by other neural organoids (Eiraku et al., 2008, 2011; Osakada et al., 2009; Kamiya et al., 2011).

Intestinal villi-like structures and crypts were the first organoids generated by inducing individual ASCs (Lgr5+) to organize in 3D suspension, giving rise to distinct cell types such as enterocytes, goblet cells, Paneth cells, and endocrine cells (Sato et al., 2009). Since then, various organoids generated from ASCs have been reported, including the liver and kidney (Lancaster et al., 2013; McCracken et al., 2014; Dye et al., 2015; Huch et al., 2015).

The methodologies used to generate an organoid vary according to which cell is best suited to initiate the process. Sequential induction steps recapitulate development to create an organoid that exhibits the desired and required characteristics. Usually, the generation of an organoid *in vitro* consists of isolating a homogeneous cell population capable of further differentiation (e.g., ASCs, ESCs, iPSCs, other progenitor cells). Next, a matrix rich in proteins, growth factors, and other culture components promotes the proliferation, adherence, and differentiation of cells seeded in a defined substrate (reviewed by Corró et al., 2020). The most used matrix is Matrigel, a mixture of complex ECM basement membrane components. This gel-like substance is obtained from mouse tumors expressing laminin, nidogen, collagen IV, and heparan sulfate proteoglycans (Kleinman and Martin, 2005). Matrigel components allow embedded cells to execute cellular functions relevant to tissue formation (Rossi et al., 2018). Under these conditions, morphogens and growth factors regulate cells to acquire a proper cellular fate, guiding them to self-organize. During

organoid formation, cells need determined physiological conditions to commit to specific-tissue cell types and develop into a 3D organized structure according to specific developmental programs (Ehrmann and Robert, 1956; Murry and Keller, 2008; Sasai, 2013). Other forms of generating organ constructs have been elaborated using bioengineering, organs-on-a-chip, and *in situ* approaches, including gene editing, interspecies chimeras, and cellular reprogramming (reviewed in Xia and Izpisua Belmonte, 2019).

Although organoids are an invaluable strategy for modeling early tissue organization characteristics *in vivo*, they have some limitations. Organoids do not fully mimic the physiological organ as they lack some tissue components, vascularization, and immune cells, limiting organ maturation and resulting in incomplete function (de Souza, 2018). Organoids are built lacking vascularization, an essential feature of all tissues to supply nutrients and allow for adequate perfusion. It may result in atypical physiology of the organoid compared to the organ to be modeled. Advances in different strategies to vascularize organoids are reviewed by Strobel et al., 2022. Furthermore, using different sources to establish organoid cultures, the heterogeneity of progenitors and differentiated cells may affect organoid formation that not necessarily corresponds to the *in vivo* counterparts.

The *in vivo* environment is complex, with multiple cell-cell and cell-matrix interactions giving rise to diverse signaling networks that dynamically change according to organ homeostasis. It is expected that attempting to model this complexity *in vitro* will be challenging.

ADVANCES IN LIMB ORGANOID GENERATION

One challenge in generating an organoid is the complexity of the organ of interest. The more complex the organ, the more difficult is the generation of the organoid. Organoid formation involves driving cell populations to spatially organize into a functional structure through exposure to morphogens and specific differentiation signals. Thus, a challenge for the generation of a limb organoid is to mimic tissue organization and function. Limb formation is a powerful model for investigating cell differentiation during development because it involves the establishment of a 3D pattern that directs the morphogenesis, shaping, and positioning of each tissue (McQueen and Towers, 2020; Royle et al., 2021). Limb buds emerge at specific positions along the flank of the embryo (Hamburger and Hamilton, 1992; Feneck and Logan, 2020). The limb bud is formed by undifferentiated mesenchymal cells derived from the lateral plate mesoderm (LPM) with an ectodermal epithelium covering these mesenchymal cells. Tissues differentiate into the limb bud in response to signals from different signaling centers that control the proximodistal [(PD), shoulder to fingers], anteroposterior [(AP), thumb to finger], and dorsoventral [(DV), from the back of the hand to palm] axes. The apical ectodermal ridge (AER) is the thickened epithelium located at the most distal limb ectoderm and

controls the PD axis. Cells from the AER express *Fgf8*, which along with *Wnt3a*, maintains the mesodermal cells underneath the AER in an undifferentiated, proliferative state (Ohuchi et al., 1997; ten Berge et al., 2008). As the limb bud grows, the undifferentiated cells underneath the AER begin to differentiate toward the chondrogenic and tenogenic lineages when they stop receiving signals from the AER (Dollé et al., 1989; Roselló-Díez et al., 2014; Marín-Llera et al., 2019; Marín-Llera et al., 2021). The zone of polarizing activity (ZPA) controls limb bud AP polarity and is located at the posterior margin of the limb bud. When the ZPA is grafted to the anterior zone of a limb bud, it induces mirror-image digit duplications. This signaling center is characterized by *Sonic hedgehog* (*Shh*) expression (Riddle et al., 1993; Fujii et al., 2021; Gamart et al., 2021). Finally, the ventral and dorsal limb bud ectoderms specify DV polarity. *Engrailed 1* (*En-1*), a transcription factor that specifies the ventral ectoderm, and *Wnt7a*, which specifies the dorsal ectoderm by inducing *Lmx1* gene activation, give rise to the DV phenotype of a limb (Loomis et al., 1996; Soshnikova et al., 2003; Haro et al., 2014). These three signaling centers are essential for patterning limbs, committing mesodermal cells to different lineages, and coordinating them within the limb to give rise to the appendicular skeletal system.

One methodology for evaluating the differentiation of limb bud progenitor cells is high-density primary limb mesenchymal culture, also known as a micromass (MM) culture (Ahrens et al., 1977). In MM cultures, the limb mesenchymal cells recapitulate the developmental process observed in limb development to give rise to cartilage cells during the formation of skeletal elements. Limb bud mesenchymal cells condense and aggregate to form 3D cartilage nodules. In long-term MM cultures, the cartilage nodules provide matrix calcification accompanied by increased alkaline phosphatase activity (Arzate et al., 1996; Mello and Tuan, 1999). Although MM cultures help study the basic mechanisms underlying the differentiation of limb bud cells and their regulation, this method has a limited ability to recapitulate the assembly of progenitors into organized tissues that span the entire limb.

Another model used to understand limb formation is the *ex vivo* limb bud culture system (Fell and Robison, 1929). At a particular stage in limb bud development, the bud contains all the elements required to develop autonomously. In this system, the embryonic limb is sectioned and placed in culture media to continue forming skeletal structures with the proper 3D organization of a mature limb, preserving all the cell-cell and cell-ECM interactions that control cell differentiation and morphogenesis (Hall, 1981; Smith et al., 2013). This methodology facilitates the study of the molecular mechanisms regulating chondrocyte differentiation (Schnabel et al., 2006; Lorda-Díez et al., 2010), toxicology testing, and aberrant embryonic limb development (Yan and Hales, 2019, 2021). Although *ex vivo* limb bud cultures provide a tool to understand skeletal and limb development, the initial commitment processes required to enter particular differentiation states remain hard to study. On the other hand, mesenchymal stromal cells (MSCs), a multipotent population

obtained from various fetal and adult tissues, differentiate into osteogenic, chondrogenic, and tenogenic lineages mainly for regenerative medicine applications (Toh et al., 2017; Xia et al., 2018; Jiang et al., 2020). MSCs' potential to differentiate into limb lineages has been investigated mainly using 2D cultures systems.

Obtaining limb-bud-like mesenchymal (LBM) cells from iPSCs or ESCs to create limb organoids is essential to recapitulate early commitment events during embryonic development. Cell differentiation of stem or progenitor cells into LBM cells can be driven by specification signals from the middle primitive streak (midPS) and the LPM. Providing induced LBM cells with the inductive signals necessary to trigger step-by-step their commitment and differentiation into a specific cell lineage ought to result in the formation of a limb organoid. One approach to inducing an LPM state relies on the transient transfection of miRNAs. In mouse ESCs, transient co-transfection of mmu-miR-126a-3p, mmu-miR-335-5p, and mmu-miR-672-5p promotes differentiation toward LPM lineages, thereby increasing the number of LPM-like cells (Tuysuz et al., 2021). Furthermore, miR-199a-3p, miR-214-3p, and miR-483-3p are enriched in mesodermal cells differentiated from human ESCs. However, their roles in specifying the mesoderm into different tissue subtypes have not yet been fully characterized (Ishikawa et al., 2017). Loh et al. (2016) established a developmental roadmap to direct the commitment of cell lineages to particular fates. The reprogramming of human adult somatic cells into human-induced pluripotent stem cells (hiPSCs) by promoting the expression of four transcription factors, including Oct4/Sox2/c-Myc/KLF4 or Oct4/Sox2/NANOG/LIN28, has also been reported (Takahashi and Yamanaka, 2006; Takahashi et al., 2007; Yu et al., 2007). Loh et al. (2016) demonstrated how to generate limb precursor cells after treating stem cells with factors that progressively regulate the formation of mesodermal lineages. They treated hiPSCs with activin, BMP4, CHIR99021, and FGF2 to induce a mid-primitive streak-like (midPS-like) state (Loh et al., 2016). Then, the administration of an ALK5 inhibitor, BMP4, and a Wnt antagonist directs the midPS-like cells down an LPM-like path (Loh et al., 2016). Thereafter, progenitor cells can differentiate into specific cell lineages. Differentiating hiPSCs into LBM cells requires a different combination of chemicals that modulate WNT, BMP, TGF- β , and hedgehog (HH) signaling added to the cells in the appropriate times resulting in PRRX1⁺ (cell-specific marker) LBM cells (Yamada et al., 2021). In addition to the Yamada factors, another study used *Prdm16*, *Zbtb16*, and *Lin28*, generally expressed in the embryonic limb bud, to reprogram mouse non-limb fibroblast into LBM progenitors (Atsuta et al., 2021). In other experimental approaches, hiPSCs seeded into high-density MM cultures treated for 21 days with BMP-2 recapitulate the osteochondrogenic transcriptional network and differentiate to the chondrogenic lineage, including articular cartilage, transient cartilage, and fibrocartilage (Guzzo et al., 2013).

One of the most recent attempts to create a limb organoid was reported by Mori et al. (2019). A polarized limb-like structure was generated from aggregates of mouse embryonic stem cells (mESCs) cultured in a scaffold of

Matrigel and treated with BMP4 and retinoic acid. While the expression of *Tbx4*, *Tbx5*, *Hand2*, *Irx3*, *Meis1*, and *Meis2*, genes involved with the induction, organization, and establishment of limb buds were found, these 3D cultures failed to generate a structure similar to the AER and, therefore, neither recapitulated the differentiation process nor the morphogenetic patterning observed during limb development.

These approaches highlight the importance of understanding the embryonic signals involved in limb development to guide the differentiation of undifferentiated cells into limb-like structures, demonstrating that the sequential activation of developmental programs is necessary for inducing differentiation into specific lineages. Undoubtedly, these works have increased our knowledge of limb organogenesis by generating limb organoids. However, these protocols still fail to recapitulate the morphogenetic processes required to form complex skeletal structures.

RECOMBINANT LIMB ASSAY AS A TOOL FOR LIMB-ORGANOID GENERATION

Edgar Zwilling (Zwilling E., 1964) developed the recombinant limb (RL) assay system to understand the interactions between limb bud ectoderm and mesenchymal cells. This technique, usually used in avian species, consists of assembling whole or dissociated-reaggregated mesodermal cells into an ectodermal cover obtained from an early limb bud to then graft into the dorsal part of a donor chick embryo (for a detailed protocol, see Marín-Llera et al., 2022; Ros et al., 2000). Patterning signals from the embryonic ectoderm induce cell differentiation of mesodermal cells in a spatial-temporal manner to form a limb-like structure following the developmental programs as occurs during limb development. This phenomenon proves that mesodermal limb cells lose their positional identity within the limb bud once they are dissociated. However, they remain competent to ectodermal signals in the RL system, re-specifying its positional values, differentiating, and generating recognizable limb structures (Zwilling E., 1964). Morphogenetic processes of the RL are enhanced by adding an intact ZPA mesoderm at one of the ectodermal edges (MacCabe et al., 1973; Crosby and Fallon, 1975; Frederick and Fallon, 1982). In this way, the RL system provides the spatial-temporal signals mimicking the embryonic limb bud allowing mesodermal cells to differentiate and pattern. RL system provides the PD signals (*Fgf8* and *Fgf4*) and DV signals (*En-1* and *Wnt7a*) of the ectoderm, promoting *Fgf10*, *Lmx-1*, and *Shh* expression in mesodermal cells (Kuhlman & Niswander, 1997; Elisa Piedra et al., 2000). The expression of patterning genes promotes positional information within RL mesodermal cells such as *Msx1*, *Msx2*, *Hoxd11*, *Hoxd12*, and *Hoxd13* (Ros et al., 1994; Cooper et al., 2011; Rosello-Diez et al., 2011). Twenty-4 hours after grafting RL, cells start the differentiation programs by committing to chondrogenic lineages by expressing *Sox9*, and muscle progenitors migrate inward RL from the somites expressing *MyoD* and *Pax3* (Cooper et al., 2011). Interestingly, in the RL assay, the patterning of these progenitors resembles

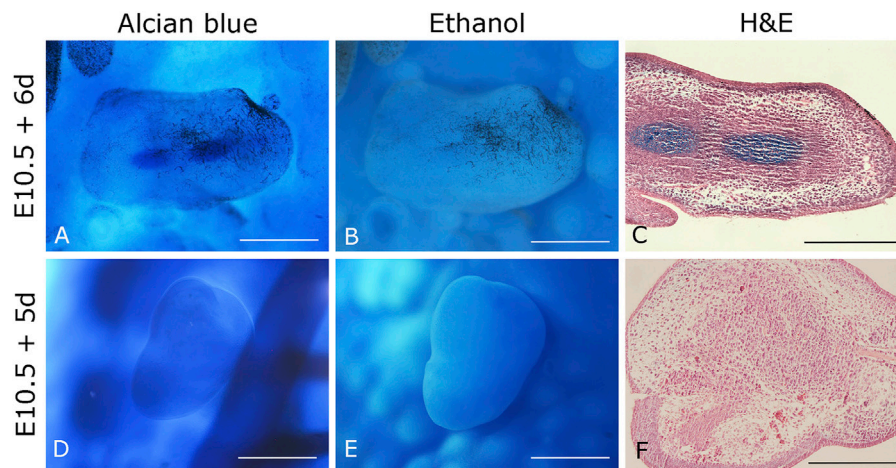


FIGURE 1 | Chimeric mouse-chicken recombinant limbs. **(A–C)** Six-day recombinant limbs. Limb bud mesodermal cells from 10.5 *dpc* mouse embryos were assembled in chicken ectoderms. **(D–F)** Five-day recombinant limbs. Limb bud mesodermal cells from 10.5 *dpc* mouse embryos were ensembled in chicken ectoderms. Chicken ectoderms and host embryos were obtained from the 22 HH stage. Data represent two independent experiments. Scale bar 100 μ m.

normal development when grafted in the somite area with high levels of retinoic acid (Fernandez-Teran et al., 1999; Cooper et al., 2011). Thus, the RL system recapitulates the differentiation, morphogenesis, and patterning programs observed in normal limb development.

One of the advantages of the RL system is the variety of combinations between its elements. It is well known that the molecular signals among vertebrate limb development are conserved throughout tetrapod evolution. Research groups have adapted Zwilling's technique to prove that cells from different species, including the turtle (Fallon & Simandl, 1984) and mouse (Kuhlman & Niswander, 1997), can interpret the signals emitted from an ectodermal jacket that is not their own. Moreover, mesenchymal cells from the anterior or posterior limbs can be placed inside the anterior or posterior ectoderm (Crosby and Fallon, 1975; Frederick and Fallon, 1982). Some points to consider about this technique are the graft efficiency that may vary between mesodermal sources and the high number of chicken embryos needed to generate the RL (mesoderm donors, ectoderm donors, and host embryos). Also, fine manipulations are needed in each step to guarantee the technique's success. Furthermore, understanding the formation of tendons and vasculature in RLs is not yet fully elucidated.

Based on these characteristics the RL model is a well-suited to evaluate the biology of stem and progenitor cells isolated directly from an organism (e.g., LBM cells). The RL system's versatility permits the creation of multiple combinations of cells from different sources, developmental stages, or positions along the limb, whole (undissociated), or reaggregated cells, even until modified LBM cells overexpress distinct molecules, as shown by Marín-Llera et al., 2021.

Data from our laboratory has demonstrated that mouse limb mesodermal cells are competent to receive chicken ectodermal signals and form skeletal elements after 6 days. Skeletal elements are organized similarly as it occurs during limb development (**Figures 1A–C**). On the other hand, in the 5-day mouse-chicken

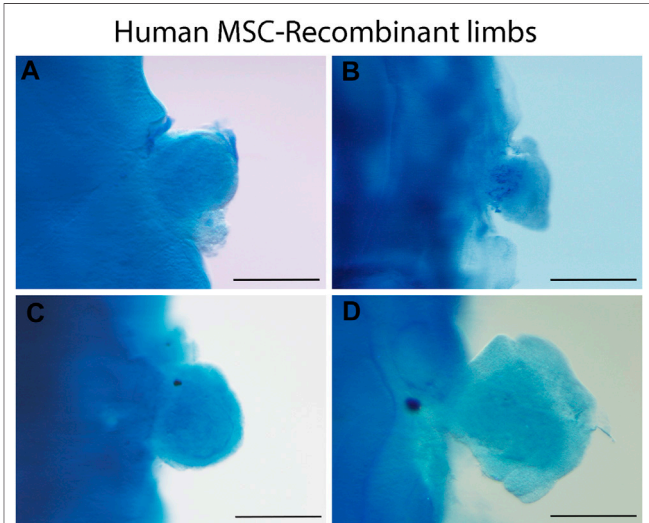


FIGURE 2 | Human MSC-derived RL from different sources. Alcian blue staining of 24 h recombinant limbs performed with human MSCs assembled in chicken ectoderms. MSCs were obtained from **(A)** bone marrow, **(B)** Wharton's jelly, **(C)** umbilical cord blood, and **(D)** placenta. Chicken ectoderms and host embryos were obtained from the 22 HH stage. Scale bar 100 μ m.

RL, mouse mesodermal cells are condensed in the center, and no skeletal elements are observed (**Figures 1D–F**). This suggests that the specification of mouse mesodermal cells in this system is delayed relative to the chicken-chicken RL. The successful generation of a chimeric RL using mouse mesoderm demonstrates the possibility of combining cells from different mammalian species, thereby creating opportunities to study morphogenesis, patterning cell-cell interactions, cell migration, and cell differentiation at the cellular and molecular levels on these cells. Notably, the source of the mesodermal component of

the RL is not limited to limb cell sources. Our unpublished work demonstrated that RL could be obtained from previously expanded cells with mesodermal differentiation capacity as adult MSCs. MSCs from bone marrow (BM), Wharton's jelly (WJ), umbilical cord blood (UCB), and placenta (P) placed under the embryonic ectodermal signals successfully formed RL after 24 h after grafting (**Figure 2**). Interestingly, MSCs are committed and spatially organized differently under these conditions depending on their origin (data not shown). These data suggest that it might be possible to generate RL from other ASCs and PSCs or stem or progenitor cells (e.g., ESCs, iPSCs) induced through *in vitro* differentiation protocols. The RL system permits us to evaluate cells' behavior in response to embryonic patterning signals and, even more relevant, to study their capacity to interpret morphogenetic signals that could lead them to form the pattern of limb bud skeletal elements *in vivo*.

The RL system exposes cells simultaneously to signaling centers, thereby physiologically mimicking the limb microenvironment and allowing undifferentiated cells to develop into distinct limb cell types simultaneously by synthesizing both the ECM and tissue-specific proteins. In addition to individual cell differentiation, groups of cells organize into a complex structure with a 3D pattern. These are essential characteristics required for a system to be considered an organoid. In this sense, the RL assay represents a powerful *in vivo* system for generating limb organoids.

CONCLUSION

Cell differentiation and morphogenesis are fine-tuned processes that lead to the formation of specialized cell types, organized tissues, and functioning organs directing cell fate from embryonic development to an independent living organism. Understanding the early cell differentiation steps is essential to model these complex processes in an experimental setting. The RL system is a powerful experimental model for studying patterning, morphogenesis, cell-cell interactions, cell migration, commitment, and cell differentiation at the cellular and molecular levels. Currently, the use of the RL model is restricted to limb developmental biology. However, this infrequently used technique represents an *in vivo* organoid system. It conserves the expression of the ectodermal limb bud signaling centers that mediate the morphogenesis and commitment of undifferentiated cells along distinct

developmental paths. This model also faithfully maintains the appropriate gene expression patterns with spatial-temporal accuracy. The RL model establishes the proper 3D polarization of limb-like structures and recapitulates the differentiation programs observed during development, resulting in correctly positioned skeletal elements. Furthermore, we consider that the RL assay system permits countless applications across numerous biological questions without being restricted to limb developmental biology and the use of LBM cells.

DATA AVAILABILITY STATEMENT

The original contributions presented in the study are included in the article/Supplementary Material, further inquiries can be directed to the corresponding authors.

ETHICS STATEMENT

The animal study was reviewed and approved by Institutional Review Board for the Care and Use of Laboratory Animals of the Instituto de Investigaciones Biomédicas, Universidad Nacional Autónoma de México (UNAM, Mexico City, Mexico).

AUTHOR CONTRIBUTIONS

RG-G, EG-P and JC-M wrote the manuscript. JCM-L conceived and wrote the manuscript.

FUNDING

This work was supported by the Dirección General de Asuntos del Personal Académico (DGAPA)-Universidad Nacional Autónoma de México (grant numbers IN211117 and IN213314) and Consejo Nacional de Ciencia y Tecnología (CONACyT) (grant number 1887 CONACyT-Fronteras de la Ciencia) awarded to JC-M, RG-G and EG-P were the recipients of an undergraduate fellowship, and JCM-L was the recipient of a postdoctoral fellowship, all from the Consejo Nacional de Ciencia y Tecnología (CONACyT-Fronteras de la Ciencia-1887).

REFERENCES

- Almohsen, F., and Al-Mudallal, S. S. (2020). Impact of Leukemia Stem Cells Phenotype Expression on Response to Induction Therapy in Acute Myeloid Leukemia Patients. *Chddt* 20, 145–151. doi:10.2174/1871529X19666190719105954
- Ahrens, P. B., Solursh, M., and Reiter, R. S. (1977). Stage-Related Capacity for Limb Chondrogenesis in Cell Culture. *Dev. Biol.* 60. doi:10.1016/0012-1606(77)90110-5
- Arzate, H., Chimal-Monroy, J., Hernández-Lagunas, L., and Leon, L. D. (1996). Human Cementum Protein Extract Promotes Chondrogenesis and Mineralization in Mesenchymal Cells. *J. Periodontal Res.* 31, 144–148. doi:10.1111/j.1600-0765.1996.tb00476.x
- Atsuta, Y., Lee, C., Rodrigues, A. R., Colle, C., Tomizawa, R. R., Lujan, E. G., et al. (2021). Direct Reprogramming of Non-limb Fibroblasts to Cells with Properties of Limb Progenitors. *bioRxiv*. doi:10.1101/2021.10.01.462632
- Capo, V., Penna, S., Merelli, I., Barcellona, M., Scala, S., Basso-Ricci, L., et al. (2020). Expanded Circulating Hematopoietic Stem/progenitor Cells as Novel Cell Source for the Treatment of TCIRG1 Osteopetrosis. *haematol* 106, 74–86. doi:10.3324/haematol.2019.238261
- Chan, C. J., Heisenberg, C.-P., and Hiiragi, T. (2017). Coordination of Morphogenesis and Cell-Fate Specification in Development. *Curr. Biol.* 27, R1024–R1035. doi:10.1016/j.cub.2017.07.010

- Cooper, K. L., Hu, J. K.-H., ten Berge, D., Fernandez-Teran, M., Ros, M. A., and Tabin, C. J. (2011). Initiation of Proximal-Distal Patterning in the Vertebrate Limb by Signals and Growth. *Science* 332, 1083–1086. doi:10.1126/science.1199499
- Corrò, C., Novellademunt, L., and Li, V. S. W. (2020). A Brief History of Organoids. *Am. J. Physiology-Cell Physiol.* 319, C151–C165. doi:10.1152/ajpcell.00120.2020
- Crosby, G. M., and Fallon, J. F. (1975). Inhibitory Effect on Limb Morphogenesis by Cells of the Polarizing Zone Coaggregated with Pre- or Postaxial wing Bud Mesoderm. *Dev. Biol.* 46, 28–39. doi:10.1016/0012-1606(75)90084-6
- de Souza, N. (2018). Organoids. *Nat. Methods* 15, 23. doi:10.1038/nmeth.4576
- Dollé, P., Izpisua-Belmonte, J.-C., Falkenstein, H., Renucci, A., and Duboule, D. (1989). Coordinate Expression of the Murine Hox-5 Complex Homoeobox-Containing Genes during Limb Pattern Formation. *Nature* 342, 767–772. doi:10.1038/342767a0
- Dye, B. R., Hill, D. R., Ferguson, M. A., Tsai, Y.-H., Nagy, M. S., Dyal, R., et al. (2015). *In Vitro* generation of Human Pluripotent Stem Cell Derived Lung Organoids. *eLife* 4, 05098. doi:10.7554/eLife.05098
- Ehrmann, L., and Robert, G. O. G. (1956). The Growth of Cells on a Transparent Gel of Reconstituted Rat-Tail Collagen. *JNCI* 16 (6), 1375–1403. doi:10.1093/jnci/16.6.1375
- Eiraku, M., Takata, N., Ishibashi, H., Kawada, M., Sakakura, E., Okuda, S., et al. (2011). Self-organizing Optic-Cup Morphogenesis in Three-Dimensional Culture. *Nature* 472, 51–56. doi:10.1038/nature09941
- Eiraku, M., Watanabe, K., Matsuo-Takasaki, M., Kawada, M., Yonemura, S., Matsumura, M., et al. (2008). Self-Organized Formation of Polarized Cortical Tissues from ESCs and its Active Manipulation by Extrinsic Signals. *Cell Stem Cell* 3, 519–532. doi:10.1016/j.stem.2008.09.002
- Escalante-Alcalde, D., and Merchant-Larios, H. (1992). Somatic and Germ Cell Interactions during Histogenetic Aggregation of Mouse Fetal Testes. *Exp. Cell Res.* 198, 150–158. doi:10.1016/0014-4827(92)90161-z
- Fallon, J., and Simandl, K. B. (1984). Interactions Between Chick Limb Bud Mesoderm and Reptile Ectoderm Result In Limb Outgrowth in the Limbless Mutant. *Anatomical Records* 208 (3), A53–A54.
- Fell, H. B., and Robison, R. (1929). The Growth, Development and Phosphatase Activity of Embryonic Avian Femora and Limb-Buds Cultivated *In Vitro*. *Biochem. J.* 23, 767–784. doi:10.1042/bj0230767
- Feneck, E., and Logan, M. (2020). The Role of Retinoic Acid in Establishing the Early Limb Bud. *Biomolecules* 10, 312. doi:10.3390/biom10020312
- Fernandez-Teran, M., Piedra, M. E., Ros, M. A., and Fallon, J. F. (1999). The Recombinant Limb as a Model for the Study of Limb Patterning, and its Application to Muscle Development. *Cell Tissue Res.* 296, 121–129. doi:10.1007/s004410051273
- Frederick, J. M., and Fallon, J. F. (1982). The Proportion and Distribution of Polarizing Zone Cells Causing Morphogenetic Inhibition when Coaggregated with Anterior Half wing Mesoderm in Recombinant Limbs. *J. Embryol. Exp. Morphol.* 67, 13–25. doi:10.1024/dev.67.1.13
- Fujii, K., Zhulyn, O., Byeon, G. W., Genuth, N. R., Kerr, C. H., Walsh, E. M., et al. (2021). Controlling Tissue Patterning by Translational Regulation of Signaling Transcripts through the Core Translation Factor eIF3c. *Dev. Cell* 56, 2928–2937.e9. doi:10.1016/j.devcel.2021.10.009
- Gamart, J., Barozzi, I., Laurent, F., Reinhardt, R., Martins, L. R., Oberholzer, T., et al. (2021). SMAD4 Target Genes Are Part of a Transcriptional Network that Integrates the Response to BMP and SHH Signaling during Early Limb Bud Patterning. *Development* 148, dev200182. doi:10.1242/dev.200182
- Guzzo, R. M., Gibson, J., Xu, R.-H., Lee, F. Y., and Drissi, H. (2013). Efficient Differentiation of Human iPSC-Derived Mesenchymal Stem Cells to Chondroprogenitor Cells. *J. Cel. Biochem.* 114, 480–490. doi:10.1002/jcb.24388
- Hall, B. K. (1981). Intracellular and Extracellular Control of the Differentiation of Cartilage and Bone. *Histochem. J.* 13, 599–614. doi:10.1007/BF01002713
- Hamburger, V., and Hamilton, H. L. (1992). A Series of normal Stages in the Development of the Chick Embryo. *Dev. Dyn.* 195, 231–272. doi:10.1002/aja.1001950404
- Haro, E., Delgado, I., Junco, M., Yamada, Y., Mansouri, A., Oberg, K. C., et al. (2014). Sp6 and Sp8 Transcription Factors Control AER Formation and Dorsal-Ventral Patterning in Limb Development. *Plos Genet.* 10, e1004468. doi:10.1371/journal.pgen.1004468
- Huang, S., Kuri, P., Aubert, Y., Brewster, M., Li, N., Farrelly, O., et al. (2021). Lgr6 marks Epidermal Stem Cells with a Nerve-dependent Role in Wound Re-epithelialization. *Cell Stem Cell* 28, 1582–1596. e6. doi:10.1016/j.stem.2021.05.007
- Huch, M., Gehart, H., van Boxtel, R., Hamer, K., Blokzijl, F., Versteegen, M. M. A., et al. (2015). Long-Term Culture of Genome-Stable Bipotent Stem Cells from Adult Human Liver. *Cell* 160, 299–312. doi:10.1016/j.cell.2014.11.050
- Ishikawa, D., Diekmann, U., Fiedler, J., Just, A., Thum, T., Lenzen, S., et al. (2017). miRNome Profiling of Purified Endoderm and Mesoderm Differentiated from hESCs Reveals Functions of miR-483-3p and miR-1263 for Cell-Fate Decisions. *Stem Cell Rep.* 9 (5), 1588–1603. doi:10.1016/j.stemcr.2017.10.011
- Jiang, M., Liu, R., Liu, L., Kot, A., Liu, X., Xiao, W., et al. (2020). Identification of Osteogenic Progenitor Cell-Targeted Peptides that Augment Bone Formation. *Nat. Commun.* 11. doi:10.1038/s41467-020-17417-9
- Kamiya, D., Banno, S., Sasai, N., Ohgushi, M., Inomata, H., Watanabe, K., et al. (2011). Intrinsic Transition of Embryonic Stem-Cell Differentiation into Neural Progenitors. *Nature* 470, 503–509. doi:10.1038/nature09726
- Kleinman, H. K., and Martin, J. R. (2005). Matrigel: Basement Membrane Matrix with Biological Activity. *Semin. Cancer Biol.* 15, 378–386. doi:10.1016/j.semcancer.2005.05.004
- Kuhlman, J., and Niswander, L. (1997). Limb Deformity Proteins: Role in Mesodermal Induction of the Apical Ectodermal ridge. *Development* 124, 133–139. doi:10.1242/dev.124.1.133
- Kumar, V., Park, S., Lee, U., and Kim, J. (2021). The Organizer and its Signaling in Embryonic Development. *Jdb* 9, 47. doi:10.3390/jdb9040047
- Lancaster, M. A., Renner, M., Martin, C.-A., Wenzel, D., Bicknell, L. S., Hurles, M. E., et al. (2013). Cerebral Organoids Model Human Brain Development and Microcephaly. *Nature* 501, 373–379. doi:10.1038/nature12517
- Loh, K. M., Chen, A., Koh, P. W., Deng, T. Z., Sinha, R., Tsai, J. M., et al. (2016). Mapping the Pairwise Choices Leading from Pluripotency to Human Bone, Heart, and Other Mesoderm Cell Types. *Cell* 166, 451–467. doi:10.1016/j.cell.2016.06.011
- Loomis, C. A., Harris, E., Michaud, J., Wurst, W., Hanks, M., and Joyner, A. L. (1996). The Mouse Engrailed-1 Gene and Ventral Limb Patterning. *Nature* 382, 360–363. doi:10.1038/382360a0
- Lorda-Diez, C. I., Montero, J. A., Garcia-Porrero, J. A., and Hurlé, J. M. (2010). Tgfb2 and 3 Are Coexpressed with Their Extracellular Regulator Ltbp1 in the Early Limb Bud and Modulate Mesodermal Outgrowth and BMP Signaling in Chicken Embryos. *BMC Dev. Biol.* 10, 69. doi:10.1186/1471-213X-10-69
- MacCabe, J. A., Saunders, J. W., and Pickett, M. (1973). The Control of the Anteroposterior and Dorsoventral Axes in Embryonic Chick Limbs Constructed of Dissociated and Reaggregated Limb-Bud Mesoderm. *Dev. Biol.* 31, 323–335. doi:10.1016/0012-1606(73)90269-8
- Marin-Llera, J. C., Fernández-Calderón, M., and Chimal-Monroy, J. (2022). Chicken Recombinant Limbs Assay to Understand Morphogenesis, Patterning, and Early Steps in Cell Differentiation. *JoVE*, e63183. doi:10.3791/63183
- Marin-Llera, J. C., Garcíadiego-Cázares, D., and Chimal-Monroy, J. (2019). Understanding the Cellular and Molecular Mechanisms that Control Early Cell Fate Decisions during Appendicular Skeletogenesis. *Front. Genet.* 10, 977. doi:10.3389/fgene.2019.00977
- Marin-Llera, J. C., Lorda-Diez, C. I., Hurlé, J. M., and Chimal-Monroy, J. (2021). SCA-1/Ly6A Mesodermal Skeletal Progenitor Subpopulations Reveal Differential Commitment of Early Limb Bud Cells. *Front. Cell Dev. Biol.* 9, 656999. doi:10.3389/fcell.2021.656999
- McCracken, K. W., Catá, E. M., Crawford, C. M., Sinagoga, K. L., Schumacher, M., Rockich, B. E., et al. (2014). Modelling Human Development and Disease in Pluripotent Stem-Cell-Derived Gastric Organoids. *Nature* 516, 400–404. doi:10.1038/nature13863
- McQueen, C., and Towers, M. (2020). Establishing the Pattern of the Vertebrate Limb. *Development* 147, dev177956. doi:10.1242/dev.177956
- Mello, M. A., and Tuan, R. S. (1999). High Density Micromass Cultures of Embryonic Limb Bud Mesenchymal Cells: An *In Vitro* Model of Endochondral Skeletal Development. *In Vitro Cell.Dev.Biol.-Animal* 35, 262–269. doi:10.1007/s11626-999-0070-0

- Montell, D. J. (2008). Morphogenetic Cell Movements: Diversity from Modular Mechanical Properties. *Science* 322, 1502–1505. doi:10.1126/science.1164073
- Mori, S., Sakakura, E., Tsunekawa, Y., Hagiwara, M., Suzuki, T., and Eiraku, M. (2019). Self-organized Formation of Developing Appendages from Murine Pluripotent Stem Cells. *Nat. Commun.* 10. doi:10.1038/s41467-019-11702-y
- Murry, C. E., and Keller, G. (2008). Differentiation of Embryonic Stem Cells to Clinically Relevant Populations: Lessons from Embryonic Development. *Cell* 132, 661–680. doi:10.1016/j.cell.2008.02.008
- Ohuchi, H., Nakagawa, T., Yamamoto, A., Araga, A., Ohata, T., Ishimaru, Y., et al. (1997). The Mesenchymal Factor, FGF10, Initiates and Maintains the Outgrowth of the Chick Limb Bud through Interaction with FGF8, an Apical Ectodermal Factor. *Development* 124, 2235–2244. doi:10.1242/dev.124.11.2235
- Osakada, F., Ikeda, H., Sasai, Y., and Takahashi, M. (2009). Stepwise Differentiation of Pluripotent Stem Cells into Retinal Cells. *Nat. Protoc.* 4, 811–824. doi:10.1038/nprot.2009.51
- Piedra, M. E., Borja Rivero, F., Fernandez-Teran, M., and Ros, M. A. (2000). Pattern Formation and Regulation of Gene Expressions in Chick Recombinant Limbs. *Mech. Dev.* 90, 167–179. doi:10.1016/S0925-4773(99)00247-6
- Riddle, R. D., Johnson, R. L., Laufer, E., and Tabin, C. (1993). Sonic Hedgehog Mediates the Polarizing Activity of the ZPA. *Cell* 75, 1401–1416. doi:10.1016/0092-8674(93)90626-2
- Río, P., Navarro, S., and Bueren, J. A. (2018). Advances in Gene Therapy for Fanconi Anemia. *Hum. Gene Ther.* 29, 1114–1123. doi:10.1089/hum.2018.124
- Ros, M. A., Lyons, G. E., Mackem, S., and Fallon, J. F. (1994). Recombinant Limbs as a Model to Study Homeobox Gene Regulation during Limb Development. *Dev. Biol.* 166, 59–72. doi:10.1006/dbio.1994.1296
- Ros, M. A., Simandl, B. K., Clark, A. W., and Fallon, J. F. (2000). Methods for Manipulating the Chick Limb Bud to Study Gene Expression, Tissue Interactions, and Patterning. *Methods Mol. Biol.* 137, 245–266. doi:10.1385/1-59259-066-7:245
- Roselló-Diez, A., Arques, C. G., Delgado, I., Giovinozzo, G., and Torres, M. (2014). Diffusible Signals and Epigenetic Timing Cooperate in Late Proximo-Distal Limb Patterning. *Development (Cambridge)* 141, 1534–1543. doi:10.1242/dev.106831
- Roselló-Diez, A., Ros, M. A., and Torres, M. (2011). Diffusible Signals, Not Autonomous Mechanisms, Determine the Main Proximodistal Limb Subdivision. *Science* 332, 1086–1088. doi:10.1126/science.1199489
- Rossi, G., Manfrin, A., and Lutolf, M. P. (2018). Progress and Potential in Organoid Research. *Nat. Rev. Genet.* 19, 671–687. doi:10.1038/s41576-018-0051-9
- Royle, S. R., Tabin, C. J., and Young, J. J. (2021). Limb Positioning and Initiation: An Evolutionary Context of Pattern and Formation. *Dev. Dyn.* 250, 1264–1279. doi:10.1002/dvdy.308
- Sasai, Y. (2013). Cytosystems Dynamics in Self-Organization of Tissue Architecture. *Nature* 493, 318–326. doi:10.1038/nature11859
- Sato, T., Vries, R. G., Snippert, H. J., van de Wetering, M., Barker, N., Stange, D. E., et al. (2009). Single Lgr5 Stem Cells Build Crypt-Villus Structures *In Vitro* without a Mesenchymal Niche. *Nature* 459, 262–265. doi:10.1038/nature07935
- Saxén, L., and Thesleff, I. (2007). Epithelial-Mesenchymal Interactions in Murine Organogenesis. *Postimplantation Dev. Mouse* 165, 183–198. Ciba Foundation Symposium. doi:10.1002/9780470514221.ch11
- Schnabel, D., Salas-Vidal, E., Narváez, V., del Rayo Sánchez-Carbente, M., Hernández-García, D., Cuervo, R., et al. (2006). Expression and Regulation of Antioxidant Enzymes in the Developing Limb Support a Function of ROS in Interdigital Cell Death. *Dev. Biol.* 291, 291–299. doi:10.1016/j.ydbio.2005.12.023
- Shu, H. S., Liu, Y. L., Tang, X. T., Zhang, X. S., Zhou, B., Zou, W., et al. (2021). Tracing the Skeletal Progenitor Transition during Postnatal Bone Formation. *Cell Stem Cell* 28, 2122–2136.e3. doi:10.1016/j.stem.2021.08.010
- Slack, J. M. W. (2008). Origin of Stem Cells in Organogenesis. *Science* 322, 1498–1501. doi:10.1126/science.1162782
- Smith, E., Kanczler, J., Kanczler, J., and Oreffo, R. (2013). A New Take on an Old story: Chick Limb Organ Culture for Skeletal Niche Development and Regenerative Medicine Evaluation. *eCM* 26, 91–106. doi:10.22203/eCM.v026a07
- Soshnikova, N., Zechner, D., Huelsken, J., Mishina, Y., Behringer, R. R., Taketo, M. M., et al. (2003). Genetic Interaction between Wnt/ β -Catenin and BMP Receptor Signaling during Formation of the AER and the Dorsal-Ventral axis in the Limb. *Genes Dev.* 17, 1963–1968. doi:10.1101/gad.263003
- Strobel, H. A., Moss, S. M., and Hoying, J. B. (2022). Methods for Vascularization and Perfusion of Tissue Organoids. *Mamm. Genome*. doi:10.1007/s00335-022-09951-2
- Takahashi, K., Tanabe, K., Ohnuki, M., Narita, M., Ichisaka, T., Tomoda, K., et al. (2007). Induction of Pluripotent Stem Cells from Adult Human Fibroblasts by Defined Factors. *Cell* 131, 861–872. doi:10.1016/j.cell.2007.11.019
- Takahashi, K., and Yamanaka, S. (2006). Induction of Pluripotent Stem Cells from Mouse Embryonic and Adult Fibroblast Cultures by Defined Factors. *Cell* 126, 663–676. doi:10.1016/j.cell.2006.07.024
- Taketo, T., and Koide, S. S. (1981). *In Vitro* development of Testis and Ovary from Indifferent Fetal Mouse Gonads. *Dev. Biol.* 84, 61–66. doi:10.1016/0012-1606(81)90370-5
- ten Berge, D., Brugmann, S. A., Helms, J. A., and Nusse, R. (2008). Wnt and FGF Signals Interact to Coordinate Growth with Cell Fate Specification During Limb Development. *Development*, 135 (19), 3247–3257. doi:10.1242/dev.023176
- Toh, W. S., Lai, R. C., Hui, J. H. P., and Lim, S. K. (2017). MSC Exosome as a Cell-free MSC Therapy for Cartilage Regeneration: Implications for Osteoarthritis Treatment. *Semin. Cel Dev. Biol.* 67, 56–64. doi:10.1016/j.semcdb.2016.11.008
- Tuysuz, E. C., Ozbey, U., Gulluoglu, S., Kuskucu, A., Sahin, F., and Bayrak, O. F. (2021). miRNAs as Cell Fate Determinants of Lateral and Paraxial Mesoderm Differentiation from Embryonic Stem Cells. *Dev. Biol.* 478, 212–221. doi:10.1016/j.ydbio.2021.07.002
- Xia, Y., and Izpisua Belmonte, J. C. (2019). Design Approaches for Generating Organ Constructs. *Cell Stem Cell* 25, 447. doi:10.1016/j.stem.2019.08.001
- Xia, Y., Sun, J., Zhao, L., Zhang, F., Liang, X.-J., Guo, Y., et al. (2018). Magnetic Field and Nano-Scaffolds with Stem Cells to Enhance Bone Regeneration. *Biomaterials* 183, 151–170. doi:10.1016/j.biomaterials.2018.08.040
- Yamada, D., Nakamura, M., Takao, T., Takihiro, S., Yoshida, A., Kawai, S., et al. (2021). Induction and Expansion of Human PRRX1+ Limb-bud-like Mesenchymal Cells from Pluripotent Stem Cells. *Nat. Biomed. Eng.* 5, 926–940. doi:10.1038/s41551-021-00778-x
- Yan, H., and Hales, B. F. (2021). Effects of an Environmentally Relevant Mixture of Organophosphate Esters Derived from House Dust on Endochondral Ossification in Murine Limb Bud Cultures. *Toxicol. Sci.* 180, 62–75. doi:10.1093/toxsci/kfaa180
- Yan, H., and Hales, B. F. (2019). Effects of Organophosphate Ester Flame Retardants on Endochondral Ossification in *Ex Vivo* Murine Limb Bud Cultures. *Toxicol. Sci.* 168, 420–429. doi:10.1093/toxsci/kfy301
- Yu, J., Vodyanik, M. A., Smuga-Otto, K., Antosiewicz-Bourget, J., Frane, J. L., Tian, S., et al. (2007). Induced Pluripotent Stem Cell Lines Derived from Human Somatic Cells. *Science* 318, 1917–1920. doi:10.1126/science.1151526
- Zhou, X., Lu, Y., Zhao, F., Dong, J., Ma, W., Zhong, S., et al. (2022). Deciphering the Spatial-Temporal Transcriptional Landscape of Human Hypothalamus Development. *Cell Stem Cell* 29, 328–343. doi:10.1016/j.stem.2021.11.009
- Zwilling, E. (1964). Development of Fragmented and of Dissociated Limb Bud Mesoderm. *Dev. Biol.* 9, 20–37. doi:10.1016/0012-1606(64)90012-0

Conflict of Interest: The authors declare that the research was conducted in the absence of any commercial or financial relationships that could be construed as a potential conflict of interest.

Publisher's Note: All claims expressed in this article are solely those of the authors and do not necessarily represent those of their affiliated organizations, or those of the publisher, the editors and the reviewers. Any product that may be evaluated in this article, or claim that may be made by its manufacturer, is not guaranteed or endorsed by the publisher.

Copyright © 2022 García-García, Garay-Pacheco, Marín-Llera and Chimal-Monroy. This is an open-access article distributed under the terms of the Creative Commons Attribution License (CC BY). The use, distribution or reproduction in other forums is permitted, provided the original author(s) and the copyright owner(s) are credited and that the original publication in this journal is cited, in accordance with accepted academic practice. No use, distribution or reproduction is permitted which does not comply with these terms.



OPEN ACCESS

EDITED BY
Daniel Ortuño-Sahagún,
University of Guadalajara, Mexico

REVIEWED BY
Michael Akam,
University of Cambridge,
United Kingdom
Prashant Sharma,
University of Wisconsin-Madison,
United States

*CORRESPONDENCE
Andres F. Sarrazin,
andres.sarrazin@pucv.cl

SPECIALTY SECTION
This article was submitted to
Morphogenesis and Patterning,
a section of the journal
Frontiers in Cell and Developmental
Biology

RECEIVED 15 May 2022
ACCEPTED 11 July 2022
PUBLISHED 05 August 2022

CITATION
Mundaca-Escobar M, Cepeda RE and
Sarrazin AF (2022), The organizing role
of Wnt signaling pathway during
arthropod posterior growth.
Front. Cell Dev. Biol. 10:944673.
doi: 10.3389/fcell.2022.944673

COPYRIGHT
© 2022 Mundaca-Escobar, Cepeda and
Sarrazin. This is an open-access article
distributed under the terms of the
[Creative Commons Attribution License](#)
(CC BY). The use, distribution or
reproduction in other forums is
permitted, provided the original
author(s) and the copyright owner(s) are
credited and that the original
publication in this journal is cited, in
accordance with accepted academic
practice. No use, distribution or
reproduction is permitted which does
not comply with these terms.

The organizing role of Wnt signaling pathway during arthropod posterior growth

Marco Mundaca-Escobar, Rodrigo E. Cepeda and
Andres F. Sarrazin*

CoDe-Lab, Instituto de Química, Pontificia Universidad Católica de Valparaíso, Valparaíso, Chile

Wnt signaling pathways are recognized for having major roles in tissue patterning and cell proliferation. In the last years, remarkable progress has been made in elucidating the molecular and cellular mechanisms that underlie sequential segmentation and axial elongation in various arthropods, and the canonical Wnt pathway has emerged as an essential factor in these processes. Here we review, with a comparative perspective, the current evidence concerning the participation of this pathway during posterior growth, its degree of conservation among the different subphyla within Arthropoda and its relationship with the rest of the gene regulatory network involved. Furthermore, we discuss how this signaling pathway could regulate segmentation to establish this repetitive pattern and, at the same time, probably modulate different cellular processes precisely coupled to axial elongation. Based on the information collected, we suggest that this pathway plays an organizing role in the formation of the body segments through the regulation of the dynamic expression of segmentation genes, *via* controlling the *caudal* gene, at the posterior region of the embryo/larva, that is necessary for the correct sequential formation of body segments in most arthropods and possibly in their common segmented ancestor. On the other hand, there is insufficient evidence to link this pathway to axial elongation by controlling its main cellular processes, such as convergent extension and cell proliferation. However, conclusions are premature until more studies incorporating diverse arthropods are carried out.

KEYWORDS

signaling pathway, segment addition zone, body segmentation, axial elongation, wnt signaling

Introduction

Panarthropods are a superphylum integrated by organisms with bilateral symmetry and a segmented body, divided into Tardigrada, Onychophora, and Arthropoda. The latter has been the most studied so far and is, in turn, grouped into Chelicerata (*e.g.*, spiders and scorpions), Myriapoda (*e.g.*, centipedes and millipedes), and Pancrustacea (*e.g.*, crustaceans and insects) (Giribet and Edgecombe, 2019). The embryonic development of panarthropods is based on the organization of a segmented body

plan, which is a shared feature in their evolutionary history (Hannibal and Patel, 2013; Chipman and Edgecombe, 2019). This developmental modality is based on the formation of similar repetitive units called segments along the anteroposterior axis (Clark et al., 2019). The establishment of this segmented patterning has been considered a significant contribution to promoting the great diversity of shapes and sizes found within panarthropods and their high adaptive success in practically all the environments on our planet (Peel et al., 2005; Auman and Chipman, 2017).

The segmented body plan of panarthropods is orchestrated by a wide variety of cellular mechanisms and genetic regulators, which can vary depending on the organism in question.

A widely conserved signaling pathway during embryonic development is the Wnt pathway, which coordinates crucial cellular processes such as proliferation, cell polarity, and the determination of cell fate (Williams and Nagy, 2017; Steinhart and Angers, 2018). Three main different Wnt signaling pathways have been described: The canonical pathway, which is dependent on β -catenin cytoplasm accumulation and subsequent nuclear translocation to the coactivation of specific gene transcription, and the noncanonical Wnt/planar cell polarity (Wnt/PCP) and Wnt/ Ca^{2+} pathways, which mediate cytoskeleton dynamics and cell movements through directional information or intracellular Ca^{2+} release, respectively (Croce and McClay, 2008; Angers and Moon, 2009). Although canonical and noncanonical pathways have different signaling mechanisms, both participate in regulating different cellular processes and genetic patterning, allowing successful embryonic development.

The first studies of the Wnt pathway in panarthropods were carried out on the vinegar fly *Drosophila melanogaster* (Nüsslein-Volhard and Wieschaus, 1980; Baker, 1987; Rijsewijk et al., 1987; Martinez et al., 1988), initiating a wide line of research that linked this pathway to embryonic development, revealing its relationship with various developmental processes. Over the years, more research has been conducted on flies and several vertebrates, including diverse developmental processes and diseases (Jenny and Basler, 2014; Bejsovec, 2018; Wiese et al., 2018), but neglecting the high number of existing arthropods and their different modes of embryogenesis (Murat et al., 2010).

In the last years, exciting advances have been made regarding the molecular and cellular mechanisms involved during sequential segmentation and axial elongation in a variety of arthropods, and the Wnt pathway has emerged as an essential factor in these processes. Some reviews have covered this topic while not focusing specifically on the role of this signaling pathway (Martin and Kimelman, 2009; Williams and Nagy, 2017; Clark et al., 2019). Thus, in a comparative approach, it remains to discuss how and when the Wnt pathway participates in establishing the segmented pattern and regulating processes such as cell proliferation or convergent extension during the posterior body growth in panarthropods. In this review, we will start with a description of the repertoire and expression pattern

of Wnt ligands in a vast number of panarthropods, including representatives of all the phyla, addressing their possible roles during germband extension. Then, we will discuss how this signaling pathway could regulate segmentation to establish this repetitive pattern and, at the same time, probably modulate different cellular processes precisely coupled to axial elongation.

The repertoire of Wnt ligands present in panarthropods

The Wnt pathway is a complex signaling pathway present in all metazoans—including placozoans and sponges—that comprises several receptors and intracellular components, as well as an established repertoire of thirteen ligand subfamilies (Holstein, 2012). In vertebrates, it has been determined that Wnt1, Wnt2, Wnt3, Wnt8, and Wnt10 ligands are activators of the canonical pathway, and that Wnt4, Wnt5, Wnt6, Wnt7, Wnt9, and Wnt11 ligands are activators attributed to the noncanonical pathways (Gajos-Michniewicz and Czyz, 2020), while Wnt16 ligand has been shown to be an activator of both, canonical and noncanonical pathways (Gori et al., 2015). WntA ligand, of an indeterminate group, has not been found in vertebrates (Prud'homme et al., 2002), although it is present in urochordates and cephalochordates (Somorjai et al., 2018), as well as in panarthropods (Janssen et al., 2010; Hogvall et al., 2014).

The analysis of the full repertoire of Wnt ligands in panarthropods published so far (Figure 1) showed that a common characteristic is the loss of the Wnt3 ligand, implying that their common ancestor most probably presented ligands from only twelve subfamilies (Hayden and Arthur, 2014; Hogvall et al., 2014; Janssen and Posnien, 2014). A significant loss also occurred in insects, where the absence of Wnt2 and Wnt4 ligands in all the representatives is observed. Interestingly, an ortholog of *wnt16* is present in the apid and absent in the other eight insects included in the analysis (Dearden et al., 2006; Bolognesi et al., 2008a; Murat et al., 2010; Shigenobu et al., 2010; Yin et al., 2015; Ding et al., 2019; Holzem et al., 2019; Panfilio et al., 2019; Vosburg et al., 2020). More losses are found in other lineages. However, they were not general to the clade, as they are mixed with other species that retained at least ten Wnt ligands from the ancestral twelve subfamilies (Figure 1). While these losses may depict specific eliminations in particular species within Arthropoda, we cannot exclude that missing ligands could represent low expression transcripts rather than losses at the genomic level when the database used is a transcriptome instead of the whole sequenced genome, as in the cases of *Cupiennius salei*, *Calanus finmarchicus* and *Thamnocephalus platyurus*, among others.

Our updated repertoire also showed that only Wnt4, Wnt5 and Wnt16 ligands were retained in all crustacean

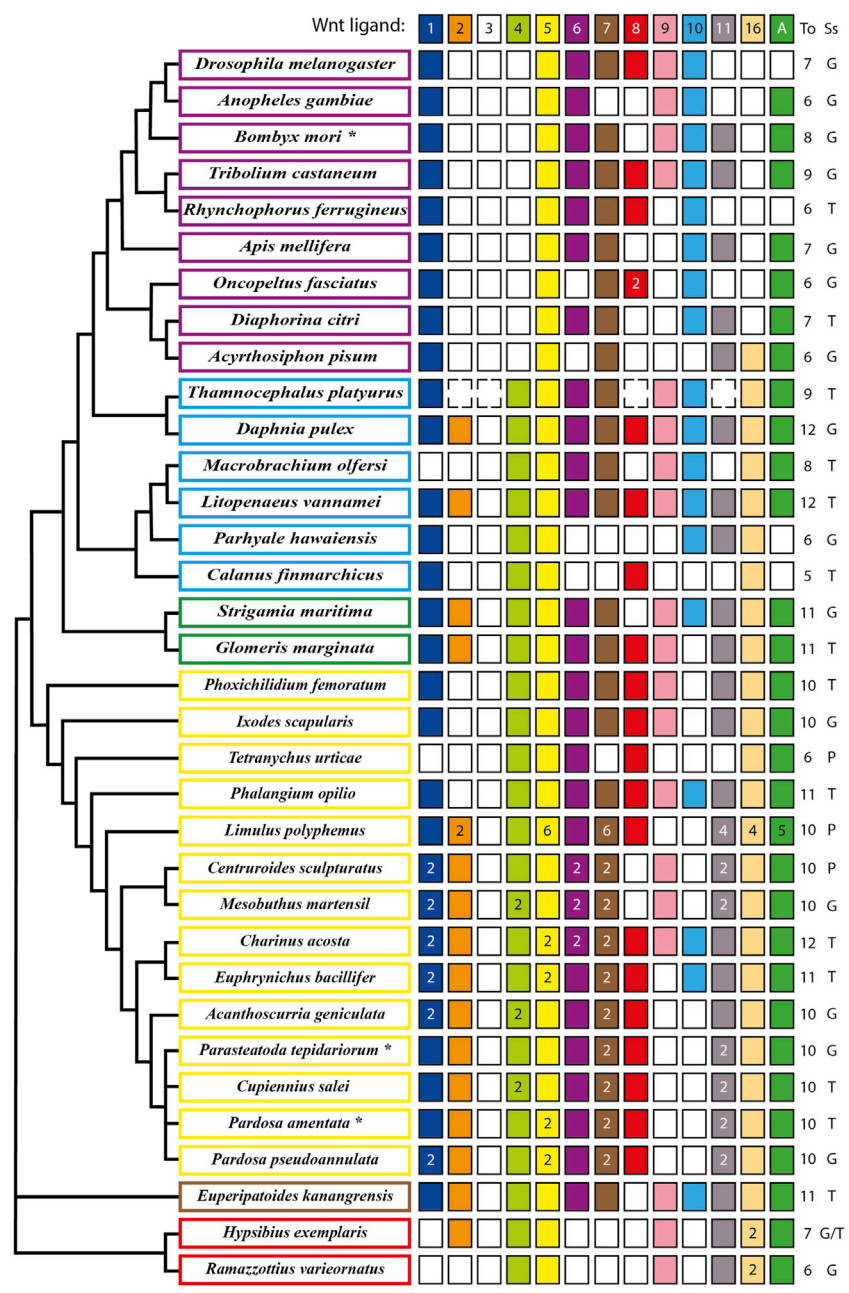


FIGURE 1
Updated repertoire and phylogenetic relationship of Wnt ligands among panarthropods. Insects are shown in purple rectangles (Dearden et al., 2006; Bolognesi et al., 2008a; Murat et al., 2010; Shigenobu et al., 2010; Yin et al., 2015; Ding et al., 2019; Holzem et al., 2019; Panfilio et al., 2019; Vosburg et al., 2020), crustaceans in pale blue (Janssen et al., 2010; Constantinou et al., 2016; Jaramillo et al., 2016; Kao et al., 2016; Du et al., 2018), myriapods in green (Janssen et al., 2010; Hayden and Arthur, 2014; Janssen and Posnien, 2014), chelicerates in yellow (Janssen et al., 2010; Pace et al., 2014; Posnien et al., 2014; Harper et al., 2021; Janssen et al., 2021; Janssen and Eriksson, 2022), onychophoran in brown (Hogvall et al., 2014) and tardigrades in red (Chavarria et al., 2021). An asterisk in the name indicates more organisms having the same repertoire. **B. mori* also includes *Bicyclus anynana*, *Amyeloides transitella*, *Calycopis cecrops*, *Danaus plexippus*, *Heliconius melpomene*, *Operophtera brumata* and *Papilio xuthus*. **P. tepidariorum* includes *Pholcus phalangioides* and **P. amentata* includes *Marpissa muscosa* and *Stegodyphus dumicola*. Filled and no-filled boxes represent the presence and the absence of the ligand, respectively. Dotted boxes represent the presence/absence of the ligand in doubt (genome not fully sequenced) and white/black numbers inside the boxes represent ligand numbers. The Wnt ligand family is indicated at the top as well as the total (To) number of ligand families. The source of the sequences (Ss) is shown as Genome (G), Transcriptome (T) or Proteome (P). Phylogenetic positions based on Koenemann et al., 2010, Misof et al., 2014, Giribet and Edgecombe, 2019, Lozano-Fernandez et al., 2019 and Ballesteros et al., 2022.

lineages—represented here by six species that belong to three of the six extant classes (Zhang, 2011) –, with a low degree of conservation of the Wnt2, Wnt8, and Wnt11 ligands (Constantinou et al., 2016; Jaramillo et al., 2016; Kao et al., 2016; Du et al., 2018).

Regarding chelicerates, they present a low loss of ligands. They also exhibit a high degree of duplications in almost all Wnt ligand subfamilies, which coincides with the whole genome duplication (WGD) that has been proposed to have taken place in the common ancestor of spiders and scorpions (Arachnopulmonata) (Schwager et al., 2017; Panfilio et al., 2019; Harper et al., 2021). Furthermore, an extreme case is found in the horseshoe crab *Limulus polyphemus*, that exhibit up to six copies of Wnt5 and Wnt7 ligands, most probably due to several rounds of WGD that have been recently documented for this order - Xiphosura - of chelicerates (Nossa et al., 2014; Nong et al., 2021). This leaves out harvestmen, sea spiders, ticks, and mites, represented in our compilation by *Phalangium opilio*, *Phoxichilidium femoratum*, *Ixodes scapularis*, and *Tetranychus urticae*, respectively, which show no duplications (Figure 1). Interestingly, *T. urticae* and the decapod crustacean *Macrobrachium olfersi* both lacks one of the most conserved ligands, Wnt1—only Wnt5 is fully present among panarthropods—and only retained one canonical ligand, Wnt8, and Wnt10, respectively. Thus, despite multiple Wnt ligand losses, there is always a canonical/noncanonical set of ligands in all reported species; however this repertoire is more variable for some ligands than for others. This diversity and variability within arthropods have been explained before by non-conserved specific functional redundancies among Wnt ligands in this and other phyla that are evident after single ligand loss-of-function experiments where no strong defects are found in or related to the site of expression (e.g., Gleason et al., 2006; Bolognesi et al., 2008a; Grigoryan et al., 2008).

Additionally, there are multiple lines of evidence of Wnt ligands signaling by canonical and noncanonical pathways. For example, *Drosophila wnt9* (*Dwnt4*) activates cell motility during ovarian morphogenesis through the noncanonical pathway and salivary gland development through the canonical pathway (Cohen et al., 2002; Harris et al., 2007). In another example, human isolated chondrocytes differentiation was triggered *in vitro* by *wnt3a* that simultaneously activated both Wnt/ β -catenin and Wnt/ Ca^{2+} signaling pathways (Nalesso et al., 2011). All this makes the interchangeability between different ligands or their combinatorial activity to regulate the same pathways or trigger similar functions even more feasible.

On the other hand, *wnt* genes duplication found almost exclusively in chelicerates has allowed this group to reach up to 14–16 ligands, keeping paralogs of the same Wnt ligand subfamily despite having several other ligands. Some authors have attributed this to an ancestral division of the function between both paralogs and acquisition of a new function by one of them (Gitelman, 2009; Cho et al., 2010). It has also been

suggested that larger sets of ligands could be an indication of morphological and functional diversification (Schwager et al., 2017). However, since numerous Wnt ligand subfamilies were found in simpler and basally branching metazoans, for example twelve in the sea anemone *Nematostella vectensis*, ten in the demosponge *Halisarca dujardini* and even 21 in the calcisponge *Sycon ciliatum*, there is no obvious relationship between higher number of ligands and morphological complexity (Kusserow et al., 2005; Borisenko et al., 2016).

The expression domains of Wnt ligands

To fully understand the wide and varied range of Wnt ligands present in the different panarthropods studied so far, it is necessary to analyze their expression patterns in a comparative manner throughout development. In this review we will focus on the period comprising the processes of axial elongation and segmentation, collectively known as posterior growth.

Published expression patterns of the complete repertoire of Wnt ligands are relatively scarce in panarthropods. However, we found such data for three representative insect species—unfortunately not including hemimetabolous insects—one branchiopod crustacean, two myriapods—a centipede and a millipede,—four chelicerates—including only arachnids: three spiders and one harvestman—and one representative for onychophorans and one for tardigrades (Figures 2,3).

The spatiotemporal analysis of *wnt* genes expression in the beetle *Tribolium castaneum* showed that several ligands overlap in the posterior zone, segments/parasegments, and head lobes, suggesting functional redundancy (Bolognesi et al., 2008a). However, when we compiled *wnt* genes expression patterns including the other panarthropods (Janssen et al., 2010; Hogvall et al., 2014; Janssen and Posnien, 2014; Constantinou et al., 2016; Holzem et al., 2019; Chavarria et al., 2021; Janssen et al., 2021), we found that overlapping is common, although diverse patterns are still observed (Figure 2). Based on the degree of patterning conservation, we were able to classify the expression of Wnt ligands as highly (Wnt1, Wnt5, Wnt6, Wnt7, and Wnt11), moderately (Wnt8, Wnt10, Wnt16, and WntA), and poorly (Wnt2, Wnt4, and Wnt9) conserved, which might suggest that the function of some of these ligands—and not others—would be essential for posterior growth in most panarthropods. Furthermore, early-branching clades, such as onychophorans—a sister group of arthropods –, chelicerates, and myriapods, showed a higher proportion of Wnt ligands in the posterior zone compared to pancrustaceans (Figure 3). Despite all this, it is unclear whether overlapping ligands fulfill similar/redundant or different/complementary functions.

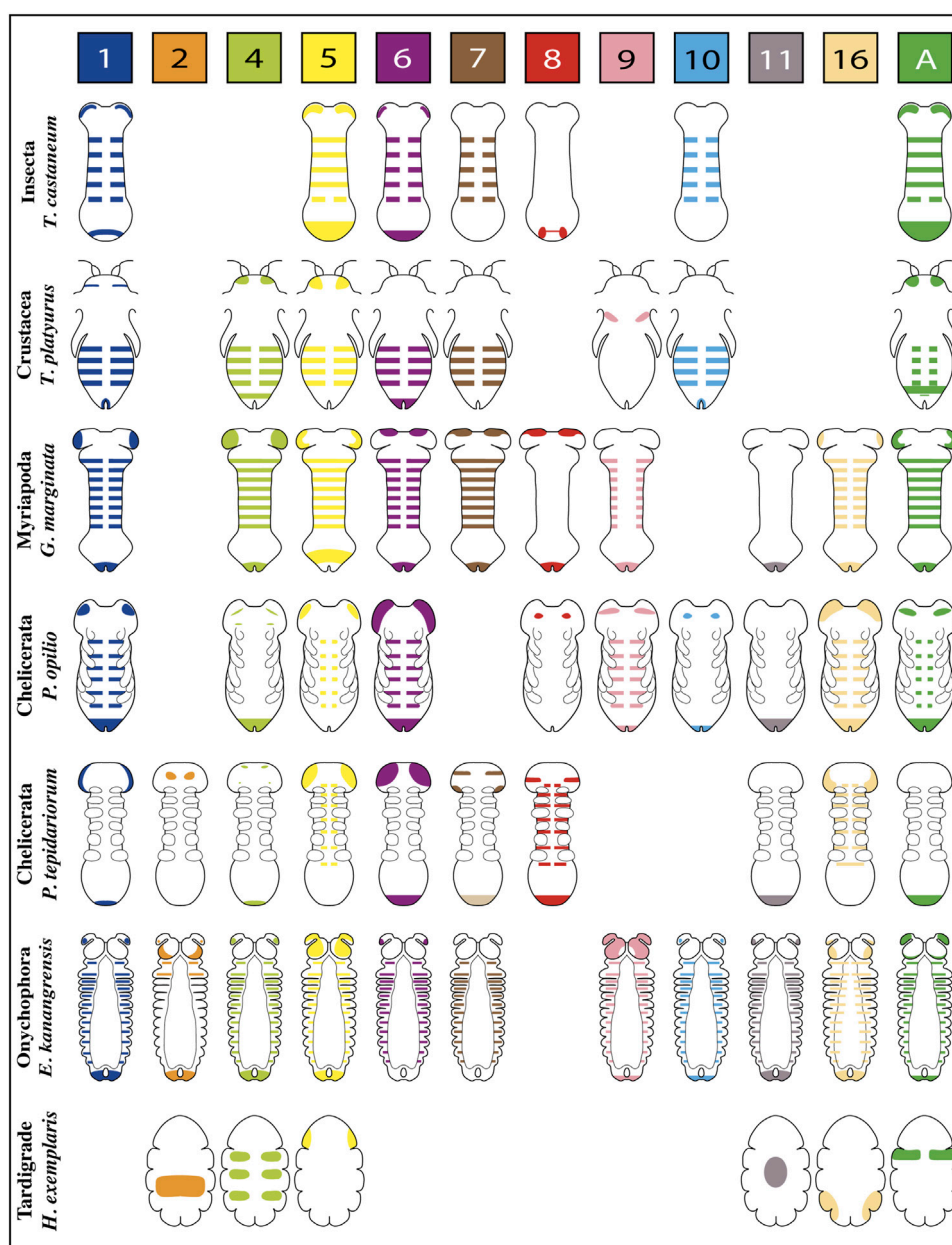


FIGURE 2

Representative expression patterns of Wnt ligands in panarthropods. Expression patterns of Wnt ligands in representative organisms of Insecta, Crustacea, Myriapoda, Chelicerata, Onychophora and Tardigrada. Each color represents one Wnt ligand as is indicated at the top. The Wnt7 ligand in *P. tepidarium* presents duplication, therefore double expression is shown in the scheme (Wnt7.1 is pale brown in the posterior, Wnt7.2 is dark brown in the head). *T. castaneum* (Bolognesi et al., 2008a); *T. platyurus* (Constantinou et al., 2016); *G. marginata* (Janssen et al., 2010; Janssen and Posnien, 2014); *P. opilio* (Janssen et al., 2021); *P. tepidarium* (Janssen et al., 2010; Janssen et al., 2021); *E. kanangrensis* (Hogvall et al., 2014); *H. exemplaris* (Chavarria et al., 2021).

wnt1 is expressed in the posterior region—known as the growth zone or, more precisely, the segment addition zone (SAZ)—of practically all the panarthropods analyzed except for the tardigrades, which do not have a proper SAZ (Chavarria et al., 2021). This suggests a leading and ancestral role of Wnt1 ligand in the regulation of the posterior growth in Panarthropoda.

Within arachnids, two *wnt1* paralogs in the tarantula *Acanthoscurria geniculata* show a clear example of posterior subfunctionalization, where one of them is only expressed on the SAZ while the other is expressed exclusively in the hindgut primordium. Interestingly, in arachnids which have retained only one paralog, *wnt1* is expressed at later stages in the putative

	Posterior zone			Segment								
Organism	1	2	4	5	6	7	8	9	10	11	16	A
<i>Drosophila melanogaster</i>	<div></div>	<div></div>	<div></div>	<div></div>	<div></div>	<div></div>	<div></div>	<div></div>	<div></div>	<div></div>	<div></div>	<div></div>
<i>Bicyclus anynana</i>	<div></div>	<div></div>	<div></div>	<div></div>	<div></div>	<div></div>	<div></div>	<div></div>	<div></div>	<div></div>	<div></div>	<div></div>
<i>Tribolium castaneum</i>	<div></div>	<div></div>	<div></div>	<div></div>	<div></div>	<div></div>	<div></div>	<div></div>	<div></div>	<div></div>	<div></div>	<div></div>
<i>Thamnocephalus platyurus</i>	<div></div>	<div></div>	<div></div>	<div></div>	<div></div>	<div></div>	<div></div>	<div></div>	<div></div>	<div></div>	<div></div>	<div></div>
<i>Strigamia maritima</i>	<div></div>	<div></div>	<div></div>	<div></div>	<div></div>	<div></div>	<div></div>	<div></div>	<div></div>	<div></div>	<div></div>	<div></div>
<i>Glomeris marginata</i>	<div></div>	<div></div>	<div></div>	<div></div>	<div></div>	<div></div>	<div></div>	<div></div>	<div></div>	<div></div>	<div></div>	<div></div>
<i>Phalangium opilio</i>	<div></div>	<div></div>	<div></div>	<div></div>	<div></div>	<div></div>	<div></div>	<div></div>	<div></div>	<div></div>	<div></div>	<div></div>
<i>Acanthoscurria geniculata</i>	<div></div>	<div></div>	<div></div>	<div></div>	<div></div>	<div></div>	<div></div>	<div></div>	<div></div>	<div></div>	<div></div>	<div></div>
<i>Pholcus phalangioides</i>	<div></div>	<div></div>	<div></div>	<div></div>	<div></div>	<div></div>	<div></div>	<div></div>	<div></div>	<div></div>	<div></div>	<div></div>
<i>Parasteatoda tepidariorum</i>	<div></div>	<div></div>	<div></div>	<div></div>	<div></div>	<div></div>	<div></div>	<div></div>	<div></div>	<div></div>	<div></div>	<div></div>
<i>Cupiennius salei</i>	<div></div>	<div></div>	<div></div>	<div></div>	<div></div>	<div></div>	<div></div>	<div></div>	<div></div>	<div></div>	<div></div>	<div></div>
<i>Euperipatoides kanangrensis</i>	<div></div>	<div></div>	<div></div>	<div></div>	<div></div>	<div></div>	<div></div>	<div></div>	<div></div>	<div></div>	<div></div>	<div></div>
<i>Hypsibius exemplaris</i>	<div></div>	<div></div>	<div></div>	<div></div>	<div></div>	<div></div>	<div></div>	<div></div>	<div></div>	<div></div>	<div></div>	<div></div>

FIGURE 3

Wnt ligands expression domains within panarthropod germbands. Blue boxes represent the expression of the corresponding Wnt ligand in the posterior zone, red boxes indicate segmental expression, and white boxes show the absence of expression. Double red and blue boxes indicate Wnt ligand expression at the posterior zone and within segments. Insects are shown in purple rectangles, crustaceans in pale blue, myriapods in green, chelicerates in yellow, onychophoran in brown and tardigrades in red. The Wnt ligand families are indicated at the top, in gray boxes. *D. melanogaster* (Murat et al., 2010); *B. anynana* (Holzem et al., 2019); *T. castaneum* (Bolognesi et al., 2008a); *T. platyurus* (Constantinou et al., 2016); *S. maritima* (Hayden and Arthur, 2014); *G. marginata* (Janssen et al., 2010; Janssen and Posnien, 2014); chelicerates (Janssen et al., 2021; Janssen and Eriksson, 2022); *E. kanangrensis* (Hogvall et al., 2014); *H. exemplaris* (Chavarria et al., 2021).

hindgut of *Parasteatoda*—without expression in the SAZ—and in the SAZ of *Pholcus* and *Phalangium*, with no expression in the hindgut primordium (Janssen et al., 2021).

Specialized functions for *wnt1* and *wnt5* are suggested by their expression patterns within the posterior region of the *Tribolium* germband (Nagy and Carroll 1994; Bolognesi et al., 2008a). *wnt1* expression is restricted to a specific domain within the SAZ—resembling the *wnt8* domain—in a region apparently covered by the broader expression of *wnt5*. Since both expression domains are not equivalents, they could be covering different functions.

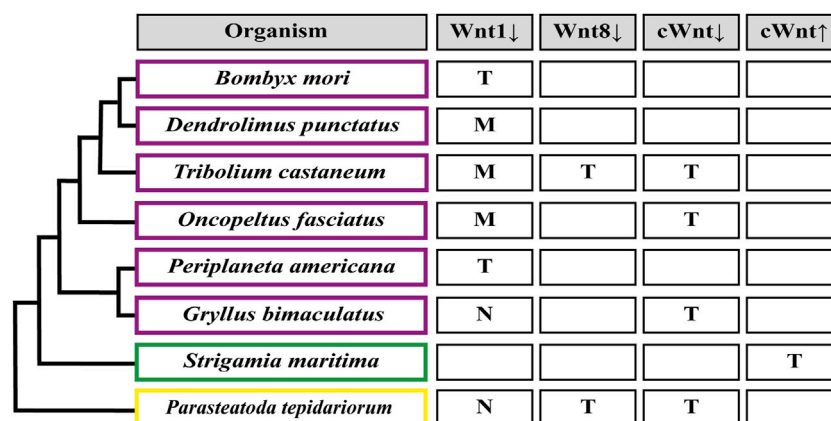
An analysis of Wnt1 and Wnt5 ligands performed in the spider *Cupiennius salei* showed their complementary expression domains within the segment, dorsal for *wnt1* and ventral for *wnt5* (Damen, 2002). However, the suggested “complementarity” in *Cupiennius* was refuted by Janssen et al. (2021) arguing that *wnt5* ventral expression is restricted to the nervous system and not related to the segment polarity establishment.

On the other hand, in the onychophoran *Euperipatoides kanangrensis*, Hogvall et al. (2014) observed that distinct Wnt ligands were expressed at different and specific regions throughout each trunk segment; *wnt5* and *wnt4* extending over the anterior and posterior domains, respectively, while *wnt1*, *wnt6*, *wnt9*, *wnt10*, *wnt11*, and *wnt16* covering the

center of the segment in adjacent or overlapping regions. However, these onychophoran *wnt* genes are expressed in a segment polarity-like pattern only at later stages, belatedly to segment polarity genes such as *engrailed*. Thus, the authors suggested that *wnt* genes were not involved in forming segmental borders in onychophorans but probably in their intrasegmental patterning.

In summary, a complete *wnt* genes repertoire is published and available in twelve panarthropods, including representatives of the main subphyla. Furthermore, many *wnt* genes are expressed in the forming segments and the posterior region during panarthropod elongation, with a general high overlapping among them. However, there is little detailed information on these expressions. Until a better resolution in the expression of various arthropods is available, both at the tissue and cellular level, it will not be possible to determine a reliable degree of functional conservation of the different Wnt ligands.

There is also an imbalance in the analysis of the different *wnt* genes, mainly concentrated in the posterior expression and function of Wnt1 and Wnt8 ligands. This analysis would be greatly benefited by incorporating the complete set of Wnt ligands in more organisms, including representatives of orders not analyzed so far (e.g., hemimetabolous insects, non-arachnid chelicerates).



Organism	Wnt1↓	Wnt8↓	cWnt↓	cWnt↑
<i>Bombyx mori</i>	T			
<i>Dendrolimus punctatus</i>	M			
<i>Tribolium castaneum</i>	M	T	T	
<i>Oncopeltus fasciatus</i>	M		T	
<i>Periplaneta americana</i>	T			
<i>Gryllus bimaculatus</i>	N		T	
<i>Strigamia maritima</i>				T
<i>Parasteatoda tepidariorum</i>	N	T	T	

FIGURE 4

Segmentation patterning phenotypes after Wnt signaling functional analysis. (M) Loss of segment boundaries. (T) Truncated embryo due to loss of abdominal segments. (N) No effect on the segmentation patterning. Down arrow indicates inhibition, up arrow indicates activation. cWnt indicates the full canonical pathway. An empty rectangle points out the absence of the corresponding functional studies in this organism. Insects are shown in purple rectangles (Miyawaki et al., 2004; Angelini and Kaufman, 2005; Bolognesi et al., 2008b; Chesebro et al., 2013; Liu et al., 2017; Nakao, 2018; Setton and Sharma, 2021); myriapods in green (Hayden et al., 2015); chelicerates in yellow (McGregor et al., 2008; Setton and Sharma, 2021).

Functional analysis of Wnt ligands during posterior growth

One of the main characteristics of panarthropods is their segmented body, the segments of which are added during development in different ways depending on the species. For example, in *Drosophila*, all segments are patterned almost simultaneously during syncytial blastoderm in what is called long germ segmentation (Peel et al., 2005). On the other hand, most arthropods and onychophorans present a short germ mode of segmentation, where anterior segments are patterned during the blastoderm stage, and the rest of segments are added sequentially from the SAZ, at the posterior end of the embryo/larva (Peel et al., 2005; Clark and Peel, 2018). This territory functions as an organizing center for posterior growth, where the mechanisms that regulate segmentation and axial elongation occur (Williams and Nagy, 2017). As was mentioned previously, the SAZ is characterized by expressing several Wnt ligands dynamically during segmentation, suggesting a role of this pathway in establishing the segmented pattern and the mechanisms controlling body elongation.

Functional studies on different components of the Wnt pathway during sequential segmentation have been performed mostly in the holometabolous insect *Tribolium castaneum* (Ober and Jockusch, 2006; Bolognesi et al., 2008b; Bolognesi et al., 2009; Beermann et al., 2011) and the spider *Parasteatoda tepidariorum* (McGregor et al., 2008; Setton and Sharma 2018; Setton and Sharma 2021), although the number of studies in other arthropod species is increasing.

Mainly, it has been observed that the loss of function of Wnt receptors in *Tribolium* (*Tc-frizzled1* and *Tc-frizzled2*), co-receptor Arrow in *Tribolium*, *Oncopeltus*, *Gryllus* and *Parasteatoda* (*Tc-arrow*, *Of-arrow*, *Gb-arrow* and *Pt-arrow*, respectively), or final effectors (the transcription factors *Gb-armadillo*/ β -catenin in *Gryllus* and *Of-pangolin* in *Oncopeltus*) of the canonical Wnt pathway, lead to the formation of truncated embryos with no posterior segments (Figure 4) (Miyawaki et al., 2004; Angelini and Kaufman 2005; Bolognesi et al., 2009; Beermann et al., 2011; Setton and Sharma, 2018; Setton and Sharma, 2021). This makes clear the essential role of this signaling pathway on the posterior growth. The same conclusion could be reached by analyzing the pharmacological inhibition of the Wnt pathway after the incubation of elongating cockroach embryos with the Inhibitor of Wnt Production-3 (IWP-3)—that blocks palmitoylation of Wnt ligands by Porcupine (Chen et al., 2009)—and after Wnt signaling activation using LiCl—that inhibits GSK3 within the β -catenin destruction complex (Hedgepeth et al., 1997)—during the elongation and segmentation of the centipede *Strigamia maritima*. After the IWP-3 treatment, the absence of Wnt signaling specifically during elongation disrupted segment formation and reduced the size of the SAZ as well as the number of proliferating cells, coinciding with the results showed by Oberhofer et al. (2014) where the Wnt signaling displays a dual role in the SAZ in growth control and posterior patterning. In the latter, the activation of the pathway generated shorter embryos with an expanded SAZ, revealing its role in the control of the segmentation clock (Chesebro et al., 2013; Hayden et al., 2015).

Regarding Wnt ligands, by far the most studied is *wnt1/wingless*, but its functional analysis has only been successful in some insects, with no loss-of-function phenotypes found in the cricket *G. bimaculatus* and the spider *P. tepidariorum* (Miyawaki et al., 2004; Setton and Sharma, 2021). Apparently, the severity of *wnt1* knockdown related to posterior growth could be linked to the presence/absence of another ligand, *wnt8*: In *Tribolium* and *Oncopeltus*—where Wnt8 ligand is present as one and two paralogs, respectively—*wnt1* RNAi only showed segmental boundary disruption without preventing elongation or the generation of the segmented pattern, as was revealed by the absence of truncated phenotypes and the regular expression of the pair-rule gene *Tc-even-skipped* (*Tc-eve*) in the beetle and a normal-sized abdomen in the case of *Oncopeltus* embryos (Angelini and Kaufman, 2005; Ober and Jockusch, 2006; Bolognesi et al., 2008b). On the other hand, in the domestic silk moth *Bombyx mori*, which do not have a *wnt8* paralog, *wnt1* RNAi produced a range of phenotypes from partially truncated embryos displaying immature legs (Yamaguchi et al., 2011) to drastically shortened embryos showing no signs of abdominal nor thoracic segments (Nakao, 2018). The idea of a (partial) functional interrelationship between both ligands is also based on the results obtained in *Tribolium* after eliminating *wnt8* alone, that generated a small proportion of truncated embryos, and the drastic increasing of the truncated phenotype frequency using the *wnt1* and *wnt8* double RNAi (Bolognesi et al., 2008b). There are other cases in which the same different results have been reported: In the cockroach *Periplaneta americana*, the loss-of-function of *wnt1* led embryos to develop posteriorly truncated germbands (Chesebro et al., 2013), while in the lepidopteran *Dendrolimus punctatus*, *wnt1* knockout using CRISPR/Cas9 showed abdominal segment fusion with no signs of posterior truncation (Liu et al., 2017). However, it is not known if Wnt8 ligand is present in these two insects. Finally, *wnt8* knockdown in the spider *Parasteatoda* (McGregor et al., 2008) caused posterior truncation or even complete absence of the opisthosomal (abdominal) region, a phenotype that resembles the effect of the RNAi against *wnt8* in *Tribolium* (Bolognesi et al., 2008b). However, given the functional redundancy between Wnt1 and Wnt8 ligands, we cannot interpret *wnt1* or *wnt8* knockdown phenotypes in any species where *wnt1/wnt8* double loss-of-function has not been analyzed.

The analysis of the phenotypes mentioned above reveals the Wnt pathway's different roles during posterior growth. On the one hand, truncated phenotypes indicate early participation in this process, although we have little evidence about the mechanisms in which it would operate. In turn, we do not have sufficient evidence to relate the Wnt signaling to maintaining gene oscillations or establishing a wavefront at the anterior SAZ, as it is well known in vertebrates (Oates et al., 2012). On the other hand, the participation of *wnt1* in the definition of segment borders is relatively conserved among arthropods and is a well-understood process at the molecular and

cellular level in the *Drosophila* fly (Nüsslein-Volhard and Wieschaus, 1980; Nagy and Carroll 1994; Ober and Jockusch, 2006).

To date, other canonical and noncanonical Wnt ligands that are expressed segmentally and/or in the posterior region have only been functionally studied in the beetle *Tribolium*. When Bolognesi et al. (2008b) RNAi screened all nine Wnt ligands expressed in *Tribolium*, they only found segmental phenotypes with *Tc-wnt1* and *Tc-wnt8*. The same result was obtained after checking different combinations of double (all combinations of *Tc-wnt1*, *Tc-wnt5*, *Tc-wnt8* and *Tc-wntA*) and triple (*Tc-wnt5*, *Tc-wnt8* and *Tc-wntA*) RNAi injections of the *wnt* genes that are most clearly expressed in the SAZ (Bolognesi et al., 2008a, b). However, we cannot rule out redundant functions during posterior growth for *wnt5* and *wntA* with *wnt6*, which is also expressed in the SAZ but was not included in their double and triple knockdown analyses.

It is also possible that in other panarthropods, different *wnt* genes fulfill the absence of specific Wnt ligands, like Wnt8 in *Thamnocephalus* (Constantinou et al., 2016), *Strigamia* (Hayden et al., 2015) or the onychophoran *Euperipatoides* (Hogvall et al., 2014). The evidence suggests redundant and partially redundant functions between arthropod Wnt ligands. Nevertheless, the relationship between a Wnt ligand and its precise function and which ligands share the same function is still unclear.

Wnt signaling as part of the genetic network underlying segmental patterning

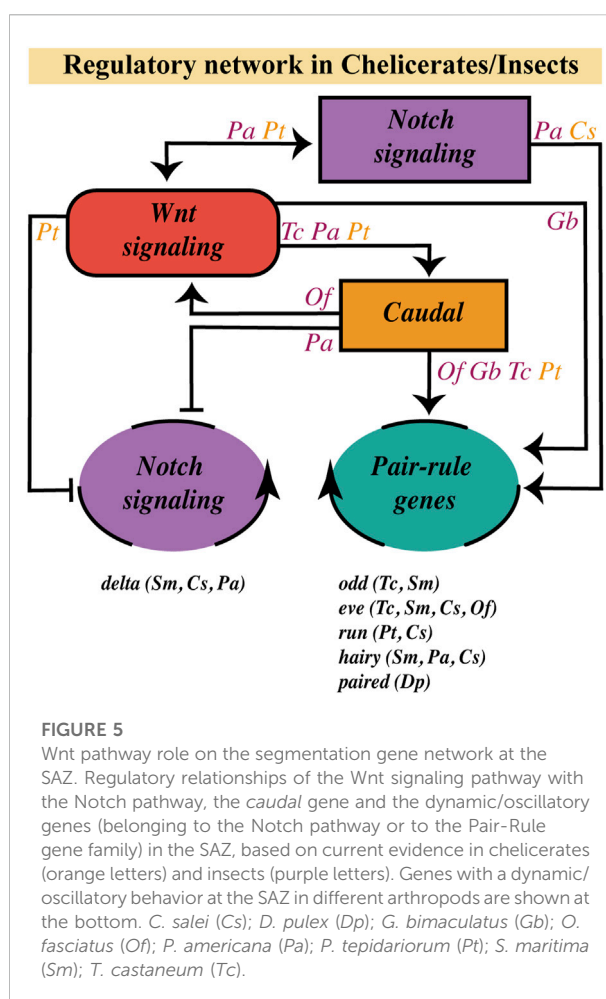
It has been established that segmentation in most arthropods and all vertebrates is driven by a cyclical mechanism where the temporal periodicity of a clock is translated into a repetitive spatial pattern (Cooke and Zeeman, 1976; Palmeirim et al., 1997; Sarrazin et al., 2012). In vertebrates, cell-autonomous oscillatory genes expression is maintained by a posterior Wnt + Fgf signaling gradient. As this gradient decreases, the generated posterior-to-anterior kinematic waves of expression are arrested, allowing the formation of a new segment (Oates et al., 2012). Furthermore, the progressive posterior elongation of the embryo moves the Wnt + Fgf gradient together with the determination front, thus linking posterior growth with segmentation. In addition, several genes related to the Wnt, Fgf, and Notch/Delta pathways oscillate and are coupled between them, which is crucial for segment generation (Dequéant et al., 2006; Krol et al., 2011; Sonnen et al., 2018). However, despite the evidence involving the Wnt signaling pathway in the vertebrate segmentation clock, its specific role is not yet fully understood.

In arthropods, *caudal*, a highly conserved gene that is expressed at the posterior half of the SAZ and is crucial for its establishment and maintenance (Dearden and Akam, 2001;

Chipman et al., 2004; Copf et al., 2004; Shinmyo et al., 2005; Chesebro et al., 2013; Janssen et al., 2015; Schönauer et al., 2016; Novikova et al., 2020), is regulated by the canonical Wnt signaling (Shinmyo et al., 2005; McGregor et al., 2008; Chesebro et al., 2013; Oberhofer et al., 2014; Schönauer et al., 2016). Recently, Clark and Peel (2018) proposed that in the SAZ, Wnt signaling would be regulating an ancient regulatory network formed by *caudal*, *dichaete*, and *odd-paired* (*opa*), which are sequentially expressed—both temporally and spatially—during segmentation in *Tribolium*, but also in the long-germ *Drosophila* embryo. Furthermore, one of the same authors proposed a transition from the posterior expression of *caudal/dichaete* to *dichaete/opa* expression at the anterior region of the SAZ, resembling the wavefront limit operating in vertebrates (Clark, 2021). Then it is possible that the Wnt pathway is regulating, through Caudal, genetic oscillations in arthropods, as occurs in vertebrates.

Two main kinds of cyclically expressed genes have been observed in arthropods (no dynamically expressed genes have been found in onychophorans; Janssen and Budd, 2013; Janssen and Budd, 2016): On one hand, the orthologs of *Drosophila* pair-rule genes as *odd-skipped* (Chipman et al., 2004; Sarrazin et al., 2012), *even-skipped* (Chipman and Akam, 2008; El-Sherif et al., 2012; Brena and Akam, 2013), *paired* (Eriksson et al., 2013), *hairy* (Chipman and Akam, 2008; Pueyo et al., 2008) and most probably *run* (Schönauer et al., 2016). On the other hand, members of the Notch signaling pathway, mainly the Delta ligand, have been shown to oscillate in cockroaches (Pueyo et al., 2008), centipedes (Chipman and Akam, 2008; Brena and Akam, 2013) and spiders (Stollewerk et al., 2003; Schönauer et al., 2016). Functional analyses in a few of these organisms appear to position Wnt signaling upstream of some cyclic genes.

In *Tribolium*, it was already shown that blocking Wnt signaling impairs the posterior expression of the three pair-rule genes (*Tc-run*, *Tc-eve*, and *Tc-odd*; Bolognesi et al., 2009; Beermann et al., 2011), which are part of the regulatory circuit involved in the segmentation clock (Choe et al., 2006). In the same insect, RNA-seq comparative analysis revealed additional pair-rule genes downregulated after knocking down the Wnt/ β -catenin pathway, such as *Tc-hairy* and *Tc-dichaete*, in addition to *Tc-odd* and *Tc-eve* (Oberhofer et al., 2014). However, the same experimental approach performed in the spider *Parasteatoda* showed no significant effect on the expression of the pair-rule genes *Pt-eve*, *Pt-run*, and *Pt-hairy*, with a mild effect on *Pt-dichaete* (Setton and Sharma, 2021). In this study, it was even seen that *caudal* expression was not interrupted in *Parasteatoda* and *Gryllus* after arrow knockdown, unlike in *Oncopeltus*, where they obtained a substantial reduction in *Of-caudal* expression. The discrepancies observed between *Tribolium* and *Parasteatoda* Wnt/ β -catenin pathway loss-of-function results could be associated with the weak penetrance of the RNAi injection (around 50% of effect; Setton and Sharma, 2021) or with a



possible low conservation of the *wnt/caudal/pair-rule* gene network among arthropods. In any case, if we consider that in the spider *Parasteatoda* *wnt8* was previously shown to be necessary for the posterior expression of *Pt-eve* and *Pt-run* (Schönauer et al., 2016) and *Pt-caudal* (McGregor et al., 2008; Schönauer et al., 2016), one alternative explanation could be that specifically in the spider, Wnt8 function acts through an Arrow-independent pathway, that is like a noncanonical ligand.

Regarding Wnt-Notch interactions, on the other hand, Chesebro et al. (2013) showed in the cockroach that *Pa-delta* expression in the posterior SAZ is completely eliminated after *Pa-wnt1* knockdown. Furthermore, they obtained similar results using the pharmacological inhibitor IWP-3 (Chesebro et al., 2013). At the same time, they observed the disruption of posterior *Pa-wnt1* expression after injecting RNAi against *Pa-notch* and its partial reduction by incubating embryos with the Notch inhibitor, DAPT.

Schönauer et al. (2016), in turn, situated this signaling pathway upstream *Pt-wnt8* in *Parasteatoda*. Depending on the SAZ region, Notch/Delta is activating (at the posterior SAZ) or inhibiting (at the anterior SAZ) this ligand. However, it was

previously found that Wnt8 would be necessary for the dynamic expression of *Pt-delta* in the same spider (McGregor et al., 2008). In addition, the RNA-seq study by Setton and Sharma (2021) exhibited *Pt-notch* "downregulation-but not *Pt delta* inhibition-after" Wnt signaling loss-of-function, although they did not check the effect of knocking down Notch signaling. So then, Notch and Wnt signaling pathways seem to display a reciprocal regulation in these two animal models, the hemimetabolous cockroach *Periplaneta* and the chelicerate *Parasteatoda*, apparently partially through their regulation of *caudal*. Nevertheless, our limited knowledge about the complexity of the SAZ in terms of cell types and tissue organization makes it hard to understand reciprocal interactions between different pathways.

As it has been suggested that the Notch pathway does not present a functional role in the segmentation process in the onychophoran *Euperipatoides kanangrensis* and the holometabolous insects *Drosophila melanogaster*, *Apis mellifera* and *Tribolium castaneum* (Aranda et al., 2008; Wilson et al., 2010; Kux et al., 2013; Janssen and Budd, 2016), the regulatory role of the Wnt pathway on the Notch signaling is limited, considering the existing evidence, to *Parasteatoda tepidariorum*, *Periplaneta americana* and the short-germ silkworm *Bombyx mori* (Liu, 2013). Thus, from the cases mentioned so far, we can conclude the following (Figure 5):

- 1) Studies in different arthropods are lacking to determine a possible ancestral regulatory route of posterior growth.
- 2) Virtually all arthropods studied to date have shown some level of dynamic/oscillatory expression in the SAZ (i.e., *odd*, *eve*, *run*, *hairy*, *paired*, *delta*), and the most widely described regulatory network involved is Wnt > Caudal > Pair-Rule/Delta - with some variations possible due to evolutionary divergences or even experimental limitations -, where Wnt signaling has a regulatory effect on the timing of segment border definition.
- 3) Notch signaling, as in vertebrates, could be involved in single-cell oscillations coupling in some arthropods and not others, where we have not yet discovered the gene(s) involved in the oscillatory synchronization.

Wnt pathway as a possible regulator of the cellular processes involved in axial elongation?

Sequential segment addition in most arthropods is accompanied by simultaneous germband extension along the anterior-posterior axis. This complex reorganization of the developing body must include, in a species-specific manner, a variable, mutually dependent, and tightly regulated arrangement of cellular behaviors, including oriented (or not) mitotic divisions, cell rearrangements,

and changes in cellular density, cell shape, and cell size, among others.

Little is known about the regulatory network behind axial elongation and the mentioned cellular processes in arthropod posterior growth. In deuterostomes, including vertebrates as well as the hemichordates that display posterior growth without segmentation, paraxial mesoderm progenitors are maintained by a posterior positive regulatory loop between *wnt* (*wnt3a* and *wnt8* in zebrafish) and *brachyury*, so that posterior elongation depends on this molecular feedback (Martin and Kimelman, 2008; Fritzenwanker et al., 2019). However, *brachyury* orthologs in insects are expressed in the SAZ but seem not necessary for posterior growth, as was shown by RNAi analysis in *Tribolium* and *Gryllus* (Shinmyo et al., 2006; Berns et al., 2008). Regardless of whether Wnt-Brachyury regulation was lost in insects or corresponds to a deuterostome evolutionary innovation, which factor is maintaining Wnt signaling at the insect SAZ is unknown.

Few direct evidence links Wnt signaling to cell proliferation during arthropod posterior growth; for example, Oberhofer et al. (2014), through genetic analyses in *Tribolium* SAZ, showed that the Wnt pathway targets some genes involved in mitotic cell cycle and spindle organization/elongation. Moreover, RNAi treatments against *wnt1* caused a decrease in cell proliferation in the cockroach SAZ, the same occurring when the pathway was inhibited by pharmacological treatment with IWP-3 (Chesebro et al., 2013). Constantinou et al. (2020), based on the cell division pattern shown by the branchiopod *Thamnocephalus*, divided the SAZ into an anterior no-proliferating region that expresses WntA ligand and a posterior slightly-but-constant proliferating region that expresses Wnt4 ligand. A similar correlation was found in *Oncopeltus* (Auman et al., 2017), where the region of cell divisions coincides with the expression of *Of-eve* and *Of-caudal* genes, two targets of Wnt signaling. The proposed model differs, however, from what was found in *Dermestes* (Xiang et al., 2017) and *Tribolium* (Cepeda et al., 2021). The proliferation region is not temporally stable in these beetles, but variable and posteriorly concentrated at specific stages. Unfortunately, no correlation has yet been found between this proliferation pattern and the expression of any gene at the SAZ, and there is evidence that the Wnt signaling target genes *Tc-caudal*, and *Tc-eve* are not involved in cell division regulation in this insect (Copf et al., 2004; Nakamoto et al., 2015). A possible mechanism that explains this patterning type would be what happens in the *Drosophila* wing, where cell proliferation is regulated by differences in the amount of Wnt1 ligand; high concentrations generate a decrease while intermediate concentrations trigger proliferation (Baena-Lopez et al., 2009). However, no changes in the expression of Wnt ligands correlating with this model have been demonstrated.

Another well-conserved cellular process among arthropods during germband elongation is the convergent extension (CE). The first studies on CE were carried out in *Drosophila*, where the

pair-rule genes *Dm-eve* and *Dm-runt* are necessary for the polarized cell movements involved (Irvine and Wieschaus, 1994; Zallen and Wieschaus, 2004). Furthermore, the necessity of *Tc-eve* and *Tc-caudal* during the intercalary cell movements seen at early stages of germband elongation in *Tribolium* was also reported (Benton et al., 2013; Nakamoto et al., 2015). In addition, the fact that *Dm-eve* regulates the expression of the Toll family receptors, which direct CE during germband elongation in *Drosophila* (Paré et al., 2014) and is conserved in *Tribolium* and *Parasteatoda* (Benton et al., 2016), leads us to wonder if the Wnt signaling pathway would have a role in this process. The Wnt signaling pathway could be involved in CE through its regulation of *eve* expression, which we have already seen occur in various arthropods during germband elongation (Bolognesi et al., 2009; Beermann et al., 2011; Oberhofer et al., 2014; Schönauer et al., 2016).

However, we will not have an answer to our question until a more significant number of studies have been carried out with a particular focus on the cellular behaviors that take place during posterior elongation in a diverse group of arthropods.

Future directions of research

After reviewing the Wnt pathway's role in axial elongation and segmentation processes in arthropods, more questions than answers arise.

We found the complete Wnt ligand repertoire from 42 species of panarthropods. However, the expression pattern of all the ligands has been published only in twelve. Thus, a more diverse palette of species is lacking in the analysis, especially non/underrepresented lineages (e.g., maxillopod crustaceans, non-insect hexapods, non-spider chelicerates). Furthermore, given the apparent overlapping between some ligands, it would be precious to have a detailed cellular-level analysis of the expression patterns, hopefully including double *in situ* hybridizations.

The incorporation of functional studies in more organisms, including non-model panarthropods with interesting phylogenetic positions as early-branching clades (e.g., onychophorans, ametabolous and hemimetabolous insects), will provide the basis for well-supported comparative analyses. In the long term, this will allow us to identify conserved and diverged aspects of the regulatory role of the Wnt pathway on posterior body elongation and segmentation. Furthermore,

adding imaging tools to this analysis, like tissue-specific transgenic lines carrying fluorescent reporters for time-lapse imaging, will be essential to understanding the contribution of Wnt signaling in the highly dynamic cellular and molecular network that organizes posterior growth in most panarthropods.

Author contributions

MM-E and RC contributed to conception and design of the study. MM-E and AS organized the database. MM-E wrote the first draft of the manuscript. MM-E and AS wrote sections of the manuscript. All authors contributed to manuscript revision, read, and approved the submitted version.

Funding

ANID/FONDECYT Agencia Nacional de Investigación y Desarrollo/Fondo Nacional de Desarrollo Científico y Tecnológico Grant (1181466); Fondo de Asignación Directa, PUCV Grant (125.729/2018)

Acknowledgments

We thank Renato V. Pardo and Valentina Núñez-Pascual for critical and constructive comments on this manuscript.

Conflict of interest

The authors declare that the research was conducted in the absence of any commercial or financial relationships that could be construed as a potential conflict of interest.

Publisher's note

All claims expressed in this article are solely those of the authors and do not necessarily represent those of their affiliated organizations, or those of the publisher, the editors and the reviewers. Any product that may be evaluated in this article, or claim that may be made by its manufacturer, is not guaranteed or endorsed by the publisher.

References

- Angelini, D. R., and Kaufman, T. C. (2005). Functional analyses in the milkweed bug *Oncopeltus fasciatus* (Hemiptera) support a role for Wnt signaling in body segmentation but not appendage development. *Dev. Biol.* 283, 409–423. doi:10.1016/j.ydbio.2005.04.034
- Angers, S., and Moon, R. T. (2009). Proximal events in Wnt signal transduction. *Nat. Rev. Mol. Cell. Biol.* 10, 468–477. doi:10.1038/nrm2717
- Aranda, M., Marques-Souza, H., Bayer, T., and Tautz, D. (2008). The role of the segmentation gene hairy in *Tribolium*. *Dev. Genes. Evol.* 218, 465–477. doi:10.1007/s00427-008-0240-1
- Auman, T., and Chipman, A. D. (2017). The evolution of gene regulatory networks that define arthropod body plans. *Integr. Comp. Biol.* 57, 523–532. doi:10.1093/icb/ixc035

- Auman, T., Vreede, B., Weiss, A., Hester, S. D., Williams, T. A., Nagy, L. M., et al. (2017). Dynamics of growth zone patterning in the milkweed bug *Oncopeltus fasciatus*. *Development* 144, 1896–1905. doi:10.1242/dev.142091
- Baena-Lopez, L. A., Franch-Marro, X., and Vincent, J. P. (2009). Wingless promotes proliferative growth in a gradient-independent manner. *Sci. Signal.* 2, ra60. doi:10.1126/scisignal.2000360
- Baker, N. E. (1987). Molecular cloning of sequences from wingless, a segment polarity gene in *Drosophila*: The spatial distribution of a transcript in embryos. *EMBO J.* 6, 1765–1773. doi:10.1002/j.1460-2075.1987.tb02429.x
- Ballesteros, J. A., Santibañez-López, C. E., Baker, C. M., Benavides, L. R., Cunha, T. J., Gainett, G., et al. (2022). Comprehensive species sampling and sophisticated algorithmic approaches refute the monophyly of Arachnida. *Mol. Biol. Evol.* 39, msac021. doi:10.1093/molbev/msac021
- Beermann, A., Prühs, R., Lutz, R., and Schröder, R. (2011). A context-dependent combination of Wnt receptors controls axis elongation and leg development in a short germ insect. *Development* 138, 2793–2805. doi:10.1242/dev.063644
- Bejsovec, A. (2018). Wingless signaling: A genetic journey from morphogenesis to metastasis. *Genetics* 208, 1311–1336. doi:10.1534/genetics.117.300157
- Benton, M. A., Akam, M., and Pavlopoulos, A. (2013). Cell and tissue dynamics during *Tribolium* embryogenesis revealed by versatile fluorescence labeling approaches. *Development* 140, 3210–3220. doi:10.1242/dev.096271
- Benton, M. A., Pechmann, M., Frey, N., Stappert, D., Conrads, K. H., Chen, Y. T., et al. (2016). Toll genes have an ancestral role in axis elongation. *Curr. Biol.* 26, 1609–1615. doi:10.1016/j.cub.2016.04.055
- Berns, N., Kusch, T., Schröder, R., and Reuter, R. (2008). Expression, function and regulation of Brachyenteron in the short germband insect *Tribolium castaneum*. *Dev. Genes. Evol.* 218, 169–179. doi:10.1007/s00427-008-0210-7
- Bolognesi, R., Beermann, A., Farzana, L., Wittkopp, N., Lutz, R., Balavoine, G., et al. (2008a). *Tribolium* wnts: Evidence for a larger repertoire in insects with overlapping expression patterns that suggest multiple redundant functions in embryogenesis. *Dev. Genes. Evol.* 218, 193–202. doi:10.1007/s00427-007-0170-3
- Bolognesi, R., Farzana, L., Fischer, T. D., and Brown, S. J. (2008b). Multiple Wnt genes are required for segmentation in the short-germ embryo of *Tribolium castaneum*. *Curr. Biol.* 18, 1624–1629. doi:10.1016/j.cub.2008.09.057
- Bolognesi, R., Fischer, T. D., and Brown, S. J. (2009). Loss of Tc-arrow and canonical Wnt signaling alters posterior morphology and pair-rule gene expression in the short-germ insect, *Tribolium castaneum*. *Dev. Genes. Evol.* 219, 369–375. doi:10.1007/s00427-009-0299-3
- Borisenko, I., Adamski, M., Ereskovsky, A., and Adamska, M. (2016). Surprisingly rich repertoire of Wnt genes in the demosponge *Halisarca dujardini*. *BMC Evol. Biol.* 16, 123. doi:10.1186/s12862-016-0700-6
- Brena, C., and Akam, M. (2013). An analysis of segmentation dynamics throughout embryogenesis in the centipede *Strigamia maritima*. *BMC Biol.* 11, 112. doi:10.1186/1741-7007-11-112
- Cepeda, R. E., Terraza, J. B., Pardo, R. V., Núñez-Pascual, V., Mundaca-Escobar, M., and Sarrazin, A. F. (2021). Spatiotemporal variation in cell proliferation patterns during arthropod axial elongation. *Sci. Rep.* 11, 327. doi:10.1038/s41598-020-79373-0
- Chavarria, R. A., Game, M., Arbelaez, B., Ramnarine, C., Snow, Z. K., and Smith, F. W. (2021). Extensive loss of wnt genes in Tardigrada. *BMC Ecol. Evol.* 21, 223. doi:10.1186/s12862-021-01954-y
- Chen, B., Dodge, M. E., Tang, W., Lu, J., Ma, Z., Fan, C. W., et al. (2009). Small molecule-mediated disruption of Wnt-dependent signaling in tissue regeneration and cancer. *Nat. Chem. Biol.* 5, 100–107. doi:10.1038/nchembio.137
- Chesebro, J. E., Pueyo, J. I., and Couso, J. P. (2013). Interplay between a Wnt-dependent organizer and the Notch segmentation clock regulates posterior development in *Periplaneta americana*. *Biol. Open* 2, 227–237. doi:10.1242/bio.20123699
- Chipman, A. D., and Akam, M. (2008). The segmentation cascade in the centipede *Strigamia maritima*: Involvement of the notch pathway and pair-rule gene homologues. *Dev. Biol.* 319, 160–169. doi:10.1016/j.ydbio.2008.02.038
- Chipman, A. D., Arthur, W., and Akam, M. (2004). A double segment periodicity underlies segment generation in centipede development. *Curr. Biol.* 14, 1250–1255. doi:10.1016/j.cub.2004.07.026
- Chipman, A. D., and Edgecombe, G. D. (2019). Developing an integrated understanding of the evolution of arthropod segmentation using fossils and evo-devo. *Proc. Biol. Sci.* 286, 20191881. doi:10.1098/rspb.2019.1881
- Cho, S. J., Vallés, Y., Giani, V. C., Seaver, E., and Weisblat, D. (2010). Evolutionary dynamics of the wnt gene family: A lophotrochozoan perspective. *Mol. Biol. Evol.* 27, 1645–1658. doi:10.1093/molbev/msq052
- Choe, C. P., Miller, S. C., and Brown, S. J. (2006). A pair-rule gene circuit defines segments sequentially in the short-germ insect *Tribolium castaneum*. *Proc. Natl. Acad. Sci. U. S. A.* 103, 6560–6564. doi:10.1073/pnas.0510440103
- Clark, E., Peel, A. D., and Akam, M. (2019). Arthropod segmentation. *Development* 146, dev170480. doi:10.1242/dev.170480
- Clark, E., and Peel, A. D. (2018). Evidence for the temporal regulation of insect segmentation by a conserved sequence of transcription factors. *Development* 145, dev155580. doi:10.1242/dev.155580
- Clark, E. (2021). Time and space in segmentation. *Interface Focus* 11, 20200049. doi:10.1098/rsfs.2020.0049
- Cohen, E. D., Mariol, M.-C., Wallace, R. M. H., Weyers, J., Kamberov, Y. G., Pradel, J., et al. (2002). DWnt4 regulates cell movement and focal adhesion kinase during *Drosophila* ovarian morphogenesis. *Dev. Cell* 2, 437–448. doi:10.1016/S1534-5807(02)00142-9
- Constantinou, S. J., Duan, N., Nagy, L. M., Chipman, A. D., and Williams, T. A. (2020). Elongation during segmentation shows axial variability, low mitotic rates, and synchronized cell cycle domains in the crustacean, *Thamnocephalus platyurus*. *EvoDevo* 11, 1. doi:10.1186/s13227-020-0147-0
- Constantinou, S. J., Pace, R. M., Stangl, A. J., Nagy, L. M., and Williams, T. A. (2016). Wnt repertoire and developmental expression patterns in the crustacean *Thamnocephalus platyurus*. *Evol. Dev.* 18, 324–341. doi:10.1111/ede.12204
- Cooke, J., and Zeeman, E. C. (1976). A clock and wavefront model for control of the number of repeated structures during animal morphogenesis. *J. Theor. Biol.* 58, 455–476. doi:10.1016/s0022-5193(76)80131-2
- Copf, T., Schröder, R., and Averof, M. (2004). Ancestral role of caudal genes in axis elongation and segmentation. *Proc. Natl. Acad. Sci. U. S. A.* 101, 17711–17715. doi:10.1073/pnas.0407327102
- Croce, J. C., and McClay, D. R. (2008). Evolution of the wnt pathways. *Methods Mol. Biol.* 469, 3–18. doi:10.1007/978-1-60327-469-2_1
- Damen, W. G. (2002). Parasegmental organization of the spider embryo implies that the parasegment is an evolutionary conserved entity in arthropod embryogenesis. *Development* 129, 1239–1250. doi:10.1242/dev.129.5.1239
- Dearden, P. K., and Akam, M. (2001). Early embryo patterning in the grasshopper, *Schistocerca gregaria*: Wingless, decapentaplegic and caudal expression. *Development* 128, 3435–3444. doi:10.1242/dev.128.18.3435
- Dearden, P. K., Wilson, M. J., Sablan, L., Osborne, P. W., Havler, M., McNaughton, E., et al. (2006). Patterns of conservation and change in honey bee developmental genes. *Genome Res.* 16, 1376–1384. doi:10.1101/gr.5108606
- Dequéant, M. L., Glynn, E., Gaudenz, K., Wahl, M., Chen, J., Mushegian, A., et al. (2006). A complex oscillating network of signaling genes underlies the mouse segmentation clock. *Science* 314, 1595–1598. doi:10.1126/science.1133141
- Ding, X., Liu, J., Zheng, L., Song, J., Li, N., Hu, H., et al. (2019). Genome-wide identification and expression profiling of Wnt family genes in the silkworm, *Bombyx mori*. *Int. J. Mol. Sci.* 20, 1221. doi:10.3390/ijms20051221
- Du, J., Zhang, X., Yuan, J., Zhang, X., Li, F., and Xiang, J. (2018). Wnt gene family members and their expression profiling in *Litopenaeus vannamei*. *Fish. Shellfish Immunol.* 77, 233–243. doi:10.1016/j.fsi.2018.03.034
- El-Sherif, E., Averof, M., and Brown, S. J. (2012). A segmentation clock operating in blastoderm and germband stages of *Tribolium* development. *Development* 139, 4341–4346. doi:10.1242/dev.085126
- Eriksson, B. J., Ungerer, P., and Stollewerk, A. (2013). The function of Notch signalling in segment formation in the crustacean *Daphnia magna* (Branchiopoda). *Dev. Biol.* 383, 321–330. doi:10.1016/j.ydbio.2013.09.021
- Fritzenwanker, J. H., Uhlinger, K. R., Gerhart, J., Silva, E., and Lowe, C. J. (2019). Untangling posterior growth and segmentation by analyzing mechanisms of axis elongation in hemichordates. *Proc. Natl. Acad. Sci. U. S. A.* 116 (17), 8403–8408. doi:10.1073/pnas.1817496116
- Gajos-Michniewicz, A., and Czyz, M. (2020). Wnt signaling in melanoma. *Int. J. Mol. Sci.* 21, 4852. doi:10.3390/ijms21144852
- Giribet, G., and Edgecombe, G. D. (2019). The phylogeny and evolutionary history of arthropods. *Curr. Biol.* 29, R592–R602. doi:10.1016/j.cub.2019.04.057
- Gitelman, I. (2009). Evolution of the vertebrate twist family and syngonization: A mechanism for differential gene loss through merging of expression domains. *Mol. Biol. Evol.* 24, 1912–1925. doi:10.1093/molbev/msm120
- Gleason, J. E., Szyleyko, E. A., and Eisenmann, D. M. (2006). Multiple redundant Wnt signaling components function in two processes during *C. elegans* vulval development. *Dev. Biol.* 298, 442–457. doi:10.1016/j.ydbio.2006.06.050
- Gori, F., Lerner, U., Ohlsson, C., and Baron, R. (2015). A new Wnt on the bone: Wnt16, cortical bone thickness, porosity and fractures. *Bonekey Rep.* 4, 669. doi:10.1038/bonekey.2015.36

- Grigoryan, T., Wend, P., Klaus, A., and Birchmeier, W. (2008). Deciphering the function of canonical wnt signals in development and disease: Conditional loss- and gain-of-function mutations of beta-catenin in mice. *Genes. Dev.* 22, 2308–2341. doi:10.1101/gad.1686208
- Hannibal, R. L., and Patel, N. (2013). What is a segment? *EvoDevo* 4, 35. doi:10.1186/2041-9139-4-35
- Harper, A., Baudouin Gonzalez, L., Schöner, A., Janssen, R., Seiter, M., Holzem, M., et al. (2021). Widespread retention of ohnologs in key developmental gene families following whole-genome duplication in arachnopholmonates. *G3 (Bethesda)* 11, jkab299. doi:10.1093/g3journal/jkab299
- Harris, K. E., and Beckendorf, S. K. (2007). Different Wnt signals act through the Frizzled and RYK receptors during *Drosophila* salivary gland migration. *Development* 134, 2017–2025. doi:10.1242/dev.001164
- Hayden, L., and Arthur, W. (2014). The centipede *Strigamia maritima* possesses a large complement of Wnt genes with diverse expression patterns. *Evol. Dev.* 16, 127–138. doi:10.1111/ede.12073
- Hayden, L., Schlosser, G., and Arthur, W. (2015). Functional analysis of centipede development supports roles for Wnt genes in posterior development and segment generation. *Evol. Dev.* 17, 49–62. doi:10.1111/ede.12112
- Hedgepeth, C. M., Conrad, L. J., Zhang, J., Huang, H.-C., Lee, V. M. Y., and Klein, P. S. (1997). Activation of the Wnt signaling pathway: a molecular mechanism for Lithium action. *Dev. Cell.* 185, 82–91. doi:10.1006/dbio.1997.8552
- Hogvall, M., Schöner, A., Budd, G. E., McGregor, A. P., Posnien, N., and Janssen, R. (2014). Analysis of the Wnt gene repertoire in an onychophoran provides new insights into the evolution of segmentation. *EvoDevo* 5, 14. doi:10.1186/2041-9139-5-14
- Holstein, T. W. (2012). The evolution of the Wnt pathway. *Cold Spring Harb. Perspect. Biol.* 4, a007922. doi:10.1101/cshperspect.a007922
- Holzem, M., Braak, N., Brattström, O., McGregor, A. P., and Breuker, C. J. (2019). Wnt gene expression during early embryogenesis in the nymphalid butterfly *Bicyclus anynana*. *Front. Ecol. Evol.* 7, 468. doi:10.3389/fevo.2019.00468
- Irvine, K. D., and Wieschaus, E. (1994). Cell intercalation during *Drosophila* germband extension and its regulation by pair-rule segmentation genes. *Development* 120, 827–841. doi:10.1242/dev.120.4.827
- Janssen, R., and Budd, G. E. (2013). Deciphering the onychophoran 'segmentation gene cascade': Gene expression reveals limited involvement of pair rule gene orthologs in segmentation, but a highly conserved segment polarity gene network. *Dev. Biol.* 382, 224–234. doi:10.1016/j.ydbio.2013.07.010
- Janssen, R., and Budd, G. E. (2016). Gene expression analysis reveals that Delta/Notch signalling is not involved in onychophoran segmentation. *Dev. Genes. Evol.* 226, 69–77. doi:10.1007/s00427-016-0529-4
- Janssen, R., Eriksson, B. J., Budd, G. E., Akam, M., and Prpic, N. M. (2010). Gene expression patterns in an onychophoran reveal that regionalization predates limb segmentation in pan-arthropods. *Evol. Dev.* 12, 363–372. doi:10.1111/j.1525-142X.2010.00423.x
- Janssen, R., and Eriksson, B. J. (2022). Embryonic expression patterns of Wnt genes in the RTA-clade spider *Cupiennius salei*. *Gene Expr. Patterns* 44, 119247. doi:10.1016/j.gexp.2022.119247
- Janssen, R., Jörgensen, M., Lagebro, L., and Budd, G. E. (2015). Fate and nature of the onychophoran mouth-anus furrow and its contribution to the blastopore. *Proc. Biol. Sci.* 282, 20142628. doi:10.1098/rspb.2014.2628
- Janssen, R., Pechmann, M., and Turetzek, N. (2021). A chelicerate wnt gene expression atlas: Novel insights into the complexity of arthropod wnt-patterning. *EvoDevo* 12, 12. doi:10.1186/s13227-021-00182-1
- Janssen, R., and Posnien, N. (2014). Identification and embryonic expression of Wnt2, Wnt4, Wnt5 and Wnt9 in the millipede glomeris marginata (Myriapoda: Diplopoda). *Gene Expr. Patterns* 14, 55–61. doi:10.1016/j.gexp.2013.12.003
- Jaramillo, M. L., Guzman, F., Paese, C. L., Margis, R., Nazari, E. M., Ammar, D., et al. (2016). Exploring developmental gene toolkit and associated pathways in a potential new model crustacean using transcriptomic analysis. *Dev. Genes. Evol.* 226, 325–337. doi:10.1007/s00427-016-0551-6
- Jenny, F. H., and Basler, K. (2014). Powerful *Drosophila* screens that paved the wingless pathway. *Fly. (Austin)* 8, 218–225. doi:10.4161/19336934.2014.985988
- Kao, D., Lai, A. G., Stamatakis, E., Rosic, S., Konstantinides, N., Jarvis, E., et al. (2016). The genome of the crustacean *Parhyale hawaiiensis*, a model for animal development, regeneration, immunity and lignocellulose digestion. *Elife* 5, e20062. doi:10.7554/eLife.20062
- Koenemann, S., Jenner, R. A., Hoenemann, M., Stemme, T., and von Reumont, B. M. (2010). Arthropod phylogeny revisited, with a focus on crustacean relationships. *Arthropod Struct. Dev.* 39, 88–110. doi:10.1016/j.asd.2009.10.003
- Krol, A. J., Roellig, D., Dequéant, M. L., Tassy, O., Glynn, E., Hattem, G., et al. (2011). Evolutionary plasticity of segmentation clock networks. *Development* 138, 2783–2792. doi:10.1242/dev.063834
- Kusserow, A., Pang, K., Sturm, C., Hrouda, M., Lentfer, J., Schmidt, H. A., et al. (2005). Unexpected complexity of the Wnt gene family in a sea anemone. *Nature* 433, 156–160. doi:10.1038/nature03158
- Kux, K., Kiparaki, M., and Delidakis, C. (2013). The two *Tribolium* E(spl) genes show evolutionarily conserved expression and function during embryonic neurogenesis. *Mech. Dev.* 130, 207–225. doi:10.1016/j.mod.2013.02.003
- Liu, H., Liu, Q., Zhou, X., Huang, Y., and Zhang, Z. (2017). Genome editing of wnt-1, a gene associated with segmentation, via CRISPR/Cas9 in the pine caterpillar moth, *Dendrolimus punctatus*. *Front. Physiol.* 7, 666. doi:10.3389/fphys.2016.00666
- Liu, W. (2013). Bmdelta phenotype implies involvement of Notch signaling in body segmentation and appendage development of silkworm, *Bombyx mori*. *Arthropod Struct. Dev.* 42, 143–151. doi:10.1016/j.asd.2012.10.002
- Lozano-Fernandez, J., Tanner, A. R., Giacomelli, M., Carton, R., Vinther, J., Edgecombe, G. D., et al. (2019). Increasing species sampling in chelicerate genomic-scale datasets provides support for monophyly of Acari and Arachnida. *Nat. Commun.* 10, 2295. doi:10.1038/s41467-019-10244-7
- Martin, B. L., and Kimelman, D. (2008). Regulation of canonical Wnt signaling by Brachyury is essential for posterior mesoderm formation. *Dev. Cell.* 15, 121–133. doi:10.1016/j.devcel.2008.04.013
- Martin, B. L., and Kimelman, D. (2009). Wnt signaling and the evolution of embryonic posterior development. *Curr. Biol.* 19, R215–R219. doi:10.1016/j.cub.2009.01.052
- Martinez, A., Baker, N. E., Ingham, P. W., and Martinez Arias, A. (1988). Role of segment polarity genes in the definition and maintenance of cell states in the *Drosophila* embryo. *Development* 103, 157–170. doi:10.1242/dev.103.1.157
- McGregor, A. P., Pechmann, M., Schwager, E. E., Feitosa, N. M., Kruck, S., Aranda, M., et al. (2008). Wnt8 is required for growth-zone establishment and development of opisthosomal segments in a spider. *Curr. Biol.* 18, 1619–1623. doi:10.1016/j.cub.2008.08.045
- Misof, B., Liu, S., Meusemann, K., Peters, R. S., Donath, A., Mayer, C., et al. (2014). Phylogenomics resolves the timing and pattern of insect evolution. *Science* 346, 763–767. doi:10.1126/science.1257570
- Miyawaki, K., Mito, T., Sarashina, I., Zhang, H., Shinmyo, Y., Ohuchi, H., et al. (2004). Involvement of Wingless/Armadillo signaling in the posterior sequential segmentation in the cricket, *Gryllus bimaculatus* (Orthoptera), as revealed by RNAi analysis. *Mech. Dev.* 121, 119–130. doi:10.1016/j.mod.2004.01.002
- Murat, S., Hopfen, C., and McGregor, A. P. (2010). The function and evolution of Wnt genes in arthropods. *Arthropod Struct. Dev.* 39, 446–452. doi:10.1016/j.asd.2010.05.007
- Nagy, L. M., and Carroll, S. (1994). Conservation of wingless patterning functions in the short-germ embryos of *Tribolium castaneum*. *Nature* 367, 460–463. doi:10.1038/367460a0
- Nakamoto, A., Hester, S. D., Constantinou, S. J., Blaine, W. G., Tewksbury, A. B., Matei, M. T., et al. (2015). Changing cell behaviours during beetle embryogenesis correlates with slowing of segmentation. *Nat. Commun.* 6, 6635. doi:10.1038/ncomms7635
- Nakao, H. (2018). A *Bombyx* homolog of ovo is a segmentation gene that acts downstream of Bm-wnt1 (*Bombyx* wnt1 homolog). *Gene Expr. Patterns* 27, 1–7. doi:10.1016/j.gexp.2017.10.002
- Nalesso, G., Sherwood, J., Bertrand, J., Pap, T., Ramachandran, M., De Bari, C., et al. (2011). Wnt-3a modulates articular chondrocyte phenotype by activating both canonical and noncanonical pathways. *J. Cell. Biol.* 193, 551–564. doi:10.1083/jcb.201011051
- Nong, W., Qu, Z., Li, Y., Barton-Owen, T., Wong, A., Yip, H. Y., et al. (2021). Horseshoe crab genomes reveal the evolution of genes and microRNAs after three rounds of whole genome duplication. *Commun. Biol.* 4, 83. doi:10.1038/s42003-020-01637-2
- Nossa, C. W., Havlak, P., Yue, J. X., Lv, J., Vincent, K. Y., Brockmann, H. J., et al. (2014). Joint assembly and genetic mapping of the Atlantic horseshoe crab genome reveals ancient whole genome duplication. *Gigascience* 3, 9. doi:10.1186/2047-217X-3-9
- Novikova, A. V., Auman, T., Cohen, M., Oleynik, O., Stahi-Hitin, R., Gil, E., et al. (2020). The multiple roles of caudal in early development of the milkweed bug *Oncopeltus fasciatus*. *Dev. Biol.* 467, 66–76. doi:10.1016/j.ydbio.2020.08.011
- Nüsslein-Volhard, C., and Wieschaus, E. (1980). Mutations affecting segment number and polarity in *Drosophila*. *Nature* 287, 795–801. doi:10.1038/287795a0
- Oates, A. C., Morelli, L. G., and Ares, S. (2012). Patterning embryos with oscillations: Structure, function and dynamics of the vertebrate segmentation clock. *Development* 139, 625–639. doi:10.1242/dev.063735

- Ober, K. A., and Jockusch, E. L. (2006). The roles of wingless and decapentaplegic in axis and appendage development in the red flour beetle, *Tribolium castaneum*. *Dev. Biol.* 294, 391–405. doi:10.1016/j.ydbio.2006.02.053
- Oberhofer, G., Grossmann, D., Siemanowski, J. L., Beissbarth, T., and Bucher, G. (2014). Wnt/ β -catenin signaling integrates patterning and metabolism of the insect growth zone. *Development* 141, 4740–4750. doi:10.1242/dev.112797
- Pace, R. M., Eskridge, P. C., Grbić, M., and Nagy, L. M. (2014). Evidence for the plasticity of arthropod signal transduction pathways. *Dev. Genes. Evol.* 224, 209–222. doi:10.1007/s00427-014-0479-7
- Palmeirim, I., Henrique, D., Ish-Horowitz, D., and Pourquié, O. (1997). Avian hairy gene expression identifies a molecular clock linked to vertebrate segmentation and somitogenesis. *Cell* 91, 639–648. doi:10.1016/s0092-8674(00)80451-1
- Panfili, K. A., Vargas Jentzsch, I. M., Benoit, J. B., Erezylmaz, D., Suzuki, Y., Colella, S., et al. (2019). Molecular evolutionary trends and feeding ecology diversification in the Hemiptera, anchored by the milkweed bug genome. *Genome Biol.* 20, 64. doi:10.1186/s13059-019-1660-0
- Paré, A. C., Vichas, A., Fincher, C. T., Mirman, Z., Farrell, D. L., Mainieri, A., et al. (2014). A positional Toll receptor code directs convergent extension in *Drosophila*. *Nature* 515, 523–527. doi:10.1038/nature13953
- Peel, A. D., Chipman, A. D., and Akam, M. (2005). Arthropod segmentation: Beyond the *Drosophila* paradigm. *Nat. Rev. Genet.* 6, 905–916. doi:10.1038/nrg1724
- Posnien, N., Zeng, V., Schwager, E. E., Pechmann, M., Hilbrant, M., Keefe, J. D., et al. (2014). A comprehensive reference transcriptome resource for the common house spider *Parasteatoda tepidariorum*. *PLoS One* 9, e104885. doi:10.1371/journal.pone.0104885
- Prud'homme, B., Lartillot, N., Balavoine, G., Adoutte, A., and Vervoort, M. (2002). Phylogenetic analysis of the Wnt gene family. Insights from lophotrochozoan members. *Curr. Biol.* 12, 1395–1400. doi:10.1016/s0960-9822(02)01068-0
- Pueyo, J. I., Lanfear, R., and Couso, J. P. (2008). Ancestral Notch-mediated segmentation revealed in the cockroach *Periplaneta americana*. *Proc. Natl. Acad. Sci. U. S. A.* 105, 16614–16619. doi:10.1073/pnas.0804093105
- Rijsewijk, F., Schuermann, M., Wagenaar, E., Parren, P., Weigel, D., and Nusse, R. (1987). The *Drosophila* homolog of the mouse mammary oncogene int-1 is identical to the segment polarity gene wingless. *Cell* 50, 649–657. doi:10.1016/0092-8674(87)90038-9
- Sarrazin, A. F., Peel, A. D., and Averof, M. (2012). A segmentation clock with two-segment periodicity in insects. *Science* 336, 338–341. doi:10.1126/science.1218256
- Schönauer, A., Paese, C. L., Hilbrant, M., Leite, D. J., Schwager, E. E., Feitosa, N. M., et al. (2016). The Wnt and Delta-Notch signalling pathways interact to direct pair-rule gene expression via caudal during segment addition in the spider *Parasteatoda tepidariorum*. *Development* 143, 2455–2463. doi:10.1242/dev.131656
- Schwager, E. E., Sharma, P. P., Clarke, T., Leite, D., Wierchin, T., Pechmann, N., et al. (2017). The house spider genome reveals an ancient whole-genome duplication during arachnid evolution. *BMC Biol.* 15, 62. doi:10.1186/s12915-017-0399-x
- Setton, E. V. W., and Sharma, P. P. (2021). A conserved role for arrow in posterior axis patterning across Arthropoda. *Dev. Biol.* 475, 91–105. doi:10.1016/j.ydbio.2021.02.006
- Setton, E. V. W., and Sharma, P. P. (2018). Cooption of an appendage-patterning gene cassette in the head segmentation of arachnids. *Proc. Natl. Acad. Sci. U. S. A.* 115, E3491–E3500. doi:10.1073/pnas.1720193115
- Shigenobu, S., Bickel, R. D., Brisson, J. A., Butts, T., Chang, C. C., Christiaens, O., et al. (2010). Comprehensive survey of developmental genes in the pea aphid, *Acyrtosiphon pisum*: Frequent lineage-specific duplications and losses of developmental genes. *Insect Mol. Biol.* 19, 47–62. doi:10.1111/j.1365-2583.2009.00944.x
- Shinmyo, Y., Mito, T., Matsushita, T., Sarashina, I., Miyawaki, K., Ohuchi, H., et al. (2005). Caudal is required for gnathal and thoracic patterning and for posterior elongation in the intermediate-germband cricket *Gryllus bimaculatus*. *Mech. Dev.* 122 (2), 231–239. doi:10.1016/j.mod.2004.10.001
- Shinmyo, Y., Mito, T., Uda, T., Nakamura, T., Miyawaki, K., Ohuchi, H., et al. (2006). Brachyenteron is necessary for morphogenesis of the posterior gut but not for anteroposterior axial elongation from the posterior growth zone in the intermediate-germband cricket *Gryllus bimaculatus*. *Development* 133, 4539–4547. doi:10.1242/dev.02646
- Somorjai, I. M., Marti-Solans, J., Diaz-Gracia, M., Nishida, H., Imai, K. S., Escrivà, H., et al. (2018). Wnt evolution and function shuffling in liberal and conservative chordate genomes. *Genome Biol.* 19, 98. doi:10.1186/s13059-018-1468-3
- Sonnen, K. F., Lauschke, V. M., Uraji, J., Falk, H. J., Petersen, Y., Funk, M. C., et al. (2018). Modulation of phase shift between Wnt and Notch signaling oscillations controls mesoderm segmentation. *Cell* 172, 1079–1090. e12. doi:10.1016/j.cell.2018.01.026
- Steinhart, Z., and Angers, S. (2018). Wnt signaling in development and tissue homeostasis. *Development* 145, dev146589. doi:10.1242/dev.146589
- Stolte, A., Schoppmeier, M., and Damen, W. G. (2003). Involvement of notch and delta genes in spider segmentation. *Nature* 423, 863–865. doi:10.1038/nature01682
- Vosburg, C., Reynold, S. M., Noel, R., Shippy, T., Hosmani, P., Flores-Gonzalez, M., et al. (2020). Characterization of wnt signaling genes in diaphorina citri, asian citrus psyllid. *bioRxiv* 2020.09.21.306100. doi:10.1101/2020.09.21.306100
- Wiese, K. E., Nusse, R., and van Amerongen, R. (2018). Wnt signalling: Conquering complexity. *Development* 145, dev165902. doi:10.1242/dev.165902
- Williams, T. A., and Nagy, L. M. (2017). Linking gene regulation to cell behaviors in the posterior growth zone of sequentially segmenting arthropods. *Arthropod Struct. Dev.* 46, 380–394. doi:10.1016/j.asd.2016.10.003
- Wilson, M. J., McKelvey, B. H., van der Heide, S., and Dearden, P. K. (2010). Notch signaling does not regulate segmentation in the honeybee, *Apis mellifera*. *Dev. Genes. Evol.* 220, 179–190. doi:10.1007/s00427-010-0340-6
- Xiang, J., Reding, K., Heffe, R. A., and Pick, L. (2017). Conservation and variation in pair-rule gene expression and function in the intermediate-germ beetle *Dermestes maculatus*. *Development* 144, 4625–4636. doi:10.1242/dev.154039
- Yamaguchi, J., Mizoguchi, T., and Fujiwara, H. (2011). siRNAs induce efficient RNAi response in *Bombyx mori* embryos. *PLoS One* 6, e25469. doi:10.1371/journal.pone.0025469
- Yin, A., Pan, L., Zhang, X., Wang, L., Yin, Y., Jia, S., et al. (2015). Transcriptomic study of the red palm weevil *Rhynchophorus ferrugineus* embryogenesis. *Insect Sci.* 22, 65–82. doi:10.1111/1744-7917.12092
- Zallen, J. A., and Wieschaus, E. (2004). Patterned gene expression directs bipolar planar polarity in *Drosophila*. *Dev. Cell* 6, 343–355. doi:10.1016/s1534-5807(04)00060-7
- Zhang, Z.-Q. (Editor) (2011). *Animal biodiversity: An outline of higher-level classification and survey of taxonomic richness* (Auckland, New Zealand: Magnolia Press. Zootaxa), 3148, 1–237. doi:10.11646/zootaxa.3703.1.1



Patched-Related Is Required for Proper Development of Embryonic *Drosophila* Nervous System

Carmen Bolatto^{1,2*}, Sofía Nieves¹, Agustina Reyes¹, Silvia Olivera-Bravo² and Verónica Cambiazo³

¹ Developmental Biology Laboratory, Histology and Embryology Department, Faculty of Medicine, Universidad de la República (UdelaR), Montevideo, Uruguay, ² Cell and Molecular Neurobiology Laboratory, Computational and Integrative Neuroscience (NCIC) Department, Instituto de Investigaciones Biológicas Clemente Estable (IIBCE), Montevideo, Uruguay, ³ Bioinformatic and Gene Expression Laboratory, Institute of Nutrition and Food Technology (INTA)-Universidad de Chile and Millennium Institute Center for Genome Regulation (CRG), Santiago, Chile

OPEN ACCESS

Edited by:

Juan Rafael Riesgo-Escovar,
Universidad Nacional Autónoma de
México, Mexico

Reviewed by:

Stefanie Schirmeier,
Dresden University of
Technology, Germany
Daniel Ríos-Barrera,
Universidad Nacional Autónoma de
México, Mexico

*Correspondence:

Carmen Bolatto
cbolatto@fmed.edu.uy

Specialty section:

This article was submitted to
Neurodevelopment,
a section of the journal
Frontiers in Neuroscience

Received: 14 April 2022

Accepted: 24 June 2022

Published: 23 August 2022

Citation:

Bolatto C, Nieves S, Reyes A,
Olivera-Bravo S and Cambiazo V
(2022) Patched-Related Is Required
for Proper Development of Embryonic
Drosophila Nervous System.
Front. Neurosci. 16:920670.
doi: 10.3389/fnins.2022.920670

Patched-related (*Ptr*), classified primarily as a neuroectodermal gene, encodes a protein with predicted topology and domain organization closely related to those of Patched (*Ptc*), the canonical receptor of the Hedgehog (*Hh*) pathway. To investigate the physiological function of *Ptr* in the developing nervous system, *Ptr* null mutant embryos were immunolabeled and imaged under confocal microscopy. These embryos displayed severe alterations in the morphology of the primary axonal tracts, reduced number, and altered distribution of the Repo-positive glia as well as peripheral nervous system defects. Most of these alterations were recapitulated by downregulating *Ptr* expression, specifically in embryonic nerve cells. Because similar nervous system phenotypes have been observed in *hh* and *ptc* mutant embryos, we evaluated the *Ptr* participation in the *Hh* pathway by performing cell-based reporter assays. Clone-8 cells were transfected with *Ptr*-specific dsRNA or a *Ptr* DNA construct and assayed for changes in *Hh*-mediated induction of a luciferase reporter. The results obtained suggest that *Ptr* could act as a negative regulator of *Hh* signaling. Furthermore, co-immunoprecipitation assays from cell culture extracts premixed with a conditioned medium revealed a direct interaction between *Ptr* and *Hh*. Moreover, *in vivo* *Ptr* overexpression in the domain of the imaginal wing disc where Engrailed and *Ptc* coexist produced wing phenotypes at the A/P border. Thus, these results strongly suggest that *Ptr* plays a crucial role in nervous system development and appears to be a negative regulator of the *Hh* pathway.

Keywords: Patched-related, *Drosophila*, embryogenesis, Hedgehog, neurodevelopment

INTRODUCTION

Patched-related (*Ptr*) is a transmembrane sterol-sensing domain (SSD) protein that is expressed in different insect and vertebrate species (Zúñiga et al., 2009). *Ptr* topology and domain organization are similar to those of the *Drosophila* segment polarity protein Patched (*Ptc*, Nüsslein-Volhard and Wieschaus, 1980). However, *Ptr* shows a distinctive expression pattern during embryogenesis (Bolatto et al., 2015). *Ptr* protein was first described in *C. elegans* (Kuwabara et al., 2000; Michaux et al., 2000), where functional studies suggested that the many *Ptr* proteins are involved in cell growth, patterning, and molting (Kuwabara et al., 2000). On the other hand, the single *Drosophila* *Ptr* gene (CG11212) was originally identified during a

subtractive hybridization screening designed to identify genes differentially expressed at the beginning of gastrulation (Zúñiga et al., 2009). In addition, our biochemical analysis revealed that *Ptr* was associated with embryo membranes, and immunohistochemistry allowed us to localize it in the growing plasma membranes of *Drosophila* blastoderms (Pastenes et al., 2008). We also demonstrated that, during the late embryonic stages, *Ptr* accumulates in hemocytes (Bolatto et al., 2015), the phagocytic cells that are closely linked to the *Drosophila* developing nervous system (NS). Hemocytes are relevant cells because they participate in two main processes necessary for the NS condensation, the removal of cellular debris, and the deposition of extracellular matrix molecules (Hortsch et al., 1998; Sears et al., 2003; Olofsson and Page, 2005).

Regarding the study of the *Ptr* presence and function in the NS, a previous report (Furlong et al., 2001) classified *Ptr* as a gene mainly expressed in the neuroectoderm. For their part, Zhao et al. (2008) observed widespread macroscopic defects in the pattern of dendritic and axonal projections in neurosecretory neurons upon the insertion of a transposable element upstream of *Ptr*, likely because of disrupted neurite pathfinding. The same authors also demonstrated that a lack of function in *Ptr* results in the loss of bilateral asymmetry in the main portions of the normal neuritic arbor and the formation of ectopic or mistargeted neurites in the adult central nervous system (CNS) immediately prior to the emergence from the puparium (Zhao et al., 2008). Thus, *Ptr* loss disrupted the branching pattern in neurons that are essential for successful head eversion (Park et al., 2003). In spite of this crucial event, the only effects reported so far for *Ptr* at the NS level refer to the morphological changes probably induced by the disruption of the neuritic guidance.

The fact that *Ptr* is a transmembrane protein with similar topology to *Ptc* suggests that *Ptr* could act as a receptor in the axonal growth and/or pathfinding processes during NS development, regulating the availability of extracellular signals as Hedgehog (Hh). The possibility of an additional/alternative receptor in the Hh pathway has been previously suggested in other reports (Méthot and Basler, 2001; Torroja et al., 2005), including a proposed direct interaction between the secreted Hh and its receptor/s to promote cell-cell signaling (Bürglin, 1996; Aspöck et al., 1999) by depending either on Smoothened (*Smo*) as suggested for the majority of organisms or on a *Smo*-independent pathway as shown in *C. elegans* (Zugasti et al., 2005). In *Drosophila*, there are also examples of Hh acting in processes using non-canonical mechanisms, some of which are linked to developmental cell migration and guidance, such as germ and glial cell migrations and axon guidance (Araújo, 2015).

Interestingly, *hh* and *ptc* mutant embryos showed severely altered CNS phenotypes. In the former, many midline cells died, and the remaining surviving cells did not differentiate (Jacobs, 2000; Bossing and Brand, 2006; Watson et al., 2011). Meanwhile, in *ptc* mutant embryos, very few commissures could be formed, and this was mainly attributed to neuronal misspecification and loss (Patel et al., 1989; Merianda et al., 2005). In addition, the axonal defects observed in both null phenotypes could be attributed to alterations in the chemoattraction and/or chemorepulsion signals that are required for proper axon

guidance (Ricolo et al., 2015). The same authors also showed that Hh is involved in axonal guidance during embryonic stages, acting in the ventral nerve cord (VNC) midline through a non-canonical *Ptc*-dependent pathway.

Considering the existing evidence, we decided to further study the *Ptr* function during the developing NS by analyzing whether embryos that lack or downregulate *Ptr* expression in embryonic neural cells show mutant NS-altered phenotypes that can be distinguished from wild-type embryos. Expected NS alterations include disruption of the NS structure, axon tract collapses or misrouting, fasciculation defects or alterations in the number or distribution of neurons.

In addition to characterize the *Ptr* role during embryogenesis, here, we also provide genetic, biochemical, and molecular evidence indicative of the *Ptr* involvement in the Hh pathway, probably acting either as an accessory component of the pathway or as an alternative receptor for the Hh signaling during NS development.

MATERIALS AND METHODS

Drosophila Strains and Genetic Manipulations

All *Drosophila* stocks were maintained and crossed at 25°C according to standard procedures. To obtain a more efficient gene silencing, the crosses involving RNAi experiments were carried out at 29°C (Brand et al., 1994). The stock *en-GAL4*, *UAS-mCD8GFP/S-T* (line *en-GAL4*), was kindly donated by A. Glavic (University of Chile, Chile), while the other *GAL4*-drivers were obtained from the Bloomington *Drosophila* Stock Center (BDSC, USA). The drivers used to express dsRNA*Ptr* were *P{GAL4::VP16-nos.UTR}MVD2* (line *nanos-GAL4*) and *w[*]*; *P{w[+mW.hs]=GawB}jinsc[Mz1407]* (line 8751), whereas the line used to overexpress *Ptr-mCherry* was *y[1] w[*]*; *P{w[+mW.hs]=en2.4-GAL4}e16E* (line 30564). To perform the control crosses *w[*]*; *P{w[+mC]=UAS-lacZ.B}melt[Bg4-2-4b]* (line *UAS-lacZ*) was used. The original *Ptr* mutant line (*Ptr*^{23c}line) balanced over *CyO*, *kr-GFP* balancer (Bolatto et al., 2015) was re-balanced using *CyO*, *twist-GAL4*, *UAS-GFP* donated by R. Cantera (Instituto Clemente Estable, Uruguay) to obtain the line *Ptr/twi-GFP*.

Determination of Hatching Rate

Adult flies of the *Ptr/twi-GFP* null mutant line were placed in cages for embryo collection for 4 h at 25°C. Eggs laid on grape juice agar plates were left for an additional 18–24 h. After that, the embryos were dechorionated with 50% commercial bleach solution in PBST (0.05% Triton X-100 in PBS), classified as GFP positive/negative and hatched/not hatched, and counted under a Nikon SMZ-10A stereomicroscope (Tokyo, Japan) using NIGHTSEA® fluorescence viewing systems (PA, USA) with a royal blue filter. Light and fluorescence images were obtained using a Discovery V8 stereomicroscope (Zeiss, Oberkochen, Germany).

Embryo Immunostaining

Patched-related null mutant embryos of stage 15/16 were collected from grape juice agar plates, dechorionated (50% commercial bleach solution in PBST) and selected by negative GFP expression. Selected embryos were fixed in a 1:1 (v/v) mixture of n-heptane and 4% paraformaldehyde (PFA) for 30 min, and their devitellinization was performed with a slow fixation procedure (Sullivan et al., 2000) using 4% PFA (Sigma-Aldrich, MO, USA) instead of 3.7% formaldehyde. The embryos were stored in methanol at -20°C until used. To perform the immunostaining, the embryos were rehydrated in PBSTA (1% BSA in 0.05% Triton X-100 in PBS) and incubated 30 min in a blocking buffer (1% BSA in 0.1% Triton X-100 in PBS). The same blocking buffer was used during the antibody incubation. Antibodies employed were: mouse anti-22C10 [1:50 22C10, Developmental Studies Hybridoma Bank (DSHB, IA, USA)] or mouse anti-FasII (1D4 anti-Fasciclin II, DSHB, diluted 1:30) or mouse anti-Repo (1:20 8D12 anti-Repo, DSHB). These antibodies were incubated together with lectin from *Arachis hypogaea* (peanut or PNA) biotin conjugate (1:200, Sigma-Aldrich) or rat anti-elav (1:50 Rat-Elav-7E8A10 anti-elav, DSHB). After overnight incubation at 4°C , embryos were washed three times with PBST and one time with a blocking buffer (15 min each) and then incubated 2 h with anti-mouse Alexa Fluor 488 (1:800, Molecular Probes, OR, USA) and anti-rat Alexa Fluor 546 (1:800, Molecular Probes) or Streptavidin Alexa Fluor 555 (1:800, Molecular Probes). After 4 washes (15 min each) with PBST, the embryos were mounted using glycerol 80% in Tris-HCl (1.5 M, pH 8.8) in a chamber made with two coverslips. The use of this chamber allowed us to rotate the embryos to locate the ventral side upward. Digital images were taken using an Olympus FV300 laser scanning confocal microscope at $1,024 \times 1,024$ or $2,048 \times 2,048$ resolution, ensuring that objective lens, brightness, laser intensities, and gain were standardized to ensure the maintenance of acquisition parameters in the samples of each experimental condition.

Cell Culture and Generation of Conditioned Medium

Cultures of clone-8 (cl-8) cells (derived from the *Drosophila* wing imaginal disc) were performed as described at the *Drosophila* RNAi Screening Center website (<http://www.flyrnai.org/DRSC-PRC.html>). The HhN conditioned medium was made by incubating S2-HhN-transfected cells (generously donated by P. Beachy, Stanford University), with a cl-8 medium plus 0.5 mM CuSO_4 for 48 h. The control medium was made by incubating S2 cells in the same culture medium and under the same conditions.

Immunostaining of cl-8 Cells

Cells were fixed with 4% PFA (20 min, RT), permeabilized with PBS containing 0.1% saponin for 15 min, and then blocked with PBS plus 5% BSA and 0.1% saponin for 45 min prior to incubation with the primary antibody mouse monoclonal anti-V5 (1:500, Sigma-Aldrich, MO, USA). The cells were washed three times in PBS with 0.1% saponin and incubated with the secondary antibody anti-mouse Alexa Fluor 546 (1:800,

Molecular Probes). Zeiss Confocal images were collected using the Confocal Laser Scanning Microscope-510 META.

dsRNA Synthesis

Pairs of primers encoding a T7 promoter sequence and gene-specific sequences were used to amplify a product from a single exon using a genomic DNA template or cDNA. These PCR products were the templates for *in vitro* dsRNA synthesis using T7 RNA polymerase (Ambion, TX, USA). See **Supplementary Material** for the table of primers used.

Constructs for Cell-Based Reporter Assays

The *ptc*-luciferase, *Renilla*, and *dally-like* constructs were kindly donated by Dr. P. Beachy. The *ptc*-luciferase (the *ptc* promoter -758 to $+130$ fragment) was generated by PCR and subsequently cloned into the MluI and HindIII sites of the pGL2-Basic firefly luciferase reporter vector (Promega, Madison, USA); the *Renilla* construct was pRL-CMV (for constitutive *Renilla* luciferase expression under CMV promoter control), and *dally-like*-3xFlag was inserted into pActSv (the cloning sites can be found by sequencing with Fw GAC ACA AAG CCG TTC CAT and reverse TTT GTC CAA TTA TGT CAC) (Chen et al., 1999).

Ptr-V5 and the control construct of overexpression experiments in cell reporter assays were obtained in Dr. V. Cambiasso's laboratory. The CG11212 fragment (residues 1–1,129) was generated by PCR and cloned into pMT/V5-His-Topo (Invitrogen, CA, USA) (Zúñiga et al., 2009). The control vector for overexpression experiments was pUASpEGFPc1 (Megraw et al., 2002). This vector derives from the pUASP vector, encoding for an enhanced green fluorescent protein and expressed in *Drosophila* cells.

Luciferase Reporter Assays

dsRNA (2 μg) and/or *Ptr*-V5 or a control vector construct (2 μg) and/or vectors that express *ptc*-luciferase, *dally-like*, and copia-*Renilla* control (to normalize transfection efficiency) were transfected into cultured cl-8 cells using the Calcium Phosphate Kit (Invitrogen) according to Chen et al. (1999) and manufacturer instructions. Transfection was followed by an incubation of 72 h to allow for protein turnover and degradation of targeted mRNA. Transfected cells cultured in 24-well plates were then split by repeated pipetting and seeded into the control medium or into the HhN-conditioned media, and the cells were incubated for additional 24 h. When required, 0.5 mM CuSO_4 was added to the cell medium to induce *Ptr* protein expression. Then, the cells were lysed, and the luciferase activity in the lysates was measured using the Dual-Luciferase Reporter Assay Kit (Promega), which enabled the sequential measurement of firefly and *Renilla* luciferase. Reporter firefly luciferase activity (L) was normalized to the *Renilla* luciferase activity (R) and expressed as the L/R ratio. Fold induction upon stimulation with Hh following transfection of pooled dsRNAs was determined by dividing the L/R ratio obtained in the presence of Hh by the L/R ratio measured in the absence of Hh (basal reporter activity). In all experiments, dsRNA targeting the *B. subtilis* *lys* gene for diaminopimelate

decarboxylase and/or a vector expressing GFP was used as a control.

Immunoprecipitation Assays

Cell extract was obtained by lysing the content of three 60 mm culture dishes of cl-8 cells expressing *Ptr-V5* with a 600 μ l cold lysis buffer [20 mM Tris, pH 7.5, 150 mM NaCl, 1 mM EDTA, 1 mM EGTA, 1% Triton X-100, and Sigma Fast, Protease Inhibitor Cocktail (Sigma-Aldrich)]. The lysate was centrifuged for 10 min at 16,000 g at 4°C and the supernatant stored at -80°C. The S2-HhN-conditioned medium was lyophilized and concentrated 10-fold. Protein determination was carried out using the Bradford method (Fermentas, MA, USA). The input sample for the immunoprecipitation was obtained by incubating equal parts of the *Ptr-V5* cl-8 cell extract and the S2-HhN-conditioned medium (each one contained 1 mg/ml of protein) over 16 h at 4°C. The premix (input sample) was immunoprecipitated with 1 μ g of a mouse anti-V5 antibody (Santa Cruz Biotechnology, TX, USA) adsorbed to 25 μ l of goat anti-mouse IgG Dynabeads (Invitrogen). For the control, Dynabeads were incubated with an alternative mouse antibody (anti-c-Myc, Santa Cruz Biotechnology). Beads were washed three times and proteins eluted in a Laemmli sample buffer. The input sample and the eluents of anti-V5 and anti-c-Myc immunocomplexes were analyzed by Western blotting as described below.

Western Blotting

To detect the presence of HhN or *Ptr-V5*, the immunocomplex was separated by SDS-PAGE and transferred to a PVDF membrane for 2 h at 100 V. Before loading the gel, the samples were incubated with a Laemmli sample buffer for 30 min at 37°C (not boiled) to avoid the formation of aggregates that impede the uniform binding of SDS to the sample proteins. The membrane was blocked (1 h, RT), with 5% low-fat milk in Tris-buffered saline (pH 7.4) and cut at the level of pre-stained molecular weight, 43 kDa (Fermentas). The piece with lower molecular weight proteins was incubated overnight at 4°C with 1:100 rabbit anti-Hh (Santa Cruz Biotechnology), diluted in 1% low-fat milk, 0.05% Tween 20 in Tris-buffered saline (pH 7.4). The rest of the membrane was incubated with a mouse anti-V5 antibody (1:2,000) in similar conditions. To detect the primary antibodies and/or the immunocomplex, the membranes were incubated with anti-mouse or anti-rabbit secondary antibodies coupled to peroxidase (1:500, Thermo Fisher Scientific, MA, USA). The product reaction was revealed using the Supersignal West Pico chemiluminescent reagent (Amersham Biosciences, Bucks, United Kingdom) and the sensitive X-ray film (Amersham Biosciences).

RNA Extraction and cDNA Synthesis

Total RNA was extracted from staged embryos ($N = 10-15$) or transfected cells using the RNA_{WIZ} reagent (Ambion). The samples were carefully homogenized in a 1.5 ml Eppendorf tube with 1 ml of RNA reagent using one insulin syringe. After 5 min at RT, 0.2 volumes of chloroform were added, and the samples were subjected to a cycle of shaking, incubation

(10 min, RT) and centrifugation (13,000 g for 15 min, 4°C). The RNA rescued from the aqueous phase was precipitated with isopropanol/glycogen by centrifugation at 14,000 g at 4°C for 15 min. The precipitate was washed with 75% ethanol and centrifuged at 14,000 g at 4°C for 5 min. Finally, the total RNA was re-suspended in 30 μ l of nuclease-free water. An average yield of 1 μ g/ μ l of RNA was obtained. RNA integrity was verified by agarose gel electrophoresis (1.2% formaldehyde-agarose gel). The samples were treated with TURBO DNA-free DNase (Ambion) to remove contaminating DNA from the RNA. For qPCR, 1 μ g of total RNA was used as a template for reverse transcription reactions to synthesize single strand (ss) cDNA using MMLV-RT reverse transcriptase (Promega) and oligo-dT primer (Invitrogen) according to standard procedures. A poly (A)-RNA was *in vitro* transcribed from the vector pGIBS-dap (ATCC 87486) and added to the embryo RNA samples prior to cDNA synthesis in a 1:1,000 ratio to be used as spike mRNA (Brand et al., 1994).

cDNA Synthesis and Quantitative Real-Time PCR

qPCR amplifications and fluorescence detection were performed using the LightCycler[®] 1.5 Instrument (Roche, Basel, Switzerland) and LightCycler[®] FastStart DNA Master SYBR[®] Green I (Roche). Reactions contained 100 ng of dsDNA or 50 ng of ssDNA. Primers were designed using Primer Premier 5.0 software (Palo Alto, CA, USA) and synthesized by Alpha DNA (Quebec, Canada). Primer sequences, annealing temperatures, and amplicon lengths are given in **Supplementary Material**. For each gene, a calibration curve was generated based on serial dilutions (101-102 pg/ μ L) of plasmid templates. The thermal cycle conditions were: denaturation at 95°C for 10 min, followed by 35 three-step cycles of template denaturation at 95°C with a 2 s hold, primer annealing at 68°C for 15 s, and extension at 72°C for 60 s/1,000 bp. The purity of amplified products was verified by melting curve analyses. Control reactions included a subset of PCR components lacking the cDNA template. The initial amount of transcript in each sample was calculated from the standard curve using the default (fit point/arithmetic) method of LightCycler Software Version 3.5 and normalized to the values of *actin*. Data represent the mean \pm SEM of three replicates from three independent experiments.

RNAi Vector Construction, Microinjection, and Generation of UAS-DsARN *Ptr* Lines

A region of the first exon of *Ptr* was generated by PCR using genomic DNA as a template with the primers indicated in **Supplementary Table 1**. To create the knockdown plasmid UAS-*PtrIR*, the PCR product was inserted into the pWiz vector (*Drosophila* Genomics Resource Center, IN, USA) at each of the AvrII and NheI restriction sites, in opposite orientations (Lee and Carthew, 2003). Clones were confirmed by sequencing. w^{1118} embryos were injected with the UAS-*PtrIR* construct at Genetic Services Inc. (MA, USA) according to standard protocols (Rubin and Spradling, 1982). Homozygous lines were generated with standard balancer chromosomes.

TABLE 1 | Penetrance of SN phenotypes.

Phenotype	CS	<i>Ptr/Ptr</i>	8751> <i>UAS-lacZ</i>	8751> <i>UAS-dsRNAPtr</i>
Longitudinal axon defects	0% (40)	20% (30)	0% (28)	30% (30)
Repo-Positive glial defects	0% (30)	≈43% (28)	0% (25)	≈53% (30)
PNS organization defects	0% (30)	≈37% (30)	0% (25)	≈44% (32)

Penetrance is defined as the percentage of embryos that present the phenotype. The total number of embryos analyzed for each condition is shown in parentheses. PNS, peripheral nervous system.

Generation of the UAS-*Ptr*-mCherry Lines

The cDNA for the *Ptr* gene was subcloned into a pUAST vector by a standard protocol and sequenced. Transgenic plasmids (with the UAS sequence and the mCherry tag fused to the C-terminal end of *Ptr*) were mixed with 100 µg/ml of helper plasmid (P {Δ2-3}) and injected into eggs [w1118] as described by Rubin and Spradling (1982). Surviving F0 males or females were individually crossed with virgin females [w1118] or males [w1118]. The progeny of these crosses (F1 generation) with colored eyes was used to establish transgenic lines through crossings with lines containing different balancer chromosomes. VectorBuilder Inc. (IL, USA) cloned the designed plasmid (pUASTattB-5 × UAS/mini_Hsp 70 > {CG11212}/mCherry) and tested its quality. BestGene Inc. (CA, USA) microinjected the embryos and balanced the transgenic lines.

Analysis of Adult Wings

Wings from male and female adult flies were removed from the thorax and incubated in a washing buffer (PBS and 0.1% Triton X-100) separately by gender. A paintbrush was used to mount the wings on a slide with 80% glycerol in PBS (Gault et al., 2012). Light images of the wings were obtained with a Nikon Eclipse E400 microscope at 10X magnification. Quantitative image processing was carried out using Fiji ImageJ software (NIH). To do this, we delimited the areas to be measured (the total wing area and the L3-L4 intervein area), with the aid of the Polygon selection tool, and the selected pixels were counted with the Analyzed option. In order to make an appropriate comparison, the quotient L3-L4 intervein area/total wing area of each wing was determined and graphed. Mean ± SEM were represented. Around 30 males and 30 females for each cross were measured.

Statistical Studies

Data are expressed as the mean ± SEM. Statistical tests used were ordinary one-way ANOVA followed by the Tukey's *post-hoc* comparisons or the unpaired two-tailed Student's *t*-test (GraphPad Prism 5.0, Mac OS X version). Statistical significance was determined at $p < 0.05$. The number of asterisks-*, **, ***- indicates $p < 0.05$, $p < 0.01$ or $p < 0.001$, respectively. Normal distribution of the data was tested using GraphPad Prism 5.0, Mac OS X version.

RESULTS

Absence of *Ptr* Elicits Alterations in Some Components of the Developing Central and Peripheral NS

Because previous studies have classified the *Ptr* coding gene sequence as a neuroectodermal gene (Furlong et al., 2001), we decided to analyze whether *Ptr* null mutants exhibit an embryonic CNS with disturbed architecture. We analyzed late homozygous embryos (stages 15/16) that were characterized by the lack of GFP fluorescence. Only ≈19% of these embryos hatched (Supplementary Figure 1), strongly reinforcing the previous evidence (Bolatto et al., 2015) that *Ptr* is critical to *Drosophila* development. In up to 100% of the cases, the larvae did not reach adulthood under standard feeding conditions.

To perform this study, we employed PNA lectin to visualize the morphology of axon tracts in the VNC as shown by D'Amico and Jacobs (1995). In *Ptr* null mutant late embryos, we detected interruptions or alterations in the regular spaces delimited by VNC commissures and connectives tracts that were analyzed in detail by combining the biotinylated lectin with specific primary antibodies. These alterations were consistently found between abdominal segments A2-A6. When anti-FASII and PNA were combined, it became evident that the alterations previously observed with the lectin (Figure 1, white arrows in images of PNA staining) correlated with FasII-positive longitudinal axons that were over-migrating and re-crossing the midline (Figure 1, the two upper rows).

Anti-Repo and PNA co-labeling indicated the co-existence of the primary axonal tract interruptions and alterations in the number and/or distribution of Repo-positive glial cells (Figure 1, the two middle rows). In addition, the combined staining using anti-22C10 and PNA enabled us to establish that the lack of *Ptr* also produces failures at the PNS branching and distribution of neurons (Figure 1, the two bottom rows).

Ptr Downregulation Using a Pan-Neural Driver Affects the Embryonic NS Structure

In a previous work, we reported differences in the number and distribution of migrating hemocytes in the *Ptr* null mutant (Bolatto et al., 2015). Considering that hemocytes are essential to NS embryogenesis (Sears et al., 2003), here, we aimed to know whether the morphological changes described above resulted directly from the lack of *Ptr* in the NS or indirectly by the reduced action of hemocytes. To elucidate this point, we expressed dsRNA

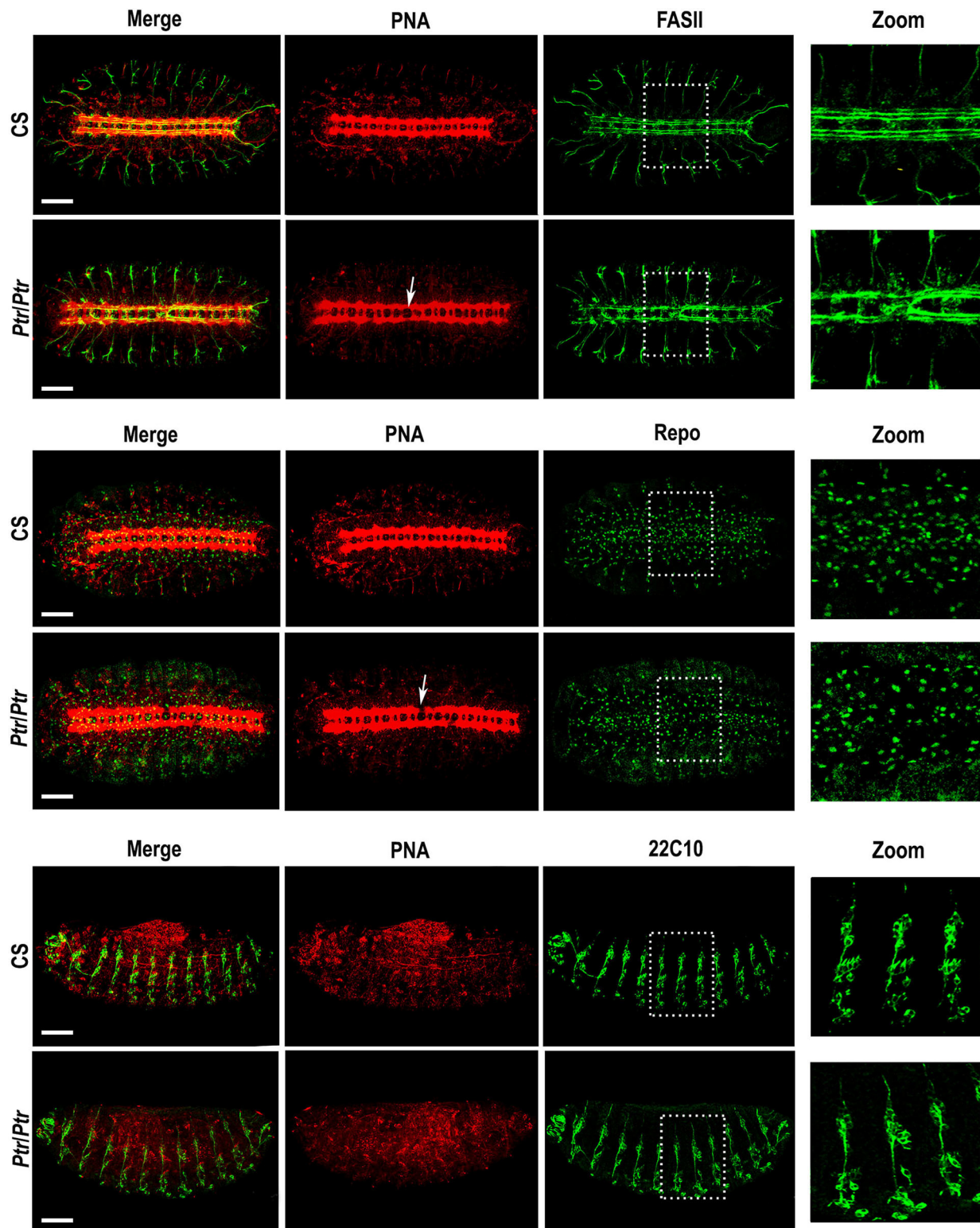
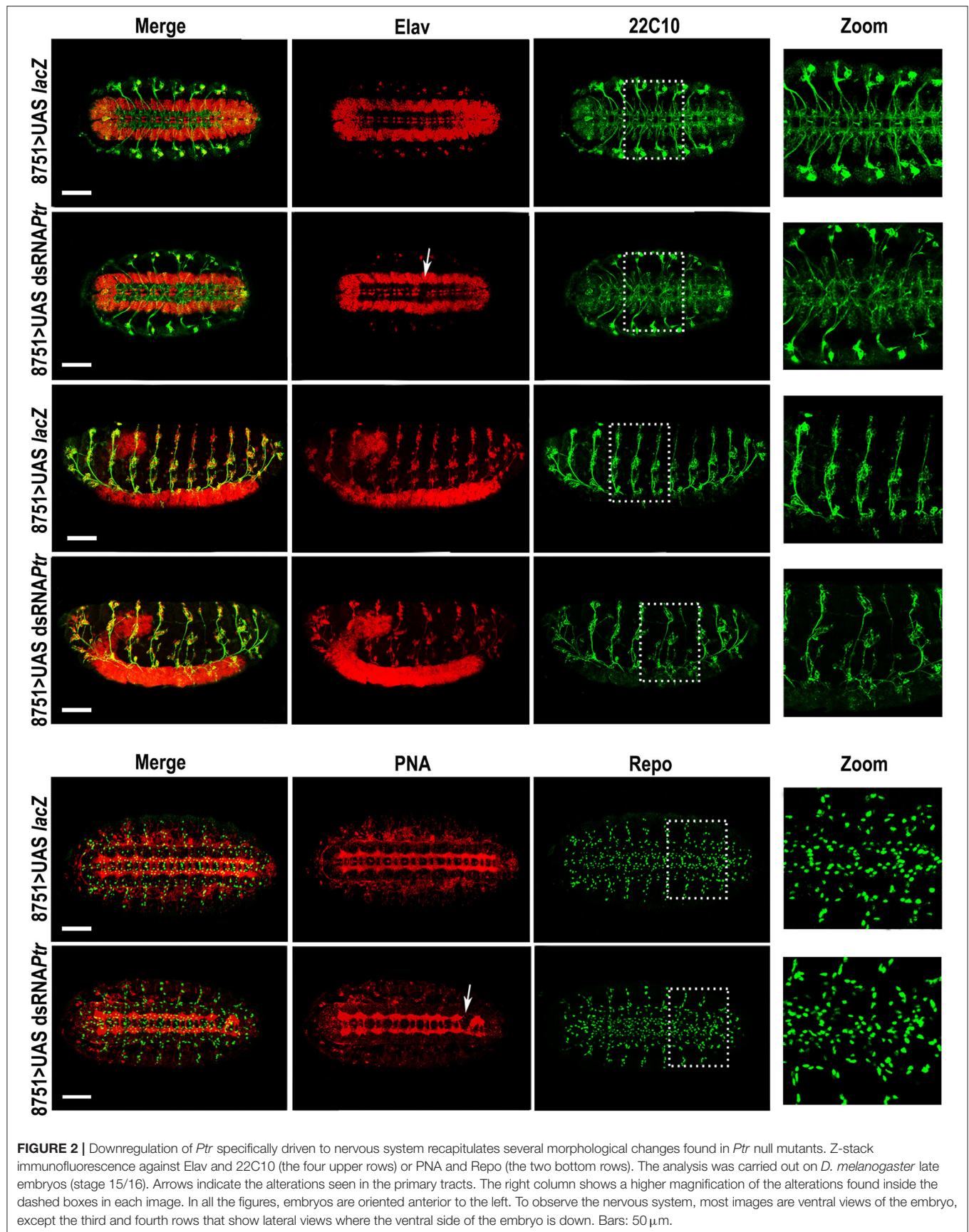
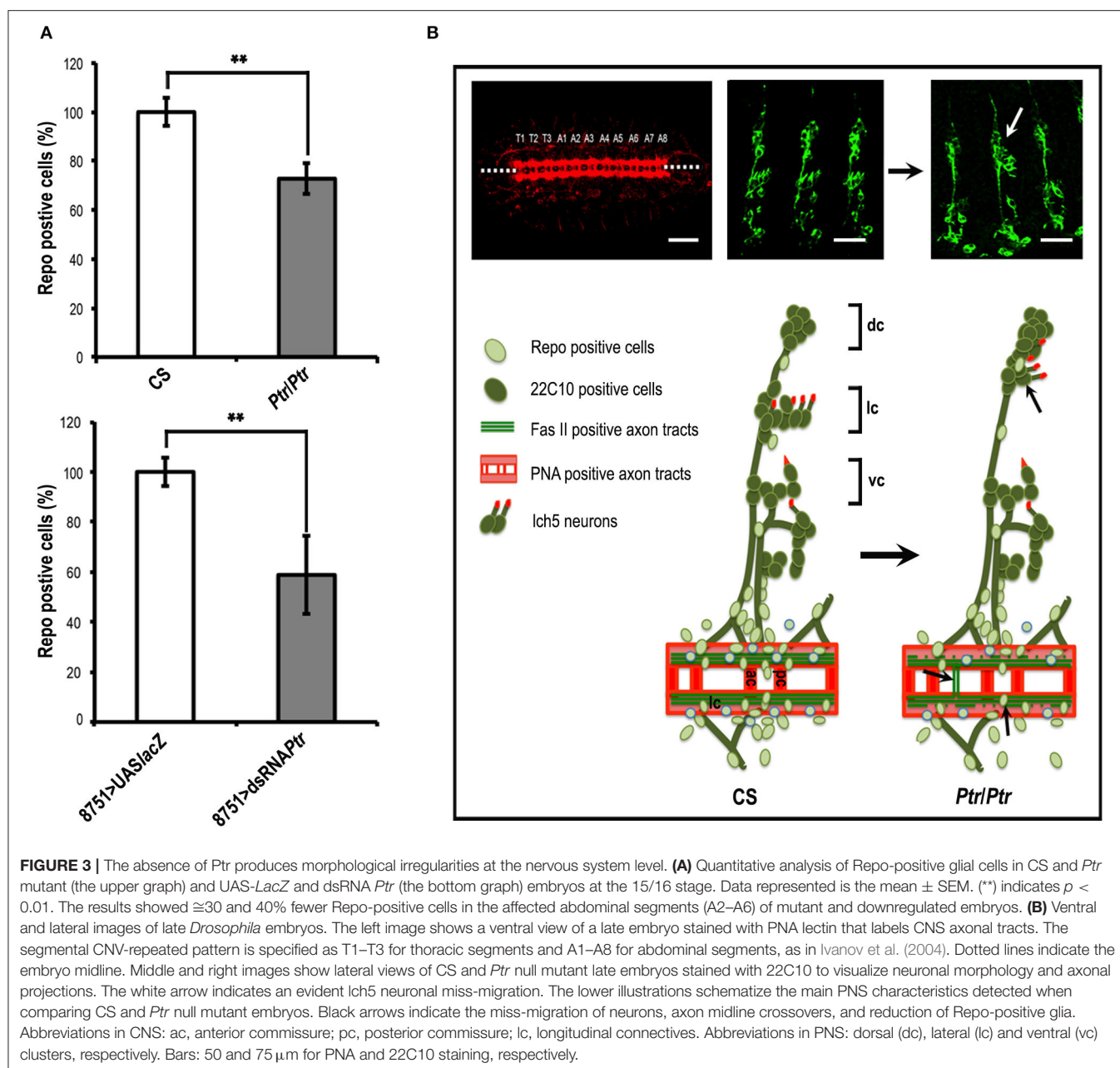


FIGURE 1 | Phenotypic analysis of the *Ptr* null mutant in whole mount embryos. Z-stack immunofluorescences against PNA and FASII (the two upper rows), PNA and Repo (the two middle rows) or PNA and 22C10 (the two bottom rows). The analysis was carried out on *D. melanogaster* late embryos (stage 15/16). Arrows indicate the alterations in the primary tracts of *Ptr* null mutants that were evidenced with PNA. The right column shows a higher magnification of the alterations found inside the dashed boxes in each image. In all the figures, embryos are oriented anterior to the left. To observe the nervous system, the first four rows of images are ventral views of the embryo, whereas, in the last two rows, the ventral side of the embryo is down. Bars: 50 μ m.





of *Ptr*, specifically in the NS using a pan-neuronal driver (line 8751 of BDSC).

First, we generated a transgenic line that expressed an inverted repeat of the first exon of the *Ptr* sequence under the control of the UAS promoter in the vector pWIZ (UAS-dsRNA*Ptr*). To determine if the construct designed was effective in silencing the *Ptr* gene, the transgenic lines were crossed with the *nanos*-GAL4 driver to activate transcription of the hairpin-encoding transgene in the progeny. As a control, GAL4 drivers were crossed with UAS-*lacZ* flies. Using qPCR analysis, we determined that the amount of *Ptr* mRNA in *nanos*>UAS-dsRNA*Ptr* embryos was reduced by about 90% of the amount found in the control embryos (*nanos*>UAS-dsRNA*Ptr*) (Supplementary Figure 2).

Regarding immunostaining, we decided to use rat anti-elav (red in Figure 2), a pan-neuronal marker for most cells in the CNS and PNS, to evidence the VNC distortions (white arrows). The use of this antibody together with anti-22C10 demonstrated that axon crossovers occurred, recapitulating the phenotype observed in the *Ptr* null mutant. In addition, the lateral view of the embryo revealed that the crosslinking resulted in the presence of fewer axons at the PNS, as well as important disorganizations in the peripheral neurons (mis-migrating and morphological irregularities in *lch5* chordotonal neurons) (Figure 2). Table 1 summarizes the penetrance of *Ptr* null mutants and NS knockdown phenotypes.

Concerning Repo-positive cells, our results showed significant reductions in both *Ptr* null mutant ($\cong 27\%$) and *Ptr* downregulation ($\cong 41\%$), specifically in the NS (**Figure 3A**). A summary of the differences found in the *Ptr* null mutant compared to the NS wild-type embryos is shown in **Figure 3B**. Given that *Ptr* downregulation produces similar alterations, it indicated that *Ptr* has a role at the NS level that is relevant for its proper organization.

Ptr Functions as a Negative Component of the Hh Pathway in cl-8 Cells

The important topological similarities between *Ptr* and the Hh pathway components, *Ptc* and Dispatched (Burke et al., 1999), prompted us to evaluate whether *Ptr* could be involved in the Hh signaling pathway. Moreover, previous reports have indicated that some of the genes associated with the Hh signal transduction pathway also develop mutant NS phenotypes, suggesting a link between the pathway and the NS developmental process (Patel et al., 1989; Merianda et al., 2005; Koizumi et al., 2007). Thus, we used a cultured cell assay developed by Philip Beachy's group (Chen et al., 1999; Lum et al., 2003), which has successfully identified new components of the Hh pathway (Yao et al., 2006). This system is quantitative and specific for cellular response because the addition of exogenous Hh, through a conditioned medium, makes the assay independent of ligand synthesis or distribution (Lum et al., 2003).

Since RNAi in *Drosophila* cultured cells is frequently used as a functional test of gene products with a known or predicted sequence (Chen et al., 1999; Lum et al., 2003; Yao et al., 2006), we treated cl-8 cells with control or *Ptr*-specific dsRNA and assayed for changes in Hh-mediated induction of a Hh pathway-responsive luciferase reporter (a *ptc*-luciferase reporter construct) (Chen et al., 1999; Lum et al., 2003). Our results indicated that the transfection of *Ptr* dsRNA caused an exclusive reduction in *Ptr* mRNA levels (**Figure 4A**) and a significant increase in the response to Hh signaling (**Figure 4B**). On the other hand, transfection of cl-8 cells with a *Ptr* DNA construct to obtain higher levels of *Ptr* protein (**Figure 4C**) produced a strong and opposite effect on the Hh pathway activity (**Figure 4D**). The observed effect suggested that normal levels of *Ptr* in cl-8 cells could act as a limiting factor in the response to Hh signaling. These results also suggested that *Ptr* can modulate the response to Hh, and the outcome depends on cellular *Ptr* levels.

To investigate the role of the *Ptr* protein in Hh signaling related to *Ptc*, we performed luciferase reporter assays in cl-8 cells to downregulate *ptc* via dsRNA together with downregulation or overexpression of *Ptr*. The overexpression of *Ptr* not only suppressed the increase in the Hh pathway activity produced by *ptc* dsRNA but also reversed it, resulting in levels of the pathway activity lower than control (**Figure 5A**). Co-transfection with *ptc* and *Ptr* dsRNA produced activation of the signaling pathway stronger than the activation produced by independent transfection with dsRNAs targeting each gene (**Figure 5B**). Thus,

these results strongly suggested that *Ptr* may act independently of *Ptc*.

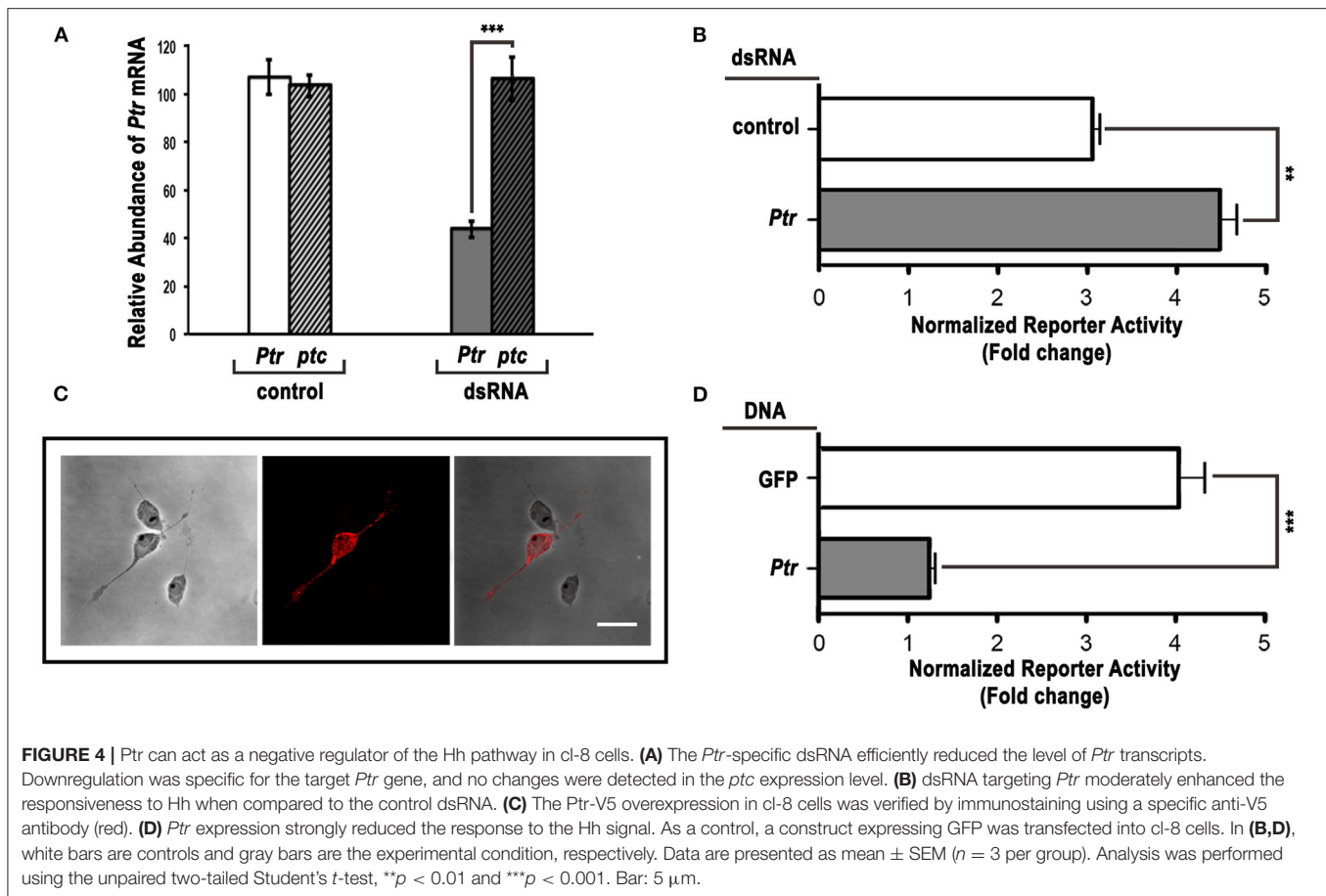
To further investigate the mechanism of *Ptr* action on the Hh signal response, we examined the effect produced by cell co-transfection with the dsRNA of *Ptr* in combination with dsRNAs targeting other known pathway components. Simultaneous transfection of *Ptr* dsRNA and either *ihog* or *smo* dsRNA had a pathway activity similar to that obtained when *ihog* and *smo* are individually silenced (**Figures 5C,D**). These results suggested that *Ptr* acts on Hh signaling upstream of these two components (*iHog* and *Smo*) of the Hh signaling pathway. Taken together, these results indicated that *Ptr* could play a role in the regulatory mechanism of the Hh signal transduction. Complementary assays are required to evaluate whether *Ptr* would be fulfilling a role similar to that of *Ptc*, especially when considering the literature reports that *iHog* acts upstream of *Ptc* (McLellan et al., 2006; Yao et al., 2006; Camp et al., 2014).

In vitro Binding of Ptr and Hh

The response observed in the cell-based reporter gene assays and the observation that *Ptr* is a transmembrane protein (Pastenes et al., 2008) raise the question of whether *Ptr* can interact directly with Hh. To test this possibility, we performed an immunoprecipitation assay in which a *Ptr*-V5 fusion protein was incubated with the conditioned-HhN medium, and the mix was immunoprecipitated with a mouse anti-V5 antibody (for details, see Methods). Co-immunoprecipitated molecules were identified with Western blot analysis using antibodies anti-V5 and anti-Hh. Both *Ptr* and HhN were identified as forming an immunocomplex, indicating a direct interaction between both proteins (**Figure 6**). The apparent molecular weights of *Ptr* and heavy/light chains of anti-V5 were slightly different than predicted (for *Ptr*-V5, a signal at 120 kDa was predicted, instead of 95 kDa). This biochemical behavior, termed "gel shifting," might derive from altered binding caused by the detergent employed (Rath et al., 2009; Nybo, 2012). Thus, the data obtained using this method indicated that *Ptr* was able to bind Hh directly.

Overexpression of Ptr Modifies the Wing A/P Border

To further evaluate the participation of *Ptr* in the Hh pathway, we overexpressed *Ptr* at the wing imaginal disc using a transgenic line that expressed *Ptr*-mCherry under the control of a UAS-activating sequence (**Supplementary Figure 3**). We used the *en*-GAL4 driver to express *Ptr* not only in the posterior compartment of the imaginal disc but also in a thin strip of cells anterior to the A/P border where *en* and *ptc* coexist (the En/*Ptc* domain). The signaling occurring in this strip of cells is important for the intervein L3-L4 area and anterior cross vein (ACV) formation (Layalle et al., 2011). As seen in **Figure 7**, we found that *Ptr* overexpression determined that adult wings have a decreased area between veins 3 and 4 related to the overall wing size. This phenotype was gender independent and reminiscent of that observed when a reduction of Hh activity occurs, since



the area between veins L3 and 4 is directly under the control of Hh (Mullor et al., 1997; Strigini and Cohen, 1997; Crozatier et al., 2004). We also noted that the overall size of the wings was reduced, while their general morphology was preserved, indicating that increased *Ptr* function leads to growth inhibition. In relation to the ACV formation, it has been observed that $\approx 19\%$ of wings overexpressing *Ptr* do not present this vein. Similar phenotypes at the A/P border have been previously observed following *ptc* overexpression (Johnson et al., 1995; Martín et al., 2001).

DISCUSSION

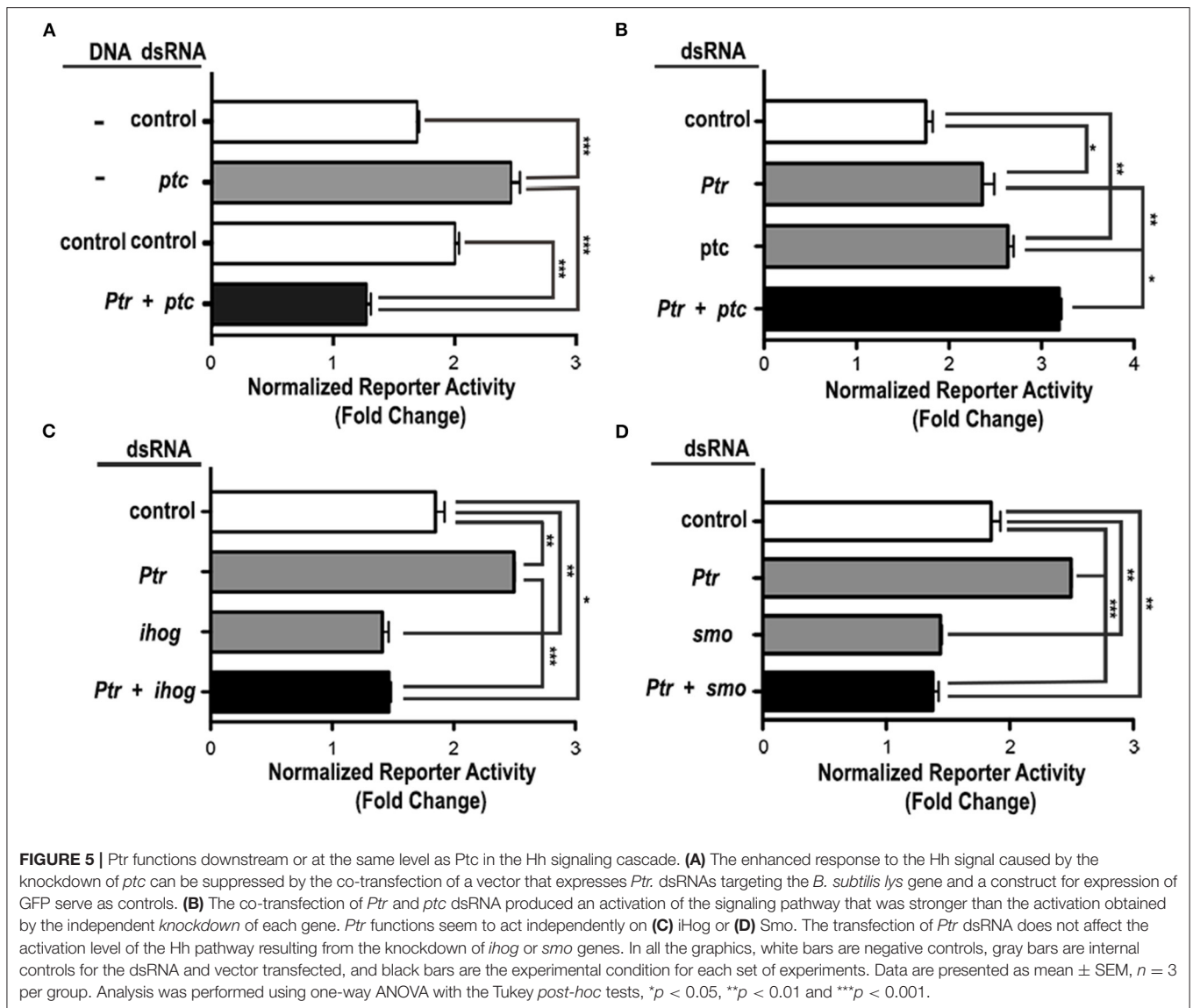
Ptr has been identified as one of 118 genes that are differentially expressed in gastrulation (Zúñiga et al., 2009). It is classified as a neuroectodermic gene (Furlong et al., 2001) that encodes an uncharacterized transmembrane protein with a predicted topology closely related to *Ptc* (Pastenes et al., 2008), the canonical Hh receptor. In this work, using *Ptr* null mutants and the UAS/GAL4 system to direct the expression of *Ptr* dsRNA specifically to neurons, we demonstrated that *Ptr* is necessary for the proper NS development.

The use of PNA lectin to label primary axonal tracts or pan-neuronal markers, such as anti-elav antibody, indicates that

Ptr absence or silencing triggers alterations in the NS general morphology. Alterations include distortions in the normal regularity of the spaces between the commissures (anterior and posterior) and the longitudinal tracts, where the axons of the longitudinal tract cross the midline. The occurrence of this kind of malformation has been previously described for *ptc* null mutants (Patel et al., 1989; Merianda et al., 2005), as well as in *hh* overexpression (Bossing and Brand, 2006; Ricolo et al., 2015).

At the antero-posterior level of VNC alterations, *Ptr* null mutants also showed changes in the number and distribution of PNS neurons and axons. These alterations resembled those observed with 22C10 immunostaining of *ptc* mutant embryos, which exhibited similar phenotypes that included the loss of neurons and defects in the organization and pathfinding (Prokopenko et al., 2000). Although experiments are still needed to establish whether peripheral alterations are a consequence of the loss of neurons at the VNC level, it is clear that *Ptr* is an essential protein for the proper organization of the developing NS.

Ptr is relevant to neuronal function in other species. For instance, *Ptr-18* (one of the 24 *ptr* genes found in *C. elegans*) is essential for establishing the capacity of neural progenitor cells to maintain quiescence in response to nutritional stresses and provides unique insights into the *Ptr* role in promoting the clearance of extracellular Hh-related protein by targeting it



to lysosomal degradation (Chiyoda et al., 2021). Interestingly, PTR-18 is structurally similar to human PTCHD1 (Chiyoda et al., 2021), which has been proposed to cause common neurodevelopmental disorders (Noor et al., 2010). Similarly, in *C. elegans*, PTR-6 participates in the formation of the glial channel that surrounds the receptive endings of the sensory neurons and likely regulates vesicular transport (Perens and Shaham, 2005; Oikonomou et al., 2011; Wallace et al., 2016; Wang et al., 2017).

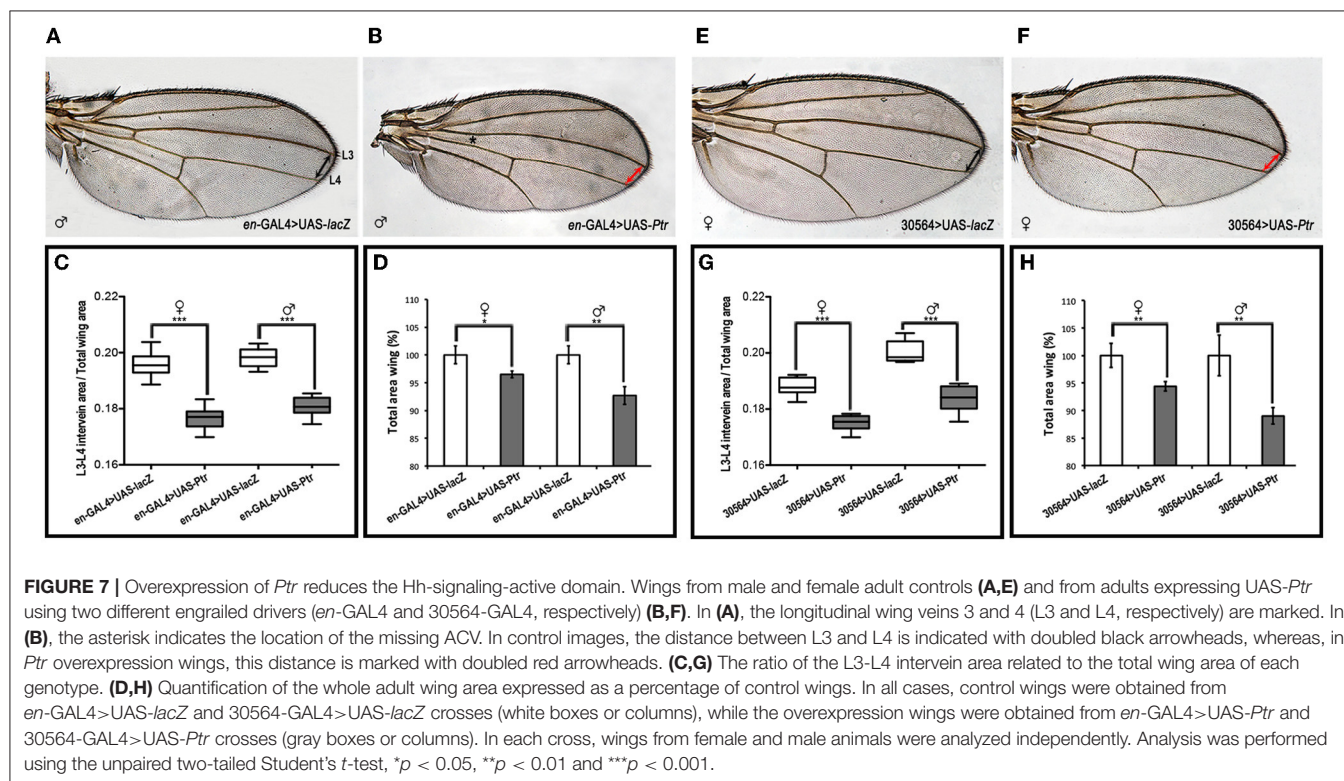
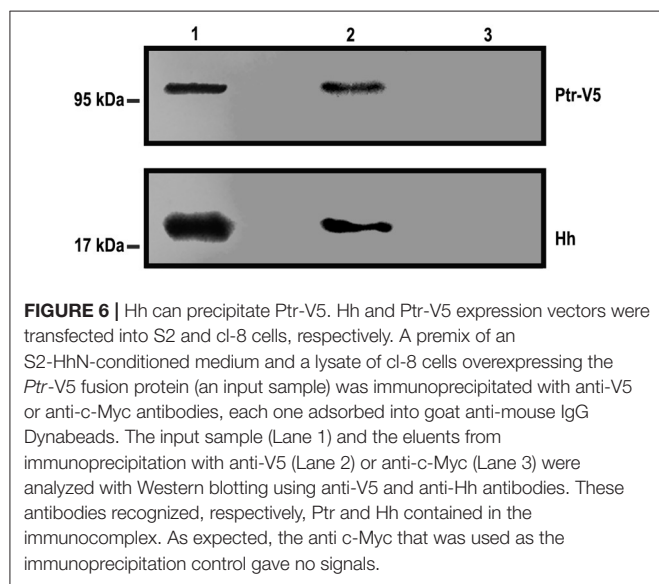
Results from this work showed that *Ptr* null mutants and knockdown embryos exhibited reduced numbers and altered distribution of Repo-positive glia around the axonal disarray previously mentioned. Although some authors described a reduction in the number of glial cells in *ptc* mutant embryos (Merianda et al., 2005), they dismissed the involvement of glial cells in axonal guidance because the mutant for the gene *glial cell missing* (or *gcm*) employed by the authors does not exhibit a *ptc*-like axon guidance phenotype (Vincent

et al., 1996; Takizawa and Hotta, 2001; Merianda et al., 2005). Nevertheless, it will be interesting to investigate whether *Ptr* dsRNA targeting to glial cells causes effects similar to those observed in the null mutant and knockdown embryos, because some aspects of the glial migration are regulated by the same ligand/receptor system that controls the axonal guidance across the CNS midline (Kinrade et al., 2001).

Ptr null and knockdown NS alterations also strongly resemble the alterations described in embryos overexpressing *hh* (Bossing and Brand, 2006; Ricolo et al., 2015). In accordance with the proposed function of *Ptr* in NS development, it has been shown that Hh is involved in several processes of cell migration and guidance (including midline axonal guidance and glial cell migration) by acting as a chemoattractant (direct or indirect) or by regulating cell physiology using both canonical and non-canonical mechanisms (Pielage et al., 2004; Araújo, 2015).

The structural similarities between *Ptr* and *Ptc*, together with the association of *Ptr* with embryo membranes and the resemblance to NS morphological alteration observed in *ptc* null mutants, raised the possibility that *Ptr* could be involved in the Hh signaling pathway. Interestingly, some reports also associated the *C. elegans* PTR-6 protein with members of the *hh-related* gen family (Aspöck et al., 1999;

Oikonomou et al., 2011; Singhal and Shaham, 2017; Wang et al., 2017). Using a cell-based reporter gene assays, we demonstrated that *Ptr* displays a response characteristic of a negative regulatory component of the pathway, since the RNAi of *Ptr* increased the reporter activity, whereas *Ptr* overexpression suppressed Hh-induced pathway activation. Applying the same experimental approach, we also showed that increased reporter activity produced by *Ptr* dsRNA was enhanced by *ptc* dsRNA, suggesting that, in this cellular system, both receptors can mediate Hh effects. The possibility that cells express receptors with different affinities has been previously suggested by experiments in which a *ptc* allele with low affinity for Hh (*Ptc^{Con}*) was co-expressed with wild-type *Ptc* in wing imaginal disks (Mullor and Guerrero, 2000). Results indicated that *Ptc^{Con}* and wild-type *Ptc* compete for Hh, so a cell containing both receptors could interpret different Hh levels. The difference between affinities implies different states of the transcription factor Cubitus interruptus and subsequent activation of different groups of genes (Mullor and Guerrero, 2000). In our case, the binding of Hh by *Ptr* could regulate its availability to *Ptc*, and, as a result, a cell that expresses both *Ptr* and *Ptc* could translate the gradient of Hh signaling into a different transcriptional readout when compared to a cell predominantly expressing *Ptc*. Thus, the possibility of expressing receptors with different or similar affinities for a ligand could enrich the signaling modulation (Yarden and Sliwkowski, 2001; Shibuya and Claesson-Welsh, 2006; Mac Gabhann and Popel, 2008).



In this sense, the results of our luciferase reporter assays suggested that normal levels of Ptr expressed by cl-8 cells are a limiting factor in the response initiated by Hh binding. These results were also consistent with the possibility that Ptr competes with Ptc, limiting Hh signaling. This option is in line with the recent report by Chiyoda et al. (2021) in *C. elegans* where the function of PTR-18 could be linked to the removal of Hh-related extracellular proteins *via* endocytosis-mediated degradation. The same authors speculated that, in *Drosophila*, Ptr might mediate the Ptc-independent Hh internalization. Given that the intracellular Ptr C-terminal contains the same highly conserved motif that is part of the Ptc SSD domain required for Smo translocation to the cell surface (Strutt et al., 2001) and for Ptc endocytosis (Hicke and Dunn, 2003), it would be interesting to know whether Ptr can mediate Hh internalization by itself. Alternatively, Ptr could sequester Hh to deliver it to the vesicular pools of Ptc, similar to the action of Megalin reported in vertebrates (McCarthy et al., 2002). This not only controls the Hh gradient but also regulates the potential of complexing vesicular Ptc with Smo.

In addition to the core components of the Hh signaling pathway in *Drosophila*, several cell surface proteins have been implicated in modulating the responses to Hh (Beachy et al., 2010), and the existence of an alternative molecule mediating the Hh signaling has been proposed. Although confirmatory experiments are needed, the present results suggested that Ptr could act upstream to Smo and iHog, in spite of the existing literature reporting iHog acting upstream of Ptc (McLellan et al., 2006; Yao et al., 2006; Camp et al., 2014). Therefore, a future challenge will be to investigate the functional interactions between these proteins. Ptr could affect the intracellular trafficking of Smo, given the alternative functions as membrane transporters proposed for proteins structurally related to Ptr (Tseng et al., 1999), or Ptr might function through a non-canonical pathway as had previously reported for Ptc (Brennan et al., 2012; Araújo, 2015; Ricolo et al., 2015).

On the other hand, the binding of Hh to Ptr might require the presence of Brother of iHog (Boi), which is essential for pathway activation but not for Hh reception and sequestration (Camp et al., 2014). It also may need Dally-like (Dlp), a glypican-type heparin sulfate proteoglycan that enhances the stability of Hh and promotes its internalization with Ptc (Yan et al., 2010). Since previous studies have demonstrated that Dlp is specifically required in the cell-based assays and in embryos (Desbordes and Sanson, 2003; Lum et al., 2003; Han et al., 2004), our cell transfection protocols were performed using an expression vector for Dlp (see Methods). Thus, it is possible to speculate that, in the cell assay model we employed, Dlp could facilitate the Ptr-Hh interaction. In spite of this possibility, immunoprecipitation assays between a lysate of cl-8 cells overexpressing Ptr and the concentrated S2-HhN-conditioned medium showed a direct interaction between Ptr and Hh. This result was obtained in conditions that facilitated their interaction, which does not rule out the existence of other molecules that collaborate with Ptr-Hh interaction, mostly when the receptor or the ligand is less available, as occurs *in vivo*.

In vivo experiments with Ptr overexpression during wing formation confirmed the involvement of Ptr in Hh signaling. Indeed, our data showed that Ptr overexpression in the Ptc/En domain of the wing imaginal disks decreased the L3–L4 intervein area, as well as the total wing area and caused the AVC loss in $\cong 19\%$ of the wings analyzed. All these features have been previously reported for *ptc* overexpression using the same types of drivers (Johnson et al., 1995; McCarthy et al., 2002). Thus, Ptr overexpression mimics *ptc* overexpression in the wing imaginal disc and corroborates the participation of Ptr as a negative regulator in the Hh pathway, which includes a possible role in sequestering Hh.

To summarize, our present results showed for the first time that the transmembrane protein Ptr is necessary for the proper NS development and suggested its functional relationship with the Hh pathway. Further *in vivo* studies are needed to explore the role of Ptr in promoting axonal guidance and glial migration, as well as to characterize its direct or indirect interaction with Hh.

DATA AVAILABILITY STATEMENT

The data will be available upon reasonable request.

AUTHOR CONTRIBUTIONS

CB and VC conceived the work. CB, VC, and SO-B wrote the manuscript. CB, SN, and AR performed the fly crosses, assembled the embryo collection, and performed all the procedures related to embryo immunofluorescences. AR and SN determined the hatched rate, obtained, imaged, measured, and analyzed wing-related data. CB and SO-B conducted the confocal microscopy and performed the statistical analysis. CB performed all the procedures related to the cl-8 luciferase reporter, including dsRNA synthesis and cl-8 immunostaining, performed immunoprecipitation and Western blot assays, as well as RNA extraction and qPCR analyses, and generated the article figures. All authors read and approved the final manuscript.

FUNDING

This work was supported by the International Brain Organization (IBRO) for its IBRO-LARC PROLAB Program that connected the groups of CB and VC, Comisión Sectorial de Investigación Científica (CSIC I+D 2020 Program, ID 313), and Programa para el Desarrollo de las Ciencias Básicas, MEC-UdelaR (PEDECIBA). SN was supported by CSIC I+D 2020, ID 313.

ACKNOWLEDGMENTS

We would like to thank Philip Beachy from the Howard Hughes Medical Institute 607 (HHMI) at Stanford University, who generously donated the vectors and HhN S2 cells to evaluate the role of Ptr in the Hh pathway using cell-based luciferase reporter assays. We are grateful to Adam Saunders, Wenchaun Liang, and Paula Quezada for their advice and/or technical

assistance; Nicolás Tobar for his help with the interpretation of results from cell reporter assays; and the Bloomington *Drosophila* Stock Center for providing the stocks used in this study. We also thank Cristina Parada for the re-balance of the *Ptr* null mutant line generating the *Ptr/twi*-GFP line and her help with immunostaining experiments and dsRNA purification. The 1D4 anti-Fasciclin II and 8D12 anti-Repo monoclonal antibodies deposited by C. Goodman; the 22C10 monoclonal antibody deposited by S. Benzer and N. Colley; and the Rat-Elav-7E8A10 anti-elav monoclonal antibody deposited by G. M. Rubin

were purchased from the Developmental Studies Hybridoma Bank, created by the NICHD of the NIH and maintained at the University of Iowa, Department of Biology, Iowa City, IA 52242.

SUPPLEMENTARY MATERIAL

The Supplementary Material for this article can be found online at: <https://www.frontiersin.org/articles/10.3389/fnins.2022.920670/full#supplementary-material>

REFERENCES

- Araújo, S. J. (2015). The hedgehog signalling pathway in cell migration and guidance: what we have learned from *Drosophila melanogaster*. *Cancers* 7, 2012–2022. doi: 10.3390/cancers7040873
- Aspöck, G., Kagoshima, H., Niklaus, G., and Bürglin, T. R. (1999). *Caenorhabditis elegans* has scores of hedgehog-related genes: sequence and expression analysis. *Genome Res.* 9, 909–923. doi: 10.1101/gr.9.10.909
- Beachy, P. A., Hymowitz, S. G., Lazarus, R. A., Leahy, D. J., and Siebold, C. (2010). Interactions between Hedgehog proteins and their binding partners come into view. *Genes Dev.* 24, 2001–2012. doi: 10.1101/gad.1951710
- Bolatto, C., Parada, C., Revello, F., Zuñiga, A., Cabrera, P., and Cambiazio, V. (2015). Spatial and temporal distribution of Patched-related protein in the *Drosophila* embryo. *Gene expression patterns: GEP* 19, 120–128. doi: 10.1016/j.gep.2015.10.002
- Bossing, T., and Brand, A. H. (2006). Determination of cell fate along the anteroposterior axis of the *Drosophila* ventral midline. *Development* 133, 1001–1012. doi: 10.1242/dev.02288
- Brand, A. H., Manoukian, A. S., and Perrimon, N. (1994). Ectopic expression in *Drosophila*. *Methods Cell Biol.* 44, 635–654. doi: 10.1016/S0091-679X(08)60936-X
- Brennan, D., Chen, X., Cheng, L., Mahoney, M., and Riobo, N. A. (2012). Noncanonical Hedgehog signaling. *Vitamins and hormones*, 88, 55–72. doi: 10.1016/B978-0-12-394622-5.00003-1
- Bürglin, T. R. (1996). Warthog and groundhog, novel families related to Hedgehog. *Curr. Biol.* 6, 1047–1050. doi: 10.1016/S0960-9822(02)70659-3
- Burke, R., Nellen, D., Bellotto, M., Hafen, E., Senti, K. A., Dickson, B. J., et al. (1999). Dispatched, a novel sterol-sensing domain protein dedicated to the release of cholesterol-modified hedgehog from signaling cells. *Cell* 99, 803–815. doi: 10.1016/S0092-8674(00)81677-3
- Camp, D., Haitian He, B., Li, S., Althaus, I. W., Holtz, A. M., Allen, B. L., et al. (2014). Ihog and Boi elicit Hh signaling via Ptc but do not aid Ptc in sequestering the Hh ligand. *Development* 141, 3879–3888. doi: 10.1242/dev.103564
- Chen, C. H., von Kessler, D. P., Park, W., Wang, B., Ma, Y., and Beachy, P. A. (1999). Nuclear trafficking of Cubitus interruptus in the transcriptional regulation of Hedgehog target gene expression. *Cell* 98, 305–316. doi: 10.1016/S0092-8674(00)81960-1
- Chiyoda, H., Kume, M., Del Castillo, C. C., Kontani, K., Spang, A., Katada, T., et al. (2021). *Caenorhabditis elegans* PTR/PTCHD PTR-18 promotes the clearance of extracellular hedgehog-related protein via endocytosis. *PLoS Genet.* 17, e1009457. doi: 10.1371/journal.pgen.1009457
- Crozatier, M., Glise, B., and Vincent, A. (2004). Patterns in evolution: veins of the *Drosophila* wing. *Trends Genet.* 20, 498–505. doi: 10.1016/j.tig.2004.07.013
- D'Amico, P., and Jacobs, J. R. (1995). Lectin histochemistry of the *Drosophila* embryo. *Tissue Cell* 27, 23–30. doi: 10.1016/S0040-8166(95)80005-0
- Desbordes, S. C., and Sanson, B. (2003). The glypican Dally-like is required for Hedgehog signalling in the embryonic epidermis of *Drosophila*. *Development* 130, 6245–6255. doi: 10.1242/dev.00874
- Furlong, E. E., Andersen, E. C., Null, B., White, K. P., and Scott, M. P. (2001). Patterns of gene expression during *Drosophila* mesoderm development. *Science*. 293, 1629–1633. doi: 10.1126/science.1062660
- Gault, W. J., Olguin, P., Weber, U., and Mlodzik, M. (2012). *Drosophila* CK1-γ, gilgamesh, controls PCP-mediated morphogenesis through regulation of vesicle trafficking. *J. Cell Biol.* 196, 605–621. doi: 10.1083/jcb.201107137
- Han, C., Belenkaya, T. Y., Wang, B., and Lin, X. (2004). *Drosophila* glypicans control the cell-to-cell movement of Hedgehog by a dynamin-independent process. *Development*. 131, 601–611. doi: 10.1242/dev.00958
- Hicke, L., and Dunn, R. (2003). Regulation of membrane protein transport by ubiquitin and ubiquitin-binding proteins. *Ann. Rev. Cell Dev. Biol.* 19, 141–172. doi: 10.1146/annurev.cellbio.19.110701.154617
- Hortsch, M., Olson, A., Fishman, S., Soneral, S. N., Marikar, Y., Dong, R., et al. (1998). The expression of MDP-1, a component of *Drosophila* embryonic basement membranes, is modulated by apoptotic cell death. *Int. J. Dev. Biol.* 42, 33–42.
- Ivanov, A. I., Rovescalli, A. C., Pozzi, P., Yoo, S., Mozer, B., Li, H. P., et al. (2004). Genes required for *Drosophila* nervous system development identified by RNA interference. *Proc. Natl. Acad. Sci. U.S.A.* 101, 16216–16221. doi: 10.1073/pnas.0407188101
- Jacobs, J. R. (2000). The midline glia of *Drosophila*: a molecular genetic model for the developmental functions of glia. *Prog. Neurobiol.* 62, 475–508. doi: 10.1016/S0304-0082(00)00016-2
- Johnson, R. L., Grenier, J. K., and Scott, M. P. (1995). Patched overexpression alters wing disc size and pattern: transcriptional and post-transcriptional effects on hedgehog targets. *Development* 121, 4161–4170. doi: 10.1242/dev.121.12.4161
- Kinrade, E. F., Brates, T., Tear, G., and Hidalgo, A. (2001). Roundabout signalling, cell contact and trophic support confine longitudinal glia and axons in the *Drosophila* CNS. *Development* 128, 207–216. doi: 10.1242/dev.128.2.207
- Koizumi, K., Higashida, H., Yoo, S., Islam, M. S., Ivanov, A. I., Guo, V., et al. (2007). RNA interference screen to identify genes required for *Drosophila* embryonic nervous system development. *Proc. Natl. Acad. Sci. U.S.A.* 104, 5626–5631. doi: 10.1073/pnas.0611687104
- Kuwabara, P. E., Lee, M. H., Schedl, T., and Jefferis, G. S. (2000). A *C. elegans* patched gene, *ptc-1*, functions in germ-line cytokinesis. *Genes Dev.* 14, 1933–1944. doi: 10.1101/gad.14.15.1933
- Layalle, S., Volovitch, M., Mugat, B., Bonneaud, N., Parmentier, M. L., Prochiantz, A., et al. (2011). Engrailed homeoprotein acts as a signaling molecule in the developing fly. *Development* 138, 2315–2323. doi: 10.1242/dev.057059
- Lee, Y. S., and Carthew, R. W. (2003). Making a better RNAi vector for *Drosophila*: use of intron spacers. *Methods*. 30, 322–329. doi: 10.1016/S1046-2023(03)00051-3
- Lum, L., Yao, S., Mozer, B., Rovescalli, A., Von Kessler, D., Nirenberg, M., et al. (2003). Identification of Hedgehog pathway components by RNAi in *Drosophila* cultured cells. *Science* 299, 2039–2045. doi: 10.1126/science.1081403
- Mac Gabhann, F., and Popel, A. S. (2008). Systems biology of vascular endothelial growth factors. *Microcirculation* 15, 715–738. doi: 10.1080/10739680802095964

- Martín, V., Carrillo, G., Torroja, C., and Guerrero, I. (2001). The sterol-sensing domain of patched protein seems to control Smoothed activity through patched vesicular trafficking. *Curr. Biol.* 11, 601–607. doi: 10.1016/S0960-9822(01)00178-6
- McCarthy, R. A., Barth, J. L., Chintalapudi, M. R., Knaak, C., and Argraves, W. S. (2002). Megalin functions as an endocytic sonic hedgehog receptor. *J. Biol. Chem.* 277, 25660–25667. doi: 10.1074/jbc.M201933200
- McLellan, J. S., Yao, S., Zheng, X., Geisbrecht, B. V., Ghirlando, R., Beachy, P. A., et al. (2006). Structure of a heparin-dependent complex of Hedgehog and Ihog. *Proc. Natl. Acad. Sci. U.S.A.* 103, 17208–17213. doi: 10.1073/pnas.0606738103
- Megraw, T. L., Kilaru, S., Turner, F. R., and Kaufman, T. C. (2002). The centrosome is a dynamic structure that ejects PCM flares. *J. Cell Sci.* 115 (Pt. 23), 4707–4718. doi: 10.1242/jcs.00134
- Merienda, T. T., Botta, V., and Bhat, K. M. (2005). Patched regulation of axon guidance is by specifying neural identity in the *Drosophila* nerve cord. *Dev. Genes Evol.* 215, 285–296. doi: 10.1007/s00427-005-0475-z
- Méhot, N., and Basler, K. (2001). An absolute requirement for cubitus interruptus in Hedgehog signaling. *Development* 128, 733–742. doi: 10.1242/dev.128.5.733
- Michaux, G., Gansmuller, A., Hindelang, C., and Labouesse, M. (2000). CHE-14, a protein with a sterol-sensing domain, is required for apical sorting in *C. elegans* ectodermal epithelial cells. *Curr. Biol.* 10, 1098–1107. doi: 10.1016/S0960-9822(00)00695-3
- Mullor, J. L., Calleja, M., Capdevila, J., and Guerrero, I. (1997). Hedgehog activity, independent of decapentaplegic, participates in wing disc patterning. *Development* 124, 1227–1237. doi: 10.1242/dev.124.6.1227
- Mullor, J. L., and Guerrero, I. (2000). A gain-of-function mutant of patched dissects different responses to the hedgehog gradient. *Dev. Biol.* 228, 211–224. doi: 10.1006/dbio.2000.9862
- Noor, A., Whibley, A., Marshall, C. R., Gianakopoulos, P. J., Piton, A., Carson, A. R., et al. (2010). Disruption at the PTCHD1 Locus on Xp22.11 in Autism spectrum disorder and intellectual disability. *Sci. Transl. Med.* 2, 49ra68. doi: 10.1126/scitranslmed.3001267
- Nüsslein-Volhard, C., and Wieschaus, E. (1980). Mutations affecting segment number and polarity in *Drosophila*. *Nature* 287, 795–801. doi: 10.1038/287795a0
- Nybo, K. (2012). Molecular biology techniques QandA. *BioTechniques* 53, 218–219. doi: 10.2144/000113935
- Oikonomou, G., Perens, E. A., Lu, Y., Watanabe, S., Jorgensen, E. M., and Shaham, S. (2011). Opposing activities of LIT-1/NLK and DAF-6/patched-related direct sensory compartment morphogenesis in *C. elegans*. *PLoS Biol.* 9, e1001121. doi: 10.1371/journal.pbio.1001121
- Olofsson, B., and Page, D. T. (2005). Condensation of the central nervous system in embryonic *Drosophila* is inhibited by blocking hemocyte migration or neural activity. *Dev. Biol.* 279, 233–243. doi: 10.1016/j.ydbio.2004.12.020
- Park, J. H., Schroeder, A. J., Helfrich-Förster, C., Jackson, F. R., and Ewer, J. (2003). Targeted ablation of CCAP neuropeptide-containing neurons of *Drosophila* causes specific defects in execution and circadian timing of ecdysis behavior. *Development* 130, 2645–2656. doi: 10.1242/dev.00503
- Pastenes, L., Ibáñez, F., Bolatto, C., Pavéz, L., and Cambiazio, V. (2008). Molecular characterization of a novel patched-related protein in *Apis mellifera* and *Drosophila melanogaster*. *Arch. Insect Biochem. Physiol.* 68, 156–170. doi: 10.1002/arch.20245
- Patel, N. H., Schafer, B., Goodman, C. S., and Holmgren, R. (1989). The role of segment polarity genes during *Drosophila* neurogenesis. *Genes Dev.* 3, 890–904. doi: 10.1101/gad.3.6.890
- Perens, E. A., and Shaham, S. (2005). *C.elegans* daf-6 encodes a patched-related protein required for lumen formation. *Dev. Cell.* 8, 893–906. doi: 10.1016/j.devcel.2005.03.009
- Pielage, J., Kippert, A., Zhu, M., and Klämbt, C. (2004). The *Drosophila* transmembrane protein fear-of-intimacy controls glial cell migration. *Dev. Biol.* 275, 245–257. doi: 10.1016/j.ydbio.2004.07.039
- Prokopenko, S. N., He, Y., Lu, Y., and Bellen, H. J. (2000). Mutations affecting the development of the peripheral nervous system in *Drosophila*: a molecular screen for novel proteins. *Genetics* 156, 1691–1715. doi: 10.1093/genetics/156.4.1691
- Rath, A., Glibowicka, M., Nadeau, V. G., Chen, G., and Deber, C. M. (2009). Detergent binding explains anomalous SDS-PAGE migration of membrane proteins. *Proc. Natl. Acad. Sci. U.S.A.* 106, 1760–1765. doi: 10.1073/pnas.0813167106
- Ricolo, D., Butí, E., and Araújo, S. J. (2015). *Drosophila melanogaster* Hedgehog cooperates with Frazzled to guide axons through a non-canonical signalling pathway. *Mech. Dev.* 137, 11–22. doi: 10.1016/j.mod.2015.04.003
- Rubin, G. M., and Spradling, A. C. (1982). Genetic transformation of *Drosophila* with transposable element vectors. *Science* 218, 348–353. doi: 10.1126/science.6289436
- Sears, H. C., Kennedy, C. J., and Garrity, P. A. (2003). Macrophage-mediated corpse engulfment is required for normal *Drosophila* CNS morphogenesis. *Development* 130, 3557–3565. doi: 10.1242/dev.00586
- Shibuya, M., and Claesson-Welsh, L. (2006). Signal transduction by VEGF receptors in regulation of angiogenesis and lymphangiogenesis. *Exp. Cell Res.* 312, 549–560. doi: 10.1016/j.yexcr.2005.11.012
- Singhal, A., and Shaham, S. (2017). Infrared laser-induced gene expression for tracking development and function of single *C. elegans* embryonic neurons. *Nat. Commun.* 8, 14100. doi: 10.1038/ncomms14100
- Strigini, M., and Cohen, S. M. (1997). A Hedgehog activity gradient contributes to AP axial patterning of the *Drosophila* wing. *Development* 124, 4697–4705. doi: 10.1242/dev.124.22.4697
- Strutt, H., Thomas, C., Nakano, Y., Stark, D., Neave, B., Taylor, A. M., et al. (2001). Mutations in the sterol-sensing domain of Patched suggest a role for vesicular trafficking in smoothed regulation. *Curr. Biol.* 11, 608–613. doi: 10.1016/S0960-9822(01)00179-8
- Sullivan, W., Ashburner, M., and Hawley, R. S. (2000). *Drosophila Protocols*. New York, NY: Cold Spring Harbor Laboratory Press.
- Takizawa, K., and Hotta, Y. (2001). Pathfinding analysis in a glia-less gcm mutant in *Drosophila*. *Dev. Genes Evol.* 211, 30–36. doi: 10.1007/s004270000117
- Torroja, C., Gorfinkel, N., and Guerrero, I. (2005). Mechanisms of Hedgehog gradient formation and interpretation. *J. Neurobiol.* 64, 334–356. doi: 10.1002/neu.20168
- Tseng, T. T., Gratwick, K. S., Kollman, J., Park, D., Nies, D. H., Goffeau, A., et al. (1999). The RND permease superfamily: an ancient, ubiquitous and diverse family that includes human disease and development proteins. *J. Mol. Microbiol. Biotechnol.* 1, 107–125.
- Vincent, S., Vonesch, J. L., and Giangrande, A. (1996). Glide directs glial fate commitment and cell fate switch between neurones and glia. *Development* 122, 131–139. doi: 10.1242/dev.122.1.131
- Wallace, S. W., Singhvi, A., Liang, Y., Lu, Y., and Shaham, S. (2016). PROS-1/prospero is a major regulator of the glia-specific secretome controlling sensory-neuron shape and function in *C. elegans*. *Cell Rep.* 15, 550–562. doi: 10.1016/j.celrep.2016.03.051
- Wang, W., Perens, E. A., Oikonomou, G., Wallace, S. W., Lu, Y., and Shaham, S. (2017). IGDB-2, an Ig/FNIII protein, binds the ion channel LGC-34 and controls sensory compartment morphogenesis in *C. elegans*. *Dev. Biol.* 430, 105–112. doi: 10.1016/j.ydbio.2017.08.009
- Watson, J. D., Wheeler, S. R., Stagg, S. B., and Crews, S. T. (2011). *Drosophila* hedgehog signaling and engrailed-run mutual repression direct midline glia to alternative ensheathing and non-ensheathing fates. *Development* 138, 1285–1295. doi: 10.1242/dev.056895
- Yan, D., Wu, Y., Yang, Y., Belenkaya, T. Y., Tang, X., and Lin, X. (2010). The cell-surface proteins dally-like and Ihog differentially regulate Hedgehog signaling strength and range during development. *Development* 137, 2033–2044. doi: 10.1242/dev.045740
- Yao, S., Lum, L., and Beachy, P. (2006). The ihog cell-surface proteins bind Hedgehog and mediate pathway activation. *Cell* 125, 343–357. doi: 10.1016/j.cell.2006.02.040
- Yarden, Y., and Slivkowsky, M. X. (2001). Untangling the ErbB signalling network. *Nat. Rev. Mol. Cell Biol.* 2, 127–137. doi: 10.1038/35052073

- Zhao, T., Gu, T., Rice, H. C., McAdams, K. L., Roark, K. M., Lawson, K., et al. (2008). A *Drosophila* gain-of-function screen for candidate genes involved in steroid-dependent neuroendocrine cell remodeling. *Genetics* 178, 883–901. doi: 10.1534/genetics.107.082487
- Zugasti, O., Rajan, J., and Kuwabara, P. E. (2005). The function and expansion of the Patched- and Hedgehog-related homologs in *C. elegans*. *Genome Res.* 15, 1402–1410. doi: 10.1101/gr.3935405
- Zúñiga, A., Hödar, C., Hanna, P., Ibáñez, F., Moreno, P., Pulgar, R., et al. (2009). Genes encoding novel secreted and transmembrane proteins are temporally and spatially regulated during *Drosophila melanogaster* embryogenesis. *BMC Biol.* 7, 61. doi: 10.1186/1741-7007-7-61

Conflict of Interest: The authors declare that the research was conducted in the absence of any commercial or financial relationships that could be construed as a potential conflict of interest.

Publisher's Note: All claims expressed in this article are solely those of the authors and do not necessarily represent those of their affiliated organizations, or those of the publisher, the editors and the reviewers. Any product that may be evaluated in this article, or claim that may be made by its manufacturer, is not guaranteed or endorsed by the publisher.

Copyright © 2022 Bolatto, Nieves, Reyes, Olivera-Bravo and Cambiazo. This is an open-access article distributed under the terms of the Creative Commons Attribution License (CC BY). The use, distribution or reproduction in other forums is permitted, provided the original author(s) and the copyright owner(s) are credited and that the original publication in this journal is cited, in accordance with accepted academic practice. No use, distribution or reproduction is permitted which does not comply with these terms.



OPEN ACCESS

EDITED BY
Daniel Ortuño-Sahagún,
University of Guadalajara, Mexico

REVIEWED BY
Olga Kopach,
University College London,
United Kingdom
Sidharth Mehan,
Indo-Soviet Friendship College of
Pharmacy, India

*CORRESPONDENCE
Bárbara S. Casas,
barbara.s.casas@gmail.com
Verónica Palma,
vpalma@uchile.cl

SPECIALTY SECTION
This article was submitted to
Morphogenesis and Patterning,
a section of the journal
Frontiers in Cell and Developmental
Biology

RECEIVED 17 May 2022
ACCEPTED 14 July 2022
PUBLISHED 24 August 2022

CITATION
Casas BS, Arancibia-Altamirano D,
Acevedo-La Rosa F, Garrido-Jara D,
Maksaev V, Pérez-Monje D and Palma V
(2022), It takes two to tango: Widening
our understanding of the onset of
schizophrenia from a neuro-
angiogenic perspective.
Front. Cell Dev. Biol. 10:946706.
doi: 10.3389/fcell.2022.946706

COPYRIGHT
© 2022 Casas, Arancibia-Altamirano,
Acevedo-La Rosa, Garrido-Jara,
Maksaev, Pérez-Monje and Palma. This
is an open-access article distributed
under the terms of the [Creative
Commons Attribution License \(CC BY\)](#).
The use, distribution or reproduction in
other forums is permitted, provided the
original author(s) and the copyright
owner(s) are credited and that the
original publication in this journal is
cited, in accordance with accepted
academic practice. No use, distribution
or reproduction is permitted which does
not comply with these terms.

It takes two to tango: Widening our understanding of the onset of schizophrenia from a neuro-angiogenic perspective

Bárbara S. Casas*, David Arancibia-Altamirano,
Franco Acevedo-La Rosa, Delia Garrido-Jara, Vera Maksaev,
Dan Pérez-Monje and Verónica Palma*

Laboratory of Stem Cells and Developmental Biology, Departamento de Biología, Facultad de Ciencias, Universidad de Chile, Santiago, Chile

Schizophrenia is a chronic debilitating mental disorder characterized by perturbations in thinking, perception, and behavior, along with brain connectivity deficiencies, neurotransmitter dysfunctions, and loss of gray brain matter. To date, schizophrenia has no cure and pharmacological treatments are only partially efficacious, with about 30% of patients describing little to no improvement after treatment. As in most neurological disorders, the main descriptions of schizophrenia physiopathology have been focused on neural network deficiencies. However, to sustain proper neural activity in the brain, another, no less important network is operating: the vast, complex and fascinating vascular network. Increasing research has characterized schizophrenia as a systemic disease where vascular involvement is important. Several neuro-angiogenic pathway disturbances have been related to schizophrenia. Alterations, ranging from genetic polymorphisms, mRNA, and protein alterations to microRNA and abnormal metabolite processing, have been evaluated in plasma, post-mortem brain, animal models, and patient-derived induced pluripotent stem cell (hiPSC) models. During embryonic brain development, the coordinated formation of blood vessels parallels neuro/gliogenesis and results in the structuration of the neurovascular niche, which brings together physical and molecular signals from both systems conforming to the Blood-Brain barrier. In this review, we offer an upfront perspective on distinctive angiogenic and neurogenic signaling pathways that might be involved in the biological causality of schizophrenia. We analyze the role of pivotal angiogenic-related pathways such as Vascular Endothelial Growth Factor and HIF signaling related to hypoxia and oxidative stress events; classic developmental pathways such as the NOTCH pathway, metabolic pathways such as the mTOR/AKT cascade; emerging neuroinflammation, and neurodegenerative processes such as UPR, and also discuss non-canonically angiogenic/axonal guidance factor signaling. Considering that all of the mentioned above pathways converge at the Blood-Brain barrier, reported neurovascular alterations could have deleterious repercussions on overall brain functioning in schizophrenia.

KEYWORDS

schizophrenia, neurogenesis, angiogenesis, brain development, blood-brain barrier, neurovascular niche, hiPSC

1 Introduction

Schizophrenia (SZ) is a complex psychiatric disorder affecting approximately 1% of the population worldwide (Owen et al., 2016). SZ is characterized by positive (e.g., delusions, hallucinations, psychotic episodes), negative (e.g., anhedonia, reduced speech or movements), and cognitive symptoms (e.g., disorganized speech, cognitive deficits). To date, the treatments for SZ mainly target the positive symptoms, leaving cognitive and negative symptoms undertreated, and are estimated to be efficient for 50–70% of patients, but with important metabolic and neurological side effects (Buckley et al., 2007; Stepnicki et al., 2018).

Despite decades of research, the causes of this disorder remain poorly understood. SZ has been described as a neurodevelopmental disease of multiple etiology, in which both genetic and environmental origins are involved (Susser and St Clair, 2013; Jaaro-Peled and Sawa, 2020). This is supported by the altered expression of development-related genes and the important brain remodeling that occurs around the age of SZ onset, during late adolescence and early adulthood (Kochunov and Hong, 2014; Weinberger, 2017; Rund, 2018).

As in most neurological disorders, the main descriptions of SZ pathophysiology have been focused on neuronal deficiencies. Altered cerebral connectivity and brain dynamics, abnormalities in the excitatory/inhibitory balance, as well as failure to specify specific neuron identities have been described (Spencer, 2009; Kantrowitz and Javitt, 2010; Inan et al., 2013; Puvogel et al., 2022). In addition to these neuronal alterations, increasing evidence has linked SZ to vascular impairments. Hypoperfusion in several areas of the brain, reduced cerebral blood flow (CBF), and Blood-Brain Barrier (BBB) dysfunctions have been described (Andreasen et al., 1997; Lopes et al., 2015; Katsel et al., 2017; Baruah and Vasudevan, 2019; Puvogel et al., 2022).

The human brain critically relies on an elaborate vascular network for its oxygen and nutrient supply (Quaeghebeur et al., 2011). This vascular network is the result of the concomitant development of both neural and vascular components in the central nervous system (CNS). Angiogenesis (formation of new blood vessels from pre-existing ones) and vasculogenesis (generation of blood vessels *de novo*) starts early in embryonic development, with the recruitment of angioblasts and endothelial cells (EC) around the newly formed brain constituting the perineural vascular plexus (PNVP) (Bautsch and James, 2009;

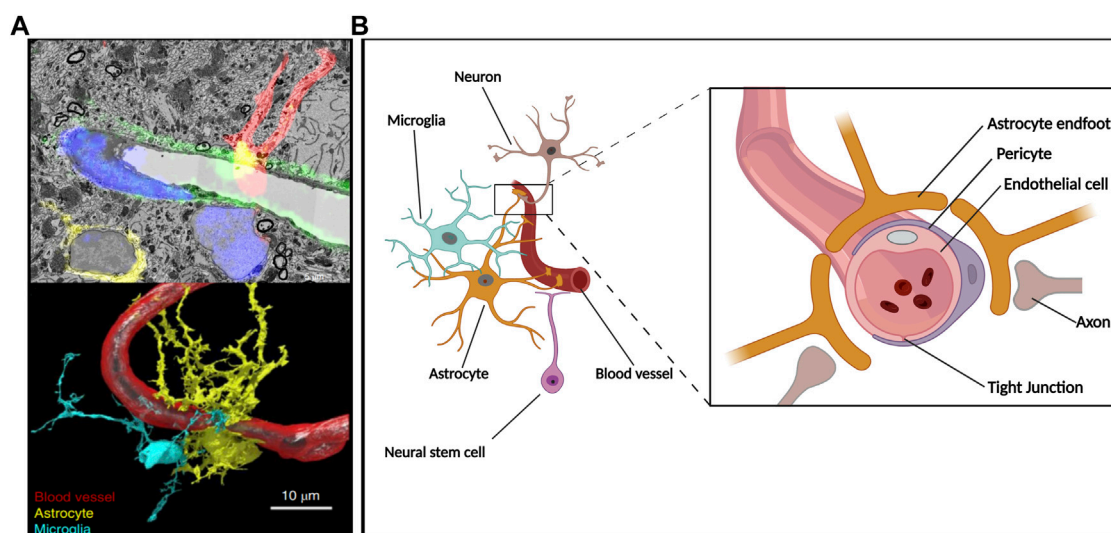


FIGURE 1

The neuro-angiogenic niche and the NVU. Constitutive components of the NVU reside in a microenvironment where secreted factors, cell-cell interactions, and vascular supply give rise to an interdependent unit. (A) Hippocampal NVU comprising blood vessels and surrounding tissue depicted throughout a composition of electron microscopy-acquired sections and its corresponding confocal microscopy fluorescence image (upper panel) as well as subsequent 3D reconstruction (lower panel); reproduced with permission (Fang et al., 2018). (B) Simplified diagram depicting components of the BBB at a neurogenic region where radial glia-like NSC are in direct contact with the vasculature.

James and Mukouyama, 2011). Then, neural stem cells (NSC) and neural progenitor cells (NPC) will induce the ingrowing of capillaries into the neural tube. Through the action of attractant and repellent molecules acting in gradients and extracellular matrix components, the spatial distribution of vascularization will occur in parallel to the brain's development and differentiation processes (Engelhardt and Liebner, 2014; Ben-Zvi and Liebner, 2021). This led to the concept of neuro-angiogenesis, which refers to the coordinated development of neurons (neurogenesis) and the formation of new blood vessels (angiogenesis). This communication will be the basis of the induction of BBB characteristics in EC of brain microvessels, as part of a greater module known as the neurovascular unit (NVU) composed of EC, pericytes, astrocytes, and neurons (Figure 1) (Tam and Watts, 2010; Engelhardt and Liebner, 2014; Segarra et al., 2019).

The synchronic development of vascular and nervous systems is orchestrated by the molecular crosstalk between both systems. Shared molecular pathways are major players in the communication of the neuronal compartment with the endothelium (Tam and Watts, 2010; Segarra et al., 2019; Peguera et al., 2021). Since neuro-angiogenic signaling plays a crucial role in the adequate structuration of the neurovascular niche, and therefore in brain functioning, SZ can be considered a systemic disease where both nervous and vascular alterations are impacting critical developmental periods (Figure 2A).

In this review, we analyze the alteration of selected signaling pathways and cascades involved in both angiogenic and neurogenic processes and their implications in SZ. We discuss some classical and emerging pathways involved in the pathophysiology of this disease, considering the interconnected network of both vascular and nervous systems as a whole. A better understanding of these processes may lead to the identification of potential biomarkers for the early diagnosis and treatment of SZ.

2 SZ is characterized by an impaired antioxidant system: The HIF pathway and oxidative stress

During CNS development, vascularization and subsequent oxygenation are key for changing stem cell behavior from proliferative to differentiative states (Morante-Redolat and Fariñas, 2016). Hypoxia-Inducible Factors (HIFs) constitute a family of heterodimeric transcription factors that regulate oxygen homeostasis, exerting transcriptional control over hundreds of genes in response to changes in oxygen supply. HIFs are also involved in processes such as glycolytic metabolism, proliferation, angiogenesis, and stemness (Semenza, 2014, 2020). Under normoxia, the subunit HIF-1 α is actively hydroxylated by an oxygen-dependent mechanism mediated by prolyl hydroxylases (PHDs) and destined for proteasomal

degradation. Under hypoxia, such degradation is rescued and HIF-1 α translocates into the nucleus where it dimerizes with HIF-1 β and regulates gene transcription through its binding to hypoxia response elements (HREs) on target genes (Dengler et al., 2014). In what could appear a counterintuitive observation, PHDs can also be inhibited in hypoxia by reactive oxygen species (ROS) (Gerald et al., 2004). ROS and mitochondrial ROS production can stabilize HIFs in non-hypoxic conditions, as is the case in hyperoxia-mediated induction of neurogenesis or non-hypoxic stabilization of HIF-1 α in cerebellar progenitors proliferation via Sonic Hedgehog (SHH)-induced ROS production (Simon, 2006; Hu et al., 2014; Eyrich et al., 2019).

Perturbations in oxygen supply have been long while associated with the physiopathology of SZ and, although there are inconsistencies in independent enzymes or metabolites, there is an overall notion that SZ is characterized by an impaired antioxidant system (J. Q. Wu et al., 2013).

Fetal hypoxia has been described as an environmental risk for SZ and the HIF pathway is considered a crucial target to understand and treat SZ (Tsuang, 2000; Katsel et al., 2017). Association studies show that many of the so-called susceptibility genes for SZ are regulated by hypoxia and/or expressed in the vasculature (Manalo et al., 2005; Schmidt-Kastner et al., 2006; Schmidt-Kastner et al., 2012). In addition, global analyses of the human brain showed that genes associated with metabolism and oxidative stress allow for discrimination of around 90% of SZ patients from healthy subjects, demonstrating the important implication of oxygen regulation in SZ physiopathology (Prabakaran et al., 2004). Given the common genic variation in these genes, the HIF-2 pathway has been proposed as a potential pharmacological target in the treatment of SZ (Reay et al., 2020). Moreover, a hindered or reduced antioxidant capacity was found in some SZ patients (Albayrak et al., 2013; Flatow et al., 2013). Antioxidant markers such as catalase and nitrite exhibited changes during the clinical course of patients, being lower at first-episode psychosis (FEP) and then increased in patients with exacerbation of psychosis and under pharmacological treatment (Flatow et al., 2013). Pharmacological agents commonly used in clinical treatment alter the systemic oxidative status and suggest a potential redox modulation in their therapeutic mechanism of action (Pandya et al., 2013; Pillai et al., 2007; J. Q. Wu et al., 2013; Z. Wu et al., 2012).

Since there is complex crosstalk between oxidative species and HIF pathways, the above-mentioned alterations could rise from a pleiotropic integration of developmental and environmental signals. As such, an increase in ROS by mitochondrial dysfunction (Prabakaran et al., 2004), could trigger events of non-hypoxic HIF stabilization, affecting both development and homeostasis of both vascular and neural lineages, and compromising brain metabolism in SZ. These dysregulations could also affect the course of the illness, for which early targeting of the HIF and ROS pathways could improve patient outcomes.

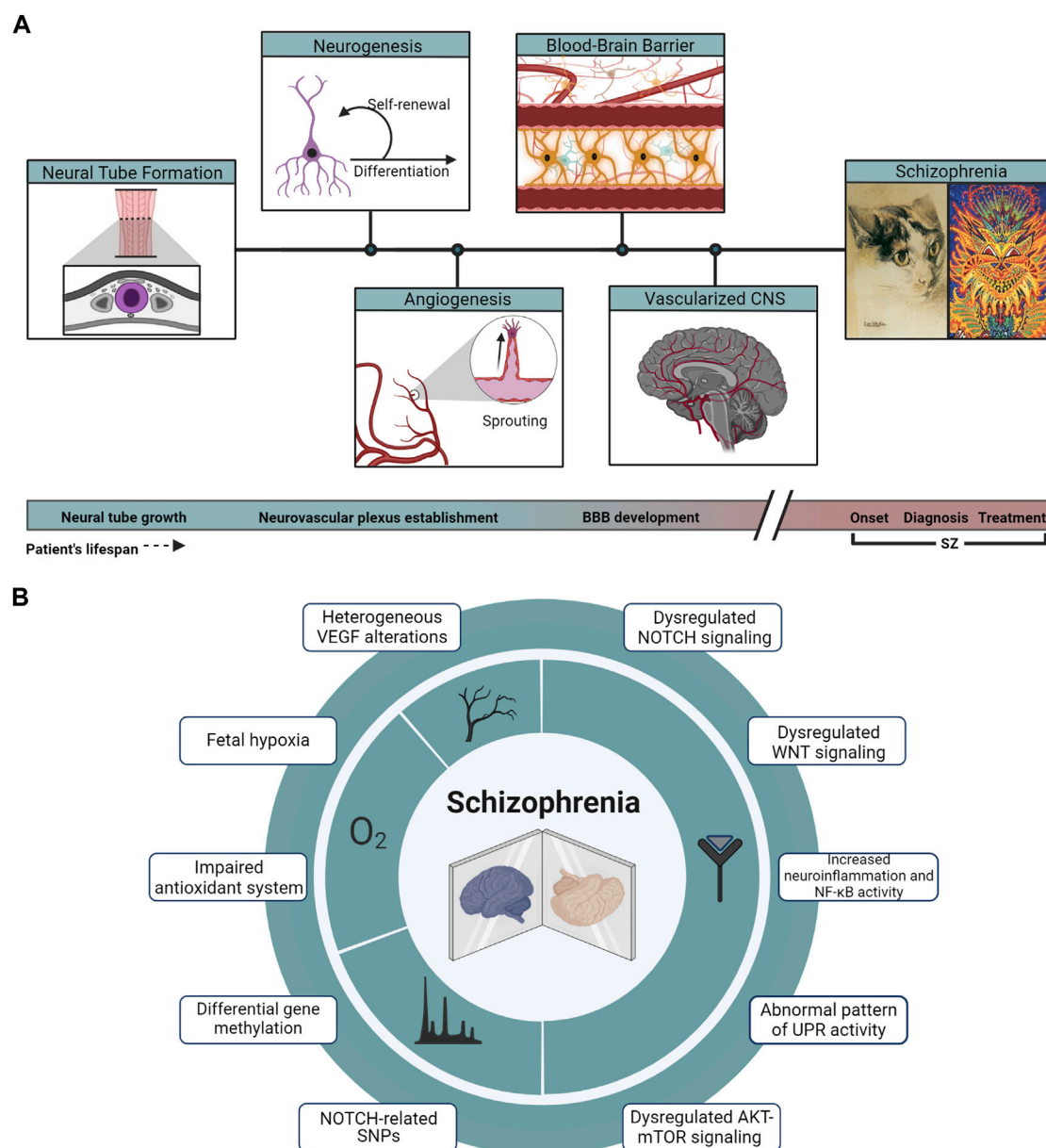


FIGURE 2

Developmental and molecular hallmarks in SZ. **(A)** From the closure and growth of the neural tube (highlighted in purple from a coronal section across the embryo's axis) to a vascularized and developed brain, events of neurogenesis and angiogenesis take place across the developing tissue, leading to the establishment of the BBB, a key component in the pathophysiology of SZ. Cat illustrations correspond to public domain paintings by Louis Wain, whose changing art style interprets as a representation of the onset and progression of the artist's SZ. **(B)** Array summarizing the main genomic, signaling, and physiological hallmarks described in the pathophysiology of SZ.

3 Aberrant NOTCH signaling pathway in SZ

The NOTCH pathway is a conserved pathway involved in multiple developmental processes including neural development (Bray, 2016; J. Liu et al., 2010). The essential steps of human

NOTCH signaling transduction involve the interaction of ligands with NOTCH receptors. Such an event triggers proteolytic cleavage and subsequent release of the NOTCH intracellular domain (NICD) which is then translocated to the nucleus where it forms a gene activating complex with the transcriptional regulator RBPJ and the co-activator MAML1 (Bray, 2016).

There are multiple human ligands and some of them constitute a canonical group defined by the presence of a Delta/Serrate/Lag-2 (DSL) domain and are denoted as Delta-like (DLL) and Jagged (JAG) families, while non-canonical ligands present a high grade of structural diversity and lack the aforementioned DSL domain, such as the well-researched Delta Like Non-Canonical Notch Ligand 1 (DLK1) (D'Souza et al., 2010).

NOTCH signaling is a relevant actor in the vascularization and remodeling of both the embryonic and postnatal brain (Jakobsson et al., 2010; Walchli et al., 2015). Inhibition of NOTCH signaling results in reduced Trans-endothelial Electrical Resistance (TEER), increased permeability, and reduction and delocalization of VE-cadherin and Claudin-5 in brain EC (Derada Troletti et al., 2018). As neural counterparts, Notch2 and 1 have shown to control quiescence and differentiation of ventricular-subventricular zone (V-SVZ) quiescent and activated NSC, respectively, in crosstalk involving the HIF pathway (Basak et al., 2012; Engler et al., 2018).

Early evidence associating NOTCH signaling and SZ came from linkage mapping reports and association studies through genotyping of blood samples. The *NOTCH4* gene at chromosome 6p has been described as a potential susceptibility gene with multiple SNPs that suggest the presence of several SZ-associated variants (S. Wang et al., 1995; Wei and Hemmings, 2000; X. Zhang et al., 2004). Further research and integration of genome-wide association studies (GWAS) in SZ have associated more variants of NOTCH pathway components, such as *NOTCH4*, *NUMBL*, and *FURIN*, describing the latter as a pleiotropic SNP also involved in major depressive disorder and bipolar disorder (Passos Gregorio et al., 2006; H. Wang et al., 2022; X. Yang et al., 2013; B. Zhang et al., 2015). In addition to the increased variants of NOTCH pathway genes in SZ, epigenetic analysis has revealed evidence of differentially methylated regions of NOTCH pathway genes in SZ patients (Shen et al., 2021).

Regarding the expression of pathway genes, it has been reported that the levels of Notch ligands DLL2 and DLK1 were higher in plasma from SZ patients, along with multiple other components of the pathway that were also differentially regulated in whole blood samples relative to healthy subjects (Hoseth et al., 2018b). The increase in the plasmatic levels of NOTCH pathway ligands is suggested to promote an attenuation of NOTCH signaling; since DLK1 is a non-canonical ligand with inhibitory effects via NOTCH1. The interpretation of the effects of an increment in plasmatic levels of DLL1 is more diffuse as the cleavage of DLL1 could relieve cis-inhibitory effects over NOTCH receptors while also yielding C-terminal fragments that compete with NOTCH receptors for proteolytic machinery and thus inhibit signaling as a result of impaired cleavage processing of receptors (Mishra-Gorur et al., 2002; LaVoie and Selkoe, 2003; Falix et al., 2012). *In vitro* modeling of SZ utilizing human-induced pluripotent stem cells (hiPSC)-derived neurons, which represent early stages of brain development, showed a decreased expression of

NOTCH pathway components such as *NOTCH1*, *HEY2* or *DLL1* when compared to healthy samples (Brennand et al., 2011).

Interestingly, while SZ patients presented reduced plasma levels of the transcriptional regulator RBPJ, its levels were significantly increased in SZ patients undergoing lithium treatment (Hoseth et al., 2018b). In an MK-801-induced murine model of SZ, the antipsychotic risperidone enhanced the Notch pathway activity and rescued cognitive deficits, effects that were abrogated by *Notch1* knockdown (Xue et al., 2017). In human NT2-differentiated neurons, other neuroleptics for SZ treatment (e.g., amisulpride, aripiprazole, and clozapine) decreased the expression of NOTCH signaling components (Panizzutti et al., 2021), for which we could be observing a contribution of treatment along with the disease progression in the expression of those genes. Therefore, the expression of NOTCH pathway genes can vary during the time course of the life of patients and may be related to epigenetic control.

Due to the increased levels of NOTCH ligand JAG1 found in the internal capsule of SZ *postmortem* brains, and its negative correlation with the expression of genes related to oligodendrocyte function, it has also been proposed that oligodendrocyte and myelin development is hindered in SZ (Kerns et al., 2010). Cuprizone intoxication has been used to establish a murine model with oligodendrogenic aberrations, white matter lesions, and behavioral changes that could mimic SZ (Xu et al., 2009; Chandran et al., 2012). In this model of demyelination, Notch components, such as Notch1 and Hes1/5 were reduced, and amelioration of cuprizone effects by the antipsychotic quetiapine was found to be Notch-dependent (H. N. Wang et al., 2015).

In summary, the Notch pathway is importantly implicated in SZ for including several high polygenic risk genes. Since this pathway also has an important role in angiogenesis and BBB function, it would be important to evaluate the effect of NOTCH pathway dysregulation in those processes, especially given the impact of SZ treatment on the pathway component expression.

4 Vascular endothelial growth factor (VEGF) signaling is highly heterogeneous between SZ patients

Vascular endothelial growth factors (VEGFs) are essential proangiogenic factors that comprise seven members: VEGFA, VEGFB, VEGFC, VEGFD, VEGFE, VEGFF, and PlGF (Hoebe et al., 2004). VEGFs exert numerous functions through their high-affinity binding to receptor tyrosine kinases VEGFR-1, -2, and -3 and co-receptors neuropilin-1 (NRP1), neuropilin-2 (NRP2), and heparan sulfate proteoglycans (HSPGs) (Simons et al., 2016). During development, CNS angiogenesis is largely controlled by neural-derived VEGF, which stimulates PNVP

formation and blood vessel sprouting from the PNVP into the CNS parenchyma. Furthermore, VEGF expression in developing brain EC is key for neurogenesis (Paredes et al., 2018). In the adult brain, VEGF also participates in neurogenesis, neuroprotection, and synaptic plasticity (Lopes et al., 2015), and has an important role in regulating vessel permeability and matching microvascular density to perfusion demands (Licht and Keshet, 2013).

A great sum of evidence relates alterations in VEGF signaling with SZ. Analysis of data obtained from the Common Mind Consortium (CMC) study has determined that VEGFA is among the genes with the greatest variability among SZ patients, compared to healthy subjects (Huang et al., 2020). But reports of VEGFA levels in SZ are rather contradictory. The first evidence pointing to alterations of VEGFA expression in SZ, described lower mRNA levels in the dorsolateral prefrontal cortex of *postmortem* SZ brains (Fulzele and Pillai, 2009). Also in *postmortem* studies, it has been found that VEGFR-2 protein levels in the prefrontal cortex are diminished in SZ in comparison with controls (Howell et al., 2011; Hino et al., 2016). This deficiency in VEGFA signaling has also been corroborated by *in vitro* SZ hiPSC modeling using NSC. Interestingly, brain microvascular EC derived from SZ-hiPSC have a decreased angiogenic response when stimulated with VEGFA (Casas et al., 2018; Casas et al., 2022). However, VEGF protein levels in the superior temporal gyrus (STG) are not significantly different between SZ and control groups (Izumi et al., 2021).

Several studies have found significantly lower plasmatic VEGFA levels in SZ patients when compared to healthy controls (Lee et al., 2015; Xiao et al., 2018; Ye et al., 2018). Nevertheless, a meta-analysis revealed no differences in VEGF blood levels between drug-naïve first-episode SZ patients and controls. Nevertheless, when the analysis was restricted to high-quality studies only, significantly increased VEGF levels were observed in these patients compared to controls (Çakici et al., 2020).

Despite basal serum levels of VEGFA, an increase in VEGFA after treatment of SZ has been reported (Pillai et al., 2016; Balótshev et al., 2017; Frydecka et al., 2018; Misiak et al., 2018; Ye et al., 2018; Xiao et al., 2019). Moreover, higher VEGFA basal levels could predict positive treatment response and VEGFA levels decrease with the severity of illness and cognitive impairment in SZ (Xiao et al., 2018; Zhao et al., 2019). Conversely, another study found that VEGF serum levels of drug-naïve FEP patients decreased after they completed 7 months of antipsychotic treatment (Haring et al., 2015).

In conclusion, heterogeneous VEGF alterations may exist between SZ patients. Given the importance of VEGF signaling in neurovascular processes, its dysregulation

could contribute to the pathophysiology of SZ, characterized by microvascular anomalies and impaired angiogenesis. Moreover, the cognitive dysfunction associated with the disease could be related to aberrant VEGF signaling impacting neurodevelopment and neural plasticity (Howell and Armstrong, 2017).

5 Dysregulation of both canonical and non-canonical WNT signaling in SZ

The canonical WNT signaling pathway is a key regulator of a large number of biological processes and, as expected, its alteration is associated with many human diseases. This signaling pathway is characterized by the activation of gene expression regulated by β -catenin. WNT proteins bind to transmembrane receptors of Frizzled (FZD) family and co-receptors Low-density lipoprotein receptor-related protein (LRP)5/6, which leads to the disassembly of the β -catenin destruction complex and prevents β -catenin proteasomal degradation. Therefore, the stabilized β -catenin accumulates in the cytoplasm and is subsequently translocated into the nucleus to form a complex with LEF/TCF proteins and regulates the expression of WNT target genes. The WNT signaling pathway is critical in processes of neural development as well as adult neurogenesis, synaptic transmission, and plasticity (Mulligan and Cheyette, 2016; Varela-Nallar and Inestrosa, 2013; K. Yang et al., 2016).

Canonical WNT signaling pathway is activated in CNS blood vessels during development and is crucial for BBB formation and the expression of many specific influx transporters, such as GLUT-1. During this process, NPC expresses WNT ligands in a regionally specific manner, while CNS EC express WNT receptors (Stenman et al., 2008; Daneman et al., 2009). This signaling is also necessary for BBB maturation and function *in vivo*. In mice, deletion of β -catenin specifically in EC at stages of BBB maturation is associated with BBB disruption (Liebner et al., 2008). There is also evidence showing that activation of this pathway supports the maintenance of BBB properties in adulthood, mainly through the secretion of WNT ligands by astrocytes (Blanchette and Daneman, 2015; Guérit et al., 2021).

Multiple studies suggest that SZ is associated with an altered canonical WNT signaling pathway. The disease has been associated with genetic variants in several pathway-related genes, including *TCF4*, *CTNNB1*, *CHD8*, *DKK1*, *DKK4*, and *KREMEN1* (Mulligan and Cheyette, 2016).

SZ patients have lower plasma levels of WNT inhibitors DKK1 and sclerostin (SOST) (Hoseth et al., 2018a). Furthermore, whole blood samples of SZ patients show reduced mRNA expression of several WNT pathway genes; pointing to an attenuated canonical WNT signaling in SZ (Kalkman, 2009; Hoseth et al., 2018a). *In vitro* models seem to support this

notion. Six-week-old neurons obtained from SZ hiPSC show alterations in transcript levels of many WNT pathway genes, such as *AXIN2*, *WNT2B*, *WNT3*, *TCF4*, *LEF1*, *LRP5*, and *WNT7A*. The same authors showed that the decreased expression of *WNT7A* in SZ neurons can be reversed with 3 weeks of treatment with the antipsychotic Loxapine, which also improved neuronal connectivity *in vitro* (Brennand et al., 2011). Also, mRNA expression of secreted WNT inhibitors DKK1, DKK2, SFRP2, and SFRP4 is increased in SZ hiPSC-derived NPC (Topol et al., 2015).

In addition to the canonical WNT/ β -catenin pathway, the WNT ligands can activate signaling cascades without interaction with β -catenin, so-called, non-canonical pathways (Montcouquiol et al., 2006). Analysis of SZ patient blood samples show enrichment of non-canonical WNT signaling components (FZD7 and NFAT) (Hoseth et al., 2018a).

In conclusion, the evidence presented highlights a dysregulation of both canonical and non-canonical WNT signaling in SZ, with an important hypofunction of the canonical pathway. This could have profound consequences on BBB structure and function, as well as neural development and connectivity.

6 AKT/mTOR defective signaling suggests systemic alterations in SZ

The AKT/mTOR signaling pathway regulates multiple cellular functions such as nutrient uptake, cell proliferation, growth, autophagy, apoptosis, and migration (L. Wang et al., 2017). This pathway has numerous components and interactors, including mTORC1, one of AKT's main downstream effectors (Rosen and She, 2006; Efeyan and Sabatini, 2010; Zoncu et al., 2011). The AKT/mTOR pathway is activated in response to inputs from regulatory molecules like growth factors, ATP, nutrient concentrations, energy, and ambient oxygen levels. Once activated, it modulates protein homeostasis via the phosphorylation of the S6K1 kinase, leading to cell proliferation and growth (Ma and Blenis, 2009; Bar-Peled et al., 2013; Ben-Sahra et al., 2013; Koehl et al., 2021).

AKT has been related to EC migration and angiogenesis via the promotion of increased VEGF secretion, due to the upregulation of HIF-1 α (Manning and Cantley, 2007; Abeyrathna and Su, 2015). The AKT/mTOR pathway acts upon and influences the cell fate lineage of NSC, thus playing a crucial role in neuronal shape and size, dendritic arborization, spine morphology, axon outgrowth, and synaptic plasticity (Götz and Huttner, 2005; Tavazoie et al., 2005). It is also implicated in numerous neurological processes such as learning, memory, and feeding (Bockaert and Marin, 2015; Garza-Lombó and Gonsebatt, 2016). mTORC1 impairments have been implicated in brain development defects like defective synaptogenesis or connectivity and in pathogenic conditions

such as epilepsy, autism, intellectual disability, dementia, traumatic brain injury, brain tumors, and ischemic injuries (Lipton and Sahin, 2014; Bockaert and Marin, 2015; Huber et al., 2015; Licausi and Hartman, 2018).

Recent reports point to the downregulation of the AKT/mTOR signaling cascade in SZ *postmortem* brains where a decreased protein expression and activity of AKT and mTOR kinases was found (Chadha and Meador-Woodruff, 2020). Interestingly, while downstream S6RP phosphorylation is reduced, downstream of mTOR complex II, PKC α phosphorylation is increased in SZ *postmortem* brains (Chadha et al., 2021). Furthermore, rats treated chronically with the antipsychotic haloperidol had increased levels of S6RP phosphorylation (Chadha et al., 2021). GSK-3 β , a major target of AKT, was also shown to be reduced at a transcriptional, protein, and phosphorylation level in *postmortem* frontal cortex and peripheral lymphocytes of SZ human patients (Kozlovsky et al., 2004; McGuire et al., 2017; Ibarra-Lecue et al., 2020). In addition to the clinical and *postmortem* data, *ex vivo* approaches using protein and mRNA data from patient-derived olfactory neurospheres have highlighted the mTOR signaling pathway as a significant dysregulated pathway in SZ (English et al., 2015).

Overall, the findings point to an important dysregulation in the AKT-mTOR signaling pathway in the SZ brain, which could lead to important functional consequences.

7 Non-canonical angiogenic signaling cues are compromised in SZ

Besides having morphological and structural similarities, with an emphasis on axonal growth cones and EC tip pathfinding, vessels and nerves share several signaling cascades. Numerous factors that were initially described as axonal guidance molecules also exert an important angiogenic function. Among these factors, we found: Netrins, Semaphorins, Ephrins, and Slits (Wälchli et al., 2015). Many also have an important role in the formation and maintenance of BBB (Blanchette and Daneman, 2015). Therefore, alterations in neurovascular communication could contribute to the development of SZ.

Netrins are secreted proteins, that regulate many cellular processes during brain development such as cell migration, adhesion, and proliferation; as well as pre and postnatal angiogenesis (Yamagishi et al., 2021). Netrin-1 (NTN1), the main netrin in CNS, can exert attractive/positive or repulsive/negative responses depending on the concentration and presence of different receptors in the target cell. Notably, NTN1 can regulate BBB function by decreasing permeability through the induction of tight junction protein expression (Podjaski et al., 2015).

Genomic studies have found an association of polymorphisms in the Deleted Colorectal Cancer gene (*DCC*),

one of the main NTN1 receptors in the CNS, in SZ (Grant et al., 2012; Z. Wang et al., 2018). These polymorphisms could alter DCC protein expression affecting NTN1 signaling (Vosberg et al., 2020). Polymorphisms of another NTN1 receptor, UNC5B, have also been correlated with SZ (J. Tang et al., 2019). Interestingly, membrane-bound Netrins, NTN-G1 and NTN-G2, were downregulated in the SZ temporal lobe; these proteins are important for neural development and synaptic activity but have not been implicated in angiogenesis so far (J. Tang et al., 2019). *In vitro* experiments using hiPSC-derived NSC and neurons have shown decreased expression of NTN1 in SZ-derived cells, compared to healthy control (Brennand et al., 2011; Casas et al., 2018).

Semaphorins are a large protein family of molecules that regulate axonal guidance and synapse formation during development (Carulli et al., 2021). They also participate in other functions including immune regulation, extracellular matrix remodeling, and angiogenesis. Canonically semaphorins have been described as chemorepellents, but some of them can also exert attractive effects (such as SEMA3D, SEMA3E, and SEMAF), an important cue for neurovascular communication (Iragavarapu-Charyulu et al., 2020). For instance, semaphorin 3G (SEMA3G) secreted from the endothelium, activates neuronal receptors neuropilin-2/ PlexinA4 regulating synaptic structure and function; SEMA4D induces BBB dysfunction by the disruption of endothelial tight junctions, glial activation, neuronal collapse and inhibition of oligodendrocyte differentiation. Neuron-derived SEMA3A can induce vascular permeability and has been proposed as a contributor to BBB disruption and brain damage (Cerani et al., 2013; Hou et al., 2015; Smith et al., 2015; Tan et al., 2019; M. Yang et al., 2019).

Analysis of *postmortem* brain shows that SEMA3A, SEMA4D, and SEMA6C as well as semaphorin receptor PlexinB1 are upregulated in SZ (Gilabert-Juan et al., 2015). The upregulation of SEMA3A has been also evidenced in the SZ cerebellum of adult subjects and by the *in vitro* modeling of SZ-hiPSC-derived NSC (Eastwood et al., 2003; Casas et al., 2018).

The Slit family comprises 3 proteins (SLIT1, SLIT2, and SLIT3) that interact with ROBO to regulate several physiologic processes during development (Tong et al., 2019). The SLIT/ROBO pathway plays an important role in neural progenitor proliferation and migration, maturation of neocortical neurons, and axonal guidance (Gonda et al., 2020). Slit2 overexpression has been proved to increase vessel density in transgenic mice. Interaction with Robo1 also reduces cell-cell adhesion of EC increasing permeability (Han and Geng, 2011). Of note, the administration of recombinant Slit2 reduced BBB disruption due to brain surgical injury (Han and Geng, 2011). Therefore, it is proposed that the Slit/ROBO pathway has a regulatory function in angiogenesis and BBB.

GWAS performed on peripheral blood cells of patients with SZ has identified *SLIT1*, *SLIT3*, and *ROBO1* as susceptibility

genes for this disease. Moreover, an SNP in one locus of *ROBO2* significantly correlates with SZ (Potkin et al., 2009; Z. Wang et al., 2018).

Ephrins and their receptors Eph are cell membrane proteins known to mediate cell-cell communication, regulate adhesion, neurogenesis, neuron migration, and axonal guidance (Laussu et al., 2014). The ephrin/Eph signaling pathways play an important role in vascular system development, regulating EC differentiation, angiogenesis, and also BBB formation and maintenance (Malik and Di Benedetto, 2018). During early vasculogenesis, VEGFA-induced Ephrin A signaling by receptor EphA2 increases angiogenesis, later on, the inhibition of EphA2 is necessary for tight junction protein expression and proper BBB formation (Zhou et al., 2011; Malik and Di Benedetto, 2018).

There is little genomic and clinical data available regarding this pathway in SZ. One study found a significant association between SNPs in the *EhprinB2* gene and SZ (R. Zhang et al., 2010). *In vitro* modeling of SZ-hiPSC-derived NSC, neurons, and astrocytes has provided more information, describing alterations in the expression of Ephrin A1, A5 and B1 (Brennand et al., 2011; Casas et al., 2018; Koskuvi et al., 2020).

All the above-cited reports are in line with current knowledge of important impairments of neuronal function in SZ. The studies describe alterations in the expression of secreted molecules for which the analysis of this data, from a new perspective that focuses on the neurovascular niche, could determine the impact of signaling alterations in these pathways on the overall functioning of BBB and neurovascular coupling.

8 Nuclear factor-kappa B (NF-κB) and inflammation in SZ

Nuclear factor-kappa B (NF-κB) transcription factors regulate the expression of numerous genes involved in pleiotropic functions, ranging from immune and inflammatory responses, apoptosis, cell proliferation, differentiation, and survival (Oeckinghaus and Ghosh, 2009). The NF-κB family consists of 5 members including RelA (p65), RelB, c-Rel, NF-κB1 (p50/p105) and NF-κB2 (p52/p100), that form different homo- or heterodimers (Chen and Greene, 2004). The canonical pathway is induced by microbial products and proinflammatory cytokines such as tumor necrosis factor α (TNFα) and interleukin-1 (IL-1), while the non-canonical pathway is activated by certain members of the TNF family (Lymphotoxin β, CD40 ligand, B cell activation factor) (Lawrence, 2009; Oeckinghaus and Ghosh, 2009). In turn, NF-κB plays a role in the expression of other proinflammatory genes including cytokines, chemokines, and adhesion molecules (T. Liu et al., 2017).

NF- κ B signaling is well known as a regulator of both embryonic and adult neurogenesis (Bortolotto et al., 2014; Y. Zhang and Hu, 2012). Indeed, it has been reported that this signaling pathway is implicated in different processes of neurogenesis, including NSC/NPC proliferation and apoptosis, differentiation, migration of neuroblasts, maturation and plasticity of nascent neurons (Y. Zhang and Hu, 2012). Cytokines, including IL-1 β and TNF α , influence neurotransmission by altering the metabolism of neurotransmitters and their release (Dunn et al., 1999). Several studies that have implicated NF- κ B in EC activation and angiogenesis, especially in the context of cancer (Tabruyn and Griffioen, 2008). There is also evidence that dysregulation of NF- κ B target genes may lead to impaired angiogenesis and reduced brain EC migration (Zhuang et al., 2017). Since inflammatory mediators have a role during brain development, several studies have investigated their involvement in neuropsychiatric disorders (Jiang et al., 2018).

There is considerable evidence showing increased levels of proinflammatory molecules in the brain, blood, and cerebrospinal fluid of SZ patients (Fillman et al., 2013; Müller, 2018). Patients with higher plasma cytokine levels, named “high inflammation” biotype, exhibit higher cognitive deficits and brain volume reductions (Fillman et al., 2016). Higher mRNA levels for NF- κ B family members RELA and c-REL, as well as for multiple receptors from both the canonical and non-canonical pathways, and their respective kinases have also been observed in SZ *postmortem* brain (Volk et al., 2019). Consistent with these reports, SZ patients exhibit increased serum levels and peripheral blood mononuclear cell (PBMC) mRNA expression of IL-1 β and TNF α . Furthermore, NF- κ B activity is higher in patients’ PBMCs than those in healthy subjects and is positively correlated with a higher mRNA expression of cytokines (Song et al., 2009). Recently, it was reported that some brain EC markers, such as intercellular adhesion molecule-1 (ICAM1) and VE-cadherin, are dysregulated in the SZ brain both in “high inflammation” and “low inflammation” subgroups (Cai et al., 2020). This endothelial altered profile is replicated *in vitro* when incubating human brain EC with IL-1 β , as ICAM1 mRNA was up-regulated in a dose-dependent manner (Cai et al., 2020), which corroborates an important detriment of endothelial function in “high inflammation” SZ patients.

These results suggest that SZ is associated with elevated pro-inflammatory cytokines in both blood and brain and, in turn, increased NF- κ B activity, constituting a positive feedback loop. This may contribute to the pathogenesis of SZ through involvement in both neurogenesis and angiogenesis during development, compromising processes such as neurotransmitter release, cell

proliferation, differentiation and migration, and BBB integrity.

9 Unfolded protein response (UPR) is disturbed in SZ

The accumulation of unfolded proteins in the endoplasmic reticulum (ER) induces the unfolded protein response (UPR), an evolutionarily conserved group of signal transduction pathways to sense and respond to ER stress (Bernales et al., 2006; Lin et al., 2008). Three major ER transmembrane stress sensors trigger the UPR signaling pathway: protein kinase RNA-like ER kinase (PERK), activating transcription factor 6 (ATF6), and inositol-requiring enzyme 1 (IRE1) (Ron and Walter, 2007). Under normal conditions, these stress transducers are in an inactive state by binding with the ER chaperone BiP (Jain, 2017). Under stress, BiP dissociates from PERK, ATF6, and IRE1, allowing UPR sensors to be activated (Malhotra and Kaufman, 2007). Each of these three signaling branches involves the activity of multiple downstream molecules, such as transcription factor X-box binding protein 1 (XBP1) or eukaryotic translation initiation factor 2 α (eIF2 α), all of which aim to restore ER homeostasis by increasing the expression of genes encoding chaperones and proteins associated with apoptosis, and by attenuating protein synthesis (Jain, 2017).

Although the UPR is commonly associated with increased cellular stress and misfolded proteins, it is required in numerous cellular functions (Hetz, 2012). For example, the UPR plays a role in the proliferation, differentiation, maturation, and viability of CNS cells, including neurons, NSC, and glial cells. UPR signaling is a mechanism that controls neurogenesis and brain development, as well as NSC self-renewal and astrogenesis (Murao and Nishitoh, 2017). Furthermore, in the context of angiogenesis, the classical pathways of the UPR have been described to have modulatory properties. Several studies suggest a role for UPR in embryonic vascularization and maintenance and survival of EC, as well as in the regulation of pro- and anti-angiogenic modulators, both in physiological and pathological contexts (Binet and Sapieha, 2015). Since cells with a high secretory load, such as neurons and glial cells, are susceptible to ER stress, fine-tuning of UPR signaling is required. There is increased sensitivity of the brain to abnormalities in the UPR, which is evidenced by its implication in many neurodegenerative diseases and psychiatric disorders, including SZ (Scheper and Hoozemans, 2015; Kim et al., 2021).

Recent reports show that the UPR is dysregulated in the dorsolateral prefrontal cortex of patients with SZ (Kim et al., 2021). The authors observed increased protein expression of BiP and decreased p-IRE1 α , the activated state of IRE1 α . They also showed decreased p-JNK2 and increased sXBP1, both

downstream targets of the IRE1 arm of the UPR (Kim et al., 2021). These findings are consistent with those obtained through proteomic studies, where BiP is dysregulated within the corpus callosum and the dorsolateral prefrontal cortex of SZ patients, suggesting the involvement of cellular stress in this psychiatric disorder (Sivagnanasundaram et al., 2007; Martins-de-Souza et al., 2009). Furthermore, as described above, the UPR is important for neural development, especially the IRE1-XBP1 pathway, as its dysregulation compromises the proper trafficking of glutamate receptors and expression of GABAergic markers during development (Shim et al., 2004; Hayashi et al., 2008). This is consistent with previous reports demonstrating protein abnormalities and may explain the dysregulation of neurotransmitter systems described in SZ (Nucifora et al., 2019; McCutcheon et al., 2020).

Altogether, these results suggest an abnormal pattern of UPR activity in SZ, specifically on the IRE1 axis, and consequent alterations in protein processing. Although evidence indicates the possible involvement of UPR dysregulation in neurodevelopment, there may also be impairment of endothelial function, a matter which should be further investigated.

10 The role of MicroRNAs (miRNAs) in SZ: The cases of miR-137 and miR-19

miRNAs, as pleiotropic post-transcriptional regulators of gene expression, have gathered interest for both their potential as biomarkers of SZ and as tools to provide more complex mechanistic and molecular explanations to the diffuse array of altered gene expression underlying SZ (Zhu et al., 2009; He et al., 2018). Overall miR-137 regulates multiple genes associated with processes such as proliferation, stemness, angiogenesis, barrier permeability, or chromatin remodeling (Y. Wang et al., 2020). miR-137 regulates the balance between proliferation and differentiation of NSC and forms a regulatory loop with transcription factors such as SOX2 (Boyer et al., 2005; Smrt et al., 2010; Szulwach et al., 2010; Channakkar et al., 2020). In an *in vitro* model of Brain Tumor Barrier, the genetic manipulation of miR-137 alters barrier permeability and expression of key actors like Occludin, ZO-1, ZO-2, and FOXC2, the latter two being a direct target of miR-137 (Yu et al., 2017).

The Psychiatric GWAS Consortium has reported a strong association between the SNP rs1625579 of miR137 and SZ (Ripke et al., 2011). Moreover, miR-137 is upregulated in SZ and several variants have been associated with its physiopathology (Lett et al., 2013; Chen et al., 2021). The SNP rs1625579 in miR-137 can be a predictor for earlier age of onset of SZ and correlates with severity of patient symptoms (PANSS score) (D. Zhang et al., 2021). The 4-repeats variable number tandem repeat variant rs58335419 (VNTR₄) has been associated with altered cortical morphology and severe cognitive deficit in SZ patients (Mahmoudi et al., 2021).

Animal models have correlated the expression of the miR-137 variant with an alteration in hippocampus-dependent learning, long-term potentiation, and expression of presynaptic proteins (Siegert et al., 2015), all phenotypes that have been described in SZ.

In addition to its direct implication in SZ, it seems that miR-137 can regulate signaling pathways that are commonly altered in SZ patients. It has been reported that *Notch1* is a target of miR-137, which acts as a regulator of Notch signaling in neurons. Consistent observations in human adipose cells have shown that miR-137 binds directly to the *NOTCH1* 3'UTR region and ultimately positively regulates *HES1* (Shi et al., 2017; Fan et al., 2021). Recent evidence provides insight into the role of miR-137 in response to oxidative damage and neuroprotection with a proposed neuroprotector and anti-inflammatory role against chemical agents and artery occlusion (Y. Tang et al., 2021; Tian et al., 2020). High levels of miR-137 are associated with mitochondrial dysfunction in SZ patients, shedding light on a mechanistic model, linking impairment of cortical parvalbumin interneuron, oxidative damage, and altered activity rhythms (Khadimallah et al., 2021).

The involvement of miR-137 in oxidative stress and the NOTCH pathway presents an interesting direction for future research given the relevant role of oxygenation in SZ when understood as a developmental and neurovascular disorder.

Another brain-specific miRNA dysregulated in SZ is miR-19, which is involved in NSC proliferation and promotes neural differentiation and migration. Recently, miR-19 has been indicated as a major hub for abnormal cellular phenotypes manifested in SZ (Balan et al., 2019). Interestingly, miR-19b, but not miR-19a, is elevated in peripheral blood of SZ patients (Horai et al., 2020).

Overall, these findings support the potential for neurodevelopmental-related miRNAs to be used as indicators for SZ.

11 Discussion

SZ is a complex multifactorial disease imparted by the polygenicity and interactions with environmental factors. For achieving an integral understanding of this mental illness, is important not to only focus on the actual state of patients, but to be able to follow its origin, onset, and visualize its outcome. From a neurodevelopmental perspective, SZ traces its origins to the early stages of brain formation, where developmental trajectories will be affected generating predisposition to SZ onset. From FEP and diagnosis, the trajectories of patients living with SZ may also take different paths: remission, mild to severe symptomatology, resistance to treatment, and so on. In all this complexity, we must keep in mind that the brain is composed of an intricate network of vessels that influences brain formation from embryogenesis to adulthood (Figure 2A).

TABLE 1 Major molecular participants underlying neurodevelopmental processes of angiogenesis, BBB formation, and neurogenesis.

Process	Key signaling molecules/pathways	References
Angiogenesis	- Hypoxia-Inducible Factors (HIFs)	(Semenza, 2014, 2020; Abeyrathna and Su, 2015)
	- VEGF/NOTCH signaling	(Jakobsson et al., 2010; Walchli et al., 2015; Paredes et al., 2018)
	- WNT/ β -catenin signaling	(Martowicz et al., 2019)
	- Non-canonical WNT ligands	(Korn et al., 2014)
	- Unfolded Protein Response (UPR) signaling	Zhuang et al. (2017)
BBB formation	- Nuclear Factor-Kappa B (NF- κ B)	(Tabruyn and Griffioen, 2008; Binet and Sapieha, 2015)
	- NOTCH signaling pathway	Derada Troletti et al. (2018)
	- Canonical WNT signaling pathway	(Liebner et al., 2008; Blanchette and Daneman, 2015; Guérit et al., 2021)
	- Nuclear Factor-Kappa B (NF- κ B)	Volk et al. (2019)
Neurogenesis	- WNT signaling pathway	(Coullery et al., 2016; Arredondo et al., 2020)
	- AKT/mTOR pathway	(Götz and Huttner, 2005; Abe et al., 2010; Polchi et al., 2018)
	- Nuclear Factor-Kappa B (NF- κ B)	(Y. Zhang and Hu, 2012)
	- Unfolded Protein Response (UPR) signaling	(Shim et al., 2004; Hayashi et al., 2008; Murao and Nishitoh, 2017)

In this review, we emphasize the importance of acknowledging the presence of this complex and dynamic neuro-angiogenic niche for the study of SZ, since both neural and vascular components are constantly interacting with each other and share several signaling pathways (Table 1). The pathways reviewed in this article have a reported function both in the nervous and endothelial components of the neurovascular niche, with reported alterations in SZ that could have deleterious repercussions on overall brain functioning.

As reported previously, SZ has an important and highly variable genetic component where more than 100 loci have been significantly associated with SZ (Ripke et al., 2011; Ripke et al., 2014). From a genetic perspective, several pathways analyzed in this review present genetic variants associated with SZ. Genes from the HIF, NOTCH, WNT, and axonal guidance pathways (NTN, ROBO, and Ephrin), present genetic variants, such as SNPs, that have been significantly associated with SZ. From these pathways, the NOTCH and WNT pathways are described as having variants in several of their pathway components, increasing the risk of developing the disease. In addition to their well-known role in neurodevelopment, these pathways are important regulators of angiogenesis, a process that is proposed to be downregulated in SZ patients (Lopes et al., 2015; Katsel et al., 2017; Casas et al., 2018; Casas et al., 2022).

Evaluating the course of illness, various studies report significant variations in analytes when analyzed at different time points of the disease, as FEP, antipsychotic treatment, and treatment resistance. In this context, antioxidants, members of the NOTCH pathway, and VEGFA exhibit changes after treatment. For the antioxidant molecules and VEGFA, these variations should not be associated with drug mechanisms but rather with the inherent characteristics of patients. In this line, it has been proposed that plasmatic levels of VEGFA, which is reported as one of the most variable expressed

genes among SZ patients, may be a predictor of patient outcome. On the other hand, the expression of RBPJ, a transcriptional regulator of the NOTCH pathway, which was found to be reduced in patient plasma, is increased after treatment. Animal models and *in vitro* studies indicate that this increment in RBPJ expression may be a direct consequence of an antipsychotic treatment. A similar observation has been reported for the phosphorylation of S6RP, a downstream mediator of the mTOR/AKT pathway, which is reduced in the SZ *postmortem* brain. Long treatments of the antipsychotic haloperidol increase S6RP phosphorylation in rats, suggesting a mechanism of action for this drug. In addition to this, the expression pattern of cytokines and inflammatory molecules is related to cognitive deficits in SZ patients.

Interestingly, for many of the pathways analyzed, except for the WNT and mTOR pathways which seem to be consistently downregulated in SZ, different studies show variations with respect to the direction of this dysregulation regarding gene or protein expression. This may be a reflection of the high genetic heterogeneity present in SZ, especially in genes described as highly variable for this disease, rather than through gene expression or variant number (Huang et al., 2020; Puvogel et al., 2022). Taking into consideration the variability in gene expression in SZ reviewed in this and other articles, we propose the existence of molecular patterns that may be related to specific symptoms, severity, and even responses to medication. We reviewed several neuro-angiogenic pathways that converge in the neurovascular niche, for which we emphasize the repercussions of their dysregulations expressed as a consistent pattern that may have different impacts on each cell type that is part of the NVU, resulting in sometimes convergent or dissimilar consequences such as biological dysfunction or symptomatology.

There are several noteworthy pathways included in this review that crosstalk and contribute to common functions. For example, NOTCH, WNT, and NF- κ B participate in BBB

formation and maintenance; HIF, VEGFA, and NOTCH cross-regulate each other in angiogenesis; ROS, WNT, and UPR promote neurogenesis; to mention only a few interactions (Table 1). We have made an effort to dissect the specific contribution of each of these pathways in SZ, in particular, in processes associated with brain angiogenesis and neurodevelopment (Figure 2B). As stated before, for many of the analyzed pathways the main conclusion may be that they are dysregulated in SZ, and whether there is a higher or lower pathway activity that may relate to the progression of the disease or be explained by the use of pharmacological treatment requires further investigation. Interestingly, many of the molecules described in this review can be obtained by peripheral samples, as plasma, which allows measurements of analytes for diagnosis and patient stratification. More effort should be made to deeply understand the specific contribution of each one of these pathways to the SZ onset and progression. miRNAs might be involved in the regulation of multiple cell signaling pathways and may affect cellular physiological functioning, and thus may be involved in the onset of SZ. As stated, recent literature suggest that miRNAs are present in human plasma and could be a potential biomarker of SZ.

In summary, we describe the current state of knowledge regarding neuro-angiogenic pathways and their dysregulation in SZ. As presented, the interpretation of the data reveals the complexity of brain interactions and the SZ physiopathology. We are eager for future research investigating the multicellularity of brain structuration as well as its systemic co-dependence, which, we believe, could be crucial for the emergence of new biomarkers and therapeutic targets in SZ.

Author contributions

BC and VP determined the scope of the manuscript. BC supervised the project. BC, FA, DA, DG, DP and VM wrote the

article. Formal analysis, editing, and general supervision were conducted by VP. All authors contributed to the manuscript and approved the submitted version.

Funding

ANID Fondecyt # 1190083 and Fondecyt # 1221522 (VP). ANID Master's fellowship No. 22211196 (DA).

Acknowledgments

We thank PhD(c) Sofia Puvogel for the critical reading of our manuscript. We thank MSc Alexandra Elbakyan for her continuous contribution to our work. We thank Jeff Lichtman and Hidde Ploegh for allowing us to reproduce images of their work. Figures created with BioRender.com.

Conflict of interest

The authors declare that the research was conducted in the absence of any commercial or financial relationships that could be construed as a potential conflict of interest.

Publisher's note

All claims expressed in this article are solely those of the authors and do not necessarily represent those of their affiliated organizations, or those of the publisher, the editors and the reviewers. Any product that may be evaluated in this article, or claim that may be made by its manufacturer, is not guaranteed or endorsed by the publisher.

References

- Abe, N., Borson, S. H., Gambello, M. J., Wang, F., and Cavalli, V. (2010). Mammalian target of rapamycin (mTOR) activation increases axonal growth capacity of injured peripheral nerves. *J. Biol. Chem.* 285 (36), 28034–28043. doi:10.1074/jbc.M110.125336
- Abeyrathna, P., and Su, Y. (2015). The critical role of Akt in cardiovascular function. *Vasc. Pharmacol.* 74, 38–48. doi:10.1016/j.vph.2015.05.008
- Albayrak, Y., Ünsal, C., Beyazyüz, M., Ünal, A., and Kuloğlu, M. (2013). Reduced total antioxidant level and increased oxidative stress in patients with deficit schizophrenia: A preliminary study. *Prog. Neuropsychopharmacol. Biol. Psychiatry* 45, 144–149. doi:10.1016/j.pnpbp.2013.04.020
- Andreasen, N. C., O'Leary, D. S., Flaum, M., Nopoulos, P., Watkins, G. L., Ponto, L. L. B., et al. (1997). Hypofrontality in schizophrenia: Distributed dysfunctional circuits in neuroleptic-naïve patients. *Lancet* 349 (9067), 1730–1734. doi:10.1016/S0140-6736(96)08258-X
- Arredondo, S. B., Guerrero, F. G., Herrera-Soto, A., Jensen-Flores, J., Bustamante, D. B., Onate-Ponce, A., et al. (2020). Wnt5a promotes differentiation and development of adult-born neurons in the hippocampus by noncanonical Wnt signaling. *Stem cells* 38 (3), 422–436. doi:10.1002/stem.3121
- Balan, S., Toyoshima, M., and Yoshikawa, T. (2019). Contribution of induced pluripotent stem cell technologies to the understanding of cellular phenotypes in schizophrenia. *Neurobiol. Dis.* 131, 104162. doi:10.1016/j.nbd.2018.04.021
- Balótsev, R., Koido, K., Vasar, V., Janno, S., Kriisa, K., Mahlapuu, R., et al. (2017). Inflammatory, cardio-metabolic and diabetic profiling of chronic schizophrenia. *Eur. Psychiatry* 39, 1–10. doi:10.1016/j.eurpsy.2016.05.010
- Bar-Peled, L., Chantranupong, L., Cherniack, A. D., Chen, W. W., Ottina, K. A., Grabiner, B. C., et al. (2013). A tumor suppressor complex with GAP activity for the Rag GTPases that signal amino acid sufficiency to mTORC1. *Science* 340 (6136), 1100–1106. doi:10.1126/science.1232044
- Baruah, J., and Vasudevan, A. (2019). The vessels shaping mental health or illness. *Open Neurol. J.* 13 (1), 1–9. doi:10.2174/1874205X01913010001
- Basak, O., Giachino, C., Fiorini, E., MacDonald, H. R., and Taylor, V. (2012). Neurogenic subventricular zone stem/progenitor cells are notch1-dependent in

their active but not quiescent state. *J. Neurosci.* 32 (16), 5654–5666. doi:10.1523/jneurosci.0455-12.2012

Bautch, V. L., and James, J. M. (2009). Neurovascular development: The beginning of a beautiful friendship. *Cell adh. Migr.* 3 (2), 199–204. doi:10.4161/cam.3.2.8397

Ben-Sahra, I., Howell, J. J., Asara, J. M., and Manning, B. D. (2013). Stimulation of de novo pyrimidine synthesis by growth signaling through mTOR and S6K1. *Science* 339 (6125), 1323–1328. doi:10.1126/science.1228792

Ben-Zvi, A., and Liebner, S. (2021). Developmental regulation of barrier- and non-barrier blood vessels in the CNS. *J. Intern. Med.* 13263, 31–46. doi:10.1111/joim.13263

Bernales, S., Papa, F. R., and Walter, P. (2006). Intracellular signaling by the unfolded protein response. *Annu. Rev. Cell Dev. Biol.* 22 (1), 487–508. doi:10.1146/annurev.cellbio.21.122303.120200

Binet, F., and Sapieha, P. (2015). ER stress and angiogenesis. *Cell Metab.* 22 (4), 560–575. doi:10.1016/j.cmet.2015.07.010

Blanchette, M., and Daneman, R. (2015). Formation and maintenance of the BBB. *Mech. Dev.*, 138, 8–16. doi:10.1016/j.mod.2015.07.007

Bockaert, J., and Marin, P. (2015). mTOR in brain physiology and pathologies. *Physiol. Rev.* 95 (4), 1157–1187. doi:10.1152/physrev.00038.2014

Bortolotto, V., Cuccurazzu, B., Canonico, P. L., and Grilli, M. (2014). NF- κ B mediated regulation of adult hippocampal neurogenesis: Relevance to mood disorders and antidepressant activity. *Biomed. Res. Int.* 2014, 612798. doi:10.1155/2014/612798

Boyer, L. A., Lee, T. I., Cole, M. F., Johnstone, S. E., Levine, S. S., Zucker, J. P., et al. (2005). Core transcriptional regulatory circuitry in human embryonic stem cells. *Cell* 122 (6), 947–956. doi:10.1016/j.cell.2005.08.020

Bray, S. J. (2016). Notch signalling in context. *Nat. Rev. Mol. Cell Biol.* 17 (11), 722–735. doi:10.1038/nrm.2016.94

Brennan, K. J., Simone, A., Jou, J., Gelboin-Burkhart, C., Tran, N., Sangar, S., et al. (2011). Modelling schizophrenia using human induced pluripotent stem cells. *Nature* 473 (7346), 221–225. doi:10.1038/nature09915

Buckley, P. F., Harvey, P. D., Bowie, C. R., and Loebel, A. (2007). The relationship between symptomatic remission and neuropsychological improvement in schizophrenia patients switched to treatment with ziprasidone. *Schizophr. Res.* 94 (1–3), 99–106. doi:10.1016/j.schres.2006.12.032

Cai, H. Q., Catts, V. S., Webster, M. J., Galletly, C., Liu, D., O'Donnell, M., et al. (2020). Increased macrophages and changed brain endothelial cell gene expression in the frontal cortex of people with schizophrenia displaying inflammation. *Mol. Psychiatry* 25 (4), 761–775. doi:10.1038/s41380-018-0235-x

Çakici, N., Sutherland, A. L., Penninx, B. W. J. H., Dalm, V. A., de Haan, L., van Beveren, N. J. M., et al. (2020). Altered peripheral blood compounds in drug-naïve first-episode patients with either schizophrenia or major depressive disorder: A meta-analysis. *Brain Behav. Immun.* 88, 547–558. doi:10.1016/J.BBI.2020.04.039

Carulli, D., de Winter, F., and Verhaagen, J. (2021). Semaphorins in adult nervous system plasticity and disease. *Front. Synaptic Neurosci.* 13, 672891. doi:10.3389/fnsyn.2021.672891

Casas, B. S., Vitória, G., do Costa, M. N., Madeiro da Costa, R., Trindade, P., Maciel, R., et al. (2018). hiPSC-derived neural stem cells from patients with schizophrenia induce an impaired angiogenesis. *Transl. Psychiatry* 8 (1), 48. doi:10.1038/s41398-018-0095-9

Casas, B. S., Vitória, G., Prieto, C. P., Casas, M., Chacón, C., Uhrig, M., et al. (2022). Schizophrenia-derived hiPSC brain microvascular endothelial-like cells show impairments in angiogenesis and blood-brain barrier function. *Mol. Psychiatry*. doi:10.1038/s41380-022-01653-0

Cerani, A., Tetreault, N., Menard, C., Lapalme, E., Patel, C., Sitaras, N., et al. (2013). Neuron-derived semaphorin 3A is an early inducer of vascular permeability in diabetic retinopathy via neuropilin-1. *Cell Metab.* 18 (4), 505–518. doi:10.1016/j.cmet.2013.09.003

Chadha, R., Alganem, K., Mccullumsmith, R. E., and Meador-Woodruff, J. H. (2021). mTOR kinase activity disrupts a phosphorylation signaling network in schizophrenia brain. *Mol. Psychiatry* 26, 6868–6879. doi:10.1038/s41380-021-01135-9

Chadha, R., and Meador-Woodruff, J. H. (2020). Downregulated AKT-mTOR signaling pathway proteins in dorsolateral prefrontal cortex in Schizophrenia. *Neuropsychopharmacology* 45 (6), 1059–1067. doi:10.1038/s41386-020-0614-2

Chandran, P., Upadhyay, J., Markosyan, S., Lisowski, A., Buck, W., Chin, C. L., et al. (2012). Magnetic resonance imaging and histological evidence for the blockade of cuprizone-induced demyelination in C57BL/6 mice. *Neuroscience* 202, 446–453. doi:10.1016/j.neuroscience.2011.10.051

Channakkar, A. S., Singh, T., Pattnaik, B., Gupta, K., Seth, P., Adlakha, Y. K., et al. (2020). MiRNA-137-mediated modulation of mitochondrial dynamics regulates human neural stem cell fate. *Stem Cells* 38 (5), 683–697. doi:10.1002/stem.3155

Chen, B. Y., Lin, J. J., Lu, M. K., Tan, H. P., Jang, F. L., Lin, S. H., et al. (2021). Neurodevelopment regulators miR-137 and miR-34 family as biomarkers for early and adult onset schizophrenia. *NPJ Schizophr.* 7 (1), 35. doi:10.1038/s41537-021-00164-1

Chen, L. F., and Greene, W. C. (2004). Shaping the nuclear action of NF- κ B. *Nat. Rev. Mol. Cell Biol.* 5 (5), 392–401. doi:10.1038/nrm1368

Coullery, R. P., Ferrari, M. E., and Rosso, S. B. (2016). Neuronal development and axon growth are altered by glyphosate through a WNT non-canonical signaling pathway. *Neurotoxicology* 52, 150–161. doi:10.1016/j.neuro.2015.12.004

Daneman, R., Agalliu, D., Zhou, L., Kuhnert, F., Kuo, C. J., Barres, B. A., et al. (2009). Wnt/beta-catenin signaling is required for CNS, but not non-CNS, angiogenesis. *Proc. Natl. Acad. Sci. U. S. A.* 106 (2), 641–646. LP – 646. doi:10.1073/pnas.0805165106

Dengler, V. L., Galbraith, M. D., and Espinosa, J. M. (2014). Transcriptional regulation by hypoxia inducible factors. *Crit. Rev. Biochem. Mol. Biol.* 49 (1), 1–15. doi:10.3109/10409238.2013.838205

Derada Troletti, C., Lopes Pinheiro, M. A., Charabati, M., Gowing, E., van Het Hof, B., van der Pol, S. M. A., et al. (2018). Notch signaling is impaired during inflammation in a Lunatic Fringe-dependent manner. *Brain Behav. Immun.* 69, 48–56. doi:10.1016/j.bbi.2017.12.016

D'Souza, B., Meloty-Kapella, L., and Weinmaster, G. (2010). Canonical and non-canonical Notch ligands. *Curr. Top. Dev. Biol.* 92, 73–129. doi:10.1016/s0070-2153(10)92003-6

Dunn, A. J., Wang, J., and Ando, T. (1999). Effects of cytokines on cerebral neurotransmission. Comparison with the effects of stress. *Adv. Exp. Med. Biol.* 461, 117–127. doi:10.1007/978-0-585-37970-8_8

Eastwood, S. L., Law, a. J., Everall, I. P., and Harrison, P. J. (2003). The axonal chemorepellant semaphorin 3A is increased in the cerebellum in schizophrenia and may contribute to its synaptic pathology. *Mol. Psychiatry* 8, 148–155. doi:10.1038/sj.mp.4001233

Efeyan, A., and Sabatini, D. M. (2010). mTOR and cancer: Many loops in one pathway. *Curr. Opin. Cell Biol.* 22 (2), 169–176. doi:10.1016/j.ccb.2009.10.007

Engelhardt, B., and Liebner, S. (2014). Novel insights into the development and maintenance of the blood-brain barrier. *Cell Tissue Res.* 355 (3), 687–699. doi:10.1007/S00441-014-1811-2

Engler, A., Rolando, C., Giachino, C., Saotome, I., Erni, A., Brien, C., et al. (2018). Notch2 signaling maintains NSC quiescence in the murine ventricular-subventricular zone. *Cell Rep.* 22 (4), 992–1002. doi:10.1016/j.celrep.2017.12.094

English, J. A., Fan, Y., Föcking, M., Lopez, L. M., Hryniewiecka, M., Wynne, K., et al. (2015). Reduced protein synthesis in schizophrenia patient-derived olfactory cells. *Transl. Psychiatry* 5, e663. doi:10.1038/tp.2015.119

Eyrich, N. W., Potts, C. R., Robinson, M. H., Maximov, V., and Kenney, A. M. (2019). Reactive oxygen species signaling promotes hypoxia-inducible factor 1a stabilization in sonic hedgehog-driven cerebellar progenitor cell proliferation. *Mol. Cell. Biol.* 39 (8), e00268–18. doi:10.1128/MCB.00268-18

Falix, F. A., Aronson, D. C., Lamers, W. H., and Gaemers, I. C. (2012). Possible roles of DLK1 in the Notch pathway during development and disease. *Biochim. Biophys. Acta* 1822 (6), 988–995. doi:10.1016/j.bbdis.2012.02.003

Fan, C., Ma, X., Wang, Y., Lv, L., Zhu, Y., Liu, H., et al. (2021). A NOTCH1/LSD1/BMP2 co-regulatory network mediated by miR-137 negatively regulates osteogenesis of human adipose-derived stem cells. *Stem Cell Res. Ther.* 12 (1), 417. doi:10.1186/s13287-021-02495-3

Fang, T., Lu, X., Berger, D., Gmeiner, C., Cho, J., Schalek, R., et al. (2018). Nanobody immunostaining for correlated light and electron microscopy with preservation of ultrastructure. *Nat. Methods* 15 (12), 1029–1032. doi:10.1038/s41592-018-0177-x

Fillman, S. G., Cloonan, N., Catts, V. S., Miller, L. C., Wong, J., McCrossin, T., et al. (2013). Increased inflammatory markers identified in the dorsolateral prefrontal cortex of individuals with schizophrenia. *Mol. Psychiatry* 18 (2), 206–214. doi:10.1038/mp.2012.110

Fillman, S. G., Weickert, T. W., Lenroot, R. K., Catts, S. V., Bruggemann, J. M., Catts, V. S., et al. (2016). Elevated peripheral cytokines characterize a subgroup of people with schizophrenia displaying poor verbal fluency and reduced Broca's area volume. *Mol. Psychiatry* 21 (8), 1090–1098. doi:10.1038/mp.2015.90

Flatow, J., Buckley, P., and Miller, B. J. (2013). Meta-analysis of oxidative stress in schizophrenia. *Biol. Psychiatry* 74 (6), 400–409. doi:10.1016/j.biopsych.2013.03.018

Frydecka, D., Krzystek-Korpacka, M., Lubeiro, A., Stramecki, F., Stańczykiewicz, B., Beszlej, J. A., et al. (2018). Profiling inflammatory signatures of schizophrenia: A

- cross-sectional and meta-analysis study. *Brain Behav. Immun.* 71, 28–36. doi:10.1016/j.bbi.2018.05.002
- Fulzele, S., and Pillai, A. (2009). Decreased VEGF mRNA expression in the dorsolateral prefrontal cortex of schizophrenia subjects. *Schizophr. Res.* 115 (2–3), 372–373. doi:10.1016/j.schres.2009.06.005
- Garza-Lombó, C., and Gensebatt, M. E. (2016). Mammalian target of rapamycin: Its role in early neural development and in adult and aged brain function. *Front. Cell. Neurosci.* 10 (JUN), 157. doi:10.3389/fncel.2016.00157
- Gerald, D., Berra, E., Frapart, Y. M., Chan, D. A., Giaccia, A. J., Mansuy, D., et al. (2004). JunD reduces tumor angiogenesis by protecting cells from oxidative stress. *Cell* 118 (6), 781–794. doi:10.1016/j.cell.2004.08.025
- Gilbert-Juan, J., Sáez, A. R., Lopez-Campos, G., Sebastián-Ortega, N., González-Martínez, R., Costa, J., et al. (2015). Semaphorin and plexin gene expression is altered in the prefrontal cortex of schizophrenia patients with and without auditory hallucinations. *Psychiatry Res.* 229 (3), 850–857. doi:10.1016/j.psychres.2015.07.074
- Gonda, Y., Namba, T., and Hanashima, C. (2020). Beyond axon guidance: Roles of slit-robo signaling in neocortical formation. *Front. Cell Dev. Biol.* 8, 607415. doi:10.3389/fcell.2020.607415
- Götz, M., and Huttner, W. B. (2005). The cell biology of neurogenesis. *Nat. Rev. Mol. Cell Biol.* 6 (10), 777–788. doi:10.1038/nrm1739
- Grant, A., Fathalli, F., Rouleau, G., Joob, R., and Flores, C. (2012). Association between schizophrenia and genetic variation in DCC: A case-control study. *Schizophr. Res.* 137 (1–3), 26–31. doi:10.1016/j.schres.2012.02.023
- Guérit, S., Fidan, E., Macas, J., Czupalla, C. J., Figueiredo, R., Vijikumar, A., et al. (2021). Astrocyte-derived Wnt growth factors are required for endothelial blood-brain barrier maintenance. *Prog. Neurobiol.* 199, 101937. doi:10.1016/j.pneurobio.2020.101937
- Han, H., and Geng, J. (2011). Over-expression of Slit2 induces vessel formation and changes blood vessel permeability in mouse brain. *Acta Pharmacol. Sin.* 32 (11), 1327–1336. doi:10.1038/aps.2011.106
- Haring, L., Koido, K., Vasar, V., Leping, V., Zilmer, K., Zilmer, M., et al. (2015). Antipsychotic treatment reduces psychotic symptoms and markers of low-grade inflammation in first episode psychosis patients, but increases their body mass index. *Schizophr. Res.* 169 (1–3), 22–29. doi:10.1016/j.schres.2015.08.027
- Hayashi, A., Kasahara, T., Kametani, M., and Kato, T. (2008). Attenuated BDNF-induced upregulation of GABAergic markers in neurons lacking Xbp1. *Biochem. Biophys. Res. Commun.* 376 (4), 758–763. doi:10.1016/j.bbrc.2008.09.059
- He, K., Guo, C., He, L., and Shi, Y. (2018). MiRNAs of peripheral blood as the biomarker of schizophrenia. *Hereditas* 155 (1), 9. doi:10.1186/s41065-017-0044-2
- Hetz, C. (2012). The unfolded protein response: Controlling cell fate decisions under ER stress and beyond. *Nat. Rev. Mol. Cell Biol.* 13 (2), 89–102. doi:10.1038/nrm3270
- Hino, M., Kunii, Y., Matsumoto, J., Wada, A., Nagaoka, A., Niwa, S., et al. (2016). Decreased VEGFR2 expression and increased phosphorylated Akt1 in the prefrontal cortex of individuals with schizophrenia. *J. Psychiatr. Res.* 82, 100–108. doi:10.1016/j.jpsychires.2016.07.018
- Hoeben, A., Landuyt, B., Highley, M. S., Wildiers, H., Van Oosterom, A. T., De Bruijn, E. A., et al. (2004). Vascular endothelial growth factor and angiogenesis. *Pharmacol. Rev.* 56 (4), 549–580. LP – 580. doi:10.1124/pr.56.4.3
- Horai, T., Boku, S., Okazaki, S., Otsuka, I., Ratta-apha, W., Mouri, K., et al. (2020). miR-19b is elevated in peripheral blood of schizophrenic patients and attenuates proliferation of hippocampal neural progenitor cells. *J. Psychiatr. Res.* 131, 102–107. doi:10.1016/j.jpsychires.2020.09.006
- Hoseth, E. Z., Krull, F., Dieset, I., Mørch, R. H., Hope, S., Gardsjord, E. S., et al. (2018a). Exploring the Wnt signaling pathway in schizophrenia and bipolar disorder. *Transl. Psychiatry* 8 (1), 55. doi:10.1038/s41398-018-0102-1
- Hoseth, E. Z., Krull, F., Dieset, I., Mørch, R. H., Hope, S., Gardsjord, E. S., et al. (2018b). Attenuated Notch signaling in schizophrenia and bipolar disorder. *Sci. Rep.* 8 (1), 5349. doi:10.1038/s41598-018-23703-w
- Hou, S. T., Nilchi, L., Li, X., Gangaraju, S., Jiang, S. X., Aylsworth, A., et al. (2015). Semaphorin3A elevates vascular permeability and contributes to cerebral ischemia-induced brain damage. *Sci. Rep.* 5 (1), 7890. doi:10.1038/srep07890
- Howell, K. R., and Armstrong, J. (2017). Vascular endothelial growth factor (VEGF) in neurodevelopmental disorders. *Curr. Behav. Neurosci. Rep.* 4 (4), 299–308. doi:10.1007/s40473-017-0130-9
- Howell, K. R., Kutianawalla, A., and Pillai, A. (2011). Long-term continuous corticosterone treatment decreases VEGF receptor-2 expression in frontal cortex. *PLoS One* 6 (5), e20198. doi:10.1371/journal.pone.0020198
- Hu, Q., Liang, X., Chen, D., Chen, Y., Doycheva, D., Tang, J., et al. (2014). Delayed hyperbaric oxygen therapy promotes neurogenesis through reactive oxygen species/hypoxia-inducible factor-1 α / β -catenin pathway in middle cerebral artery occlusion rats. *Stroke* 45 (6), 1807–1814. doi:10.1161/STROKEAHA.114.005116
- Huang, G., Osorio, D., Guan, J., Ji, G., and Cai, J. J. (2020). Overdispersed gene expression in schizophrenia. *NPJ Schizophr.* 6 (1), 9. doi:10.1038/s41537-020-0097-5
- Huber, K. M., Klann, E., Costa-Mattioli, M., and Zukin, R. S. (2015). Dysregulation of mammalian target of rapamycin signaling in mouse models of autism. *J. Neurosci.* 35 (41), 13836–13842. doi:10.1523/JNEUROSCI.2656-15.2015
- Ibarra-Lecue, I., Díez-Alarcia, R., Morentin, B., Meana, J. J., Callado, L. F., Urigüen, L., et al. (2020). Ribosomal protein S6 hypofunction in postmortem human brain links mTORC1-dependent signaling and schizophrenia. *Front. Pharmacol.* 11, 344. doi:10.3389/fphar.2020.00344
- Inan, M., Petros, T. J., and Anderson, S. A. (2013). Losing your inhibition: Linking cortical GABAergic interneurons to schizophrenia. *Neurobiol. Dis.* 53, 36–48. doi:10.1016/j.nbd.2012.11.013
- Iragavarapu-Charyulu, V., Wojcikiewicz, E., and Urdaneta, A. (2020). Semaphorins in angiogenesis and autoimmune diseases: Therapeutic targets? *Front. Immunol.* 11, 346. doi:10.3389/fimmu.2020.00346
- Izumi, R., Hino, M., Wada, A., Nagaoka, A., Kawamura, T., Mori, T., et al. (2021). Detailed postmortem profiling of inflammatory mediators expression revealed post-inflammatory alternation in the superior temporal gyrus of schizophrenia. *Front. Psychiatry* 12, 653821. doi:10.3389/fpsy.2021.653821
- Jaaro-Peled, H., and Sawa, A. (2020). Neurodevelopmental factors in schizophrenia. *Psychiatr. Clin. North Am.* 43 (2), 263–274. doi:10.1016/j.psc.2020.02.010
- Jain, B. P. (2017). An overview of unfolded protein response signaling and its role in cancer. *Cancer biother. Radiopharm.* 32 (8), 275–281. doi:10.1089/cbr.2017.2309
- Jakobsson, L., Franco, C. A., Bentley, K., Collins, R. T., Ponsioen, B., Aspalter, I. M., et al. (2010). Endothelial cells dynamically compete for the tip cell position during angiogenic sprouting. *Nat. Cell Biol.* 12 (10), 943–953. doi:10.1038/ncb2103
- James, J. M., and Mukoyama, Y. (2011). Neuronal action on the developing blood vessel pattern. *Semin. Cell Dev. Biol.* 22 (9), 1019–1027. doi:10.1016/j.semcdb.2011.09.010
- Jiang, N. M., Cowan, M., Moonah, S. N., and Petri, W. A. (2018). The impact of systemic inflammation on neurodevelopment. *Trends Mol. Med.* 24 (9), 794–804. doi:10.1016/j.molmed.2018.06.008
- Kalkman, H. O. (2009). Altered growth factor signaling pathways as the basis of aberrant stem cell maturation in schizophrenia. *Pharmacol. Ther.* 121 (1), 115–122. doi:10.1016/j.pharmthera.2008.11.002
- Kantrowitz, J. T., and Javitt, D. C. (2010). N-methyl-D-aspartate (NMDA) receptor dysfunction or dysregulation: The final common pathway on the road to schizophrenia? *Brain Res. Bull.* 83 (3–4), 108–121. doi:10.1016/j.brainresbull.2010.04.006
- Katsel, P., Roussos, P., Pletnikov, M., and Haroutunian, V. (2017). Microvascular anomaly conditions in psychiatric disease. Schizophrenia – angiogenesis connection. *Neurosci. Biobehav. Rev.* 77, 327–339. doi:10.1016/j.neubiorev.2017.04.003
- Kerns, D., Vong, G. S., Barley, K., Dracheva, S., Katsel, P., Casaccia, P., et al. (2010). Gene expression abnormalities and oligodendrocyte deficits in the internal capsule in schizophrenia. *Schizophr. Res.* 120 (1–3), 150–158. doi:10.1016/j.schres.2010.04.012
- Khadimallah, I., Jenni, R., Cabungcal, J. H., Cleusix, M., Fournier, M., Beard, E., et al. (2021). Mitochondrial, exosomal miR137-COX6A2 and gamma synchrony as biomarkers of parvalbumin interneurons, psychopathology, and neurocognition in schizophrenia. *Mol. Psychiatry* 27, 1192–1204. doi:10.1038/s41380-021-01313-9
- Kim, P., Scott, M. R., and Meador-Woodruff, J. H. (2021). Dysregulation of the unfolded protein response (UPR) in the dorsolateral prefrontal cortex in elderly patients with schizophrenia. *Mol. Psychiatry* 26 (4), 1321–1331. doi:10.1038/s41380-019-0537-7
- Kochunov, P., and Hong, L. E. (2014). Neurodevelopmental and neurodegenerative models of schizophrenia: White matter at the center stage. *Schizophr. Bull.* 40 (4), 721–728. doi:10.1093/schbul/sbu070
- Koehl, M., Ladevèze, E., Catania, C., Cota, D., and Abrous, D. N. (2021). Inhibition of mTOR signaling by genetic removal of p70 S6 kinase 1 increases anxiety-like behavior in mice. *Transl. Psychiatry* 11 (1), 165. doi:10.1038/s41398-020-01187-5
- Korn, C., Scholz, B., Hu, J., Srivastava, K., Wojtarowicz, J., Arnsperger, T., et al. (2014). Endothelial cell-derived non-canonical Wnt ligands control vascular pruning in angiogenesis. *Development* 141 (8), 1757–1766. doi:10.1242/dev.104422

- Koskivi, M., Lehtonen, Š., Trontti, K., Keuters, M., Wu, Y. C., Koivisto, H., et al. (2020). Patient iPSC-astrocytes show transcriptional and functional dysregulation in schizophrenia. *BioRxiv* 1, 1–45. doi:10.1101/2020.10.23.350413
- Kozlovsky, N., Shanon-Weickert, C., Tomaskovic-Crook, E., Kleinman, J. E., Belmaker, R. H., Agam, G., et al. (2004). Reduced GSK-3 β mRNA levels in postmortem dorsolateral prefrontal cortex of schizophrenic patients. *J. Neural Transm.* 111 (12), 1583–1592. doi:10.1007/s00702-004-0166-3
- Laussu, J., Khuong, A., Gautrais, J., and Davy, A. (2014). Beyond boundaries—Eph-ephrin signaling in neurogenesis. *Cell adh. Migr.* 8 (4), 349–359. doi:10.4161/19336918.2014.969990
- LaVoie, M. J., and Selkoe, D. J. (2003). The Notch ligands, Jagged and Delta, are sequentially processed by α -secretase and presenilin/ γ -secretase and release signaling fragments. *J. Biol. Chem.* 278 (36), 34427–34437. doi:10.1074/jbc.M302659200
- Lawrence, T. (2009). The nuclear factor NF- κ B pathway in inflammation. *Cold Spring Harb. Perspect. Biol.* 1 (6), a001651. doi:10.1101/cshperspect.a001651
- Lee, B. H., Hong, J. P., Hwang, J. A., Ham, B. J., Na, K. S., Kim, W. J., et al. (2015). Alterations in plasma vascular endothelial growth factor levels in patients with schizophrenia before and after treatment. *Psychiatry Res.* 228 (1), 95–99. doi:10.1016/j.psychres.2015.04.020
- Lett, T. A., Chakavarty, M. M., Felsky, D., Brandl, E. J., Tiwari, A. K., Gonçalves, V. F., et al. (2013). The genome-wide supported microRNA-137 variant predicts phenotypic heterogeneity within schizophrenia. *Mol. Psychiatry* 18 (4), 443–450. doi:10.1038/mp.2013.17
- Licausi, F., and Hartman, N. W. (2018). Role of mTOR complexes in neurogenesis. *Int. J. Mol. Sci.* 19 (5), E1544. doi:10.3390/ijms19051544
- Licht, T., and Keshet, E. (2013). Delineating multiple functions of VEGF-A in the adult brain. *Cell. Mol. Life Sci.* 70 (10), 1727–1737. doi:10.1007/s00018-013-1280-x
- Liebner, S., Corada, M., Bangsow, T., Babbage, J., Taddei, A., Czapalla, C. J., et al. (2008). Wnt/ β -catenin signaling controls development of the blood-brain barrier. *J. Cell Biol.* 183 (3), 409–417. doi:10.1083/jcb.200806024
- Lin, J. H., Walter, P., and Yen, T. S. B. (2008). Endoplasmic reticulum stress in disease pathogenesis. *Annu. Rev. Pathol.* 3 (1), 399–425. doi:10.1146/annurev.pathmechdis.3.121806.151434
- Lipton, J. O., and Sahin, M. (2014). The Neurology of mTOR. *Neuron* 2 (84), 275–291. doi:10.1016/j.neuron.2014.09.034
- Liu, J., Sato, C., Cerletti, M., and Wagers, A. (2010). Notch signaling in the regulation of stem cell self-renewal and differentiation. *Curr. Top. Dev. Biol.* 92, 367–409. doi:10.1016/S0070-2153(10)92012-7
- Liu, T., Zhang, L., Joo, D., and Sun, S.-C. (2017). NF- κ B signaling in inflammation. *Signal Transduct. Target. Ther.* 2 (1), 17023. doi:10.1038/sigtrans.2017.23
- Lopes, R., Soares, R., Coelho, R., and Figueiredo-Braga, M. (2015). Angiogenesis in the pathophysiology of schizophrenia — a comprehensive review and a conceptual hypothesis. *Life Sci.* 128, 79–93. doi:10.1016/j.lfs.2015.02.010
- Ma, X. M., and Blenis, J. (2009). Molecular mechanisms of mTOR-mediated translational control. *Nat. Rev. Mol. Cell Biol.* 10 (5), 307–318. doi:10.1038/nrm2672
- Mahmoudi, E., Atkins, J. R., Quidé, Y., Reay, W. R., Cairns, H. M., Fitzsimmons, C., et al. (2021). The MIR137 VNTR rs58335419 is associated with cognitive impairment in schizophrenia and altered cortical morphology. *Schizophr. Bull.* 47 (2), 495–504. doi:10.1093/schbul/sbaa123
- Malhotra, J. D., and Kaufman, R. J. (2007). The endoplasmic reticulum and the unfolded protein response. *Semin. Cell Dev. Biol.* 18 (6), 716–731. doi:10.1016/j.semcdb.2007.09.003
- Malik, V. A., and Di Benedetto, B. (2018). The blood-brain barrier and the EphR/ephrin system: Perspectives on a link between neurovascular and neuropsychiatric disorders. *Front. Mol. Neurosci.* 11, 127. doi:10.3389/fnmol.2018.00127
- Manalo, D. J., Rowan, A., Lavoie, T., Natarajan, L., Kelly, B. D., Ye, S. Q., et al. (2005). Transcriptional regulation of vascular endothelial cell responses to hypoxia by HIF-1. *Blood* 105 (2), 659–669. doi:10.1182/blood-2004-07-2958
- Manning, B. D., and Cantley, L. C. (2007). AKT/PKB signaling: Navigating downstream. *Cell* 129 (7), 1261–1274. doi:10.1016/j.cell.2007.06.009
- Martins-de-Souza, D., Gattaz, W. F., Schmitt, A., Rewerts, C., Maccarrone, G., Dias-Neto, E., et al. (2009). Prefrontal cortex shotgun proteome analysis reveals altered calcium homeostasis and immune system imbalance in schizophrenia. *Eur. Arch. Psychiatry Clin. Neurosci.* 259 (3), 151–163. doi:10.1007/s00406-008-0847-2
- Martowicz, A., Trusohamm, M., Jensen, N., Wisniewska-Kruk, J., Corada, M., Ning, F. C., et al. (2019). Endothelial β -catenin signaling supports postnatal brain and retinal angiogenesis by promoting sprouting, tip cell formation, and VEGFR (Vascular Endothelial Growth Factor Receptor) 2 expression. *Arterioscl. Thromb. Vasc. Biol.* 39 (11), 2273–2288. doi:10.1161/ATVBAHA.119.312749
- McCutcheon, R. A., Krystal, J. H., and Howes, O. D. (2020). Dopamine and glutamate in schizophrenia: Biology, symptoms and treatment. *World Psychiatry* 19 (1), 15–33. doi:10.1002/wps.20693
- McGuire, J. L., Depasquale, E. A., Funk, A. J., O'Donovan, S. M., Hasselfeld, K., Marwaha, S., et al. (2017). Abnormalities of signal transduction networks in chronic schizophrenia. *NPJ Schizophr.* 3 (1), 30. doi:10.1038/s41537-017-0032-6
- Mishra-Gorur, K., Rand, M. D., Perez-Villamil, B., and Artavanis-Tsakonas, S. (2002). Down-regulation of Delta by proteolytic processing. *J. Cell Biol.* 159 (2), 313–324. doi:10.1083/jcb.200203117
- Misiak, B., Stramecki, F., Stańczykiewicz, B., Frydecka, D., and Lubeiro, A. (2018). Vascular endothelial growth factor in patients with schizophrenia: A systematic review and meta-analysis. *Prog. Neuropsychopharmacol. Biol. Psychiatry* 86, 24–29. doi:10.1016/j.pnpbp.2018.05.005
- Montcouquiol, M., Crenshaw, E. B., and Kelley, M. W. (2006). Noncanonical Wnt signaling and neural polarity. *Annu. Rev. Neurosci.* 29, 363–386. doi:10.1146/annurev.neuro.29.051605.112933
- Morante-Redolat, J. M., and Fariñas, I. (2016). Fetal neurogenesis: Breathe HIF you can. *Embo J.* 35 (9), 901–903. doi:10.15252/embj.201694238
- Müller, N. (2018). Inflammation in schizophrenia: Pathogenetic aspects and therapeutic considerations. *Schizophr. Bull.* 44 (5), 973–982. doi:10.1093/schbul/sby024
- Mulligan, K. A., and Cheyette, B. N. R. (2016). Neurodevelopmental perspectives on wnt signaling in psychiatry. *Mol. Neuropsychiatry* 2 (4), 219–246. doi:10.1159/000453266
- Murao, N., and Nishitoh, H. (2017). Role of the unfolded protein response in the development of central nervous system. *J. Biochem.* 162 (3), 155–162. doi:10.1093/jb/mvx047
- Nucifora, L. G., MacDonald, M. L., Lee, B. J., Peters, M. E., Norris, A. L., Orsburn, B. C., et al. (2019). Increased protein insolubility in brains from a subset of patients with schizophrenia. *Am. J. Psychiatry* 176 (9), 730–743. doi:10.1176/appi.ajp.2019.18070864
- Oeckinghaus, A., and Ghosh, S. (2009). The NF- κ B family of transcription factors and its regulation. *Cold Spring Harb. Perspect. Biol.* 1 (4), a000034. doi:10.1101/cshperspect.a000034
- Owen, M. J., Sawa, A., and Mortensen, P. B. (2016). Schizophrenia. *Lancet* 388 (10039), 86–97. doi:10.1016/S0140-6736(15)01121-6
- Pandya, C. D., Howell, K. R., and Pillai, A. (2013). Antioxidants as potential therapeutics for neuropsychiatric disorders. *Prog. Neuropsychopharmacol. Biol. Psychiatry* 46, 214–223. doi:10.1016/j.pnpbp.2012.10.017
- Panizzutti, B., Bortolasci, C. C., Spolding, B., Kidnapillai, S., Connor, T., Richardson, M. F., et al. (2021). Transcriptional modulation of the hippo signaling pathway by drugs used to treat bipolar disorder and schizophrenia. *Int. J. Mol. Sci.* 22 (13), 7164. doi:10.3390/ijms22137164
- Paredes, I., Himmels, P., and Ruiz de Almodóvar, C. (2018). Neurovascular communication during CNS development. *Dev. Cell* 45 (1), 10–32. doi:10.1016/j.devcel.2018.01.023
- Passos Gregorio, S., Gattaz, W. F., Tavares, H., Kieling, C., Timm, S., Wang, A. G., et al. (2006). Analysis of coding polymorphisms in NOTCH-related genes reveals NUMBL poly-glutamine repeat to be associated with schizophrenia in Brazilian and Danish subjects. *Schizophr. Res.* 88 (1–3), 275–282. doi:10.1016/j.schres.2006.06.036
- Peguera, B., Segarra, M., and Acker-Palmer, A. (2021). Neurovascular crosstalk coordinates the central nervous system development. *Curr. Opin. Neurobiol.* 69, 202–213. doi:10.1016/j.conb.2021.04.005
- Pillai, A., Parikh, V., Terry, A. V., Jr., and Mahadik, S. P. (2007). Long-term antipsychotic treatments and crossover studies in rats: Differential effects of typical and atypical agents on the expression of antioxidant enzymes and membrane lipid peroxidation in rat brain. *J. Psychiatr. Res.* 41 (5), 372–386. doi:10.1016/j.jpsychires.2006.01.011
- Pillai, A., Howell, K. R., Ahmed, A. O., Weinberg, D., Allen, K. M., Bruggemann, J., et al. (2016). Association of serum VEGF levels with prefrontal cortex volume in schizophrenia. *Mol. Psychiatry* 21 (5), 686–692. doi:10.1038/mp.2015.96
- Podjaski, C., Alvarez, J. I., Bourbonniere, L., Larouche, S., Terouz, S., Bin, J. M., et al. (2015). Netrin 1 regulates blood-brain barrier function and neuroinflammation. *Brain* 138 (6), 1598–1612. doi:10.1093/brain/awv092
- Polchi, A., Magini, A., Meo, D. D., Tancini, B., and Emiliani, C. (2018). mTOR signaling and neural stem cells: The tuberous sclerosis complex model. *Int. J. Mol. Sci.* 19 (5), 1474. doi:10.3390/ijms19051474

- Potkin, S. G., Turner, J. A., Guffanti, G., Lakatos, A., Fallon, J. H., Nguyen, D. D., et al. (2009). A genome-wide association study of schizophrenia using brain activation as a quantitative phenotype. *Schizophr. Bull.* 35 (1), 96–108. doi:10.1093/schbul/sbn155
- Prabakaran, S., Swatton, J. E., Ryan, M. M., Huffaker, S. J., Huang, J. T., Griffin, J. L., et al. (2004). Mitochondrial dysfunction in schizophrenia: Evidence for compromised brain metabolism and oxidative stress. *Mol. Psychiatry* 9 (7643), 684–697. doi:10.1038/sj.mp.4001511
- Puvogel, S., Palma, V., and Sommer, I. E. C. (2022). Brain vasculature disturbance in schizophrenia. *Curr. Opin. Psychiatry* 35, 146. Publish Ah. doi:10.1097/YCO.0000000000000789
- Quaeghebeur, A., Lange, C., and Carmeliet, P. (2011). The neurovascular link in health and disease: Molecular mechanisms and therapeutic implications. *Neuron* 71 (3), 406–424. doi:10.1016/j.neuron.2011.07.013
- Reay, W. R., Atkins, J. R., Carr, V. J., Green, M. J., and Cairns, M. J. (2020). Pharmacological enrichment of polygenic risk for precision medicine in complex disorders. *Sci. Rep.* 10 (1), 879. doi:10.1038/s41598-020-57795-0
- Ripke, S., Neale, B. M., Corvin, A., Walters, J. T. R., Farh, K. H., Holmans, P. A., et al. (2014). Biological insights from 108 schizophrenia-associated genetic loci. *Nature* 511 (7510), 421–427. doi:10.1038/nature13595
- Ripke, S., Sanders, A. R., Kendler, K. S., Levinson, D. F., Sklar, P., Holmans, P. A., et al. (2011). Genome-wide association study identifies five new schizophrenia loci. *Nat. Genet.* 43 (10), 969–976. doi:10.1038/ng.940
- Ron, D., and Walter, P. (2007). Signal integration in the endoplasmic reticulum unfolded protein response. *Nat. Rev. Mol. Cell Biol.* 8 (7), 519–529. doi:10.1038/nrm2199
- Rosen, N., and She, Q.-B. (2006). AKT and cancer—is it all mTOR? *Cancer Cell* 10 (4), 253–254. doi:10.1016/j.ccr.2006.09.010
- Rund, B. R. (2018). The research evidence for schizophrenia as a neurodevelopmental disorder. *Scand. J. Psychol.* 59 (1), 49–58. doi:10.1111/sjop.12414
- Scheper, W., and Hoozemans, J. J. M. (2015). The unfolded protein response in neurodegenerative diseases: A neuropathological perspective. *Acta Neuropathol.* 130 (3), 315–331. doi:10.1007/s00401-015-1462-8
- Schmidt-Kastner, R., van Os, J., H. W. M. S., and Schmitz, C. (2006). Gene regulation by hypoxia and the neurodevelopmental origin of schizophrenia. *Schizophr. Res.* 84 (2–3), 253–271. doi:10.1016/j.schres.2006.02.022
- Schmidt-Kastner, R., van Os, J., Esquivel, G., Steinbusch, H. W. M., and Rutten, B. P. F. (2012). An environmental analysis of genes associated with schizophrenia: Hypoxia and vascular factors as interacting elements in the neurodevelopmental model. *Mol. Psychiatry* 17 (12), 1194–1205. doi:10.1038/mp.2011.183
- Segarra, M., Aburto, M. R., Hefendehl, J., and Acker-Palmer, A. (2019). Neurovascular interactions in the nervous system. *Annu. Rev. Cell Dev. Biol.* 35 (1), 615–635. doi:10.1146/annurev-cellbio-100818-125142
- Semenza, G. L. (2014). Oxygen sensing, hypoxia-inducible factors, and disease pathophysiology. *Annu. Rev. Pathol.* 9 (1), 47–71. doi:10.1146/annurev-pathol-012513-104720
- Semenza, G. L. (2020). The genomics and genetics of oxygen homeostasis. *Annu. Rev. Genomics Hum. Genet.* 21 (1), 183–204. doi:10.1146/annurev-genom-111119-073356
- Shen, L., Lv, X., Huang, H., Li, M., Huai, C., Wu, X., et al. (2021). Genome-wide analysis of DNA methylation in 106 schizophrenia family trios in Han Chinese. *EBioMedicine* 72, 103609. doi:10.1016/j.ebiom.2021.103609
- Shi, F., Dong, Z., Li, H., Liu, X., Liu, H., Dong, R., et al. (2017). MicroRNA-137 protects neurons against ischemia/reperfusion injury through regulation of the Notch signaling pathway. *Exp. Cell Res.* 352 (1), 1–8. doi:10.1016/j.yexcr.2017.01.015
- Shim, J., Umemura, T., Nothstein, E., and Rongo, C. (2004). The unfolded protein response regulates glutamate receptor export from the endoplasmic reticulum. *Mol. Biol. Cell* 15 (11), 4818–4828. doi:10.1091/mbc.e04-02-0108
- Siebert, S., Seo, J., Kwon, E. J., Rudenko, A., Cho, S., Wang, W., et al. (2015). The schizophrenia risk gene product miR-137 alters presynaptic plasticity. *Nat. Neurosci.* 18 (7), 1008–1016. doi:10.1038/nn.4023
- Simon, M. C. (2006). Mitochondrial reactive oxygen species are required for hypoxic HIF alpha stabilization. *Adv. Exp. Med. Biol.* 588, 165–170. doi:10.1007/978-0-387-34817-9_15
- Simons, M., Gordon, E., and Claesson-Welsh, L. (2016). Mechanisms and regulation of endothelial VEGF receptor signalling. *Nat. Rev. Mol. Cell Biol.* 17 (10), 611–625. doi:10.1038/nrm.2016.87
- Sivagnanasundaram, S., Crossett, B., Dedova, I., Cordwell, S., and Matsumoto, I. (2007). Abnormal pathways in the genu of the corpus callosum in schizophrenia pathogenesis: A proteome study. *Proteomics. Clin. Appl.* 1 (10), 1291–1305. doi:10.1002/prca.200700230
- Smith, E. S., Jonason, A., Reilly, C., Veeraghavan, J., Fisher, T., Doherty, M., et al. (2015). SEMA4D compromises blood–brain barrier, activates microglia, and inhibits remyelination in neurodegenerative disease. *Neurobiol. Dis.* 73, 254–268. doi:10.1016/j.nbd.2014.10.008
- Smrt, R. D., Szulwach, K. E., Pfeiffer, R. L., Li, X., Guo, W., Pathania, M., et al. (2010). MicroRNA miR-137 regulates neuronal maturation by targeting ubiquitin ligase mind bomb-1. *Stem Cells* 28 (6), 1060–1070. doi:10.1002/stem.431
- Song, X.-Q., Lv, L.-X., Li, W.-Q., Hao, Y.-H., and Zhao, J.-P. (2009). The interaction of nuclear factor-kappa B and cytokines is associated with schizophrenia. *Biol. Psychiatry* 65 (6), 481–488. doi:10.1016/j.biopsych.2008.10.018
- Spencer, K. M. (2009). The functional consequences of cortical circuit abnormalities on gamma oscillations in schizophrenia: Insights from computational modeling. *Front. Hum. Neurosci.* 3 (OCT), 33. doi:10.3389/neuro.09.033.2009
- Stenman, J. M., Rajagopal, J., Carroll, T. J., Ishibashi, M., McMahon, J., McMahon, A. P., et al. (2008). Canonical Wnt signaling regulates organ-specific assembly and differentiation of CNS vasculature. *Sci. (New York, N.Y.)* 322 (5905), 1247–1250. doi:10.1126/science.1164594
- Stepnicki, P., Kondej, M., and Kaczor, A. A. (2018). Current concepts and treatments of schizophrenia. *Molecules* 23 (8), 2087. doi:10.3390/molecules23082087
- Susser, E., and St Clair, D. (2013). Prenatal famine and adult mental illness: Interpreting concordant and discordant results from the Dutch and Chinese Famines. *Soc. Sci. Med.* 97, 325–330. doi:10.1016/j.socscimed.2013.02.049
- Szulwach, K. E., Li, X., Smrt, R. D., Li, Y., Luo, Y., Lin, L., et al. (2010). Cross talk between microRNA and epigenetic regulation in adult neurogenesis. *J. Cell Biol.* 189 (1), 127–141. doi:10.1083/jcb.200908151
- Tabruyn, S. P., and Griffioen, A. W. (2008). NF-κB: A new player in angiostatic therapy. *Angiogenesis* 11 (1), 101–106. doi:10.1007/s10456-008-9094-4
- Tam, S. J., and Watts, R. J. (2010). Connecting vascular and nervous system development: Angiogenesis and the blood–brain barrier. *Annu. Rev. Neurosci.* 33 (1), 379–408. doi:10.1146/annurev-neuro-060909-152829
- Tan, C., Lu, N.-N., Wang, C.-K., Chen, D.-Y., Sun, N.-H., Lyu, H., et al. (2019). Endothelium-derived semaphorin 3G regulates hippocampal synaptic structure and plasticity via neuropilin-2/PlexinA4. *Neuron* 101 (5), 920–937. e13. doi:10.1016/j.neuron.2018.12.036
- Tang, J., Chen, X., Cai, B., and Chen, G. (2019). A logical relationship for schizophrenia, bipolar, and major depressive disorder. Part 4: Evidence from chromosome 4 high-density association screen. *J. Comp. Neurol.* 527 (2), 392–405. doi:10.1002/cne.24543
- Tang, Y., Li, Y., Yu, G., Ling, Z., Zhong, K., Zilundu, P. L. M., et al. (2021). MicroRNA-137-3p protects PC12 cells against oxidative stress by downregulation of calpain-2 and nNOS. *Cell. Mol. Neurobiol.* 41 (6), 1373–1387. doi:10.1007/s10571-020-00908-0
- Tavazoei, S. F., Alvarez, V. A., Ridenour, D. A., Kwiatkowski, D. J., and Sabatini, B. L. (2005). Regulation of neuronal morphology and function by the tumor suppressors Tsc1 and Tsc2. *Nat. Neurosci.* 8 (12), 1727–1734. doi:10.1038/nn1566
- Tian, R., Wu, B., Fu, C., and Guo, K. (2020). miR-137 prevents inflammatory response, oxidative stress, neuronal injury and cognitive impairment via blockade of Src-mediated MAPK signaling pathway in ischemic stroke. *Aging (Albany NY)* 12 (11), 10873–10895. doi:10.18632/aging.103301
- Tong, M., Jun, T., Nie, Y., Hao, J., and Fan, D. (2019). The role of the slit/robo signaling pathway. *J. Cancer* 10 (12), 2694–2705. doi:10.7150/jca.31877
- Topol, A., Zhu, S., Tran, N., Simone, A., Fang, G., Brennand, K. J., et al. (2015). Altered WNT signaling in human induced pluripotent stem cell neural progenitor cells derived from four schizophrenia patients. *Biol. Psychiatry* 78 (6), e29–34. doi:10.1016/j.biopsych.2014.12.028
- Tsuang, M. (2000). Schizophrenia: Genes and environment. *Biol. Psychiatry* 47 (3), 210–220. doi:10.1016/s0006-3223(99)00289-9
- Varela-Nallar, L., and Inestrosa, N. (2013). Wnt signaling in the regulation of adult hippocampal neurogenesis. *Front. Cell. Neurosci.* 7, 100. doi:10.3389/fncel.2013.00100
- Volk, D. W., Moroco, A. E., Roman, K. M., Edelson, J. R., and Lewis, D. A. (2019). The role of the nuclear factor-kb transcriptional complex in cortical immune activation in schizophrenia. *Biol. Psychiatry* 85 (1), 25–34. doi:10.1016/j.biopsych.2018.06.015
- Vosberg, D. E., Leyton, M., and Flores, C. (2020). The netrin-1/DCC guidance system: Dopamine pathway maturation and psychiatric disorders emerging in adolescence. *Mol. Psychiatry* 25 (2), 297–307. doi:10.1038/s41380-019-0561-7

- Wälchli, T., Wacker, A., Frei, K., Regli, L., Schwab, M. E., Hoerstrup, S. P., et al. (2015). Wiring the vascular network with neural cues: A CNS perspective. *Neuron* 87 (2), 271–296. doi:10.1016/j.neuron.2015.06.038
- Wang, S., Sun, C. E., Walczak, C. A., Ziegler, J. S., Kipps, B. R., Goldin, L. R., et al. (1995). Evidence for a susceptibility locus for schizophrenia on chromosome 6pter-p22. *Nat. Genet.* 10 (1), 41–46. doi:10.1038/ng0595-41
- Wang, H. N., Liu, G. H., Zhang, R. G., Xue, F., Wu, D., Chen, Y. C., et al. (2015). Quetiapine ameliorates schizophrenia-like behaviors and protects myelin integrity in cuprizone intoxicated mice: The involvement of notch signaling pathway. *Int. J. Neuropsychopharmacol.* 19 (2), pyv088. doi:10.1093/ijnp/pyv088
- Wang, L., Zhou, K., Fu, Z., Yu, D., Huang, H., Zang, X., et al. (2017). Brain development and akt signaling: The crossroads of signaling pathway and neurodevelopmental diseases. *J. Mol. Neurosci.* 61 (3), 379–384. doi:10.1007/s12031-016-0872-y
- Wang, Z., Li, P., Wu, T., Zhu, S., Deng, L., Cui, G., et al. (2018). Axon guidance pathway genes are associated with schizophrenia risk. *Exp. Ther. Med.* 16 (6), 4519–4526. doi:10.3892/etm.2018.6781
- Wang, Y., Chen, R., Zhou, X., Guo, R., Yin, J., Li, Y., et al. (2020). miR-137: A novel therapeutic target for human glioma. *Mol. Ther. Nucleic Acids* 21, 614–622. doi:10.1016/j.omtn.2020.06.028
- Wang, H., Yi, Z., and Shi, T. (2022). Novel loci and potential mechanisms of major depressive disorder, bipolar disorder, and schizophrenia. *Sci. China. Life Sci.* 65 (1), 167–183. doi:10.1007/s11427-020-1934-x
- Wei, J., and Hemmings, G. P. (2000). The NOTCH4 locus is associated with susceptibility to schizophrenia. *Nat. Genet.* 25 (4), 376–377. doi:10.1038/78044
- Weinberger, D. R. (2017). Future of days past: Neurodevelopment and schizophrenia. *Schizophr. Bull.* 43 (6), 1164–1168. doi:10.1093/schbul/sbx118
- Wu, Z., Zhang, X. Y., Wang, H., Tang, W., Xia, Y., Zhang, F., et al. (2012). Elevated plasma superoxide dismutase in first-episode and drug naive patients with schizophrenia: Inverse association with positive symptoms. *Prog. Neuropsychopharmacol. Biol. Psychiatry* 36 (1), 34–38. doi:10.1016/j.pnpbp.2011.08.018
- Wu, J. Q., Kosten, T. R., and Zhang, X. Y. (2013). Free radicals, antioxidant defense systems, and schizophrenia. *Prog. Neuropsychopharmacol. Biol. Psychiatry* 46, 200–206. doi:10.1016/j.pnpbp.2013.02.015
- Xiao, W., Zhan, Q., Ye, F., Tang, X., Li, J., Dong, H., et al. (2018). Baseline serum vascular endothelial growth factor levels predict treatment response to antipsychotic medication in patients with schizophrenia. *Eur. Neuropsychopharmacol.* 28(5), 603–609. doi:10.1016/j.euroneuro.2018.03.007
- Xiao, W., Zhan, Q., Ye, F., Tang, X., Li, J., Dong, H., et al. (2019). Elevated serum vascular endothelial growth factor in treatment-resistant schizophrenia treated with electroconvulsive therapy: Positive association with therapeutic effects. *World J. Biol. Psychiatry* 20 (2), 150–158. doi:10.1080/15622975.2018.1459048
- Xu, H., Yang, H. J., Zhang, Y., Clough, R., Browning, R., Li, X. M., et al. (2009). Behavioral and neurobiological changes in C57BL/6 mice exposed to cuprizone. *Behav. Neurosci.* 123 (2), 418–429. doi:10.1037/a0014477
- Xue, F., Chen, Y.-C., Zhou, C.-H., Wang, Y., Cai, M., Yan, W.-J., et al. (2017). Risperidone ameliorates cognitive deficits, promotes hippocampal proliferation, and enhances Notch signaling in a murine model of schizophrenia. *Pharmacol. Biochem. Behav.* 163, 101–109. doi:10.1016/j.pbb.2017.09.010
- Yamagishi, S., Bando, Y., and Sato, K. (2021). Involvement of netrins and their receptors in neuronal migration in the cerebral cortex. *Front. Cell Dev. Biol.* 8, 590009. doi:10.3389/fcell.2020.590009
- Yang, X., Zhu, A., Li, F., Zhang, Z., and Li, M. (2013). Neurogenic locus notch homolog protein 4 and brain-derived neurotrophic factor variants combined effect on schizophrenia susceptibility. *Acta Neuropsychiatr.* 25 (6), 356–360. doi:10.1017/neu.2013.13
- Yang, K., Wang, X., Zhang, H., Wang, Z., Nan, G., Li, Y., et al. (2016). The evolving roles of canonical WNT signaling in stem cells and tumorigenesis: Implications in targeted cancer therapies. *Lab. Invest.* 96 (2), 116–136. doi:10.1038/labinvest.2015.144
- Yang, M., Wang, X., Fan, Y., Chen, Y., Sun, D., Xu, X., et al. (2019). Semaphorin 3A contributes to secondary blood–brain barrier damage after traumatic brain injury. *Front. Cell. Neurosci.* 13, 117. doi:10.3389/fncel.2019.00117
- Ye, F., Zhan, Q., Xiao, W., Tang, X., Li, J., Dong, H., et al. (2018). Altered serum levels of vascular endothelial growth factor in first-episode drug-naïve and chronic medicated schizophrenia. *Psychiatry Res.* 264, 361–365. doi:10.1016/j.psychres.2018.04.027
- Yu, H., Xue, Y., Wang, P., Liu, X., Ma, J., Zheng, J., et al. (2017). Knockdown of long non-coding RNA XIST increases blood-tumor barrier permeability and inhibits glioma angiogenesis by targeting miR-137. *Oncogenesis* 6 (3), e303. doi:10.1038/oncsis.2017.7
- Zhang, X., Wei, J., Yu, Y.-Q., Liu, S.-Z., Shi, J.-P., Liu, L.-L., et al. (2004). Is NOTCH4 associated with schizophrenia? *Psychiatr. Genet.* 14 (1), 43–46. doi:10.1097/00041444-200403000-00007
- Zhang, R., Zhong, N.-N., Liu, X.-G., Yan, H., Qiu, C., Han, Y., et al. (2010). Is the EFNB2 locus associated with schizophrenia? Single nucleotide polymorphisms and haplotypes analysis. *Psychiatry Res.* 180 (1), 5–9. doi:10.1016/j.psychres.2010.04.037
- Zhang, B., Fan, Q. R., Li, W. H., Lu, N., Fu, D. K., Kang, Y. J., et al. (2015). Association of the NOTCH4 gene polymorphism rs204993 with schizophrenia in the Chinese han population. *Biomed. Res. Int.* 2015, 408096. doi:10.1155/2015/408096
- Zhang, D., Li, H., Ding, K., Zhang, Z., Luo, S., Li, G., et al. (2021). Polymorphisms in MicroRNA genes associated with schizophrenia susceptibility but not with effectiveness of MECT. *Comput. Math. Methods Med.* 2021, 1959172. doi:10.1155/2021/1959172
- Zhang, Y., and Hu, W. (2012). NFκB signaling regulates embryonic and adult neurogenesis. *Front. Biol.* 7 (4), 277–291. doi:10.1007/s11515-012-1233-z
- Zhao, Y., Xiao, W., Chen, K., Zhan, Q., Ye, F., Tang, X., et al. (2019). Neurocognition and social cognition in remitted first-episode schizophrenia: Correlation with VEGF serum levels. *BMC Psychiatry* 19 (1), 403. doi:10.1186/s12888-019-2397-8
- Zhou, N., Zhao, W.-D., Liu, D.-X., Liang, Y., Fang, W.-G., Li, B., et al. (2011). Inactivation of EphA2 promotes tight junction formation and impairs angiogenesis in brain endothelial cells. *Microvasc. Res.* 82 (2), 113–121. doi:10.1016/j.mvr.2011.06.005
- Zhu, Y., Kalbfleisch, T., Brennan, M. D., and Li, Y. (2009). A MicroRNA gene is hosted in an intron of a schizophrenia-susceptibility gene. *Schizophr. Res.* 109 (1–3), 86–89. doi:10.1016/j.schres.2009.01.022
- Zhuang, S.-F., Liu, D.-X., Wang, H.-J., Zhang, S.-H., Wei, J.-Y., Fang, W.-G., et al. (2017). Atg7 regulates brain angiogenesis via NF-κB-Dependent IL-6 production. *Int. J. Mol. Sci.* 18 (5), 968. doi:10.3390/ijms18050968
- Zoncu, R., Efeyan, A., and Sabatini, D. M. (2011). Mtor: From growth signal integration to cancer, diabetes and ageing. *Nat. Rev. Mol. Cell Biol.* 12 (1), 21–35. doi:10.1038/nrm3025



OPEN ACCESS

EDITED BY
De-Li Shi,
Sorbonne University, France

REVIEWED BY
Suleyman Yildirim,
Istanbul Medipol University, Turkey
James Monaghan,
Northeastern University, United States

*CORRESPONDENCE
Belfran Carbonell-M,
belfran.carbonell@udea.edu.co
Jean Paul Delgado,
jean.delgado@udea.edu.co

SPECIALTY SECTION
This article was submitted to
Morphogenesis and Patterning,
a section of the journal
Frontiers in Cell and Developmental
Biology

RECEIVED 23 April 2022
ACCEPTED 28 July 2022
PUBLISHED 26 August 2022

CITATION
Carbonell-M B, Zapata Cardona J and
Delgado JP (2022), Post-amputation
reactive oxygen species production is
necessary for axolotls
limb regeneration.
Front. Cell Dev. Biol. 10:921520.
doi: 10.3389/fcell.2022.921520

COPYRIGHT
© 2022 Carbonell-M, Zapata Cardona
and Delgado. This is an open-access
article distributed under the terms of the
[Creative Commons Attribution License
\(CC BY\)](https://creativecommons.org/licenses/by/4.0/). The use, distribution or
reproduction in other forums is
permitted, provided the original
author(s) and the copyright owner(s) are
credited and that the original
publication in this journal is cited, in
accordance with accepted academic
practice. No use, distribution or
reproduction is permitted which does
not comply with these terms.

Post-amputation reactive oxygen species production is necessary for axolotls limb regeneration

Belfran Carbonell-M^{1,2*}, Juliana Zapata Cardona³ and
Jean Paul Delgado^{1*}

¹Grupo de Genética, Regeneración y Cáncer, Universidad de Antioquia, Sede de Investigación Universitaria, Medellín, Colombia, ²Departamento de Estudios Básicos Integrados, Facultad de Odontología, Universidad de Antioquia, Medellín, Colombia, ³Grupo de Investigación en Patobiología Quiron, Escuela de Medicina Veterinaria, Universidad de Antioquia, Medellín, Colombia

Introduction: Reactive oxygen species (ROS) represent molecules of great interest in the field of regenerative biology since several animal models require their production to promote and favor tissue, organ, and appendage regeneration. Recently, it has been shown that the production of ROS such as hydrogen peroxide (H₂O₂) is required for tail regeneration in *Ambystoma mexicanum*. However, to date, it is unknown whether ROS production is necessary for limb regeneration in this animal model. **Methods:** forelimbs of juvenile animals were amputated proximally and the dynamics of ROS production was determined using 2',7'-dichlorofluorescein diacetate (DCFDA) during the regeneration process. Inhibition of ROS production was performed using the NADPH oxidase inhibitor apocynin. Subsequently, a rescue assay was performed using exogenous hydrogen peroxide (H₂O₂). The effect of these treatments on the size and skeletal structures of the regenerated limb was evaluated by staining with alcian blue and alizarin red, as well as the effect on blastema formation, cell proliferation, immune cell recruitment, and expression of genes related to proximal-distal identity. **Results:** our results show that inhibition of post-amputation limb ROS production in the *A. mexicanum* salamander model results in the regeneration of a miniature limb with a significant reduction in the size of skeletal elements such as the ulna, radius, and overall autopod. Additionally, other effects such as decrease in the number of carpals, defective joint morphology, and failure of integrity between the regenerated structure and the remaining tissue were identified. In addition, this treatment affected blastema formation and induced a reduction in the levels of cell proliferation in this structure, as well as a reduction in the number of CD45⁺ and CD11b⁺ immune system cells. On the other hand, blocking ROS production affected the expression of proximo-distal identity genes such as *Aldha1a1*, *Rarb*, *Prod1*, *Meis1*, *Hoxa13*, and other genes such as *Agr2* and *Yap1* in early/mid blastema. Of great interest, the failure in blastema formation, skeletal alterations, as well as the expression of the genes evaluated were rescued by the application of exogenous H₂O₂, suggesting that ROS/H₂O₂ production is

necessary from the early stages for proper regeneration and patterning of the limb.

KEYWORDS

axolotl, reactive oxygen species, hydrogen peroxide, blastema, limb regeneration, *Ambystoma mexicanum*, macrophages, immune cells

Introduction

The ability to regenerate structures is widely distributed throughout the animal kingdom including vertebrates and invertebrates (Brockes and Kumar, 2008; Daponte et al., 2021; Elchaninov et al., 2021). Accordingly, understanding the mechanisms underlying this regenerative capacity has become one of the major challenges in developmental and regenerative biology, with the firm purpose of providing new insights and directions for the development of new therapies in the field of regenerative medicine (Brockes and Kumar, 2005; Poss, 2010; Dolan et al., 2018; Iismaa et al., 2018; Arenas Gómez and Echeverri, 2021; Grigoryan, 2021). Within vertebrates, salamanders possess an exceptional ability to regenerate a variety of tissues, organs, and appendages including tail and limbs (Joven et al., 2019). Limb regeneration is a fascinating process and given the complexity of this structure, its regeneration represents one of the main and most conventional models for the study of regenerative response, control of morphogenesis, and final patterning of the regenerated structure (Simon and Tanaka, 2013; Brockes and Gates, 2014; Tanaka, 2016; Dwaraka and Voss, 2019). Among salamanders, Urodeles such as *A. mexicanum* is considered a primary reference model for the study of limb regeneration, given its capacity to regenerate this structure throughout its life (Kragl et al., 2009; Voss et al., 2009, 2015; Haas and Whited, 2017a).

Amputation of a limb in Salamanders including *A. mexicanum* consequently promotes a regenerative response characterized in the first instance by the migration of epithelial cells from the edge of the wound, giving rise to the wound epithelium, which subsequently thickens to form the apical epithelial cap (AEC), which covers the remnant tissue and acts as a signaling center (Tank et al., 1976; Satoh et al., 2012; McCusker et al., 2015; Stocum, 2017; Aztekin, 2021). Simultaneously to the formation of the AEC, other processes such as histolysis and remodeling of the extracellular matrix of the remnant tissue take place, favoring its dedifferentiation, re-entry into the cell cycle, and consequently, the accumulation of progenitor cells (including resident stem cells) between the wound epithelium and the remnant tissue to form the blastema (Tank et al., 1976; McCusker et al., 2015; Voss et al., 2015; Stocum, 2017). Finally, following the growth and patterning of the blastema, a phase of morphogenesis and growth of the regenerating structure takes place to form the lost or amputated limb (McCusker et al., 2015; Voss et al., 2015; Stocum, 2017). During limb regeneration, a wide group of signals

has been identified from the immediate amputation to the formation, growth, and patterning of the blastema, as well as signals involved in the morphogenesis of blastema-derived structures (Yokoyama, 2008; Kumar et al., 2010; Makanae and Satoh, 2012; Tanaka, 2016; Haas and Whited, 2017b; Stocum, 2017). Within these signals, we can mention Bioelectrical signals, TGF β , FGF, SHH, WNT, Retinoic Acid (RA) signaling, and other neurotrophic factors that promote blastema formation and growth, such as n(AG), among others (Borgens et al., 1984; Jenkins et al., 1996; Kawakami et al., 2006; Kumar et al., 2007, 2010; Satoh et al., 2011; Makanae et al., 2014; Nacu et al., 2016; Wischin et al., 2017; Vieira et al., 2019; Maden, 2020; Sader and Roy, 2021). However, other signaling mechanisms are subject to future studies to determine their potential requirement during limb regeneration.

Interestingly, although reactive oxygen species (ROS) have been listed as deleterious molecules for cellular and tissue homeostasis, today they represent molecules of great interest in the field of developmental biology and regeneration, given their capacity to regulate events such as apoptosis, migration, cell proliferation, and differentiation, among other cellular processes (Covarrubias et al., 2008; Hernández-García et al., 2010; Meda et al., 2018; Rampon et al., 2018; Sies and Jones, 2020a). Notably, ROS can regulate the activity of various molecules including transcription factors and kinases (Marinho et al., 2014; Sies, 2017; Rhee et al., 2018)). Previous studies have identified ROS production as a pro-regenerative signal post-amputation of various structures in both vertebrates and invertebrates (Pirotte et al., 2015; Rampon et al., 2018). In vertebrate models, ROS have been extensively involved in the regeneration of appendages such as tail in Gecko (Zhang et al., 2016), tail fin in zebrafish (Yoo et al., 2012; Gauron et al., 2013; Romero et al., 2018; Thauvin et al., 2022), and tail regeneration in *Xenopus* (Love et al., 2013; Ferreira et al., 2016, 2018). Of great interest, in several of these models, it has been evidenced that ROS regulate the activity of signals such as Wnt, Fgf, Shh, and kinases which are described as necessary signals for limb regeneration (Yoo et al., 2012; Love et al., 2013; Romero et al., 2018; Thauvin et al., 2022). In salamanders, studies performed in axolotl embryos show that ROS are necessary for tail regeneration (Al Haj Baddar et al., 2019). In addition, we have recently identified that ROS, particularly H₂O₂, promotes tail regeneration in juvenile axolotls by regulating blastema formation and growth through activation of the transcriptional co-activator of the Hippo signaling pathway, Yap1, as well as regulating *Agr2* expression and AKT kinase

activation (Carbonell et al., 2021). Of great interest, a recent study in *Xenopus* shows that ROS production induced by melanocortin receptor 4 (*Melanocortin four receptor (Mc4r)*) is necessary to promote limb regeneration (Zhang et al., 2018). However, to date, it is unknown whether ROS production is necessary for axolotl limb regeneration.

Therefore, considering the background of ROS during appendage regeneration in different species, particularly, its implication during tail regeneration in the *A. mexicanum* model, and considering the need to identify whether this signaling mechanism is conserved during regeneration of other structures in this animal model, our aim was to evaluate whether ROS-mediated redox signaling is necessary during axolotl limb regeneration.

Here we show for the first time that post-amputation ROS production is necessary for proper limb regeneration in the *A. mexicanum* model. Thus, ROS production, particularly H_2O_2 is required for blastema formation and growth, and blocking NADPH oxidases (NOXs)-dependent ROS production induces regeneration of a miniaturized limb. Additionally, as a first approach to the function of ROS during limb regeneration, it was observed that ROS regulate the expression of several proximal-distal identity genes such as *Meis1*, *Meis2*, *Prod1*, *Hoxa13*, *Aldh1a1*, *Rarb* and other genes such as *Agr2* and *Yap1* during blastema formation. In addition, ROS were necessary to promote the recruitment of CD45⁺ leukocytes and CD11b⁺ monocytes/macrophages, as well as their phagocytic activity. These results suggest a potential regulation and interaction between ROS production and these signaling pathways during *A. mexicanum* limb regeneration.

Materials and methods

Animal handling and ethical aspects

Leucistic Juvenile axolotls (10 cm snout to tail) were used for this research. Animals were obtained from the *Ambystoma* Genetic Stock Center (AGSC) of the University of Kentucky and bred at the SIU (Sede de Investigación Universitaria) of the University of Antioquia, Colombia. All animals were maintained under the same conditions and fed ad libitum with protein pellets at a temperature between 19 and 21°C in 20% Holtfreter's solution. The animal experimentation procedures were previously approved by the Ethics and Animal Experimentation Committee of the University of Antioquia under the animal experimentation protocol registered in Acta No. 121.

Limb amputation surgery and regeneration assays

Juvenile axolotls were anesthetized by immersion in 0.1% ethyl-3-aminobenzoate methanesulfonate (Sigma Aldrich, Louis, MO) dissolved in 20% Holtfreter's solution for all surgical

procedures. Bilateral proximal forelimb amputations were performed at the medial humerus level with microsurgical scissors and the protruding bone tissue was regularized with iridectomy scissors to promote proper wound epithelium formation as previously suggested (Kragl and Tanaka, 2009; Arenas Gómez et al., 2017a). Subsequently, the animals were placed in their respective treatments and, once the treatments were completed, they remained in a 20% Holtfreter solution. Each limb was photographed under the same magnification parameters for each of the experimental groups using a stereomicroscope (Olympus SZ×16, Tokyo, Japan) with a digital camera (MotiCAM 5, Kowloon, Hong Kong) pre-amputation, immediate post-amputation, and during the time course of regeneration. The size of the blastema and the regenerated limb was obtained by using Motic Images Plus software (Version 2.0, Kowloon, Hong Kong). Blastema size was determined by subtracting the size of the post-amputation remnant tissue from the distance obtained from the most distal and medial point of the blastema to the most proximal region of the limb at 11, 14, and 21 dpa. The size of the regenerated limbs was determined by subtracting the size of the post-amputation remnant from the distance obtained from the most proximal region of the humerus to the elbow and from the elbow to the most distal point regenerated the second digit at 62 dpa.

Reactive oxygen species detection

In vivo detection of ROS production was performed using 2',7'-dichlorofluorescein diacetate (H_2DCFDA , Sigma). Animals were incubated for 2 h in 50 μM of H_2DCFDA in a dark environment before image acquisition by confocal microscopy as previously described (Carbonell M et al., 2021). Subsequently, animals were immersed in 40% Holtfreter solution to remove excess H_2DCFDA and anesthetized in 0.1% ethyl-3-aminobenzoate methanesulfonate (Tricaine) for image acquisition. The animals used for each point were different and were not reused for subsequent analyses. In this way, the potential accumulation of DCFDA residues that could interfere with subsequent detections of ROS production was avoided. Fluorescence generated by oxidation of H_2DCFDA was acquired on a confocal microscope (Olympus FV1000 MPE, FV10-ASW software) using the mosaic stitching tool given the size of the limb area to be imaged. Samples were excited with a 488 nm laser and the emitted fluorescence was detected using a 520/39 nm filter. Given the thickness of the samples and the difficulty that this can generate to detect the global fluorescence in each sample, a semiquantitative approximation of fluorescence intensity with ImageJ software according to previous studies was performed (Schneider et al., 2012; Jensen, 2013). Thus, a region of interest (ROI) was determined for each acquired image. The area of interest extended from the most distal point of the regenerated tissue to 500 μm proximal to the amputation

plane. The intensity of the gray pixels was measured, and the background was subtracted according to previous studies (Schneider et al., 2012; Jensen, 2013; Al Haj Baddar et al., 2019). The gray intensity obtained for each day assessed was compared with pre-amputation levels using a one-way ANOVA and a Tukey's post hoc analysis between each point assessed was performed to determine differences between these. In addition, fluorescence levels obtained for animals in the control group (0.1% DMSO) and exposed to NOX inhibitors (400 μ M apocynin) were compared using Student's t-test. An $n = 6$ was used for each point, and a p -value < 0.05 was considered statistically significant.

Chemical inhibition of NOX activity and rescue treatment by exogenous H_2O_2 during axolotl's limb regeneration

For all the tests, the experimental groups remained submerged in each treatment for 1 h before amputation. After the amputation process, animals were incubated in 400 μ M apocynin (NOX activity inhibitor, Santa Cruz, SC-203321) for incremental time intervals of 0 dpa - 3 dpa and 0 dpa - 11 dpa. Apocynin inhibits the production of ROS by blocking the formation of the NOX complex (Stefanska and Pawliczak, 2008). Control animals were incubated in 0.1% DMSO for the same time intervals. For the rescue assay, after amputation, animals were incubated from 0 dpa to 11 dpa in 400 μ M apocynin combined with 50 μ M H_2O_2 . For the rescue group, a control group exposed to the same concentration of H_2O_2 in the absence of the inhibitor was included. A $n = 10$ animals group was used for each experimental group. Each treatment was changed every 24 h. The size of the regenerated structure was evaluated at 72 dpa and the values obtained were compared by one-way ANOVA and Tukey's post-hoc analysis to establish the differences between each group evaluated. Similarly, blastema size at 11, 14, and 21 dpa was compared between each group evaluated. A value of $p < 0.05$ was considered statistically significant.

Histology and immunofluorescence

Regenerated tissues were collected at 11 dpa for histological analysis and stained with Hematoxylin-Eosin (H-E) to evaluate blastema formation and immunofluorescence for cell proliferation assay. Similarly, regenerated limbs were analyzed histologically by H-E staining and Masson's Trichrome staining at 72 dpa for identification of regenerated tissues including the joint between the stylopod and zeugopod.

After tissue collection, tissues were fixed in 4% paraformaldehyde for 24 h and embedded in paraffin. Subsequently, 5 μ m histological sections were stained with

H-E or Masson's Trichrome stain to evaluate the effect of the different experimental conditions. For immunofluorescence, blastemas at 11 dpa from control animals in 0.1% DMSO, exposed to 400 μ M apocynin and from the rescue assay group (50 μ M H_2O_2 + 400 μ M apocynin) were collected. Briefly, tissues were fixed in 4% PFA for 24 h, embedded in paraffin, and 5 μ m histological sections were made on a microtome. Histological sections were deparaffinized, rehydrated, postfixed in 4% PF4 for 5 min, and washed 3 times for 5 min in 1X TBST (1X Tris-buffered Saline, 0.1% Tween 20). All sections were incubated in blocking solution (10% fetal bovine serum in 1X TBST) for 3 h at room temperature and then incubated with anti-BrdU primary antibody (1:500) diluted in blocking solution at 4°C overnight. The next day, histological sections were washed with 1X TBST and incubated with anti-mouse Alexa fluor 594 secondary antibody (1:200, Abcam #ab 150120). To detect leukocyte recruitment direct immunofluorescence was performed using anti-CD45 FITC Mouse anti-CD45 (1:500, BD Pharmingen), additionally direct immunofluorescence against CD11b was performed using APC mouse anti-CD11b (1:1,000, Invitrogen ref 17-0118-42) to detect monocytes/macrophages. Finally, nuclear counterstaining was performed with Hoechst, and photographs were acquired on an AXIO Vision Zoom V16 stereomicroscope (Carl Zeiss) using ZEN software. An $n = 5$ was used for each group.

In vivo BrdU labeling assay

5-Bromo-2-deoxyuridine (BrdU) (Sigma, United States) was used as an S-phase proliferative marker during blastema formation. Control animals exposed to 0.1% DMSO ($n = 5$), animals exposed to 400 μ M apocynin inhibitor treatment, and animals exposed to rescue treatment (50 μ M H_2O_2 + 400 μ M apocynin) were injected with BrdU intraperitoneally (0, 4 mg/g body weight) in two pulses (24 and 48 h before blastema tissue collection) at 9 dpa and 10 dpa according to Arenas et al and Carbonell et al (Arenas Gómez et al., 2017b; Carbonell et al., 2021). Blastema tissues collected at 11 dpa were processed for immunofluorescence as described in the previous item "histology and immunofluorescence". A total of five to six histological sections were analyzed for each replicate. The percentage of BrdU-positive cells was determined by dividing the number of BrdU-positive cells by the number of Hoechst-labeled nuclei.

Skeletal preparations

To visualize skeletal structures, alcian blue and alizarin red staining was performed as previously described (Depew, 2008). Whole limbs were fixed in 4% PFA in 1X PBS for 48 h. Subsequently, the samples were washed in distilled water for 24 h, with water replacement every 8 h. Carefully, skin and

muscle tissue were removed with dissecting forceps. The samples were then immersed in 0.3% alcian blue solution for 48 h at 37°C, rehydrated in ethanol series (75%, 40%, and 15%), and washed in distilled water for 2 h. Then, the samples were left in 1% trypsin/sodium borate solution for 24 h and exposed to 0.5% alizarin red/KOH solution for 24 h. Finally, washings were performed with 0.5% KOH, clearing over the next several days by carrying through a 1% KOH/glycerol solution for 24 h at 3:1, 1:1, and 1:3 ratios, and the samples were left in 87% glycerol for photography. Photographs were acquired using stereomicroscopy (Olympus SZX16, Tokyo, Japan) with a digital camera (MotiCAM 5, Kowloon, Hong Kong). Measurements of skeletal structures were performed using Motic Images Plus software (Version 2.0, Kowloon, Hong Kong).

Phagocytic activity

For the evaluation of phagocytic activity, live neutral red staining was used according to previous studies (Herbomel et al., 2001; Godwin et al., 2013; Franklin et al., 2017). Neutral red stains phagocytic cell populations and has a high affinity for macrophages. This method has been used with great efficiency to label macrophages in zebrafish as well as to identify macrophage phagocytic activity during tail and limb regeneration in *A. mexicanum* (Herbomel et al., 2001; Godwin et al., 2013; Franklin et al., 2017). The animals were immersed in neutral red solution 5 µg/ml in Holtfreter's solution for 6 h. Subsequently, the animals were left for 24 h in Holtfreter's solution to destain them. Finally, the animals were photographed under a brightfield stereomicroscope with prior anesthesia. Counting of cells per unit area (1mm²) was performed using ImageJ.

RNA extraction and RT/Q-PCR

Total RNA was isolated from limb blastema at 11 dpa using Trizol reagent (Ambion, 15,596-026) according to the manufacturer's protocol. Subsequently, cDNA was synthesized using the RevertAid H minus Strand cDNA Synthesis kit (Thermo Scientific #K1632) from 500 ng of total RNA, pretreated with RNase-free DNase I. The cDNA was diluted 1:10 before qPCR assays. The q-PCR reactions were performed using iQ SYBER Green supermix and an iCycler iQTM detection system (Bio-Rad). Gene expression levels were normalized to endogenous 18S reference gene expression as previously reported (Zhu et al., 2012). Three independent experiments ($n = 3$) with respective biological replicates ($n = 3$) and technical triplicates for each experimental point and condition were performed. In addition, negative controls without the first cDNA strand were performed for each gene evaluated. Gene expression levels were calculated by the comparative CT ($2^{-\Delta\Delta CT}$)

method (Schmittgen and Livak, 2008) and between-group comparisons were performed by one-way ANOVA and Tukey's post-hoc. The sequences of the primers are listed in Table 1 together with the respective reference where they were previously described. All protocols and information necessary for the reproducibility of the experiments will be available to all interested researchers upon request.

An illustrative diagram of the Overall experimental design is presented (See Supplementary Figure S1)

Results

ROS production during axolotl limb regeneration

As a first step to identify whether ROS are necessary during limb regeneration, we set out to characterize the dynamics of ROS production during the regeneration of this structure using 2',7'-dichlorofluorescein diacetate (DCFDA). Following limb amputation, at 1 dpa high levels of ROS were detected at the level of the amputation plane and remnant tissue (Figure 1A). ROS production was confined to the *epidermis* covering the wound. These levels increased at 2 dpa maintaining the same localization pattern; however, at 3 dpa and 5 dpa ROS production decreased and ROS production remains localized in the wound epithelium. (Figures 1A,B). At 7 dpa, a new increase in ROS production was detected in the area circumscribed to thickened epithelium covering the wound now called the apical epithelial cap (AEC). These levels were maintained between 9 and 11 dpa when blastema formation takes place. At 9 dpa ROS remained in the AEC and at 11 dpa, in addition to localization in the AEC, signals are detected in presumptive blastema cells (Figure 1A). Finally, ROS levels decreased at 18 dpa reaching basal levels at 21 dpa (Figures 1A,B). Although ROS levels are less detectable at 18 dpa, ROS can be detected in both AEC and presumptive blastemal cells. Fluorescence semiquantification shows that ROS production was detected for at least 18 dpa (Figure 1B). These results indicate that limb amputation significantly induces substantial ROS production during the first 2 weeks post-amputation suggesting a potential role of these molecules during limb regeneration both in the early stages of the regenerative response up to blastema formation and growth.

NOXs-dependent ROS production is required for proper limb regeneration and exogenous H₂O₂ rescues limb regeneration impaired by NOX inhibition

To evaluate the requirement of ROS during limb regeneration, we blocked the activity of NOXs using the inhibitor apocynin. Considering the ROS production

TABLE 1 List of primers used for Q-PCR.

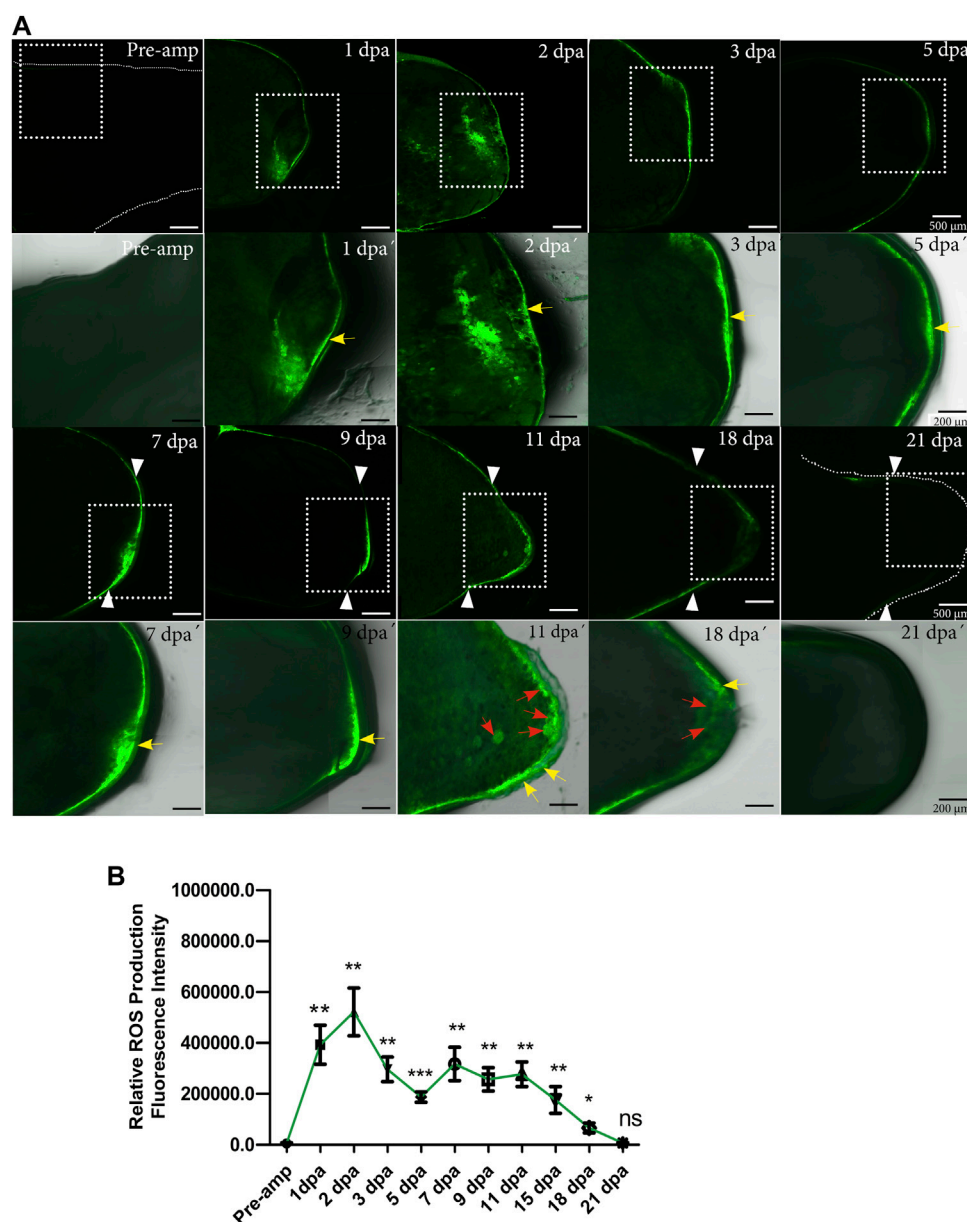
Gen	Forward 5'-3'	Reverse 5'-3'	References
<i>Meis1</i>	CCATCTACGGACACCCCT	GGAAGAACACACGTCCCG	Mercader et al. (2005)
<i>Meis2</i>	AGTGGAGGGACGCTTCT	GCTTCTTGCTTTGTCCGGT	Mercader et al. (2005)
<i>Hoxa13</i>	TCTGGAAGTCTCTCTGCCG	TCAGCTGGACCTTGGTGACG	Mercader et al. (2005)
<i>Prod1</i>	GGTGGCAGTGAGCACAGGT	TGGCATTCTGTATCAGAGT	Shaikh et al. (2011)
<i>RARA</i>	ATACTTGGCAGCCAGAAGGT	GCCAACGTTGTATGCATCTC	Nguyen et al. (2017)
<i>RARB</i>	AAAACCTCTGAGGGGCTTGAA	CTGGTGTGGATTCTCCTGTG	Nguyen et al. (2017)
<i>RARG</i>	CTTCTGCGTTTGATCCTTCA	AGTGAGTATGGGGCTGTTC	Nguyen et al. (2017)
<i>Aldh1a1</i>	AAGACATCGACAAGGCACTG	CCAAAGGACACTGTGAGGA	Nguyen et al. (2017)
<i>Aldh1a2</i>	GCCAAGACGGTCACAATAAA	CATTCTGAGTGCTGTTGCT	Nguyen et al. (2017)
<i>Yap1</i>	TACCATACCTTCCCAACAAACC	TACATTCATTGCTTCTCCGTCT	(Carbonell M et al., 2021)
<i>Agr2</i>	GCTTTCAACAAACACCTTCTTCA	CCTCCACAGAGCCCAGAC	(Carbonell M et al., 2021)
<i>18S</i>	AGGCCCTGCCTGCC	TTACGCTACCTTGCACGGTC	Zhu et al. (2012)

dynamics characterized above, animals were exposed to 400 μ M apocynin and the resulting phenotype was evaluated at 72 dpa. Initially, considering that early blockade of post-amputation tail and caudal fin ROS production in zebrafish larvae and adult animals as well as in *Xenopus* tails and *A. mexicanum* affects the regeneration of these appendages (Gauron et al., 2013; Love et al., 2013; Tauzin et al., 2014; Al Haj Baddar et al., 2019; Carbonell M et al., 2021), we hypothesized that given this background and early detection of post-amputation limb ROS production, ROS blockade of 0 dpa-3pa would generate some perturbation in limb regeneration in *A. mexicanum*. The animals were incubated in apocynin from 0 to 3 dpa corresponding to the first wave of ROS production; however, the animals regenerated their limbs correctly, without any alteration (See Supplementary Figure S2). Subsequently, it was decided to increase the apocynin inhibitor exposure interval from 0 to 11 dpa, covering the second wave of ROS production according to the ROS production dynamics (Figure 1B) and to previous studies showing that extended blockade of ROS production impacts later events during appendage regeneration (Gauron et al., 2013; Love et al., 2013; Carbonell M et al., 2021). The results show that animals exposed to the inhibitor regenerated limbs of reduced size, resembling a miniature structure when compared to control animals exposed to 0.1% DMSO (Figures 2A,B). Additionally, the external morphology of the limbs of apocynin-treated animals showed no apparent intersegmental boundary between the regenerated autopod, zeugopod and stylopod (Figure 2A).

Considering that H_2O_2 is one of the main products of NOXs activity and one molecule involved in ROS-mediated redox signaling and that in a previous study we have shown that H_2O_2 is required for tail regeneration in *A. mexicanum* (Carbonell M et al., 2021), this prompted us to perform a rescue assay using 50 μ M H_2O_2 in combination with the inhibitor apocynin from 0 dpa to 11 dpa. The results show

that exogenous H_2O_2 allows to rescue the phenotype generated by the inhibition of NOXs activity (Figures 2A,B). The regenerated limb in the rescue group presents a larger size compared to animals treated only with the inhibitor apocynin and present an external morphology like that observed in controls exposed to DMSO 0.1%, without apparent syndactyly or supernumerary digits (Figures 2A,B). Animals exposed to exogenous H_2O_2 + 0.1% DMSO showed no differences when compared to controls in 0.1% DMSO, indicating that the animals can tolerate this concentration of H_2O_2 without affecting the regeneration process (Figures 2A,B). To evaluate whether the defects observed in animals exposed to the inhibitor were permanent, re-amputation of the affected limbs was performed. After re-amputation, the limbs regenerated similarly to controls exposed to 0.1% DMSO (Figures 2A,B). This indicates that the defects generated were the result of transient inhibition of ROS production and that the remaining tissues still retain the ability to induce a regenerative response.

On the other hand, to evaluate whether the regenerated limb with miniature appearance was due to an apparent delay in the speed of the regenerative process post-exposure to the inhibitor, a group of animals exposed to apocynin was evaluated at a longer time corresponding to 124 dpa (approximately twice the time initially evaluated). The results show that this additional time was not sufficient for the miniature limbs to reach a similar size to the controls in DMSO and the rescue group evaluated at 72 dpa (Figures 2A,B). These results suggest that early-stage ROS production potentially influences the determination of the final size of the regenerated structure. Additionally, to ratify that the phenotype observed post apocynin treatment was a product of decreased ROS production, post apocynin treatment, the ROS levels were quantified from 0 dpa to 11 dpa. The results show a significant reduction in ROS levels when compared to the control group (Figure 2C).

**FIGURE 1**

ROS production during limb regeneration in *A. mexicanum*. **(A)** representative images of ROS production acquired by confocal microscopy. The pre-amputation image represents the medial area of the non-amputated humerus (basal level of ROS production). ROS production was detected at the amputation plane at 1, 2, 3, and 5 dpa. At 7 dpa and 9 dpa ROS was detected in the apical epithelial cap (AEC) and at 11 dpa in the AEC and developing blastema region. White arrowheads represent the amputation plane. A white box with a dashed line is shown at higher magnification in lower panel images acquired with differential interference contrast (DIC) in conjunction with fluorescence images for anatomical details. Yellow arrows indicate epithelial localization of ROS and red arrows localization in blastema cells. **(B)**, Semi-quantification of relative fluorescence intensity. Fluorescence levels show two apparent waves of ROS production between 1 dpa and 3 dpa for the first wave, and between 7 and 15 dpa, for the second wave of ROS production. One-way ANOVA with a Tukey post-hoc was performed to compare each point with basal levels of pre-amputation ROS production ($n = 10$ for each point, 5 animals per point). Data are expressed as mean \pm SEM (mean standard error). *** $p < 0.001$, ** $p < 0.01$, * $p < 0.05$.

Finally, to confirm whether the rescue effect observed in the treatments from 0 to 11 dpa was due to H_2O_2 as such and not to potential interference between H_2O_2 and apocynin, we performed another new rescue assay. Thus, we treated two

groups of animals with apocynin from 0 to 11 dpa and withdrew the apocynin treatment. Subsequently, one of these groups previously treated with apocynin was treated with 50 μM exogenous H_2O_2 for 7 days until 18 dpa and the

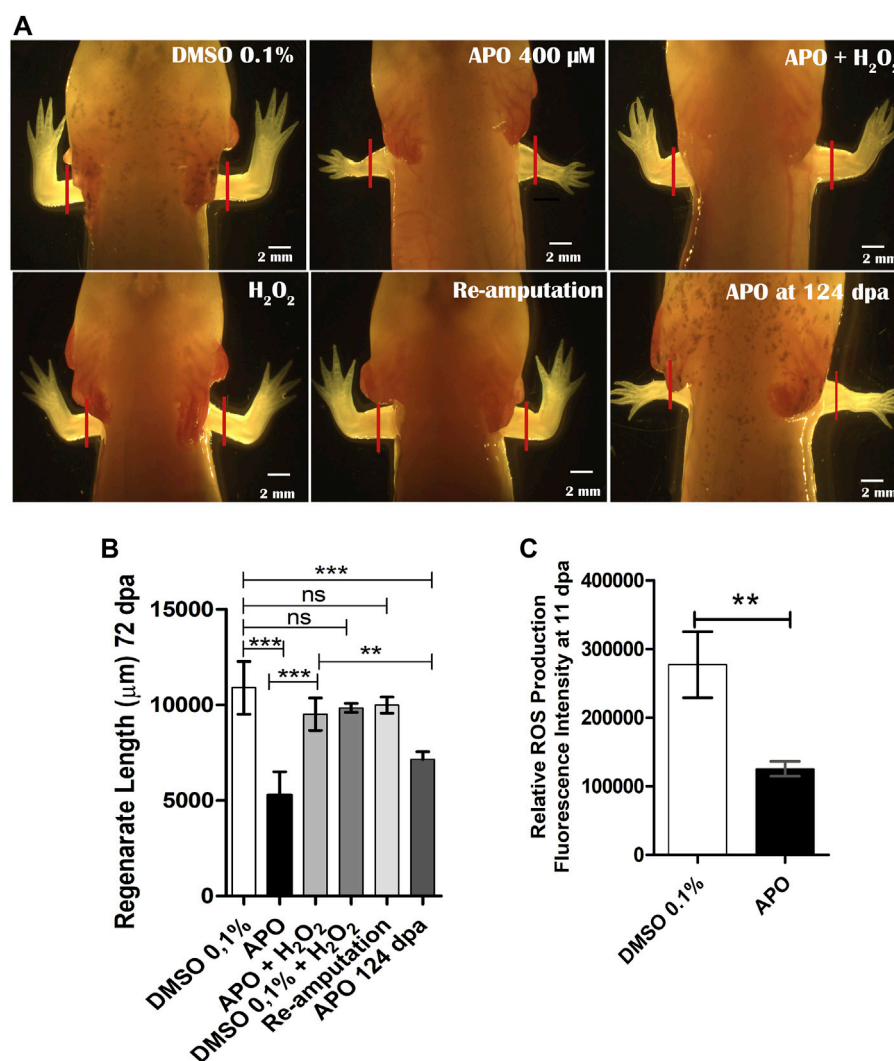


FIGURE 2

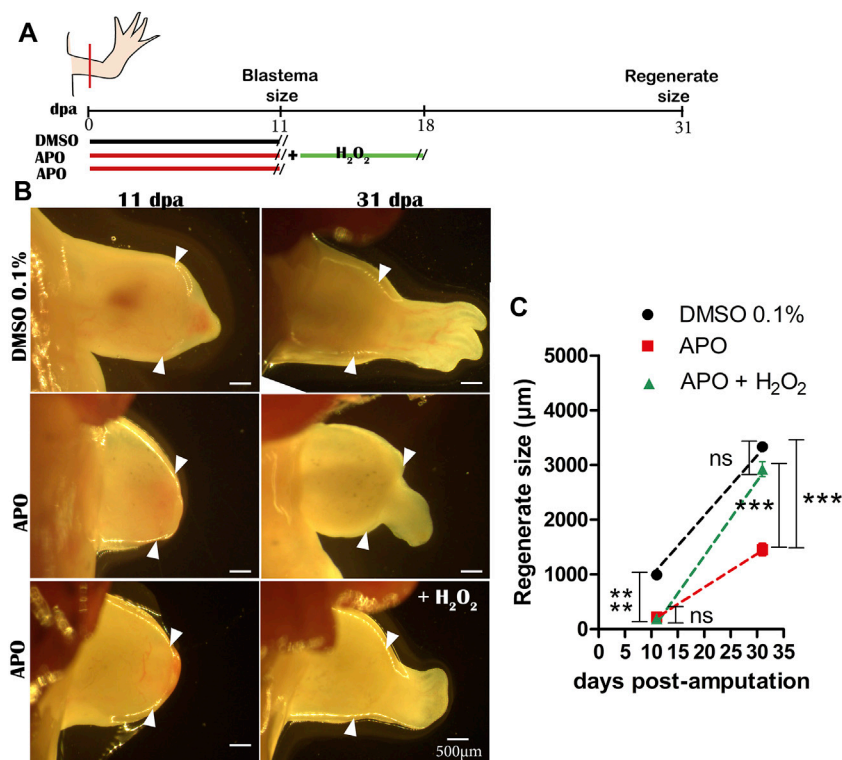
Blocking ROS production by apocynin affects limb regeneration in *A. mexicanum*. **(A)**, Representative images of animals exposed to different treatments compared to the control group in 0.1% DMSO. Defects generated by inhibition of NOX activity and rescue treatments (apocynin 400 μ M + H_2O_2) are shown. Solid red lines represent the amputation plane. **(B)**, Quantification of regenerated limb size at 72 dpa. Apocynin-exposed group evaluated at 124 dpa was included. One-way ANOVA and post-hoc Tukey were performed to compare the evaluated groups ($n = 10$ per group). **(C)**, Semi-quantification of ROS levels post-exposure to apocynin inhibitor ($n = 7$). ROS levels decrease significantly under inhibitory treatment. Student's t-test was performed to compare the two groups. Data are expressed as mean \pm SEM. *** $p < 0.001$, ** $p < 0.01$, * $p < 0.05$.

other group was not treated at all (Figure 3A). At 31 dpa, we were able to determine that the treatment with 50 μ M exogenous H_2O_2 effectively promoted a rescue effect on the regenerating structure in contrast to the group not exposed to this treatment, which presented an apparent delay in digit formation and a reduction in the size of the regenerate (Figures 3B,C). This confirms that the rescue effect previously observed when apocynin was administered simultaneously with exogenous H_2O_2 was due to the effect of exogenous H_2O_2 , and not to interference with the inhibitor apocynin (see new

Figure 3). This latter result suggests that exogenous H_2O_2 can regulate the regenerative response.

Exogenous H_2O_2 rescues skeletal alterations generated by blocking NOX-dependent ROS production

Given our previous observations regarding the post-inhibition effect of ROS production on the size and external morphogenesis of regenerated limbs, we proceeded to perform

**FIGURE 3**

Exogenous H₂O₂ induces a rescue effect on the regenerating structure. **(A)** Illustrative scheme of the rescue assay performed. **(B)** Representative images of regenerating tissues at 11 and 31 dpa of controls in 0.1% DMSO, inhibitory treatments with apocynin and without rescue, and inhibitory treatments rescued with exogenous H₂O₂. **(C)** Quantification of regenerate size at 31 dpa. White arrowheads represent the amputation plane. One-way ANOVA and post-hoc Tukey were performed to compare the evaluated groups ($n = 10$ per group). Data are expressed as mean \pm SEM. *** $p < 0.001$, ** $p < 0.01$, * $p < 0.05$.

a skeletal analysis using alcian blue and alizarin red staining. The results showed that animals exposed to apocynin inhibitor from 0 to 11 dpa regenerated the skeletal structures that make up the stylopod (humerus), zeugopod (radius and ulna), and autopod (carpal bones, metacarpals, and phalanges) with a discernible number of four digits (Figure 4A). However, it can be globally identified that the skeleton of the regenerated limb shows a size reduction, recapitulating the external phenotype of a miniature limb described above (Figure 2A). Of great importance, treatment with exogenous H₂O₂ was able to rescue the size of the skeleton affected by the inhibition of ROS production, generating a phenotype like that observed in the control group (Figure 4A). A discriminative analysis for each skeletal structure shows that treatment with apocynin generated a proximal-distal reduction in the size of the humerus, radius, ulna, and zeugopodium when compared to the control group in 0.1% DMSO (Figures 4B–E). Similarly, it was identified that the application of exogenous H₂O₂ peroxide significantly rescued the size of the affected skeletal structures (Figures 4B–E). These results suggest that redox signaling mediated by ROS/H₂O₂ production during the early stages

of limb regeneration is necessary to regulate the size of regenerated skeletal structures.

On the other hand, it was identified that inhibition of NOXs activity resulted in a decrease in the number of carpals in 70% of the animals treated with the inhibitor, compared to the controls in 0.1% DMSO, in which a decrease in the number of carpals was identified in 10% of these animals (less than 8 carpals was considered as a reduction in the number of these structures). Of great interest, only 30% of the animals treated with exogenous H₂O₂ showed a decrease in the number of carpals, indicating rescue of the phenotype generated by the inhibition of NOXs activity (Figures 4F,G). Additionally, the treatments of the control group exposed to 0.1% DMSO + exogenous H₂O₂ did not differ from the control group exposed only to 0.1% DMSO, confirming that the concentration of H₂O₂ used does not affect the regeneration process (Figures 4A–G). These results suggest that the inhibition of ROS/H₂O₂ production not only affects the proximal-distal size of the regenerate but also disturbs the number of skeletal elements of the autopodium.

Additionally, we observed that the group of animals treated with the inhibitor apocynin presented failure in the integration

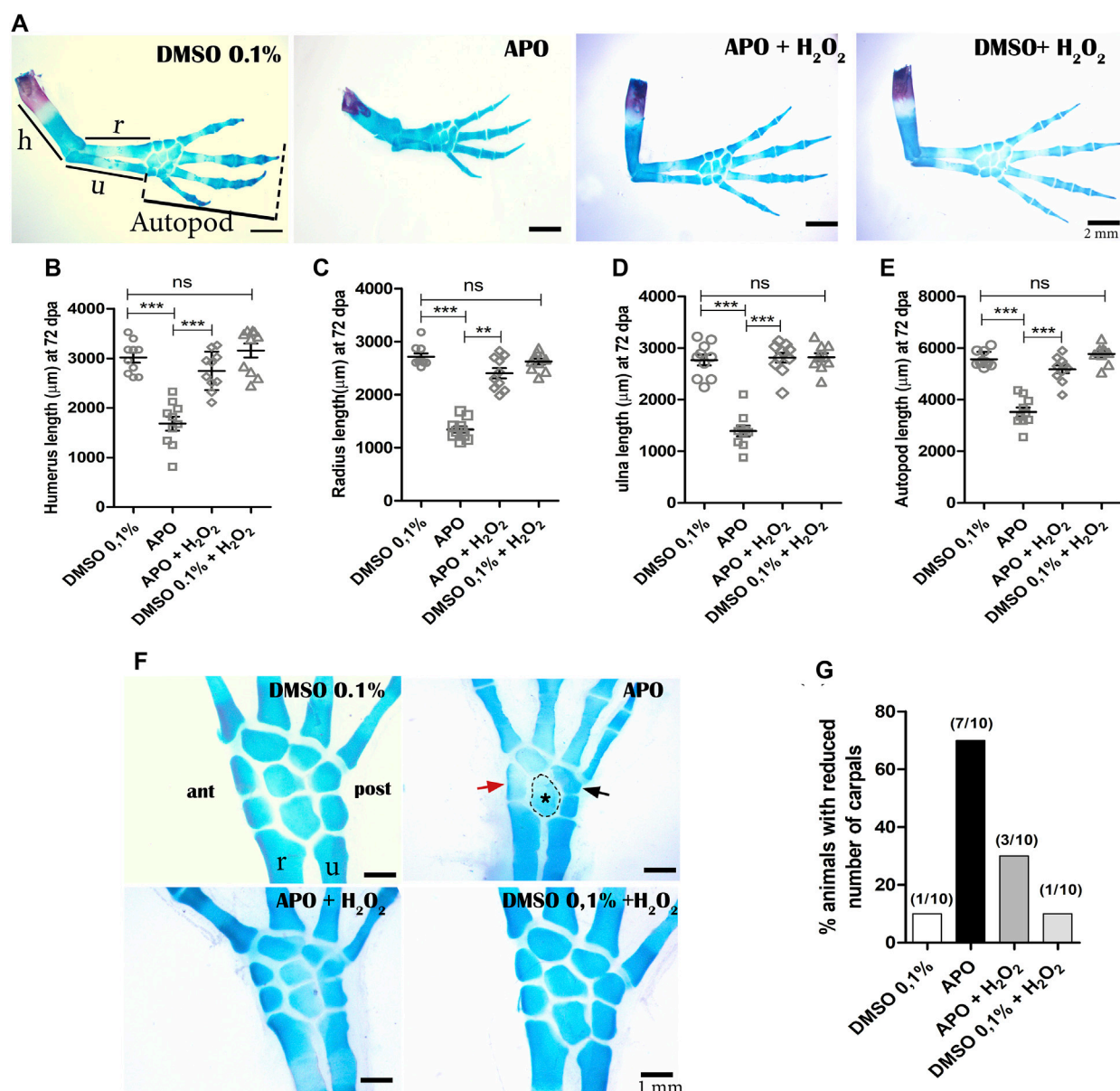


FIGURE 4

Inhibition of NOXs activity reduces the size of the regenerated skeleton and induces a decrease in the number of carpal bones in *A. mexicanum* at 72 dpa. (A), Representative images of the treatments evaluated. The skeleton of apocynin (APO)-treated limbs confirms a miniature limb phenotype. Treatments with exogenous H_2O_2 partially rescue the phenotype generated by NOXs inhibition. (B–E), Quantification of the skeletal elements of the stylopod (humerus), zeugopod (radius and ulna), and autopod (carpals, metacarpals, and phalanges). One-way and post-hoc Tukey ANOVA was performed to compare the evaluated groups ($n = 10$ per group). (F), inhibition of ROS production by APO generated a decrease in the number of carpal bones (5 animals had only 5 carpal bones and 2 animals had six carpal bones out of 10 animals evaluated). Red arrow, black arrow and dotted circle indicate apparent ectopic fusions in anterior (ant), posterior (post), and intermediate carpal, respectively. (G), Percentage of animals with reduction in the number of carpal bones observed in the different experimental groups. h, humerus; r, radius; u, ulna. Data are expressed as mean \pm SEM. *** $p < 0.001$, ** $p < 0.01$, * $p < 0.05$.

between the regenerated skeletal tissue and the remaining skeletal tissue compared to the control group in 0.1% DMSO (Figures 5A–C). For better identification of this defect by using alcian blue and alizarin red staining, we identified a region that we called the “area of integration (ai)”, which corresponds to the area where the

regenerated skeletal tissue integrates with the remnant tissue (junction between the most proximal region of the regenerated humerus and the distal region of the remnant humerus) (Figure 5A). Control animals in 0.1% DMSO show an area of integrity characterized by continuity between the remnant

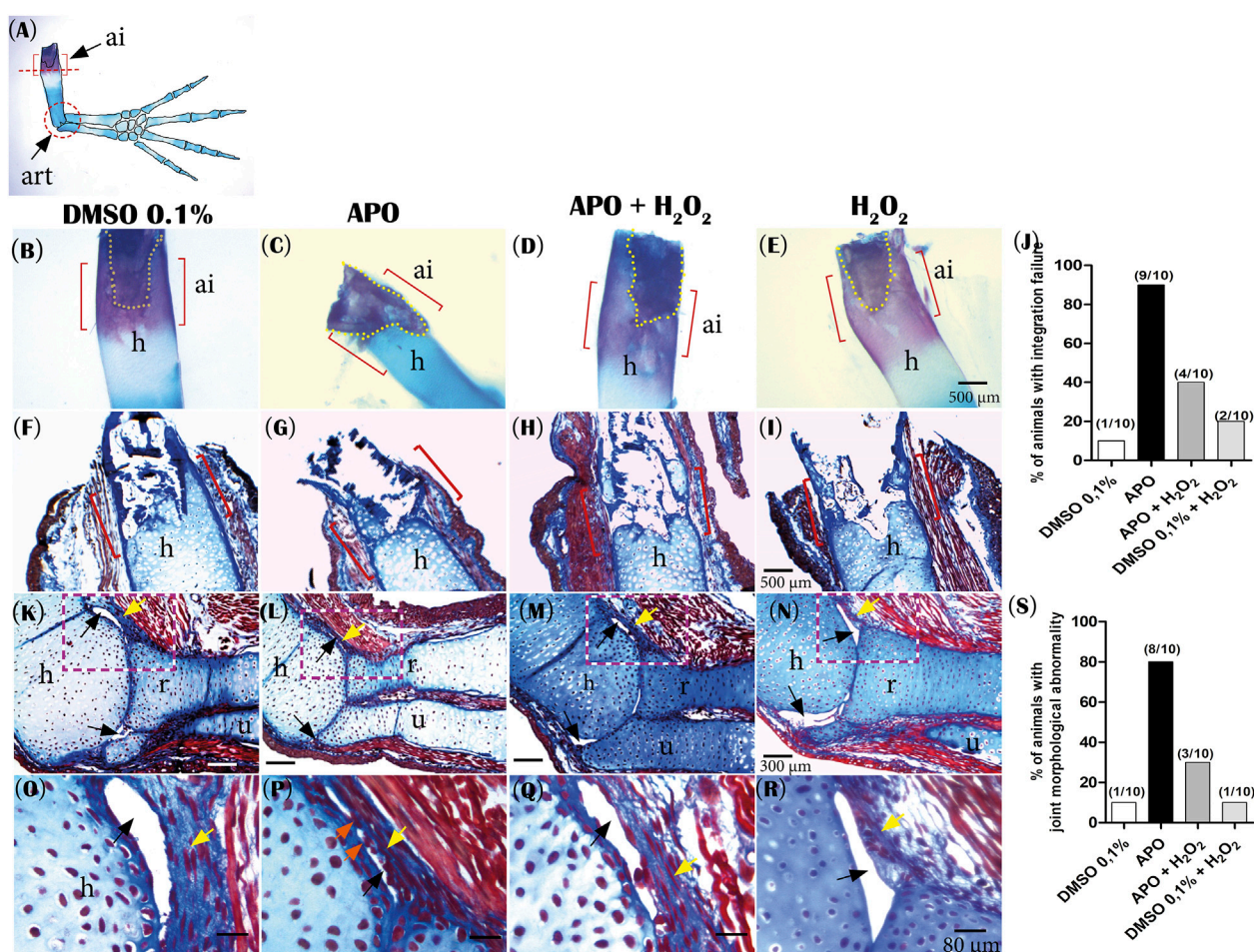
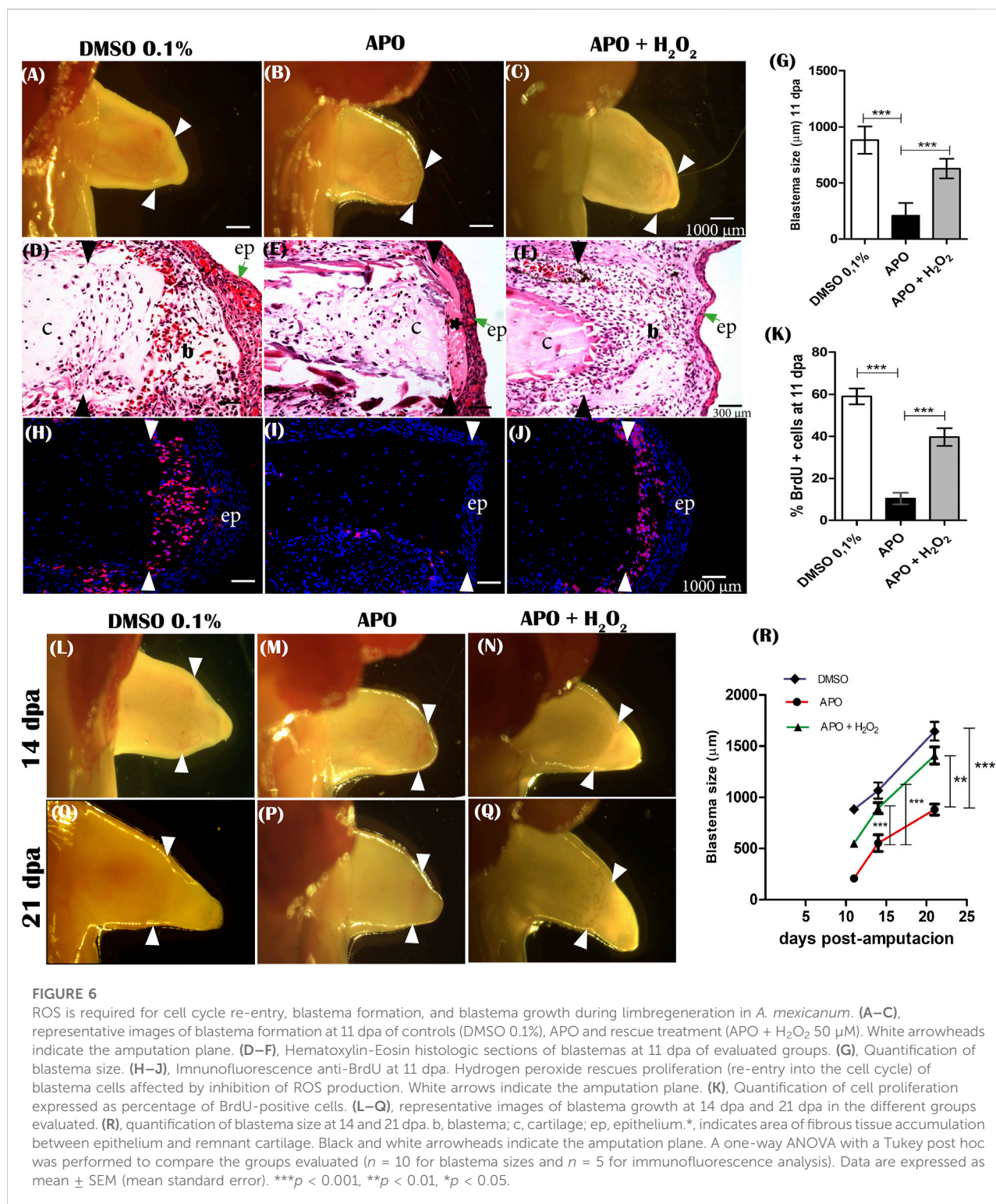


FIGURE 5

Inhibitory treatment of NOXs-dependent ROS production affects the integration of the regenerated skeleton and joint morphology in *A. mexicanum* at 72 dpa. (A), Illustration of the areas of interest evaluated: ai (integration area) delimited with red brackets. The red circle indicates the joint area studied. (B–E), representative images of the experimental groups evaluated by alcian blue and alizarin red staining: Controls in 0.1% DMSO, apocynin (APO) treatment, rescue assay (APO + H₂O₂) and control exposed to 0.1% DMSO + 50 μ M H₂O₂. Yellow dotted lines indicate remnant bone tissue. (F–I), Histological sections with Masson's trichrome staining at 5 μ m. (F), shows continuity between the regenerated humerus and remnant skeletal tissue in the "ai". (G), the integration area shows discontinuity between the regenerated and remnant humerus. (H), application of exogenous H₂O₂ rescues the phenotype affected by ROS inhibition. (I), Control animals exposed to 0.1% DMSO + H₂O₂ show integration between regenerated skeletal tissue and remnant skeletal tissue. (J), Percentage of animals that presented integration failure in the different experimental groups. (K, L), Representative images of joint morphology. (K), typical synovial joint morphology. (L), APO treatment affects the joint capsule and generates constriction of synovial spaces. (M), treatment with exogenous H₂O₂ rescues the articular morphology. (N), DMSO + H₂O₂ treatments do not affect typical joint morphology. (O–R), magnification of area delimited with red dotted lines in K, L, M, and N. (O) A well-defined synovial space can be observed. (P) Animals treated with apocynin show a fairly constricted synovial space with apparent continuity between the connective tissue of the articular capsule and the articular surface of the regenerated humerus (orange arrows). (Q) Similar to controls, a more defined synovial space is observed. (R) An articular morphology as seen in the DMSO controls can be observed. (S), Percentage of animals that presented joint morphological abnormality in the evaluated groups. Yellow arrows indicate connective tissue joint capsule. Black arrows indicate synovial spaces. ai, integration area; h, regenerated humerus; r, radius; u, ulna.

humerus and the regenerated humerus (Figure 5B). Histological sections show continuity between the perichondrium of the regenerated humerus, periosteum of the regenerating ossified humerus, and periosteum of the remnant humerus (Figure 5F). In contrast, 90% of the animals treated with apocynin (9/10 animals) present integration failure characterized by the discontinuity between the regenerated humerus and the

remnant humerus (Figures 5C,J). This discontinuity can be observed as an angular junction between these two skeletal components; in addition, histological sections show that the perichondrium of the regenerated humerus does not continue with the periosteum of the remaining humerus (Figures 5C,G). Of great importance, rescue treatment with exogenous H₂O₂ reduced to 40% (4/10 animals) the



integrity failure between the regenerated skeletal tissue and the remnant skeleton generated by inhibition of ROS production (Figures 5D,H). Additionally, only 20% ($n = 2/10$) of the control animals exposed to 0.1% DMSO + H₂O₂ presented integration

failure (Figures 5E,I,J). Taken together, these results suggest that ROS production during the first 11 dpa is necessary to promote integration between regenerated skeletal tissue and the remnant skeleton.

Finally, considering that the animals that regenerated miniature limbs did not present a defined boundary between the stylopod and zeugopod, this prompted us to perform an analysis of the joint morphology between these two segments. The results show that control animals exposed to 0.1% DMSO (90%, $n = 9/10$) presented a typical synovial joint with defined acellular synovial cavities and bounded externally by a connective tissue joint capsule and internally by the articular surfaces of the humerus, radius, and ulna bones (Figures 5K,O,S). In contrast to the controls, the animals treated with apocynin presented an altered articular morphology, characterized by a reduced articular capsule and apparently absent synovial spaces (superior and inferior) (80%, 8/10) (Figures 5L,P,S). On the other hand, animals exposed to rescue treatment with exogenous H_2O_2 regenerated a joint with a morphology like controls, and only 30% ($n = 3/10$ joints) presented morphological alterations as those reported in the apocynin-treated group (Figures 5M,Q,S). Additionally, animals exposed to 0.1% DMSO + H_2O_2 (90%, $n = 9/10$) presented a typical synovial joint morphology comparable to controls in 0.1% DMSO (Figures 5N,R). These results suggest a potential role of ROS in the early patterning of precursors that will form the articular region between the stylopod and zeugopod.

NOX-dependent ROS production is required to induce cell cycle re-entry and blastema formation during limb regeneration

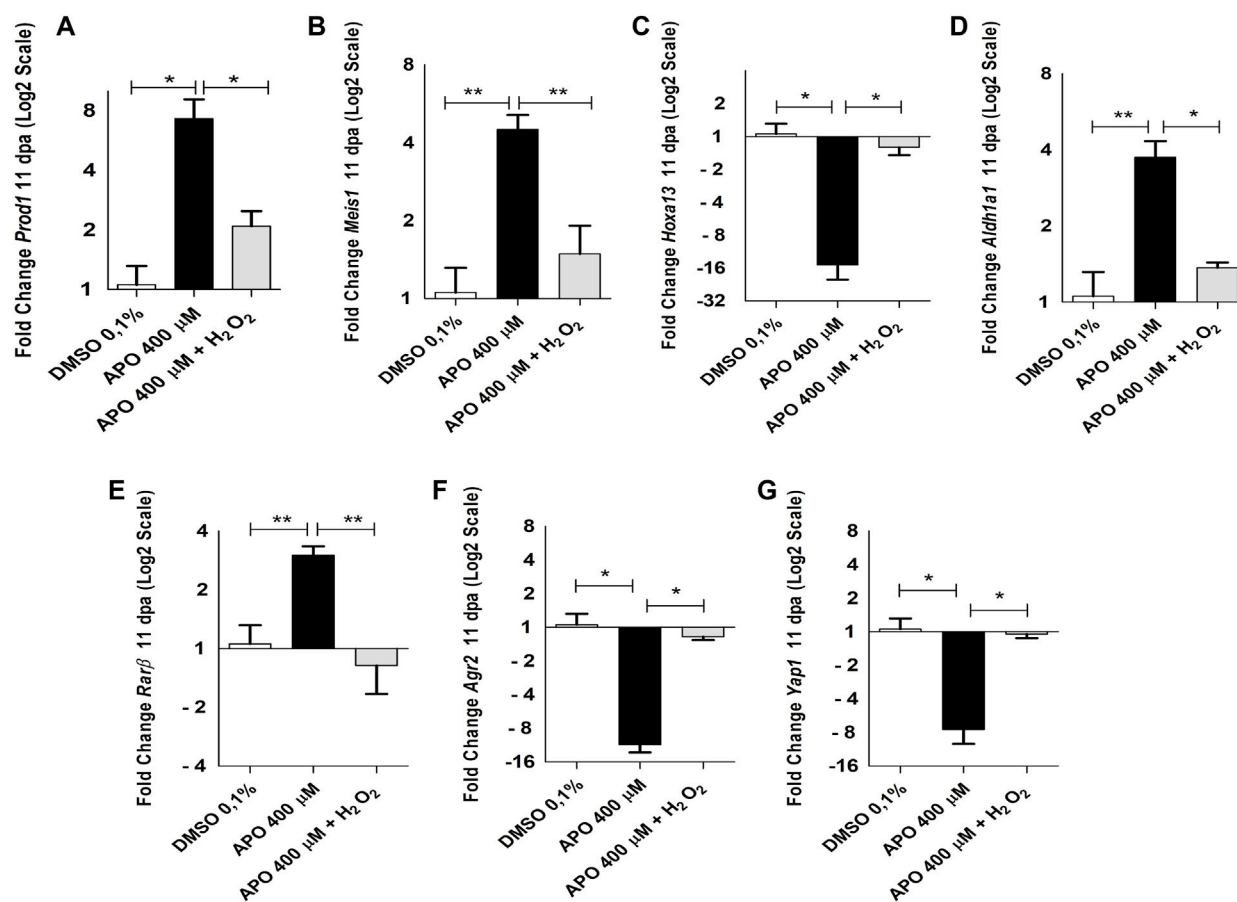
One of the prominent features during limb regeneration is blastema formation. The formation of the blastema and the proliferation of the cells forming this structure are considered fundamental events for the growth of the regenerating structure (McCusker et al., 2015). Therefore, considering that inhibition of ROS production caused a significant reduction in the final size of the regenerated limb, the next step was to evaluate the effect of inhibition of NOXs activity on blastema formation. The results show that at 11 dpa, control animals in 0.1% DMSO formed an early blastema characterized by the accumulation of mesenchymal cells between the apical epithelial layer and the remnant cartilage (Figures 6A,D). In contrast, the apocynin-treated group of animals from 0 to 11 dpa showed an apparent absence of blastema formation (Figure 6B). Histological sections show sparse blastema cells between the epithelium and remnant cartilage in this experimental group (Figure 6E). Of great interest, between the epithelial layer and the remnant cartilage, a predominant deposition of connective tissue was identified overlying the accumulation of blastema mesenchymal cells (Figure 6E). Accordingly, we decided to evaluate whether the application of exogenous H_2O_2 could rescue blastema formation. The results show that exogenous H_2O_2 from 0 to 11 dpa induced the formation of a blastema similar in size and

shape to the control group, favoring the accumulation of mesenchymal cells between the epithelium and the remnant cartilage (Figures 6C,F,G). This shows that exogenous H_2O_2 is sufficient to rescue the size of the blastema affected by ROS inhibition. Finally, although at 11 dpa blastema formation was affected by apocynin treatments, we followed up with these animals and identified the formation of a late blastema whose size was smaller compared to the control group in DMSO at 14 and 21 dpa. However, blastema growth in the rescue group animals experienced similar growth to the control group in DMSO (Figures 6L–R). These results show that although there is a delayed blastema formation in apocynin-treated animals, its size was smaller compared to controls, which correlates with the final size and miniaturized appearance of the regenerated limb.

Additionally, considering the deficient blastema formation in apocynin-treated animals, the effect of ROS inhibition on blastema cell proliferation by BrdU incorporation was evaluated. The results show that apocynin-treated animals showed a significant reduction in the percentage of cells incorporating BrdU compared with the control group in 0.1% DMSO (Figures 6H,I). Few BrdU-positive cells were detected at the amputation plane, whereas only a small percentage of positive cells were detected lateral to the amputation plane in apocynin-treated animals (Figure 6I). Of great importance, rescue treatment with exogenous H_2O_2 increased BrdU incorporation levels like controls in 0.1% DMSO. Therefore, H_2O_2 can rescue the effect generated by inhibition of ROS production (Figures 6J,K). These results suggest that ROS production is required for cell cycle re-entry and subsequent blastema formation and growth during limb regeneration in axolotls.

Identifying potential target genes regulated by ROS production during axolotl limb regeneration

In order to approach a potential explanation for the phenotypic alterations observed upon inhibition of ROS production such as failure of blastema formation, shortening of regenerated skeletal structures, decrease in the number of carpals, alteration in joint morphogenesis and failure of the integrity of the new regenerated structure to the remnant, we set out to evaluate the effect of ROS on the expression of genes related to blastema formation and growth in axolotls, we set out to evaluate the effect of ROS on the expression of genes related to blastema formation and growth (*Agr2* and *Yap1*), positional identity and tissue integrity such as Retinoic Acid (RA) pathway genes such as *Aldh1a1*, *Aldh1a2*, *Rarb*, *Rara*, *Rarg*, and other positional identity genes such as *Meis1*, *Meis2*, *Prod1* and *Hoxa13*. Accordingly, the expression of these genes was evaluated by RT-qPCR after blocking NOX-dependent ROS production and after exposure to rescue assay with exogenous H_2O_2 from 0 to 11 dpa.

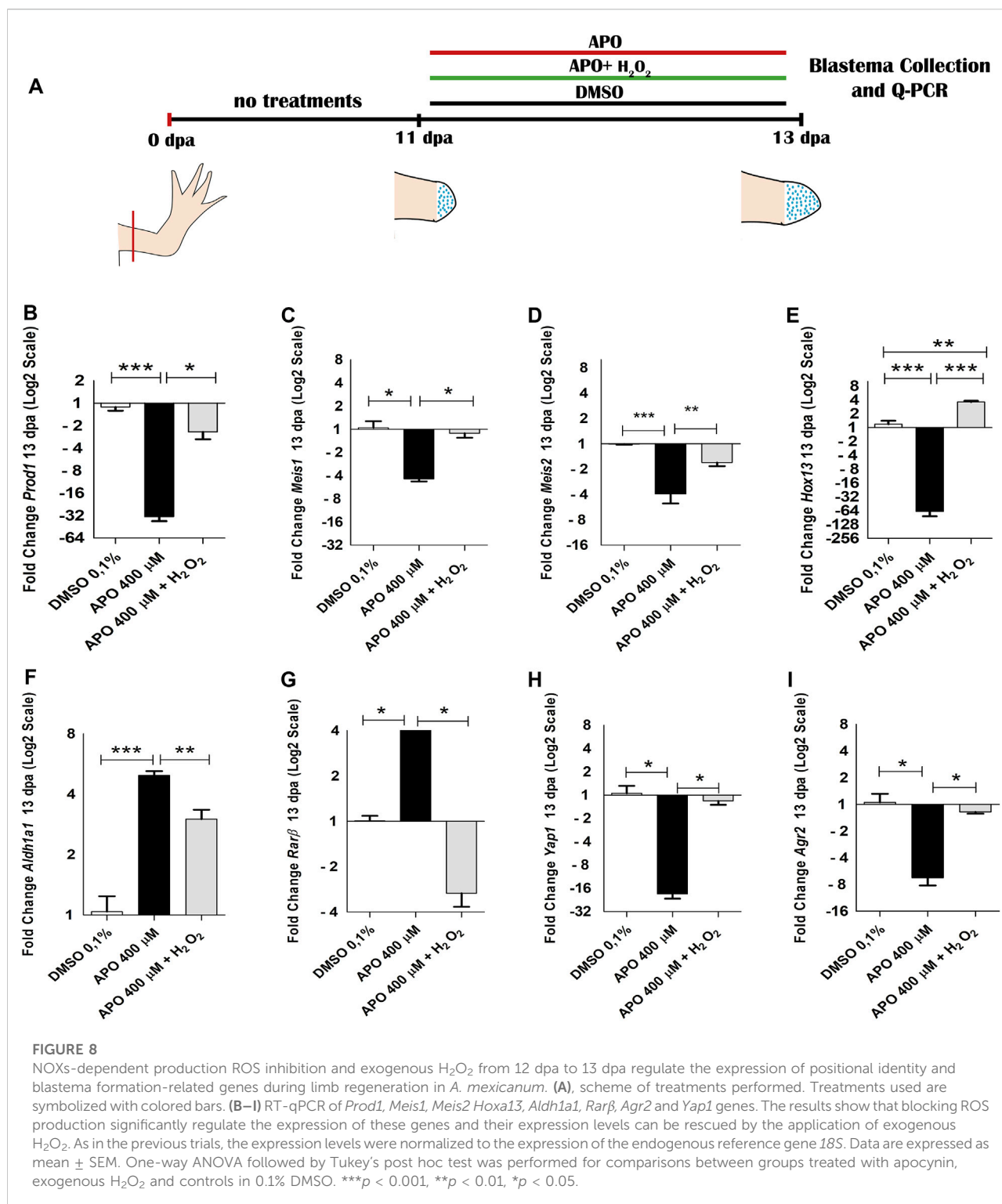
**FIGURE 7**

NOXs-dependent production ROS inhibition and exogenous H₂O₂ induces expression changes of genes related to blastema formation and positional identity during limb regeneration in *A. mexicanum* at 11 dpa. (A–G), RT-qPCR of *Prod1*, *Meis1*, *Hoxa13*, *Aldh1a1*, *Rarb*, *Agr2* and *Yap1* genes. The results show that blocking ROS production significantly affects the expression of the genes described here and their expression levels can be rescued by the application of exogenous H₂O₂. Gene expression levels were normalized to the expression of the endogenous reference gene *18S*. Data are expressed as mean \pm SEM. One-way ANOVA followed by Tukey's post hoc test was performed for comparisons between groups treated with apocynin, exogenous H₂O₂ and controls in 0.1% DMSO. *** p < 0.001, ** p < 0.01, * p < 0.05.

The results show a significant increase in *Prod1* expression levels upon blocking ROS production compared to the control group in 0.1% DMSO. Of great relevance, rescue assay with exogenous H₂O₂ was able to significantly reduce *Prod1* expression to similar levels as those observed for the control group in 0.1% DMSO (Figure 7A). In addition, we also identified that like *Prod1*, *Meis1*, another gene involved in proximal identity, increased its expression post-inhibition of ROS production and its expression levels decreased upon rescue treatment with exogenous H₂O₂ (Figure 7B). No significant effects on *Meis2* expression were observed (Supplementary Figure S3). Considering the presence of skeletal alterations in the distal region such as decrease in the number of carpals, the effect of ROS on *Hoxa13* gene expression was evaluated. In contrast to *Prod1* and *Meis1*, it was found that inhibitory treatments with apocynin significantly reduced *Hoxa13*

expression levels when compared to the control group. However, rescue treatment with exogenous H₂O₂ rescued the expression of this gene (Figure 7C).

On the other hand, considering the function of the retinoic acid pathway on the specification of the identity of the proximo-distal axis and previous reports linking the expression of *Prod1* and *Meis1* with this signaling pathway (Da Silva et al., 2002; Mercader et al., 2005; Kumar et al., 2015) as well as previous studies showing a regulatory effect of ROS on the activity and expression of some retinoic acid receptors (Casadevall and Sarkar, 1998; Demary et al., 2001; Park et al., 2009), we decided to evaluate the effect of ROS on the expression of some RA signaling component genes. Inhibition of ROS production generated an increase in the expression levels of *Aldh1a1* and *Rarb* genes, which were rescued by rescue treatment with exogenous H₂O₂ when compared with the



control group in 0.1% DMSO (Figures 7D,E). No significant differences were found in the expression of *Aldh1a2*, *Rara*, and *RarG* (Supplementary Figure S3). Finally, considering previous results describing the effect of *Agr2* and *Yap1* on blastema

formation and the regulation of events such as proliferation during appendage regeneration in vertebrates and their relationship with ROS production, we proceeded to evaluate their expression under conditions of loss and gain of ROS activity

(Kumar et al., 2007; Hayashi et al., 2014b; Carbonell M et al., 2021). The results show that ROS inhibition significantly decreased the expression levels of *Agr2* and *Yap1* at 11 dpa. Of great interest, exogenous H_2O_2 treatments rescued the expression levels of these genes (Figures 7F,G). These results suggest that ROS are necessary to regulate the expression of proximo-distal identity genes. Additionally, these results also suggest *Agr2* and *Yap1* as potential mediators of redox signaling during limb regeneration in *A. mexicanum*. However, the cell population in the blastema of apocynin-treated animals was more reduced than that of the control and rescue groups which could promote a greater accumulation of proximal identity cells and consequently a higher expression of proximal identity genes as shown above (Figures 7A–E). Therefore, to corroborate whether ROS have a real effect on the expression of proximo-distal identity genes during blastema development, we allowed the blastema to grow until 11 dpa and then apply treatments with the inhibitor apocynin, as well as rescue assays with exogenous hydrogen peroxide from 12 dpa to 13 dpa (48 h of treatment), and again evaluated the impact of ROS on the expression of the genes previously evaluated (Figure 8A).

The results of this new assay show that blocking ROS production from 12 dpa to 13 dpa induced a decrease in the expression of *Prod1* and *Meis1* differing from the results obtained at 11 dpa, where apocynin treatment promoted an increase in the expression of these genes (Figures 8B,C). In addition, an increase in *Meis2* expression was now identified (Figure 8D). Like what was observed at 11 dpa, a decrease in the expression of the distal identity marker *Hoxa13* was identified (Figure 8E). On the other hand, an increase in the expression of RA pathway component genes such as *Aldh1a1* and *Rarb* was similar to that observed at 11 dpa (Figures 8F,G). Of great relevance, H_2O_2 rescued the expression of each of the genes regulated by blocking NOXs activity.

Therefore, considering that the effect on the expression of proximal identity genes (*Prod1* and *Meis1*) was contrasting at 11 and 13 dpa, the data obtained suggest that the increase in the expression of these genes and the decrease in *Hoxa13* expression at 11 dpa was potentially attributed in this case, more to a predominant accumulation of proximal identity cells and a probable lack of distal identity cells as a consequence of the failure of blastema cell formation generated by the effect of ROS inhibition, than to an effect of ROS/ H_2O_2 -mediated transcriptional regulation. However, given that assays blocking ROS production from 12 to 13 dpa, when presumably proximal and distal identity cell populations are already present generated changes in the expression of several genes (including *Prod1*, *Meis1*, *Meis2*, *Hoxa13*, *Rarb* and *Aldh1a1*) when compared to the control group, and their expression was rescued by exogenous H_2O_2 treatments, the data further suggest, that ROS/ H_2O_2 does indeed regulate the expression of these proximal-distal identity genes during blastema formation and growth. Thus, ROS

production is necessary for the formation of blastema cells and the expression of their proximo-distal identity genes necessary for the growth of the blastema and its derivatives. In addition to proximodistal identity genes, blocking ROS production from 12 to 13 dpa reduced the expression levels of *Yap1* and *Agr2*, which were rescued by exogenous H_2O_2 treatments corroborating the transcriptional regulation of these genes by ROS (Figures 8H,I).

Inhibitory treatments of NOXs by apocynin and exogenous H_2O_2 treatments impact inflammatory cell recruitment and phagocytic activity

Inflammatory cell recruitment represents a prominent feature following tissue injury or appendage amputation in different vertebrate animal models such as zebrafish and *Xenopus* (Niethammer et al., 2009; Love et al., 2013). In zebrafish, NOX-dependent ROS production is required to promote leukocyte recruitment following tail amputation (Niethammer et al., 2009; Yoo et al., 2011). Of great interest, post-amputation of limbs in *A. mexicanum*, macrophage recruitment is required for proper regeneration of this structure (Godwin et al., 2013), and previous studies during tail regeneration in this animal model have shown that NADPH oxidase-dependent ROS production is required to promote leukocyte recruitment (Carbonell M et al., 2021). In addition, several studies have shown that apocynin possesses anti-inflammatory properties mediated by the regulation of NADPH oxidases and oxidative stress, which has been explored in several inflammatory diseases. (Kim et al., 2012; Hwang et al., 2019; Boshtam et al., 2021). This background motivated us to question whether inhibitory treatments of ROS production using the NOX inhibitor apocynin have any effect on the inflammatory response after limb amputation. To address this question, we first evaluated the effect of blocking ROS production from 0 dpa to 11 dpa on leukocyte recruitment using a leukocyte pan marker, CD45 (Im et al., 2011). The results show a significant reduction in CD45⁺ leukocyte recruitment in animals treated with the inhibitor apocynin compared to controls in DMSO (Figures 9A,B,G). Of great interest, rescue treatment with exogenous H_2O_2 rescued the recruitment of these cells and even promoted higher recruitment of CD45⁺ cells when compared to controls in 0.1% DMSO (Figures 9C,G). The CD45⁺ cells were predominantly located in the region underlying the amputation plane (Figures 9A–C). Subsequently, to evaluate the effect of blocking ROS production on monocyte/macrophage recruitment, we used the CD11b marker, previously used in this animal model for the same purpose (Godwin et al., 2013). Similar to what was observed previously, treatment with apocynin reduced the number of CD11b⁺ cells compared to the control group, and relevantly, treatment with exogenous H_2O_2 promoted a greater increase in monocyte/macrophage recruitment compared to both the group exposed to the

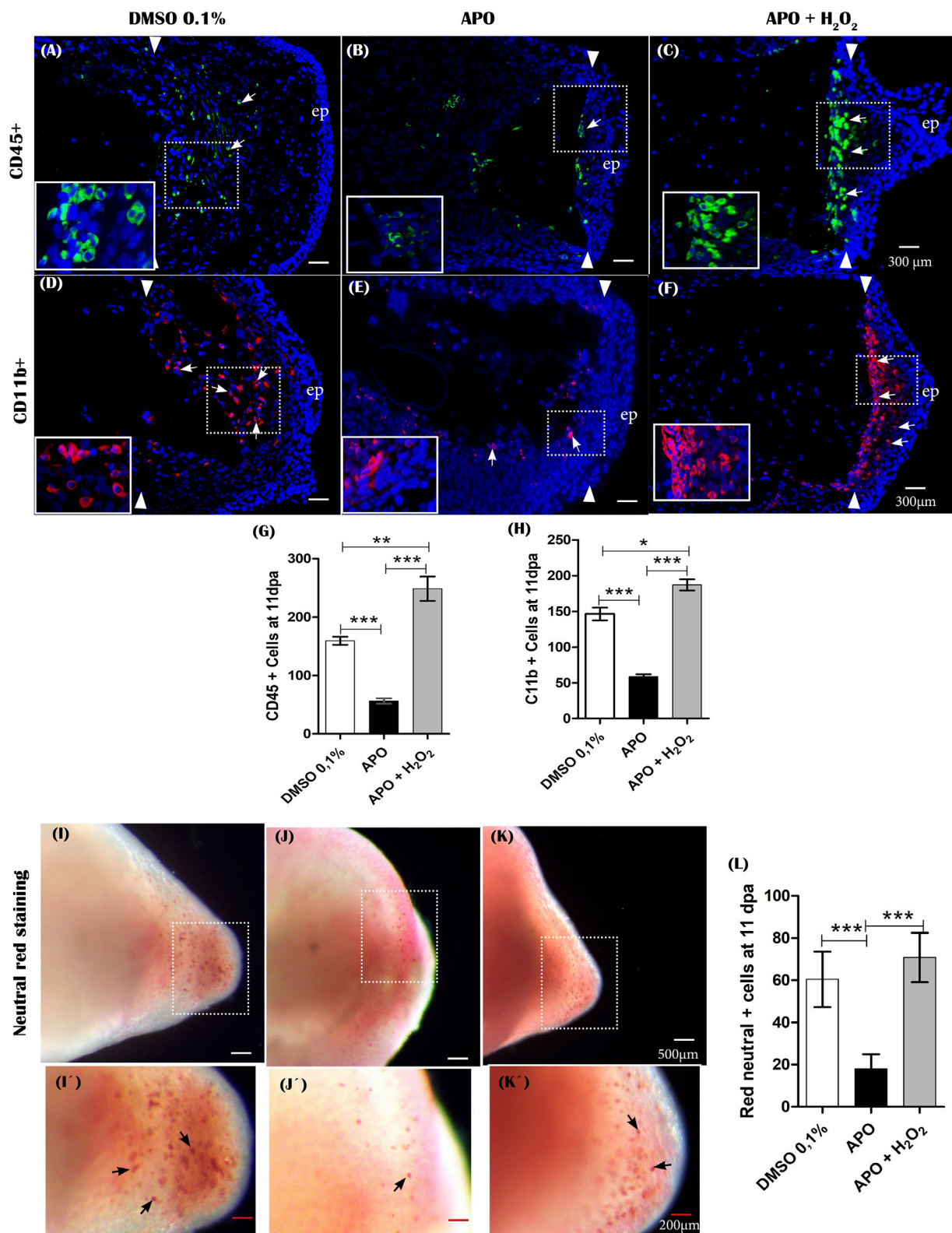


FIGURE 9
The production of ROS generated post-amputation of the limb is necessary for the recruitment and phagocytic activity of inflammatory cells.
(A–C), Representative immunofluorescence images against the leukocyte pan marker CD45 at 11 dpa. Boxes in white dotted lines are shown at
(Continued)

FIGURE 9

higher magnification in solid line boxes for each image. (A) CD45⁺ cells are predominantly located in the blastema region adjacent to the amputation plane. (B) A reduced number of CD45⁺ cells are observed near the amputation plane. (C) a notable increase of CD45⁺ cells are observed in the region of the blastema and the amputation plane. (D–F), Representative immunofluorescence images against CD11b. A higher presence of CD11b⁺ cells can be seen in the control group compared with the apocynin-treated group. Animals exposed to rescue treatment show a prominent accumulation of CD11b⁺ cells in the blastema and amputation plane. (G,H), quantification of CD45 and CD11b⁺ positive cells, respectively. (I–K), vital staining with neutral red at 11 dpa. Representative images of control animals in 0.1% DMSO, exposed to apocynin inhibitor (APO) and rescue assays. Boxes in dotted white lines are shown at higher magnification in (I',J',K') for each experimental group. (L), quantification of cells positive for neutral red staining. Data are expressed as mean \pm SEM. One-way ANOVA followed by Tukey's post hoc test was performed for comparisons between groups treated with apocynin, exogenous H₂O₂ and controls in 0.1% DMSO. *** p < 0.001, ** p < 0.01, * p < 0.05.

inhibitory treatment and the control group in DMSO (Figures 9D–F,H). Finally, we set out to evaluate the effect of inhibitory treatment with apocynin on macrophage phagocytic activity using the neutral red labeling method previously used in this animal model (Godwin et al., 2013; Franklin et al., 2017). The results show a remarkable accumulation of phagocytic cells in the blastema of control animals in 0.1% DMSO (Figures 9I, 9I'). In contrast, treatment with apocynin reduced the number of phagocytes (Figures 9J,J',L). On the other hand, treatment with exogenous H₂O₂ rescued the number of phagocytic cells, which were widely located in the blastema region (Figures 9K,K',L). Consistently, neutral red-positive cells were located at sites comparable to CD11b⁺ cells. In the first instance, these results suggest that NADPH oxidase-dependent ROS production is required for the recruitment and activity of inflammatory cells whether leukocytes or monocytes/macrophages. This then suggests that the inflammatory response represents a potential mechanism for mediating ROS function during limb regeneration in *A. mexicanum*.

Discussion

ROS production and signaling are conserved during the regeneration of appendages such as tail and limbs in vertebrates

Recently, ROS have emerged as a group of key molecules in redox signaling, among them H₂O₂ (Sies, 2017; Sies and Jones, 2020b). ROS are highlighted because they can regulate a wide range of cellular processes including proliferation, migration, differentiation, and apoptosis, among others (Milkovic et al., 2019; Sies and Jones, 2020b; Sun et al., 2020). This has promoted a growing interest in the requirement of these molecules during biological processes such as the regeneration of tissues and complex structures such as appendages, including tails and limbs in vertebrates (Meda et al., 2017, 2018; Rampon et al., 2018). Our results show that post-amputation of limbs in axolotl, ROS production was detected up to 18 dpa, with peaks of production at 2, 7, and 11 dpa which correlates with events such as wound closure, blastema formation, and growth. These results are comparable with previous results obtained in our

group where after tail amputation in juvenile salamanders, ROS production was also detected at these stages of the regenerative process (Carbonell M et al., 2021). Similarly, another study performed in embryos of the same species shows that ROS production is also detected during wound closure and blastema formation (Al Haj Baddar et al., 2019). In the present study, NOX-dependent blockade of ROS production affected the size and patterning of the regenerated limb. Consistent with these results, blocking ROS production during tail regeneration in embryonic and juvenile axolotls also perturbed regeneration of this structure (Al Haj Baddar et al., 2019). This suggests that NOX-dependent ROS signaling represents a conserved mechanism during regeneration of appendages such as tail and limb in the salamander *A. mexicanum*. On the other hand, studies in other vertebrate species show that post-amputation of tail in *Xenopus*, Gecko, and tail fin in zebrafish, ROS production is also part of an immediate response which is sustained during the early stages of the regeneration process (Gauron et al., 2013; Love et al., 2013; Ferreira et al., 2016, 2018; Meda et al., 2016; Zhang et al., 2016; Romero et al., 2018). Similarly, blocking ROS production during regeneration in these species disrupts the regeneration of the amputated structure. Additionally, studies in *Xenopus* tadpoles during stages 52–53 show that ROS production is necessary for regeneration of amputated limbs (Zhang et al., 2018). Taken together, our results suggest that NOXs-dependent ROS/H₂O₂ signaling is a conserved mechanism during appendage regeneration among different vertebrate species with regenerative capacity, and in particular, its production is required during limb regeneration in urodele amphibians such as axolotls, and other amphibians such as *Xenopus*.

NOX-dependent ROS production is necessary for cell cycle re-entry and blastema formation during limb regeneration

Blastema formation and growth are critical steps during epimorphic limb regeneration (Tassava et al., 1987; McCusker et al., 2015; Stocum, 2019). Thus, the recruitment of progenitor cells from remnant “Stump” tissues and the re-entry of these cells

into the cell cycle are necessary events for blastema development (Tassava et al., 1987; Heber-Katz et al., 2013; McCusker et al., 2015). In the present study, blocking NOX-dependent ROS production from 0 dpa to 11 dpa affected blastema formation (failure of blastema progenitor recruitment) and significantly decreased BrdU incorporation, reflecting a reduction in cell cycle reentry. Consistent with our results, previous studies show that blocking ROS production during tail regeneration in embryonic and juvenile axolotls disrupts blastema formation and reduces cell proliferation (Al Haj Baddar et al., 2019). Additionally, studies in other vertebrates such as *Xenopus* and zebrafish show that ROS production induced post-amputation of tail and tail fin is necessary to promote blastema cell formation and proliferation (Yoo et al., 2012; Gauron et al., 2013; Love et al., 2013). Relevantly, our results show that the application of exogenous H_2O_2 rescues blastema formation and increases cell proliferation levels in limbs exposed to the inhibitor apocynin. These findings are consistent with previous results showing that overexpression of *cyba*, an inducer of ROS production, rescues blastema formation inhibited by *mcr4* receptor activity-dependent reduction in ROS production during limb regeneration in *Xenopus* (Zhang et al., 2018). Similarly, during tail regeneration in this animal model, H_2O_2 production induced by *cyba* overexpression rescues blastema formation (Love et al., 2013). Like our results, the application of exogenous H_2O_2 rescues blastema formation, proliferation, and growth inhibited by NOXs complex blockade during tail regeneration in axolotls (Carbonell M et al., 2021). On the other hand, during zebrafish tail fin regeneration, exogenous H_2O_2 treatments rescue cell proliferation levels and blastema formation in denervated fins or fins exposed to SHH signaling inhibitors (Meda et al., 2016; Thauvin et al., 2022). Accordingly, our results suggest that ROS, particularly H_2O_2 , are required as early signals for blastema formation and re-entry into the cell cycle of blastema progenitors during limb regeneration in axolotl like that observed in other vertebrates.

To date, the molecular and cellular mechanisms by which ROS/ H_2O_2 regulate blastema formation and proliferation in vertebrates are still under study and a small number of studies show some evidence of interactions between ROS and other signaling pathways (Yoo et al., 2012; Gauron et al., 2013; Love et al., 2013; Romero et al., 2018; Thauvin et al., 2022). Our results show that inhibition of ROS production generated a reduction in *Agr2* (*nAG*) and *Yap1* expression at 11 dpa during early/mid blastema formation, positioning these genes as new potential mediators of ROS signaling. Of great interest, the expression of these genes was rescued post-treatment with exogenous H_2O_2 . These results agree with previous studies, where post-amputation of tails in axolotls, similar treatments generate a similar effect on *Agr2* and *Yap1* expression during early blastema formation (Carbonell M et al., 2021). Additionally, in this animal model, blocking ROS-dependent YAP1 signaling decreases cell cycle re-entry and mitotic index, affecting blastema formation and growth

(Carbonell M et al., 2021). Of great relevance, during limb regeneration in axolotls, YAP1 has been detected at the nuclear level in proliferating blastema dedifferentiated cells, and blocking its activity, delays blastema formation and growth, like what was observed in the present study by blocking ROS production (Erler, 2017). Likewise, YAP1 activity is necessary to promote blastema proliferation and formation during tail and limb regeneration in *Xenopus* (Hayashi et al., 2014b; 2014a). In addition, several studies demonstrate that *Yap1* expression and transcriptional activity is regulated by ROS, particularly H_2O_2 (Delaunay et al., 2000; Veal et al., 2003; Dixit et al., 2014; Tung et al., 2018; Shome et al., 2020). Regarding *Agr2*, consistent with our results, previous studies show that ROS can regulate its expression in regeneration and cancer contexts (Zweitzig et al., 2007; Chevet et al., 2013; Carbonell M et al., 2021) and *nAG* can promote regeneration of denervated limbs, as well as induce a high mitogenic response on blastema cells in newts (Kumar et al., 2007; Grassme et al., 2016). Therefore, our results and the above results suggest that ROS signaling could potentially be mediated by YAP1 and AGR2 to induce blastema formation during limb regeneration.

Finally, taking into account the localization of ROS production detected in this study and that its blockade led to alterations in gene expression and failure of blastema formation, and the fact that in salamanders signals from the epithelium and from the blastema itself are necessary to induce its formation and growth, respectively (Mullen et al., 1996; Han et al., 2001; Christensen et al., 2002; Stocum, 2017; Lovely et al., 2022), we propose two potential ways by which ROS can regulate the expression and potential activity of signals required for blastema formation. 1) according to the remarkable ability of ROS, especially hydrogen peroxide to diffuse with great ease across membranes (Veal et al., 2007; Miller et al., 2010; Bienert and Chaumont, 2014; Sies, 2017; Ledo et al., 2022), it could potentially regulate the expression and activity of genes and signaling pathways directly on blastema cells at the expense of its outstanding diffusion capacity from the epithelium to the blastema and between cells of the same blastema. 2) On the other hand, although in our work we did not evaluate the effect of ROS on the activity and expression of genes and activation of signaling pathways with epithelial predominance, ROS could also regulate the expression of soluble factors from the epithelium (AEC), which in turn can influence signaling pathways in the remaining tissue and the blastema itself to regulate its formation and growth. Additionally, considering that the localization of ROS was persistent in the AEC and the blockade of NOXs only slowed the rate of blastema formation without completely blocking its formation, then the function of the AEC as an inducer of blastema formation was not blocked in its entirety but transiently. Further studies are required to evaluate the effect of ROS on the expression and activity of epithelial and mesenchymal localized genes in the blastema.

ROS/H₂O₂ an early signal potentially involved in the determination of regenerated limb size

The regulation of growth and determination of the final size of a developing structure or during regeneration represents an area of great interest and the underlying mechanisms are still debated (Hafen and Stocker, 2003; Tornini and Poss, 2014; Penzo-Mendez and Stanger, 2015; Vollmer et al., 2017; Wells et al., 2022). Our results show that blocking ROS production during the early stages of regeneration (early/mid blastema formation) generated a significant shortening in the final size of the regenerate and its skeletal components, simulating a miniature limb. We hypothesize that a first potential explanation for this phenotype can be attributed to the formation of a reduced blastema size caused by decreased cell cycle re-entry and decreased amount of progenitor cells post-blockade of ROS production. This approach is consistent with previous results showing that the reduction in proliferation levels and progenitor cell numbers in axolotl limb buds by colchicine results in the development of miniature limbs as a product of a decrease in the embryonic field “limb bud area” (Alberch and Gale, 1983). Therefore, the reduction in this embryonic field could be equivalent to the decrease in blastema size observed in the present study. Similarly, other studies have shown that repeated amputations during limb regeneration in axolotls generate a miniature limb phenotype, which developed from a reduced blastema size, similar to that observed in our study (Bryant et al., 2017). Of great interest, the authors showed that re-amputation of the miniaturized limb generates a reduced size blastema and consequently, a new miniaturized limb, suggesting that local blastema tissue size and cellular bias represent a major force for size determination during regeneration (Bryant et al., 2017). Supporting our approach, similar to our results, blocking ROS production during regeneration of other appendages such as tail in salamanders, *Xenopus*, Gecko, and tail fin in Zebrafish reduces the size of the regenerated appendage (Gauron et al., 2013; Love et al., 2013; Zhang et al., 2016; Carbonell M et al., 2021). Accordingly, our results suggest that ROS production is necessary as an early signal to promote an adequate number of progenitor cells in the blastema to support its growth and the final size of the regenerated structure.

Several studies show that from early stages the presence of the nerve is necessary to promote blastema formation and growth, and denervation of a mid-stage blastema (Singer, 1978; Mullen et al., 1996; Stocum, 2019), as well as blockade of early nerve-regulated signals (Farkas et al., 2016; Satoh et al., 2016; Purushothaman et al., 2019) result in miniature limbs, indicating that from early stages the nerve and other signals regulate the size of the regenerate. Wells *et al* demonstrated that nerve fiber thickness as well as factors produced from the nerve are determinants from the early tiny stage in regulating the growth rate and determining the final size of the regenerated

limb (Wells et al., 2021). Similar to the requirement of the nerve to regulate the size of the regenerate, our results show that ROS blockade from 0 dpa to 11 dpa, affects the final size of the regenerated limb. Additionally, this phenotype is rescued by the addition of exogenous H₂O₂ and relevantly, previous reports have suggested an integration between ROS signaling and nerve (Meda et al., 2018). Therefore, it is feasible to hypothesize that ROS production could regulate the production of factors from the nerve affecting the size of the regenerate. Previous studies in Zebrafish show that ROS production regulates *Shha* expression in Schwann cells and reciprocally, HH (*shha*) signaling from these cells controls ROS levels and rescues the size of the regenerated caudal fin in animals treated with ROS production inhibitors (Meda et al., 2016; Thauvin et al., 2022). Of great relevance, our results show that blocking ROS production and exogenous H₂O₂ affect *Agr2* expression levels, which has been previously detected in Schwann cells during limb regeneration in axolotls (Kumar et al., 2010) and overexpression of this gene promotes blastema formation and denervated limb regeneration in newts (Kumar et al., 2007). Notably, limb denervation in *Xenopus* reduces the ROS production required for the regeneration of this structure and *Agr2* inhibition reduces the regenerated tail area in this same animal model (Zhang et al., 2018; Ivanova et al., 2021). Additionally, during tail regeneration in salamanders, blocking ROS production reduces *Agr2* expression levels and the final size of the regenerate (Carbonell M et al., 2021). Therefore, these findings suggest that from early stages ROS could regulate the production of *Agr2* from the Schwann cells, without excluding the production of other factors such as Shh, Fgf, Wnt and Bmp also necessary for limb regeneration (Mullen et al., 1996; Kawakami et al., 2006; Guimond et al., 2010; Wischin et al., 2017; Purushothaman et al., 2019) and regulated by ROS during the regeneration of other appendages (Love et al., 2013; Meda et al., 2016; Satoh et al., 2016; Romero et al., 2018) to favor an adequate regenerative response that contributes to growth control and size of the regenerate.

On the other hand, several of the genes regulated by blocking ROS production, such as *Prod1* and *Yap1*, have been previously implicated in the regeneration of shortened structures. The shortening of skeletal structures of regenerated limbs in axolotl has also been evidenced after overexpression of *Prod1*, which also reduces proliferation levels in the blastema (Echeverri and Tanaka, 2005). Consistent with our results, *Yap1* expression and its transcriptional activity are regulated by ROS/H₂O₂ production (Delaunay et al., 2000; Veal et al., 2003; Kim and Hahn, 2013; Tung et al., 2018; Shome et al., 2020), and of great interest, its activity has been implicated in the control of organ and appendage size in contexts such as development and generation (Camargo et al., 2007; Dong et al., 2007; Halder and Johnson, 2011; Hayashi et al., 2015). Particularly, during tail regeneration in *Xenopus* and axolotls, blocking *Yap1* transcriptional activity causes regeneration of reduced size tails and in the axolotls model, its activity was dependent on

ROS production (Hayashi et al., 2014a). Considering the above, our results suggest that ROS signaling can regulate growth and size determination through Yap1 signaling and *Prod1* during limb regeneration. Furthermore, although in our study we did not evaluate the effect of ROS on tissue differentiation, a premature differentiation of tissues with a reduction in tissue growth is not excluded as a potential mechanism to explore as a cause for this phenotype. Accordingly, our results propose ROS signaling as a new candidate for regulating regenerate size early in the regenerative process, potentially participating in blastema patterning and proliferation. Further studies are required to elucidate the mechanisms proposed here.

Regulation of positional identity genes by ROS and their potential relationship to skeletal defects generated post-inhibition of NADPH oxidases

Our results show that blockade of ROS production from 0 dpa to 11 dpa generated a series of skeletal alterations that included in addition to proximal-distal shortening of skeletal structures: failure of integration between the regenerated structure and the remnant tissue, and decrease in the number of carpals, and alteration in joint morphogenesis. Likewise, blocking ROS production generated overexpression of gene *Meis1*, *Meis2*, *Prod1*, *Rarb*, and *Aldh1a1*, and a reduction in the expression of the *Hoxa13*. Of great relevance, both skeletal alterations and expression levels of these genes were rescued by exogenous H_2O_2 treatments, suggesting that ROS/ H_2O_2 production from early stages is required for the final patterning of skeletal structures and its function, may potentially be mediated by the activity of these positional identity genes.

Comparable to our results, integration failures have been reported when regenerating limbs are exposed to different exogenous treatments such as vitamin D and RA (Niazi et al., 1985; McCusker et al., 2014; Vieira et al., 2018). The application of exogenous RA during early/late blastema formation generates ectopic integration characterized by hypertrophic growth and a discontinuity in the area of integration between the newly regenerated humerus and the remnant tissue, similar to what was observed in our study when ROS production is blocked (Niazi et al., 1985). Although to date, the mechanisms responsible for the failure of integration have not been elucidated, several authors suggest that a potential explanation may be related to disturbances in positional identity (McCusker and Gardiner, 2014; Vieira and McCusker, 2018). Accordingly, overexpression of several proximal identity genes such as *Mes1*, *Prod1*, *Rarb*, and *Aldh1a1* after ROS inhibition may, on the one hand, affect the positional values of proximal cells that potentially contribute to the integration between the new regenerate and the remaining tissues and, on the other hand, may promote some

degree of proximalization of more distal cells, which by preserving part of their distal identity, may affect integration by a “discontinuity of positional values” as has been previously proposed (McCusker and Gardiner, 2014).

Accordingly, ROS function could be mediated by RA and previous studies have shown a relationship between the redox state and RA signaling (Casadevall and Sarkar, 1998; Demary et al., 2001; Cao et al., 2015). Studies performed in melanoma tumor cell lines and fibroblasts show that antioxidant treatments or overexpression of antioxidant enzymes increase the binding of RA receptors (RAR α /RAR β) to RARE (Retinoic Acid Response Elements) and the application of exogenous H_2O_2 stabilizes RA signaling by decreasing the affinity of its receptors to RARE (Demary et al., 2001; Park et al., 2009). Additionally, *Rarb* expression levels are increased by reducing ROS levels and rescued post-application of exogenous H_2O_2 , similar to what was observed in our results (Park et al., 2009). Of great interest, during AR-dependent nephrogenesis in *Xenopus*, peroxiredoxin 1 (Prdx1) functions as a modulator of AR signaling by regulating ROS levels (Chae et al., 2017). Therefore, we hypothesize that optimal levels of ROS are necessary to maintain balanced RA signaling (including RAR α) and consequently, the expression of other genes such as *Meis1*, *Meis2* and *Prod1* for the establishment of positional identity values that favor integration between the regenerated structure and the remnant tissue during limb regeneration in axolotls.

On the other hand, inhibition of ROS production also generated decrease in the number of carpals and alterations in elbow joint morphogenesis. Previous studies show that the specification of intersegmental precursor cells (stylopod, zeugopod, and autopod) during limb regeneration in axolotls is progressively defined during blastema formation and growth (from early, middle, to late blastema) and follows a pattern similar to that reported during development (Echeverri and Tanaka, 2005; Roensch et al., 2013). Previous studies show that this specification is regulated by HoxA family genes. Particularly *Hoxa13*-positive cells located more distally in the mid blastema are determined to form autopod structures (Gardiner and Bryant, 2004; Roensch et al., 2013). Our results show that ROS blockade during early/mid blastema formation reduced *Hoxa13* gene expression and generated a decrease in the number of carpals; additionally, these alterations and *Hoxa13* expression were rescued by the application of exogenous H_2O_2 . Although there are no previous reports evidencing transcriptional regulation of Hox genes by ROS, a previous study shows that the transcriptional activity of the HoxB5 factor is dependent on its ROS-mediated oxidation (Galang and Hauser, 1993). Therefore, this background and our results suggest that ROS, specifically H_2O_2 , could regulate distal cell identity by mediating activity and *Hoxa13* factor expression for the correct patterning of blastema cells destined to form distal structures such as carpal bones either directly or indirectly through RA signaling. Additionally, the phenotype of

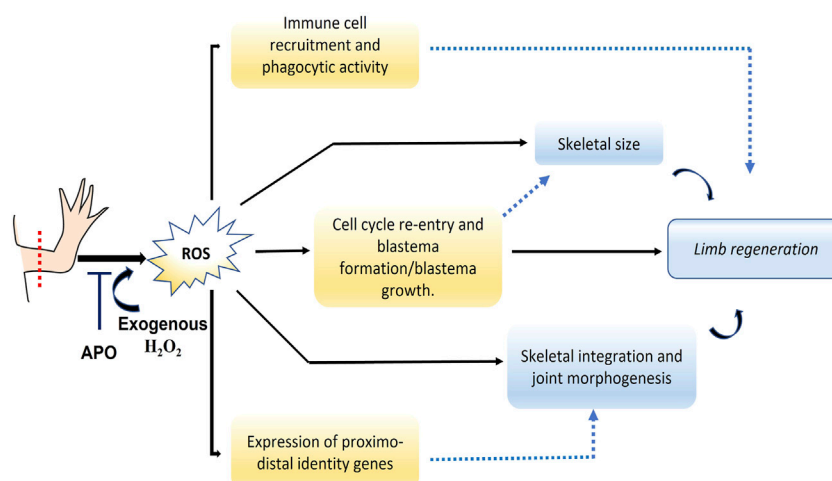


FIGURE 10

Graphical abstract of the results obtained and putative mechanistic insight of ROS in regeneration. Following limb amputation, ROS are produced. The production of ROS is necessary for the re-entry into the cell cycle of the remaining tissues and consequently for the formation and growth of the blastema. ROS also regulates the expression of genes previously involved in blastema formation such as *Yap1* and *Agr2*. This suggests that ROS production-dependent blastema size influences the final size of the limb and its regenerating skeleton. Moreover, ROS regulates the expression of proximal-distal identity genes, suggesting that the obtained phenotype of integration failure between the regenerated and remnant skeleton as well as alterations in joint morphogenesis could be regulated by ROS production. In addition, ROS are necessary to promote the recruitment of inflammatory cells such as leukocytes including monocytes/macrophages during blastema formation, as well as their phagocytic activity. Therefore, we hypothesize that the regulation of the inflammatory response represents a potential mechanism by which ROS mediate its function during axolotl limb regeneration. The solid black lines represent the results obtained in this work and the dotted blue lines represent the proposed relationships according to previous studies and those obtained in this work.

reduced carpal number could be due to decreased levels of cell proliferation, or potentially, to a differentiation defect, such as “premature differentiation” as proposed above for skeletal shortening, which would not allow the formation of the correct number of carpals. Further trials evaluating this approach are needed.

ROS production as a potential regulatory mechanism of the inflammatory response during limb regeneration

Following amputation of appendages in different vertebrate models, several responses of adjacent tissues have been identified (Yoo et al., 2012; Ferreira et al., 2016; Liu et al., 2021). Within these responses, ROS production and activation of the inflammatory response top the list of major events (Niethammer et al., 2009; Yoo et al., 2011; Godwin et al., 2013; Meda et al., 2018; Niethammer, 2018; Al Haj Baddar et al., 2019; Carbonell M et al., 2021; Liu et al., 2021).

Our results show that ROS production is required for blastema formation and proper regeneration of the limb. Additionally, our data show that blocking ROS production affects the recruitment of cells such as leukocytes (CD45⁺) including CD11b + monocytes/macrophages, as well as phagocytic activity. The relationship between ROS production and the inflammatory response has

been described in principle under the fact that polymorphonuclear leukocytes generate ROS from NADPH oxidase activity as an antimicrobial mechanism (Gabig and Babior, 1979; Panday et al., 2015). However, in the context of regeneration, the functional relationship between ROS production and the inflammatory response is still unclear. Previous studies in Zebrafish show that NADPH oxidase Duox-dependent ROS production is necessary to promote leukocyte recruitment favoring their directionality and tissue infiltration during tail regeneration (Niethammer et al., 2009). On the other hand, in adult zebrafish and larvae it has been identified that H₂O₂ production from the wound epithelium is necessary to activate the redox sensor protein Lyn in neutrophils favoring the recruitment of these cells (Yoo et al., 2011). Previous results in our group have shown that during tail regeneration in *A. mexicanum* blocking ROS production reduces leukocyte recruitment to the site of blastema formation (Carbonell M et al., 2021). Therefore, our results and the aforementioned studies suggest that ROS production acts as a necessary signal to promote post-amputation inflammatory cell recruitment of appendages such as tails and limbs. This function would be predominantly regulated from the wound epithelium and AEC from where the main source of ROS concerning limb regeneration in *A. mexicanum* was identified. However, although the inflammatory response has been suggested as a determinant factor for the regenerative response, several studies show some contrasting results among vertebrates (Godwin and Brockes,

2006; Mescher and Neff, 2006; Godwin et al., 2017). Studies in Zebrafish show that immune system cell depletion does not affect caudal and tail fin regeneration in embryos and adults of this species (Mathew et al., 2007; Yoo et al., 2012). On the other hand, similar results have been reported in the *Xenopus* model, where myeloid precursor depletion does not affect tail regeneration (Love et al., 2013). Thus, although in each of these models ROS production is necessary to promote regeneration and recruitment of these cells, in these species it appears that the inflammatory response is not the mechanism by which ROS mediate their role in the regenerative response. However, in other vertebrate models, the recruitment of inflammatory cells is required for the regenerative response. Studies in *A. mexicanum* show that monocyte/macrophage recruitment is required for limb regeneration (Godwin et al., 2013). Thus, early macrophage depletion blocks regeneration and promotes scar tissue formation between the remnant tissue and the wound epithelium affecting blastema formation. On the other hand, macrophage depletion at a later stage generates a delay in regeneration and reduce the expression of *Mmp9/Mmp3* and failure of extracellular matrix remodeling. Additionally, it reduces the expression of blastema markers such as *Prrx1* and *Sp9*, as well as reduces the activation of TGF β , necessary for blastema formation and progression of the regenerative response (Godwin et al., 2013). Interestingly, our results show that blocking ROS production, in addition to generating a decrease in monocyte/macrophage (CD11b+) recruitment and a reduction in their phagocytic activity, affected blastema formation. ROS blockade promoted the formation of a fibrous tissue between the epithelium and the remnant tissue, similar to that reported when macrophage depletion is induced (Godwin et al., 2013). These findings suggest that in the case of limb regeneration in *A. mexicanum*, regulation of the inflammatory response could represent a potential mechanism by which ROS may be mediating processes such as extracellular matrix remodeling necessary for blastema formation. In support of this, in contexts other than regeneration such as cancer, ROS have been implicated during extracellular matrix remodeling by mediating the expression of several metalloproteinases (Svineng et al., 2008; Shin et al., 2015; Hsieh et al., 2017). Further assays are needed to assess whether ROS blockade affects the activity of the metalloproteinases MMP9 and MMP3, as well as the expression and activation of other pathways regulated by macrophage activity during limb regeneration in the *A. mexicanum* model.

Conclusion

Overall, our results propose ROS, particularly H₂O₂ as an early signal necessary for proper limb regeneration in salamanders, mediating in the first instance the formation and growth of the blastema. Likewise, it was evidenced that ROS/H₂O₂ are necessary for the correct morphogenesis and size of the skeletal structures, as well as for the correct integration between the new regenerated structure and the remaining tissue. Finally,

according to the transcriptional regulation evidenced in the present work, the function of ROS/H₂O₂ would be potentially related to the proximal-distal specification of intersegmental precursors for stylopod, zeugopod, and autopod formation. Additionally, our results show for the first time that ROS are necessary to promote the recruitment of inflammatory cells such as leukocytes including monocytes/macrophages during blastema formation, as well as their phagocytic activity (Figure 10). Future studies are needed to further decipher the mechanism by which ROS such as H₂O₂ participate in limb regeneration and how their activity relates to signaling pathways involved in proximal-distal and anterior-posterior specification during limb regeneration.

Data availability statement

The original contributions presented in the study are included in the article/Supplementary Material, further inquiries can be directed to the corresponding authors.

Ethics statement

The animal study was reviewed and approved by the Ethics and Animal Experimentation Committee of the University of Antioquia under the animal experimentation protocol registered in Acta No. 121.

Author contributions

BC-M: Conceptualization; data curation; formal analysis; investigation; methodology; validation; visualization; writing—original draft; writing—review and editing. JZ: Formal analysis; methodology. JD: Conceptualization; funding acquisition; project administration; supervision; writing review and editing. All authors contributed to manuscript revision, read and approved the submitted version.

Funding

This work was financed with resources from the Universidad de Antioquia, Colombia and by the student instructor grant (No. 1000235120) from the Faculty of Exact and Natural Sciences of the Universidad de Antioquia.

Acknowledgments

We thank the Universidad de Antioquia for providing us with the financial sources and laboratory infrastructure to

conduct this research. We also thank Professor Miguel Mendivil P of the Neuroscience Research Group of Antioquia, University of Antioquia, for his support in the acquisition of images and the donation of the anti-CD45 antibody and Professor Diego Uribe Yunda for providing us the equipment to perform q-PCR. We also thank Felipe Valdez of the GICIB research group for the donation of cd11b antibody.

Conflict of interest

The authors declare that the research was conducted in the absence of any commercial or financial relationships that could be construed as a potential conflict of interest.

References

- Al Haj Baddar, N. W., Chithrala, A., and Voss, S. R. (2019). Amputation-induced reactive oxygen species signaling is required for axolotl tail regeneration. *Dev. Dyn.* 248, 189–196. doi:10.1002/dvdy.5
- Alberch, P., and Gale, E. A. (1983). Size dependence during the development of the amphibian foot. Colchicine-induced digital loss and reduction. *Development* 76, 177–197. doi:10.1242/dev.76.1.177
- Arenas Gómez, C. M., and Echeverri, K. (2021). Salamanders: The molecular basis of tissue regeneration and its relevance to human disease. *Curr. Top. Dev. Biol.* 145, 235–275. doi:10.1016/BS.CTDB.2020.11.009
- Arenas Gómez, C. M., Gómez Molina, A., Zapata, J. D., and Delgado, J. P. (2017b). 4. Oxford, England, 227–235. doi:10.1002/reg.2.93 Limb regeneration in a direct-developing terrestrial salamander, *Bolitoglossa ramosi* (Caudata: Plethodontidae): Limb regeneration in plethodontid salamanders *Regeneration*
- Arenas Gómez, C. M., Gomez Molina, A., Zapata, J. D., and Delgado, J. P. (2017a). Limb regeneration in a direct-developing terrestrial salamander, *Bolitoglossa ramosi* (Caudata: Plethodontidae): Limb regeneration in plethodontid salamanders. *Regeneration* 4, 227–235. doi:10.1002/reg.2.93
- Aztekin, C. (2021). Tissues and cell types of appendage regeneration: A detailed look at the wound epidermis and its specialized forms. *Front. Physiol.* 12, 2047. doi:10.3389/fphys.2021.771040
- Bienert, G. P., and Chaumont, F. (2014). Aquaporin-facilitated transmembrane diffusion of hydrogen peroxide. *Biochim. Biophys. Acta* 1840, 1596–1604. doi:10.1016/j.bbaagen.2013.09.017
- Borgens, R. B., McGinnis, M. E., Vanable, J. W., and Miles, E. S. (1984). Stump currents in regenerating salamanders and newts. *J. Exp. Zool.* 231, 249–256. doi:10.1002/JEZ.1402310209
- Boshtam, M., Kouhpayeh, S., Amini, F., Azizi, Y., Najafu, M., Shariati, L., et al. (2021). Anti-inflammatory effects of apocynin: A narrative review of the evidence. *Pharmacol. Pharm.* 14, 997–1010. doi:10.1080/26895293.2021.1990136
- Brookes, J. F., and Kumar, A. (2005). Appendage regeneration in adult vertebrates and implications for regenerative medicine. *Science* 80310, 1919–1923. doi:10.1126/SCIENCE.1115200
- Brookes, J. P., and Gates, P. B. (2014). Mechanisms underlying vertebrate limb regeneration: Lessons from the salamander. *Biochem. Soc. Trans.* 42, 625–630. doi:10.1042/BST20140002
- Brookes, J. P., and Kumar, A. (2008). Comparative aspects of animal regeneration. *Annu. Rev. Cell Dev. Biol.* 24, 525–549. doi:10.1146/annurev.cellbio.24.110707.175336
- Bryant, D. M., Sousounis, K., Farkas, J. E., Bryant, S., Thao, N., Guzowski, A. R., et al. (2017). Repeated removal of developing limb buds permanently reduces appendage size in the highly-regenerative axolotl. *Dev. Biol.* 424, 1–9. doi:10.1016/j.ydbio.2017.02.013
- Camargo, F. D., Gokhale, S., Johnnidis, J. B., Fu, D., Bell, G. W., Jaenisch, R., et al. (2007). YAP1 increases organ size and expands undifferentiated progenitor cells. *Curr. Biol.* 17, 2054–2060. doi:10.1016/j.CUB.2007.10.039
- Cao, Y., Wei, W., Zhang, N., Yu, Q., Xu, W.-B., Yu, W.-J., et al. (2015). Oridonin stabilizes retinoic acid receptor alpha through ROS-activated NF- κ B signaling. *BMC Cancer* 15, 248. doi:10.1186/S12885-015-1219-8
- Carbonell, M. B., Zapata Cardona, J., and Delgado, J. (2021). Hydrogen peroxide is necessary during tail regeneration in juvenile axolotl. *Dev. Dyn.* 251, 1054–1076. doi:10.1002/DVDY.386
- Casadevall, M., and Sarkar, B. (1998). Effect of redox conditions on the DNA-binding efficiency of the retinoic acid receptor zinc-finger. *J. Inorg. Biochem.* 71, 147–152. doi:10.1016/S0162-0134(98)10046-6
- Chae, S., Lee, H. K., Kim, Y. K., Jung Sim, H., Ji, Y., Kim, C., et al. (2017). Peroxiredoxin1, a novel regulator of pronephros development, influences retinoic acid and Wnt signaling by controlling ROS levels. *Sci. Rep.* 7, 8874. doi:10.1038/S41598-017-09262-6
- Chevet, E., Fessart, D., Delom, F., Mulot, A., Vojtesek, B., Hrstka, R., et al. (2013). Emerging roles for the pro-oncogenic anterior gradient-2 in cancer development. *Oncogene* 32, 2499–2509. doi:10.1038/onc.2012.346
- Christensen, R. N., Weinstein, M., and Tassava, R. A. (2002). Expression of fibroblast growth factors 4, 8, and 10 in limbs, flanks, and blastemas of Ambystoma. *Dev. Dyn.* 223, 193–203. doi:10.1002/DVDY.10049
- Covarrubias, L., Hernández-García, D., Schnabel, D., Salas-Vidal, E., and Castro-Obregón, S. (2008). Function of reactive oxygen species during animal development: Passive or active? *Dev. Biol.* 320, 1–11. doi:10.1016/j.ydbio.2008.04.041
- Da Silva, S. M., Gates, P. B., and Brookes, J. P. (2002). The newt ortholog of CD59 is implicated in proximodistal identity during amphibian limb regeneration. *Dev. Cell* 3, 547–555. doi:10.1016/S1534-5807(02)00288-5
- Daponte, V., Tytlanowski, P., and Forlino, A. (2021). Appendage regeneration in vertebrates: What makes this possible? *Cells* 10, 242. doi:10.3390/CELLS10020242
- Delanay, A., Isnard, A. D., and Toledano, M. B. (2000). H₂O₂ sensing through oxidation of the Yap1 transcription factor. *EMBO J.* 19, 5157–5166. doi:10.1093/emboj/19.19.5157
- Demary, K., Wong, L., Liou, J. S., Faller, D. V., and Spanjaard, R. A. (2001). Redox control of retinoic acid receptor activity: A novel mechanism for retinoic acid resistance in melanoma cells. *Endocrinology* 142, 2600–2605. doi:10.1210/ENDO.142.6.8201
- Depew, M. J. (2008). Analysis of skeletal ontogenesis through differential staining of bone and cartilage. *Methods Mol. Biol.* 461, 37–45. doi:10.1007/978-1-60327-483-8_5
- Dixit, D., Ghildiyal, R., Anto, N. P., and Sen, E. (2014). Chaetocin-induced ROS-mediated apoptosis involves ATM-YAP1 axis and JNK-dependent inhibition of glucose metabolism. *Cell Death Dis.* 5, e1212. doi:10.1038/cddis.2014.179
- Dolan, C. P., Dawson, L. A., and Muneoka, K. (2018). Digit tip regeneration: Merging regeneration biology with regenerative medicine. *Stem Cells Transl. Med.* 7, 262–270. doi:10.1002/SCTM.17-0236
- Dong, J., Feldmann, G., Huang, J., Wu, S., Zhang, N., Comerford, S. A., et al. (2007). Elucidation of a universal size-control mechanism in Drosophila and mammals. *Cell* 130, 1120–1133. doi:10.1016/j.CELL.2007.07.019
- Dwaraka, V. B., and Voss, S. R. (2019). Towards comparative analyses of salamander limb regeneration. *J. Exp. Zool. B Mol. Dev. Evol.* 336, 129–144. doi:10.1002/jez.b.22902

Publisher's note

All claims expressed in this article are solely those of the authors and do not necessarily represent those of their affiliated organizations, or those of the publisher, the editors and the reviewers. Any product that may be evaluated in this article, or claim that may be made by its manufacturer, is not guaranteed or endorsed by the publisher.

Supplementary material

The Supplementary Material for this article can be found online at: <https://www.frontiersin.org/articles/10.3389/fcell.2022.921520/full#supplementary-material>

- Echeverri, K., and Tanaka, E. M. (2005). Proximodistal patterning during limb regeneration. *Dev. Biol.* 279, 391–401. doi:10.1016/j.ydbio.2004.12.029
- Elchaninov, A., Sukhikh, G., and Fatkhudinov, T. (2021). Evolution of regeneration in animals: A tangled story. *Front. Ecol. Evol.* 0, 121. doi:10.3389/FEVO.2021.621686
- Erler, P. (2017). Role of proto-oncogenes, *Pi3K*, *Her2*, *braf* and *Yap1* and adult stem cells in regeneration.
- Farkas, J. E., Freitas, P. D., Bryant, D. M., Whited, J. L., and Monaghan, J. R. (2016). Neuregulin-1 signaling is essential for nerve-dependent axolotl limb regeneration. *Development* 143, 2724–2731. doi:10.1242/DEV.133363
- Ferreira, F., Luxardi, G., Reid, B., and Zhao, M. (2016). Early bioelectric activities mediate redox-modulated regeneration. *Development* 143, 4582–4594. doi:10.1242/dev.142034
- Ferreira, F., Raghunathan, V. K., Luxardi, G., Zhu, K., and Zhao, M. (2018). Early redox activities modulate *Xenopus* tail regeneration. *Nat. Commun.* 9, 4296. doi:10.1038/s41467-018-06614-2
- Franklin, B. M., Voss, S. R., and Osborn, J. L. (2017). Ion channel signaling influences cellular proliferation and phagocyte activity during axolotl tail regeneration. *Mech. Dev.* 146, 42–54. doi:10.1016/j.mod.2017.06.001
- Gabig, T. G., and Babior, B. M. (1979). The O₂(-) -forming oxidase responsible for the respiratory burst in human neutrophils. Properties of the solubilized enzyme. *J. Biol. Chem.* 254, 9070–9074. doi:10.1016/s0021-9258(19)86810-2
- Galang, C. K., and Hauser, C. A. (1993). Cooperative DNA binding of the human HoxB5 (Hox-2.1) protein is under redox regulation *in vitro*. *Mol. Cell. Biol.* 13, 4609–4617. doi:10.1128/mcb.13.8.4609
- Gardiner, D. M., and Bryant, S. V. (2004). Molecular mechanisms in the control of limb regeneration: The role of homeobox genes. *Int. J. Dev. Biol.* 40, 797–805. doi:10.1387/IJDB.8877453
- Gauron, C., Rampon, C., Bouzaffour, M., Ipendey, E., Teillon, J., Volovitch, M., et al. (2013). Sustained production of ROS triggers compensatory proliferation and is required for regeneration to proceed. *Sci. Rep.* 3, 2084. doi:10.1038/srep02084
- Godwin, J., Pinto, A., and Rosenthal, N. (2013). Macrophages are required for adult salamander limb regeneration. *Proc. Natl. Acad. Sci. U. S. A.* 110, 9415–9420. doi:10.1073/pnas.1300290110
- Godwin, J. W., and Brookes, J. P. (2006). Regeneration, tissue injury and the immune response. *J. Anat.* 209, 423–432. doi:10.1111/J.1469-7580.2006.00626.X
- Godwin, J. W., Pinto, A. R., and Rosenthal, N. A. (2017). Chasing the recipe for a pro-regenerative immune system. *Semin. Cell Dev. Biol.* 61, 71–79. doi:10.1016/J.SEMCDB.2016.08.008
- Grassme, K. S., Garza-Garcia, A., Delgado, J. P., Godwin, J. W., Kumar, A., Gates, P. B., et al. (2016). Mechanism of action of secreted newt anterior gradient protein. *PLoS One* 11, e0154176. doi:10.1371/journal.pone.0154176
- Grigoryan, E. N. (2021). Study of natural longlife juvenility and tissue regeneration in caudate Amphibians and potential application of resulting data in biomedicine. *J. Dev. Biol.* 9, 2–19. doi:10.3390/JDB9010002
- Guimond, J. C., Lévesque, M., Michaud, P. L., Berdugo, J., Finnson, K., Philip, A., et al. (2010). BMP-2 functions independently of SHH signaling and triggers cell condensation and apoptosis in regenerating axolotl limbs. *BMC Dev. Biol.* 10, 15. doi:10.1186/1471-213X-10-15
- Haas, B. J., and Whited, J. L. (2017a). Advances in decoding axolotl limb regeneration. *Trends Genet.* 33, 553–565. doi:10.1016/j.tig.2017.05.006
- Haas, B. J., and Whited, J. L. (2017b). Advances in decoding axolotl limb regeneration. *Trends Genet.* 33, 553–565. doi:10.1016/j.tig.2017.05.006
- Hafen, E., and Stocker, H. (2003). How are the sizes of cells, organs, and bodies controlled? *PLoS Biol.* 1, E86. doi:10.1371/JOURNAL.PBIO.0000086
- Halder, G., and Johnson, R. L. (2011). Hippo signaling: Growth control and beyond. *Development* 138, 9–22. doi:10.1242/dev.045500
- Han, M.-J., An, J.-Y., and Kim, W.-S. (2001). Expression patterns of fgf-8 during development and limb regeneration of the axolotl. *Dev. Dyn.* 220(1):40–48. doi:10.1002/1097-0177(2000)9999:9999<AID-DVDY1085>3.0.CO;2-8
- Hayashi, S., Ochi, H., Ogino, H., Kawasumi, A., Kamei, Y., Tamura, K., et al. (2014a). Transcriptional regulators in the Hippo signaling pathway control organ growth in *Xenopus* tadpole tail regeneration. *Dev. Biol.* 396, 31–41. doi:10.1016/j.ydbio.2014.09.018
- Hayashi, S., Tamura, K., and Yokoyama, H. (2014b). Yap1, transcription regulator in the Hippo signaling pathway, is required for *Xenopus* limb bud regeneration. *Dev. Biol.* 388, 57–67. doi:10.1016/j.ydbio.2014.01.018
- Hayashi, S., Yokoyama, H., and Tamura, K. (2015). Roles of Hippo signaling pathway in size control of organ regeneration. *Dev. Growth Differ.* 57, 341–351. doi:10.1111/dgd.12212
- Heber-Katz, E., Zhang, Y., Bedelbaeva, K., Song, F., Chen, X., and Stocum, D. L. (2013). Cell cycle regulation and regeneration. *Curr. Top. Microbiol. Immunol.* 367, 253–276. doi:10.1007/82_2012_294
- Herbomel, P., Thisse, B., and Thisse, C. (2001). Zebrafish early macrophages colonize cephalic mesenchyme and developing brain, retina, and epidermis through a M-CSF receptor-dependent invasive process. *Dev. Biol.* 238, 274–288. doi:10.1006/DBIO.2001.0393
- Hernández-García, D., Wood, C. D., Castro-Obregón, S., and Covarrubias, L. (2010). Reactive oxygen species: A radical role in development? *Free Radic. Biol. Med.* 49, 130–143. doi:10.1016/j.freeradbiomed.2010.03.020
- Hsieh, C. L., Liu, C. M., Chen, H. A., Yang, S. T., Shigemura, K., Kitagawa, K., et al. (2017). Reactive oxygen species-mediated switching expression of MMP-3 in stromal fibroblasts and cancer cells during prostate cancer progression. *Sci. Rep.* 7(1), 1–14. doi:10.1038/s41598-017-08835-9
- Hwang, Y. J., Nam, S. J., Chun, W., Kim, S. I., Park, S. C., Kang, C. D., et al. (2019). Anti-inflammatory effects of apocynin on dextran sulfate sodium-induced mouse colitis model. *PLoS One* 14, e0217642. doi:10.1371/JOURNAL.PONE.0217642
- Iismaa, S. E., Kaidonis, X., Nicks, A. M., Bogush, N., Kikuchi, K., Naqvi, N., et al. (2018). Comparative regenerative mechanisms across different mammalian tissues. *npj Regen. Med.* 3, 6–20. doi:10.1038/s41536-018-0044-5
- Im, M., Chae, H., Kim, T., Park, H. H., Lim, J., Oh, E. J., et al. (2011). Comparative quantitative analysis of cluster of differentiation 45 antigen expression on lymphocyte subsets. *Korean J. Lab. Med.* 31, 148–153. doi:10.3343/KJLM.2011.31.3.148
- Ivanova, A. S., Tereshina, M. B., Araslanova, K. R., Martynova, N. Y., and Zaraisky, A. G. (2021). The secreted protein disulfide isomerase Ag1 lost by ancestors of poorly regenerating vertebrates is required for *Xenopus laevis* tail regeneration. *Front. Cell Dev. Biol.* 9, 2725. doi:10.3389/fcell.2021.738940
- Jenkins, L., Duerstock, B., and Borgens, R. (1996). Reduction of the current of injury leaving the amputation inhibits limb regeneration in the red spotted newt. *Dev. Biol.* 178, 251–262. doi:10.1006/DBIO.1996.0216
- Jensen, E. C. (2013). Quantitative analysis of histological staining and fluorescence using ImageJ. *Anat. Rec.* 296, 378–381. doi:10.1002/ar.22641
- Joven, A., Elewa, A., and Simon, A. (2019). Model systems for regeneration: Salamanders. *Development* 146, dev167700. doi:10.1242/dev.167700
- Kawakami, Y., Esteban, C. R., Raya, M., Kawakami, H., Martí, M., Dubova, I., et al. (2006). Wnt/beta-catenin signaling regulates vertebrate limb regeneration. *Genes Dev.* 20, 3232–3237. doi:10.1101/GAD.1475106
- Kim, D., and Hahn, J.-S. (2013). Roles of the *Yap1* transcription factor and antioxidants in *Saccharomyces cerevisiae*'s tolerance to furfural and 5-hydroxymethylfurfural, which function as thiol-reactive electrophiles generating oxidative stress. doi:10.1128/AEM.00643-13
- Kim, S. Y., Moon, K. A., Jo, H. Y., Jeong, S., Seon, S. H., Jung, E., et al. (2012). Anti-inflammatory effects of apocynin, an inhibitor of NADPH oxidase, in airway inflammation. *Immunol. Cell Biol.* 90, 441–448. doi:10.1038/ICB.2011.60
- Kragl, M., Knapp, D., Nacu, E., Khattak, S., Maden, M., Epperlein, H. H., et al. (2009). Cells keep a memory of their tissue origin during axolotl limb regeneration. *Nature* 460, 60–65. doi:10.1038/nature08152
- Kragl, M., and Tanaka, E. M. (2009). Axolotl (*Ambystoma mexicanum*) limb and tail amputation. *Cold Spring Harb. Protoc.* 4, pdb.prot5267. doi:10.1101/pdb.prot5267
- Kumar, A., Gates, P. B., Czarkwiani, A., and Brookes, J. P. (2015). An orphan gene is necessary for preaxial digit formation during salamander limb development. *Nat. Commun.* 6, 8684. doi:10.1038/NCOMMS9684
- Kumar, A., Godwin, J. W., Gates, P. B., Garza-Garcia, A. A., and Brookes, J. P. (2007). Molecular basis for the nerve dependence of limb regeneration in an adult vertebrate. *Science* 318, 772–777. doi:10.1126/science.1147710
- Kumar, A., Nevill, G., Brookes, J. P., and Forge, A. (2010). A comparative study of gland cells implicated in the nerve dependence of salamander limb regeneration. *J. Anat.* 217, 16–25. doi:10.1111/J.1469-7580.2010.01239.X
- Ledo, A., Fernandes, E., Salvador, A., Laranjinha, J., and Barbosa, R. M. (2022). *In vivo* hydrogen peroxide diffusivity in brain tissue supports volume signaling activity. *Redox Biol.* 50, 102250. doi:10.1016/J.REDOX.2022.102250
- Liu, Y., Lou, W. P. K., and Fei, J. F. (2021). 10, London, England, 12. doi:10.1186/S13619-020-00073-1The engine initiating tissue regeneration: Does a common mechanism exist during evolution? *Cell Regen.*
- Love, N. R., Chen, Y., Ishibashi, S., Kritsiligkou, P., Lea, R., Koh, Y., et al. (2013). Amputation-induced reactive oxygen species are required for successful *Xenopus* tadpole tail regeneration. *Nat. Cell Biol.* 15, 222–228. doi:10.1038/ncb2659
- Lovely, A. M., Duerr, T. J., Qiu, Q., Galvan, S., Voss, S. R., and Monaghan, J. R. (2022). Wnt signaling coordinates the expression of limb patterning genes during

axolotl forelimb development and regeneration. *Front. Cell Dev. Biol.* 10, 742. doi:10.3389/fcell.2022.814250

Maden, M. (2020). RA signaling in limb development and regeneration in different species. *Subcell. Biochem.* 95, 87–117. doi:10.1007/978-3-030-42282-0_4

Makanae, A., Mitogawa, K., and Satoh, A. (2014). Co-operative Bmp- and Fgf-signaling inputs convert skin wound healing to limb formation in urodele amphibians. *Dev. Biol.* 396, 57–66. doi:10.1016/j.ydbio.2014.09.021

Makanae, A., and Satoh, A. (2012). Early regulation of axolotl limb regeneration. *Anat. Rec. Hob.* 295, 1566–1574. doi:10.1002/AR.22529

Marinho, H. S., Real, C., Cyrne, L., Soares, H., and Antunes, F. (2014). Hydrogen peroxide sensing, signaling and regulation of transcription factors. *Redox Biol.* 2, 535–562. doi:10.1016/j.redox.2014.02.006

Mathew, L. K., Sengupta, S., Kawakami, A., Andreasen, E. A., Löhr, C. V., Loynes, C. A., et al. (2007). Unraveling tissue regeneration pathways using chemical genetics. *J. Biol. Chem.* 282, 35202–35210. doi:10.1074/JBC.M706640200

McCusker, C., Bryant, S., and Gardiner, D. (2015). 2. Oxford, England, 54–71. doi:10.1002/REG2.32 The axolotl limb blastema: Cellular and molecular mechanisms driving blastema formation and limb regeneration in tetrapods *Regeneration*

McCusker, C. D., and Gardiner, D. M. (2014). Understanding positional cues in salamander limb regeneration: Implications for optimizing cell-based regenerative therapies. *Dis. Model. Mech.* 7, 593–599. doi:10.1242/DMM.013359

McCusker, C., Lehrberg, J., and Gardiner, D. (2014). Position-specific induction of ectopic limbs in non-regenerating blastemas on axolotl forelimbs. *Regeneration* 1, 27–34. doi:10.1002/REG2.10

Meda, F., Gauron, C., Rampon, C., Teillon, J., Volovitch, M., and Vriza, S. (2016). Nerves control redox levels in mature tissues through Schwann cells and Hedgehog signaling. *Antioxid. Redox Signal.* 24, 299–311. doi:10.1089/ars.2015.6380

Meda, F., Joliet, A., and Vriza, S. (2017). Nerves and hydrogen peroxide: How old enemies become new friends. *Neural Regen. Res.* 12, 568–569. doi:10.4103/1673-5374.205088

Meda, F., Rampon, C., Dupont, E., Gauron, C., Mourtou, A., Queguiner, I., et al. (2018). Nerves, H₂O₂ and Shh: Three players in the game of regeneration. *Semin. Cell Dev. Biol.* 80, 65–73. doi:10.1016/j.semcdb.2017.08.015

Mercader, N., Tanaka, E. M., and Torres, M. (2005). Proximodistal identity during vertebrate limb regeneration is regulated by Meis homeodomain proteins. *Development* 132, 4131–4142. doi:10.1242/DEV.01976

Mescher, A. L., and Neff, A. W. (2006). Limb regeneration in Amphibians: Immunological considerations. *ScientificWorldJournal*. 6, 1–11. doi:10.1100/TSW.2006.323

Milkovic, L., Cipak Gasparovic, A., Cindric, M., Mouthuy, P. A., and Zarkovic, N. (2019). Short overview of ROS as cell function regulators and their implications in therapy concepts. *Cells* 8. doi:10.3390/CELLS8080793

Miller, E. W., Dickinson, B. C., and Chang, C. J. (2010). Aquaporin-3 mediates hydrogen peroxide uptake to regulate downstream intracellular signaling. *Proc. Natl. Acad. Sci. U. S. A.* 107, 15681–15686. doi:10.1073/PNAS.1005776107

Mullen, L. M., Bryant, S. V., Torok, M. A., Blumberg, B., and Gardiner, D. M. (1996). Nerve dependency of regeneration: The role of distal-less and FGF signaling in amphibian limb regeneration. *Development* 122, 3487–3497. doi:10.1242/DEV.122.11.3487

Nacu, E., Gromberg, E., Oliveira, C. R., Drechsel, D., and Tanaka, E. M. (2016). FGF8 and SHH substitute for anterior–posterior tissue interactions to induce limb regeneration. *Nature* 533, 407–410. doi:10.1038/nature17972

Nguyen, M., Singhal, P., Piet, J. W., Shefelbine, S. J., Maden, M., Voss, S. R., et al. (2017). Retinoic acid receptor regulation of epimorphic and homeostatic regeneration in the axolotl. *Development* 144, 601–611. doi:10.1242/DEV.139873

Niazi, I. A., Pescitelli, M. J., and Stocum, D. L. (1985). Stage-dependent effects of retinoic acid on regenerating urodele limbs. *Wilhelm Roux' Arch.* 194, 355–363. doi:10.1007/BF00877373

Niethammer, P., Grabher, C., Look, A. T., and Mitchison, T. J. (2009). A tissue-scale gradient of hydrogen peroxide mediates rapid wound detection in zebrafish. *Nature* 459, 996–999. doi:10.1038/nature08119

Niethammer, P. (2018). Wound redox gradients revisited. *Semin. Cell Dev. Biol.* 80, 13–16. doi:10.1016/j.semcdb.2017.07.038

Panday, A., Sahoo, M. K., Osorio, D., and Batra, S. (2015). NADPH oxidases: An overview from structure to innate immunity-associated pathologies. *Cell. Mol. Immunol.* 12, 5–23. doi:10.1038/CMI.2014.89

Park, U. H., Han, H. S., Um, E., An, X. H., Kim, E. J., and Um, S. J. (2009). Redox regulation of transcriptional activity of retinoic acid receptor by thioredoxin glutathione reductase (TGR). *Biochem. Biophys. Res. Commun.* 390, 241–246. doi:10.1016/J.BBRC.2009.09.097

Penzo-Mendez, A. I., and Stanger, B. Z. (2015). Organ-size regulation in mammals. *Cold Spring Harb. Perspect. Biol.* 7, a019240. doi:10.1101/CSHPERSPECT.A019240

Pirotte, N., Stevens, A. S., Fraguas, S., Plusquin, M., Van Roten, A., Van Belleghem, F., et al. (2015). Reactive oxygen species in planarian regeneration: An upstream necessity for correct patterning and brain formation. *Oxid. Med. Cell. Longev.* 2015, 392476. doi:10.1155/2015/392476

Poss, K. D. (2010). Advances in understanding tissue regenerative capacity and mechanisms in animals. *Nat. Rev. Genet.* 11, 710–722. doi:10.1038/nrg2879

Purushothaman, S., Elewa, A., and Seifert, A. W. (2019). Fgf-signaling is compartmentalized within the mesenchyme and controls proliferation during salamander limb development. *Elife* 8, e48507. doi:10.7554/ELIFE.48507

Rampon, C., Volovitch, M., Joliet, A., and Vriza, S. (2018). Hydrogen peroxide and redox regulation of developments. *Antioxidants* 7, E159. doi:10.3390/antiox7110159

Rhee, S. G., Woo, H. A., and Kang, D. (2018). The role of peroxiredoxins in the transduction of H₂O₂ signals. *Antioxid. Redox Signal.* 28, 537–557. doi:10.1089/ars.2017.7167

Roensch, K., Tazaki, A., Chara, O., and Tanaka, E. M. (2013). Progressive specification rather than intercalation of segments during limb regeneration. *Science* 342, 1375–1379. doi:10.1126/SCIENCE.1241796

Romero, M. M. G., McCathie, G., Jankun, P., and Roehl, H. H. (2018). Damage-induced reactive oxygen species enable zebrafish tail regeneration by repositioning of Hedgehog expressing cells. *Nat. Commun.* 9, 4010. doi:10.1038/s41467-018-06460-2

Sader, F., and Roy, S. (2021). Tgf- β superfamily and limb regeneration: Tgf- β to start and Bmp to end. *Dev. Dyn.* 251, 973–987. doi:10.1002/DVDY.379

Satoh, A., Bryant, S. V., and Gardiner, D. M. (2012). Nerve signaling regulates basal keratinocyte proliferation in the blastema apical epithelial cap in the axolotl (*Ambystoma mexicanum*). *Dev. Biol.* 366, 374–381. doi:10.1016/j.ydbio.2012.03.022

Satoh, A., makanae, A., Hirata, A., and Satou, Y. (2011). Blastema induction in aneuregenic state and Prx-1 regulation by MMPs and FGFs in *Ambystoma mexicanum* limb regeneration. *Dev. Biol.* 355, 263–274. doi:10.1016/j.ydbio.2011.04.017

Satoh, A., Makanae, A., Nishimoto, Y., and Mitogawa, K. (2016). FGF and BMP derived from dorsal root ganglia regulate blastema induction in limb regeneration in *Ambystoma mexicanum*. *Dev. Biol.* 417, 114–125. doi:10.1016/j.ydbio.2016.07.005

Schmittgen, T. D., and Livak, K. J. (2008). Analyzing real-time PCR data by the comparative CT method. *Nat. Protoc.* 3, 1101–1108. doi:10.1038/nprot.2008.73

Schneider, C. A., Rasband, W. S., and Eliceiri, K. W. (2012). NIH image to ImageJ: 25 years of image analysis. *Nat. Methods* 9, 671–675. doi:10.1038/nmeth.2089

Shaikh, N., Gates, P. B., and Brockes, J. P. (2011). The Meis homeoprotein regulates the axolotl Prod 1 promoter during limb regeneration. *Gene* 484, 69–74. doi:10.1016/j.gene.2011.06.003

Shin, D. H., Dier, U., Melendez, J. A., and Hempel, N. (2015). Regulation of MMP-1 expression in response to hypoxia is dependent on the intracellular redox status of metastatic bladder cancer cells. *Biochim. Biophys. Acta* 1852, 2593–2602. doi:10.1016/j.bbdis.2015.09.001

Shome, D., Von Woedtk, T., Riedel, K., and Masur, K. (2020). The HIPPO transducer YAP and its targets CTGF and Cyr61 drive a paracrine signalling in cold atmospheric plasma-mediated wound healing. *Oxid. Med. Cell. Longev.* 2020, 4910280. doi:10.1155/2020/4910280

Sies, H. (2017). Hydrogen peroxide as a central redox signaling molecule in physiological oxidative stress: Oxidative eustress. *Redox Biol.* 11, 613–619. doi:10.1016/j.redox.2016.12.035

Sies, H., and Jones, D. P. (2020a). Reactive oxygen species (ROS) as pleiotropic physiological signalling agents. *Nat. Rev. Mol. Cell Biol.* 21, 363–383. doi:10.1038/s41580-020-0230-3

Sies, H., and Jones, D. P. (2020b). Reactive oxygen species (ROS) as pleiotropic physiological signalling agents. *Nat. Rev. Mol. Cell Biol.* 21, 363–383. doi:10.1038/s41580-020-0230-3

Simon, A., and Tanaka, E. M. (2013). Limb regeneration. *Wiley Interdiscip. Rev. Dev. Biol.* 2, 291–300. doi:10.1002/wdev.73

Singer, M. (1978). On the nature of the neurotrophic phenomenon in urodele limb regeneration. *Am. Zool.* 18, 829–841. doi:10.1093/ICB/18.4.829

Stefanska, J., and Pawliczak, R. (2008). Apocynin: Molecular aptitudes. *Mediat. Inflamm.* 2008, 106507. doi:10.1155/2008/106507

Stocum, D. L. (2019). Nerves and proliferation of progenitor cells in limb regeneration. *Dev. Neurobiol.* 79, 468–478. doi:10.1002/DNEU.22643

- Stocum, D. (2017)., 4. Oxford, England, 159–200. doi:10.1002/REG2.92Mechanisms of urodele limb regeneration*Regeneration*
- Sun, Y., Lu, Y., Saredy, J., Wang, X., Drummer IV, C., Shao, Y., et al. (2020). ROS systems are a new integrated network for sensing homeostasis and alarming stresses in organelle metabolic processes. *Redox Biol.* 37, 101696. doi:10.1016/j.REDOX.2020.101696
- Svineng, G., Ravuri, C., Rikardsen, O., Huseby, N. E., and Winberg, J. O. (2008). The role of reactive oxygen species in integrin and matrix metalloproteinase expression and function. *Connect. Tissue Res.* 49, 197–202. doi:10.1080/03008200802143166
- Tanaka, E. M. (2016). The molecular and cellular choreography of appendage regeneration. *Cell* 165, 1598–1608. doi:10.1016/j.cell.2016.05.038
- Tank, P. W., Carlson, B. M., and Connelly, T. G. (1976). A staging system for forelimb regeneration in the axolotl, *Ambystoma mexicanum*. *J. Morphol.* 150, 117–128. doi:10.1002/JMOR.1051500106
- Tassava, R. A., Goldhamer, D. J., and Tomlinson, B. L. (1987). Cell cycle controls and the role of nerves and the regenerate epithelium in urodele forelimb regeneration: Possible modifications of basic concepts. *Biochem. Cell Biol.* 65, 739–749. doi:10.1139/O87-097
- Tauzin, S., Starnes, T. W., Becker, F. B., Lam, P. Y., and Huttenlocher, A. (2014). Redox and Src family kinase signaling control leukocyte wound attraction and neutrophil reverse migration. *J. Cell Biol.* 207, 589–598. doi:10.1083/jcb.201408090
- Thauvin, M., Matias de Sousa, R., Alves, M., Volovitch, M., Vriz, S., and Rampon, C. (2022). *SHH-H2O2-RECIPROCAL-REGULATORY*, 135. doi:10.1242/JCS.259664/274206/AM/AN-EARLY-An early Shh-H2O2 reciprocal regulatory interaction controls the regenerative program during zebrafish fin regeneration*J. Cell Sci.*
- Tornini, V. A., and Poss, K. D. (2014). Keeping at arm's length during regeneration. *Dev. Cell* 29, 139–145. doi:10.1016/j.DEVCEL.2014.04.007
- Tung, J. N., Lin, P. L., Wang, Y. C., Wu, D. W., Chen, C. Y., and Lee, H. (2018). PD-L1 confers resistance to EGFR mutation-independent tyrosine kinase inhibitors in non-small cell lung cancer via upregulation of YAP1 expression. *Oncotarget* 9, 4637–4646. doi:10.18632/oncotarget.23161
- Veal, E. A., Day, A. M., and Morgan, B. A. (2007). Hydrogen peroxide sensing and signaling. *Mol. Cell* 26, 1–14. doi:10.1016/j.MOLCEL.2007.03.016
- Veal, E. A., Ross, S. J., Malakasi, P., Peacock, E., and Morgan, B. A. (2003). Ybp1 is required for the hydrogen peroxide-induced oxidation of the Yap1 transcription factor. *J. Biol. Chem.* 278, 30896–30904. doi:10.1074/jbc.M303542200
- Vieira, W. A., and McCusker, C. D. (2018). Regenerative models for the integration and regeneration of head skeletal tissues. *Int. J. Mol. Sci.* 19, E3752. doi:10.3390/ijms19123752
- Vieira, W. A., Wells, K. M., Milgrom, R., and McCusker, C. D. (2018). Exogenous Vitamin D signaling alters skeletal patterning, differentiation, and tissue integration during limb regeneration in the axolotl. *Mech. Dev.* 153, 1–9. doi:10.1016/j.MOD.2018.08.004
- Vieira, W., Wells, K., Raymond, M., De Souza, L., Garcia, E., and McCusker, C. (2019). FGF, BMP, and RA signaling are sufficient for the induction of complete limb regeneration from non-regenerating wounds on *Ambystoma mexicanum* limbs. *Dev. Biol.* 451, 146–157. doi:10.1016/j.YDBIO.2019.04.008
- Vollmer, J., Casares, F., and Iber, D. (2017). Growth and size control during development. *Open Biol.* 7, 170190. doi:10.1098/RSOB.170190
- Voss, S. R., Epperlein, H. H., and Tanaka, E. M. (2009). *Ambystoma mexicanum*, the axolotl: A versatile amphibian model for regeneration, development, and evolution studies. *Cold Spring Harb. Protoc.* 2009, emo128. doi:10.1101/pdb.emo128
- Voss, S. R., Palumbo, A., Nagarajan, R., Gardiner, D. M., Muneoka, K., Stromberg, A. J., et al. (2015). Gene expression during the first 28 days of axolotl limb regeneration I: Experimental design and global analysis of gene expression. *Regeneration* 2, 120–136. doi:10.1002/reg2.37
- Wells, K. M., Baumel, M., and McCusker, C. D. (2022). The regulation of growth in developing, homeostatic, and regenerating tetrapod limbs: A minireview. *Front. Cell Dev. Biol.* 0, 768505. doi:10.3389/FCELL.2021.768505
- Wells, K. M., Kelley, K., Baumel, M., Vieira, W. A., and McCusker, C. D. (2021). Neural control of growth and size in the axolotl limb regenerate. *Elife* 10, e68584. doi:10.7554/ELIFE.68584
- Wischnin, S., Castañeda-Patlán, C., Robles-Flores, M., and Chimal-Monroy, J. (2017). Chemical activation of Wnt/ β -catenin signalling inhibits innervation and causes skeletal tissue malformations during axolotl limb regeneration. *Mech. Dev.* 144, 182–190. doi:10.1016/j.MOD.2017.01.005
- Yokoyama, H. (2008). Initiation of limb regeneration: The critical steps for regenerative capacity. *Dev. Growth Differ.* 50, 13–22. doi:10.1111/J.1440-169X.2007.00973.X
- Yoo, S. K., Freisinger, C. M., LeBert, D. C., and Huttenlocher, A. (2012). Early redox, Src family kinase, and calcium signaling integrate wound responses and tissue regeneration in zebrafish. *J. Cell Biol.* 199, 225–234. doi:10.1083/jcb.201203154
- Yoo, S. K., Starnes, T. W., Deng, Q., and Huttenlocher, A. (2011). Lyn is a redox sensor that mediates leukocyte wound attraction *in vivo*. *Nature* 480, 109–112. doi:10.1038/nature10632
- Zhang, M., Chen, Y., Xu, H., Yang, L., Yuan, F., Li, L., et al. (2018). Melanocortin receptor 4 signaling regulates vertebrate limb regeneration. *Dev. Cell* 46, 397–409. e5. doi:10.1016/j.DEVCEL.2018.07.021
- Zhang, Q., Wang, Y., Man, L., Zhu, Z., Bai, X., Wei, S., et al. (2016). Reactive oxygen species generated from skeletal muscles are required for gecko tail regeneration. *Sci. Rep.* 6, 20752. doi:10.1038/srep20752
- Zhu, W., Pao, G. M., Satoh, A., Cummings, G., Monaghan, J. R., Harkins, T. T., et al. (2012). Activation of germline-specific genes is required for limb regeneration in the Mexican axolotl. *Dev. Biol.* 370, 42–51. doi:10.1016/j.ydbio.2012.07.021
- Zweitig, D. R., Smirnov, D. A., Connelly, M. C., Terstappen, L. W. M. M., O'Hara, S. M., and Moran, E. (2007). Physiological stress induces the metastasis marker AGR2 in breast cancer cells. *Mol. Cell. Biochem.* 306, 255–260. doi:10.1007/s11010-007-9562-y



OPEN ACCESS

EDITED BY

Juan Rafael Riesgo-Escovar,
Universidad Nacional Autónoma de
México, Mexico

REVIEWED BY

Elizabeth Jenness Duncan,
University of Leeds, United Kingdom
Alexandra Chittka,
University College London,
United Kingdom
Tomas Erban,
Crop Research Institute (CRI), Czechia

*CORRESPONDENCE

Francis Morais Franco Nunes,
francis.nunes@ufscar.br

SPECIALTY SECTION

This article was submitted to
Morphogenesis and Patterning,
a section of the journal
Frontiers in Cell and Developmental
Biology

RECEIVED 15 April 2022

ACCEPTED 01 August 2022

PUBLISHED 29 August 2022

CITATION

Bataglia L, Simões ZLP and Nunes FMF
(2022), Transcriptional expression of
m⁶A and m⁵C RNA methyltransferase
genes in the brain and fat body of honey
bee adult workers.
Front. Cell Dev. Biol. 10:921503.
doi: 10.3389/fcell.2022.921503

COPYRIGHT

© 2022 Bataglia, Simões and Nunes.
This is an open-access article
distributed under the terms of the
[Creative Commons Attribution License
\(CC BY\)](https://creativecommons.org/licenses/by/4.0/). The use, distribution or
reproduction in other forums is
permitted, provided the original
author(s) and the copyright owner(s) are
credited and that the original
publication in this journal is cited, in
accordance with accepted academic
practice. No use, distribution or
reproduction is permitted which does
not comply with these terms.

Transcriptional expression of m⁶A and m⁵C RNA methyltransferase genes in the brain and fat body of honey bee adult workers

Luana Bataglia¹, Zilá Luz Paulino Simões^{1,2} and
Francis Morais Franco Nunes^{1,3*}

¹Departamento de Genética, Faculdade de Medicina de Ribeirão Preto, Universidade de São Paulo, Ribeirão Preto, Brazil, ²Departamento de Biologia, Faculdade de Filosofia Ciências e Letras de Ribeirão Preto, Universidade de São Paulo, Ribeirão Preto, Brazil, ³Departamento de Genética e Evolução, Centro de Ciências Biológicas e da Saúde, Universidade Federal de São Carlos, São Carlos, Brazil

Honey bee (*Apis mellifera*) adult workers change behaviors and nutrition according to age progression. Young workers, such as nurses, perform in-hive tasks and consume protein-rich pollen, while older workers (foragers) leave the colony to search for food, and consume carbohydrate-rich nectar. These environmentally stimulated events involve transcriptional and DNA epigenetic marks alterations in worker tissues. However, post-transcriptional RNA modifications (epitranscriptomics) are still poorly explored in bees. We investigated the transcriptional profiles of m⁶A and m⁵C RNA methyltransferases in the brain and fat body of adult workers of 1) different ages and performing different tasks [nurses of 8 days-old (N-8D) and foragers of 29 days-old (F-29D), sampled from wild-type colonies], and 2) same-aged young workers caged in an incubator and treated with a pollen-rich [PR] or a pollen-deprived [PD] diet for 8 days. In the brain, METTL3, DNMT2, NOP2, NSUN2, NSUN5, and NSUN7 genes increased expression during adulthood (from N-8D to F-29D), while the opposite pattern was observed in the fat body for METTL3, DNMT2, and NSUN2 genes. Regarding diet treatments, high expression levels were observed in the brains of the pollen-deprived group (DNMT2, NOP2, and NSUN2 genes) and the fat bodies of the pollen-rich group (NOP2, NSUN4, and NSUN5 genes) compared to the brains of the PR group and the fat bodies of the PD group, respectively. Our data indicate that RNA epigenetics may be an important regulatory layer in the development of adult workers, presenting tissue-specific signatures of RNA methyltransferases expression in response to age, behavior, and diet content.

KEYWORDS

RNA methylation, m⁶A, m⁵C, epitranscriptomics, bee, nutrition, aging, behavior

Introduction

The adult life of honey bee (*Apis mellifera*) workers is characterized by a temporal polyethism, in which individuals progressively experience different tasks and behaviors during their lifetime. This age-related polyethism is accompanied by alteration of the feeding regimes. Young workers feed on pollen, a predominant source of protein, lipids, vitamins, and minerals (Brodschneider and Crailsheim, 2010). During this period, they perform in-hive tasks, such as feeding the developing larvae, a behavior that characterizes them as nurses (Winston, 1987; Page and Peng, 2001). Around the third week of adulthood, workers start to go outside the colony to collect pollen, nectar, resins, and water, a behavior that characterizes them as foragers (Winston, 1987; Page and Peng, 2001). The foragers consume nectar, a diet rich in carbohydrates and low in proteins, which increases the bee's energy metabolism, necessary for flight activity and resource gathering (Winston, 1987). This behavioral transition in honey bees involves transcriptional and metabolic changes in tissues, especially in the brain and the fat body (Ament et al., 2011). Foragers have an increase in cognitive capacity (memory and learning) compared to young workers performing in-hive tasks (Zayed and Robinson, 2012), and their brain transcriptomes differ significantly (Whitfield et al., 2003). The fat body is a metabolic center and during the behavior transition, the foragers lose half of their lipid stores and the capacity to metabolize these molecules (Toth and Robinson, 2005).

Epigenetics is proposed to be a plastic mechanism for regulating gene expression in response to environmental conditions (Vaiserman, 2014; Abdul et al., 2017). Diet is one of the external factors that alters gene expression through epigenetic modifications of the genomic DNA (epigenomics). The nutrients and bioactive components present in food can alter the activity of genes involved in DNA methylation or histone modifications or can change the availability of substrates required for these modifications' reactions (reviewed by Abdul et al., 2017). In honey bees, the different diets consumed by workers and queens' larvae trigger distinct abundance and patterns of DNA methylation between castes (Kucharski et al., 2008). In workers, several DNA CpG sites are differentially methylated comparing the brains of nurses and foragers (Herb et al., 2012; Lockett et al., 2012). Although knowledge in bee epigenomics has advanced in recent years, little has been explored about how epitranscriptomics, an emerging field of investigation, acts in bee development.

Epitranscriptomics is the study of RNA post-transcriptional modifications. More than 170 chemical modifications present in RNAs are currently known (Boccalletto et al., 2017; Huang et al., 2020). Two of them, the methylation of the nitrogen N6 of adenosine (N6-methyladenosine, m⁶A) and the methylation of the carbon C5 of cytosine (5-methylcytosine, m⁵C) are the most studied and regulate several biological processes such as development in mouse (Tuorto et al., 2012) and *Drosophila*

melanogaster (Lence et al., 2016), behavioral adaptation in mammals (Meyer et al., 2012), aging and response to environmental (feeding, temperature) stimuli in *D. melanogaster*, *Caenorhabditis elegans* and *Saccharomyces cerevisiae* (Schosserer et al., 2015). Interestingly, these biological processes are closely related to those observed in the context of age polyethism such that RNA modifications have become excellent candidates to be explored in honey bees.

To date, over 1,000 RNA epigenetic studies were published, however, only 3% of them investigated insects (source: PubMed, June 2022). Most of them used *D. melanogaster*, with RNA methylation being related to sex determination (Hausmann, et al., 2016; Kan et al., 2017), fertility (Hongay and Orr-Weaver, 2011), and nervous system development (Lence et al., 2016). In *Bombyx mori*, m⁶A was reported to control gene expression and cell cycle progression (Li et al., 2019). In honey bees, two studies revealed RNA modifications acting in caste differentiation (Bataglia et al., 2021; Wang et al., 2021). Our group recently identified the orthologs of RNA methyltransferase genes in the *A. mellifera* genome, being METTL3 (methyltransferase like 3) and METTL14 (methyltransferase like 14) for m⁶A methylation, and DNMT2 (DNA methyltransferase 2) and the NSUN (NOP2/Sun RNA methyltransferase member) family encoding genes (NOP2, NSUN2, NSUN4, NSUN5, and NSUN7) for m⁵C methylation (Bataglia et al., 2021).

Here, we verified if the expression of m⁶A and m⁵C RNA methyltransferase genes vary in the development of *A. mellifera* adult workers according to age-related behavior (nurses of 8 days-old versus foragers of 29 days-old), diet content (pollen-rich or pollen-deprived), or tissue (brain or fat body). We found that the expression of some RNA methyltransferase transcripts is modulated during temporal polyethism in a tissue-specific and nutrition-dependent manner.

Materials and methods

Samples

Apis mellifera workers were collected from three queenright colonies maintained at the experimental apiary of the Universidade de São Paulo in Ribeirão Preto, Brazil. Three independent biological experiments were performed, each one starting with 1 day of difference, on three consecutive days, each day with bees from a different colony. For each experiment, combs containing pharate adults close to emergence (Pbd stage) were placed in an incubator at 34°C and ~80% relative humidity for 8 h to obtain at least 400 newly-emerged adult workers.

Each experiment was performed according to the following design. A total of 100 newly-emerged workers were divided (day 1) into two cages ($n = 50$ per cage of 20 cm × 13 cm × 13 cm) and kept in the incubator, with food and water *ad libitum* for 8 days. Every day, the food and the water were replaced, and the dead

bees were removed. The bees of one cage received a pollen-deprived (PD) diet (a mix of 20% honey plus 80% powdered sugar, named candy), and the bees of the other cage received a pollen-rich (PR) diet (a mix of 70% candy and 30% of fresh poly floral pollen collected from the same apiary). On day 8, five individuals per cage were collected. The newly-emerged workers that were not placed in cages (at least 300 workers), were then marked on the thorax with uni POSCA non-toxic pens (1.8–2.5 mm), for age control, and returned to their original colony. We collected five nurses of 8 days-old visiting larval cells and five foragers of 29 days-old returning to the colony (N-8D and F-29D, respectively).

The collected workers were anesthetized at 4°C for 5 min for tissue dissection. Then, we quickly dissected the brain and the fat body of each worker. Brains were dissected using a Leica M125 stereomicroscope and all glands and adjacent tissues were removed. For sampling the fat body, we pulled the sting along with the last abdominal segment, to remove the venom gland, the intestine, and adjacent tissues (such as the ovaries), leaving only the abdominal carcass. The abdominal carcass is internally lined by the fat body (Ament et al., 2011). Each individual brain or abdominal fat body was placed separately in tubes containing TRIzol® (Invitrogen) for RNA extraction.

Total RNA extraction, cDNA synthesis, and real-time PCR

The total RNA was extracted from individual brains and fat bodies according to Trizol® protocol. To avoid genomic DNA contamination, the total RNA was treated with DNase (DNase I Amplification Grade—Invitrogen). Next, cDNA was synthesized by reverse transcription catalyzed by SuperScript II reverse transcriptase (200 U/μL, Invitrogen) and oligo (dT) 12–18 primers.

Real-time PCR was performed with 60 brain samples and 60 fat body samples. Among these 60 samples of each tissue, 15 samples represent each condition (PD, PR, N-8D, F-29D), being five samples of each experiment. The expression of the following methyltransferase genes was evaluated: for m⁶A, METTL3 (NCBI Gene ID: 551911) and METTL14 (409900), and for m⁵C, DNMT2 (410512), NOP2 (726212), NSUN2 (411579), NSUN4 (102655259), NSUN5 (410262), and NSUN7 (413907).

We perform the real-time PCR following the PowerUP™ SYBR™ Green Master Mix (2X) protocol and cycling (Applied Biosystems). For each sample, reactions were assembled in triplicate, and every single reaction consisted of a final volume of 20 μL, containing: 10 μL of PowerUP™ SYBR™ Green Master Mix (2X) solution (Applied Biosystems), 6.4 μL of water, 0.8 μL of each primer, forward and reverse (10 pmol/μL), and 2 μL of the cDNA solution (10 ng/μL). The primer pairs used are listed in [Supplementary Table S1](#), including the pair used for

amplification of the ribosomal protein L32 (RpL32) encoding gene, used as a reference for data normalization (Groizinger et al., 2003; Lourenço et al., 2008). The amplification reactions were conducted on a 7,500 Real-Time PCR System (Applied Biosystems). For primer pairs with optimal efficiency at 60°C, the following cycling conditions were used: 50°C for 2 min, 95°C for 10 min, followed by 40 cycles of 95°C for 15 s and 60°C for 1 min. For primer pairs with annealing temperature lower than 60°C, the following cycle was used: 50°C for 2 min, 95°C for 10 min, followed by 40 cycles of 95°C for 15 s, primer annealing temperature for 15 s, and 72°C for 1 min.

The relative expressions were calculated using the $2^{-\Delta\Delta CT}$ method (Livak and Schmittgen, 2001). The statistical analyses were performed in R (version 4.1.3). We applied the Generalized Linear Mixed (GLM) models (package lme4 version 1.1–29) followed by the Anova function (package car version 3.0.12) to compare the different diets or ages with gene expression, using colony or cage replicate as a random effect. Significant outliers were removed [Grubbs' test (alpha = 0.05)] when detected.

Results

The expression of METTL3, DNMT2, NOP2, NSUN2, NSUN5, and NSUN7 methyltransferases statistically vary in the brain of workers of different ages, performing different tasks (N-8D versus F-29D comparison). Also, DNMT2, NOP2, and NSUN2 were differentially expressed in the brain of same-aged young workers that consumed distinct diets (PR versus PD comparison). In the fat body, the expression of METTL3, DNMT2, and NSUN2 genes were influenced by age/task (N-8D versus F-29D comparison), while the expression of NOP2, NSUN4, and NSUN5 was influenced by diet (PR versus PD comparison). All these results are graphically represented in [Figure 1](#) (and the results of the statistical analyses are in [Supplementary Table S2](#)).

A clear expression pattern for methyltransferase genes should be highlighted. Regarding the gene set that presented significant transcriptional differences in the brain, we observed lower levels in both N-8D and PR groups when compared to F-29D and PD groups. In addition, an opposite pattern was observed in the fat body, with increased expression in N-8D and PR groups in relation to F-29D and PD groups.

Discussion

The adult life progression of *A. mellifera* workers is marked by changes ranging from behavior to nutrition, mainly in the brain and the fat body (Ament et al., 2011). Despite the age-related division of labor in workers (temporal polyethism) being well-documented (Page et al., 2006), the participation of RNA modifications in these processes remains largely unknown

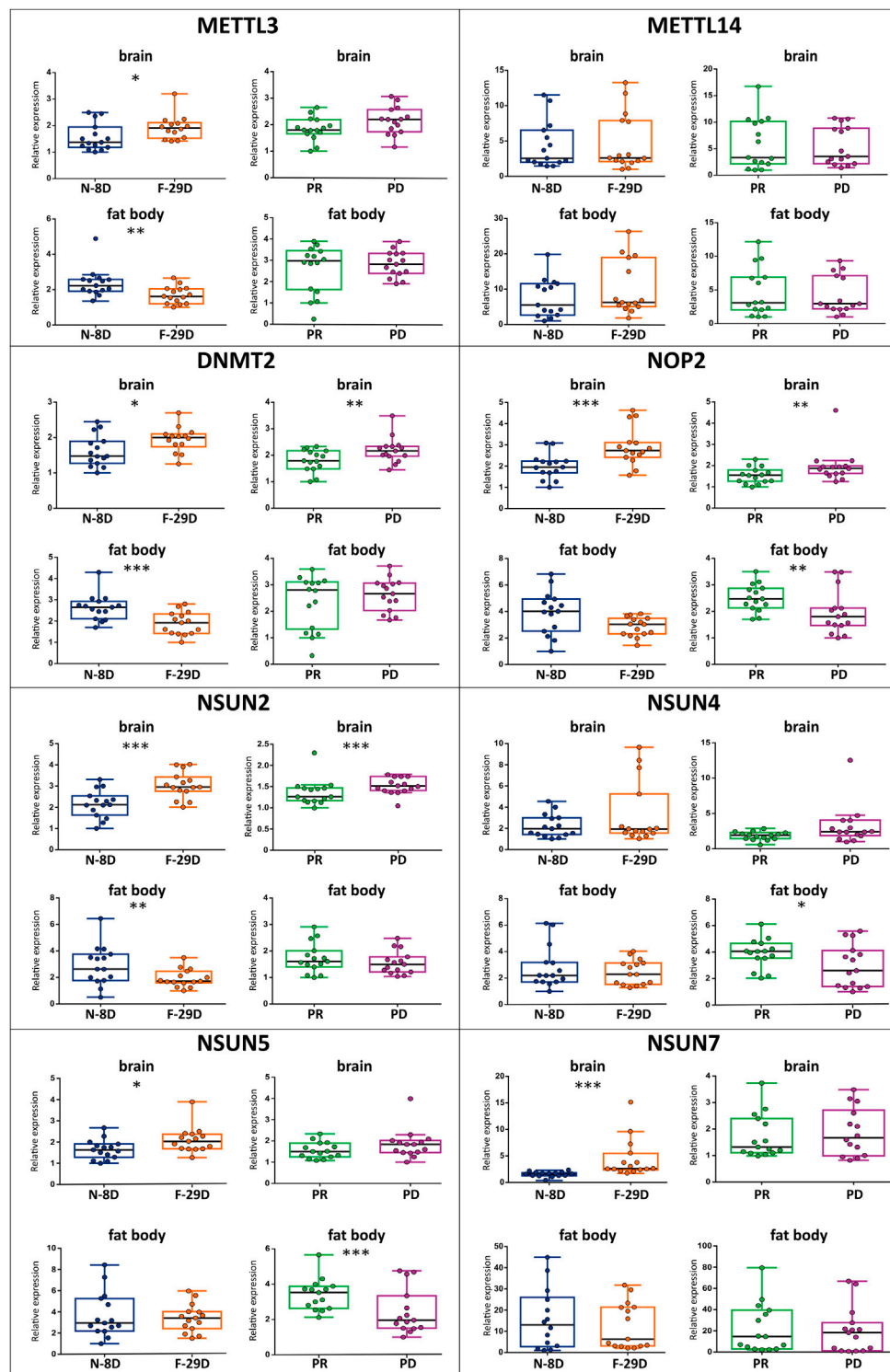


FIGURE 1

Relative expression of m⁶A (METTL3 and METTL14) and m⁵C (DNMT2, NOP2, NSUN2, NSUN4, NSUN5, and NSUN7) RNA methyltransferase genes, measured by real-time PCR in the brain and fat body samples from workers of different ages/behaviors (N-8D for 8 days-old nurses—blue—and F-29D for 29 days-old foragers—orange) and under different dietary regimes (PR for pollen-rich diet—green—and PD for pollen-deprived—purple), $n = 15$ per condition. The boxplots represent the minimum, maximum, and median values. The presence of asterisks indicates a significant difference in expression, $*p < 0.05$, $*p < 0.01$, $**p < 0.001$.

(Bataglia et al., 2021). To advance this knowledge, we have investigated the transcriptional expression of m⁶A and m⁵C RNA methyltransferases in the brain and fat body of workers of different ages, performing different tasks, or same-aged young workers that consumed a pollen-deprived or a pollen-rich diet.

Foraging tasks of workers require well-developed brain abilities such as, recognizing the environment, identifying food resources, and communicating this information with nestmates. During the transition from in-hive to outside tasks, structural modifications such as the increase of the mushroom bodies (Withers et al., 1993; Durst et al., 1994) and the neuronal dendritic arborization (Farris et al., 2001) are observed. Higher expression levels of METTL3, DNMT2, NOP2, NSUN2, NSUN5, and NSUN7 transcripts were found in the brain of foragers compared to nurses. All these genes are reported in the literature as being involved in brain development, memory formation, or increase of cognitive capacity. The overexpression of METTL3 enhances hippocampus-dependent long-term memory in mice (Zhang et al., 2018) while its depletion perturbs short-term memory formation in flies (Kan et al., 2021). High abundance of mRNAs of DNMT2 (Rai et al., 2007) and NOP2 (Kosi et al., 2015) are related to neurogenesis in zebrafish brains and neural stem cell proliferation in mammals, respectively. The lack of NSUN2 expression inhibits normal brain development by reducing the number of differentiated neurons in mice (Flores et al., 2017) and short-term memory deficits in *Drosophila* (Abbasi-Moheb et al., 2012). NSUN5 mutant mice showed deficits in spatial cognitive abilities (Zhang et al., 2019) and in cerebral cortex development (Chen et al., 2019). Transcriptomic evidence suggests that NSUN7 may act on the cognitive processes of mammals (Chi and Delgado-Olguin, 2013; Tang et al., 2019). It is increasingly evident that the development of the nervous system, cognitive and behavioral aspects, and learning and memory abilities, in different organisms, are associated with a reprogramming (spatial and temporal) of the epitranscriptome (Jung and Goldman, 2018; Leighton et al., 2018). Our study supports and extends such evidence.

The main function of fat body of insects is the metabolism of macromolecules (reviewed by Skowronek et al., 2021). RNA methylation acts on nutritional metabolism, mainly on glucose and lipid metabolism (Wu et al., 2020). For example, METTL3 knockdown decreased lipid accumulation in human liver cell culture (Zhong et al., 2018). The difference in the expression of RNA methyltransferases in the fat body of nurses and foragers found here may be integrated into the gene regulatory network associated with the conversion of a protein-lipid metabolism in younger workers to a carbohydrate metabolism in older ones (Ament et al., 2011). Our data showed that not only age, but diet also influenced the expression of some methyltransferases. NOP2, NSUN4, and NSUN5 were differentially expressed in the fat body of same-aged workers that fed on different diets under caged conditions and did not

perform behavioral tasks. Thus, these genes are excellent candidates for further studies about nutritional metabolism uncoupled to social interactions in honey bees. Moreover, in the worker brains, DNMT2, NOP2, and NSUN2 expression levels were diet-responsive. Our data are further corroborated by a study performed with rats fed on high or low-calorie diets, that showed the nutritional influence on the differential expression of RNA methyltransferases depending on the tissue analyzed (D'Aquila et al., 2022). It is important to highlight that the pollen-rich (PR) diet mimics that consumed by nurses while the pollen-deprived (PD) diet is similar to the nutritional content of foragers. Recently, Martelli et al. (2022) showed that young honey bee workers fed on PD diet age precociously and present biological parameters similar to foragers. Here, we observed corresponding expression profiles of some m⁵C genes (DNMT2, NOP2, and NSUN2) between N-8D + PR groups, which contrast with data from F-29D + PD groups. These genes will be tested in the future as potential candidates for aging markers in adult worker brains.

The fat body is also important for the production of energy and for the synthesis of immune system proteins (reviewed by Skowronek et al., 2021). Changes in the activity of methyltransferases have already been observed in response to stressful conditions. METTL3 plays a crucial role in oxidative stress, glycolytic stress, and DNA damage, and promotes an increased lipid metabolism in different mammalian cell lines (reviewed by Wilkinson et al., 2021). DNMT2 integrates stress response pathways by protecting tRNAs against ribonuclease cleavage induced by heat shock conditions in *Drosophila* (Schaefer et al., 2010), while NOP2 is involved with resistance to heat stress in *C. elegans* (Heissenberger et al., 2020). In mice, NSUN2 is required in cellular adaptation in response to toxic compounds and UV radiation (Gkatza et al., 2019). In honey bees, nurses have a more robust immune response to stress conditions compared to foragers (Amdam et al., 2004; Lourenço et al., 2019). In addition, our findings on the higher expression of some methyltransferases in the fat body of young bees compared to old ones seem somewhat coherent with this immunological scenario. Further research is needed to check if this suggestive crosstalk between immunity and epitranscriptomics is also true for bees.

This scientific topic is promising and some studies already involve epigenetic mechanisms to the xenobiotic response in insects. Epigenomic marks are associated with modulation of the expression of pesticide resistant genes in the beetle *Meligethes aeneus* (Erban et al., 2017). Also, strong evidence suggests that the expression of METTL3, METTL14 and a set of detoxification P450 genes along with increased levels of m⁶A marks confer thiamethoxam resistance to a strain of whitefly crop pest, *Bemisia tabaci* (Yang et al., 2021). It is important to consider that pollen is a common source of pesticides in agricultural sites and the contamination can be the cause of poisoning incidents of honey bees (Kiljanek et al., 2016). Although we did not screen

the pollen for pesticides, our apiary is located within a non-agricultural area of a University with six million m² containing an abundance of flowering plants representing nearly 300 species, and no poisoning effects were observed on bees we used as a source for the experiments. Furthermore, it is known that pollen consumption reduces the toxicity of pesticides in *Apis mellifera* (Barascou et al., 2021) and that diets influence the expression of genes of the epitranscriptomic machinery (this study). Perspectives are open to investigate whether RNA modifications respond to the detrimental impacts of insecticides and/or whether they confer some resistance to these pollinators.

Here we observed co-expression of RNA methyltransferase genes in all tested contexts in worker bees irrespective of their nutrition or age. Does this co-expression indicate functional redundancy? Do RNA methyltransferases have specific or integrated actions? It is widely accepted that all RNA methyltransferases have the canonical function of methylating RNAs, and RNA modifications are found in viruses (Kennedy et al., 2017), prokaryotes (Deng et al., 2015), yeasts (Clancy et al., 2002), plants (Fray & Simpson 2015), invertebrates (Hongay & Orr-Weaver, 2011), and vertebrates (D'Aquila et al., 2022). Despite METTL3 gene silencing in human embryonic stem cells is not sufficient for a complete reduction of m⁶A methylation levels, this knockdown at least removes the methylation marks of a specific subset of pluripotency-related genes, influencing the process of cell differentiation (Batista et al., 2014). This suggests a co-working, but it is also true that an individual RNA methyltransferase may have preferential RNA species as targets. NSUN2 preferentially methylates mRNA, tRNAs, and mitochondrial tRNAs (Tuorto et al., 2012; Shinoda et al., 2019), whereas NSUN5 preferentially methylates rRNA (Schosserer et al., 2015). Also, m⁶A sites are found mainly in mRNAs and affect the physical interaction of RNA with proteins or regulatory factors, resulting in altered translation or changes in mRNA stability (Meyer et al., 2015). This methylation also participates in alternative splicing (Zhao et al., 2014) and miRNA processing (Alarcón et al., 2015) events. The m⁵C marks are more frequent in non-protein-coding RNAs (ncRNAs, mainly tRNAs, and rRNAs) and maintain the stability of their secondary structures for the correct translation events (Micura et al., 2001; Schaefer et al., 2010). We believe that new findings should emerge in the coming years to clarify both species-specific or conserved functional issues related to epitranscriptomics. This is the case of a recent article that studied the m⁵C methylation patterns of maternal mRNAs in six species (five vertebrates: zebrafish, *Xenopus laevis*, *Xenopus tropicalis*, mouse, human, and one invertebrate: *D. melanogaster*) spanning ~800 million years of evolution. For all tested species, they found a massive methylation of maternal mRNAs occurring in early embryonic development, and the rates drop dramatically after the mater-zygotic transition. This data shows an extremely conserved pattern in animals. On the other hand, they also

observed regulatory innovations, such as the gain of m⁵C sites in mRNAs during evolution (Liu et al., 2022).

Concerning the differences we found in the expression of m⁶A and m⁵C methyltransferases between honey bee tissues, we speculate that they may reflect in the regulation of tissue-specific splicing variants previously found in the brain and fat body (Kannan et al., 2019), and/or several differentially expressed coding-genes and miRNA from workers performing different behaviors (Whitfield et al., 2003; Behura and Whitfield, 2010).

Bataglia et al. (2021) reported that global levels of m⁶A and m⁵C methylation quantified in the total RNA from brain and fat body samples increases in age progression. In this study we observed an increase in the expression of RNA methyltransferases in brain which is in accordance with the overall increase in global m⁶A and m⁵C methylation levels (Bataglia et al., 2021). However, in the fat body, although the higher expression of RNA methyltransferases is found in younger bees, the global m⁶A and m⁵C methylation levels are lower in young bees when compared with older bees. This point may sound contradictory, but it is important to emphasize that epitranscriptomic machinery is not only composed of RNA methyltransferases (named as writers) but also of readers and demethylases (erasers), and these last two sets of enzymes act in the recognition and removal of methyl groups, respectively (Schaefer et al., 2017). So, when the global methylation levels are accessed, we are measuring the resulting action of the whole machinery (writers, readers, and erasers) on the analyzed transcriptome.

We conclude that the adult life progression of *A. mellifera* workers is accompanied by changes in the expression of m⁶A and m⁵C RNA methyltransferases. It is possible that the mRNA methylome is dynamically regulated all through the lifespan of workers. We found that brain and fat body influence the transcriptional levels of these methyltransferases in opposite ways. Further the transcript levels of some of these genes are impacted by the protein content of food consumed as well as by the age-related behavior performed. Our results point to a tissue-specific transcriptional signature of RNA methyltransferases during the progression of adulthood.

Data availability statement

The raw data supporting the conclusions of this article will be made available by the authors, without undue reservation.

Author contributions

FMFN conceived and supervised the study. LB performed sampling, experiments, data collection, and analysis. ZLPS provided materials and reagents. FMFN and ZLPS acquired

funding. FMFN and LB wrote the manuscript. All authors performed data interpretation, reviewed, and edited the manuscript, and approved its final version.

Funding

This research was financially supported by the Conselho Nacional de Desenvolvimento Científico e Tecnológico (CNPq, universal grant, process number 461711/2014-1), the Fundação de Amparo à Pesquisa do Estado de São Paulo (FAPESP, processes number 16/06657-0 and 19/02374-1), the Coordenação de Aperfeiçoamento de Pessoal de Nível Superior—Brasil (CAPES, Finance Code 001), and a fellowship for LB (CNPq, process number 130285/2016-1).

Acknowledgments

We are very grateful to Marcela Laure, Luís Aguiar, and Vera Figueiredo for their valuable technical assistance, to Kate Ihle, Felipe Martelli and Carlos Cardoso Jr for statistical advice, and to Navdeep Mutti for critical reading.

References

- Abbasi-Moheb, L., Mertel, S., Gonsior, M., Nouri-Vahid, L., Kahrizi, K., Cirak, S., et al. (2012). Mutations in NSUN2 cause autosomal-recessive intellectual disability. *Am. J. Hum. Genet.* 90 (5), 847–855. doi:10.1016/j.ajhg.2012.03.021
- Abdul, Q. A., Yu, B. P., Chung, H. Y., Jung, H. A., and Choi, J. S. (2017). Epigenetic modifications of gene expression by lifestyle and environment. *Arch. Pharm. Res.* 40 (11), 1219–1237. doi:10.1007/s12272-017-0973-3
- Alarcón, C. R., Lee, H., Goodarzi, H., Halberg, N., and Tavazoie, S. F. (2015). N6-methyladenosine marks primary microRNAs for processing. *Nature* 519 (7544), 482–485. doi:10.1038/nature14281
- Amdam, G. V., Simões, Z. L., Hagen, A., Norberg, K., Schröder, K., Mikkelsen, Ø., et al. (2004). Hormonal control of the yolk precursor vitellogenin regulates immune function and longevity in honeybees. *Exp. Gerontol.* 39 (5), 767–773. doi:10.1016/j.exger.2004.02.010
- Ament, S. A., Chan, Q. W., Wheeler, M. M., Nixon, S. E., Johnson, S. P., Rodriguez-Zas, S. L., et al. (2011). Mechanisms of stable lipid loss in a social insect. *J. Exp. Biol.* 214 (22), 3808–3821. doi:10.1242/jeb.060244
- Barascou, L., Sene, D., Barraud, A., Michez, D., Lefebvre, V., Medrzycki, P., et al. (2021). Pollen nutrition fosters honeybee tolerance to pesticides. *R. Soc. Open Sci.* 18 (9), 210818. doi:10.1098/rsos.210818
- Bataglia, L., Simões, Z. L. P., and Nunes, F. M. F. (2021). Active genic machinery for epigenetic RNA modifications in bees. *Insect Mol. Biol.* 30 (6), 566–579. doi:10.1111/imb.12726
- Batista, P. J., Molinier, B., Wang, J., Qu, K., Zhang, J., Li, L., et al. (2014). m(6)A RNA modification controls cell fate transition in mammalian embryonic stem cells. *Cell Stem Cell* 15 (6), 707–719. doi:10.1016/j.stem.2014.09.019
- Behura, S. K., and Whitfield, C. W. (2010). Correlated expression patterns of microRNA genes with age-dependent behavioural changes in honeybee. *Insect Mol. Biol.* 19 (4), 431–439. doi:10.1111/j.1365-2583.2010.01010.x
- Boccaletto, P., Machnicka, M. A., Purta, E., Piatkowski, P., Baginski, B., Wirecki, T. K., et al. (2017). Modomics: A database of RNA modification pathways. 2017 update. *Nucleic Acids Res.* 46 (1), D303–D307. doi:10.1093/nar/gkx1030
- Brodshneider, R., and Crailsheim, K. (2010). Nutrition and health in honey bees. *Apidologie* 41 (3), 278–294. doi:10.1051/apido/2010012
- Chen, P., Zhang, T., Yuan, Z., Shen, B., and Chen, L. (2019). Expression of the RNA methyltransferase Nsun5 is essential for developing cerebral cortex. *Mol. Brain* 12 (1), 74. doi:10.1186/s13041-019-0496-6
- Chi, L., and Delgado-Olguín, P. (2013). Expression of NOL1/NOP2/sun domain (Nsun) RNA methyltransferase family genes in early mouse embryogenesis. *Gene Expr. Patterns* 13 (8), 319–327. doi:10.1016/j.gep.2013.06.003
- Clancy, M. J., Shambaugh, M. E., Timpte, C. S., and Bokar, J. A. (2002). Induction of sporulation in *Saccharomyces cerevisiae* leads to the formation of N6-methyladenosine in mRNA: A potential mechanism for the activity of the IME4 gene. *Nucleic Acids Res.* 30 (20), 4509–4518. doi:10.1093/nar/gkf573
- D'Aquila, P., De Rango, F., Paparazzo, E., Mandalà, M., Bellizzi, D., and Passarino, G. (2022). Impact of nutrition on age-related epigenetic RNA modifications in rats. *Nutrients* 14 (6), 1232. doi:10.3390/nu14061232
- Deng, X., Chen, K., Luo, G. Z., Weng, X., Ji, Q., Zhou, T., et al. (2015). Widespread occurrence of N6-methyladenosine in bacterial mRNA. *Nucleic Acids Res.* 43 (13), 6557–6567. doi:10.1093/nar/gkv596
- Durst, C., Eichmüller, S., and Menzel, R. (1994). Development and experience lead to increased volume of subcompartments of the honeybee mushroom body. *Behav. Neural Biol.* 62 (3), 259–263. doi:10.1016/s0163-1047(05)80025-1
- Erban, T., Harant, K., Chalupnikova, J., Kocourek, F., and Stara, J. (2017). Beyond the survival and death of the deltamethrin-threatened pollen beetle *Meligethes aeneus*: An in-depth proteomic study employing a transcriptome database. *J. Proteomics* 50, 281–289. doi:10.1016/j.jprot.2016.09.016
- Farris, S. M., Robinson, G. E., and Fahrback, S. E. (2001). Experience- and age-related outgrowth of intrinsic neurons in the mushroom bodies of the adult worker honeybee. *J. Neurosci.* 21 (16), 6395–6404. doi:10.1523/JNEUROSCI.21-16-06395.2001
- Flores, J. V., Cordero-Espinoza, L., Oetzuerk-Winder, F., Andersson-Rolf, A., Selmi, T., Blanco, S., et al. (2017). Cytosine-5 RNA methylation regulates neural stem cell differentiation and motility. *Stem Cell Rep.* 8 (1), 112–124. doi:10.1016/j.stemcr.2016.11.014
- Fray, R. G., and Simpson, G. G. (2015). The *Arabidopsis* epitranscriptome. *Curr. Opin. Plant Biol.* 27, 17–21. doi:10.1016/j.pbi.2015.05.015
- Gkatza, N. A., Castro, C., Harvey, R. F., Heiß, M., Popis, M. C., Blanco, S., et al. (2019). Cytosine-5 RNA methylation links protein synthesis to cell metabolism. *PLoS Biol.* 17 (6), e3000297. doi:10.1371/journal.pbio.3000297

Conflict of interest

The authors declare that the research was conducted in the absence of any commercial or financial relationships that could be construed as a potential conflict of interest.

Publisher's note

All claims expressed in this article are solely those of the authors and do not necessarily represent those of their affiliated organizations, or those of the publisher, the editors and the reviewers. Any product that may be evaluated in this article, or claim that may be made by its manufacturer, is not guaranteed or endorsed by the publisher.

Supplementary material

The Supplementary Material for this article can be found online at: <https://www.frontiersin.org/articles/10.3389/fcell.2022.921503/full#supplementary-material>

- Grozinger, C. M., Sharabash, N. M., Whitfield, C. W., and Robinson, G. E. (2003). Pheromone-mediated gene expression in the honey bee brain. *Proc. Natl. Acad. Sci. U. S. A.* 100 (2), 14519–14525. doi:10.1073/pnas.2335884100
- Hausmann, I. U., Bodi, Z., Sanchez-Moran, E., Mongan, N. P., Archer, N., Fray, R. G., et al. (2016). m6A potentiates Sxl alternative pre-mRNA splicing for robust *Drosophila* sex determination. *Nature* 540 (7632), 301–304. doi:10.1038/nature20577
- Heissenberger, C., Rollins, J. A., Krammer, T. L., Nagelreiter, F., Stocker, I., Wacheul, L., et al. (2020). The ribosomal RNA m5C methyltransferase NSUN-1 modulates healthspan and oogenesis in *Caenorhabditis elegans*. *Elife* 9, e56205. doi:10.7554/eLife.56205
- Herb, B. R., Wolschin, F., Hansen, K. D., Aryee, M. J., Langmead, B., Irizarry, R., et al. (2012). Reversible switching between epigenetic states in honeybee behavioral subcastes. *Nat. Neurosci.* 15 (10), 1371–1373. doi:10.1038/nn.3218
- Hongay, C. F., and Orr-Weaver, T. L. (2011). *Drosophila* Inducer of MEiosis 4 (IME4) is required for Notch signaling during oogenesis. *Proc. Natl. Acad. Sci. U. S. A.* 108 (36), 14855–14860. doi:10.1073/pnas.1111577108
- Huang, H., Weng, H., and Chen, J. (2020). The biogenesis and precise control of RNA m6A methylation. *Trends Genet.* 36 (1), 44–52. doi:10.1016/j.tig.2019.10.011
- Jung, Y., and Goldman, D. (2018). Role of RNA modifications in brain and behavior. *Genes Brain Behav.* 17 (3), e12444. doi:10.1111/gbb.12444
- Kan, L., Grozhik, A. V., Vedanayagam, J., Patil, D. P., Pang, N., Lim, K. S., et al. (2017). The m6A pathway facilitates sex determination in *Drosophila*. *Nat. Commun.* 8, 15737. doi:10.1038/ncomms15737
- Kan, L., Ott, S., Joseph, B., Park, E. S., Dai, W., Kleiner, R. E., et al. (2021). A neural m6A/Ythdf pathway is required for learning and memory in *Drosophila*. *Nat. Commun.* 12 (1), 1458. doi:10.1038/s41467-021-21537-1
- Kannan, K., Shook, M., Li, Y., Robinson, G. E., and Ma, J. (2019). Comparative analysis of brain and fat body gene splicing patterns in the honey bee, *Apis mellifera*. *G3 (Bethesda)* 9 (4), 1055–1063. doi:10.1534/g3.118.200857
- Kennedy, E. M., Courtney, D. G., Tsai, K., and Cullen, B. R. (2017). Viral epitranscriptomics. *J. Virol.* 91 (9), e02263–16. doi:10.1128/JVI.02263-16
- Kiljanek, T., Niewiadowska, A., and Posyniak, A. (2016). Pesticide poisoning of honeybees: A review of symptoms, incident classification, and causes of poisoning. *J. Apic. Sci.* 60 (2), 5–24. doi:10.1515/jas-2016-0024
- Kosi, N., Alić, I., Kolačević, M., Vrsaljko, N., Jovanov Milošević, N., Sobol, M., et al. (2015). Nop2 is expressed during proliferation of neural stem cells and in adult mouse and human brain. *Brain Res.* 1597, 65–76. doi:10.1016/j.brainres.2014.11.040
- Kucharski, R., Maleszka, J., Foret, S., and Maleszka, R. (2008). Nutritional control of reproductive status in honeybees via DNA methylation. *Science* 319 (5871), 1827–1830. doi:10.1126/science.1153069
- Leighton, L. J., Ke, K., Zajackowski, E. L., Edmunds, J., Spitale, R. C., and Bredy, T. W. (2018). Experience-dependent neural plasticity, learning, and memory in the era of epitranscriptomics. *Genes Brain Behav.* 17 (3), e12426. doi:10.1111/gbb.12426
- Lence, T., Akhtar, J., Bayer, M., Schmid, K., Spindler, L., Ho, C. H., et al. (2016). m6A modulates neuronal functions and sex determination in *Drosophila*. *Nature* 540 (7632), 242–247. doi:10.1038/nature20568
- Li, B., Wang, X., Li, Z., Lu, C., Zhang, Q., Chang, L., et al. (2019). Transcriptome-wide analysis of N6-methyladenosine uncovers its regulatory role in gene expression in the lepidopteran *Bombyx mori*. *Insect Mol. Biol.* 28 (5), 703–715. doi:10.1111/imb.12584
- Liu, J., Huang, T., Chen, W., Ding, C., Zhao, T., Zhao, X., et al. (2022). Developmental mRNA m5C methylation and regulatory innovations of massive m5C modification of maternal mRNAs in animals. *Nat. Commun.* 13 (1), 2484. doi:10.1038/s41467-022-30210-0
- Livak, K. J., and Schmittgen, T. D. (2001). Analysis of relative gene expression data using real-time quantitative PCR and the 2(-Delta Delta C(T)) Method. *Methods* 25 (4), 402–408. doi:10.1006/meth.2001.1262
- Lockett, G. A., Kucharski, R., and Maleszka, R. (2012). DNA methylation changes elicited by social stimuli in the brains of worker honey bees. *Genes Brain Behav.* 11 (2), 235–242. doi:10.1111/j.1601-183X.2011.00751.x
- Lourenço, A. P., Mackert, A., Cristino, A. S., and Simões, Z. L. P. (2008). Validation of reference genes for gene expression studies in the honey bee, *Apis mellifera*, by quantitative real-time RT-PCR. *Apidologie* 39, 372–385. doi:10.1051/apido:2008015
- Lourenço, A. P., Martins, J. R., Torres, F. A. S., Mackert, A., Aguiar, L. R., Hartfelder, K., et al. (2019). Immunosenescence in honey bees (*Apis mellifera* L.) is caused by intrinsic senescence and behavioral physiology. *Exp. Gerontol.* 119, 174–183. doi:10.1016/j.exger.2019.02.005
- Martelli, F., Falcon, T., Pinheiro, D. G., Simões, Z. L. P., and Nunes, F. M. F. (2022). Worker bees (*Apis mellifera*) deprived of pollen in the first week of adulthood exhibit signs of premature aging. *Insect Biochem. Mol. Biol.* 146, 103774. doi:10.1016/j.ibmb.2022.103774
- Meyer, K. D., Patil, D. P., Zhou, J., Zinoviev, A., Skabkin, M. A., Elemento, O., et al. (2015). 5' UTR m(6)A promotes cap-independent translation. *Cell* 163 (4), 999–1010. doi:10.1016/j.cell.2015.10.012
- Meyer, K. D., Saletore, Y., Zumbo, P., Elemento, O., Mason, C. E., and Jaffrey, S. R. (2012). Comprehensive analysis of mRNA methylation reveals enrichment in 3' UTRs and near stop codons. *Cell* 149 (7), 1635–1646. doi:10.1016/j.cell.2012.05.003
- Micura, R., Pils, W., Höbartner, C., Grubmayr, K., Ebert, M. O., and Jaun, B. (2001). Methylation of the nucleobases in RNA oligonucleotides mediates duplex-hairpin conversion. *Nucleic Acids Res.* 29 (19), 3997–4005. doi:10.1093/nar/29.19.3997
- Page, R. E., Jr., and Peng, C. Y. (2001). Aging and development in social insects with emphasis on the honey bee, *Apis mellifera* L. *Exp. Gerontol.* 36 (4–6), 695–711. doi:10.1016/s0531-5565(00)00236-9
- Page, R. E., Jr., Scheiner, R., Erber, J., and Amdam, G. V. (2006). The development and evolution of division of labor and foraging specialization in a social insect (*Apis mellifera* L.). *Curr. Top. Dev. Biol.* 74, 253–286. doi:10.1016/S0070-2153(06)74008-X
- Rai, K., Chidester, S., Zavala, C. V., Manos, E. J., James, S. R., Karpf, A. R., et al. (2007). Dnmt2 functions in the cytoplasm to promote liver, brain, and retina development in zebrafish. *Genes Dev.* 21 (3), 261–266. doi:10.1101/gad.1472907
- Schaefer, M., Kapoor, U., and Jantsch, M. F. (2017). Understanding RNA modifications: The promises and technological bottlenecks of the 'epitranscriptome'. *Open Biol.* 7 (5), 170077. doi:10.1098/rsob.170077
- Schaefer, M., Pollex, T., Hanna, K., Tuorto, F., Meusburger, M., Helm, M., et al. (2010). RNA methylation by Dnmt2 protects transfer RNAs against stress-induced cleavage. *Genes Dev.* 24 (15), 1590–1595. doi:10.1101/gad.586710
- Schossere, M., Minois, N., Angerer, T. B., Amring, M., Dellago, H., Harreither, E., et al. (2015). Methylation of ribosomal RNA by NSUN5 is a conserved mechanism modulating organismal lifespan. *Nat. Commun.* 6, 6158. doi:10.1038/ncomms7158
- Shinoda, S., Kitagawa, S., Nakagawa, S., Wei, F. Y., Tomizawa, K., Araki, K., et al. (2019). Mammalian NSUN2 introduces 5-methylcytidines into mitochondrial tRNAs. *Nucleic Acids Res.* 47 (16), 8734–8745. doi:10.1093/nar/gkz575
- Skowronek, P., Wójcik, L., and Strachecka, A. (2021). Fat body-multifunctional insect tissue. *Insects* 12 (6), 547. doi:10.3390/insects12060547
- Tang, J., Chen, X., Cai, B., and Chen, G. (2019). A logical relationship for schizophrenia, bipolar, and major depressive disorder. Part 4: Evidence from chromosome 4 high-density association screen. *J. Comp. Neurol.* 527 (2), 392–405. doi:10.1002/cne.24543
- Toth, A. L., and Robinson, G. E. (2005). Worker nutrition and division of labour in honeybees. *Anim. Behav.* 69 (2), 427–435. doi:10.1016/j.anbehav.2004.03.017
- Tuorto, F., Liebers, R., Musch, T., Schaefer, M., Hofmann, S., Kellner, S., et al. (2012). RNA cytosine methylation by Dnmt2 and NSun2 promotes tRNA stability and protein synthesis. *Nat. Struct. Mol. Biol.* 19 (9), 900–905. doi:10.1038/nsmb.2357
- Vaiserman, A. (2014). Developmental epigenetic programming of caste-specific differences in social insects: An impact on longevity. *Curr. Aging Sci.* 7 (3), 176–186. doi:10.2174/1874609807666141129173749
- Wang, M., Xiao, Y., Li, Y., Wang, X., Qi, S., Wang, Y., et al. (2021). RNA m6A modification functions in larval development and caste differentiation in honeybee (*Apis mellifera*). *Cell Rep.* 34 (1), 108580. doi:10.1016/j.celrep.2020.108580
- Whitfield, C. W., Cziko, A. M., and Robinson, G. E. (2003). Gene expression profiles in the brain predict behavior in individual honey bees. *Science* 302 (5643), 296–299. doi:10.1126/science.1086807
- Wilkinson, E., Cui, Y. H., and He, Y. Y. (2021). Context-dependent roles of RNA modifications in stress responses and diseases. *Int. J. Mol. Sci.* 22 (4), 1949. doi:10.3390/ijms22041949
- Winston, M. L. (1987). "The honey bee colony: Life history," in *The hive and the honey bee*. Editor J. M. Graham (Illinois: Dadant & Sons-Hamilton).

- Withers, G. S., Fahrbach, S. E., and Robinson, G. E. (1993). Selective neuroanatomical plasticity and division of labour in the honeybee. *Nature* 364 (6434), 238–240. doi:10.1038/364238a0
- Wu, J., Frazier, K., Zhang, J., Gan, Z., Wang, T., and Zhong, X. (2020). Emerging role of m6A RNA methylation in nutritional physiology and metabolism. *Obes. Rev.* 21 (1), e12942. doi:10.1111/obr.12942
- Yang, X., Wei, X., Yang, J., Du, T., Yin, C., Fu, B., et al. (2021). Epitranscriptomic regulation of insecticide resistance. *Sci. Adv.* 7 (19), eabe5903. doi:10.1126/sciadv.abe5903
- Zayed, A., and Robinson, G. E. (2012). Understanding the relationship between brain gene expression and social behavior: Lessons from the honey bee. *Annu. Rev. Genet.* 46, 591–615. doi:10.1146/annurev-genet-110711-155517
- Zhang, T., Chen, P., Li, W., Sha, S., Wang, Y., Yuan, Z., et al. (2019). Cognitive deficits in mice lacking Nsun5, a cytosine-5 RNA methyltransferase, with impairment of oligodendrocyte precursor cells. *Glia* 67 (4), 688–702. doi:10.1002/glia.23565
- Zhang, Z., Wang, M., Xie, D., Huang, Z., Zhang, L., Yang, Y., et al. (2018). METTL3-mediated N6-methyladenosine mRNA modification enhances long-term memory consolidation. *Cell Res.* 28 (11), 1050–1061. doi:10.1038/s41422-018-0092-9
- Zhao, X., Yang, Y., Sun, B. F., Shi, Y., Yang, X., Xiao, W., et al. (2014). FTO-dependent demethylation of N6-methyladenosine regulates mRNA splicing and is required for adipogenesis. *Cell Res.* 24 (12), 1403–1419. doi:10.1038/cr.2014.151
- Zhong, X., Yu, J., Frazier, K., Weng, X., Li, Y., Cham, C. M., et al. (2018). Circadian clock regulation of hepatic lipid metabolism by modulation of m6A mRNA methylation. *Cell Rep.* 25 (7), 1816–1828.e4. doi:10.1016/j.celrep.2018.10.068



OPEN ACCESS

EDITED BY

Juan Rafael Riesgo-Escovar,
Universidad Nacional Autónoma de
México, Mexico

REVIEWED BY

Emma Louise Dempster,
University of Exeter, United Kingdom
Mufeng Hu,
AbbVie, United States

*CORRESPONDENCE

Nestor Emmanuel Diaz-Martinez,
ediaz@ciatej.mx

SPECIALTY SECTION

This article was submitted to
Morphogenesis and Patterning,
a section of the journal
Frontiers in Cell and Developmental
Biology

RECEIVED 19 May 2022

ACCEPTED 01 August 2022

PUBLISHED 02 September 2022

CITATION

Barragán-Álvarez CP,
Flores-Fernandez JM,
Hernández-Pérez OR,
Ávila-González D, Díaz NF,
Padilla-Camberos E, Dublan-García O,
Gómez-Oliván LM and
Diaz-Martinez NE (2022), Recent
advances in the use of CRISPR/Cas for
understanding the early development of
molecular gaps in glial cells.
Front. Cell Dev. Biol. 10:947769.
doi: 10.3389/fcell.2022.947769

COPYRIGHT

© 2022 Barragán-Álvarez, Flores-
Fernandez, Hernández-Pérez, Ávila-
González, Díaz, Padilla-Camberos,
Dublan-García, Gómez-Oliván and
Diaz-Martinez. This is an open-access
article distributed under the terms of the
[Creative Commons Attribution License](#)
(CC BY). The use, distribution or
reproduction in other forums is
permitted, provided the original
author(s) and the copyright owner(s) are
credited and that the original
publication in this journal is cited, in
accordance with accepted academic
practice. No use, distribution or
reproduction is permitted which does
not comply with these terms.

Recent advances in the use of CRISPR/Cas for understanding the early development of molecular gaps in glial cells

Carla Patricia Barragán-Álvarez¹,
José Miguel Flores-Fernandez^{2,3}, Oscar R. Hernández-Pérez,
Daniela Ávila-González^{1,4}, Nestor Fabian Díaz⁴,
Eduardo Padilla-Camberos¹, Octavio Dublan-García⁵,
Leobardo Manuel Gómez-Oliván⁵ and
Nestor Emmanuel Diaz-Martinez^{1*}

¹Laboratorio de Reprogramación Celular y Bioingeniería de Tejidos, Biotecnología Médica y Farmacéutica, Centro de Investigación y Asistencia en Tecnología y Diseño Del Estado de Jalisco, Guadalajara, Mexico, ²Departamento de Investigación e Innovación, Universidad Tecnológica de Oriental, Oriental, Mexico, ³Department of Biochemistry & Centre for Prions and Protein Folding Diseases, University of Alberta, Edmonton, AB, Canada, ⁴Departamento de Fisiología y Desarrollo Celular, Instituto Nacional de Perinatología, México City, Mexico, ⁵Laboratorio de Alimentos y Toxicología Ambiental, Facultad de Química, Universidad Autónoma Del Estado de México, Toluca, México

Glial cells are non-neuronal elements of the nervous system (NS) and play a central role in its development, maturation, and homeostasis. Glial cell interest has increased, leading to the discovery of novel study fields. The CRISPR/Cas system has been widely employed for NS understanding. Its use to study glial cells gives crucial information about their mechanisms and role in the central nervous system (CNS) and neurodegenerative disorders. Furthermore, the increasingly accelerated discovery of genes associated with the multiple implications of glial cells could be studied and complemented with the novel screening methods of high-content and single-cell screens at the genome-scale as Perturb-Seq, CRISP-seq, and CROPseq. Besides, the emerging methods, GESTALT, and LINNAEUS, employed to generate large-scale cell lineage maps have yielded invaluable information about processes involved in neurogenesis. These advances offer new therapeutic approaches to finding critical unanswered questions about glial cells and their fundamental role in the nervous system. Furthermore, they help to better understanding the significance of glial cells and their role in developmental biology.

KEYWORDS

glial cells, CRISPR/Cas, lineage tracing, gliogenesis-related genes, screening platforms, large-scale maps of cell lineage

Introduction

The central nervous system (CNS) is made up of a complex cell network comprised of diverse types of neurons, macroglia, and microglial cells that play a fundamental role in its proper function (Ceprian and Fulton, 2019; Nott et al., 2019; Wright-Jin and Gutmann, 2019). Glial cells can be described as progenitor cells as well as differentiated populations. Radial glial cells (RGCs) are the primary stem cells during neural development. The differentiated population involves astrocytes, oligodendrocytes, ependymal cells, Schwann cells, microglia, and among others (Arai and Lo, 2017).

While neurons have always been the protagonists of the nervous system because they are involved in synaptic interactions and electrical signaling, it was not until recently that the role of glial cells received the same attention (Wang and Gao, 2019). For many years, glial cells were considered connective tissue with the sole function of preserving nervous system junctions. However, more functions have been discovered in recent years, such as their role in neurotransmission, nutrient transport, brain functions, pathological conditions, and early development of the nervous system (Hirbec et al., 2020).

The interest in glial cell roles in neurological function has increased, focusing specifically on their dynamic interaction and involvement in neurological disorders. Moreover, recent findings open up a wide range of new opportunities for modeling early development and diseases; additionally, the discovery of biomarkers to understand pathologies causing neurodegeneration (McAvoy and Kawamata, 2019; Raikwar et al., 2019; Wang and Gao, 2019; Hidalgo-Lanussa et al., 2020; Dang et al., 2021), as well as the development of new drugs (Möller and Boddeke, 2016).

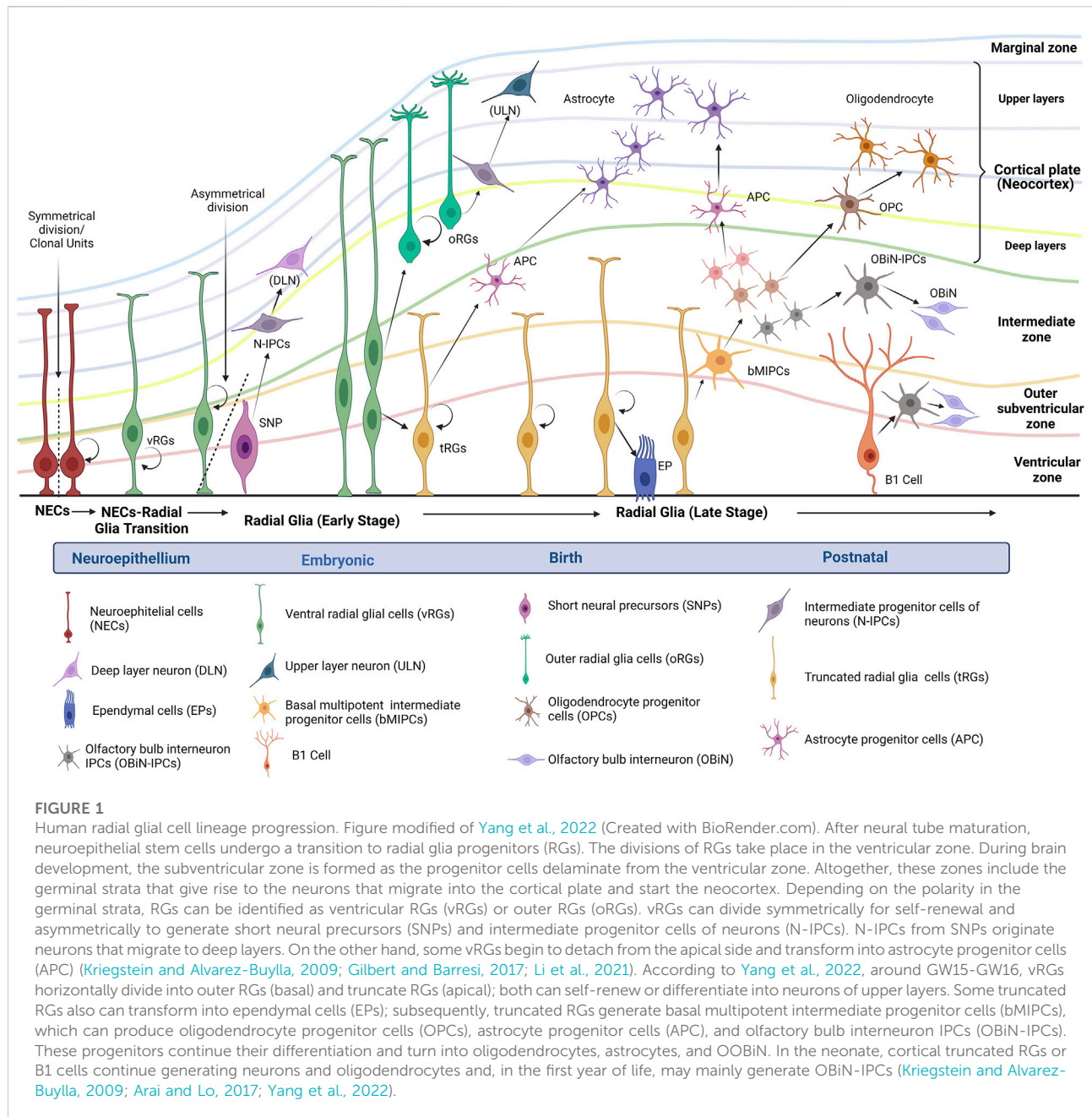
Genome engineering for modeling neuronal diseases is an emerging clinical application with a significant public health impact. However, in terms of glial cells, there is still a considerable gap in understanding origins, lineage progression, and molecular properties (Yang et al., 2022). The widely described Clustered Regularly Interspaced Short Palindromic Repeats (CRISPR)/Cas system has become a key tool for genome editing since it provides advantages such as design simplicity, considerable cost reduction, and enhanced efficiency than its analogs, Zinc Finger Nucleases (ZFN) and Transcription Activator-like Effector Nucleases (TALENs) (Moon et al., 2019). In addition, CRISPR/Cas system offers other potential clinical applications, such as gene screening or combination with orthogonal methods, thereby increasing its potential for developing new diagnostic or research tools. For instance, screening methods such as Perturb-Seq, CRISP-seq, and CROP seq, examine how diverse mutations affect specific cell types; the method Genome Editing of Synthetic Target Arrays for Lineage Tracing (GESTALT) can be combined with single-cell RNA sequencing (scRNA-seq) to find/analyze cellular lineage relationships and catalog the cell identities in different tissues;

similarly, the LINEage Tracing by Nuclease-Activated Editing of Ubiquitous Sequences (LINNAEUS) is a strategy for simultaneous lineage tracing and transcriptome profiling in thousands of single cells (McKenna et al., 2016; Raj et al., 2018; Spanjaard et al., 2018; So et al., 2019; Jin et al., 2020). On the other hand, recent studies have established the basis for CRISPR/Cas9 genome editing frameworks that seem promising for neuroscience knowledge and neurological disorders treatment (Cota-Coronado et al., 2019a; Dever et al., 2019; Hirbec et al., 2020; Jin et al., 2020). Although scRNA-seq has been applied for the study of different cell phenotypes in the CNS, there are still multiple gaps in fully understanding the molecular mechanisms of glial-neuron interactions during development, as well as the role of glial cells in neuroinflammation, neurodegenerative diseases, and inherited mental disorders (Menon et al., 2019; Nott et al., 2019; Hidalgo-Lanussa et al., 2020). Therefore, this review highlights recent advances in using CRISPR technology for a better comprehension of glial cells and their role in developmental biology.

Glial cell types and functions

Glial cells are defined as non-neuronal cells in the CNS and derive from different origins; for example, macroglia (astrocytes, oligodendrocytes, and NG2 glia) origin is the ectoderm and arise from neuroepithelial progenitor cells (NPCs); in contrast, the origin of microglia is the mesoderm, specifically from the yolk sac and its precursors are fetal macrophages (Zuchero and Barres, 2015; Arcuri et al., 2017; Yildirim et al., 2019; Patro and Patro, 2022). Glial cells are involved in nervous system regulation from development to maturation. On the other hand, they can influence nervous system plasticity and are implicated in the appearance of neurodegenerative diseases (Vallejo et al., 2019; Dietz et al., 2020). Research on glial cells began in the second half of the 19th century. However, it was not until 1919 that Rio-Hortega described for the first time the three main types of glial cells present in the CNS: astrocytes, oligodendrocytes, and microglia (Sierra et al., 2016; Sierra et al., 2019).

The nervous system development implies complex processes with extensive nuclear movements and cell migration. During early embryonic development, the neural tube emerges from the neural plate, where neuroepithelial cells (NECs) reside. These cells give rise to the radial glial cells (RGs), cornerstones of neurogenesis and gliogenesis (Arai and Lo, 2017; Bertipaglia et al., 2018). RGs nuclei exhibit a particular form of cell cycle-dependent oscillatory behavior known as interkinetic nuclear migration (INM), where the nucleus migrates within the cytoplasm basally or apically, depending on the cell cycle stage. RGs are present during most of the cortical development and divide symmetrically for self-proliferation or asymmetrically to generate neurons and glial



cells (Arai and Lo, 2017; Bertipaglia et al., 2018; Lin et al., 2021).

Currently, three different types of RGs have been identified: ventricular RGs (vRGs), outer RGs (oRGs), and truncated RGs (tRGs). Yang et al., 2022 have proposed that tRGs give rise to progenitor cells of pyramidal neurons (PyN-IPCs) becoming upper layer Pyramidal neurons (PyNs). Then they produce basal multipotent intermediate progenitor cells (bMIPCs). However, there are multiple gaps related to the role of the developing cortex and the series of steps required to generate the remaining types of cells during gliogenesis (Yang et al., 2022).

In addition to serving as stem cells, RGs provide the scaffolding for the movement of progenitor cells and newborn neurons to superficial layers (Gilbert & Barresi, 2017). Figure 1 describes the general radial glial cell lineage progression known and proposed to date in humans.

Glial cells are also found in the peripheral nervous system (PNS) as Schwann cells, satellite glial cells, olfactory ensheathing cells, and enteric glia, whose origin is the neural crest but with at least a subset coming from the CNS that migrates to the PNS (Suter and Jaworski, 2019; Verkhratsky et al., 2019). The function of the glial cell begins at the early stages of life during brain

development since glial cells facilitate neuron interactions and synaptic pruning at the final stage of brain development, as well as releasing essential gliotransmitters and cytokines during neural development (Neniskyte and Gross, 2017). In the course of embryogenesis, the microglia colonize the early embryonic neuroepithelium and give rise to the primary immune cells of the CNS (Deverman and Patterson, 2009; Neniskyte and Gross, 2017; Kim et al., 2017).

As the major components of CNS, glial cells perform multiple activities that allow homeostatic maintenance. An example is astrocytes, which modulate synaptic structure and function and promote neuronal survival. As an outcome of their interaction with blood vessels, glial cells enable nutrient intake and metabolic support; on the other hand, they can control blood flow in the brain aside from regulating the flow of cerebral spinal fluid (Zuchero and Barres, 2015; Butt and Verkhratsky, 2018; Simhal et al., 2019). Oligodendrocytes and Schwann cells are involved in the process of myelination, which is essential for neurotransmission (Kuhn et al., 2019; Verkhratsky et al., 2019). Microglia possess numerous functions and activities beyond immune surveillance in the brain; these cells can, for instance, instruct progenitor cells about cell fate decisions, establish communication with other glial cells, influence the formation of synapses and promote neurite formation, regulate neuronal function, and even ease the myelination process (Wright-Jin and Gutmann, 2019).

Glial cells-associated neurological disorders

Glial cells are intrinsically associated in the formation or development of the nervous system since they are involved in synaptic pruning. This process is a crucial step in maturing synaptic connections during the early stages of brain development, and if key signaling pathways between glial cells and neurons do not function properly can cause several neurodevelopmental disorders like autism, schizophrenia, and epilepsy (Neniskyte and Gross, 2017; Allen and Lyons, 2018; Lehrman et al., 2018; Sellgren et al., 2019; Yanuck, 2019). Accumulated evidence suggests that excessive synaptic pruning by microglia could contribute to synapse density reduction in patients with autism and schizophrenia (Sellgren et al., 2017; Sellgren et al., 2019; Li et al., 2020; Scott-Hewitt et al., 2020). To study interactions between microglia and neural cells, Sellgren et al. (2017) validated a model system combining reprogrammed microglia-like cells with neural progenitor cells (NPCs); their results showed the ability of microglia-like cells to engulf synaptosomes and NPCs *in vitro*; moreover, they reported risk schizophrenia variants in the human complement component 4 locus causing an excessive neuronal complement deposition by C4A, a factor associated with increased microglial synapse engulfment (Sellgren et al., 2017; Sellgren et al., 2019; Li et al., 2020; Scott-Hewitt et al., 2020).

It has been reported that microglial complement receptor CR3/Mac1 and triggering receptor expressed on myeloid cells 2 (TREM2) contribute to synaptic pruning (Qin et al., 2022). Scott-Hewitt et al. (2020) proposed that the recognition of exposed phosphatidylserine in neurons is crucial for microglial-mediated pruning, and some possible candidates as synapse pruning mediators are the isoform of adhesion G protein-coupled receptor (ADGRG1/GPR56) and TREM2; however, the molecular mechanisms involved in microglia target neuron selection are unknown (Li et al., 2020; Scott-Hewitt et al., 2020; Qin et al., 2022). On the other hand, it should be noted that TREM2 and the complement cascade have been associated with the progression of Alzheimer's disease (AD), as mouse models have shown the importance of TREM2 for the microglial phagocytosis response in amyloid seeds (Smidt et al., 2007; Flores-Fernández et al., 2018; Parhizkar et al., 2019; Ewers et al., 2020; Meilandt et al., 2020; Scott-Hewitt et al., 2020; Yang et al., 2020). The increased presence of soluble TREM2 (sTREM2) in cerebrospinal fluid (CSF) has also been associated with an attenuated decline in memory and cognition among patients with mild cognitive impairment (MCI) and AD (Ewers et al., 2019; Suárez-Calvet et al., 2019). In addition to TREM2, genome-wide association studies (GWAS) have identified other important AD and Parkinson's disease (PD) risk genes expressed or associated with reactivity in glial cells, such as the transmembrane protein CD33, box-dependent-interacting protein 1 (BIN1), complement receptor 1 (CR1), apolipoprotein E (ApoE), GBA1, and stearoyl-CoA-desaturase (SCD) (Park et al., 2018; Bartels et al., 2020).

Similar to AD, a recent study reported increased levels of sTREM2 in PD patients, proposing sTREM2 as a potential biomarker in both conditions. Furthermore, current evidence suggests astroglial cells as the primary source of inflammatory mediators in the brain, as well as the microglia response to pro-inflammatory signals of mast cells, where glia maturation factor (GMF) could have a central role during neuroinflammation. GMF is a growth and differentiation factor majorly expressed in CNS; it has been indicated as a pro-inflammatory protein playing a central role in neuroinflammatory and neurodegenerative diseases such as AD, PD, and multiple sclerosis (MS) (Kempuraj et al., 2018a; Kempuraj et al., 2018b; Fan et al., 2018; Raikwar et al., 2019). To date, the exact mechanism by which GMF acts on diseases is unknown; however, there is considerable evidence that helps to understand its relationship with neuroinflammation and neurodegeneration (Fan et al., 2018; Yin et al., 2018; Ramaswamy et al., 2019; Lee et al., 2021). Some reports indicate that GMF is involved in the secretion of granulocyte-macrophage colony-stimulating factor (GM-CSF); overexpression of GM-CSF may lead to the activation of microglia and the secretion of TNF- α , IL-1 β , and MIP-1 β triggering an inflammatory process. In addition, GMF can activate mast cells which also release inflammatory mediators (Kempuraj et al., 2018b; Lee et al., 2021).

Moreover, GMF is involved in oxidative stress signaling. It has been reported that GMF is closely related to the dysregulation of copper-zinc superoxide dismutase (Cu-Zn SOD) and catalase

and glutathione peroxidase (GPX), enhancing neurotoxicity through oxidative stress (Fan et al., 2018; Selvakumar et al., 2018). Microglia activation leads to reactive oxygen species (ROS) production, which can exacerbate oxidative stress, causing neuroinflammation and cell death (Fan et al., 2018; Selvakumar et al., 2018). On the other hand, some studies have demonstrated that in GMF-KO neurons or glial cells, the activation and release of chemokine (C-C motif) ligand 2 (CCL2) is reduced, and they are more tolerant of 1-methyl-4-phenylpyridinium (MPP+) toxicity. CCL2 is expressed in glia, neurons, and mast cells; its relevance resides in its role in PD. Up-regulation of this chemoattractant can lead to microglia over-activation leading to neuron damage and neuroinflammation. Furthermore, CCL2 released from brain cells and mast cells could be involved in infiltrating other inflammatory cells into the substantia nigra, potentiating the damage (Kempuraj et al., 2018a; Kempuraj et al., 2018b; Shen et al., 2019).

Glial cells play an essential role in the development and progression of other neurological disorders, such as amyotrophic lateral sclerosis (ALS), Fragile X Syndrome (FXS), and brain tumors (Kempuraj et al., 2018a; McAvoy and Kawamata, 2019; Raikwar et al., 2019; Selvakumar et al., 2019; Wright-Jin and Gutmann, 2019; Wilson et al., 2020). ALS is characterized by motor neuron degeneration and gliosis. New reports have been described that aberrant glial cells with highly proliferative and neurotoxic properties promotes the disease progression (Martínez-Palma et al., 2019; Filipi et al., 2020). The FXS disorder is caused by the loss of Fragile X Mental Retardation Protein (FMRP) that triggers alterations in glial cells, as demonstrated in FMRP knockout (KO) mice models where decreased hippocampal and neocortical circuitry synapses associated with astrocytes were observed (Simhal et al., 2019). On the other hand, the most common primary malignant brain tumor, glioblastoma, can modulate glial cells to regulate the microenvironment surrounding the tumor by multiple intercellular communication pathways. This tumor possesses a high infiltrative growth pattern since its boundary is composed of tumor cells, immune cells, and reactive glial cells. Several studies have demonstrated that microglial cells and astrocytes are essential for tumor progression. However, many unanswered questions still need to be clarified to improve understanding of the crosstalk role between glioblastoma and glial cells (Oliveira et al., 2017; Yekula et al., 2019; Belykh et al., 2020).

Advances and new CRISPR/Cas applications

CRISPR/Cas system enhancement and common uses

The CRISPR/Cas systems are considered the adaptive immune prokaryote machinery against bacteriophages and mobile genetic elements; their applications have gone beyond

genome editing in a wide variety of organisms by enhancing and renewing biotechnological tools through the specific DNA-binding ability of Cas to perform transcriptional control, modulate epigenetic modifications, live-cell imaging studies, identification of gene targets or gene signatures, cell lineage mapping, and diagnostic platforms, among other, uses (McKenna et al., 2016; Murugan et al., 2017; Duan et al., 2019; Kellner et al., 2019; Manghwar et al., 2019; Pickar-Oliver and Gersbach, 2019). The range of Cas9 variants has increased since the first use of the well-characterized *Streptococcus pyogenes* Cas9 (SpCas9). As a result of current research, we know more about new CRISPR–Cas systems than ever before, and the last classification considered two classes, six types, and 33 subtypes. Nonetheless, there is a huge reservoir of unknown CRISPR/Cas systems that could have enormous potential. Cas9 recognition depends on base pairing between the target sequence and the single-guide RNA (sgRNA) and the presence of an adjacent protospacer motif (PAM) sequence flanking the target site (Murugan et al., 2017; Manghwar et al., 2019; Makarova et al., 2020).

CRISPR/Cas9 systems are the most widely known and used. However, they have limitations, such as their large protein size, *in vivo* restrictions to optimal viral delivery, limited PAM sites, presence of off-target mutations, and low homology-directed repair (HDR) efficiency. As a way of overcoming these limitations, several studies have explored the natural diversity of the CRISPR/Cas9 system, finding suitable variants, such as the CjCas9 isolated from *Campylobacter jejuni*, which boast several benefits such as lower protein size compared to other Cas9 orthologues, having major specificity, including its ability efficient to modify the genome both *in vitro* and *in vivo* (Edraki et al., 2019; Hua, Tao, Han, Wang, & Zhu, 2019; E. Kim et al., 2017; Kleinstiver et al., 2016; Manghwar et al., 2019). Furthermore, the *Neisseria meningitidis* Cas9 variants (Nme1Cas9 and Nme2Cas9) have emerged as other options for an all-in-one delivery method because their compact size can be packet in an adeno-associated virus (AAV) with a guide RNA targeting for *in vivo* applications. Additionally, Nme2Cas9 can recognize a simple dinucleotide PAM (N4CC), providing a higher target site density of genomic sites with minimal or null off-target mutagenesis (Amrani et al., 2018; Edraki et al., 2019). PAM interaction is one of the significant restrictions of Cas9 recognition since it can be challenging to generate precise genome editing if it depends on a specific PAM; a clear example is HDR, where efficiency is improved when the double-stranded breaks (DSBs) are made between 10 and 20 base pairs of the desired target (Kleinstiver et al., 2016). According to a recent study involving 79 Cas9 proteins, 50 different PAM sequences can be recognized. Most orthologs can recognize a PAM greater than 2 bp; orthologs that recognize a PAM of ≥ 3 bp are likely to provide a major degree of specificity. However, it is essential to be careful with a complex PAM since access will also be more restricted (Hua et al., 2019; Gasiunas et al., 2020).

TABLE 1 Examples of SpCas9 and SaCas9 PAM engineered variants.

Variants	Origin Specie	PAM	Tested organisms	Advantages	Strategy for engineered	References
VRER-Cas9 VQR-Cas9	<i>Streptococcus pyogenes</i>	NGCG and NGA	Human cells (U2OS cells)	Similar (or better) genome-wide specificities compared to wild-type SpCas9	Bacterial selection-based directed evolution, and combinatorial design	Kleinstiver et al. (2016)
KKH SaCas9	<i>Staphylococcus aureus</i>	NNNRRT	Human cells (U2OS cells)	Comparable or slightly lower levels of mutagenesis compared with SaCas9 wild type	Molecular evolution	Kleinstiver et al. (2016)
SaCas9-HF	<i>Staphylococcus aureus</i>	NNNRRT	Human retinal pigmented epithelium cell line	Reduced off-target effects than SaCas9	Site-directed mutagenesis	Tan et al. (2019)
SpCas9-NRRH SpCas9-NRCH SpCas9-NRTH	<i>Streptococcus pyogenes</i>	NRRH, NRCH and NRTH	Human cells (HEK293T cells)	Higher on-target activity and similar or fewer numbers of detected off-target sites compared to SpCas9	Phage-assisted evolution	Miller et al. (2020)
xCas9 SpCas9-NG	<i>Streptococcus pyogenes</i>	GAT and NG	Rice	Higher specificity than SpCas9	Codon-optimization by PCR	Hua et al. (2019)

The Cas9 PAM interaction domain can be engineered to recognize multiple sequence motifs due to its extraordinary flexibility. Currently, the two widely used Cas9 orthologs, *Staphylococcus aureus* Cas9 (SaCas9) and SpCas9, have been modified to have different specificity and recognize new PAM sequences; some of them are shown in Table 1. For example, xCas9 and SpCas9-NG are two newly engineered SpCas9 variants that can identify more relaxed NG PAMs (Hu et al., 2018; Hua et al., 2019; Karvelis et al., 2019; Gasiunas et al., 2020). Altogether, these new evolved variants enable targeting multiple PAM sequences and making approachable genomic sites that were previously inaccessible (Miller et al., 2020). Cas9 recognizes GC-rich PAM sequences, but Cas12a (or Cpf1) and Cas12b (or C2c1) belonging to class 2 type V of the CRISPR/Cas system offer a new option for genome engineering by recognizing AT-rich PAM sequences. Furthermore, the newly described anti-CRISPR proteins AcrIIA2, AcrIIA4, and AcrIIC2Nme with Cas inhibition effect could be used as genetically encodable “off-switch” tools for Cas9 activity (Yang and Patel, 2017; Hua et al., 2019; Sun et al., 2019; Thavalingam et al., 2019). More recently, Cas 13 protein has been described as a nuclease capable of targeting and cleaving single-stranded RNA molecules (Shmakov et al., 2015; Abudayyeh et al., 2016; Wolter and Puchta, 2018). It must also be noted that these proteins possess two enzymatically distinct RNase activities since they can cleave the pre-crRNA array to form mature Cas13-crRNA and an RNA target complementary to the crRNA. These qualities make Cas 13 proteins optimal for RNA interference assays and potential diagnostic and treatment tools for viral diseases (Tambe et al., 2018; Fricke et al., 2020; Yin et al., 2020; Dang et al., 2021).

Since CRISPR/Cas is recognized as a natural genome editing tool, targeting a DNA/RNA sequence to monitor, break down, or

replace, reverting the versions of diseased genes to a healthy version of the gene. This technology has been widely used to treat human genetic disorders, diagnose human diseases, and help detect diseases early. Beyond those usages, it has been used for creating animal genetic models to assist in the understanding of human genetic diseases; however, it is potential usage for understanding the early development of molecular gaps in glial cells, gene editing of human neural stem cells (NSC), and RGs have been poorly studied (Abdelnour, Xie, Hassanin, Zuo, & Lu, 2021; Cota-Coronado et al., 2019b; Ramírez-Rodríguez, et al., 2019).

CRISPR/Cas is strategy to study glial cells

CRISPR applications for the study of glial cells-associated neurological disorders

Due to its enormous potential for multiple applications, the CRISPR/Cas system has been widely used to study neurodegenerative diseases. The system has assisted in understanding the molecular processes involved in the dynamic interaction between CNS cells and neurodegeneration. Genome examination with the CRISPR/Cas system leads to the discovery of potential markers in the early stages of neurodegeneration; on the other hand, epigenetic and gene editing can drive precision-targeted regenerative therapies (Cota-Coronado et al., 2019a; Raikwar et al., 2019; Kampmann, 2020; Ruetz et al., 2021).

The mechanisms and role of glial cells in the CNS and in treating neurodegenerative disorders could be understood using CRISPR/Cas. As mentioned above, critical glial genes are involved in neurological pathologies like the TREM2 gene. An

innovative study employing CRISPR/Cas in an induced pluripotent stem cell (iPSC) model differentiated to microglia, demonstrated that TREM2-KO reduces microglial survival, alters its phagocytosis function, and results in an impaired response to beta-amyloid plaques, thus revealing possible mechanisms that may have an essential role in AD progression (McQuade et al., 2020). However, other mechanisms related to TREM2 signaling must be elucidated as possible participation in synaptic pruning. A dual role has been proposed since TREM2 may contribute to plaque containment and clearance or aberrant synaptic loss (Scott-Hewitt et al., 2020). Hence, attention to TREM2 has been remarked on as a therapeutic target for its ability to modulate the microglial function and as a biomarker in the early stages of AD (Ewers et al., 2019; Ewers et al., 2020). Another target gene studied using the CRISPR/Cas9 method is GMF since it possesses a proinflammatory effect and is significantly upregulated in different zones of the AD brain. GMF expression is predominant in the reactive glial cells surrounding the amyloid plaques (APs). Raikwar et al. (2019) inhibited GMF expression in the microglial cell line BV2 by transducing them with lentiviral vectors that expressed SpCas9 and GMF-sgRNAs; they observed a reduction of microglial activation and suggested that *in vivo* GMF gene editing could be considered as a novel AD therapy (Raikwar et al., 2019). In addition, it has been demonstrated that GMF-KO in microglial cells ameliorates microgliosis as a consequence of improved mitochondrial dynamics and oxidative stress. In accordance with this, Selvakumar et al. (2019) shown that oxidative stress generated for microglial cells is associated with PD.

CRISPR approaches in the early development of glial cells

The CRISPR/Cas system allows the study of genes associated with neurodegenerative diseases and offers therapeutic approaches such as gene editing of NSC and RGs. As mentioned above, RGs are the primary stem cells during neural development and play a crucial role in neurogenesis and gliogenesis. However, it is necessary to extend our understanding of these cells' origins, lineage relationships, the timing of differentiation, and molecular properties (Li et al., 2021; Yang et al., 2022). The electroporation is a common technique employed for a rapid and efficient *in vivo* delivery of CRISPR/Cas9 system components into neural stem cells of the embryonic neocortex by *in utero* electroporation and/or microinjection into single neural stem cells in neocortical tissue, to investigate the function of specific genes during embryonic brain development (Kalebic et al., 2016). A similar approach known as Easi-CRISPR (Efficient additions with ssDNA inserts-CRISPR) has recently been adapted to target the developing brain by electroporating neurons with ribonucleoprotein complexes (Cas9 + crRNA + tracrRNA) which allows the editing of neural clonal lineages to be

selective. Similar Breasi-CRISPR can reveal protein-protein interactions in the developing cortex, tagged proteins by immunoblot analysis in a single cortex just 2 days after electroporation and, by immunohistochemistry in 24 h. Using these techniques, we can elucidate protein-protein interactions. Thus, we can analyze the role played by endogenous proteins during early brain development (Meyerink et al., 2022).

A recent study of integrating analysis of single-cell RNA-Seq datasets from human fetal brain samples concluded that “the developmental origins of human cortical glial cells are similar to that in the mouse cortex” (Yang et al., 2022). With these data, Yang et al. (2022) could establish a general model of RGs lineage progression (Figure 1) and the molecular identity of tRGs, which express many hallmarks of cells in the astrocyte lineage. Some molecular markers identified appear to have a central role in specific progenitors, such as epidermal growth factor receptor (EGFR) expressed in tRGs but not in vRGs or oRGs. In addition, tRGs expressing EGFR give rise to PyN-IPCs and bMIPCs positives at this marker, too (Yang et al., 2022). Previous studies have revealed that EGF is a vital mitogen to enhance oligodendroglial development (Yang et al., 2016; Yang et al., 2017). More recently, some findings provided strong evidence that EGF facilitates the transdifferentiation of astrocytes to oligodendrocytes and that the EGF-EGFR-Erk1/2 pathway could be essential in this process (Liu et al., 2022). Furthermore, markers such as HOPX, FAM107A, TNC, and LIFR have been identified in the three RGs (vRGs, oRGs, and tRGs) (Yang et al., 2022).

Understanding processes involved in gliogenesis can help define and manipulate specific subsets of neurons and glial cells, as shown in recent research where an atlas was generated from a developing zebrafish brain employing the method GESTALT. The model encompasses 12 stages of the diversification of neurons and progenitors from embryo to larva and has shown differences with other species in neurogenic programs of CNS, as well as between zebrafish and mammalian neurogenesis. For example, in zebrafish, radial glial cells persist into adulthood and contribute to neurogenesis, in contrast to mammals, where a shift from neuronal to glial programs exists. Based on the optimized GESTALT method, cell lineage trees can be constructed and adapted for barcoding lineages on specific development windows corresponding to different branches of the specification trees or tag Campo's interest populations (Raj et al., 2020).

Gliogenesis-related genes of interest

Some genes of interest still need to be studied in more detail using the techniques described in this review to determine their essential role in gliogenesis. For instance, since quite a while ago; it has been known that in different animal models, such as lampreys, Nkx2.2, PDGFR, and SoxE (the lamprey Sox10 ortholog) genes might be involved in gliogenesis (Yuan et al., 2018), but it wasn't until the CRISPR/Cas9 gene was used in

the year 2021 that it was determined SOX10 plays similar roles, but not the same ones, in the development, migration, and differentiation of the neural crest. SOX10 is essential in human neural crest development for the transition of premigratory cells to migrating neural crest, it is vital for neural crest survival, and it is required for Schwann cell development as well (Lai et al., 2021). Similarly, the Olig1 and Olig2 genes in animal models have been suggested as necessary and sufficient for oligodendrocyte precursor development in the brain of Olig2 gene null mice, but Olig1 is insufficient for the formation of motor neurons or oligodendrocytes in the embryonic spinal cord in the absence of Olig2. However, both genes have not been studied yet using technologies described in this review to elucidate their roles in the RGs, which is extremely important since these genes are located on chromosome 21 and could be associated with Down syndrome (Lu et al., 2002).

Furthermore, RGs can be studied in tissue organoid models such as a 3D cortical spheroid differentiation, a recent *in vitro* model in which mTORC1 hyperactivation was induced, resulted in greater production of glial-lineage cells, which include astrocytes. In contrast, mTORC1 suppression strongly promoted neurogenesis and impaired gliogenesis, meaning mTORC1 is required for normal gliogenesis. Still, more studies are needed to uncover its central role in the RGs (Blair et al., 2018). In addition to this, considering studying the RGs shape is another essential factor to perform its proper function, that is why further morphological studies by technologies using CRISPR/Cas need it; for example, in one study, Pax2a gene mutants of the zebrafish resulted in defects in many aspects of the Müller glial cell morphology (Charlton-Perkins et al., 2019). Furthermore, 3D brain organoid technology allows for studying human microglia functions (Cakir et al., 2022). However, most of the methods employed for brain organoid generation are based on the neuroectoderm differentiation of pluripotent stem cells. These methods hinder mesodermal lineage cell obtention and, therefore, microglia emerging (Ormel et al., 2018; Fagerlund et al., 2021; Cakir et al., 2022). Currently, some models have been developed for functional microglia representing as described in the recent work of Cakir et al. (2022) that generated microglia-containing human cortical organoids (macOS) using PU.1-induction. They proposed mhCOs as a novel platform to study the microglia-specific function; to exemplify it, they performed a pooled CRISPRi screening of AD-related genes in microglia; their findings suggested an association with dysregulation of cholesterol metabolism *via* the Sorl1 gene (Cakir et al., 2022).

It is worth mentioning that in a human neural stem cell model of astrocyte pathology, other genes of interest were found upregulated. They were associated with neurological system processes (CHRNA1, CRYZ, EYA1, NPY, PCDHB5), synapse organization, biogenesis (CHRNA1, PCDHB5) and synaptic transmission (CHRNA1, NPY, PCDHB5), founding ANXA2 gene significantly expressed in the pathology

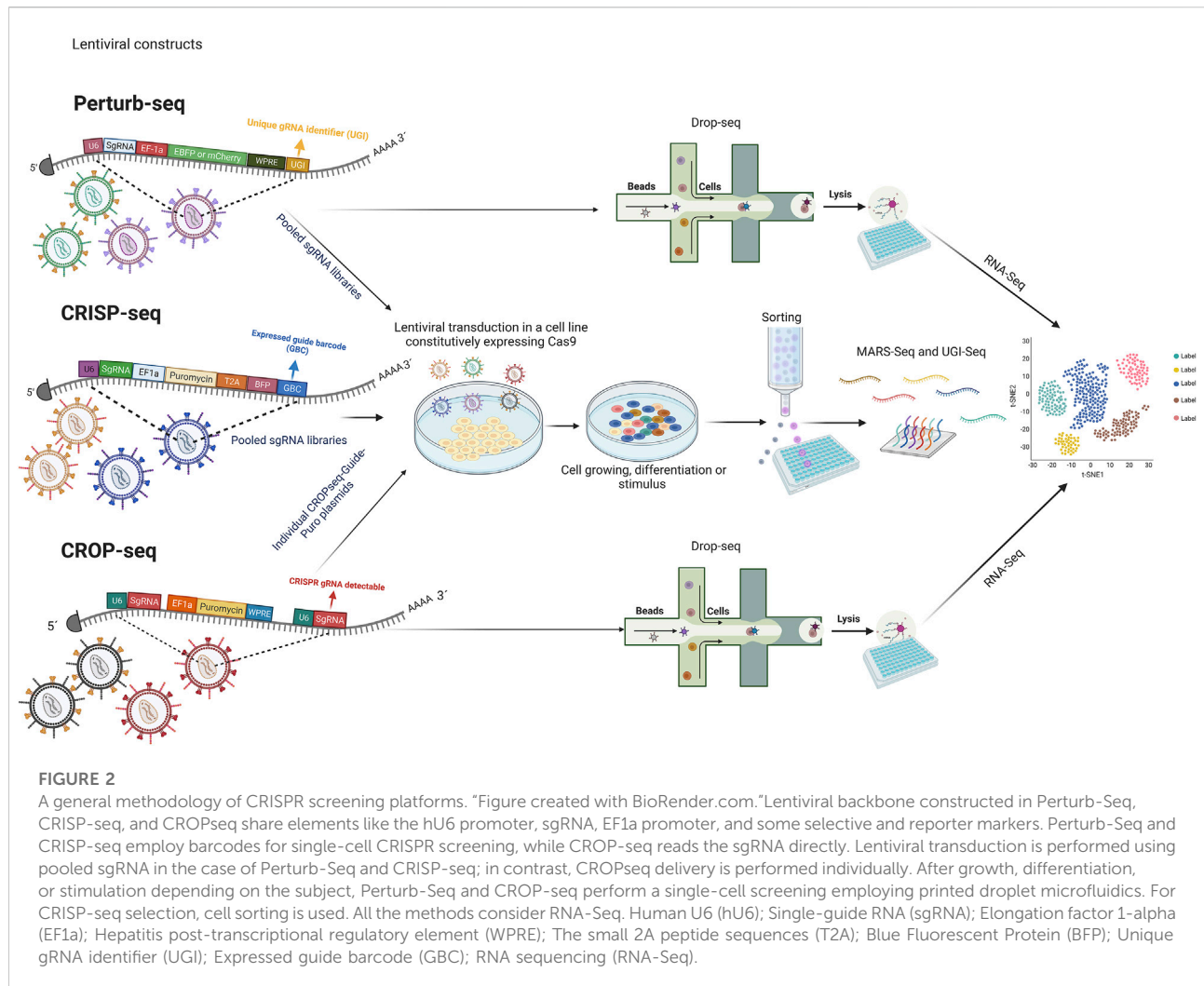
(Hallmann et al., 2017). However, its primary function is still a gap open to elucidation.

CRISPR screening platforms, panels, and large-scale maps of cell lineage

The latest advances in pooled screening provide a powerful approach to illustrating gene function and association in a biological process, disease, or disorder. These kinds of studies are challenging due to the enormous list of genes at the genome-scale. In some cases, pooled screening has been delimited to phenotypic average properties of a population by considering only a few exogenous reporters or effects on cell viability, thus limiting the understanding of genetic perturbations of impact or the distinction between different perturbations with similar responses (Adamson et al., 2016; de Groot et al., 2018; Parekh et al., 2018; Jin et al., 2020).

Facing these challenges, CRISPR screens have emerged, enabling a new efficient perturbation tool with multiple applications. There are two major kinds of CRISPR screens, the pooled and the arrayed. A pooled CRISPR screen typically involves a library that is introduced in bulk into a single or a group of cells under a specific treatment that leads to selecting cells whose perturbations confers a particular advantage. In contrast, arrayed CRISPR screens separate perturbations throughout the screen for a more controlled study (Bock et al., 2022). In the next few years, novel screening methods with high-content and single-cell screening at the genome-scale will be necessary. Currently, some methods have been described: Perturb-Seq, CRISP-seq, and CROPseq; their base resides on CRISPR knockout or knockdown screening in combination with single-cell-based RNA-seq, doing possible research at a single-cell level and with the projection of the study of a large-scale gene perturbation (Adamson et al., 2016; Dixit et al., 2016; Jaitin et al., 2016; Datlinger et al., 2017; Parekh et al., 2018; Duan et al., 2019; Schraivogel et al., 2020). The review work of Bock et al. (2022) describes concepts of CRISPR screening, experimental design, and applications extensively. The major difference between CROP-seq compared to Perturb-seq and CRISP-seq is that guide RNA is directly read, simplifying the single-cell CRISPR screening with large guide RNA libraries (Datlinger et al., 2017). The general mechanism through which these methodologies work can be seen in Figure 2. In addition to these approaches, the pooled genetic screens based on the CRISPR interference (CRISPRi) system allow the study of a wide range of genetic perturbations and mutagenesis for identifying gene function and gene-phenotype interactions (Schuster et al., 2019).

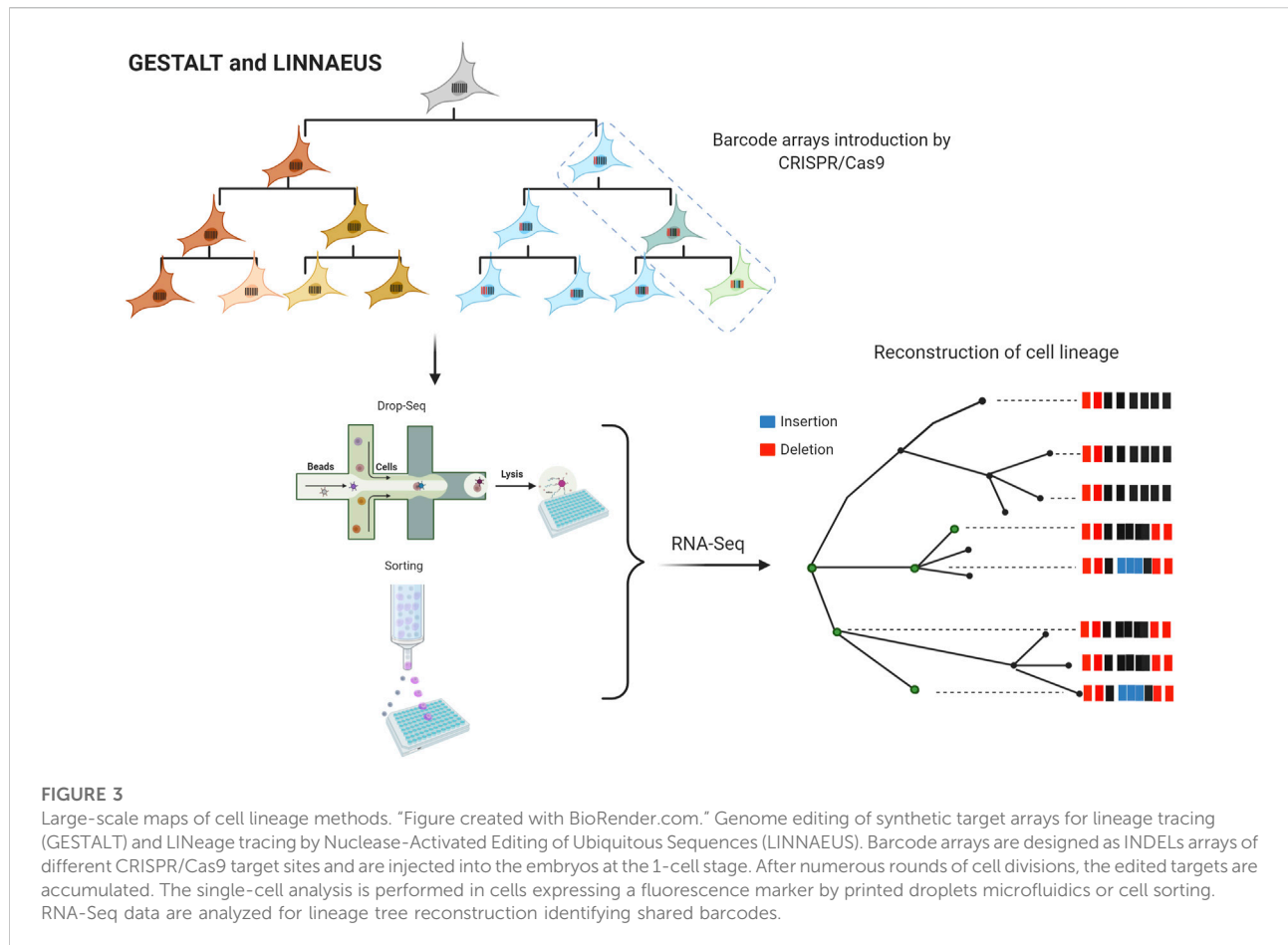
Like current research on single glial gene function, large gene panels in the neurobiological context are arising. Jin et al. (2020) developed a scalable genetic screen approach applying *in vivo* Perturb-Seq for the study of 35 loss-of-function risk genes for



autism spectrum disorder (ASD), and they identified specific cell gene signatures in both neuronal and glial cells that are affected by genetic perturbations (Jin et al., 2020). A recent study performed with the CRISPR/Cas9 platform for gene targeting at multiple loci of NSCs for galactosylceramidase (GALC) overexpressing, a vital enzyme whose loss is associated with the death of myelin-producing oligodendrocytes and Schwann cells, gene editing allowed the reestablishment of GALC activity when edited NSCs were transplanted into oligodendrocyte mutant shiverer-immunodeficient mice (Dever et al., 2019). On the other hand, Lalli et al. (2020) studied a set of 13 ASD-associated genes by coupling pooled dCas9-based transcriptional repression to single-cell RNA-seq in a human model of neuron differentiation; their findings evidenced unique and overlapping consequences on transcriptional networks and pathways of these genes on cell-cycle, and five of them (ADNP, ARID1B, ASH1L, CHD2, and DYRK1A) were identified as the cause of delay neuron differentiation. Additionally, they predicted that PTEN (phosphatase and tensin homolog) repression could have a

positive effect by increasing proliferation and neuron projection (Lalli et al., 2020).

Meanwhile, cellular barcoding strategies and single-cell sequencing have led to the development of new methodologies for lineage tracing. GESTALT and LINNAEUS are two other emerging methods with the potential to generate large-scale cell lineage maps. Using these methods is possible to introduce barcode arrays that can be traced in future generations using multiple CRISPR/Cas target sites (Figure 3) (McKenna et al., 2016). These barcodes consist of combinations of insertions and deletions (INDELs) generated by CRISPR/Cas9 and are designed to have multiple targets in the genome. After numerous rounds of cell divisions, there is an accumulation of edited targets. It is assumed that targets are independent of each other, which allows lineage tracing; shared barcodes reconstruct cell lineage trees. LINNAEUS and GESTALT methods employ fluorescence intensity of GFP or RFP for INDELs detection; however, LINNAEUS designs are more limited in comparison to GESTALT designs since their arrays are performed in the



3'UTR of GFP or RFP, facilitating the simultaneous detection of multiple targets (Chen et al., 2022). In the long term, all these new approaches will generate invaluable information, representing new challenges due to the amount of data to process and analyze. In other words, the evolution of informatics platforms for understanding single-cell CRISPR screening data is also being considered; MUSIC, scMAGeCK, and SCEPTRE are clear examples of these advances in data analysis (Duan et al., 2019; Yang et al., 2020; Barry et al., 2021; Watson et al., 2021).

Glial cell's potential applications in regenerative medicine

In regenerative medicine, constructing cell lineage trees could enhance the therapeutic approaches for converting glial cells into functional neurons, which could benefit a wide range of medicinal purposes. Recently, Zhou et al. (2020) reported an efficient conversion of Müller glia into retinal ganglion cells (RGCs) by downregulation of the polypyrimidine tract-binding protein 1 (Ptp1), employing an *in vivo* viral delivery and the CRISPR-Cas13d (CasRx), in this research was proven induction

of neurons with dopaminergic features in the striatum that contrasted motor defects in a PD mouse model (Zhou et al., 2020). Ptp1 encodes an RNA binding protein whose depletion is sufficient to convert cultured mouse fibroblasts and N2a cells into functional neurons (Xue et al., 2013; Qian et al., 2020). More recently, the conversion of midbrain astrocytes to dopaminergic neurons with the ability to reconstruct the nigrostriatal circuit in an induced mouse PD model has been demonstrated (Qian et al., 2020). These findings further incentivize the potential applications of glial cells as a source of neurons to replace those that lose their function in neurodegenerative diseases.

The use of technologies involving CRISPR/Cas would not just enable the elucidation of the current gaps in glial cells. Still, it would also be a great way to generate fast and reliable models for glial cell studies, as an existing method that allowed to reduce the differentiating time of hPSCs to astrocytes from 3–6 months to generate functional astrocytes from hESCs and hiPSCs in 4–7 weeks, meaning NF1A and SOX9 dispensable at the early stage of neural differentiation (Li et al., 2018). Besides, iPSC-based disease models are a powerful tool for understanding neurodegenerative disorders in a relevant genetic and cellular context. Recently, Guan et al. (2022) reported a promising iPSC

generation method with small molecules. Chemical reprogramming has advantages compared to existing reprogramming methods: it is non-integrative to the genome, controllable, and easy to optimize, standardize and manufacture. In addition, differentiation employing small molecules has shown better epigenome reprogramming which is essential for reliable iPSC-based models (Meneghini et al., 2021; Guan et al., 2022).

Perspectives and remarks

Although the study of glial cells has been delayed by a lack of interest in the past, the use of new biotechnological tools, such as those employing CRISPR/Cas, will decrease the existing knowledge gap in the glial cells. The CRISPR/Cas enhancements and their CRISPR screening platforms along the large-scale maps of cell lineage methods make new genomic sites that were previously inaccessible for genome engineering to study genes of interest in bulk; in addition, emerging Cas proteins could be used in the all-in-one delivery method, which is crucial for success *in vivo* delivery experiments. However, it is essential to consider the limitations of using this technology, which is still improving. For example, introducing specific INDELS tends to be less efficient than KO experiments. On the other hand, the outcomes after genome edition can vary in differentiated neural tissue since the nonhomologous end-joining (NHEJ) DNA repair is the most common in this type of cell, and the CRISPR/Cas system has been optimized in dividing cell lines that generally use the HDR repair. Additionally, the NHEJ pathway is more active and error-prone, facilitating frame-shift mutations in the coding sequence. Although new approaches have been developed such as the strategy “HiTi” (homology-independent targeted integration) to improve DNA knock-in in dividing and nondividing cells (Vesikansa, 2018; Meneghini et al., 2021).

Even though CRISPR specificity has improved over time, it is still a critical concern for clinical applications. On the other hand, it has been reported toxicity after an induced double-strand break (DSB), and there is no information about it in neurons and glial cells. In addition, the complex and diverse architecture of the brain limits accesses to the CRISPR/Cas system (Vesikansa, 2018; Meneghini et al., 2021).

Next-generation sequencing technologies have led to the discovery of novel genes associated with the multiple functions of glial cells as well as their role in the appearance of neurodegenerative diseases without forgetting genes of paramount interest that have been somehow overlooked or

not sufficiently investigated; the use of pooled screening, single-cell CRISPR screening, lineage tracing, and transcriptome profiling are powerful strategies to facilitate gene function evaluation to define and manipulate specific subsets of neurons and glial cells, and thus find critical unanswered questions. However, there are some challenges to a successful CRISPR screen study; for example, the appropriate screen design as well as the biological model selection, optimization of the delivery of Cas protein, and the gRNAs, and noise associated or not associated with CRISPR screens (Bock et al., 2022). The use of these technologies is vital to expand current knowledge and go beyond one of the functions most described by microglia, namely, synaptic pruning during development and synaptic modulation, and begin to add missing pieces when it comes to functions, cellular origins, differentiation time, morphology, along with the discovery of new cell types involved in embryogenesis and the CNS.

Author contributions

CB-A, JF-F, and OH-P wrote the manuscript, DA-G, OD-G, and LG-O revised the manuscript, FD-M, EP-C, and ED-M outlined the concept for this review and approved the final version of the manuscript.

Acknowledgments

The authors would like to thank Michele Brennan for advising on academic writing.

Conflict of interest

The authors declare that the research was conducted in the absence of any commercial or financial relationships that could be construed as a potential conflict of interest.

Publisher's note

All claims expressed in this article are solely those of the authors and do not necessarily represent those of their affiliated organizations, or those of the publisher, the editors and the reviewers. Any product that may be evaluated in this article, or claim that may be made by its manufacturer, is not guaranteed or endorsed by the publisher.

References

- Abdelnour, S. A., Xie, L., Hassanin, A. A., Zuo, E., and Lu, Y. (2021). The potential of CRISPR/Cas9 gene editing as a treatment strategy for inherited diseases. *Front. Cell Dev. Biol.* 9, 699597. doi:10.3389/fcell.2021.699597
- Abudayyeh, O. O., Gootenberg, J. S., Konermann, S., Joung, J., Slaymaker, I. M., Cox, D. B., et al. (2016). C2c2 is a single-component programmable RNA-guided RNA-targeting CRISPR effector. *Science* 353 (6299), aaf5573. doi:10.1126/science.aaf5573
- Adamson, B., Norman, T. M., Jost, M., Cho, M. Y., Nuñez, J. K., Chen, Y., et al. (2016). A Multiplexed single-cell CRISPR screening platform enables systematic dissection of the unfolded protein response. *Cell* 167 (7), 1867–1882.e21. doi:10.1016/j.cell.2016.11.048
- Allen, N. J., and Lyons, D. A. (2018). Glia as architects of central nervous system formation and function. *Science* 362 (6411), 181–185. doi:10.1126/science.aat0473
- Amrani, N., Gao, X. D., Liu, P., Edraki, A., Mir, A., Ibrahim, R., et al. (2018). NmeCas9 is an intrinsically high-fidelity genome-editing platform. *Genome Biol.* 19 (1), 214. doi:10.1186/s13059-018-1591-1
- Arai, K., and Lo, E. H. (2017). “Chapter 18 - gliogenesis,” in *Primer on cerebrovascular diseases*. Editors L. R. Caplan, J. Biller, M. C. Leary, E. H. Lo, A. J. Thomas, M. Yenari, et al. Second Edition (San Diego: Academic Press), 91–95.
- Arcuri, C., Mecca, C., Bianchi, R., Giambanco, I., and Donato, R. (2017). The pathophysiological role of microglia in dynamic surveillance, phagocytosis and structural remodeling of the developing CNS. *Front. Mol. Neurosci.* 10, 191. doi:10.3389/fnmol.2017.00191
- Barry, T., Wang, X., Morris, J. A., Roeder, K., and Katsevich, E. (2021). SCEPTRE improves calibration and sensitivity in single-cell CRISPR screen analysis. *Genome Biol.* 22 (1), 344. doi:10.1186/s13059-021-02545-2
- Bartels, T., De Schepper, S., and Hong, S. (2020). Microglia modulate neurodegeneration in Alzheimer's and Parkinson's diseases. *Science* 370 (6512), 66–69. doi:10.1126/science.abb8587
- Belykh, E., Shaffer, K. V., Lin, C., Byvalts, V. A., Preul, M. C., and Chen, L. (2020). Blood-brain barrier, blood-brain tumor barrier, and fluorescence-guided neurosurgical oncology: Delivering optical labels to brain tumors. *Front. Oncol.* 10, 739. doi:10.3389/fonc.2020.00739
- Bertapaglia, C., Gonçalves, J. C., and Vallee, R. B. (2018). Nuclear migration in mammalian brain development. *Semin. Cell Dev. Biol.* 82, 57–66. doi:10.1016/j.semcdb.2017.11.033
- Blair, J. D., Hockemeyer, D., and Bateup, H. S. (2018). Genetically engineered human cortical spheroid models of tuberous sclerosis. *Nat. Med.* 24 (10), 1568–1578. doi:10.1038/s41591-018-0139-y
- Bock, C., Datlinger, P., Chardon, F., Coelho, M. A., Dong, M. B., Lawson, K. A., et al. (2022). High-content CRISPR screening. *Nat. Rev. Methods Prim.* 2 (1), 8. doi:10.1038/s43586-021-00093-4
- Butt, A., and Verkhratsky, A. (2018). Neuroglia: Realising their true potential. *Brain Neurosci. Adv.* 2, 2398212818817495. doi:10.1177/2398212818817495
- Cakir, B., Tanaka, Y., Kiral, F. R., Xiang, Y., Dagliyan, O., Wang, J., et al. (2022). Expression of the transcription factor PU.1 induces the generation of microglia-like cells in human cortical organoids. *Nat. Commun.* 13 (1), 430. doi:10.1038/s41467-022-28043-y
- Ceprian, M., and Fulton, D. (2019). Glial cell AMPA receptors in nervous system health, injury and disease. *Int. J. Mol. Sci.* 20 (10), E2450. doi:10.3390/ijms20102450
- Charlton-Perkins, M., Almeida, A. D., MacDonald, R. B., and Harris, W. A. (2019). Genetic control of cellular morphogenesis in Müller glia. *Glia* 67 (7), 1401–1411. doi:10.1002/glia.23615
- Chen, C., Liao, Y., and Peng, G. (2022). Connecting past and present: Single-cell lineage tracing. *Protein Cell* 13, 790–807. doi:10.1007/s13238-022-00913-7
- Cota-Coronado, A., Díaz-Martínez, N. F., Padilla-Camberos, E., and Díaz-Martínez, N. E. (2019a). Editing the central nervous system through CRISPR/Cas9 systems. *Front. Mol. Neurosci.* 12, 110. doi:10.3389/fnmol.2019.00110
- Cota-Coronado, A., Ramírez-Rodríguez, P. B., Padilla-Camberos, E., Díaz, E. F., Flores-Fernández, J. M., Ávila-González, D., et al. (2019b). Implications of human induced pluripotent stem cells in metabolic disorders: From drug discovery toward precision medicine. *Drug Discov. Today* 24 (1), 334–341. doi:10.1016/j.drudis.2018.10.001
- Dang, J., Tiwari, S. K., Agrawal, K., Hui, H., Qin, Y., and Rana, T. M. (2021). Glial cell diversity and methamphetamine-induced neuroinflammation in human cerebral organoids. *Mol. Psychiatry* 26 (4), 1194–1207. doi:10.1038/s41380-020-0676-x
- Datlinger, P., Rendeiro, A. F., Schmidl, C., Krausgruber, T., Traxler, P., Klughammer, J., et al. (2017). Pooled CRISPR screening with single-cell transcriptome readout. *Nat. Methods* 14 (3), 297–301. doi:10.1038/nmeth.4177
- de Groot, R., Lüthi, J., Lindsay, H., Holtackers, R., and Pelkmans, L. (2018). Large-scale image-based profiling of single-cell phenotypes in arrayed CRISPR-Cas9 gene perturbation screens. *Mol. Syst. Biol.* 14 (1), e8064. doi:10.15252/msb.20178064
- Dever, D. P., Scharenberg, S. G., Camarena, J., Kildebeck, E. J., Clark, J. T., Martin, R. M., et al. (2019). CRISPR/Cas9 genome engineering in engraftable human brain-derived neural stem cells. *iScience* 15, 524–535. doi:10.1016/j.isci.2019.04.036
- Deverman, B. E., and Patterson, P. H. (2009). Cytokines and CNS development. *Neuron* 64 (1), 61–78. doi:10.1016/j.neuron.2009.09.002
- Dietz, A. G., Goldman, S. A., and Nedergaard, M. (2020). Glial cells in schizophrenia: A unified hypothesis. *Lancet. Psychiatry* 7 (3), 272–281. doi:10.1016/s2215-0366(19)30302-5
- Dixit, A., Parnas, O., Li, B., Chen, J., Fulco, C. P., Jerby-Arnon, L., et al. (2016). Perturb-Seq: Dissecting molecular circuits with scalable single-cell RNA profiling of pooled genetic screens. *Cell* 167 (7), 1853–1866.e17. doi:10.1016/j.cell.2016.11.038
- Duan, B., Zhou, C., Zhu, C., Yu, Y., Li, G., Zhang, S., et al. (2019). Model-based understanding of single-cell CRISPR screening. *Nat. Commun.* 10 (1), 2233. doi:10.1038/s41467-019-10216-x
- Edraki, A., Mir, A., Ibrahim, R., Gainetdinov, I., Yoon, Y., Song, C. Q., et al. (2019). A compact, high-accuracy Cas9 with a dinucleotide PAM for *in vivo* genome editing. *Mol. Cell* 73 (4), 714–726.e4. e714. doi:10.1016/j.molcel.2018.12.003
- Ewers, M., Biechele, G., Suárez-Calvet, M., Sacher, C., Blume, T., Morenas-Rodríguez, E., et al. (2020). Higher CSF sTREM2 and microglia activation are associated with slower rates of beta-amyloid accumulation. *EMBO Mol. Med.* 12 (9), e12308. doi:10.15252/emmm.202012308
- Ewers, M., Franzmeier, N., Suárez-Calvet, M., Morenas-Rodríguez, E., Caballero, M. A. A., Kleinberger, G., et al. (2019). Increased soluble TREM2 in cerebrospinal fluid is associated with reduced cognitive and clinical decline in Alzheimer's disease. *Sci. Transl. Med.* 11 (507), eaav6221. doi:10.1126/scitranslmed.aav6221
- Fagerlund, I., Dougali, A., Shakirzyanova, A., Gómez-Budia, M., Pelkonen, A., Kontinen, H., et al. (2021). Microglia-like cells promote neuronal functions in cerebral organoids. *Cells* 11 (1), 124. doi:10.3390/cells11010124
- Fan, J., Fong, T., Chen, X., Chen, C., Luo, P., and Xie, H. (2018). Glia maturation factor-β: A potential therapeutic target in neurodegeneration and neuroinflammation. *Neuropsychiatr. Dis. Treat.* 14, 495–504. doi:10.2147/ndt.S157099
- Filipi, T., Hermanova, Z., Tureckova, J., Vanatko, O., and Anderova, A. M. (2020). Glial cells-the strategic targets in amyotrophic lateral sclerosis treatment. *J. Clin. Med.* 9 (1), E261. doi:10.3390/jcm9010261
- Flores-Fernández, J. M., Rathod, V., and Wille, H. (2018). Comparing the folds of prions and other pathogenic amyloids. *Pathogens* 7 (2), E50. doi:10.3390/pathogens7020050
- Fricke, T., Smalakyte, D., Lapinski, M., Pateria, A., Weige, C., Pastor, M., et al. (2020). Targeted RNA knockdown by a type III CRISPR-cas complex in zebrafish. *Crispr J.* 3 (4), 299–313. doi:10.1089/crispr.2020.0032
- Gasiunas, G., Young, J. K., Karvelis, T., Kazlauskas, D., Urbaitis, T., Jasnauskaitė, M., et al. (2020). A catalogue of biochemically diverse CRISPR-Cas9 orthologs. *Nat. Commun.* 11 (1), 5512. doi:10.1038/s41467-020-19344-1
- Gilbert, S. F., and Barresi, M. J. F. (2017). Developmental biology. *Am. J. Med. Genet. A* 173, 1430. doi:10.1002/ajmg.a.3816611th Edition
- Guan, J., Wang, G., Wang, J., Zhang, Z., Fu, Y., Cheng, L., et al. (2022). Chemical reprogramming of human somatic cells to pluripotent stem cells. *Nature* 605, 325–331. doi:10.1038/s41586-022-04593-5
- Hallmann, A. L., Araúzo-Bravo, M. J., Mavrommatis, L., Ehrlich, M., Röpke, A., Brockhaus, J., et al. (2017). Astrocyte pathology in a human neural stem cell model of frontotemporal dementia caused by mutant TAU protein. *Sci. Rep.* 7, 42991. doi:10.1038/srep42991
- Hidalgo-Lanusa, O., Baez-Jurado, E., Echeverría, V., Ashraf, G. M., Sahebkar, A., García-Segura, L. M., et al. (2020). Lipotoxicity, neuroinflammation, glial cells and oestrogenic compounds. *J. Neuroendocrinol.* 32 (1), e12776. doi:10.1111/jne.12776
- Hirbec, H., Déglon, N., Foo, L. C., Goshen, I., Grutzendler, J., Hangen, E., et al. (2020). Emerging technologies to study glial cells. *Glia* 68 (9), 1692–1728. doi:10.1002/glia.23780
- Hu, J. H., Miller, S. M., Geurts, M. H., Tang, W., Chen, L., Sun, N., et al. (2018). Evolved Cas9 variants with broad PAM compatibility and high DNA specificity. *Nature* 556 (7699), 57–63. doi:10.1038/nature26155

- Hua, K., Tao, X., Han, P., Wang, R., and Zhu, J.-K. (2019). Genome engineering in rice using Cas9 variants that recognize NG PAM sequences. *Mol. Plant* 12 (7), 1003–1014. doi:10.1016/j.molp.2019.03.009
- Jaitin, D. A., Weiner, A., Yofe, I., Lara-Astiaso, D., Keren-Shaul, H., David, E., et al. (2016). Dissecting immune circuits by linking CRISPR-pooled screens with single-cell RNA-seq. *Cell* 167 (7), 1883–1896.e15. e1815. doi:10.1016/j.cell.2016.11.039
- Jin, X., Simmons, S. K., Guo, A., Shetty, A. S., Ko, M., Nguyen, L., et al. (2020). *In vivo* Perturb-Seq reveals neuronal and glial abnormalities associated with autism risk genes. *Science* 370 (6520), eaaz6063. doi:10.1126/science.aaz6063
- Kalebic, N., Taverna, E., Tavano, S., Wong, F. K., Suchold, D., Winkler, S., et al. (2016). CRISPR/Cas9-induced disruption of gene expression in mouse embryonic brain and single neural stem cells *in vivo*. *EMBO Rep.* 17 (3), 338–348. doi:10.15252/embr.201541715
- Kampmann, M. (2020). CRISPR-based functional genomics for neurological disease. *Nat. Rev. Neurol.* 16 (9), 465–480. doi:10.1038/s41582-020-0373-z
- Karvelis, T., Young, J. K., and Siksnys, V. (2019). A pipeline for characterization of novel Cas9 orthologs. *Methods Enzymol.* 616, 219–240. doi:10.1016/bs.mie.2018.10.021
- Kellner, M. J., Koob, J. G., Gootenberg, J. S., Abudayyeh, O. O., and Zhang, F. (2019). Sherlock: Nucleic acid detection with CRISPR nucleases. *Nat. Protoc.* 14 (10), 2986–3012. doi:10.1038/s41596-019-0210-2
- Kempuraj, D., Selvakumar, G. P., Thangavel, R., Ahmed, M. E., Zaheer, S., Kumar, K. K., et al. (2018a). Glia maturation factor and mast cell-dependent expression of inflammatory mediators and proteinase activated receptor-2 in neuroinflammation. *J. Alzheimers Dis.* 66 (3), 1117–1129. doi:10.3233/jad-180786
- Kempuraj, D., Selvakumar, G. P., Zaheer, S., Thangavel, R., Ahmed, M. E., Raikwar, S., et al. (2018b). Cross-talk between glia, neurons and mast cells in neuroinflammation associated with Parkinson's disease. *J. Neuroimmune Pharmacol.* 13 (1), 100–112. doi:10.1007/s11481-017-9766-1
- Kim, E., Koo, T., Park, S. W., Kim, D., Kim, K., Cho, H. Y., et al. (2017). *In vivo* genome editing with a small Cas9 orthologue derived from *Campylobacter jejuni*. *Nat. Commun.* 8. doi:10.1038/ncomms14500
- Kleinstiver, B. P., Pattanayak, V., Prew, M. S., Tsai, S. Q., Nguyen, N. T., Zheng, Z., et al. (2016). High-fidelity CRISPR-Cas9 nucleases with no detectable genome-wide off-target effects. *Nature* 529, 490–495. doi:10.1038/nature16526
- Kriegstein, A., and Alvarez-Buylla, A. (2009). The glial nature of embryonic and adult neural stem cells. *Annu. Rev. Neurosci.* 32, 149–184.
- Kuhn, S., Gritti, L., Crooks, D., and Dombrowski, Y. (2019). Oligodendrocytes in development, myelin generation and beyond. *Cells* 8 (11), E1424. doi:10.3390/cells8111424
- Lai, X., Liu, J., Zou, Z., Wang, Y., Wang, Y., Liu, X., et al. (2021). SOX10 ablation severely impairs the generation of postmigratory neural crest from human pluripotent stem cells. *Cell Death Dis.* 12 (9), 814. doi:10.1038/s41419-021-04099-4
- Lalli, M. A., Avey, D., Dougherty, J. D., Milbrandt, J., and Mitra, R. D. (2020). High-throughput single-cell functional elucidation of neurodevelopmental disease-associated genes reveals convergent mechanisms altering neuronal differentiation. *Genome Res.* 30 (9), 1317–1331. doi:10.1101/gr.262295.120
- Lee, J. W., Chun, W., Lee, H. J., Kim, S. M., Min, J. H., Kim, D. Y., et al. (2021). The role of microglia in the development of neurodegenerative diseases. *Biomedicines* 9 (10), 1449. doi:10.3390/biomedicines9101449
- Lehrman, E. K., Wilton, D. K., Litvina, E. Y., Welsh, C. A., Chang, S. T., Frouin, A., et al. (2018). CD47 protects synapses from excess microglia-mediated pruning during development. *Neuron* 100 (1), 120–134.e6. e126. doi:10.1016/j.neuron.2018.09.017
- Li, T., Chiou, B., Gilman, C. K., Luo, R., Koshi, T., Yu, D., et al. (2020). A splicing isoform of GPR56 mediates microglial synaptic refinement via phosphatidylserine binding. *Embo J.* 39 (16), e104136. doi:10.15252/emboj.2019104136
- Li, X., Liu, G., Yang, L., Li, Z., Zhang, Z., Xu, Z., et al. (2021). Decoding cortical glial cell development. *Neurosci. Bull.* 37 (4), 440–460. doi:10.1007/s12264-021-00640-9
- Li, X., Tao, Y., Bradley, R., Du, Z., Tao, Y., Kong, L., et al. (2018). Fast generation of functional subtype Astrocytes from human pluripotent stem cells. *Stem Cell Rep.* 11 (4), 998–1008. doi:10.1016/j.stemcr.2018.08.019
- Lin, Y., Yang, J., Shen, Z., Ma, J., Simons, B. D., and Shi, S. H. (2021). Behavior and lineage progression of neural progenitors in the mammalian cortex. *Curr. Opin. Neurobiol.* 66, 144–157. doi:10.1016/j.conb.2020.10.017
- Liu, X., Li, C., Li, J., Xie, L., Hong, Z., Zheng, K., et al. (2022). EGF signaling promotes the lineage conversion of astrocytes into oligodendrocytes. *Mol. Med.* 28 (1), 50. doi:10.1186/s10020-022-00478-5
- Lu, Q. R., Sun, T., Zhu, Z., Ma, N., Garcia, M., Stiles, C. D., et al. (2002). Common developmental requirement for Olig function indicates a motor neuron/oligodendrocyte connection. *Cell* 109 (1), 75–86. doi:10.1016/s0092-8674(02)00678-5
- Makarova, K. S., Wolf, Y. I., Iranzo, J., Shmakov, S. A., Alkhnbashi, O. S., Brouns, S. J. J., et al. (2020). Evolutionary classification of CRISPR-cas systems: A burst of class 2 and derived variants. *Nat. Rev. Microbiol.* 18 (2), 67–83. doi:10.1038/s41579-019-0299-x
- Manghwar, H., Lindsey, K., Zhang, X., and Jin, S. (2019). CRISPR/Cas system: Recent advances and future prospects for genome editing. *Trends Plant Sci.* 24 (12), 1102–1125. doi:10.1016/j.tplants.2019.09.006
- Martínez-Palma, L., Miquel, E., Lagos-Rodríguez, V., Barbeito, L., Cassina, A., and Cassina, P. (2019). Mitochondrial modulation by dichloroacetate reduces toxicity of aberrant glial cells and gliosis in the SOD1G93A rat model of amyotrophic lateral sclerosis. *Neurotherapeutics* 16 (1), 203–215. doi:10.1007/s13311-018-0659-7
- McAvoy, K., and Kawamata, H. (2019). Glial mitochondrial function and dysfunction in health and neurodegeneration. *Mol. Cell. Neurosci.* 101, 103417. doi:10.1016/j.mcn.2019.103417
- McKenna, A., Findlay, G. M., Gagnon, J. A., Horwitz, M. S., Schier, A. F., and Shendure, J. (2016). Whole-organism lineage tracing by combinatorial and cumulative genome editing. *Science* 353 (6298), aaf7907. doi:10.1126/science.aaf7907
- McQuade, A., Kang, Y. J., Hasselmann, J., Jairaman, A., Sotelo, A., Coburn, M., et al. (2020). Gene expression and functional deficits underlie TREM2-knockout microglia responses in human models of Alzheimer's disease. *Nat. Commun.* 11 (1), 5370. doi:10.1038/s41467-020-19227-5
- Meilandt, W. J., Ngu, H., Gogineni, A., Lalehzadeh, G., Lee, S. H., Srinivasan, K., et al. (2020). Trem2 deletion reduces late-stage amyloid plaque accumulation, elevates the Aβ42:Aβ40 ratio, and exacerbates axonal dystrophy and dendritic spine loss in the PS2APP Alzheimer's mouse model. *J. Neurosci.* 40 (9), 1956–1974. doi:10.1523/jneurosci.1871-19.2019
- Meneghini, V., Peviani, M., Luciani, M., Zambonini, G., and Gritti, A. (2021). Delivery platforms for CRISPR/Cas9 genome editing of glial cells in the central nervous system. *Front. genome Ed.* 3, 644319. doi:10.3389/fgeed.2021.644319
- Menon, M., Mohammadi, S., Davila-Velderrain, J., Goods, B. A., Cadwell, T. D., Xing, Y., et al. (2019). Single-cell transcriptomic atlas of the human retina identifies cell types associated with age-related macular degeneration. *Nat. Commun.* 10 (1), 4902. doi:10.1038/s41467-019-12780-8
- Meyerink, B. L., Pratiksha, K., Tiwari, N. K., Kittock, C. M., Klein, A., Evans, C., et al. (2022). Breasi-CRISPR: An efficient genome editing method to interrogate protein localization and protein-protein interactions in the embryonic mouse cortex. *bioRxiv* [Preprint]. Available at: <https://www.biorxiv.org/content/10.1101/2022.02.02.478837v1>, 478837. doi:10.1101/2022.02.02.478837
- Miller, S. M., Wang, T., Randolph, P. B., Arbab, M., Shen, M. W., Huang, T. P., et al. (2020). Continuous evolution of SpCas9 variants compatible with non-G PAMs. *Nat. Biotechnol.* 38 (4), 471–481. doi:10.1038/s41587-020-0412-8
- Möller, T., and Boddeke, H. W. G. M. (2016). Glial cells as drug targets: What does it take? *Glia* 64, 1742–1754. doi:10.1002/glia.22993
- Moon, S. B., Kim, D. Y., Ko, J. H., and Kim, Y. S. (2019). Recent advances in the CRISPR genome editing tool set. *Exp. Mol. Med.* 51 (11), 1–11. doi:10.1038/s12276-019-0339-7
- Murugan, K., Babu, K., Sundaresan, R., Rajan, R., and Sashital, D. G. (2017). The revolution continues: Newly discovered systems expand the CRISPR-cas toolkit. *Mol. Cell* 68 (1), 15–25. doi:10.1016/j.molcel.2017.09.007
- Neniskyte, U., and Gross, C. T. (2017). Errant gardeners: Glial-cell-dependent synaptic pruning and neurodevelopmental disorders. *Nat. Rev. Neurosci.* 18 (11), 658–670. doi:10.1038/nrn.2017.110
- Nott, A., Holtman, I. R., Coufal, N. G., Schlachetzki, J. C. M., Yu, M., Hu, R., et al. (2019). Brain cell type-specific enhancer-promoter interactome maps and disease-risk association. *Science* 366 (6469), 1134–1139. doi:10.1126/science.aay0793
- Oliveira, A. I., Anjo, S. I., Vieira de Castro, J., Serra, S. C., Salgado, A. J., Manadas, B., et al. (2017). Crosstalk between glial and glioblastoma cells triggers the "go-or-grow" phenotype of tumor cells. *Cell Commun. Signal.* 15 (1), 37. doi:10.1186/s12964-017-0194-x
- Ormel, P. R., Vieira de Sá, R., van Bodegraven, E. J., Karst, H., Harschnitz, O., Sneeboer, M. A. M., et al. (2018). Microglia innately develop within cerebral organoids. *Nat. Commun.* 9 (1), 4167. doi:10.1038/s41467-018-06684-2
- Parekh, U., Wu, Y., Zhao, D., Worlikar, A., Shah, N., Zhang, K., et al. (2018). Mapping cellular reprogramming via pooled overexpression screens with paired fitness and single-cell RNA-sequencing readout. *Cell Syst.* 7 (5), 548–555.e8. e548. doi:10.1016/j.cels.2018.10.008

- Parhizkar, S., Arzberger, T., Brendel, M., Kleinberger, G., Deussing, M., Focke, C., et al. (2019). Loss of TREM2 function increases amyloid seeding but reduces plaque-associated ApoE. *Nat. Neurosci.* 22 (2), 191–204. doi:10.1038/s41593-018-0296-9
- Park, J., Wetzel, I., Marriott, I., Dréau, D., D'Avanzo, C., Kim, D. Y., et al. (2018). A 3D human triculture system modeling neurodegeneration and neuroinflammation in Alzheimer's disease. *Nat. Neurosci.* 21 (7), 941–951. doi:10.1038/s41593-018-0175-4
- Patro, N., and Patro, I. (2022). "Generation and maturation of macroglia in the central nervous system," in *The biology of glial cells: Recent advances*. Editors I. Patro, P. Seth, N. Patro, and P. N. Tandon (Singapore: Springer Singapore), 115–142.
- Pickar-Oliver, A., and Gersbach, C. A. (2019). The next generation of CRISPR-Cas technologies and applications. *Nat. Rev. Mol. Cell Biol.* 20 (8), 490–507. doi:10.1038/s41580-019-0131-5
- Qian, H., Kang, X., Hu, J., Zhang, D., Liang, Z., Meng, F., et al. (2020). Reversing a model of Parkinson's disease with *in situ* converted nigral neurons. *Nature* 582, 550–556. doi:10.1038/s41586-020-2388-4
- Qin, Q., Wang, M., Yin, Y., and Tang, Y. (2022). The specific mechanism of TREM2 regulation of synaptic clearance in Alzheimer's disease. *Front. Immunol.* 0, 845897. doi:10.3389/fimmu.2022.845897
- Raikwar, S. P., Thangavel, R., Dubova, I., Selvakumar, G. P., Ahmed, M. E., Kempuraj, D., et al. (2019). Targeted gene editing of glia maturation factor in microglia: A novel alzheimer's disease therapeutic target. *Mol. Neurobiol.* 56 (1), 378–393. doi:10.1007/s12035-018-1068-y
- Raj, B., Farrell, J. A., Liu, J., El Kholtei, J., Carte, A. N., Navajas Acedo, J., et al. (2020). Emergence of neuronal diversity during vertebrate brain development. *Neuron* 108 (6), 1058–1074.e6. doi:10.1016/j.neuron.2020.09.023
- Raj, B., Wagner, D. E., McKenna, A., Pandey, S., Klein, A. M., Shendure, J., et al. (2018). Simultaneous single-cell profiling of lineages and cell types in the vertebrate brain. *Nat. Biotechnol.* 36 (5), 442–450. doi:10.1038/nbt.4103
- Ramaswamy, S. B., Bhagavan, S. M., Kaur, H., Giler, G. E., Kempuraj, D., Thangavel, R., et al. (2019). Glia maturation factor in the pathogenesis of alzheimer's disease. *Open Access J. Neurol. Neurosurg.* 12 (3), 79–82. doi:10.19080/oajnn.2019.12.555840
- Ruetz, T. J., Kashiwagi, C. M., Morton, B., Yeo, R. W., Leeman, D. S., Morgens, D. W., et al. (2021). Vitro and *in vivo* CRISPR-Cas9 screens reveal drivers of aging in neural stem cells of the brain. *bioRxiv* 11, 469762. doi:10.1101/2021.11.23.469762
- Schraivogel, D., Gschwind, A. R., Milbank, J. H., Leonce, D. R., Jakob, P., Mathur, L., et al. (2020). Targeted Perturb-seq enables genome-scale genetic screens in single cells. *Nat. Methods* 17 (6), 629–635. doi:10.1038/s41592-020-0837-5
- Schuster, A., Erasimus, H., Fritah, S., Nazarov, P. V., van Dyck, E., Niclou, S. P., et al. (2019). RNAi/CRISPR screens: From a pool to a Valid Hit. *Trends Biotechnol.* 37 (1), 38–55. doi:10.1016/j.tibtech.2018.08.002
- Scott-Hewitt, N., Perrucci, F., Morini, R., Erreni, M., Mahoney, M., Witkowska, A., et al. (2020). Local internalization of phosphatidylserine mediates developmental synaptic pruning by microglia. *Embo J.* 39 (16), e105380. doi:10.15252/embj.2020105380
- Sellgren, C. M., Gracias, J., Watmuff, B., Biag, J. D., Thanos, J. M., Whittredge, P. B., et al. (2019). Increased synapse elimination by microglia in schizophrenia patient-derived models of synaptic pruning. *Nat. Neurosci.* 22 (3), 374–385. doi:10.1038/s41593-018-0334-7
- Sellgren, C. M., Sheridan, S. D., Gracias, J., Xuan, D., Fu, T., and Perlis, R. H. (2017). Patient-specific models of microglia-mediated engulfment of synapses and neural progenitors. *Mol. Psychiatry* 22 (2), 170–177. doi:10.1038/mp.2016.220
- Selvakumar, G. P., Ahmed, M. E., Raikwar, S. P., Thangavel, R., Kempuraj, D., Dubova, I., et al. (2019). CRISPR/Cas9 editing of glia maturation factor regulates mitochondrial dynamics by attenuation of the NRF2/HO-1 dependent ferritin activation in glial cells. *J. Neuroimmune Pharmacol.* 14 (4), 537–550. doi:10.1007/s11481-019-09833-6
- Selvakumar, G. P., Iyer, S. S., Kempuraj, D., Raju, M., Thangavel, R., Saeed, D., et al. (2018). Glia maturation factor dependent inhibition of mitochondrial PGC-1 α triggers oxidative stress-mediated apoptosis in N27 rat dopaminergic neuronal cells. *Mol. Neurobiol.* 55 (9), 7132–7152. doi:10.1007/s12035-018-0882-6
- Shen, R., Lin, S., He, L., Zhu, X., Zhou, Z., Chen, S., et al. (2019). Association of two polymorphisms in CCL2 with Parkinson's disease: A case-control study. *Front. Neurol.* 10, 35. doi:10.3389/fneur.2019.00035
- Shmakov, S., Abudayyeh, O. O., Makarova, K. S., Wolf, Y. I., Gootenberg, J. S., Semenova, E., et al. (2015). Discovery and functional characterization of diverse class 2 CRISPR-cas systems. *Mol. Cell* 60 (3), 385–397. doi:10.1016/j.molcel.2015.10.008
- Sierra, A., de Castro, F., Del Río-Hortega, J., Rafael Iglesias-Rozas, J., Garrosa, M., and Kettenmann, H. (2016). The "Big-Bang" for modern glial biology: Translation and comments on Pío del Río-Hortega 1919 series of papers on microglia. *Glia* 64 (11), 1801–1840. doi:10.1002/glia.23046
- Sierra, A., Paolicelli, R. C., and Kettenmann, H. (2019). Cien años de Microglía: Milestones in a century of microglial research. *Trends Neurosci.* 42 (11), 778–792. doi:10.1016/j.tins.2019.09.004
- Simhal, A. K., Zuo, Y., Perez, M. M., Madison, D. V., Sapiro, G., and Micheva, K. D. (2019). Multifaceted changes in synaptic composition and astrocytic involvement in a mouse model of fragile X syndrome. *Sci. Rep.* 9 (1), 13855. doi:10.1038/s41598-019-50240-x
- Smidt, K., Pedersen, S. B., Brock, B., Schmitz, O., Fisker, S., Bendix, J., et al. (2007). Zinc-transporter genes in human visceral and subcutaneous adipocytes: Lean versus obese. *Mol. Cell. Endocrinol.* 264 (1–2), 68–73. doi:10.1016/j.mce.2006.10.010
- So, R. W. L., Chung, S. W., Lau, H. H. C., Watts, J. J., Gaudette, E., Al-Azzawi, Z. A. M., et al. (2019). Application of CRISPR genetic screens to investigate neurological diseases. *Mol. Neurodegener.* 14 (1), 41. doi:10.1186/s13024-019-0343-3
- Spanjaard, B., Hu, B., Mitic, N., Olivares-Chauvet, P., Janjua, S., Ninov, N., et al. (2018). Simultaneous lineage tracing and cell-type identification using CRISPR-Cas9-induced genetic scars. *Nat. Biotechnol.* 36 (5), 469–473. doi:10.1038/nbt.4124
- Sun, W., Yang, J., Cheng, Z., Amrani, N., Liu, C., Wang, K., et al. (2019). Structures of Neisseria meningitidis Cas9 complexes in catalytically poised and anti-CRISPR-inhibited States. *Mol. Cell* 76 (6), 938–952.e5. e935. doi:10.1016/j.molcel.2019.09.025
- Suter, T., and Jaworski, A. (2019). Cell migration and axon guidance at the border between central and peripheral nervous system. *Science* 365 (6456), eaaw8231. doi:10.1126/science.aaw8231
- Suárez-Calvet, M., Morenas-Rodríguez, E., Kleinberger, G., Schlepckow, K., Caballero, M. Á. A., Franzmeier, N., et al. (2019). Early increase of CSF sTREM2 in Alzheimer's disease is associated with tau related-neurodegeneration but not with amyloid- β pathology. *Mol. Neurodegener.* 14, 1.
- Tambe, A., East-Seletsky, A., Knott, G. J., Doudna, J. A., and O'Connell, M. R. (2018). RNA binding and HEPN-nuclease activation are decoupled in CRISPR-cas13a. *Cell Rep.* 24 (4), 1025–1036. doi:10.1016/j.celrep.2018.06.105
- Tan, Y., Chu, A. H. Y., Bao, S., Hoang, D. A., Kebede, F. T., Xiong, W., et al. (2019). Rationally engineered Staphylococcus aureus Cas9 nucleases with high genome-wide specificity. *Proc. Natl. Acad. Sci. USA* 116 (42), 20969–20976. doi:10.1073/pnas.1906843116
- Thavalingam, A., Cheng, Z., Garcia, B., Huang, X., Shah, M., Sun, W., et al. (2019). Inhibition of CRISPR-Cas9 ribonucleoprotein complex assembly by anti-CRISPR AcrIIIC2. *Nat. Commun.* 10 (1), 2806. doi:10.1038/s41467-019-10577-3
- Vallejo, R., Platt, D. C., Rink, J. A., Jones, M. A., Kelley, C. A., Gupta, A., et al. (2019). Electrical stimulation of C6 glia-precursor cells *in vitro* differentially modulates gene expression related to chronic pain pathways. *Brain Sci.* 9 (11), E303. doi:10.3390/brainsci9110303
- Verkhatsky, A., Ho, M. S., Zorec, R., and Parpura, V. (2019). The concept of neuroglia. *Adv. Exp. Med. Biol.* 1175, 1–13. doi:10.1007/978-981-13-9913-8_1
- Vesikansa, A. (2018). Unraveling of central nervous system disease mechanisms using CRISPR genome manipulation. *J. Cent. Nerv. Syst. Dis.* 10, 1179573518787469. doi:10.1177/1179573518787469
- Wang, Y. F., and Gao, Y. J. (2019). 2019 academic annual Meeting and the frontier seminar on "glial cell function and disease" (nantong, China). *ASN Neuro* 11, 1759091419863576. doi:10.1177/1759091419863576
- Watson, E. R., Taherian Fard, A., and Mar, J. C. (2021). Computational methods for single-cell imaging and omics data integration. *Front. Mol. Biosci.* 8, 768106. doi:10.3389/fmolb.2021.768106
- Wilson, E. N., Swarovski, M. S., Linortner, P., Shahid, M., Zuckerman, A. J., Wang, Q., et al. (2020). Soluble TREM2 is elevated in Parkinson's disease subgroups with increased CSF tau. *Brain* 143 (3), 932–943. doi:10.1093/brain/awaa021
- Wolter, F., and Puchta, H. (2018). The CRISPR/Cas revolution reaches the RNA world: Cas13, a new Swiss Army knife for plant biologists. *Plant J.* 94 (5), 767–775. doi:10.1111/tjpi.13899
- Wright-Jin, E. C., and Gutmann, D. H. (2019). Microglia as dynamic cellular mediators of brain function. *Trends Mol. Med.* 25 (11), 967–979. doi:10.1016/j.molmed.2019.08.013
- Xue, Y., Ouyang, K., Huang, J., Zhou, Y., Ouyang, H., Li, H., et al. (2013). Direct conversion of fibroblasts to neurons by reprogramming PTB-regulated microRNA circuits. *Cell* 152 (1–2), 82–96. doi:10.1016/j.cell.2012.11.045
- Yang, H., and Patel, D. J. (2017). Inhibition mechanism of an anti-CRISPR suppressor AcrIIA4 targeting SpyCas9. *Mol. Cell* 67 (1), 117–127.e5. e115. doi:10.1016/j.molcel.2017.05.024

- Yang, J., Cheng, X., Qi, J., Xie, B., Zhao, X., Zheng, K., et al. (2017). EGF enhances oligodendrogenesis from glial progenitor cells. *Front. Mol. Neurosci.* 10, 106. doi:10.3389/fnmol.2017.00106
- Yang, J., Cheng, X., Shen, J., Xie, B., Zhao, X., Zhang, Z., et al. (2016). A novel approach for amplification and purification of mouse oligodendrocyte progenitor cells. *Front. Cell. Neurosci.* 10, 203. doi:10.3389/fncel.2016.00203
- Yang, J., Fu, Z., Zhang, X., Xiong, M., Meng, L., and Zhang, Z. (2020). TREM2 ectodomain and its soluble form in Alzheimer's disease. *J. Neuroinflammation* 17 (1), 204. doi:10.1186/s12974-020-01878-2
- Yang, L., Li, Z., Liu, G., Li, X., and Yang, Z. (2022). Developmental origins of human cortical oligodendrocytes and astrocytes. *Neurosci. Bull.* 38 (1), 47–68. doi:10.1007/s12264-021-00759-9
- Yanuck, S. F. (2019). Microglial phagocytosis of neurons: Diminishing neuronal loss in traumatic, infectious, inflammatory, and autoimmune CNS disorders. *Front. Psychiatry* 10, 712. doi:10.3389/fpsyt.2019.00712
- Yekula, A., Yekula, A., Muralidharan, K., Kang, K., Carter, B. S., and Balaj, L. (2019). Extracellular vesicles in glioblastoma tumor microenvironment. *Front. Immunol.* 10, 3137. doi:10.3389/fimmu.2019.03137
- Yildirim, K., Petri, J., Kottmeier, R., and Klämbt, C. (2019). *Drosophila* glia: Few cell types and many conserved functions. *Glia* 67 (1), 5–26. doi:10.1002/glia.23459
- Yin, G., Du, M., Li, R., Li, K., Huang, X., Duan, D., et al. (2018). Glia maturation factor beta is required for reactive gliosis after traumatic brain injury in zebrafish. *Exp. Neurol.* 305, 129–138. doi:10.1016/j.expneurol.2018.04.008
- Yin, L., Zhao, F., Sun, H., Wang, Z., Huang, Y., Zhu, W., et al. (2020). CRISPR-Cas13a inhibits HIV-1 infection. *Mol. Ther. Nucleic Acids* 21, 147–155. doi:10.1016/j.omtn.2020.05.030
- Yuan, T., York, J. R., and McCauley, D. W. (2018). Gliogenesis in lampreys shares gene regulatory interactions with oligodendrocyte development in jawed vertebrates. *Dev. Biol.* 441 (1), 176–190. doi:10.1016/j.ydbio.2018.07.002
- Zhou, H., Su, J., Hu, X., Zhou, C., Li, H., Chen, Z., et al. (2020). Glia-to-Neuron conversion by CRISPR-CasRx alleviates symptoms of neurological disease in mice. *Cell* 181 (3), 590–603.e16. e516. doi:10.1016/j.cell.2020.03.024
- Zuchero, J. B., and Barres, B. A. (2015). Glia in mammalian development and disease. *Development* 142 (22), 3805–3809. doi:10.1242/dev.129304



OPEN ACCESS

EDITED BY

Juan Rafael Riesgo-Escovar,
Universidad Nacional Autónoma
de México, Mexico

REVIEWED BY

Ariel Ávila,
Universidad Católica de la Santísima
Concepción, Chile
Giovanni Morelli,
Italian Institute of Technology (IIT), Italy

*CORRESPONDENCE

Rocío Salceda
rsalceda@ifc.unam.mx

SPECIALTY SECTION

This article was submitted to
Neurodevelopment,
a section of the journal
Frontiers in Neuroscience

RECEIVED 18 May 2022

ACCEPTED 30 August 2022

PUBLISHED 16 September 2022

CITATION

Salceda R (2022) Glycine
neurotransmission: Its role
in development.
Front. Neurosci. 16:947563.
doi: 10.3389/fnins.2022.947563

COPYRIGHT

© 2022 Salceda. This is an
open-access article distributed under
the terms of the [Creative Commons
Attribution License \(CC BY\)](#). The use,
distribution or reproduction in other
forums is permitted, provided the
original author(s) and the copyright
owner(s) are credited and that the
original publication in this journal is
cited, in accordance with accepted
academic practice. No use, distribution
or reproduction is permitted which
does not comply with these terms.

Glycine neurotransmission: Its role in development

Rocío Salceda*

Departamento de Neurodesarrollo y Fisiología, Instituto de Fisiología Celular, Universidad Nacional Autónoma de México, Juriquilla, Mexico

The accurate function of the central nervous system (CNS) depends of the consonance of multiple genetic programs and external signals during the ontogenesis. A variety of molecules including neurotransmitters, have been implied in the regulation of proliferation, survival, and cell-fate of neurons and glial cells. Among these, neurotransmitters may play a central role since functional ligand-gated ionic channel receptors have been described before the establishment of synapses. This review argues on the function of glycine during development, and show evidence indicating it regulates morphogenetic events by means of their transporters and receptors, emphasizing the role of glycinergic activity in the balance of excitatory and inhibitory signals during development. Understanding the mechanisms involved in these processes would help us to know the etiology of cognitive dysfunctions and lead to improve brain repair strategies.

KEYWORDS

glycine, glycine receptor, development, neurotransmission, GlyR isoforms

Introduction

The central nervous system (CNS) development is a long process that starts early during embryogenesis and takes years to be completed in humans. The initial steps involve precise coordination of cell proliferation, differentiation, and cell migration. A tight control of these processes is achieved by integration of the intrinsic genetic program with the extracellular signals present in the environment (Platel et al., 2010; Caronia-Brown and Grove, 2011; Káradóttir and Kuo, 2018; Ali and von Gall, 2022). Many factors have been identified as regulators of neurogenesis; among these, extracellular molecules, neurotransmitters, and their receptors have been found to be present in the developing brain well before synaptogenesis occurs (Casanova and Trippe, 2006; Metzger, 2010; Carulli and Verhaagen, 2021), suggesting that they could mediate signaling unrelated to classical neurotransmission.

Early neurotransmitter signaling has been implicated in a range of developmental processes, such as differentiation, migration, neurite outgrowth, axon pathfinding,

synaptogenesis, and survival of nascent neurons (Nguyen et al., 2002; Heng et al., 2007; Platel et al., 2010; Spitzer, 2012). The inhibitory neurotransmitter, glycine and its receptors are not only present but also functional in the developing brain before synaptogenesis occurs, suggesting their involvement in development (Chalpin and Saha, 2010).

Adult glycinergic neurotransmission

In addition to its role in cell metabolism, being the structurally simplest amino acid, glycine, acting through ionotropic receptors, also serves as an important and widely distributed inhibitory neurotransmitter that is most prominently expressed in adult brainstem, spinal cord, and retina of animals from several phyla (Aprison and Werman, 1965; Werman et al., 1968).

The biosynthesis of glycine for its use in neurotransmission is mediated by the serine hydroxymethyl transferase, which uses pyridoxal phosphate and tetra hydrofolate as cofactors of the reaction. In nervous system, glycine is also synthesized by the glycine synthase (glycine cleavage, GCS) enzyme, which catalyzes a readily reversible reaction between carbon dioxide, ammonium ion, N5- N10-methylene tetrahydrofolate, NADH and a proton to produce glycine, tetrahydrofolate and NAD⁺ (Daly and Aprison, 1974). Immunohistochemistry and *in situ* hybridization studies in rats revealed that the glycine cleavage enzyme is also expressed in embryonic neural stem/progenitor cells, neuroepithelial cells, and astrocytes (Ichinohe et al., 2004).

Glycinergic transmission requires of high-affinity specific transporters GlyT1 and GlyT2 for the reuptake of glycine from the synaptic cleft into cells. These proteins are members of the Na⁺/Cl⁻ dependent neurotransmitter transporter family, with GlyT1 expressed predominantly in glial cells and GlyT2 by neurons (Zafra and Giménez, 2008; Eulenburg and Gomez, 2010). In addition to glycinergic transmission, GlyT1 can modulate glutamatergic neurotransmission through NMDA receptors, supporting its role in brain function and in various diseases (Marques et al., 2020).

Glycine action is mediated by a strychnine-sensitive ligand gated chloride channel glycine receptor (GlyR), which belongs to the cys-loop ligand-gated ion channel superfamily that are composed of five protein subunits that form homomeric or heteromeric pentamers assemble around a central ion-conducting pore (Langosch et al., 1988; Schmieden et al., 1992; Betz et al., 1993; Lynch, 2004). GlyRs are anchored postsynaptically by gephyrin, which binds to the β receptor subunit and tubulin, resulting in the receptor clustering (Feng et al., 1998; Kneussel and Betz, 2000). Four α subunits (1–4) and one β subunit have been characterized to date, with a stoichiometry reported first as 3 α /2 β (Becker et al., 1988; Kuhse et al., 1993; Burzomato et al., 2003; Durisic et al., 2012) and later

as 2 α /3 β (Grudzinska et al., 2005); although an stoichiometry of 4 α /1 β was recently reported (Yu et al., 2021; Zhu and Gouaux, 2021). The α 2 subunit is expressed in the immature spinal cord, which switches to α 1 in the adult, where the α 1 and α 3 subunits are expressed. In the adult brain the α 1 and α 3 subunits are mainly expressed; α 4 has been demonstrated in mouse, chick and zebrafish, being a pseudogene in humans (Becker et al., 1988; Betz et al., 1993; Lynch, 2004). The adult retina expresses the four α subunits (Grünert, 2000; Haverkamp et al., 2004; Heinze et al., 2007; Sánchez-Chávez et al., 2017).

Role of glycine during nervous system development

A variety of studies have focused to characterize the developmental expression of the glycine receptor and transporters as well as glycine immunoreactivity as means to recognize the process whereby cells adopt a glycinergic phenotype.

Glycine levels

In cortical neuroepithelium, levels of glycine increase by twofold during embryogenesis, reach a peak around birth, and gradually decrease to about 60% during the first 2 weeks of postnatal development, time in which the GSC enzyme is highly expressed (Ichinohe et al., 2004).

In rodents, glycinergic neurons tend to appear during embryonic development in the rostral spinal cord, followed by increased expression caudally in the spinal cord and rostrally into the hindbrain, midbrain and retina (Van Den Pol and Gorcs, 1988; Allain et al., 2006). In the mice spinal cord, glycine immunoreactivity was found from E11.5 to E15.5 (Scain et al., 2010). Also, glycine immunoreactivity occurs in the inner retina since P1, and by P3-P5 in the outer retina; adult expression was found at P11 (Fletcher and Kalloniatis, 1997; Sharma et al., 2003).

Glycine immunoreactivity has also been examined in zebra fish (Moly et al., 2014), and chick embryos with positive staining, first observed at E8 in the dorsal and ventral spinal cord (Berki et al., 1995). In *Xenopus laevis* the first glycine positive cells appear in the rostral spinal cord and caudal hindbrain at stage 22, a few hours after the neural tube closes (Roberts et al., 1988).

Glycine uptake

Glycine transporters appear early during embryonic brain development in rats. GlyT1 is predominant in the embryonic cortex and can be detected in radial glial cells (Jursky and Nelson, 1996).

Immunoreactivity for GlyT 1 and GlyT 2 glycine transporters was first observed at E10–12 in the midbrain floor plate. By E17, GlyT 1 expression is evident at the borders between the thalamus and hypothalamus, as well as at the border of the dorsal thalamus. GlyT 2 staining increases in the ventral spinal cord at E14 and in several brain regions at E17 (Jursky and Nelson, 1995; Lall et al., 2012). *In situ* hybridization studies in the zebra fish revealed the expression of GlyT1 and GlyT 2 in the rostral spinal cord at 18 and 20-h post-fertilization (Ganser and Dallman, 2009). Expression studies in *Xenopus laevis* showed the appearance of GlyT1 first in the proliferative ventricular layer of the hindbrain and the anterior spinal cord during early tail bud stages (stage 24) (Wester et al., 2008). In rat retina, pharmacological studies revealed the presence of both GlyT1 and GlyT 2 before final synaptogenesis has occurred (Salceda, 2006).

The role of GlyT 1 in glycine signaling was proved in E12.5 spinal cord cells, in which the decay rate of glycine current was increased by the presence of the GlyT 1 ALX-5407 inhibitor (Scain et al., 2010).

On the other hand, development of neurons in different regions of the brain is controlled by transcription factors. In this context, the expression of Ptf1a, Lbx1 and Pax2 transcription factors was described to be necessary for the expression of glycinergic phenotype in the spinal cord. Ptf1a, Lbx1, and Pax2 coordinate glycinergic and peptidergic transmitter phenotypes in dorsal spinal inhibitory neurons (Huang et al., 2008). Even more, transcription of GlyT 2 is activated by Pax2 (Batista and Lewis, 2008).

Glycine receptors

During development, the GlyRs properties undergo molecular changes resulting in modifications of their physiological function; however, biochemical and molecular cloning studies have indicated heterogeneity of GlyRs subunits during development (Aguayo et al., 2004; Avila et al., 2013a).

Immunostaining for the $\alpha 1$ subunit is first seen in the rat spinal cord at E14, after which time the mRNA levels gradually increase in the ventral and dorsal horns until leveling off at P15. In the brain, $\alpha 1$ is detected at near adult levels by P5. The $\alpha 2$ subunit is expressed since E15 in the telencephalon, diencephalon, midbrain and cortex, and remains through early postnatal stages (P5) (Malosio et al., 1991; Watanabe and Akagi, 1995).

GlyRs $\alpha 2$ -homomers, are found throughout the CNS during development and its expression markedly decreases after birth (Watanabe and Akagi, 1995), switching for the expression of the adult, $\alpha 1\beta$ heteromer (Lynch, 2004). The GlyRs subunit, $\alpha 3$, is observed until relatively late in development (P5), but it remains throughout life. The β subunit of GlyRs is first expressed

at E14 in both the telencephalon and the ventral and dorsal horns of the spinal cord.

The postnatal rat retina shows GlyRs expression in the neuroblastic layer, while GlyR in the adults is only observed in the inner nuclear layer (INL) (Sassoè-Pognetto and Wässle, 1997). GlyR $\alpha 2$ subunit was found to be expressed in retinal progenitor cells at birth (Young and Cepko, 2004). Besides, a continuing increase of mRNA and protein expression of $\alpha 1$, $\alpha 3$, $\alpha 4$, and β subunits was found during postnatal retinal development, while $\alpha 2$ showed high levels in developing and adult retina (Sánchez-Chávez et al., 2017).

GlyRs are not only present during development but also functional. Whole-cell patch clamp motoneurons recordings in embryonic spinal cord show the first synaptic activity at E12.5; and demonstrate that radial cells release glycine, being the main source of it in the embryonic spinal cord (Scain et al., 2010). Likewise glycine elicited currents in different zones of the embryonic cortex were demonstrated at E19 (Flint et al., 1998). Moreover, it was shown that glycine application triggers a massive calcium influx in the upper-layer of pyramidal neurons at E17, effect that was blocked by strychnine and absent in the GlyR-knockout animals (Young-Pearse et al., 2006).

The expression of functional $\alpha 2$ -containing GlyRs in cortical progenitors was demonstrated by whole-cell patch clamp recordings, where application of glycine triggered fast-activating currents. Moreover, *Gla2*-knockout mice show a reduced number of excitatory projection neurons in deep and upper layers of the cortex, leading to a modest reduction in brain size (Avila et al., 2013b, 2014; Ávila et al., 2020).

Glycine signaling

It is noteworthy that during development, glycine undergoes modifications of its kinetics and pharmacological properties (Aguayo et al., 2004). While glycine is an inhibitor neurotransmitter in the adult, it is excitatory in immature tissues (Rivera et al., 1999; Kandler et al., 2002; Kilb et al., 2002).

During development, chloride gradients change according to the expression of chloride transporters (Watanabe and Fukuda, 2015). In embryonic neurons, the sodium-potassium-chloride co-transporter (NKCC1) increases the intracellular concentration of chloride, then glycine binding to GlyRs causes a release of chloride ions and, therefore, induces a depolarization of the cell (Avila et al., 2014; Theisen et al., 2018). The switch from excitation to inhibition originates through the expression of the neural-specific potassium-chloride co-transporter 2 (KCC2), which actively reduces the intracellular concentration of chloride, transforming the opening of a chloride channel into a hyperpolarizing stimulus (Blaesse et al., 2006; Reynolds et al., 2008; Gonzalez-Islas et al., 2009; Liu and Wong-Riley, 2012). In other way, blocking GlyRs by strychnine decrease expression

of KCC2 in ventral spinal networks without interfering with NKCC1; in addition, blockage of GlyRs led to decrease of KCC2 at the cell membrane (Allain et al., 2016), suggesting that glycine modulates KCC2.

In consequence, GlyRs activation during embryonic and early postnatal development induces a depolarization of the cell membrane (Flint et al., 1998; Kilb et al., 2002, 2008) which in turn may activate calcium influx (Platel et al., 2005). In fact, this depolarization activates voltage-sensitive sodium channels that subsequently activate sodium-sensitive calcium transporters, leading to the increase in intracellular calcium, which in turn may induce the release of glutamate (Kullmann et al., 2002; Platel et al., 2005; Brustein et al., 2013). In accordance with that, it was shown that applying glycine triggers a calcium influx in pyramidal and cortical neurons at E17 and E13, respectively (Platel et al., 2005). This effect was blocked by strychnine and disappears in the GlyR-knockout (KO) animals (Jimmy Zhou, 2001; Young-Pearse et al., 2006), supporting the specific effect of glycine through GlyRs.

Excitatory postsynaptic potentials produced by glycine have been observed since fetal to P7 in gerbils and rats. During this period neuronal growth occurs as well as the establishment of dendritic arbors (Sanes and Friauf, 2000). Glycinergic neurotransmission has been shown to influence neural maturation via modulating intracellular Ca^{+2} concentrations in the respiratory brainstem nuclei, hippocampus, and the lateral superior olive of the auditory system (Ben-Ari, 2001, 2013; Soria and Valdeolmillos, 2002; Ávila et al., 2020). In this regard, growing evidence is connecting the glycine induced depolarization with lateral superior olive (LSO) network maturation via modulating intracellular Ca^{+2} concentrations (Malenka and Nicoll, 1993; Sanes and Friauf, 2000; Kandler et al., 2002).

Similarly, the blockage of glycinergic transmission since the beginning of development by either embryonic glycine receptor knockdown (McDermid et al., 2006), reversing the depolarizing chloride gradient by over expression of human KCC2 (Reynolds et al., 2008; Schwale et al., 2016), or by blocking GlyRs with strychnine (Côté and Drapeau, 2012) resulted in a selective reduction in the interneuron population with minimal changes in motoneurons and spinal sensory neuron populations.

This excitatory effect of glycine during embryonic development appears to be necessary for a broad range of neurogenic processes including formation and maturation of neuronal circuits (Ben-Ari, 2001; Ávila et al., 2020). Evidence indicate that GlyR $\alpha 2$ subunits are involved in the regulation of interneuron differentiation during spinal cord development (McDermid et al., 2006) and synaptogenesis (Avila et al., 2013a,b; Lin et al., 2017; Ávila et al., 2020).

The role of glycinergic neurotransmission in the optimal balance of excitatory and inhibitory synaptic inputs during development is highlighted by the increase in dendritic arbors

and dendritic spines found in motoneurons from gephyrin-deficient mice. These increases were associated with an increase of excitatory synaptic neurotransmission and a decrease of inhibitory neurotransmission (Banks et al., 2005; Fogarty et al., 2016). Also, it was demonstrated that GlyR $\alpha 2$ is needed for correct maturation and function of the glutamatergic striatum medium spiny neurons (Comhair et al., 2018).

In spite of that, glycine levels in the nervous tissue are assumed to be too low to allow normal neurotransmission during development (Van Den Pol and Gorcs, 1988; Zafra and Giménez, 2008) and it is hypothesized that the amino-sulfonic acid taurine, a partial agonist of GlyRs (Schmieden et al., 1992; Hussy et al., 1997; Mori et al., 2002; Jiang et al., 2004) may act as a ligand for the receptor. Supporting this hypothesis, it was shown that taurine function as a ligand for GlyR via non-synaptic signaling in the early neocortex (Flint et al., 1998). However, although the concentration of taurine progressively increases during embryogenesis and its levels are 10–20-fold higher than the levels of glycine and GABA (Benítez-Díaz et al., 2003), GlyRs in the developing cortex are 10 times less sensitive to taurine (Schmieden et al., 1992; Hussy et al., 1997; Okabe et al., 2004), strongly suggesting that glycine is acting on its own receptors.

On the other hand, glycine transporters may well play an important role controlling the extracellular level of glycine through GlyT1. In fact, it has been proposed that this could be the primarily role of GlyT1 during the spinal cord development, where this transporter is active in the removal of glycine from the extracellular compartment in extra synaptic locations (Gomez et al., 2003).

In addition, glycine concentrations are influenced by the GCS that catalyzes the degradation of glycine and provides the developing brain with other metabolites, such as 5,10-methylenetetrahydrofolate, which is essential for DNA synthesis (Ichinohe et al., 2004).

Role of glycine in cell proliferation and specification

Pioneering studies in the immature retina revealed a glycinergic transmission role in directing the proliferation of rod photoreceptor cells as well as in the light-dependent maturation of retinal ganglion and bipolar cells. Outstanding, overexpression of the $\alpha 2$ GlyR subunit leads to the development of a high percentage of rod photoreceptors at the expense of Muller glial cells (Young and Cepko, 2004).

Similarly, knockout of the $\alpha 2$ subunit at the onset of development reduces the number as well as the differentiation of spinal interneurons, thus affecting the formation of rhythm-generating networks (McDermid et al., 2006). Moreover, $\alpha 2$ -GlyRs were found to control the proliferation of progenitor cells

during corticogenesis (Avila et al., 2014) and to promote the migration of cortical interneurons (Avila et al., 2013b).

Cells may be differentially affected depending on the type of GlyR subunit expressed as well as the cell type at different places compared to migrating interneurons (Ávila et al., 2020). In this context, glial cells can modulate neurotransmission by secretion of soluble factors; in fact, microglia secrete glycine and enhance NMDA receptor-mediated responses (Hayashi and Nakanishi, 2013).

Although glia are non-excitabile, they express many of the same receptors for neurotransmitters, and these can induce membrane depolarization, increase in intracellular calcium, and proliferation (Domingues et al., 2010); indeed, GlyRs can modulate action potential conduction in white matter (Constantinou and Fern, 2009). Therefore, glial cells may also through these receptors modulate synaptic development.

Remarkably, glycine has been showed to be related to the rapid cancer cell proliferation and could reverse the expression of aging phenotypes. This effect is thought to be related to glycine metabolism (Pan et al., 2021); glycine biosynthesis enzymes are more highly expressed in proliferating cells, where they are incorporated in purine nucleotides. In addition, depleting extracellular glycine or knocking down the SHMT2 glycine-synthesizing enzyme blocked rapid proliferation by prolonging the G1 phase of the cell cycle (Nguyen et al., 2002; Yang et al., 2018). Besides, $\alpha 1$ and $\alpha 3$ GlyR subunits were found to be expressed in human brain tumor biopsies (Förster et al., 2014). Moreover, knockdown of $\alpha 1$ GlyR protein expression impaired the self-renewal capacity and tumorigenicity of GL261 glioma cells (Förster et al., 2014), supporting a non-synaptic role of GlyRs. In this respect, outstandingly, $\alpha 1$ and $\alpha 3$ GlyR subunits were found to contain a nuclear localization signal in the large cytosolic loop domain (Melzer et al., 2010).

In addition, two inhibitors of the Wnt pathway (WIF1 and DKK1B) were upregulated upon GlyRs knockdown in neural stem cells (NSCs), suggesting that a Wnt-dependent neurogenic process could be silenced in NSCs when glycine signaling is impaired (Samarut et al., 2016, 2019). Moreover, the P53 tumor suppressor protein was upregulated upon GlyR knockdown, suggesting that cells might die in the absence of glycine signaling. Similarly, the activation of the Hedgehog signaling pathway reduces GlyT 2 expression *in vitro* in rodent primary spinal cord neurons or *in vivo* in zebrafish embryos (de la Rocha-Muñoz et al., 2021). These results define a link between development signaling pathways and glycine action.

Pathophysiological consequences of glycinergic action during development

There is considerable evidence supporting the role of glycine on the CNS development. GlyRs are expressed in dorsal

progenitors and migratory neurons, contributing to the cell cycle control, cell migration and morphological development (Tapia et al., 2000, 2001; Nimmervoll et al., 2011; Avila et al., 2013b; Avila et al., 2014), which impairs the formation of cortical circuits (Morelli et al., 2017). Therefore, the lack of GlyRs may affect the development process, including circuit formation that may lead to different disorders in adulthood (Ruediger and Bolz, 2007).

Indeed, defects in glycinergic signaling during neural development can result in the neurological motor disorders hyperekplexia, hypertonia, and episodic neonatal apnea (Lewis et al., 1998; Lape et al., 2012; Bode and Lynch, 2013). The hyperekplexia-causing mutations in *GLRA1* and *GLRB* result either in disrupted surface expression or altered glycine efficacy (Bode and Lynch, 2013).

Likewise, mutations in genes either encoding GlyRs (Piton et al., 2013; Pilorge et al., 2016), KCC2 (Merner et al., 2015), or the amino methyltransferase enzyme (AMT) involved in glycine degradation (Yu et al., 2013), were reported in patients affected by autism, supporting the glycine role in neurogenesis. Furthermore, recently Chen et al. (2022) using a combination of molecular modeling and electrophysiology recordings for four novel missense variants in *GLRA2* associated with autism spectrum disorder (ASD), identified *GLRA2* as the cause of autism spectrum neurodevelopmental phenotypes. The missense variants cause either loss, gain or altered function of GlyR $\alpha 2$ subunit, enlightening the clinical forms associated with human ASD (Chen et al., 2022).

Similarly, failure in GCS activity leads to serious malformations, such as agenesis of the corpus callosum, gyral malformation, and cerebellar hypoplasia. Moreover, alternative splicing variants of GlyRs have been detected in patients suffering from temporal lobe epilepsy (Eichler et al., 2008). Also, *GLRA2* knockout mice showed disruption of the excitation/inhibition balance, resulting in enhanced susceptibility to epileptic seizures (Morelli et al., 2017). Remarkably, pharmacological inhibition of GlyR $\alpha 2$ decreased the proliferation of hippocampal adult NSCs, and its genetic deletion leads to impaired and spatial memory in the adult mice (Lin et al., 2017).

Furthermore, the $\alpha 4$ subunit and the β subunit were recently found to be expressed in mouse embryos, where were implicated in the regulation of embryo implantation (Nishizono et al., 2020).

Conclusion

CNS development involved precise coordination of cell proliferation, differentiation and cell migration; in

addition to an intrinsic genetic program, these processes are controlled by extracellular signals. Among these, neurotransmitters have been found to have an important role. In the adulthood, glycinergic neurotransmission is limited to the spinal cord, retina and few brain areas; however, functional GlyRs have been found almost everywhere in the developing brain.

Moreover a variety of evidence strongly support a relevant role of glycine signaling during development; even more, alterations in this signaling has been associated to pathologies in the adulthood (Eichler et al., 2008; Bode and Lynch, 2013; Piton et al., 2013; Pilorge et al., 2016; Morelli et al., 2017; Chen et al., 2022) supporting glycinergic function in proliferation and cell specification and circuit formation. Though, few studies have been carried out to analyze the mechanisms involved. Although these findings should be extended, they open new insights to understand the role of glycine during early neural development and its role in different pathologies, information which will improve adult brain healing.

Author contributions

The author confirms being the sole contributor of this work and has approved it for publication.

References

- Aguayo, L. G., Van Zundert, B., Tapia, J. C., Carrasco, M. A., and Alvarez, F. J. (2004). Changes on the properties of glycine receptors during neuronal development. *Brain Res. Brain Res. Rev.* 47, 33–45. doi: 10.1016/j.brainresrev.2004.06.007
- Ali, A. A. H., and von Gall, C. (2022). Adult neurogenesis under control of the circadian system. *Cells* 11:764. doi: 10.3390/cells11050764
- Allain, A. E., Baïri, A., Meyrand, P., and Branchereau, P. (2006). Expression of the glycinergic system during the course of embryonic development in the mouse spinal cord and its co-localization with GABA immunoreactivity. *J. Comp. Neurol.* 496, 832–846. doi: 10.1002/cne.20967
- Allain, A. E., Cazenave, W., Delpy, A., Exertier, P., Barthe, C., Meyrand, P., et al. (2016). Nonsynaptic glycine release is involved in the early KCC2 expression. *Dev. Neurobiol.* 76, 764–779. doi: 10.1002/dneu.22358
- Aprison, M. H., and Werman, R. (1965). The distribution of glycine in cat spinal cord and roots. *Life Sci.* 4, 2075–2083. doi: 10.1016/0024-3205(65)90325-5
- Avila, A., Nguyen, L., and Rigo, J. M. (2013a). Glycine receptors and brain development. *Front. Cell. Neurosci.* 7:184. doi: 10.3389/fncel.2013.00184
- Avila, A., Vidal, P. M., Dear, T. N., Harvey, R. J., Rigo, J. M., and Nguyen, L. (2013b). Glycine receptor $\alpha 2$ subunit activation promotes cortical interneuron migration. *Cell Rep.* 4, 738–750. doi: 10.1016/j.celrep.2013.07.016
- Avila, A., Vidal, P. M., Tielens, S., Morelli, G., Laguesse, S., Harvey, R. J., et al. (2014). Glycine receptors control the generation of projection neurons in the developing cerebral cortex. *Cell Death Dif.* 21, 1696–1708. doi: 10.1038/cdd.2014.75
- Ávila, D., Aedo, E., Sánchez-Hechavarria, M., Ávila, C., and Ávila, A. (2020). Glycine receptor inhibition differentially affect selected neuronal populations of the developing embryonic cortex, as evidenced by the analysis of spontaneous calcium oscillations. *Int. J. Mol. Sci.* 21, 1–14. doi: 10.3390/ijms21218013
- Banks, G. B., Kanjhan, R., Wiese, S., Kneussel, M., Wong, L. M., O'Sullivan, G., et al. (2005). Glycinergic and GABAergic synaptic activity differentially regulate motoneuron survival and skeletal muscle innervation. *J. Neurosci.* 25, 1249–1259. doi: 10.1523/JNEUROSCI.1786-04.2005
- Batista, M. F., and Lewis, K. E. (2008). Pax2/8 act redundantly to specify glycinergic and GABAergic fates of multiple spinal interneurons. *Dev. Biol.* 323, 88–97. doi: 10.1016/j.ydbio.2008.08.009
- Becker, C. M., Hoch, W., and Betz, H. (1988). Glycine receptor heterogeneity in rat spinal cord during postnatal development. *EMBO J.* 7, 3717–3726. doi: 10.1002/j.1460-2075.1988.tb03255.x
- Ben-Ari, Y. (2001). Developing networks play a similar melody. *Trends Neurosci.* 24, 353–360. doi: 10.1016/S0166-2236(00)01813-0
- Ben-Ari, Y. (2013). The developing cortex. *Handb. Clin. Neurol.* 111, 417–426. doi: 10.1016/B978-0-444-52891-9.00045-2
- Benítez-Díaz, P., Miranda-Contreras, L., Mendoza-Briceño, R. V., Peña-Contreras, Z., and Palacios-Prü, E. (2003). Prenatal and postnatal contents of amino acid neurotransmitters in mouse parietal cortex. *Dev. Neurosci.* 25, 366–374. doi: 10.1159/000073514
- Berki, Á.C., O'Donovan, M. J., and Antal, M. (1995). Developmental expression of glycine immunoreactivity and its colocalization with gaba in the embryonic chick lumbosacral spinal cord. *J. Comp. Neurol.* 362, 583–596. doi: 10.1002/cne.903620411
- Betz, H., Langosch, D., Rundström, N., Bormann, J., Kuryatov, A., Kuhse, J., et al. (1993). Structure and biology of inhibitory glycine receptors. *Ann. N.Y. Acad. Sci.* 707, 109–115. doi: 10.1111/j.1749-6632.1993.tb38046.x
- Blaesse, P., Guillemain, I., Schindler, J., Schweizer, M., Delpire, E., Khiroug, L., et al. (2006). Oligomerization of KCC2 correlates with development of inhibitory neurotransmission. *J. Neurosci.* 26, 10407–10419. doi: 10.1523/JNEUROSCI.3257-06.2006

Acknowledgments

The author want to thank Gustavo Sánchez-Chávez and Miguel A. Velázquez-Flores for comments and editing the text. The author recognize DGAPA/PAPIIT-UNAM project IN203520.

Conflict of interest

The author declares that the research was conducted in the absence of any commercial or financial relationships that could be construed as a potential conflict of interest.

The handling editor JR-E declared a past collaboration with the author.

Publisher's note

All claims expressed in this article are solely those of the authors and do not necessarily represent those of their affiliated organizations, or those of the publisher, the editors and the reviewers. Any product that may be evaluated in this article, or claim that may be made by its manufacturer, is not guaranteed or endorsed by the publisher.

- Bode, A., and Lynch, J. W. (2013). Analysis of hyperekplexia mutations identifies transmembrane domain rearrangements that mediate glycine receptor activation. *J. Biol. Chem.* 288, 33760–33771. doi: 10.1074/jbc.M113.513804
- Brustein, E., Côté, S., Ghislain, J., and Drapeau, P. (2013). Spontaneous glycine-induced calcium transients in spinal cord progenitors promote neurogenesis. *Dev. Neurobiol.* 73, 168–175. doi: 10.1002/dneu.22050
- Burzomato, V., Groot-Kormelink, P. J., Sivilotti, L. G., and Beato, M. (2003). Stoichiometry of recombinant heteromeric glycine receptors revealed by a pore-lining region point mutation. *Recept. Channels* 9, 353–361. doi: 10.3109/174041016
- Caronia-Brown, G., and Grove, E. A. (2011). Timing of cortical interneuron migration is influenced by the cortical hem. *Cereb. Cortex* 21, 748–755. doi: 10.1093/cercor/bhq142
- Carulli, D., and Verhaagen, J. (2021). An extracellular perspective on cns maturation: Perineuronal nets and the control of plasticity. *Int. J. Mol. Sci.* 22, 1–26. doi: 10.3390/ijms22052434
- Casanova, M. F., and Trippe, J. (2006). Regulatory mechanisms of cortical laminar development. *Brain Res. Rev.* 51, 72–84. doi: 10.1016/j.brainresrev.2005.10.002
- Chalpin, A. V., and Saha, M. S. (2010). The specification of glycinergic neurons and the role of glycinergic transmission in development. *Front. Mol. Neurosci.* 3:11. doi: 10.3389/fnmol.2010.00011
- Chen, X., Wilson, K. A., Schaefer, N., De Hayr, L., Windsor, M., Scalais, E., et al. (2022). Loss, gain and altered function of GlyR $\alpha 2$ subunit mutations in neurodevelopmental disorders. *Front. Mol. Neurosci.* 15:886729. doi: 10.3389/fnmol.2022.886729
- Comhair, J., Devoght, J., Morelli, G., Harvey, R. J., Briz, V., Borrie, S. C., et al. (2018). Alpha2-containing glycine receptors promote neonatal spontaneous activity of striatal medium spiny neurons and support maturation of glutamatergic inputs. *Front. Mol. Neurosci.* 11:380. doi: 10.3389/fnmol.2018.0380
- Constantinou, S., and Fern, R. (2009). Conduction block and glial injury induced in developing central white matter by glycine, GABA, noradrenalin, or nicotine, studied in isolated neonatal rat optic nerve. *Glia* 57, 1168–1177. doi: 10.1002/glia.20839
- Côté, S., and Drapeau, P. (2012). Regulation of spinal interneuron differentiation by the paracrine action of glycine. *Dev. Neurobiol.* 72, 208–214. doi: 10.1002/dneu.20972
- Daly, E. C., and Aprison, M. H. (1974). Distribution of serine Hydroxymethyltransferase and glycine transaminase in several areas of the central nervous system of the rat. *J. Neurochem.* 22, 877–885. doi: 10.1111/j.1471-4159.1974.tb04312.x
- de la Rocha-Muñoz, A., Núñez, E., Vishwanath, A. A., Gómez-López, S., Dhanasobhon, D., Rebola, N., et al. (2021). The presynaptic glycine transporter GlyT2 is regulated by the Hedgehog pathway in vitro and in vivo. *Commun. Biol.* 4, 1–10. doi: 10.1038/s42003-021-02718-6
- Domingues, A. M., de, J., Taylor, M., and Fern, R. (2010). Glia as transmitter sources and sensors in health and disease. *Neurochem. Int.* 57, 359–366. doi: 10.1016/j.neuint.2010.03.024
- Durisic, N., Godin, A. G., Wever, C. M., Heyes, C. D., Lakadamyali, M., and Dent, J. A. (2012). Stoichiometry of the human glycine receptor revealed by direct subunit counting. *J. Neurosci.* 32, 12915–12920. doi: 10.1523/JNEUROSCI.2050-12.2012
- Eichler, S. A., Kirischuk, S., Jüttner, R., Schafermeier, P. K., Legendre, P., Lehmann, T. N., et al. (2008). Glycinergic tonic inhibition of hippocampal neurons with depolarizing GABAergic transmission elicits histopathological signs of temporal lobe epilepsy. *J. Cell. Mol. Med.* 12, 2848–2866. doi: 10.1111/j.1582-4934.2008.00357.x
- Eulenburg, V., and Gomez, J. (2010). Neurotransmitter transporters expressed in glial cells as regulators of synapse function. *Brain Res. Rev.* 63, 103–112. doi: 10.1016/j.brainresrev.2010.01.003
- Feng, G., Tintrup, H., Kirsch, J., Nichol, M. C., Kuhse, J., Betz, H., et al. (1998). Dual requirement for gephyrin in glycine receptor clustering and molybdoenzyme activity. *Science* 282, 1321–1324. doi: 10.1126/science.282.5392.1321
- Fletcher, E. L., and Kalloniatis, M. (1997). Localisation of amino acid neurotransmitters during postnatal development of the rat retina. *J. Comp. Neurol.* 380, 449–471. doi: 10.1002/(SICI)1096-9861(19970421)380:4<449::AID-CNE3>3.0.CO;2-1
- Flint, A. C., Liu, X., and Kriegstein, A. R. (1998). Nonsynaptic glycine receptor activation during early neocortical development. *Neuron* 20, 43–53. doi: 10.1016/S0896-6273(00)80433-X
- Fogarty, M. J., Kanjhan, R., Bellingham, M. C., and Noakes, P. G. (2016). Glycinergic neurotransmission: A potent regulator of embryonic motor neuron dendritic morphology and synaptic plasticity. *J. Neurosci.* 36, 80–87. doi: 10.1523/JNEUROSCI.1576-15.2016
- Förstera, B., Dzaye, O. D. A., Winkelmann, A., Semtner, M., Benedetti, B., Markovic, D. S., et al. (2014). Intracellular glycine receptor function facilitates glioma formation: In vivo. *J. Cell Sci.* 127, 3687–3698. doi: 10.1242/jcs.146662
- Ganser, L. R., and Dallman, J. E. (2009). Glycinergic synapse development, plasticity, and homeostasis in zebrafish. *Front. Mol. Neurosci.* 2:30. doi: 10.3389/fnmo.02.030.2009
- Gomez, J., Hülsmann, S., Ohno, K., Eulenburg, V., Szöke, K., Richter, D., et al. (2003). Inactivation of the glycine transporter 1 gene discloses vital role of glial glycine uptake in glycinergic inhibition. *Neuron* 40, 785–796. doi: 10.1016/S0896-6273(03)00672-X
- Gonzalez-Islas, C., Chub, N., and Wenner, P. (2009). NKCC1 and AE3 appear to accumulate chloride in embryonic motoneurons. *J. Neurophysiol.* 101, 507–518. doi: 10.1152/jn.90986.2008
- Grudzinska, J., Schemm, R., Haeger, S., Nicke, A., Schmalzing, G., Betz, H., et al. (2005). The β subunit determines the ligand binding properties of synaptic glycine receptors. *Neuron* 45, 727–739. doi: 10.1016/j.neuron.2005.01.028
- Grünert, U. (2000). Distribution of GABA and glycine receptors on bipolar and ganglion cells in the mammalian retina. *Microsc. Res. Tech.* 50, 130–140. doi: 10.1002/1097-0029(20000715)50:2<130::AID-JEMT5>3.3.CO;2-9
- Haverkamp, S., Müller, U., Zeilhofer, H. U., Harvey, R. J., and Wässle, H. (2004). Diversity of glycine receptors in the mouse retina: Localization of the $\alpha 2$ subunit. *J. Comp. Neurol.* 477, 399–411. doi: 10.1002/cne.20267
- Hayashi, Y., and Nakanishi, H. (2013). Synaptic plasticity and synaptic reorganization regulated by microglia. *Japanese J. Neuropsychopharmacol.* 33, 211–216.
- Heinze, L., Harvey, R. J., Haverkamp, S., and Wässle, H. (2007). Diversity of glycine receptors in the mouse retina: Localization of the $\alpha 4$ subunit. *J. Comp. Neurol.* 500, 693–707. doi: 10.1002/cne.21201
- Heng, J. I. T., Moonen, G., and Nguyen, L. (2007). Neurotransmitters regulate cell migration in the telencephalon. *Eur. J. Neurosci.* 26, 537–546. doi: 10.1111/j.1460-9568.2007.05694.x
- Huang, M., Huang, T., Xiang, Y., Xie, Z., Chen, Y., Yan, R., et al. (2008). Ptf1a, Lbx1 and Pax2 coordinate glycinergic and peptidergic transmitter phenotypes in dorsal spinal inhibitory neurons. *Dev. Biol.* 322, 394–405. doi: 10.1016/j.ydbio.2008.06.031
- Hussy, N., Deleuze, C., Pantaloni, A., Desarménien, M. G., and Moos, F. (1997). Agonist action of taurine on glycine receptors in rat supraoptic magnocellular neurones: Possible role in osmoregulation. *J. Physiol.* 502, 609–621. doi: 10.1111/j.1469-7793.1997.609bj.x
- Ichinohe, A., Kure, S., Mikawa, S., Ueki, T., Kojima, K., Fujiwara, K., et al. (2004). Glycine cleavage system in neurogenic regions. *Eur. J. Neurosci.* 19, 2365–2370. doi: 10.1111/j.0953-816X.2004.03345.x
- Jiang, Z., Krnjević, K., Wang, F., and Ye, J. H. (2004). Taurine activates strychnine-sensitive glycine receptors in neurons freshly isolated from nucleus accumbens of young rats. *J. Neurophysiol.* 91, 248–257. doi: 10.1152/jn.00106.2003
- Jimmy Zhou, Z. (2001). A critical role of the strychnine-sensitive glycinergic system in spontaneous retinal waves of the developing rabbit. *J. Neurosci.* 21, 5158–5168. doi: 10.1523/jneurosci.21-14-05158.2001
- Jursky, F., and Nelson, N. (1995). Localization of glycine neurotransmitter transporter (GLYT2) Reveals correlation with the distribution of glycine receptor. *J. Neurochem.* 64, 1026–1033. doi: 10.1046/j.1471-4159.1995.64031026.x
- Jursky, F., and Nelson, N. (1996). Developmental expression of the glycine transporters GLYT1 and GLYT2 in mouse brain. *J. Neurochem.* 67, 336–344. doi: 10.1046/j.1471-4159.1996.67010336.x
- Kandler, K., Kullmann, P. H. M., Ene, F. A., and Kim, G. (2002). Excitatory action of an immature glycinergic/GABAergic sound localization pathway. *Physiol. Behav.* 77, 583–587. doi: 10.1016/S0031-9384(02)00905-8
- Kárádóttir, R. T., and Kuo, C. T. (2018). Neuronal activity-dependent control of postnatal neurogenesis and gliogenesis. *Ann. Rev. Neurosci.* 41, 139–161. doi: 10.1146/annurev-neuro-072116-031054
- Kilb, W., Hanganu, I. L., Okabe, A., Sava, B. A., Shimizu-Okabe, C., Fukuda, A., et al. (2008). Glycine receptors mediate excitation of subplate neurons in neonatal rat cerebral cortex. *J. Neurophysiol.* 100, 698–707. doi: 10.1152/jn.00657.2007
- Kilb, W., Ikeda, M., Uchida, K., Okabe, A., Fukuda, A., and Luhmann, H. J. (2002). Depolarizing glycine responses in Cajal-Retzius cells of neonatal rat cerebral cortex. *Neuroscience* 112, 299–307. doi: 10.1016/S0306-4522(02)00071-4

- Kneussel, M., and Betz, H. (2000). Clustering of inhibitory neurotransmitter receptors at developing postsynaptic sites: The membrane activation model. *Trends Neurosci.* 23, 429–435. doi: 10.1016/S0166-2236(00)01627-1
- Kuhse, J., Laube, B., Magalei, D., and Betz, H. (1993). Assembly of the inhibitory glycine receptor: Identification of amino acid sequence motifs governing subunit stoichiometry. *Neuron* 11, 1049–1056. doi: 10.1016/0896-6273(93)90218-G
- Kullmann, P. H. M., Ene, F. A., and Kandler, K. (2002). Glycinergic and GABAergic calcium responses in the developing lateral superior olive. *Eur. J. Neurosci.* 15, 1093–1104. doi: 10.1046/j.1460-9568.2002.01946.x
- Lall, D., Armbruster, A., Ruffert, K., Betz, H., and Eulenburg, V. (2012). Transport activities and expression patterns of glycine transporters 1 and 2 in the developing murine brain stem and spinal cord. *Biochem. Biophys. Res. Commun.* 423, 661–666. doi: 10.1016/j.bbrc.2012.06.007
- Langosch, D., Thomas, L., and Betz, H. (1988). Conserved quaternary structure of ligand-gated ion channels: The postsynaptic glycine receptor is a pentamer. *Proc. Natl. Acad. Sci. U.S.A.* 85, 7394–7398. doi: 10.1073/pnas.85.19.7394
- Lape, R., Plested, A. J. R., Moroni, M., Colquhoun, D., and Sivilotti, L. G. (2012). The $\alpha 1$ K276E startle disease mutation reveals multiple intermediate states in the gating of glycine receptors. *J. Neurosci.* 32, 1336–1352. doi: 10.1523/JNEUROSCI.4346-11.2012
- Lewis, T. M., Sivilotti, L. G., Colquhoun, D., Gardiner, R. M., Schoepfer, R., and Rees, M. (1998). Properties of human glycine receptors containing the hyperkplexia mutation $\alpha 1$ (K276E), expressed in *Xenopus* oocytes. *J. Physiol.* 507, 25–40. doi: 10.1111/j.1469-7793.1998.025bu.x
- Lin, M. S., Xiong, W. C., Li, S. J., Gong, Z., Cao, X., Kuang, X. J., et al. (2017). A2-Glycine Receptors Modulate Adult Hippocampal Neurogenesis and Spatial Memory. *Dev. Neurobiol.* 77, 1430–1441. doi: 10.1002/dneu.22549
- Liu, Q., and Wong-Riley, M. T. T. (2012). Postnatal development of Na⁺-K⁺-2Cl⁻ co-transporter 1 and K⁺-Cl⁻ co-transporter 2 immunoreactivity in multiple brain stem respiratory nuclei of the rat. *Neuroscience* 210, 1–20. doi: 10.1016/j.neuroscience.2012.03.018
- Lynch, J. W. (2004). Molecular structure and function of the glycine receptor chloride channel. *Physiol. Rev.* 84, 1051–1095. doi: 10.1152/physrev.00042.2003
- Malenka, R. C., and Nicoll, R. A. (1993). NMDA-receptor-dependent synaptic plasticity: Multiple forms and mechanisms. *Trends Neurosci.* 16, 521–527. doi: 10.1016/0166-2236(93)90197-T
- Malosio, M. L., Marqu  e-Pouey, B., Kuhse, J., and Betz, H. (1991). Widespread expression of glycine receptor subunit mRNAs in the adult and developing rat brain. *EMBO J.* 10, 2401–2409. doi: 10.1002/j.1460-2075.1991.tb07779.x
- Marques, B. L., Oliveira-Lima, O. C., Carvalho, G. A., de Almeida Chiarelli, R., Ribeiro, R. I., Parreira, R. C., et al. (2020). Neurobiology of glycine transporters: From molecules to behavior. *Neurosci. Biobehav. Rev.* 118, 97–110. doi: 10.1016/j.neubiorev.2020.07.025
- McDearmid, J. R., Liao, M., and Drapeau, P. (2006). Glycine receptors regulate interneuron differentiation during spinal network development. *Proc. Natl. Acad. Sci. U.S.A.* 103, 9679–9684. doi: 10.1073/pnas.0504871103
- Melzer, N., Villmann, C., Becker, K., Harvey, K., Harvey, R. J., Vogel, N., et al. (2010). Multifunctional basic motif in the glycine receptor intracellular domain induces subunit-specific sorting. *J. Biol. Chem.* 285, 3730–3739. doi: 10.1074/jbc.M109.030460
- Merner, N. D., Chandler, M. R., Bourassa, C., Liang, B., Khanna, A. R., Dion, P., et al. (2015). Regulatory domain or CPG site variation in SLC12A5, encoding the chloride transporter KCC2, in human autism and schizophrenia. *Front. Cell. Neurosci.* 9:386. doi: 10.3389/fncel.2015.00386
- Metzger, F. (2010). Molecular and cellular control of dendrite maturation during brain development. *Curr. Mol. Pharmacol.* 3, 1–11. doi: 10.2174/1874467211003010001
- Moly, P. K., Ikenaga, T., Kamihagi, C., Islam, A. F. M. T., and Hatta, K. (2014). Identification of initially appearing glycine-immunoreactive neurons in the embryonic zebrafish brain. *Dev. Neurobiol.* 74, 616–632. doi: 10.1002/dneu.22158
- Morelli, G., Avila, A., Ravanidis, S., Aourz, N., Neve, R. L., Smolders, I., et al. (2017). Cerebral cortical circuitry formation requires functional glycine receptors. *Cereb. Cortex* 27, 1863–1877. doi: 10.1093/cercor/bhw025
- Mori, M., G  hwiler, B. H., and Gerber, U. (2002). β -Alanine and taurine as endogenous agonists at glycine receptors in rat hippocampus in vitro. *J. Physiol.* 539, 191–200. doi: 10.1113/jphysiol.2001.013147
- Nguyen, L., Malgrange, B., Belachew, S., Rogister, B., Rocher, V., Moonen, G., et al. (2002). Functional glycine receptors are expressed by postnatal nestin-positive neural stem/progenitor cells. *Eur. J. Neurosci.* 15, 1299–1305. doi: 10.1046/j.1460-9568.2002.01966.x
- Nimmervoll, B., Denter, D. G., Sava, I., Kilb, W., and Luhmann, H. J. (2011). Glycine receptors influence radial migration in the embryonic mouse neocortex. *Neuroreport* 22, 509–513. doi: 10.1097/WNR.0b013e328348aaf6
- Nishizono, H., Darwish, M., Endo, T. A., Uno, K., Abe, H., and Yasuda, R. (2020). Glycine receptor $\alpha 4$ subunit facilitates the early embryonic development in mice. *Reproduction* 159, 41–48. doi: 10.1530/REP-19-0312
- Okabe, A., Kilb, W., Shimizu-Okabe, C., Hanganu, I. L., Fukuda, A., and Luhmann, H. J. (2004). Homogenous glycine receptor expression in cortical plate neurons and Cajal-Retzius cells of neonatal rat cerebral cortex. *Neuroscience* 123, 715–724. doi: 10.1016/j.neuroscience.2003.10.014
- Pan, S., Fan, M., Liu, Z., Li, X., and Wang, H. (2021). Serine, glycine and one-carbon metabolism in cancer (Review). *Int. J. Oncol.* 58, 158–170. doi: 10.3892/ijo.2020.5158
- Pilorge, M., Fassier, C., Le Corronc, H., Potey, A., Bai, J., De Gois, S., et al. (2016). Genetic and functional analyses demonstrate a role for abnormal glycinergic signaling in autism. *Mol. Psychiatry* 21, 936–945. doi: 10.1038/mp.2015.139
- Piton, A., Jouan, L., Rochefort, D., Dobrzyniecka, S., Lachapelle, K., Dion, P. A., et al. (2013). Analysis of the effects of rare variants on splicing identifies alterations in GABA A receptor genes in autism spectrum disorder individuals. *Eur. J. Hum. Genet.* 21, 749–756. doi: 10.1038/ejhg.2012.243
- Platel, J. C., Boisseau, S., Dupuis, A., Brocard, J., Poupard, A., Savasta, M., et al. (2005). Na⁺ channel-mediated Ca²⁺ entry leads to glutamate secretion in mouse neocortical preplate. *Proc. Natl. Acad. Sci. U.S.A.* 102, 19174–19179. doi: 10.1073/pnas.0504540102
- Platel, J. C., Stambouliau, S., Nguyen, I., and Bordey, A. (2010). Neurotransmitter signaling in postnatal neurogenesis: The first leg. *Brain Res. Rev.* 63, 60–71. doi: 10.1016/j.brainresrev.2010.02.004
- Reynolds, A., Bruste, E., Liao, M., Mercado, A., Babilonia, E., Mount, D. B., et al. (2008). Neurogenic role of the depolarizing gradient revealed by global overexpression of KCC2 from the onset of development. *J. Neurosci.* 28, 1588–1597. doi: 10.1523/JNEUROSCI.3791-07.2008
- Rivera, C., Voipio, J., Payne, J. A., Ruusuvuori, E., Lahtinen, H., Lamsa, K., et al. (1999). The K⁺/Cl⁻ co-transporter KCC2 reverses GABA hyperpolarizing during neuronal maturation. *Nature* 397, 251–255. doi: 10.1038/16697
- Roberts, A., Dale, N., Ottersen, O. P., and Storm-Mathisen, J. (1988). Development and characterization of commissural interneurons in the spinal cord of *Xenopus laevis* embryos revealed by antibodies to glycine. *Development* 103, 447–461. doi: 10.1242/dev.103.3.447
- Ruediger, T., and Bolz, J. (2007). Neurotransmitters and the development of neuronal circuits. *Adv. Exp. Med. Biol.* 621, 104–115. doi: 10.1007/978-0-387-76715-4_8
- Salceda, R. (2006). Pharmacological properties of glycine uptake in the developing rat retina. *Neurochem. Int.* 49, 342–346. doi: 10.1016/j.neuint.2006.02.006
- Samarut, E., Bekri, A., and Drapeau, P. (2016). Transcriptomic analysis of purified embryonic neural stem cells from zebrafish embryos reveals signaling pathways involved in glycine-dependent neurogenesis. *Front. Mol. Neurosci.* 9:22. doi: 10.3389/fnmol.2016.00022
- Samarut, E., Chalopin, D., Rich  , R., Allard, M., Liao, M., and Drapeau, P. (2019). Individual knock out of glycine receptor alpha subunits identifies a specific requirement of glr1a for motor function in zebrafish. *PLoS One* 14:e0216159. doi: 10.1371/journal.pone.0216159
- S  nchez-Ch  vez, G., Vel  zquez-Flores, M.   , Ruiz Esparza-Garrido, R., and Salceda, R. (2017). Glycine receptor subunits expression in the developing rat retina. *Neurochem. Int.* 108, 177–182. doi: 10.1016/j.neuint.2017.03.013
- Sanes, D. H., and Friauf, E. (2000). Development and influence of inhibition in the lateral superior olivary nucleus. *Hear. Res.* 147, 46–58. doi: 10.1016/S0378-5955(00)00119-2
- Sass  e-Pognetto, M., and W  ssle, H. (1997). Synaptogenesis in the rat retina: Subcellular localization of glycine receptors, GABA(A) receptors, and the anchoring protein gephyrin. *J. Comp. Neurol.* 381, 158–174. doi: 10.1002/(SICI)1096-9861(19970505)381:2<158::AID-CNE4<3.0.CO;2-2
- Scain, A. L., Le Corronc, H., Allain, A. E., Muller, E., Rigo, J. M., Meyrand, P., et al. (2010). Glycine release from radial cells modulates the spontaneous activity and its propagation during early spinal cord development. *J. Neurosci.* 30, 390–403. doi: 10.1523/JNEUROSCI.2115-09.2010
- Schmieden, V., Kuhse, J., and Betz, H. (1992). Agonist pharmacology of neonatal and adult glycine receptor α subunits: Identification of amino acid residues involved in taurine activation. *EMBO J.* 11, 2025–2032. doi: 10.1002/j.1460-2075.1992.tb05259.x

- Schwale, C., Schumacher, S., Bruehl, C., Titz, S., Schlicksupp, A., Kokocinska, M., et al. (2016). KCC2 knockdown impairs glycinergic synapse maturation in cultured spinal cord neurons. *Histochem. Cell Biol.* 145, 637–646. doi: 10.1007/s00418-015-1397-0
- Sharma, R. K., O'Leary, T. E., Fields, C. M., and Johnson, D. A. (2003). Development of the outer retina in the mouse. *Dev. Brain Res.* 145, 93–105. doi: 10.1016/S0165-3806(03)00217-7
- Soria, J. M., and Valdeolmillos, M. (2002). Receptor-activated calcium signals in tangentially migrating cortical cells. *Cereb. Cortex* 12, 831–839. doi: 10.1093/cercor/12.8.831
- Spitzer, N. C. (2012). Activity-dependent neurotransmitter respecification. *Nat. Rev. Neurosci.* 13, 94–106. doi: 10.1038/nrn3154
- Tapia, J. C., Cárdenas, A. M., Nualart, F., Mentis, G. Z., Navarrete, R., and Aguayo, L. G. (2000). Neurite outgrowth in developing mouse spinal cord neurons is modulated by glycine receptors. *Neuroreport* 11, 3007–3010. doi: 10.1097/00001756-200009110-00036
- Tapia, J. C., Mentis, G. Z., Navarrete, R., Nualart, F., Figueroa, E., Sánchez, A., et al. (2001). Early expression of glycine and GABA_A receptors in developing spinal cord neurons. Effects on neurite outgrowth. *Neuroscience* 108, 493–506. doi: 10.1016/S0306-4522(01)00348-7
- Theisen, U., Hey, S., Hennig, C. D., Schnabel, R., and Köster, R. W. (2018). Glycine is able to induce both a motility speed in- and decrease during zebrafish neuronal migration. *Commun. Integr. Biol.* 11, 1–7. doi: 10.1080/19420889.2018.1493324
- Van Den Pol, A. N., and Gorcs, T. (1988). Glycine and glycine receptor immunoreactivity in brain and spinal cord. *J. Neurosci.* 8, 472–492. doi: 10.1523/jneurosci.08-02-00472.1988
- Watanabe, E., and Akagi, H. (1995). Distribution patterns of mRNAs encoding glycine receptor channels in the developing rat spinal cord. *Neurosci. Res.* 23, 377–382. doi: 10.1016/0168-0102(95)00972-V
- Watanabe, M., and Fukuda, A. (2015). Development and regulation of chloride homeostasis in the central nervous system. *Front. Cell. Neurosci.* 9:371. doi: 10.3389/fncel.2015.00371
- Werman, R., Davidoff, R. A., and Aprison, M. H. (1968). Inhibitory of glycine on spinal neurons in the cat. *J. Neurophysiol.* 31, 81–95. doi: 10.1152/jn.1968.31.1.81
- Wester, M. R., Teasley, D. C., Byers, S. L., and Saha, M. S. (2008). Expression patterns of glycine transporters (xGlyT1, xGlyT2, and xVIAAT) in *Xenopus laevis* during early development. *Gene Expr. Patterns* 8, 261–270. doi: 10.1016/j.gep.2007.12.005
- Yang, X., Wang, Z., Li, X., Liu, B., Liu, M., Liu, L., et al. (2018). Shmt2 desuccinylation by SIRT5 drives cancer cell proliferation. *Cancer Res.* 78, 372–386. doi: 10.1158/0008-5472.CAN-17-1912
- Young, T. L., and Cepko, C. L. (2004). A role for ligand-gated ion channels in rod photoreceptor development. *Neuron* 41, 867–879. doi: 10.1016/S0896-6273(04)00141-2
- Young-Pearse, T. L., Ivic, L., Kriegstein, A. R., and Cepko, C. L. (2006). Characterization of mice with targeted deletion of glycine receptor Alpha 2. *Mol. Cell. Biol.* 26, 5728–5734. doi: 10.1128/mcb.00237-06
- Yu, H., Bai, X. C., and Wang, W. (2021). Characterization of the subunit composition and structure of adult human glycine receptors. *Neuron* 109, 2707.e–2716.e. doi: 10.1016/j.neuron.2021.08.019
- Yu, T. W., Chahrouh, M. H., Coulter, M. E., Jiralerspong, S., Okamura-Ikeda, K., Ataman, B., et al. (2013). Using whole-exome sequencing to identify inherited causes of Autism. *Neuron* 77, 259–273. doi: 10.1016/j.neuron.2012.11.002
- Zafra, F., and Giménez, C. (2008). Glycine transporters and synaptic function. *IUBMB Life* 60, 810–817. doi: 10.1002/iub.128
- Zhu, H., and Gouaux, E. (2021). Architecture and assembly mechanism of native glycine receptors. *Nature* 599, 513–517. doi: 10.1038/s41586-021-04022-z



OPEN ACCESS

EDITED BY

Daniel Ortuño-Sahagún,
University of Guadalajara, Mexico

REVIEWED BY

Kanta Mizusawa,
Kitasato University, Japan
Ryota Matsuo,
Fukuoka Women's University, Japan

*CORRESPONDENCE

Patricia N. Schneider
pschneider@lsu.edu

SPECIALTY SECTION

This article was submitted to
Neurodevelopment,
a section of the journal
Frontiers in Neuroscience

RECEIVED 15 July 2022

ACCEPTED 08 September 2022

PUBLISHED 29 September 2022

CITATION

Salgado D, Mariluz BR, Araujo M,
Lorena J, Perez LN, Ribeiro RdL,
Sousa JdF and Schneider PN (2022)
Light-induced shifts in opsin gene
expression in the four-eyed fish
Anableps anableps.
Front. Neurosci. 16:995469.
doi: 10.3389/fnins.2022.995469

COPYRIGHT

© 2022 Salgado, Mariluz, Araujo,
Lorena, Perez, Ribeiro, Sousa and
Schneider. This is an open-access
article distributed under the terms of
the [Creative Commons Attribution
License \(CC BY\)](#). The use, distribution
or reproduction in other forums is
permitted, provided the original
author(s) and the copyright owner(s)
are credited and that the original
publication in this journal is cited, in
accordance with accepted academic
practice. No use, distribution or
reproduction is permitted which does
not comply with these terms.

Light-induced shifts in opsin gene expression in the four-eyed fish *Anableps anableps*

Daniele Salgado¹, Bertha R. Mariluz¹, Maysa Araujo¹,
Jamilly Lorena², Louise N. Perez³, Rafaela de L. Ribeiro⁴,
Josane de F. Sousa³ and Patricia N. Schneider^{1,3*}

¹Instituto de Ciências Biológicas, Universidade Federal do Pará, Belém, Brazil, ²Department of Integrative Biology, Michigan State University, East Lansing, MI, United States, ³Department of Biological Sciences, Louisiana State University, Baton Rouge, LA, United States, ⁴Instituto Tecnológico Vale, Belém, Brazil

The development of the vertebrate eye is a complex process orchestrated by several conserved transcriptional and signaling regulators. Aside from partial or complete loss, examples of exceptional modifications to this intricate organ are scarce. The unique eye of the four-eyed fish *Anableps anableps* is composed of duplicated corneas and pupils, as well as specialized retina regions associated with simultaneous aerial and aquatic vision. In a previous transcriptomic study of the *A. anableps* developing eye we identified expression of twenty non-visual and eleven visual opsin genes. Here, we surveyed the expression territories of three non-visual melanopsins genes (*opn4x1*, *opn4x2*, *opn4m3*), one teleost multiple tissue opsin (*tmt1b*) and two visual opsins (*lws* and *rh2-1*) in dorsal and ventral retinas. Our data showed that asymmetry of non-visual opsin expression is only established after birth. During embryonic development, while inside pregnant females, the expression of *opn4x1*, *opn4x2*, and *tmt1b* spans the whole retina. In juvenile fish (post birth), the expression of *opn4x1*, *opn4x2*, *opn4m3*, and *tmt1b* genes becomes restricted to the ventral retina, which receives aerial light. Raising juvenile fish in clear water instead of the murky waters found in its natural habitat is sufficient to change gene expression territories of *opn4x1*, *opn4x2*, *opn4m3*, *tmt1b*, and *rh2-1*, demonstrating that different lighting conditions can shift opsin expression and potentially contribute to changes in spectral sensitivity in the four eyed fish.

KEYWORDS

evolution, opsin, plasticity, retina, *Anableps*

Introduction

Change in environmental light is an important driving force for the diversity of visual systems in vertebrates. Aquatic animals occupy a great range of visual environments and have evolved adaptations to increase sensitivity to the availability of light (Collin, 2009). Evolutionary and developmental adaptations to the visual system have ensured success in avoiding predation, establishing feeding behavior and finding sexual partners (Jeffery, 2020; Thomas et al., 2020). For example, cichlid fishes show a versatile visual system with a complex sensory plasticity that regulates reproductive, feeding, and social behavior (Butler et al., 2019; Maruska and Butler, 2021). Substantial changes to the general structure of the vertebrate eye are rare, and include total or partial loss of the eyes, as seen in cavefishes, and the specialized retinas of the deep-water fish (Warrant and Locket, 2004; Biagioni et al., 2016; Lunghi et al., 2019).

Attempt in eye duplication is a rare event observed in only a few fish lineages such as *Dialommus fuscus* and *Dialommus macrocephalus*, also known as “Rockskipper,” these fish are terrestrial predators and have a vertically split cornea that allows them to remain upright with one cornea in and the other out of the water. In addition, *Bathylachnops exilis*, inhabits depths between 600 and 3,000 ft, and has an auxiliary globe in addition to the main eyeball directed toward the ocean floor (Schwab et al., 2001). Species from the genus *Anableps* are also a remarkable example of extreme adaptation of the visual system. With a partially duplicated eye, simultaneous aerial and aquatic vision, and a single optic nerve, *Anableps* consists in a unique model to understand the genetic bases of eye duplication (Figure 1A; Schwab et al., 2001; Owens et al., 2012; Perez et al., 2017).

Morphological innovations to the visual system require molecular changes in photoreception regulation. The distribution of photoreceptor cells and the composition of rods and cones play an important role in spectral sensitivity in teleost fish (Okano et al., 1994; Collin, 2009; Sato et al., 2018).

Membrane proteins known as visual opsins are present in retina cells and act as light sensors. Coupled with chromophores, these proteins mediate light detection and the initiation of visual processing in the photoreceptor cells (Wald, 1968; Yokoyama, 2000). Conversely, non-visual opsins, although expressed in the inner retina among other tissues in the vertebrate body, do not participate directly in image formation and instead respond to light by activating a series of non-visual sensory responses. In fish, these proteins are present in the pineal complex, epidermal photoreceptors and in the retina nuclear layers and play an important role in light detection, neural development and control of the circadian rhythm (Okano et al., 1994; Kojima and Fukada, 1999; Van Gelder, 2001; Peirson et al., 2009).

The melanopsins are the most widely studied non-visual opsins (Peirson et al., 2009; Diaz et al., 2016; Van Gelder

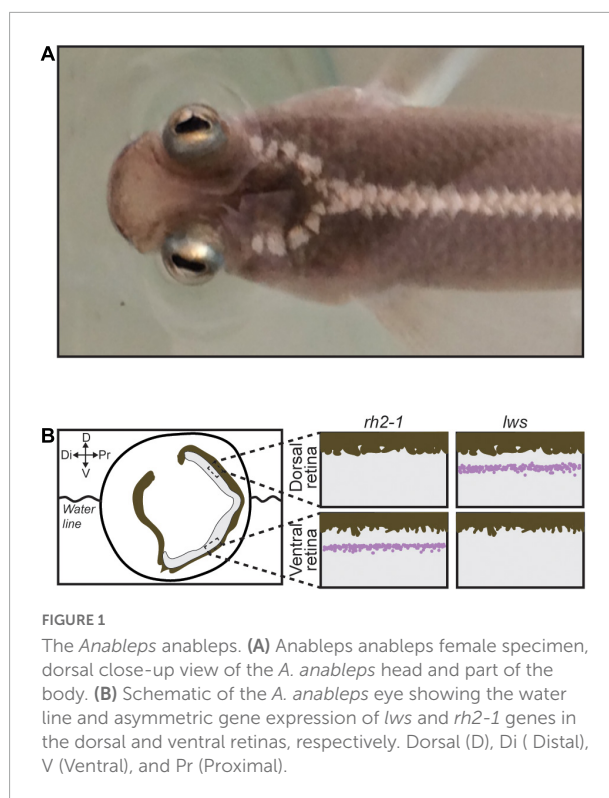


FIGURE 1

The *Anableps anableps*. (A) *Anableps anableps* female specimen, dorsal close-up view of the *A. anableps* head and part of the body. (B) Schematic of the *A. anableps* eye showing the water line and asymmetric gene expression of *lws* and *rh2-1* genes in the dorsal and ventral retinas, respectively. Dorsal (D), Di (Distal), V (Ventral), and Pr (Proximal).

and Buhr, 2016; Guido et al., 2020). In zebrafish (*Danio rerio*), expression of *opn4x1a*, *opn4x1b*, and *opn4m3* are detected in horizontal, bipolar and amacrine cells while a small subgroup of retinal ganglion cells expresses *opn4x1* and *opn4m3*. The expression of *opn4m3* was also detected in the zebrafish retinal pigment epithelial (RPE) (Davies et al., 2011). In the retina cells of salmon fish (*Salmo salar*), five melanopsin genes were observed: *opn4x1a* and *opn4x1b*, *opn4m1a1*, *opn4m1a2*, and *opn4m2* (Sandbakken et al., 2012). The non-visual opsin multiple tissue of teleosts (*tmt*) is expressed in the eyes, brain, liver, kidneys, and heart of fugu (*Fugu rubripes*) and zebrafish and in the brain and eyes of medaka (*Oryzias latipes*) (Moutsaki et al., 2003; Fischer et al., 2013). Previous studies have demonstrated that *tmt1* and *tmt2* opsins act as a blue light-sensitive Gi/Go-coupled receptors but exhibited spectral properties and photo-convertibility of the active state different from each other (Diaz et al., 2016; Guido et al., 2020). While non-visual opsins are expressed in the retina cells of many fish species, the exact role of these proteins and their physiological functions remain to be elucidated (Diaz et al., 2016; Guido et al., 2020).

Asymmetric gene expression of opsin genes is another way of modulating visual sensitivity, and this mechanism plays an important role in the diversification of visual pigments in fish, leading to changes in spectral sensitivity (Hofmann and Carleton, 2009; Hauser and Chang, 2017). In addition,

modulation of spectral sensitivity could also occur as part of a short-term plastic response to environmental changes, as observed in the eyes of the four eyed fish *Anableps anableps*.

Anableps are livebearers; female fish give birth to fully developed progeny, similarly to mammals. Previous work from our group has shown that the establishment of asymmetric expression of visual opsins (*rh2-1* and *lws*) occurs prior to birth and is independent of photic input, suggesting that it is genetically programmed (Perez et al., 2017). Here, we show that *opn4x1*, *opn4x2*, and *tmt1b* are expressed symmetrically in the entire retina of the developing eye of the *A. anableps* during larval stages. In the juvenile fish, *tmt1b*, *opn4x1*, *opn4x2*, and *opn4m3* shift the expression domain and become restricted to the ventral retina. *A. anableps* inhabit murky waters of the Amazon River and its tributaries (Supplementary Video 1). However, when animals were maintained in aquaria with clear water, we observed loss of *opn4x2* expression in the retina, and a shift in *opn4x1*, *opn4m3*, and *tmt1b* expression domains, from being restricted to the ventral retina, to being expanded dorsally and occupying the entire retina, recapitulating the expression pattern of the developing eye during larval stages.

Materials and methods

Sample collection

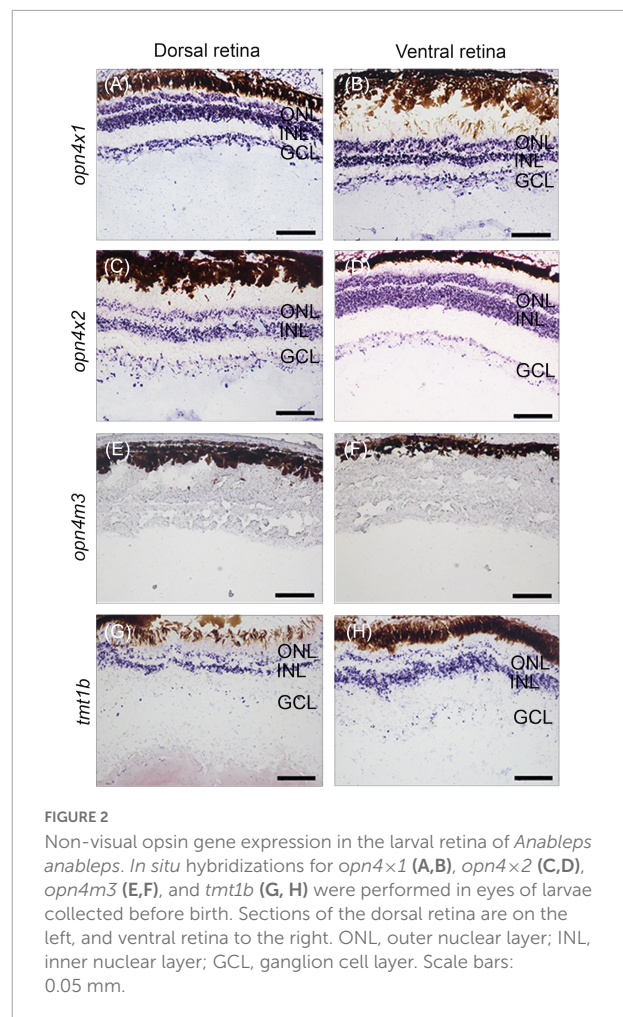
Specimens of *A. anableps* were collected by seine net in two locations: Abaetetuba, Pará, Brazil (1°42'24.9"S 48°53'46.4"W) and Bragança, Pará, Brazil (0°53'27.6"S 46°39'21.9"W). Animals were euthanized using MS-222 (Sigma-Aldrich Corp., Milwaukee, WI, USA) followed by decapitation.

Histological analysis

Eyes of wild-caught *A. anableps* juvenile (up to 15 cm long) and larvae were collected and flash frozen in Tissue-Tek® O.C.T TM embedding medium (Sakura Finetek USA Inc., Torrance, CA, USA). Sagittal cryosections (20 µm) of the eyes were obtained using CM1850 UV cryostat (Leica Biosystems Nussloch GmbH, Nussloch, BW, Germany) and collected on ColorFrost Plus microscope slides (Thermo Fisher Scientific, Pittsburgh, PA, USA), fixed in 3% paraformaldehyde (Sigma-Aldrich Inc., St. Louis, MO, USA) and stored at −80°C for further use.

Lighting environment conditions

Eight juvenile fish were kept in a 75 Gallon glass aquarium with UV filter and standard fluorescent light (40 watts);



fish were kept in dechlorinated tap water at 28°C with aeration and biological and mechanical filtration and fed daily with fish ration. Fish were exposed to a day and night cycle of 12 h for 30 days followed by euthanasia, according to Fuller and Claricoates (Fuller and Claricoates, 2011; Supplementary Video 2).

Sagittal sections (20 µm) were obtained using CM1850 UV cryostat (Leica Biosystems Nussloch GmbH, Nussloch, BW, Germany), placed on ColorFrost Plus microscope slides (Thermo Fisher Scientific, Pittsburgh, PA, USA) and stored at −80°C for further use. Eight wild-caught juvenile fish were used as control for these experiments.

Riboprobe synthesis

To produce riboprobes for *in situ* hybridization for the genes *opn4m3*, *opn4x1*, *opn4x2*, and *tmt1b*, we adapted a PCR-based technique for the preparation of riboprobe templates (David and Wedlich, 2001). First, vectors containing target gene sequences were synthesized in pBlueScript II SK(+) by

BioCat GmbH (Heidelberg, Germany). Next, these vectors were used as a template on a PCR reaction. The T7 promoter sequence was included at the 5' end of each gene-specific forward primer, whereas the SP6 promoter sequence was added to the 5' end of each gene-specific reverse primer. The resulting amplicons for each target gene were subsequently used as template for sense (T7) or antisense (SP6) riboprobe synthesis. Primers (with promoter sequences underlined) were: *opn4m3*-Forward: 5' TAATACGACTCACTATAGGCTCGTCTGAG GTGGTTT TAGG 3' and reverse: 5' ATTTAGGTGACAC TATAGTGTAGGAGCAGGGTGGAGAAG 3', *opn4x1*-Forward: 5' TAATACGACTCACTATAGCAAAGAAGGCAAC GATGTAGTGA 3' and reverse: 5' ATTTAGGTGACACTA TAGACACGGATTCTATCGGCATGT 3', *opn4x2*-Forward: 5' TAATACGACTCACTATAGCCATTCCTTGTAGAGGCAGTT GATA 3' and reverse: 5' ATTTAGGTGACACTATAGGCGACT TCCTCATGGCTTTC3', *tmt1b*-Forward: 5' TAATACGA CTCACTATAGCAGTGGTTCGTCGAAAATGG 3' and reverse: 5' ATTTAGGTGACACTATAGGCGGTTCAAAGGG ATTACTGT 3'.

To produce riboprobes for the visual opsins *lws* and *rh2-1*, we used as templates vectors previously described (Perez et al., 2017). The pCRII-TOPO vector (Thermo Fisher Scientific, Pittsburgh, PA, USA) containing the target gene sequence was used as a template in a PCR reaction with M13 forward (5' TAAAACGACGCCAG-3') and M13 reverse (5'-CAGGAAACAGCTATGAC 3') primers. The resulting amplicon contained the sequence of the gene of interest flanked by an upstream T7 promoter and a downstream SP6 promoter. Sense and antisense probes were produced using T7 and SP6 RNA polymerases, respectively. Riboprobe reaction was performed using DIG-labeling mix (Roche Diagnostics Deutschland GmbH, Mannheim, BW., GER.) and according to manufacturer's protocol (mMESSAGE mMACHINE Transcription kits, Ambion, Carlsbad, CA, USA).

In situ hybridization

In situ hybridization was performed according to previously established protocol (Lovell et al., 2013; Carleton et al., 2014; De Lima et al., 2015). Cryosections from heads *A. anableps* specimens were acetylated for 10 min in a solution of 0.33% acetic anhydride in DEPC-treated water, rinsed with 2× SSPE buffer (0.02 M EDTA and 2.98 M NaCl in 0.2 M phosphate buffer) and dehydrated in 70, 95, and 100% RNase-free ethanol. Each section was then hybridized with a solution (32 µL) containing 50% formamide, 2× SSPE, 1 µg/µL BSA, 1 µg/µL poly(A) (Sigma-Aldrich Corp., Milwaukee, WI, USA) in DEPC-treated water, and 1 µL of the DIG-labeled riboprobe. Slides were cover slipped, sealed by immersion in mineral oil, and incubated overnight at 65°C. Next, sections were rinsed in chloroform, de-cover slipped in 2× SSPE, and incubated serially

in 2× SSPE/50% formamide, and in 0.1× SSPE at 65°C. Sections were then blocked for 30 min at RT in blocking buffer with 1% skim milk and incubated overnight with an alkaline phosphatase-conjugated anti-DIG antibody (Roche Diagnostics Deutschland GmbH, Mannheim, BW, Germany). Slides were washed twice for 15 min in TMN (100 mM Tris, pH 9.5; 150 mM NaCl, 0.05 M MgCl₂), and incubated in a detection solution containing the alkaline phosphatase substrates Nitro-Blue Tetrazolium Chloride (NBT) (Roche Diagnostics Deutschland GmbH, Mannheim, BW, Germany). and 5-Bromo-4-Chloro-3-Indolyl-phosphate p-Toluidine Salt (BCIP) (Roche Diagnostics Deutschland GmbH, Mannheim, BW, Germany). Slides were washed overnight, fixed in 4% paraformaldehyde (dissolved in PBS) and cover slipped with Cytoseal (Thermo Fisher Scientific, Pittsburgh, PA, USA). Slides were imaged using a Nikon SMZ1500 microscope and processed on NIS-Elements D 4.10.01 program (Nikon Instruments Inc., Melville, NY, USA).

Results

Non-visual opsins are expressed symmetrically in the developing eye of *Anableps anableps* prior to birth

Our previous work identified twenty non-visual and eleven visual opsins expressed during the development of the eye in the four-eyed fish (Beaudry et al., 2017; Perez et al., 2017). Here, *in situ* hybridization was performed to examine the expression domains of three types of melanopsin subfamily of genes, *opn4x1*, *opn4x2*, *opn4m3*, and one type of teleost multiple tissue opsin, *tmt1b*, in the developing retina of pre-birth larvae. Our results showed that *opn4x1*, *opn4x2*, and *tmt1b* are expressed uniformly in the outer nuclear layer (ONL), inner nuclear layer (INL), and ganglion cell layer (GCL) in both dorsal and ventral regions of the retina (Figures 2A–D,G,H). The expression of *opn4m3* was not detected by *in situ* hybridization at stage 5 (Figures 2E,F).

Expression domains of visual and non-visual opsins change upon different lighting conditions in juvenile *Anableps anableps*

We have previously shown that in the *A. anableps*, asymmetric expression of *lws* and *rh2.1* in the dorsal and ventral regions of the retina, respectively, is established prior to birth in photoreceptor cells (Perez et al., 2017). Here, we wanted to investigate the plasticity of visual and non-visual opsins in the retina upon changes in environmental lighting. To this end,

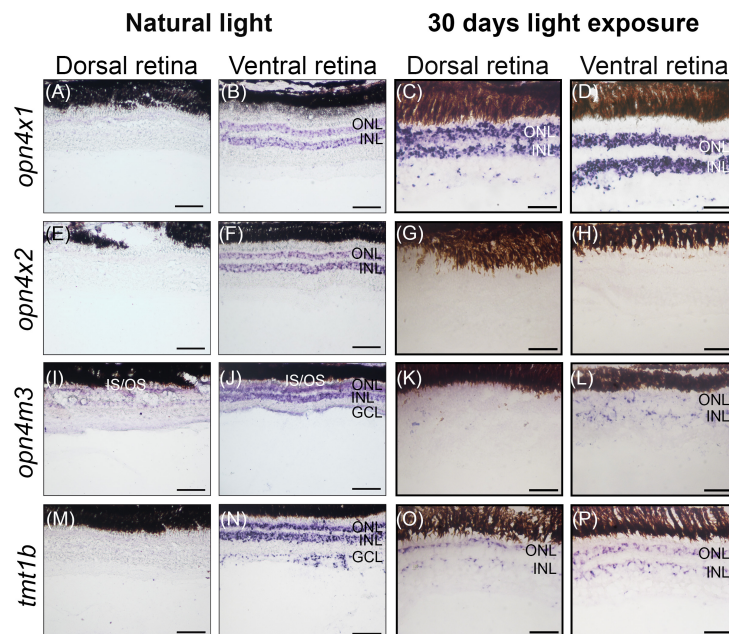


FIGURE 3

Non-visual opsin gene expression in the juvenile retina of *Anableps anableps*. *In situ* hybridizations of *opn4x1* (A–D), *opn4x2* (E–H), *opn4m3* (I–L), and *tmt1b* (M–P) were performed in *A. anableps*' eyes from wild-caught juvenile fish under natural light conditions (A,B,E,F,I,J,M,N) and juveniles that were kept for 30 days in light exposure from above and below the water (C,D,G,H,K,L,O,P). The panel shows sections of the dorsal retina and ventral retina. ONL, outer nuclear layer; INL, inner nuclear layer; GCL, ganglion cell layer; IS, photoreceptor inner segments; OS, photoreceptor outer segments. Scale bars: 0.05 mm.

juvenile fish were maintained in clear water for 30 days and surveyed for visual and non-visual opsin gene expression using RNA *in situ* hybridization.

In wild-caught juvenile *A. anableps* found in murky river water, the expression of *opn4x1* (Figures 3A,B) and *opn4x2* (Figures 3E,F) is restricted to the ONL and INL of the ventral retina while *opn4m3* and *tmt1b* are expressed in the INL, ONL and GCL of the ventral retina (Figures 3I,J,M,N). We next used a 30-day light-induced cycle and assayed opsin gene expression. Our results showed that expression of *opn4x1* and *tmt1b*, restricted to the ONL and INL in the ventral retina in wild-caught fish, expands to the ONL, INL and GCL in the dorsal retina (Figures 3C,D,O,P); *opn4x2* expression is lost in the entire retina (Figures 3G,H) while *opn4m3* expression becomes sparse in the ONL, INL and GCL of the ventral retina (Figures 3K,L).

We next assayed the *lws* and *rh2-1* visual opsins, which show expression domains restricted to the dorsal and ventral retinas, respectively (Perez et al., 2017). Upon light-induced exposure, *in situ* hybridization showed that *lws* expression remained in the photoreceptor layer of the dorsal retina, however, *rh2-1* expression expanded to the photoreceptor layer of ventral and dorsal retina territories (Figures 1B, 4A–D for reference).

Altogether, our results show that *lws* and *rh2-1* visual opsin expression is established without environmental light stimuli, prior to birth. However, changes in light input can modulate the expression of *rh2-1* and cause a shift the expression

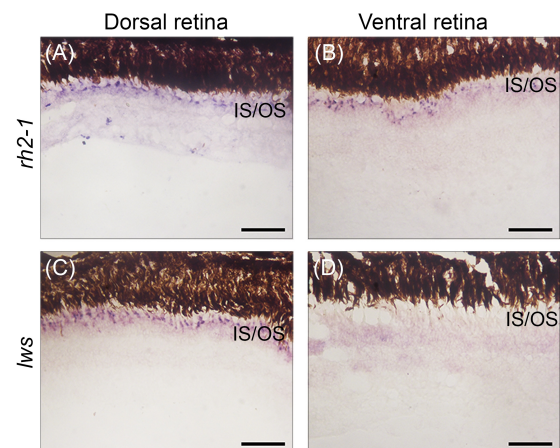


FIGURE 4

Gene expression of visual opsins in the retina of juvenile *A. anableps* under light stimuli for 30 days. *In situ* hybridizations of *rh2-1* (A,B) and *lws* (C,D) in dorsal and ventral retinas from juveniles of *A. anableps*. Scale bars: 0.05 mm.

domain, from being restricted to the ventral retina, to being expanded to the entire retina. Non-visual opsins also show asymmetric expression in the nuclear layer of the retina in juvenile fish. Although established only after birth, changes in the environmental lighting caused a shift in the expression domains of *opn4x1*, *opn4m3*, and *tmt1b*, suggesting that both

visual and non-visual opsins can be modulated by changes in the photic input.

Discussion

In this work, we surveyed the expression of three melanopsins *opn4x1*, *opn4x2*, *opn4m3*, and one *tmt1b* in the nuclear layers of the *A. anableps* retina. The spatial pattern observed pre-birth diverges from that seen in free-swimming juvenile individuals, which express *opn4x1* and *opn4x2* in the ONL and INL of the ventral retina while *opn4m3* and *tmt1b* are expressed in the INL, ONL and GCL of the ventral retina.

In zebrafish, melanopsin genes are expressed in different regions of the retina and have been associated with the regulation of negative phototaxis (Matos-Cruz et al., 2011; Fernandes et al., 2012). In teleost fish, the expression of melanopsin in various types of neuronal cells can directly influence retinal function in a dependent and/or independent way from intrinsically photosensitive retinal ganglion cells (Matos-Cruz et al., 2011). In other vertebrates, including teleost fish, *tmt* expression is distributed across many tissues including internal organs where light can hardly penetrate, suggesting that *tmt* opsin may have both photosensitive and non-photosensitive functions (Fischer et al., 2013; Sakai et al., 2015). In our work, we speculate that light-induced changes in non-visual opsins expression could be due to the indirect regulation of visual opsins in the photoreceptor cells of the retina.

Previous studies from our group and others have shown asymmetric expression of *lws* and *rh2.1* in the photoreceptor cells in the dorsal and ventral domains of the developing retina, respectively, with the establishment of asymmetric expression of *lws* and *rh2.1* occurring before birth, suggesting that it is genetically programmed and independent of light stimuli (Owens et al., 2012; Perez et al., 2017). This asymmetry allows the partial duplicated eye of the *A. anableps* to optimize the absorption of different wavelengths coming simultaneously from the aerial and aquatic environment. In this work, we manipulated light input by changing the turbid water where the *A. anableps* is normally found and replacing it with clear water. We tested the plasticity of *lws* and *rh2.1* in the photoreceptor cells in the retina of juvenile fish after a 30 day period and our results showed that, despite being established before light stimuli reach the retina (Perez et al., 2017), the expression of *rh2.1* (normally expressed in the ventral retina) shifted and became uniformly expressed in the entire retina, while the expression of *lws* remained unchanged and restricted to the photoreceptor cells in the dorsal retina. While in captivity, animals were maintained in tanks with average temperature of 28°C, which closely mirrors that of their natural environment. The commercial diet provided for the animals in captivity, however, differs from their diet in natural settings. In the wild, the stomach content of *A. anableps* ranges from micro and macroalgae, insects, crustaceans, molluscs, fishes, to mud and

detritus (Figueiredo et al., 2019). While we cannot rule out a potential feeding behavior of food content impact on opsin gene expression, we have no knowledge of a documented link between the former and the latter.

In zebrafish and guppies, the expression patterns of different subtypes of *rh2* and *lws* vary according to the developmental stage and region of the retina (Takechi and Kawamura, 2005; Owens et al., 2012). Several studies have demonstrated that opsin expression is subject to phenotypic plasticity (Fuller et al., 2005; Shand et al., 2008; Veen et al., 2017). Several teleost species placed under altered light conditions, such as damselfish and cardinal fish (Luehrmann et al., 2018), African cichlids (Wright et al., 2019), guppies (Kranz et al., 2018), and Senegalese sole (Frau et al., 2020) can alter the expression of opsin genes to adapt to the environmental changes. Here we show that shift in opsin expression happens in the dorsal and ventral domains of the retina in *A. anableps* within a 30-day period, our results do not exclude the possibility that the change in the expression pattern of opsin genes occurs in a shorter period. Here, we show that after a 30-day period of exposure to clear water, opsin expression changes in the dorsal and ventral retinas, given that, this shift happens in portions of the retina for both visual and non-visual opsin genes, our results suggest that the regulatory control of the expression of opsins in the eye of the *A. anableps* is complex and compartmentalized in the dorsal and ventral retinas.

Conclusion

Our study shows that the expression of visual opsins in the retina of *A. anableps* can be modulated by spectral and intensity changes in ambient light. These adjustments allow for a quick adaptation of the visual system to different water turbidity and environmental luminosity. Our findings indicate that the *A. anableps* exhibits great potential to modulate its vision according to the environment, allowing this organism to adjust its vision to different photic conditions. Furthermore, our findings suggest that the expression of non-visual opsins can also be altered upon changes in environmental light, suggesting a regulatory correlation between visual and non-visual opsin regulation of physiological functions responsive to light.

Data availability statement

The raw data supporting the conclusions of this article will be made available by the authors, without undue reservation.

Ethics statement

This study was approved by IBAMA/SISBIO under license number 47206-1 and the Ethics Committee for Animal Research at the Universidade Federal do Pará (protocol number 037-2015).

Author contributions

DS, MA, JL, LP, and PS designed the research. LP, MA, JL, and BM performed *in situ* hybridizations (ISH) of *A. anableps* larvae. RR and JS designed the riboprobes for ISH. DS and LP performed light-induced experiments and analysis. DS, LP, and PS wrote the manuscript with input from BM, MA, JL, RR, and JS. All authors contributed to the article and approved the submitted version.

Acknowledgments

We thank Jeferson Carneiro and Karen Pinto for help in fish collection. We also thank Iracilda Sampaio for logistical support at the collection site. We would also like to thank Igor Schneider for critical reading of the manuscript.

Conflict of interest

The authors declare that the research was conducted in the absence of any commercial or financial relationships that could be construed as a potential conflict of interest.

References

- Baudry, F. E. G., Iwanicki, T. W., Mariluz, B. R. Z., Darnet, S., Brinkmann, H., Schneider, P., et al. (2017). The non-visual opsins: Eighteen in the ancestor of vertebrates, astonishing increase in ray-finned fish, and loss in amniotes. *J. Exp. Zool. Part B Mol. Dev. Evol.* 328, 685–696. doi: 10.1002/jez.b.22773
- Biagioni, L. M., Hunt, D. M., and Collin, S. P. (2016). Morphological Characterization and Topographic Analysis of Multiple Photoreceptor Types in the Retinae of Mesopelagic Hatchetfishes with Tubular Eyes. *Front. Ecol. Evol.* 4:25. doi: 10.3389/fevo.2016.00025
- Butler, J. M., Whitlow, S. M., Rogers, L. S., Putland, R. L., Mensinger, A. F., and Maruska, K. P. (2019). Reproductive state-dependent plasticity in the visual system of an African cichlid fish. *Horm. Behav.* 114:104539. doi: 10.1016/j.yhbeh.2019.06.003
- Carleton, J. B., Lovell, P. V., Mchugh, A., Marzulla, T., Horback, K. L., and Mello, C. V. (2014). An optimized protocol for high-throughput *in situ* hybridization of zebra finch brain. *Cold Spring Harb. Protoc.* 2014, 1249–1258. doi: 10.1101/pdb.prot084582
- Collin, S. P. (2009). "Evolution of the Visual System in Fishes," in *Encyclopedia of Neuroscience*, eds M. D. Binder, N. Hirokawa, and U. Windhorst (Berlin: Springer), 1459–1466. doi: 10.1007/978-3-540-29678-2_3178
- David, R., and Wedlich, D. (2001). Pcr-based Rna probes: A quick and sensitive method to improve whole mount embryo *in situ* hybridizations. *Biotechniques* 30:74. doi: 10.2144/01304st02
- Davies, W. I., Zheng, L., Hughes, S., Tamai, T. K., Turton, M., Halford, S., et al. (2011). Functional diversity of melanopsins and their global expression in the teleost retina. *Cell. Mol. Life Sci.* 68, 4115–4132. doi: 10.1007/s00018-011-0785-4
- De Lima, J. L., Soares, F. A., Remedios, A. C., Thom, G., Wirthlin, M., Aleixo, A., et al. (2015). A putative Ra-like region in the brain of the scale-backed antbird, *Willisornis poecilinotus* (Furnariidae, Suboscines, Passeriformes, Thamnophilidae). *Genet. Mol. Biol.* 38, 249–254. doi: 10.1590/S1415-475738320150010
- Diaz, N. M., Morera, L. P., and Guido, M. E. (2016). Melanopsin and the Non-visual Photochemistry in the Inner Retina of Vertebrates. *Photochem. Photobiol.* 92, 29–44. doi: 10.1111/php.12545
- Fernandes, A. M., Fero, K., Arrenberg, A. B., Bergeron, S. A., Driever, W., and Burgess, H. A. (2012). Deep brain photoreceptors control light-seeking behavior in zebrafish larvae. *Curr. Biol.* 22, 2042–2047. doi: 10.1016/j.cub.2012.08.016
- Figueiredo, M. B., Nunes, J. L., Almeida, Z. S., Paz, A. C., Piorski, N. M., and Reis, M. R. (2019). Feeding ecology of *Anableps Anableps* (Actinopterygii: Cyprinodontiformes: Anablepidae) off the north-eastern coast of Brazil. *Acta Ichthyol. Piscat.* 49, 213–219. doi: 10.3750/AIEP/02477
- Fischer, R. M., Fontinha, B. M., Kirchmaier, S., Steger, J., Bloch, S., Inoue, D., et al. (2013). Co-expression of Val- and Tmt-opsins uncovers ancient photosensory interneurons and motoneurons in the vertebrate brain. *PLoS Biol.* 11:e1001585. doi: 10.1371/journal.pbio.1001585
- Frau, S., Loentgen, G., Martin-Robles, A. J., and Munoz-Cueto, J. A. (2020). Ontogenetic expression rhythms of visual opsins in senegalese sole are modulated by photoperiod and light spectrum. *J. Comp. Physiol. B* 190, 185–204. doi: 10.1007/s00360-020-01264-7
- Fuller, R. C., and Claricoates, K. M. (2011). Rapid light-induced shifts in opsin expression: Finding new opsins, discerning mechanisms of change, and implications for visual sensitivity. *Mol. Ecol.* 20, 3321–3335. doi: 10.1111/j.1365-294X.2011.05180.x
- Fuller, R. C., Carleton, K. L., Fadool, J. M., Spady, T. C., and Travis, J. (2005). Genetic and environmental variation in the visual properties of bluefin killifish, *Lucania goodei*. *J. Evol. Biol.* 18, 516–523. doi: 10.1111/j.1420-9101.2005.00886.x

Publisher's note

All claims expressed in this article are solely those of the authors and do not necessarily represent those of their affiliated organizations, or those of the publisher, the editors and the reviewers. Any product that may be evaluated in this article, or claim that may be made by its manufacturer, is not guaranteed or endorsed by the publisher.

Supplementary material

The Supplementary Material for this article can be found online at: <https://www.frontiersin.org/articles/10.3389/fnins.2022.995469/full#supplementary-material>

SUPPLEMENTARY FIGURE 1

In situ hybridization showing the sense control riboprobes for the non-visual opsins: *opn4x1*, *opn4x2*, *opn4m3*, *tmt1b*.

SUPPLEMENTARY FIGURE 2

In situ hybridization showing the sense control riboprobes for the visual opsins *lws* and *rh2-1*.

SUPPLEMENTARY VIDEO 1

A group of five *Anableps anableps* specimens in the wild. Movie was recorded in the estuarine region of Bragança, Pará, Brazil (0°53'27.6"S 46°39'21.9"W).

SUPPLEMENTARY VIDEO 2

A fish tank with *Anableps anableps* specimens during the 30-day light induced experiments.

- Guido, M. E., Marchese, N. A., Rios, M. N., Morera, L. P., Diaz, N. M., Garbarino-Pico, E., et al. (2020). Non-visual Opsins and Novel Photo-Detectors in the Vertebrate Inner Retina Mediate Light Responses Within the Blue Spectrum Region. *Cell. Mol. Neurobiol.* 42, 59–83. doi: 10.1007/s10571-020-00997-x
- Hauser, F. E., and Chang, B. S. W. (2017). Insights into visual pigment adaptation and diversity from model ecological and evolutionary systems. *Curr. Opin. Genet. Dev.* 47, 110–120. doi: 10.1016/j.gde.2017.09.005
- Hofmann, C. M., and Carleton, K. L. (2009). Gene duplication and differential gene expression play an important role in the diversification of visual pigments in fish. *Integr. Comp. Biol.* 49, 630–643. doi: 10.1093/icb/icp079
- Jeffery, W. R. (2020). Astyanax surface and cave fish morphs. *Evodevo* 11:14. doi: 10.1186/s13227-020-00159-6
- Kojima, D., and Fukada, Y. (1999). Non-visual photoreception by a variety of vertebrate opsins. *Novartis Found Symp.* 224, 265–279. doi: 10.1002/9780470515693.ch15
- Kranz, A. M., Forgan, L. G., Cole, G. L., and Endler, J. A. (2018). Light environment change induces differential expression of guppy opsins in a multi-generational evolution experiment. *Evolution* 72, 1656–1676. doi: 10.1111/evo.13519
- Lovell, P. V., Carleton, J. B., and Mello, C. V. (2013). Genomics analysis of potassium channel genes in songbirds reveals molecular specializations of brain circuits for the maintenance and production of learned vocalizations. *BMC Genom.* 14:470. doi: 10.1186/1471-2164-14-470
- Luehrmann, M., Stieb, S. M., Carleton, K. L., Pietzker, A., Cheney, K. L., and Marshall, N. J. (2018). Short-term colour vision plasticity on the reef: Changes in opsin expression under varying light conditions differ between ecologically distinct fish species. *J. Exp. Biol.* 221:jeb175281. doi: 10.1242/jeb.175281
- Lunghi, E., Zhao, Y., Sun, X., and Zhao, Y. (2019). Morphometrics of eight Chinese cavefish species. *Sci. Data* 6:233. doi: 10.1038/s41597-019-0257-5
- Maruska, K. P., and Butler, J. M. (2021). Reproductive- and Social-State Plasticity of Multiple Sensory Systems in a Cichlid Fish. *Integr. Comp. Biol.* 61, 249–268. doi: 10.1093/icb/icab062
- Matos-Cruz, V., Blasic, J., Nickle, B., Robinson, P. R., Hattar, S., and Halpern, M. E. (2011). Unexpected diversity and photoperiod dependence of the zebrafish melanopsin system. *PLoS One* 6:e25111. doi: 10.1371/journal.pone.0025111
- Moutsaki, P., Whitmore, D., Bellingham, J., Sakamoto, K., David-Gray, Z. K., and Foster, R. G. (2003). Teleost multiple tissue (tmt) opsin: A candidate photopigment regulating the peripheral clocks of zebrafish? *Brain Res. Mol. Brain Res.* 112, 135–145. doi: 10.1016/S0169-328X(03)00059-7
- Okano, T., Yoshizawa, T., and Fukada, Y. (1994). Pinopsin is a chicken pineal photoreceptive molecule. *Nature* 372, 94–97. doi: 10.1038/372094a0
- Owens, G. L., Rennison, D. J., Allison, W. T., and Taylor, J. S. (2012). In the four-eyed fish (*Anableps anableps*), the regions of the retina exposed to aquatic and aerial light do not express the same set of opsin genes. *Biol. Lett.* 8, 86–89. doi: 10.1098/rsbl.2011.0582
- Peirson, S. N., Halford, S., and Foster, R. G. (2009). The evolution of irradiance detection: Melanopsin and the non-visual opsins. *Philos. Trans. R. Soc. Lond. B Biol. Sci.* 364, 2849–2865. doi: 10.1098/rstb.2009.0050
- Perez, L. N., Lorena, J., Costa, C. M., Araujo, M. S., Frota-Lima, G. N., Matos-Rodrigues, G. E., et al. (2017). Eye development in the four-eyed fish *Anableps anableps*: Cranial and retinal adaptations to simultaneous aerial and aquatic vision. *Proc. Biol. Sci.* 284:20170157. doi: 10.1098/rspb.2017.0157
- Sakai, K., Yamashita, T., Imamoto, Y., and Shichida, Y. (2015). Diversity of Active States in Tmt Opsins. *PLoS One* 10:e0141238. doi: 10.1371/journal.pone.0141238
- Sandbakken, M., Ebbesson, L., Stefansson, S., and Helvik, J. V. (2012). Isolation and characterization of melanopsin photoreceptors of Atlantic salmon (*Salmo salar*). *J. Comp. Neurol.* 520, 3727–3744. doi: 10.1002/cne.23125
- Sato, K., Yamashita, T., Kojima, K., Sakai, K., Matsutani, Y., Yanagawa, M., et al. (2018). Pinopsin evolved as the ancestral dim-light visual opsin in vertebrates. *Commun. Biol.* 1:156. doi: 10.1038/s42003-018-0164-x
- Schwab, I. R., Ho, V., Roth, A., Blankenship, T. N., and Fitzgerald, P. G. (2001). Evolutionary attempts at 4 eyes in vertebrates. *Trans. Am. Ophthalmol. Soc.* 99, 145–156.
- Shand, J., Davies, W. L., Thomas, N., Balmer, L., Cowing, J. A., Pointer, M., et al. (2008). The influence of ontogeny and light environment on the expression of visual pigment opsins in the retina of the black bream, *Acanthopagrus butcheri*. *J. Exp. Biol.* 211, 1495–1503. doi: 10.1242/jeb.012047
- Takechi, M., and Kawamura, S. (2005). Temporal and spatial changes in the expression pattern of multiple red and green subtype opsin genes during zebrafish development. *J. Exp. Biol.* 208, 1337–1345. doi: 10.1242/jeb.01532
- Thomas, K. N., Gower, D. J., Bell, R. C., Fujita, M. K., Schott, R. K., and Streicher, J. W. (2020). Eye size and investment in frogs and toads correlate with adult habitat, activity pattern and breeding ecology. *Proc. Biol. Sci.* 287:20201393. doi: 10.1098/rspb.2020.1393
- Van Gelder, R. N. (2001). Non-visual ocular photoreception. *Ophthalmic Genet.* 22, 195–205. doi: 10.1076/opge.22.4.195.2215
- Van Gelder, R. N., and Buhr, E. D. (2016). Melanopsin: The Tale of the Tail. *Neuron* 90, 909–911. doi: 10.1016/j.neuron.2016.05.033
- Veen, T., Brock, C., Rennison, D., and Bolnick, D. (2017). Plasticity contributes to a fine-scale depth gradient in sticklebacks' visual system. *Mol. Ecol.* 26, 4339–4350. doi: 10.1111/mec.14193
- Wald, G. (1968). The molecular basis of visual excitation. *Nature* 219, 800–807. doi: 10.1038/219800a0
- Warrant, E. J., and Locket, N. A. (2004). Vision in the deep sea. *Biol. Rev. Camb. Philos. Soc.* 79, 671–712. doi: 10.1017/S1464793103006420
- Wright, D. S., Meijer, R., Van Eijk, R., Vos, W., Seehausen, O., and Maan, M. E. (2019). Geographic variation in opsin expression does not align with opsin genotype in Lake Victoria cichlid populations. *Ecol. Evol.* 9, 8676–8689. doi: 10.1002/ece3.5411
- Yokoyama, S. (2000). Phylogenetic analysis and experimental approaches to study color vision in vertebrates. *Methods Enzymol.* 315, 312–325. doi: 10.1016/S0076-6879(00)15851-3



OPEN ACCESS

EDITED BY
Daniel Ortuño-Sahagún,
University of Guadalajara, Mexico

REVIEWED BY
Olga Zueva,
Carnegie Mellon University,
United States
Yury Morozov,
Yale University, United States
Aixa Victoria Morales,
Cajal Institute (CSIC), Spain

*CORRESPONDENCE
José E. García-Arrarás
jegarcia@hpcf.upr.edu

SPECIALTY SECTION
This article was submitted to
Neurodevelopment,
a section of the journal
Frontiers in Neuroscience

RECEIVED 28 July 2022
ACCEPTED 21 October 2022
PUBLISHED 16 November 2022

CITATION
Miranda-Negrón Y and
García-Arrarás JE (2022) Radial glia
and radial glia-like cells: Their role
in neurogenesis and regeneration.
Front. Neurosci. 16:1006037.
doi: 10.3389/fnins.2022.1006037

COPYRIGHT
© 2022 Miranda-Negrón and
García-Arrarás. This is an open-access
article distributed under the terms of
the [Creative Commons Attribution
License \(CC BY\)](#). The use, distribution
or reproduction in other forums is
permitted, provided the original
author(s) and the copyright owner(s)
are credited and that the original
publication in this journal is cited, in
accordance with accepted academic
practice. No use, distribution or
reproduction is permitted which does
not comply with these terms.

Radial glia and radial glia-like cells: Their role in neurogenesis and regeneration

Yamil Miranda-Negrón and José E. García-Arrarás*

Department of Biology, College of Natural Sciences, University of Puerto Rico, San Juan, Puerto Rico

Radial glia is a cell type traditionally associated with the developing nervous system, particularly with the formation of cortical layers in the mammalian brain. Nonetheless, some of these cells, or closely related types, called radial glia-like cells are found in adult central nervous system structures, functioning as neurogenic progenitors in normal homeostatic maintenance and in response to injury. The heterogeneity of radial glia-like cells is nowadays being probed with molecular tools, primarily by the expression of specific genes that define cell types. Similar markers have identified radial glia-like cells in the nervous system of non-vertebrate organisms. In this review, we focus on adult radial glia-like cells in neurogenic processes during homeostasis and in response to injury. We highlight our results using a non-vertebrate model system, the echinoderm *Holothuria glaberrima* where we have described a radial glia-like cell that plays a prominent role in the regeneration of the holothurian central nervous system.

KEYWORDS

regeneration, echinoderm, spinal cord, radial nerve cord, radial glia (RG), radial glia like cells

Origin and description of radial glia cell

Radial glial cells (RGCs) were initially described around the mid-late 1800s in several mammalian species by [Bentivoglio and Mazzarello \(1999\)](#). Using the Golgi impregnation technique, these and other investigators reported that RGCs were found in the developing nervous system (NS) at different embryonic and neonatal stages ([Figure 1](#)). Ever since then, RGCs have been associated with: (1) characteristic morphological features, (2) their occurrence in nervous tissue, specifically in the central nervous system (CNS), and (3) their transient presence during embryonic development. Over one century later, multiple studies have confirmed the original findings and have extended them to incorporate the molecular basis of cellular phenotypes and their functions. RGCs, or cells with similar properties termed radial glia-like cells (RGLCs), have been documented in adults of various species, where functions, additional to their embryological role, have been described. In this review, we focus on the presence of

RGLC's in adult organisms and their roles in NS regeneration, we highlight the work of our group in studying the RGLCs in echinoderms and their prominent role during regeneration of the radial nerve cord (RNC).

Radial glia in vertebrates

Magini's original description of RGCs consisted solely of the cell's morphological features and the changes they displayed during vertebrate NS development. In one of his Golgi-stained sections, [Bentivoglio and Mazzarello \(1999\)](#) describes them as "very long and thin filaments, mostly directed toward the white matter, where they often get lost after having traversed the entire thickness of the gray matter". This description, with emphasis on the apico-basal radial morphology, has been substantiated using many other techniques. Among them immunohistochemical and transgenic tools ([Figure 2](#)). Many of these tools have also served to study the cell's origin.

Radial glial cells originate from the early neural tube neuroepithelial cells (NECs) by a transition that involves acquiring astroglia characteristics. NECs are known for their apico-basal polarity and interkinetic nuclear migration associated with their cell cycle progression. At the beginning of neural tube formation, NECs divide symmetrically, populating and supporting the development of the neural tube. Eventually, most NECs will differentiate into RGCs. At this point, gene expression changes are observed, and unique markers for the RGCs are expressed. For example, tight junction occludins are replaced by cell adhesion proteins such as N-cadherins ([Aaku-Saraste et al., 1996](#)). Similarly, cytoplasmic glycogen granules begin to appear ([Gadisieux and Evrard, 1985](#)). Other changes can be seen at the transcriptional level, where the involvement of repressor-type basic helix-loop-helix (bHLH) gene *Hes3* is downregulated while *Hes5* expression increases ([Hatakeyama et al., 2004](#); [Kageyama et al., 2008](#)). RGC progenitor cells will divide asymmetrically, self-renewing, giving rise to progenitor cells and eventually differentiating into neuronal and glial cells ([Haubensak et al., 2004](#); [Noctor et al., 2004](#); [Rowitch and Kriegstein, 2010](#)).

Radial glial cells identification has evolved from recognition solely based on morphology to the identification of RGC markers and, more recently, RGC gene expression profiles. In these studies, it has been shown that RGCs change their morphology and gene expression during the developmental process. Thus, the description of their gene expression profile and/or their specific marker expression has been used to define RGC subpopulations that are found at specific developmental stages or in certain regions of the CNS.

Historically, at the gene expression level, cells that expressed glutamate aspartate transporter (GLAST) (*SCL1A3*), glutamate synthase (GS), S100 β , tenascin C (TN-C), brain lipid binding protein (BLBP), SCO-spondin, and the intermediate filaments

glial fibrillary acidic protein (GFAP), Nestin, and Vimentin (VIM) were generally considered RGCs ([Mori et al., 2005](#); [März et al., 2010](#); [Diotel et al., 2020](#)). Therefore, these markers have been adopted as the "typical" RGC markers. However, not all of them are RGC specific. For example, BLBP, S100 β , GFAP, and GS are also expressed by NECs and some astrocytes ([Robel et al., 2011](#); [Lattke and Guillemot, 2022](#)). Moreover, some of these markers are only expressed transiently in RGCs, depending on the differentiation stage ([Gotz et al., 2013](#)). In view of these provisos, the repertoire of RGC markers is continuously expanding with the discovery of new gene products. Among these are Sox2, PAX6, Hes1, Hes5, and N-cadherin, that are considered markers that can be of use to identify RGC populations in rodents and humans ([Levitt and Rakic, 1980](#); [Kageyama et al., 2008](#); [Malatesta et al., 2008](#); [März et al., 2010](#); [Krencik and Zhang, 2011](#); [Johnson et al., 2016](#)). In the last few years, our knowledge of RGCs has expanded significantly due to the use of single-cell RNA-sequencing (sc-RNAseq) technology. Additional putative markers for RGCs have been proposed, such as PDGFD, HOPX, and ITGB5, identified in human stem cells of the ventricular and outer subventricular neocortex. These markers still need to be further characterized to determine their specificity to RGCs ([Pollen et al., 2015](#)).

Differences between cell cycle, markers, and neuronal fate have made it clear that RGCs comprise a heterogenic population ([Pinto and Götz, 2007](#); [Malatesta et al., 2008](#); [Pollen et al., 2015](#); [Scott et al., 2021](#)). This was well established in the early 2000 when colocalization analysis reveal different RGC marker expressions within the RGCs ([Hartfuss et al., 2001](#)). In both the zebrafish and human CNS, studies have shown that RGCs are more heterogenic than originally thought. For example, sc-RNAseq experiment of the zebrafish spinal cord revealed a small subset of RGCs to be oligodendrocyte progenitor cells given their Sox19a and olig2 marker expression ([Scott et al., 2021](#)). Similarly, in the human telencephalon, nine different RGC progenitor clusters were identified via a combination of VIM, SOX2, Hes5, and DLK1 gene expression profiling and immunostaining ([Eze et al., 2021](#)). Human cortical RGC also showed a transcriptional diversity that apical versus non-apical RGCs which were then classified as pro-neural or multipotent RGC ([Johnson et al., 2015](#)). It is expected that the growing identification of markers increases the likelihood of presenting a comprehensive characterization of RGC origin, development, and possible differences between species, brain regions, and/or developmental stages.

As is evident, the remaining challenge is to characterize cellular populations that might differ among developmental stages, anatomical regions and/or species in their gene expression, to determine developmental, evolutionary and functional homologies. In [Table 1](#) we have listed some markers commonly used to identify RGC and RGLC and the species where they have been detected.

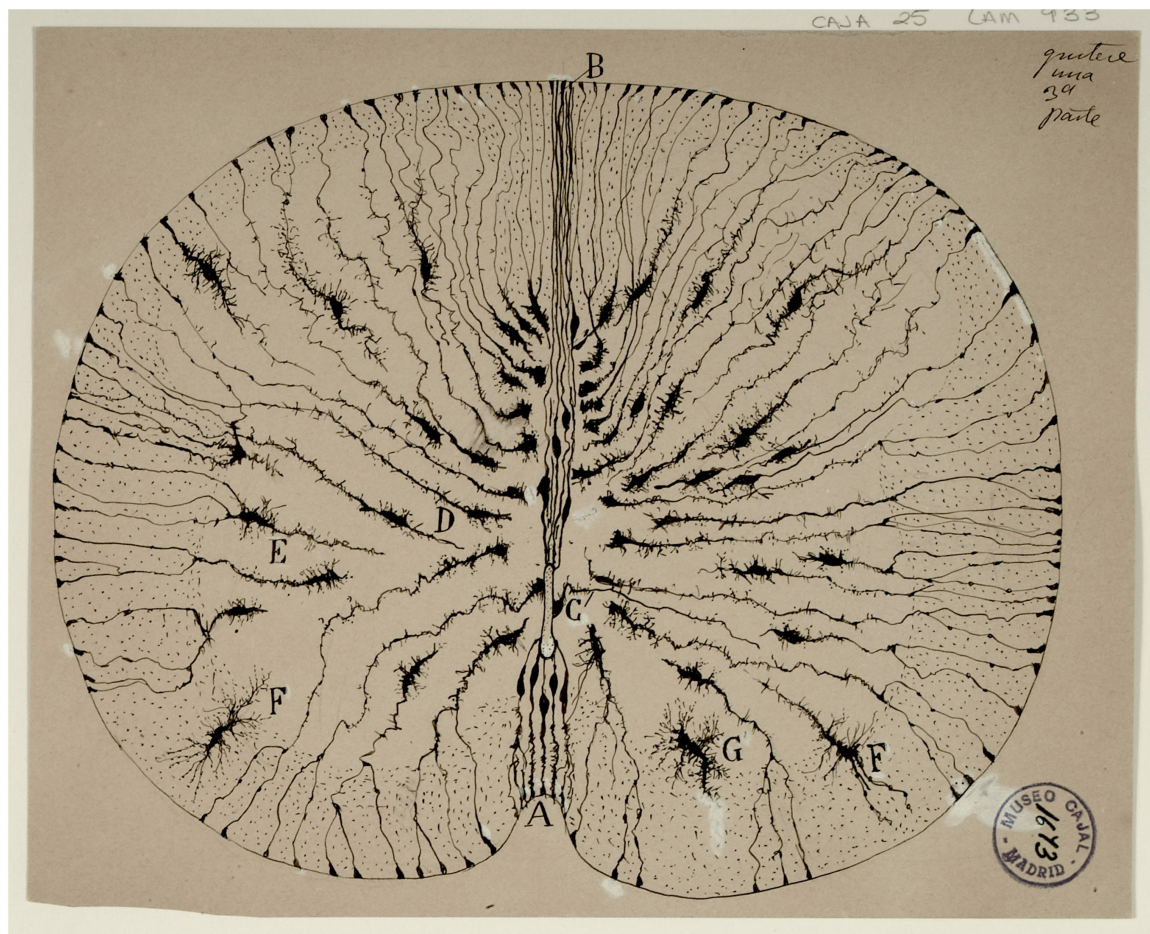


FIGURE 1

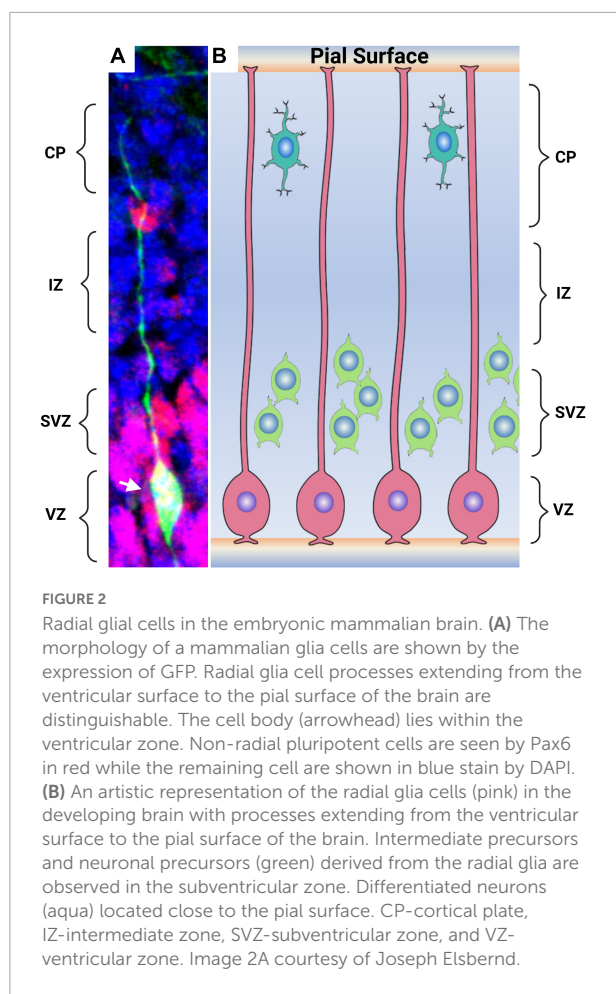
Original drawing by Santiago Ramón y Cajal depicting the radial glia cells in Golgi-stained neonatal mouse spinal cord sections. The radial morphology of the cells, extending from the central canal to the outside perimeter of the cord is clearly observed. Reproduced with permission from the Cajal Institute, Madrid.

Radial glia-like cells in vertebrates

Due to their initial association with embryological development, the term RGC has not been well accepted to name cells that express radial morphology and RGC markers in the adult vertebrate CNS. The nomenclature used to name these cells mostly depends on the species or on the anatomical region where they are found. For example, radial ependymoglia cells, Bergmann radial glia, and Müller glial cells are terms used to describe them in the spinal cord, cerebellum, and retina, respectively (Goldman, 2014; Gao et al., 2021; Walker and Echeverri, 2022). Similarly, cells that share these characteristics in the subventricular zone (SVZ) and subgranular zone (SGZ) of adult mammals have been interchangeably addressed in the literature as neural stem cells (NSC), RGLC, and radial astrocyte (RA) (Gebara et al., 2016; Berg et al., 2018; Joven and Simon, 2018; Lust and Tanaka, 2019; Obernier and Alvarez-Buylla, 2019; Urbán et al., 2019; Zambusi and Ninkovic, 2020). Given

their original description as a glial cell lineage, in this review we will use the term RGLC when referring to these adult cells, while the term RGC will be reserved to name the embryonic cells.

The best case to consider RGLCs in adult vertebrates is probably the existence of cells that continue to proliferate throughout the animal's life in the hippocampal dentate gyrus (DG) and in the SVZ of the lateral ventricle (Götz and Barde, 2005; Urbán et al., 2016, 2019; Obernier and Alvarez-Buylla, 2019; Figure 3). Those that reside in the SGZ have long processes that reach the granule cell layer and extend into the inner molecular layer. Extensive studies on this region have categorized the RGLC population into type I and type II cells also known as quiescent NSC (qNSC) and active NSC (aNSC) (Gonçalves et al., 2016; Urbán et al., 2016). Besides their morphological resemblance to embryonic RGCs, they also share distinctive marker expressions, such as BLBP, Sox2, GFAP, and Nestin (Bonaguidi et al., 2011).



Similar to what has been observed in the SGZ, the adult SVZ niche also contains cells expressing astroglia markers and having radial glial-like morphology. These cells, called B cells, were initially thought to be proliferating astrocytes given their astroglial marker expression (Doetsch et al., 1999; Capilla-Gonzalez et al., 2015). However, they were eventually demonstrated to be neurogenic progenitors, resembling types I and II RGLCs of the SGZ niche (Rushing and Ihrie, 2016). Due to their progenitor capacity, they are also commonly addressed in the literature as NSC, while others have used the term “radial astrocytes” or “SVZ astrocyte” (Kriegstein and Alvarez-Buylla, 2009). The B cells also share with SGZ cells their distinction by proliferative capacity, where qNSC give rise to aNSCs and differ in some of the markers that they express (Berg et al., 2018; Ruddy and Morshead, 2018). For example, upon activation, quiescent B cells upregulate Nestin and EGFR (Ruddy and Morshead, 2018).

Radial glia-like cells have also been extensively studied in the adult zebrafish brain, mainly in the telencephalon but also in the hindbrain, mesencephalon, cerebellum, medulla oblongata, and retina (Grandel et al., 2006; Than-Trong and Bally-Cuif, 2015; Barbosa and Ninkovic, 2016; Diotel et al., 2020; Figure 3). The best studied region is the pallial zone, located in the dorsal

telencephalon. Given that this region is on the brain’s outer surface, it is more accessible for experimental procedures. It has been documented that some of the residing cells within this region bear a morphology reminiscent of mammalian RGCs (Barbosa and Ninkovic, 2016). They show a polarized morphology with their bodies within the ventricular surface and their processes spanning through the parenchyma. Cells in the pallial region express GFAP, BLBP, Fabp7a, Sox2, Her4.1, Hey1, and Nestin, meeting the accepted distinctive RGC molecular profile (Barbosa et al., 2004; Dray et al., 2015; Than-Trong et al., 2018). Heterogeneity between cells in the pallial niche has also been proven, classifying them as type I and type II cells based on their proliferative status (März et al., 2010). Analogous to adult rodent cells in the SGZ, most RGLCs in the zebrafish are in a quiescent state (known as type I cells) while only 5% are actively proliferating (known as type II cells) as shown by PCNA or MCM2/5 expression (Adolf et al., 2006; Diotel et al., 2010, 2020; Rodriguez Viales et al., 2015; Labusch et al., 2020).

In summary, the present evidence strongly suggests that an RGC-like population persists through vertebrate development and can be found in certain specialized niches in the adult brain.

Radial glia in invertebrates

While RGCs have been described in all vertebrate classes, establishing the occurrence of RGC in invertebrates has been a challenge. Studies of radial glia in invertebrates can be described, at their best as patchy, where some animal groups have been studied while others have been largely ignored. These studies also suffer from differences in the use of scientific tools or markers to characterize the cells. Nonetheless, some bona fide RGLCs have been described in invertebrate organisms, and most of these reports can be found in the review of glia evolution authored by Verkhratsky et al. (2019).

Probably, the most extensive comparative study of RGLCs in invertebrates was done using transmission electron microscopy (TEM) and immunolabeling for SCO-spondin glycoprotein (Helm et al., 2017). Researchers analyzed two invertebrate protostomes (the annelid *Owenia fusiformis* and the priapulid worm *Pirapulus caudatus*) and two invertebrate deuterostomes, the non-chordate sea star *Asteria rubens* and the hemichordate acorn worm *Balanoglossus misakiensis*. They reported cells with prominent radial morphology in all species. The radial morphology correlated with the presence of immunoreactivity to Reissner’s substance (the major component of Reissner’s substance is SCO-spondin). Although positive immunoreactivity was observed in all organisms, extensive data was provided only for *O. fusiformis*, where positive labeling for RGLCs was found in larval, juvenile, and adult animals (Helm et al., 2017). Thus, RGLCs expressing at least one RGC marker were found in protostomes. A different study, focusing on another annelid, the earthworm *Eisenia fetida* identified two

TABLE 1 Radial glia and radial glia-like cell markers.

Gene/Marker/ Antigen	Rodents				Zebrafish			Axolotl
	Embryonic	Adult SGZ	Adult SVZ	Müller glia	Larvae	Adult VZ	Müller Glia	
Radial morphology	+	+/-	+	+	+	+	+	ND
BLBP	+	+	+	—	—	+	—	ND
Cyp19a1b (aromatase B)	—	—	—	—	+	+	—	ND
GFAP	—	+	+	+	+	+	+	+
GLAST	+	+	+	+	ND	ND	+	ND
GS	+	ND	ND	+	ND	+	+	ND
Her4.1	—	—	—	—	—	+	—	ND
Hes1	+	+	+	+	—	—	—	ND
Hes5	+	+	+	+	—	—	—	ND
Nestin	+	+	+	ND	+	+	ND	+
Pax6	+	ND	+	+	—	—	+	+
S100B	+	—	—	ND	ND	+	ND	ND
Sox2	+	+	+	+	+	+	+	+
Tenascin—C	+	ND	+	ND	ND	ND	ND	ND
Vimentin	+	ND	+	+	+	+	+	+

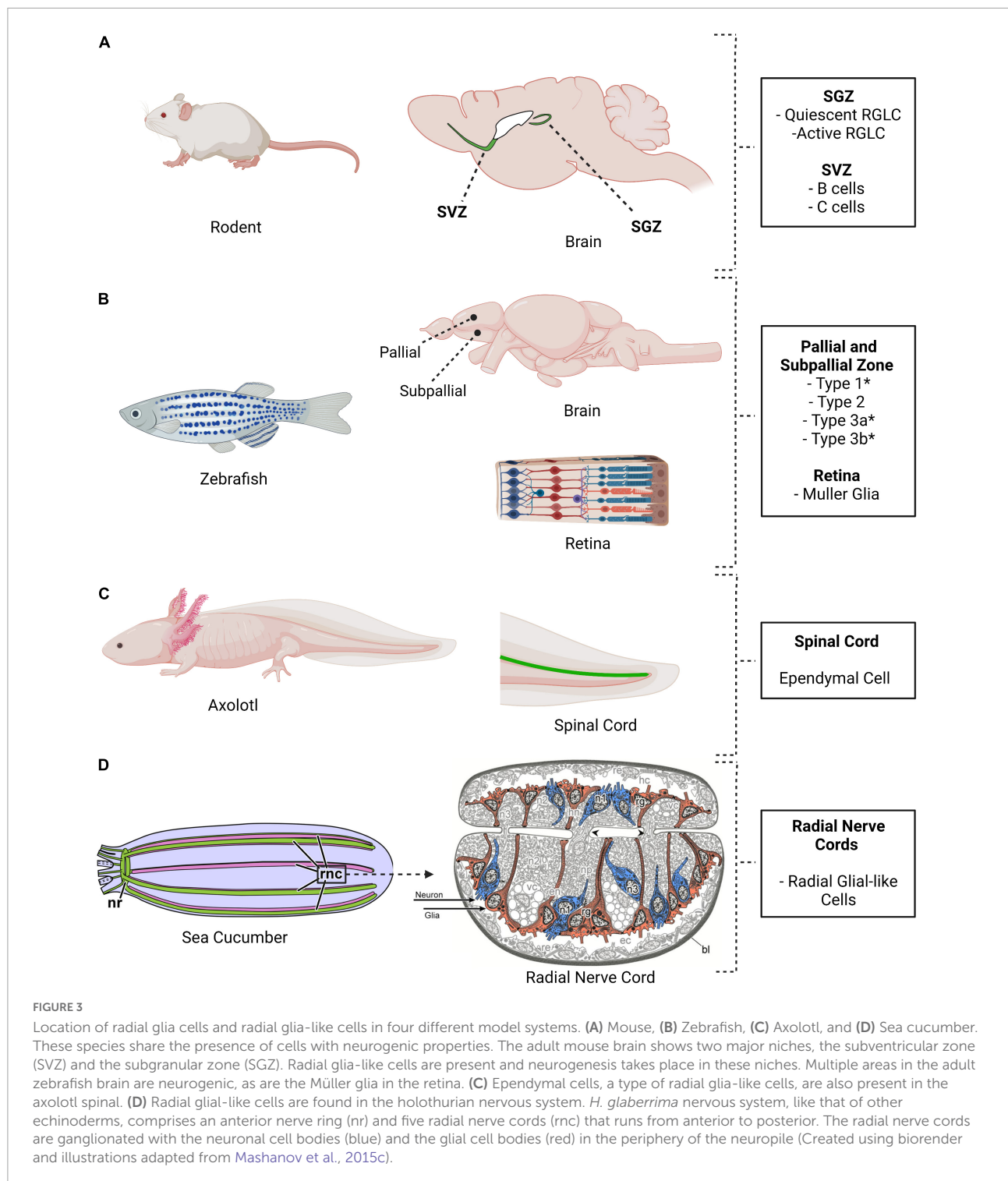
+, marker is expressed only in response to injury. +/-, two types of glia are found in this region. One with radial morphology and another non-radial. ND, no information regarding marker was found in these cells. The table illustrates radial glia markers' presence during development and radial glia-like cells of adults in different cerebral regions. It takes into consideration markers found for rodents, zebrafish, and axolotl's spinal cord. Table was created using the following references: Holder et al. (1990), Akimoto et al. (1993), Walder et al. (2003), Bernardos et al. (2007), Kageyama et al. (2008), Thummel et al. (2008), März et al. (2010), Hutton and Pevny (2011), Gotz et al. (2013), Sundholm-Peters et al. (2004), Patro et al. (2015), and Tazaki et al. (2017), among others already cited in this article.

types of cells: the long process glial cells (named neurilemmal glial cells) in the ventral ganglion periphery and another glial cell (supporting-nutritory cells) (Csoknya et al., 2012). However, in this case, they reported positive GFAP immunoreactivity in the supporting cells and not in the cells with radial morphology. Thus, showing some of the inconsistencies that plague the protostome reports.

In contrast to the invertebrate protostomes, RGLCs have been reported in the three major groups of invertebrate deuterostomes: the Echinodermata, the Hemichordata and the non-vertebrate Chordata. In fact, some investigators propose that it is within the deuterostomes that RGCs first appeared and undertake a pivotal role in the formation of the CNS (Verkhatsky et al., 2019). For example, RGLCs have been identified in the Amphioxus CNS (Bozzo et al., 2021). Amphioxus is a cephalochordate (a subphylum that groups non-vertebrate considered the closest relatives of the Vertebrata). One study analyzed the expression of RGC markers (EAAT2, GFAP/vimentin, and SCO-spondin) by cells in the developing CNS, asserting that some of these markers are expressed by cells with radial morphology (Bozzo et al., 2021). Moreover, these embryonic cells are the progenitors of RGLCs found in the adult lancelet CNS in regions that are known to sustain neurogenesis (Bozzo et al., 2021).

There is also strong experimental support for the presence of RGLCs in the echinoderms (Mashanov and Zueva, 2020).

Studies performed by our group in the sea cucumber *Holothuria glaberrima* have identified RGLCs by employing a combination of cell morphology, Reissner's substance immunolabeling, and the expression of a yet to be characterized antigen recognized by monoclonal antibodies (Mashanov et al., 2010, 2013). The RGLCs were described in radial nerve cords (RNCs), which are ganglionated nerves that, like the vertebrate spinal cord, contain neuronal and glial cell bodies and extensive fiber tracts. In the echinoderms, the neuronal and glial cell bodies are localized toward the periphery of the cords, while the fibers are mainly found in a neuropile in the center (Figures 3, 4). In *H. glaberrima*, RGLCs represent 60–70% of the cells in the RNCs consisting of most, if not all, glial cells present (Mashanov et al., 2010; Mashanov and Zueva, 2020). Mashanov et al. (2015a) outlined the general similarities of the echinoderm RGLC and vertebrate RGCs in their published chapter on the NS of the Echinodermata: “(i) orthogonal orientation of the cell's main axis to the plane of the neuroepithelium; (ii) highly elongated shape of the cells allowing them to span the entire thickness of the neuroepithelium between the apical and basal surfaces, (iii) long thick bundles of intermediate filaments, which run mostly along the main axis of the cell and fill almost the entire intracellular space of the glial processes, (iv) short protrusions branching off at a right angles from the main processes and penetrating into the surrounding neural parenchyma” and (v) the expression of a “material similar to the so-called Reissner's substance of chordates”.



The holothurian RGLCs constantly proliferate in the adult sea cucumber RNC lateral regions (Mashanov et al., 2005). However, it is still unknown whether these cells proliferate symmetrically or asymmetrically, nor the type of cells produced under homeostatic conditions (Mashanov et al., 2015c). Differential expression patterns were documented by *in situ*

hybridization studies identifying *Myc* transcripts, suggesting that RGLCs are a heterogeneous population. Nonetheless, additional validations are required for a more in-depth characterization of RGLC subpopulations.

In summary, cells with radial glial morphology have been described in several invertebrate groups, however, in

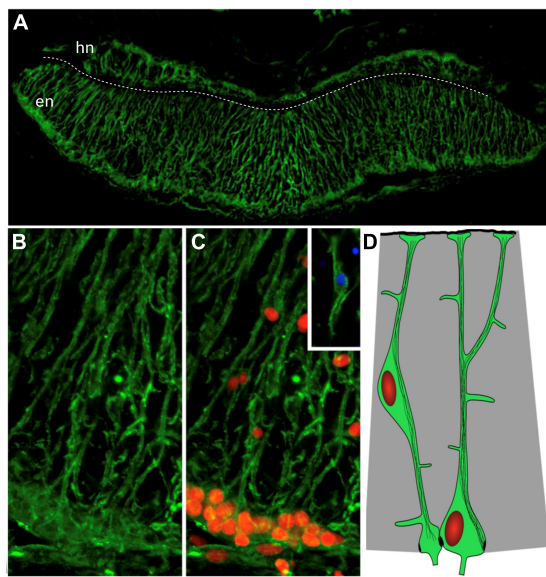


FIGURE 4

Radial glia-like cells in the holothurian radial nerve cord.

(A) Cross section of the radial nerve cord of the sea cucumber *H. glaberrima* showing immunoreactivity to ERG1 antibody. This antibody recognizes the radial glia-like cells full extension from the apical to the basal borders. (B,C) Magnification of the ectoneural band highlighting the radial morphology of the cell extensions and the presence of the nuclei (red) within the cell bodies. Insert shows the cell body of a glial cell found within the neuropile. The white dash line divides the hyponeural region (hn) from the ectoneural region (en) of the radial nerve cord. (D) Diagram depicting the cell body and extensions with cytoskeletal filaments (Adapted from Mashanov et al., 2010).

many cases, the typical RGC vertebrate molecular markers are not documented. Most of the early studies identifying these cells in invertebrates focus on their radial morphology but are hindered by the possible limited cross-reactivity of antibodies that recognize vertebrate RGC markers when used against invertebrate tissues. Thus, identifying their presence in invertebrates remains an enduring process. However, the availability of transcriptome studies promises to advance the comparative studies needed to characterize invertebrate RGLCs. Future experiments using new and evolving techniques will improve invertebrate RGLC identification and serve to elucidate their relationship to the vertebrate RGC and RGLC populations (Csoknya et al., 2012; Verkhatsky et al., 2019).

Roles and functions of radial glia cells

Their defining developmental role

The roles of RGCs were first described in mammals during embryonic development. The original descriptions and putative

roles were based on histological and anatomical data and, as such, were subject to different interpretations (Bentivoglio and Mazzarello, 1999). RGCs were easily identified at different developmental stages by their elongated fibers that traversed the neural tube from the ventricular zone, where the cell bodies are located, to the pial surface (Figure 5). The functions of these morphological features were elucidated in the early 1970s by Pasko Rakic in a series of trailblazing experiments (Rakic, 1971; Bentivoglio and Mazzarello, 1999; Shu and Richards, 2001; Barresi et al., 2005; Johnson et al., 2016). Using electron microscopy, he and colleagues showed that in rhesus monkeys, RGCs were responsible for guiding and distributing migrating newborn neurons from the ventricular zone to the developing cortex. Thus, they proposed that RGCs function as scaffolding cells for migrating cerebral cortex neurons. In addition to the scaffolding functions, RGCs were subsequently found to divide and eventually give rise to many brain components. These include not only cells but functional structures, such as their interaction with endothelial cells to form what will become the blood-brain barrier (BBB) (Johnson et al., 2016).

In the developing mammalian brain, RGCs divide symmetrically and asymmetrically, self-renewing, and giving rise to other cell populations (Figure 5; Haubensak et al., 2004; Noctor et al., 2004). Some of these cells are neurons, while others are ependymal cells, glial cells (astrocytes and oligodendrocytes), and stem cells (here considered RGLCs) that will continue to reside in specific niches of the adult brain (Rakic, 1995; Malatesta et al., 2003; Merkle et al., 2004; Spassky et al., 2005). The RGC behavior is greatly influenced by intrinsic cell signaling and local environmental signals (Götz et al., 2002). It is now accepted that RGCs consist of a heterogeneous population of progenitor cells, some with a predetermined capacity to differentiate into neurons (Malatesta et al., 2000, 2008; Howard et al., 2008). Other populations are more prone to give rise to glial cells. For example, at the end of the human embryonic developmental period, approximately 20 weeks after fertilization, some RGCs begin their transformation into GFAP⁺ astrocytes, losing their ventricular contacts while acquiring the astrocytic morphology (deAzevedo et al., 2003; Howard et al., 2008). Thus, a relationship between RGC disappearance and astrocyte number increase has been demonstrated by cell birth lineage tracing experiments (Voigt, 1989).

Roles of vertebrate radial glia-like cells

The main role associated with all RGLCs is homeostatic neurogenesis. Neurogenesis is the birth of new neurons via precursor cells (intermediate progenitors and neuroblasts) that originate from RGLC proliferation and maturation (Encinas et al., 2011; Berg et al., 2018). Although neurogenesis is mainly associated with embryonic development, some animals

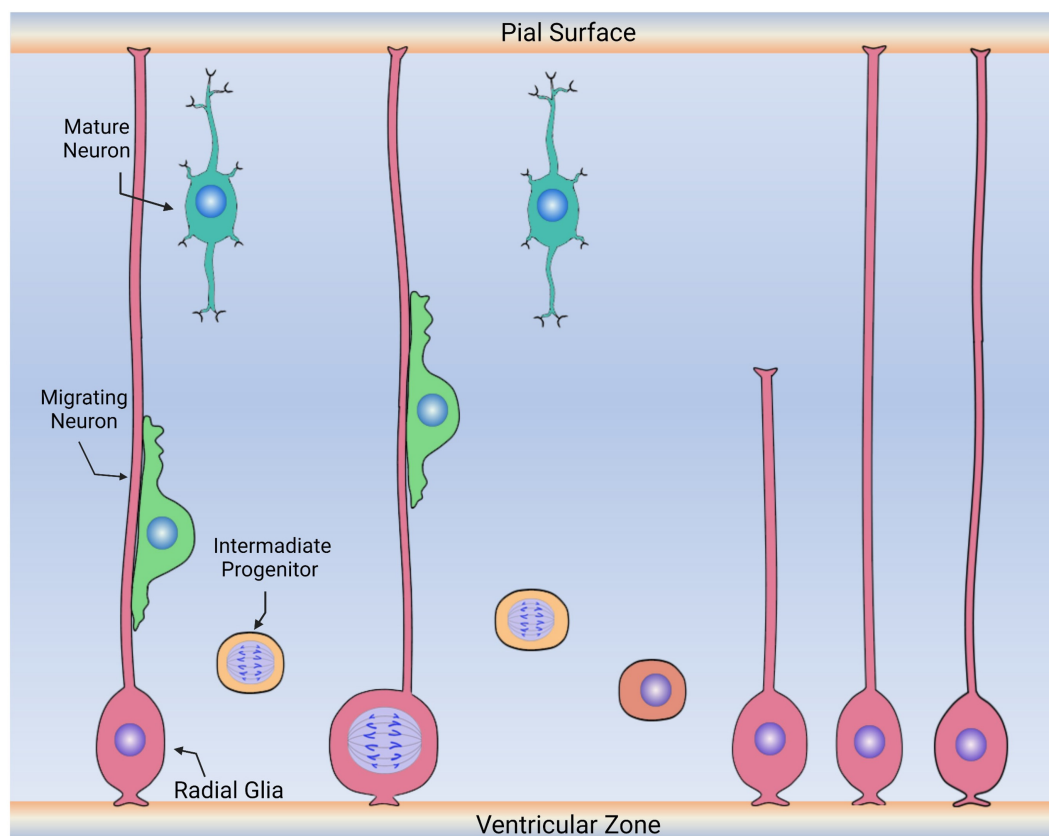


FIGURE 5

Diagram depicting the embryonic roles of radial glia cells. During embryonic development, radial glia cells (pink) divide symmetrically and asymmetrically, generating other radial glia and intermediate progenitors (labeled in yellow) that will continue to migrate, proliferate and differentiate into new neurons or glia. Radial glia cells also serve as the scaffold for the migration of neuronal precursors (green) to the upper layers of the cerebral cortex. Following migration, these cells then differentiate into neurons (aqua) or other glia (not shown).

maintain a homeostatic neurogenic process throughout most, if not all, their life span (Lust and Tanaka, 2019; Abbott and Nigussie, 2020; Zambusi and Ninkovic, 2020). In fact, one of the earliest examples of adult neurogenesis was reported to occur during the breeding season in the CNS of adult canaries (Nottebohm, 1989). In adult rodents, RGLCs of the SGZ have been shown to produce excitatory neurons that might be involved in memory formation and learning capacity (Ming and Song, 2011; Berg et al., 2018). Similarly, the RGLC of the SVZ are associated with adult neurogenesis. But in this case with the formation of inhibitory neurons that contribute to odor discrimination and odor-reward association (Grelat et al., 2018; Li et al., 2018). It is important to consider that, despite their proliferative capacities, most of these cells are in a dormant or quiescent state (Bonaguidi et al., 2011; Berg et al., 2018). In fact, the study of quiescence and proliferation of RGCLs has become an important area of study (Urbán et al., 2016, 2019; Lattke and Guillemot, 2022). It is believed that the quiescent state is necessary to conserve stemness, therefore maintaining the cell's neurogenic potential. The hypothesis being, that this cell state

avoids DNA, protein, or mitochondrial damage that might lead to premature cell senescence, eliminating the stem cell niche (Urbán et al., 2019; Labusch et al., 2020). Particular attention has been placed on identifying the local niche signals that control quiescence, such as the Notch pathway or *ASCL1* (Geribaldi-Doldán et al., 2018; Harris and Guillemot, 2019; Dray et al., 2021; Harris et al., 2021; Terreros-Roncal et al., 2021). Other experiments are focused on signaling pathways that channel the newly generated cells toward a neuronal versus a glial phenotype (Domínguez-García et al., 2020, 2021).

In the adult zebrafish brain, sixteen RCLC niches provide the organism with lifelong neuron replacement sites (Labusch et al., 2020). In the telencephalon, cell types I, II, IIIa, and IIIb have been suggested to be the main neurogenic cells (März et al., 2010; Diotel et al., 2020). Type I and II cells have been characterized as quiescent and proliferative, respectively, while type IIIa/b are thought to be higher committed progenitor cells (Diotel et al., 2020). These classifications highlight the similar roles of RGLCs in zebrafish and rodents, where quiescent cells maintain niche and stemness while active cells replenish the tissue

with new neurons. Breakthroughs in single-cell transcriptomic sequencing have provided important information on RGLC progeny and cell heterogeneity. In particular, experiments performed with transgenic zebrafish have shown that the RGLC population is able to generate a diverse pool of newborn neurons (Lange et al., 2020). Moreover, some of these RGLC also expressed *olig2* marker suggesting the presence of a RGLC subpopulation that will transition to oligodendrocyte progenitors (Lange et al., 2020). Thus, these studies demonstrate the heterogeneity of the RGLC population in the vertebrate brain.

In summary, RGLCs in adult organisms appear to be associated with the formation of new neurons. The present evidence strongly suggests that an RGLC population persists through vertebrate development and is involved in neurogenesis in the adult brain. The limitations in neurogenesis, or its absence in most regions of the adult vertebrate brain and spinal cord, account for the limited regeneration abilities of the vertebrate CNS. Therefore, the second part of this review will focus on the role of RGLCs in NS regenerative processes. We begin this section with an overview of NS regeneration, the models where it has been studied, and the mechanisms that take place.

Principles of nervous system regeneration

Nervous system regeneration, or the lack of it, remains one of the least understood and most diverse areas of study in the field of regeneration biology. Many species can regenerate their NS components, though the cellular and molecular machinery they employ to attain their regeneration capacities can differ. Hence, understanding the fundamental biological processes by which regeneration-competent species achieve regeneration has been the field's holy grail for quite some time. Given the diverse nature of regeneration, understanding these processes will greatly benefit from a comparative/evolutionary analysis using a highly diverse subset of species.

NS regeneration is defined as the process by which damaged nervous tissue undergoes regrowth or renewal, restoring the system's morphology and physiological functions. At the cellular level, NS regeneration can be divided into two independent processes: axonogenesis and neurogenesis. Axonogenesis is the process by which the axon of a pre-existing neuron regrows after suffering an injury, re-establishing the original connection. In vertebrates, axon regeneration is commonly seen in the peripheral nervous system (PNS); however, the same phenomenon is highly limited or fails to occur in the CNS. Axonogenesis does not fall within the scope of this review. For those interested in axonogenesis, we recommend some publications on the topic (Chisholm et al., 2016; Wahane et al., 2019).

Our focus is mainly on injury-induced neurogenesis and the mechanisms by which adult organisms activate neurogenesis

in response to injury. Similar to the processes of cellular homeostasis or regeneration in other organs or tissues, new nerve cells originate from: (1) a reservoir of stem cells that can proliferate and differentiate to maintain tissue physiology or restore and repair an injury site or (2) by dedifferentiation, where a cell population reverts to a less-differentiated state by losing some of their differentiated properties (Tanaka, 2016; Yao and Wang, 2020; Walker and Echeverri, 2022). These cells can eventually divide and produce replacement cells for the organ or tissue in question. (3) A third mechanism has been proposed where tissues can generate new cells via trans-differentiation. In this case, similar to dedifferentiation, the cells lose their specific phenotypic characteristics and then acquire the phenotype of a different cell type without transiting through a "less differentiated stage" (Walker and Echeverri, 2022).

Regeneration is a dynamic process that can vary significantly from one species to another. A common mechanistic link to achieve NS regeneration has not been elucidated and, in fact, there might not be one common mechanism, but mechanisms might differ according to the animal groups. For example, protostomes with extensive regenerating abilities, such as Hydra or Planaria, are known to have pluripotent stem cells that can give rise to the NS cells and other cell types (Cebrià et al., 2002; Agata and Umesono, 2008). Crayfish, a well-studied crustacean, possess neurogenic niches with primary precursor neural progenitors (Sullivan and Beltz, 2005; Ventura et al., 2019). These cells can divide into secondary precursors that migrate to the olfactory structures and later differentiate into olfactory interneurons or projection neurons. The primary precursors cannot self-renew and depend on a re-supply of circulating hemocytes to replenish the precursor cell stock (Chaves da Silva et al., 2013; Benton et al., 2014). A comprehensive review on crustacean and insect adult neurogenesis and their regenerative mechanism can be found in Simões and Rhiner (2017).

Radial glia-like cell role in adult vertebrate regeneration

In most vertebrates, CNS neuroregenerative capacities have been associated with the presence of RGLCs. These cells are well-known to repopulate and replenish injured tissues. Thus, organisms that retain RGLCs in their adult stages are associated with higher CNS regenerative abilities (Alvarez-Buylla et al., 1987; Malatesta et al., 2000; Malatesta and Götz, 2013; Hartfuss et al., 2001; Jurisch-Yaksi et al., 2020). For example, RGCs in rodents normally disappear soon after birth. In neonatal rodents whose brains have been injured, RGCs persist for a more extended period, suggesting that after neonatal brain injury, RGCs serve as scaffolds for neuroblasts to migrate and populate the lesioned site (Jinnou et al., 2018). Several studies have addressed the concept of proliferation and neurogenesis in adult rodents' SVZ and SGZ after inducing focal ischemia or traumatic brain injury (Kernie and Parent,

2010). Following these injuries, progenitor cells on both niches respond by proliferating. Whether the cells generated by RGLC survive, migrate, and incorporate into CNS circuits remain controversial. Studies have determined that, in mammals, most of the cells generated in response to cerebral cortex injury do not survive and those that do are unable to successfully migrate to the lesion site and differentiate (Chang et al., 2016). However, cell extrinsic factors have been shown to increase cell survivability and/or migration. For example, SVZ cell exposure to fibroblast growth factor (FGF2) increased cell survivability while inhibition of ADAM17 metalloprotease increased not only survival but also migration to the injured primary motor cortex (Chang et al., 2016; Geribaldi-Doldán et al., 2018).

While these studies expose the neurogenetic response to injury of adult RGLCs and their potential for facilitating CNS repair, these capacities in mammals are highly limited. Thus, the reason to focus on alternative model systems where the role of RGLCs in CNS regeneration can be explored extensively. Here we provide information on three of them, two vertebrate animals, the axolotl, the zebrafish, and an invertebrate, the sea cucumber.

Regeneration in axolotl and zebrafish spinal cord

The spinal cord is a component of the CNS whose regenerative capacities have been intensively probed. While the formation of a glial scar hinders spinal cord regeneration in mammals, in some amphibians and fishes, morphological and functional recovery is possible. In the two best studied species, axolotl and zebrafish, new neurons are formed by so called “ependymal cells” surrounding the central spinal canal (Chernoff et al., 2003; Reimer et al., 2008). These ependymal cells clearly fulfill our description of RGLCs. First, they are derived from RGCs during development, Second, they retain their radial morphology and third they express some of the RG markers (GFAP and Sox2) (Hui et al., 2015b). In addition, several markers associated with RGCs are expressed by the proliferating cells following spinal cord injury (Hui et al., 2015a). After injury, these cells have been shown to retract their radial processes, proliferate and differentiate to form new spinal cord neurons (Reimer et al., 2008; Ribeiro et al., 2017; Cura Costa et al., 2021; Klatt Shaw et al., 2021; Walker and Echeverri, 2022). In fact, some researchers have suggested that these RGLCs undergo dedifferentiation during regeneration, as can be determined by the changes in cell morphology, the loss of the radial extensions, and the differential expression of genes associated with neural stem cell properties (Walder et al., 2003; Ribeiro et al., 2017; Walker and Echeverri, 2022).

It is important to contrast these RGLCs/ependymal cells of zebrafish and axolotl to those in adult mammals. In the latter, the ependymal cells are cuboidal and multiciliated and usually

do not divide after differentiation or in some cases, give rise only to glia (Spassky et al., 2005; Meletis et al., 2008). Moreover, transcriptomic studies have shown that ependymal cells in mice are transcriptionally different from neural stem cells and are not induced to divide by brain injury (Shah et al., 2018).

Recent single-cell transcriptomics have identified distinct precursor populations that generate neuronal and glial cells during zebrafish embryonic development (Scott et al., 2021). Likewise, single cell transcriptomics have shown several populations of RGLCs to be present in the developing and adult axolotl brain, and one of these appears to be activated by injury (Wei et al., 2022). Thus, we expect that future experiments will provide crucial information on the ependymal populations in the adult zebrafish and axolotl and the transitions they undergo during spinal cord regeneration.

Nervous system regeneration in zebrafish brain

Zebrafish RGLCs in different niches can generate new neurons under normal homeostatic conditions and in response to injury (Barbosa et al., 2004; Dray et al., 2015). However, there are differences between homeostatic neuron production and their formation in response to injury. In the former, newborn neurons remain below the progenitor zone while in the latter, newborn neurons migrate to populate injured brain regions (Barbosa et al., 2004; Dray et al., 2015). During normal conditions, only type II zebrafish RGLCs are in the active proliferative state (Dray et al., 2015). Their proliferation modes have been shown to be symmetric and asymmetric, providing self-renewing and progenitor-generating properties (Barbosa et al., 2004; Barbosa and Ninkovic, 2016; Rothenaigier et al., 2011; Dray et al., 2015). Most of the RGLC proliferation capacities are enhanced in response to injury. For example, using an engineered neurotoxic amyloid- β 42 (A β 42)-dependent zebrafish, which represents degenerative neurotoxicity similar to that observed in Alzheimer's disease, researchers found that some RGLCs responded to this injury by extensive proliferation and enhanced neurogenesis (Bhattarai et al., 2016). One unique difference between homeostatic- and injury-generated neurons is that the latter have enhanced migratory capacities, rendering them able to restore damaged tissue (Barbosa et al., 2015; Barbosa and Ninkovic, 2016).

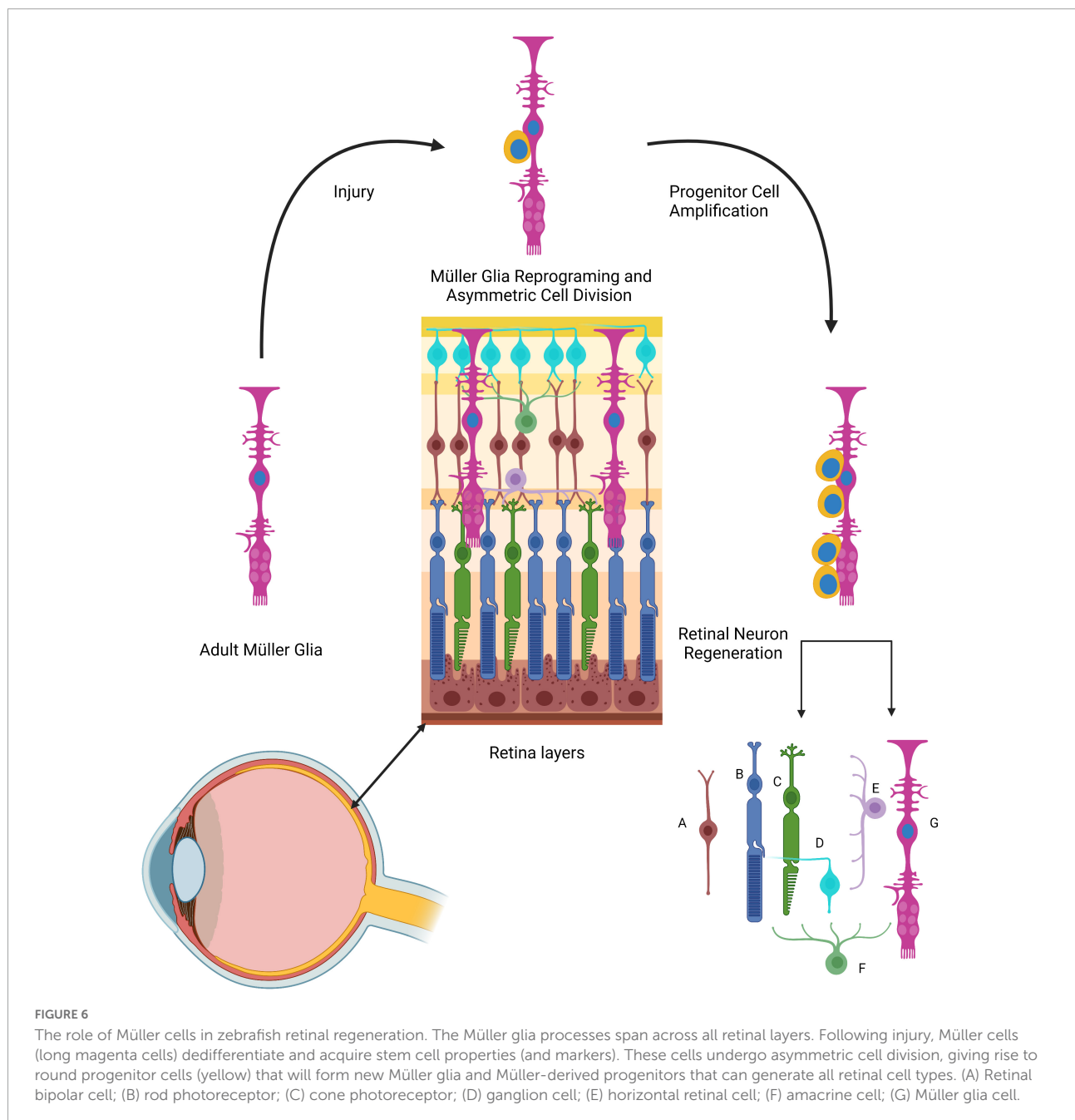
Müller glia and regeneration of zebrafish retina

Zebrafish also display an impressive ability to regenerate their retina. The zebrafish retina, typical of vertebrate retinas, is composed of three cellular layers, six principal neuron

population types, and four types of glial cells (Fadool and Dowling, 2008). One of the glial cells, the Müller glia, stands out in that it plays a unique role in retinal regeneration (Figure 6). The Müller glia apico-basal morphology enables structural and metabolic support for the retinal neuron population (Reichenbach and Bringmann, 2013; Lenkowski and Raymond, 2014). Müller glia are considered mature, differentiated cells. Under normal retinal physiology, they contribute to retinal synaptic activity by recycling GABA and glutamate neurotransmitters. Moreover, these cells support neurons by regulation of extracellular volume and molecular

composition, transporting metabolic waste, and providing neurons with nutrients (Lenkowski and Raymond, 2014; Gao et al., 2021).

Müller glia have been proclaimed as being the retinal RGLC, mainly because of their radial morphology but also because they share some of the RGC markers, such as GS, GFAP, GLAST, and VIM (Linser and Moscona, 1979; Malchow et al., 1989; Lenkowski and Raymond, 2014; Gao et al., 2021). In response to injury, Müller glia play a pivotal role in retina regeneration. This process has been extensively studied at both cellular and molecular levels. It has been documented



that these RGLCs respond to injury in the following manner: (i) Müller glia sense injury in the retina, (ii) The cells dedifferentiate or reprogram, (iii) Dedifferentiated Müller glia divide asymmetrically, producing one Müller glia cell and one Müller glia-derived progenitor cell, (iv) The progenitor cells divide and populate the injury site creating neurogenic clusters.

Transgenic zebrafish lines have provided crucial data to acknowledge Müller glia as the neural stem cell source for retinal regeneration (Bernardos and Raymond, 2006; Fimbel et al., 2007; Thummel et al., 2008). A study assessing their proliferation capacity by BrdU incorporation or PCNA immunodetection determined, that although there are proliferating Müller glia in the uninjured retina, most of the cells are in a quiescent state that is regulated by Notch signaling (Bernardos et al., 2007). As a response to injury, Notch expression decreases, facilitating Müller glia proliferation (Ruddy and Morshead, 2018; Sahu et al., 2021). Similar to other RGLCs, the Müller glia are also a source of neurons, as demonstrated by using transgenic reporter lines showing that proliferating Müller glia gave rise to rod progenitors (Bernardos et al., 2007).

Among the events that involve Müller glia in the regeneration process, we would like to highlight the dedifferentiation response since cell dedifferentiation stands out as a process by which RGLCs in various organisms appear to contribute to NS regeneration. Müller glia dedifferentiation has been assessed by the re-expression of retinal progenitor neurogenic markers, such as BLBP, ALCAMA, Rx1, six3b, and Pax6 (Fimbel et al., 2007; Thummel et al., 2008; Nagashima et al., 2013). In addition, Sox2 role has been functionally assessed in the regenerating zebrafish retina, demonstrating it to be an essential factor regulating Müller glia proliferation and reprogramming (Gorsuch et al., 2017; Elsaiedi et al., 2018). Even though progenitor marker re-expression is observed, it has been suggested that Müller glia cells only partially dedifferentiate, given that mature Müller glial cell markers persist at a lower level during dedifferentiation. Nonetheless, dedifferentiation enables Müller glia cells to divide asymmetrically producing a neural progenitor cell that proliferates and builds neurogenic clusters that will differentiate into the retina neural cell types (Bernardos et al., 2007).

Conserved functions of the Müller glia mediating ocular regeneration have also been documented in other vertebrates (Fischer and Bongini, 2010; Goldman, 2014). In the early 2000s, Fischer and Reh (2001) demonstrated that, in chickens, following retinal injury by injection of *N*-methyl-D-aspartate (NMDA), Müller glia cells re-entered the cell cycle and could differentiate into retinal neurons as determined by co-labeling of BrdU and retinal markers. The available data point to Müller glia cells as the essential cell for retinal repair (Fischer and Reh, 2003).

Nervous system regeneration in echinoderms

Radial glia-like cells also play a major role in the regeneration of the echinoderm NS following transection of the RNC. Immediately after transection, the injured edges of the RNCs begin to swell, nerve fibers become distorted, and programmed cell death occurs. This initial phase is characterized by extracellular matrix (ECM) deposition at the wound site and elongation of the RNC ectoneural component (Mashanov et al., 2008, 2014). At the cellular level, evidence using electron and fluorescence microscopy strongly suggests that the RGLCs dedifferentiate and provide the precursors for the new nervous tissue (Figure 7; San Miguel-Ruiz et al., 2009; Mashanov et al., 2010, 2013). Two observations have been key to outline the RGLCs role: First, the degradation of the RGLC radial cytoskeletal fibers during regeneration and second, BrdU experiments demonstrating the dedifferentiated RGLC proliferative capacities. The morphological changes are key features consistent with other known dedifferentiating cells. Hence, by losing their complex radial extensions, they transition into a less specialized state and proliferate. The dedifferentiated cells also migrate toward the injury gap and participate in one of the main events in RNC regeneration: the reconnection of the transected stumps. During this phase, both RNC edges from each side of the transected side close together until they reconnect and restore the RNC. This is thought to be one of the most complex processes involving signaling molecules that control growth, migration, axial polarity, and cell-to-cell interactions (San Miguel-Ruiz et al., 2009; Mashanov et al., 2013).

Following RNC reconnection, dedifferentiated cells in the regenerative zone redifferentiate, which is reflected by the growth in the size of the “new” tissue between the stumps. Birth dating experiments have shown that dedifferentiated RGLCs cells play a role in this event by giving rise to both RGLCs and neuronal populations in the regenerated structure (Mashanov et al., 2013). What regulates RGLC redifferentiation to neuronal or non-neuronal lineage still needs to be studied. However, many researchers have suggested that this process is mainly intrinsically regulated, while still having extrinsic signaling molecules and/or cell-to-cell interaction that could influence the outcome (Mashanov et al., 2008, 2013; San Miguel-Ruiz et al., 2009). By the end of the regenerative response, cell proliferation and apoptosis return to basal levels, and cellular and anatomical organization of the “new” RNC segment resembles that of the non-transected cords.

Much of what is known of RNC regeneration in holothurians has been provided by histological analyses, including immunohistochemistry, *in situ* RNA hybridizations, and RNA sequencing analysis. The transcriptomics data analyses have provided a list of differentially expressed genes that are possible candidates for genes controlling or modulating

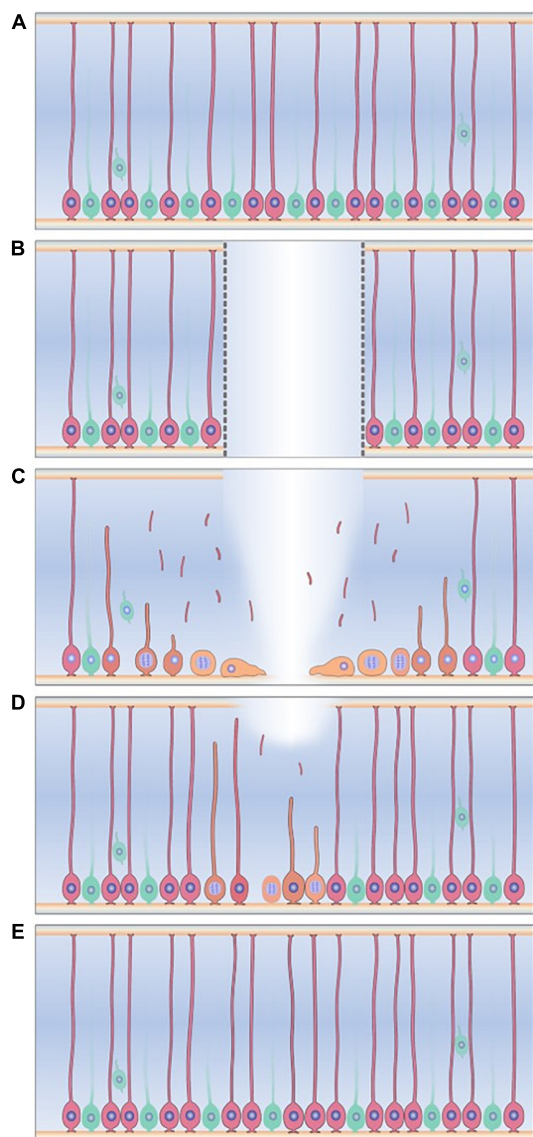


FIGURE 7

Radial glia-like cells response to injury in the sea cucumber *Holothuria glaberrima*. (A) Radial glia-like cells (pink) are the main glial cell found adjacent to neurons (green) in the holothurian radial nerve cord. (B) Transection of the radial nerve cord causes gap between two ends of the RNC (C) Radial glia-like cells adjacent to the injury dedifferentiate, as seen by degradation of cytoskeletal structures and loss of the radial processes. The dedifferentiated cells (yellow) are now able to proliferate and migrate to the injury gap. (D) The dedifferentiated cells and their progenitors give rise to the new radial glia-like cells and neurons that repopulate and restores the new tissue. (E) The regeneration process is completed when the progenitors of these cells differentiate into the new neurons and glia.

the regeneration response (Mashanov et al., 2014). For example, ECM-related genes were among the most differentially expressed transcripts in all regeneration stages. Many other genes have been targeted as possible candidates and even

transposable elements have been suggested to be associated with RNC regeneration (Mashanov et al., 2012).

Specific genes have been probed to modulate particular cellular events, for example, the process of RGLC dedifferentiation. The first candidate genes to be evaluated as promoters of RGLC dedifferentiation were the Yamanaka pluripotency factors Oct1/2/11, c-Myc, Sox 2, and Klf1/2/4 homologs (Mashanov et al., 2015b). The study demonstrated that (i) all four factors were expressed during early and late stages of RNC regeneration, (ii) Myc was significantly overexpressed during all the stages of regeneration, suggesting that it played an important role in the regeneration process (iii) Oct1/2/11 and SoxB1 (sox 1 homolog) were significantly downregulated at the late stages of RNC regeneration (Mashanov et al., 2015b). These findings were further explored by evaluating the role of *Myc* via RNA knockdown in regenerating RNC. The results demonstrated that *Myc* regulated programmed cell death and RGLC cell dedifferentiation, two major events known to occur during the initial regeneration response (Mashanov et al., 2015c). Therefore, it has been assumed that the *in vivo* de-differentiation observed in the RGLCs is more akin to a partial reprogramming that partially dedifferentiates cells to a precursor-like phenotype than to the total reprogramming that produces pluripotent stem cells.

New advances

Two recent advances open the possibility for new findings on the regeneration of the echinoderm CNS and the possible role of the RGLCs. The first is the development of an *in vitro* RNC explant preparation (Quesada-Díaz et al., 2021). Most, if not all, of the previously performed studies were done using the holothurian RNC complex, that in addition to the RNC is composed of longitudinal muscle bands, water vascular canal, and the body wall. This has made it almost impossible to directly target the RNC without affecting the surrounding tissues. Using an isolated RNC explant that can be cultured provides a unique opportunity to study cellular events associated with dedifferentiation and regeneration without the influence of adjacent tissues (Quesada-Díaz et al., 2021). Moreover, it has been documented that in *in vitro* cultures, RGLCs within the RNC continue to exhibit the same morphological changes shown to occur during *in vivo* RGC dedifferentiation. Hence, this method provides a tool to study the dedifferentiation process while excluding other cellular events in the surrounding tissues. This culture system is presently being used to provide a transcriptomic profile of regenerating RNC explants.

The second advancement with a significant impact on RNC regeneration studies is the sequencing of the *H. glaberrima* genome. This was published as a draft genome, providing a tool that can benefit both the regenerative and developmental

biology fields (Medina-Feliciano et al., 2021). The genome serves as a database to identify potential genes and molecules that are key to the regeneration process. In addition, for researchers working with *H. glaberrima* that have obtained transcriptomic data from regenerating intestine and nerve complex at different time points, the genome provides a reference to the identification of the differentially-expressed genes. The impacts of these results will reach their full potential when a reference genome becomes available.

Concluding remarks

Radial glial cells are found in all developing vertebrate CNS studied to date, and RGLCs are found in adult CNS components of vertebrates and invertebrates. The morphological data accumulated over decades, together with the avalanche of new molecular data provided by new sequencing methods is molding our view of these cells. In fact, we can describe the RG/RGLCs in terms of Ernst Haeckel dictum “Ontogeny recapitulates Phylogeny” where their evolution and their presence in different animal species parallels their embryological development. In this scenario, the RGCs that form in the early deuterostome embryo can be considered the precursors of both neurons and glia of the adult CNS. In invertebrate deuterostomes, these cells remain in the adult CNS, retaining morphological properties and particular molecular markers along with their competence to undergo neurogenesis. Thus, organisms where RGLCs are found are capable of robust CNS regeneration. A similar situation is observed in some amphibians and fishes, where the progeny of RGCs is retained as RGLCs and are responsible for both homeostatic and regenerative neurogenesis in adults. In contrast, in mammals, only certain areas of the adult CNS retain RGLCs. The cells in these niches might express specific markers along with more general RGLC markers, giving rise to particular subpopulations. Nonetheless, these RGLC subpopulations are able to undergo homeostatic neurogenesis and, after injury, these RGLCs are activated and appear to participate in some, albeit limited, CNS restoration. One last example will serve to strengthen the evolution/regeneration comparison. It is well documented that in most vertebrates, the capacity for CNS regeneration is lost during the developmental process. Nowhere is this better shown than in the *Xenopus* model where the ability to regenerate their transected spinal cord changes dramatically as the animal undergoes metamorphosis. In this respect, the work by the Larraín lab (Edwards-Faret et al., 2018, 2021) has correlated the regenerative capacity to the presence of RGLCs, expressing certain molecular markers and showing neurogenic capacity found in the regenerative stage but lost or greatly diminished in the non-regenerative stage.

In addition to the neurogenic regenerative potentials of RGLCs, there are also parallels in the processes by which RGLCs

in different species or different regions of the CNS respond to injury. Specifically, changes observed in their radial morphology and, at the molecular level, in their gene expression profile point out toward a degree of dedifferentiation, where a mature cell reverts into a progenitor/stem cell phenotype as described by Walker and Echeverri (2022). Dedifferentiation allows cells to enter the cell cycle and give rise to new tissue cells. In this respect, it is interesting that activated astrocytes, following trauma to the adult mammalian brain, have also been shown to re-express markers of more immature precursors suggesting a degree of dedifferentiation (Zambusi et al., 2020; Lattke and Guillemot, 2022).

To fully understand the RGCs and RGLCs it becomes crucial to determine the lineage and evolutionary relationship of these cell types. Are all adult RGLCs remnants of the embryonic RGC population that persist in certain areas of the adult brain? Are the invertebrate RGLCs evolutionarily related to the vertebrate RGCs? What, if any, specific marker can be used to identify the RGLC and RGC subpopulations? Modern cell-typing techniques will be important in answering these and other questions. The use of gene expression markers will be decisive in determining the expression profile of the different cell types and the changes that might take place during developmental or functional stages. Equally important will be to determine the factors that induce the neurogenic activity in these cells and the process by which cells might dedifferentiate and/or enter the cell cycle.

The possibility exists that the neurogenic abilities of these cells can be manipulated to respond to traumatic injury so that they serve as proliferating neurogenic progenitors in favor of CNS repair. Apropos to this, dedifferentiation is also being explored as a potential therapy to regenerate the CNS. The idea is to be able to transform the state of the brain into a regeneration-promoting state by, for example, converting terminally differentiated astrocytes into a precursor type cell that could give rise to neurons (Yao and Wang, 2020; Zamboni et al., 2020; Robel et al., 2011; Lattke and Guillemot, 2022). Nonetheless, it is imperative to first lay a foundational understanding of RGC roles, their pathways of regulation, and possible differentiation stages. Key information could be obtained from comparative studies using non-traditional model animals that show extraordinary regeneration abilities. Therefore, we propose that the study of the RGLCs in the echinoderms, particularly in the sea cucumber *H. glaberrima* will provide important information to elucidate neurogenesis activation in adult animals.

Author contributions

YM-N and JG-A wrote part of the manuscript, contributed to the article, and approved the submitted version.

Funding

This study was supported by the National Institute of Health (grant numbers: R21AG057974 and R15NS01686). YM-N was funded by National Science Foundation Bridge to the Doctorate Program (Grant Number: HRD-1906130), and the Research Initiative for Scientific Enhancement (RISE) (grant number: 5R25GM061151-21).

Acknowledgments

We would like to acknowledge Giselle Valentin-Tirado for her significant contributions in the preparation of **Figures 2, 5, 7** and Edwin Peña-Martínez for his support and contributions to the remaining figures.

References

- Aaku-Saraste, E., Hellwig, A., and Huttner, W. B. (1996). Loss of occludin and functional tight junctions, but not ZO-1, during neural tube closure–remodeling of the neuroepithelium prior to neurogenesis. *Dev. Biol.* 180, 664–679. doi: 10.1006/dbio.1996.0336
- Abbott, L. C., and Nigussie, F. (2020). Adult neurogenesis in the mammalian dentate gyrus. *Anat. Histol. Embryol.* 49, 3–16. doi: 10.1111/ahc.12496
- Adolf, B., Chapouton, P., Lam, C. S., Topp, S., Tannhäuser, B., Strähle, U., et al. (2006). Conserved and acquired features of adult neurogenesis in the zebrafish telencephalon. *Dev. Biol.* 295, 278–293. doi: 10.1016/j.ydbio.2006.03.023
- Agata, K., and Umesono, Y. (2008). Brain regeneration from pluripotent stem cells in planarian. *Philos. Trans. R. Soc. Lond B Biol. Sci.* 363, 2071–2078. doi: 10.1098/rstb.2008.2260
- Akimoto, J., Itoh, H., Miwa, T., and Ikeda, K. (1993). Immunohistochemical study of glutamine synthetase expression in early glial development. *Brain Res. Dev. Brain Res.* 72, 9–14. doi: 10.1016/0165-3806(93)90154-3
- Alvarez-Buylla, A., Buskirk, D. R., and Noweborn, F. (1987). Monoclonal antibody reveals radial glia in adult avian brain. *J. Comp. Neurol.* 264, 159–170. doi: 10.1002/cne.902640203
- Barbosa, J., Sanchez-Gonzalez, R., Di-Giaimo, R., Violette, E., Theis, F., Gotz, M., et al. (2004). Live Imaging of adult neural stem cell behavior in the intact and injured zebrafish brain. *Comp. Biochem. Physiol.* 429, 157–173. doi: 10.5061/dryad.hq4v0
- Barbosa, J. S., and Ninkovic, J. (2016). Adult neural stem cell behavior underlying constitutive and restorative neurogenesis in zebrafish. *Neurogenesis* 3:e1148101. doi: 10.1080/23262133.2016.1148101
- Barbosa, J. S., Sanchez-Gonzalez, R., Di-Giaimo, R., Baumgart, E. V., Theis, F. J., Götz, M., et al. (2015). Neurodevelopment. Live imaging of adult neural stem cell behavior in the intact and injured zebrafish brain. *Science* 348, 789–793. doi: 10.1126/science.aaa2729
- Barresi, M. J., Hutson, L. D., Chien, C. B., and Karlstrom, R. O. (2005). Hedgehog regulated Slit expression determines commissure and glial cell position in the zebrafish forebrain. *Development* 132, 3643–3656. doi: 10.1242/dev.01929
- Bentivoglio, M., and Mazzarello, P. (1999). The history of radial glia. *Brain Res. Bull.* 49, 305–315. doi: 10.1016/s0361-9230(99)00065-9
- Benton, J. L., Kery, R., Noonin, C., Söderhäll, I., and Beltz, B. S. (2014). Cells from the immune system generate adult-born neurons in crayfish. *Dev. Cell* 30, 322–333. doi: 10.1016/j.devcel.2014.06.016
- Berg, D. A., Bond, A. M., Ming, G. L., and Song, H. (2018). Radial glial cells in the adult dentate gyrus: What are they and where do they come from? *F1000Res* 7:277. doi: 10.12688/f1000research.12684.1
- Bernardos, R. L., Barthel, L. K., Meyers, J. R., and Raymond, P. A. (2007). Late-stage neuronal progenitors in the retina are radial Müller glia that function as retinal stem cells. *J. Neurosci.* 27, 7028–7040. doi: 10.1523/JNEUROSCI.1624-07.2007
- Bernardos, R. L., and Raymond, P. A. (2006). GFAP transgenic zebrafish. *Gene Expr. Patterns* 6, 1007–1013. doi: 10.1016/j.modgep.2006.04.006
- Bhattarai, P., Thomas, A. K., Cosacak, M. I., Papadimitriou, C., Mashkaryan, V., Froc, C., et al. (2016). IL4/STAT6 signaling activates neural stem cell proliferation and neurogenesis upon amyloid-β42 aggregation in adult zebrafish brain. *Cell Rep.* 17, 941–948. doi: 10.1016/j.celrep.2016.09.075
- Bonaguidi, M. A., Wheeler, M. A., Shapiro, J. S., Stadel, R. P., Sun, G. J., Ming, G. L., et al. (2011). In vivo clonal analysis reveals self-renewing and multipotent adult neural stem cell characteristics. *Cell* 145, 1142–1155. doi: 10.1016/j.cell.2011.05.024
- Bozzo, M., Lacalli, T. C., Obino, V., Caicci, F., Marcenaro, E., Bachetti, T., et al. (2021). Amphioxus neuroglia: Molecular characterization and evidence for early compartmentalization of the developing nerve cord. *Glia* 99, 1654–1678. doi: 10.1002/glia.23982
- Capilla-Gonzalez, V., Herranz-Pérez, V., and García-Verdugo, J. M. (2015). The aged brain: Genesis and fate of residual progenitor cells in the subventricular zone. *Front. Cell. Neurosci.* 9:365. doi: 10.3389/fncel.2015.00365
- Cebrià, F., Kudome, T., Nakazawa, M., Mineta, K., Ikeo, K., Gojobori, T., et al. (2002). The expression of neural-specific genes reveals the structural and molecular complexity of the planarian central nervous system. *Mech. Dev.* 116, 199–204. doi: 10.1016/s0925-4773(02)00134-x
- Chang, E. H., Adorjan, I., Mundim, M. V., Sun, B., Dizon, M. L., Szele, F. G., et al. (2016). Traumatic brain injury activation of the adult subventricular zone neurogenic niche. *Front. Neurosci.* 10:332. doi: 10.3389/fnins.2016.00332
- Chaves da Silva, P. G., Benton, J. L., Sandeman, D. C., and Beltz, B. S. (2013). Adult neurogenesis in the crayfish brain: The hematopoietic anterior proliferation center has direct access to the brain and stem cell niche. *Stem Cells Dev.* 22, 1027–1041. doi: 10.1089/scd.2012.0583
- Chernoff, E. A., Stocum, D. L., Nye, H. L., and Cameron, J. A. (2003). Urodele spinal cord regeneration and related processes. *Dev. Dyn.* 226, 295–307. doi: 10.1002/dvdy.10240
- Chisholm, A. D., Hutter, H., Jin, Y., and Wadsworth, W. G. (2016). The genetics of axon guidance and axon regeneration in *Caenorhabditis elegans*. *Genetics* 204, 849–882. doi: 10.1534/genetics.115.186262
- Csoknya, M., Dénes, V., and Wilhelm, M. (2012). Glial cells in the central nervous system of earthworm, *Eisenia fetida*. *Acta Biol. Hung.* 63, 114–128. doi: 10.1556/ABiol.63.2012.Suppl.1.11

Conflict of interest

The authors declare that the research was conducted in the absence of any commercial or financial relationships that could be construed as a potential conflict of interest.

Publisher's note

All claims expressed in this article are solely those of the authors and do not necessarily represent those of their affiliated organizations, or those of the publisher, the editors and the reviewers. Any product that may be evaluated in this article, or claim that may be made by its manufacturer, is not guaranteed or endorsed by the publisher.

- Cura Costa, E., Otsuki, L., Rodrigo Albors, A., Tanaka, E. M., and Chara, O. (2021). Spatiotemporal control of cell cycle acceleration during axolotl spinal cord regeneration. *eLife* 10:e55665. doi: 10.7554/eLife.55665
- deAzevedo, L. C., Fallet, C., Moura-Neto, V., Dumas-Duport, C., Hedin-Pereira, C., Lent, R., et al. (2003). Cortical radial glial cells in human fetuses: Depth-correlated transition into astrocytes. *J. Neurobiol.* 55, 288–298. doi: 10.1002/neu.10205
- Diotel, N., Lübke, L., Strähle, U., and Rastegar, S. (2020). Common and distinct features of adult neurogenesis and regeneration in the telencephalon of zebrafish and mammals. *Front. Neurosci.* 14:568930. doi: 10.3389/fnins.2020.568930
- Diotel, N., Vaillant, C., Gueguen, M. M., Mironov, S., Anglade, I., Servili, A., et al. (2010). Cxcr4 and Cxcl12 expression in radial glial cells of the brain of adult zebrafish. *J. Comp. Neurol.* 518, 4855–4876. doi: 10.1002/cne.22492
- Doetsch, F., Caillé, I., Lim, D. A., García-Verdugo, J. M., and Alvarez-Buylla, A. (1999). Subventricular zone astrocytes are neural stem cells in the adult mammalian brain. *Cell* 97, 703–716. doi: 10.1016/s0092-8674(00)80783-7
- Dominguez-García, S., Geribaldi-Doldán, N., Gómez-Oliva, R., Ruiz, F. A., Carrascal, L., Bolívar, J., et al. (2020). A novel PKC activating molecule promotes neuroblast differentiation and delivery of new neurons in brain injuries. *Cell Death Dis.* 11:262. doi: 10.1038/s41419-020-2453-9
- Dominguez-García, S., Gómez-Oliva, R., Geribaldi-Doldán, N., Hierro-Bujalance, C., Sendra, M., Ruiz, F. A., et al. (2021). Effects of classical PKC activation on hippocampal neurogenesis and cognitive performance: Mechanism of action. *Neuropsychopharmacology* 46, 1207–1219. doi: 10.1038/s41386-020-00934-y
- Dray, N., Bedu, S., Vuillemin, N., Alunni, A., Coolen, M., Krecsmarik, M., et al. (2015). Large-scale live imaging of adult neural stem cells in their endogenous niche. *Development* 142, 3592–3600. doi: 10.1242/dev.123018
- Dray, N., Than-Trong, E., and Bally-Cuif, L. (2021). Neural stem pools in the vertebrate adult brain: Homeostasis from cell-autonomous decisions or community rules? *BioEssays* 43:2000228. doi: 10.1002/bies.202000228
- Edwards-Faret, G., Cebrián-Silla, A., Méndez-Olivos, E. E., González-Pinto, K., García-Verdugo, J. M., Larrain, J., et al. (2018). Cellular composition and organization of the spinal cord central canal during metamorphosis of the frog *Xenopus laevis*. *J. Comp. Neurol.* 526, 1712–1732. doi: 10.1002/cne.24441
- Edwards-Faret, G., González-Pinto, K., Cebrián-Silla, A., Peñailillo, J., García-Verdugo, J. M., Larrain, J., et al. (2021). Cellular response to spinal cord injury in regenerative and non-regenerative stages in *Xenopus laevis*. *Neural Dev.* 16:2. doi: 10.1186/s13064-021-00152-2
- Elsaedi, F., Macpherson, P., Mills, E. A., Jui, J., Flannery, J. G., and Goldman, D. (2018). Notch suppression collaborates with Ascl1 and Lin28 to unleash a regenerative response in fish retina, but not in mice. *J. Neurosci.* 38, 2246–2261. doi: 10.1523/JNEUROSCI.2126-17.2018
- Encinas, J. M., Michurina, T. V., Peunova, N., Park, J. H., Tordo, J., Peterson, D. A., et al. (2011). Division-coupled astrocytic differentiation and age-related depletion of neural stem cells in the adult hippocampus. *Cell Stem Cell* 8, 566–579. doi: 10.1016/j.stem.2011.03.010
- Eze, U. C., Bhaduri, A., Haessler, M., Nowakowski, T. J., and Kriegstein, A. R. (2021). Single-cell atlas of early human brain development highlights heterogeneity of human neuroepithelial cells and early radial glia. *Nat. Neurosci.* 24, 584–594. doi: 10.1038/s41593-020-00794-1
- Fadool, J. M., and Dowling, J. E. (2008). Zebrafish: A model system for the study of eye genetics. *Prog. Retin. Eye Res.* 27, 89–110. doi: 10.1016/j.preteyeres.2007.08.002
- Fimbel, S. M., Montgomery, J. E., Burket, C. T., and Hyde, D. R. (2007). Regeneration of inner retinal neurons after intravitreal injection of ouabain in zebrafish. *J. Neurosci.* 27, 1712–1724. doi: 10.1523/JNEUROSCI.5317-06.2007
- Fischer, A. J., and Bongini, R. (2010). Turning Müller glia into neural progenitors in the retina. *Mol. Neurobiol.* 42, 199–209. doi: 10.1007/s12035-010-8152-2
- Fischer, A. J., and Reh, T. (2001). Müller glia are a potential source of neural regeneration in the postnatal chicken retina. *Nat. Neurosci.* 4, 247–252. doi: 10.1038/85090
- Fischer, A. J., and Reh, T. A. (2003). Potential of Müller glia to become neurogenic retinal progenitor cells. *Glia* 43, 70–76. doi: 10.1002/glia.10218
- Gadisseux, J. F., and Evrard, P. (1985). Glial-neuronal relationship in the developing central nervous system: A histochemical-electron microscope study of radial glial cell particulate glycogen in normal and reeler mice and the human fetus. *Dev. Neurosci.* 7, 12–32. doi: 10.1159/000112273
- Gao, H. A. L., Huang, X., Chen, X., and Xu, H. (2021). Müller Glia-Mediated Retinal Regeneration. *Mol. Neurobiol.* 58, 2342–2361. doi: 10.1007/s12035-020-02274-w
- Gebara, E., Bonaguidi, M. A., Beckervordersandforth, R., Sultan, S., Udry, F., Gijis, P. J., et al. (2016). Heterogeneity of radial glia-like cells in the adult hippocampus. *Stem Cells* 34, 997–1010. doi: 10.1002/stem.2266
- Geribaldi-Doldán, N., Carrasco, M., Murillo-Carretero, M., Domínguez-García, S., García-Cózar, F. J., Muñoz-Miranda, J. P., et al. (2018). Specific inhibition of ADAM17/TACE promotes neurogenesis in the injured motor cortex. *Cell Death Dis.* 9:862. doi: 10.1038/s41419-018-0913-2
- Goldman, D. (2014). Müller glial cell reprogramming and retina regeneration. *Nat. Rev. Neurosci.* 15, 431–442. doi: 10.1038/nrn3723
- Gonçalves, J. T., Schafer, S. T., and Gage, F. H. (2016). Adult neurogenesis in the hippocampus: From stem cells to behavior. *Cell* 167, 897–914. doi: 10.1016/j.cell.2016.10.021
- Gorsuch, R. A., Lahne, M., Yarka, C. E., Petravick, M. E., Li, J., Hyde, D. R., et al. (2017). Sox2 regulates Müller glia reprogramming and proliferation in the regenerating zebrafish retina via Lin28 and Ascl1a. *Exp. Eye Res.* 161, 174–192. doi: 10.1016/j.exer.2017.05.012
- Götz, M., and Barde, Y. A. (2005). Radial glial cells defined and major intermediates between embryonic stem cells and CNS neurons. *Neuron* 46, 369–372. doi: 10.1016/j.neuron.2005.04.012
- Götz, M., Hartfuss, E., and Malatesta, P. (2002). Radial glial cells as neuronal precursors: A new perspective on the correlation of morphology and lineage restriction in the developing cerebral cortex of mice. *Brain Res. Bull.* 57, 777–788. doi: 10.1016/s0361-9230(01)00777-8
- Gotz, M., Ransom, B., and Kettenmann, H. (2013). *Neuroglia*. Oxford: Oxford University Press. doi: 10.1093/med/9780199794591.001.0001
- Grandel, H., Kaslin, J., Ganz, J., Wenzel, I., and Brand, M. (2006). Neural stem cells and neurogenesis in the adult zebrafish brain: Origin, proliferation dynamics, migration and cell fate. *Dev. Biol.* 295, 263–277. doi: 10.1016/j.ydbio.2006.03.040
- Grelat, A., Benoit, L., Wagner, S., Moigneu, C., Lledo, P.-M., and Alonso, M. (2018). Adult-born neurons boost odor-reward association. *Proc. Natl. Acad. Sci. U. S. A.* 115, 2514–2519. doi: 10.1073/pnas.1716400115
- Harris, L., and Guillemot, F. (2019). HES1, two programs: Promoting the quiescence and proliferation of adult neural stem cells. *Genes. Dev.* 33, 479–481. doi: 10.1101/gad.325761.119
- Harris, L., Rigo, P., Stieh, T., Gaber, Z. B., Austin, S. H. L., and Edwards, A. (2021). Coordinated changes in cellular behavior ensure the lifelong maintenance of the hippocampal stem cell population. *Cell Stem Cell* 28, 863–879. doi: 10.1016/j.stem.2021.01.003
- Hartfuss, E., Galli, R., Heins, N., and Götz, M. (2001). Characterization of CNS precursor subtypes and radial glia. *Dev. Biol.* 229, 15–30. doi: 10.1006/dbio.2000.9962
- Hatakeyama, J., Bessho, Y., Katoh, K., Ookawara, S., Fujioka, M., Guillemot, F., et al. (2004). Hes genes regulate size, shape and histogenesis of the nervous system by control of the timing of neural stem cell differentiation. *Development* 131, 5539–5550. doi: 10.1242/dev.01436
- Haubensack, W., Attardo, A., Denk, W., and Huttner, W. B. (2004). Neurons arise in the basal neuroepithelium of the early mammalian telencephalon: A major site of neurogenesis. *Proc. Natl. Acad. Sci. U. S. A.* 101, 3196–3201. doi: 10.1073/pnas.0308600100
- Helm, C., Karl, A., Beckers, P., Kaul-Strehlow, S., Ulbricht, E., Kourtesis, I., et al. (2017). Early evolution of radial glial cells in Bilateria. *Proc. Biol. Sci.* 284:20170743. doi: 10.1098/rspb.2017.0743
- Holder, N., Clarke, J. D. W., Kamalati, T., and Lane, E. B. (1990). Heterogeneity in spinal radial glia demonstrated by intermediate filament expression and HRP labelling. *J. Neurocytol.* 19, 915–928. doi: 10.1007/BF01186819
- Howard, B. M., Mo, Z., Filipovic, R., Moore, A. R., Antic, S. D., Zecevic, N., et al. (2008). Radial glia cells in the developing human brain. *Neuroscientist* 14, 459–473. doi: 10.1177/1073858407313512
- Hui, S. P., Nag, T. C., and Ghosh, S. (2015b). Neural cells and their progenitors in regenerating zebrafish spinal cord. *Int. J. Dev. Biol.* 64, 353–366. doi: 10.1387/ijdb.190130sg
- Hui, S. P., Nag, T. C., and Ghosh, S. (2015a). Characterization of proliferating neural progenitors after spinal cord injury in adult zebrafish. *PLoS One* 10:e0143595. doi: 10.1371/journal.pone.0143595
- Hutton, S. R., and Pevny, L. H. (2011). SOX2 expression levels distinguish between neural progenitor populations of the developing dorsal telencephalon. *Dev. Biol.* 352, 40–47. doi: 10.1016/j.ydbio.2011.01.015
- Jinnou, H., Sawada, M., Kawase, K., Kaneko, N., Herranz-Pérez, V., Miyamoto, T., et al. (2018). Radial glial fibers promote neuronal migration and functional

- recovery after neonatal brain injury. *Cell Stem Cell* 22, 128–137.e9. doi: 10.1016/j.stem.2017.11.005
- Johnson, K., Barragan, J., Bashiruddin, S., Smith, C. J., Tyrrell, C., Parsons, M. J., et al. (2016). Gfap-positive radial glial cells are an essential progenitor population for later born neurons and glia in the zebrafish spinal cord. *Glia* 64, 1170–1189. doi: 10.1002/glia.22990
- Johnson, M. B., Wang, P. P., Atabay, K. D., Murphy, E. A., Doan, R. N., Hecht, J. L., et al. (2015). Single-cell analysis reveals transcriptional heterogeneity of neural progenitors in human cortex. *Nat. Neurosci.* 18, 637–646. doi: 10.1038/nn.3980
- Joven, A., and Simon, A. (2018). Homeostatic and regenerative neurogenesis in salamanders. *Prog. Neurobiol.* 170, 81–98. doi: 10.1016/j.pneurobio.2018.04.006
- Jurisch-Yaksi, N., Yaksi, E., and Kizil, C. (2020). Radial glia in the zebrafish brain: Functional, structural, and physiological comparison with the mammalian glia. *Glia* 68, 2451–2470. doi: 10.1002/glia.23849
- Kageyama, R., Ohtsuka, T., and Kobayashi, T. (2008). Roles of Hes genes in neural development. *Dev. Growth Differ.* 50, S97–S103. doi: 10.1111/j.1440-169X.2008.00993.x
- Kernie, S. G., and Parent, J. M. (2010). Forebrain neurogenesis after focal ischemic and traumatic brain injury. *Neurobiol. Dis.* 37, 267–274. doi: 10.1016/j.nbd.2009.11.002
- Klatt Shaw, D., Saraswathy, V. M., Zhou, L., McAdow, A. R., Burris, B., Butka, E., et al. (2021). Localized EMT reprograms glial progenitors to promote spinal cord repair. *Dev. Cell* 56, 613–626.e7. doi: 10.1016/j.devcel.2021.01.017
- Krencik, R., and Zhang, S. C. (2011). Directed differentiation of functional astroglial subtypes from human pluripotent stem cells. *Nat. Protoc.* 6, 1710–1717. doi: 10.1038/nprot.2011.405
- Kriegstein, A., and Alvarez-Buylla, A. (2009). The glial nature of embryonic and adult neural stem cells. *Annu. Rev. Neurosci.* 32, 149–184. doi: 10.1146/annurev.neuro.051508.135600
- Labusch, M., Mancini, L., Morizet, D., and Bally-Cuif, L. (2020). Conserved and Divergent Features of Adult Neurogenesis in Zebrafish. *Front. Cell Dev. Biol.* 8:525. doi: 10.3389/fcell.2020.00525
- Lange, C., Rost, F., Machate, A., Reinhardt, S., Lesche, M., Weber, A., et al. (2020). Single cell sequencing of radial glia progeny reveals the diversity of newborn neurons in the adult zebrafish brain. *Development* 147:dev185595. doi: 10.1242/dev.185595
- Lattke, M., and Guillemot, F. (2022). Understanding astrocyte differentiation: Clinical relevance, technical challenges, and new opportunities in the omics era. *WIREs Mech. Dis.* 14:e1557. doi: 10.1002/wsbm.1557
- Lenkowski, J. R., and Raymond, P. A. (2014). Müller glia: Stem cells for generation and regeneration of retinal neurons in teleost fish. *Prog. Retin. Eye Res.* 40, 94–123. doi: 10.1016/j.preteyeres.2013.12.007
- Levitt, P., and Rakic, P. (1980). Immunoperoxidase localization of glial fibrillary acidic protein in radial glial cells and astrocytes of the developing rhesus monkey brain. *J. Comp. Neurol.* 193, 815–840. doi: 10.1002/cne.901930316
- Li, W. L., Chu, M. W., Wu, A., Suzuki, Y., Imayoshi, I., and Komiyama, T. (2018). Adult-born neurons facilitate olfactory bulb pattern separation during task engagement. *eLife* 7:e33006. doi: 10.7554/eLife.33006
- Linsler, P., and Moscona, A. A. (1979). Induction of glutamine synthetase in embryonic neural retina: Localization in Müller fibers and dependence on cell interactions. *Proc. Natl. Acad. Sci. U. S. A.* 76, 6476–6480. doi: 10.1073/pnas.76.12.6476
- Lust, K., and Tanaka, E. M. (2019). A comparative perspective on brain regeneration in amphibians and teleost fish. *Dev. Neurobiol.* 79, 424–436. doi: 10.1002/dneu.22665
- Malatesta, P., Appolloni, I., and Calzolari, F. (2008). Radial glia and neural stem cells. *Cell Tissue Res.* 331, 165–178. doi: 10.1007/s00441-007-0481-8
- Malatesta, P., and Götz, M. (2013). Radial glia from boring cables to stem cell stars. *Development* 140, 483–486. doi: 10.1242/dev.085852
- Malatesta, P., Hack, M. A., Hartfuss, E., Kettenmann, H., Klinkert, W., Kirchhoff, F., et al. (2003). Neuronal or glial progeny: Regional differences in radial glia fate. *Neuron* 37, 751–764. doi: 10.1016/s0896-6273(03)00116-8
- Malatesta, P., Hartfuss, E., and Götz, M. (2000). Isolation of radial glial cells by fluorescent-activated cell sorting reveals a neuronal lineage. *Development* 127, 5253–5263. doi: 10.1242/dev.127.24.5253
- Malchow, R. P., Qiant, H., and Ripps, H. (1989). Gamma-Aminobutyric acid (GABA)-induced currents of skate Müller (glial) cells are mediated by neuronal-like GABAA receptors. *Proc. Natl. Acad. Sci. U. S. A.* 86, 4326–4330. doi: 10.1073/pnas.86.11.4326
- März, M., Chapouton, P., Diotel, N., Vaillant, C., Hesl, B., Takamiya, M., et al. (2010). Heterogeneity in progenitor cell subtypes in the ventricular zone of the zebrafish adult telencephalon. *Glia* 58, 870–888. doi: 10.1002/glia.20971
- Mashanov, V., and Zueva, O. (2020). Radial glia in echinoderms. *Dev. Neurobiol.* 79, 396–405. doi: 10.1002/dneu.22659
- Mashanov, V. S., Zueva, O. R., and García-Arrarás, J. E. (2005). Heterogeneous generation of new cells in the adult echinoderm nervous system. *Front. Neuroanat.* 9:123. doi: 10.3389/fnana.2015.00123
- Mashanov, V. S., Zueva, O. R., and García-Arrarás, J. E. (2010). Organization of glial cells in the adult sea cucumber central nervous system. *Glia* 58, 1581–1593. doi: 10.1002/glia.21031
- Mashanov, V. S., Zueva, O. R., and García-Arrarás, J. E. (2012). Posttraumatic regeneration involves differential expression of long terminal repeat (LTR) retrotransposons. *Dev. Dyn.* 241, 1625–1636. doi: 10.1002/dvdy.23844
- Mashanov, V. S., Zueva, O. R., and García-Arrarás, J. E. (2013). Radial glial cells play a key role in echinoderm neural regeneration. *BMC Biol.* 11:49. doi: 10.1186/1741-7007-11-49
- Mashanov, V. S., Zueva, O. R., and García-Arrarás, J. E. (2014). Transcriptomic changes during regeneration of the central nervous system in an echinoderm. *BMC Genomics* 15:357. doi: 10.1186/1471-2164-15-357
- Mashanov, V. S., Zueva, O. R., and García-Arrarás, J. E. (2015a). “Echinodermata,” in *Structure and Evolution of Invertebrate Nervous Systems*, eds A. Schmidt-Rhaesa, S. Harzsch, and G. Purschke (Oxford: Oxford Scholarship University Press), (655–668), doi: 10.1093/acprof:oso/9780199682201.003.0051
- Mashanov, V. S., Zueva, O. R., and García-Arrarás, J. E. (2015c). Myc regulates programmed cell death and radial glia dedifferentiation after neural injury in an echinoderm. *BMC Dev. Biol.* 15:24. doi: 10.1186/s12861-015-0071-z
- Mashanov, V. S., Zueva, O. R., and García-Arrarás, J. E. (2015b). Expression of pluripotency factors in echinoderm regeneration. *Cell Tissue Res.* 359, 521–536. doi: 10.1007/s00441-014-2040-4
- Mashanov, V. S., Zueva, O. R., and Heinzeller, T. (2008). Regeneration of the radial nerve cord in a holothurian: A promising new model system for studying post-traumatic recovery in the adult nervous system. *Tissue Cell* 40, 351–372. doi: 10.1016/j.tice.2008.03.004
- Medina-Feliciano, J. G., Pirro, S., García-Arrarás, J. E., Mashanov, V., and Ryan, J. F. (2021). Draft genome of the sea cucumber *Holothuria glaberrima*, a model for the study of regeneration. *Front. Mar. Sci.* 8:603410. doi: 10.3389/fmars.2021.603410
- Meletis, K., Barnabé-Heider, F., Carlén, M., Evergren, E., Tomilin, N., Shupliakov, O., et al. (2008). Spinal cord injury reveals multilineage differentiation of ependymal cells. *PLoS Biol.* 6:e182. doi: 10.1371/journal.pbio.0060182
- Merkle, F. T., Tramontin, A. D., García-Verdugo, J. M., and Alvarez-Buylla, A. (2004). Radial glia give rise to adult neural stem cells in the subventricular zone. *Proc. Natl. Acad. Sci. U. S. A.* 101, 17528–17532. doi: 10.1073/pnas.0407893101
- Ming, G.-L., and Song, H. (2011). Adult neurogenesis in the mammalian brain: Significant answers and significant questions. *Neuron* 70, 687–702.
- Mori, T., Buffo, A., and Götz, M. (2005). The novel roles of glial cells revisited: The contribution of radial glia and astrocytes to neurogenesis. *Curr. Top. Dev. Biol.* 69, 67–99. doi: 10.1016/S0070-2153(05)69004-7
- Nagashima, M., Barthel, L. K., and Raymond, P. A. (2013). A self-renewing division of zebrafish Müller glial cells generates neuronal progenitors that require N-cadherin to regenerate retinal neurons. *Development* 140, 4510–4521. doi: 10.1242/dev.090738
- Noctor, S. C., Martínez-Cerdeño, V., Ivic, L., and Kriegstein, A. R. (2004). Cortical neurons arise in symmetric and asymmetric division zones and migrate through specific phases. *Nat. Neurosci.* 7, 136–144. doi: 10.1038/nn1172
- Nottebohm, F. (1989). From Bird Song to Neurogenesis. *Sci. Am.* 260, 74–79. doi: 10.1038/scientificamerican0289-74
- Obnier, K., and Alvarez-Buylla, A. (2019). Neural stem cells: Origin, heterogeneity and regulation in the adult mammalian brain. *Development* 146:dev156059. doi: 10.1242/dev.156059
- Patro, N., Naik, A., and Patro, I. K. (2015). Differential temporal expression of S100β in developing rat brain. *Front. Cell Neurosci.* 9:87. doi: 10.3389/fncel.2015.00087
- Pinto, L., and Götz, M. (2007). Radial glial cell heterogeneity-The source of diverse progeny in the CNS. *Prog. Neurobiol.* 83, 2–23. doi: 10.1016/j.pneurobio.2007.02.010
- Pollen, A. A., Nowakowski, T. J., Chen, J., Retallack, H., Sandoval-Espinosa, C., Nicholas, C. R., et al. (2015). Molecular identity of human outer radial glia during cortical development. *Cell* 163, 55–67. doi: 10.1016/j.cell.2015.09.004
- Quesada-Díaz, E., Figueroa-Delgado, P., García-Rosario, R., Sirfa, A., and García-Arrarás, J. E. (2021). Dedifferentiation of radial glia-like cells is observed in

in vitro explants of holothurian radial nerve cord. *J. Neurosci. Methods* 364:109358. doi: 10.1016/j.jneumeth.2021.109358

Rakic, P. (1971). Neuron-glia relationship during granule cell migration in developing cerebellar cortex. A golgi and electron microscopic study in Macacus Rhesus. *J. Comp. Neurol.* 141, 283–312. doi: 10.1002/cne.901410303

Rakic, P. (1995). A small step for the cell, a giant leap for mankind: A hypothesis of neocortical expansion during evolution. *Trends Neurosci.* 18, 383–388. doi: 10.1016/0166-2236(95)93934-p

Reichenbach, A., and Bringmann, A. (2013). New functions of Müller cells. *Glia* 61, 651–678. doi: 10.1002/glia.22477

Reimer, M. M., Sörensen, I., Kuscha, V., Frank, R. E., Liu, C., Becker, C. G., et al. (2008). Motor neuron regeneration in adult zebrafish. *J. Neurosci.* 28, 8510–8516. doi: 10.1523/JNEUROSCI.1189-08.2008

Ribeiro, A., Monteiro, J. F., Certal, A. C., Cristovão, A. M., and Saúde, L. (2017). Foxj1a is expressed in ependymal precursors, controls central canal position and is activated in new ependymal cells during regeneration in zebrafish. *Open Biol.* 7:170139. doi: 10.1098/rsob.170139

Robel, S., Berninger, B., and Götz, M. (2011). The stem cell potential of glia: Lessons from reactive gliosis. *Nat. Rev.* 12, 88–104. doi: 10.1038/nrn2978

Rodriguez Viales, R., Diotel, N., Ferg, M., Armant, O., Eich, J., Alunni, A., et al. (2015). The helix-loop-helix protein id1 controls stem cell proliferation during regenerative neurogenesis in the adult zebrafish telencephalon. *Stem Cells* 33, 892–903. doi: 10.1002/stem.1883

Rothengraber, I., Krecsmarik, M., Hayes, J. A., Bahn, B., Lepier, A., Fortin, G., et al. (2011). Clonal analysis by distinct viral vectors identifies bona fide neural stem cells in the adult zebrafish telencephalon and characterizes their division properties and fate. *Development* 138, 1459–1469. doi: 10.1242/dev.058156

Rowitch, D. H., and Kriegstein, A. R. (2010). Developmental genetics of vertebrate glial-cell specification. *Nature* 468, 214–222. doi: 10.1038/nature09611

Ruddy, R. M., and Morshead, C. M. (2018). Home sweet home: The neural stem cell niche throughout development and after injury. *Cell Tissue Res.* 371, 125–141. doi: 10.1007/s00441-017-2658-0

Rushing, G., and Ihrie, R. A. (2016). Neural stem cell heterogeneity through time and space in the ventricular-subventricular zone. *Front. Biol.* 11:261–284. doi: 10.1007/s11515-016-1407-1

Sahu, A., Devi, S., Jui, J., and Goldman, D. (2021). Notch signaling via Hey1 and Id2b regulates Müller glia's regenerative response to retinal injury. *Glia* 69, 2882–2898. doi: 10.1002/glia.24075

San Miguel-Ruiz, J. E., Maldonado-Soto, A. R., and García-Arrarás, J. E. (2009). Regeneration of the radial nerve cord in the sea cucumber *Holothuria glaberrima*. *BMC Dev. Biol.* 9:3. doi: 10.1186/1471-213X-9-3

Scott, K., O'Rourke, R., Winkler, C. C., Kearns, C. A., and Appel, B. (2021). Temporal single-cell transcriptomes of zebrafish spinal cord pMN progenitors reveal distinct neuronal and glial progenitor populations. *Dev. Biol.* 479, 37–50. doi: 10.1016/j.ydbio.2021.07.010

Shah, P. T., Stratton, J. A., Stykel, M. G., Abbasi, S., Sharma, S., Mayr, K. A., et al. (2018). Single-cell transcriptomics and fate mapping of ependymal cells reveals an absence of neural stem cell functions. *Cell* 173, 1045–1057. doi: 10.1016/j.cell.2018.03.063

Shu, T., and Richards, L. J. (2001). Cortical axon guidance by the glial wedge during the development of the corpus callosum. *J. Neurosci.* 21, 2749–2758. doi: 10.1523/JNEUROSCI.21-08-02749.2001

Simões, A. R., and Rhiner, C. (2017). A cold-blooded view on adult neurogenesis. *Front. Neurosci.* 11:327. doi: 10.3389/fnins.2017.00327

Spassky, N., Merkle, F. T., Flames, N., Tramontin, A. D., García-Verdugo, J. M., Alvarez-Buylla, A., et al. (2005). Adult ependymal cells are postmitotic and are derived from radial glial cells during embryogenesis. *J. Neurosci.* 25, 10–18. doi: 10.1523/JNEUROSCI.1108-04.2005

Sullivan, J. M., and Beltz, B. S. (2005). Newborn cells in the adult crayfish brain differentiate into distinct neuronal types. *J. Neurobiol.* 65, 157–170. doi: 10.1002/neu.20195

Sundholm-Peters, N. L., Yang, H. K., Goings, G. E., Walker, A. S., and Szele, F. G. (2004). Radial glia-like cells at the base of the lateral ventricles in adult mice. *J. Neurocytol.* 33, 153–164. doi: 10.1023/B:NEUR.0000029654.70632.3a

Tanaka, E. M. (2016). The molecular and cellular choreography of appendage regeneration. *Cell* 165, 1598–1608. doi: 10.1016/j.cell.2016.05.038

Tazaki, A., Tanaka, E. M., and Fei, J. F. (2017). Salamander spinal cord regeneration: The ultimate positive control in vertebrate spinal cord regeneration. *Dev. Biol.* 432, 63–71. doi: 10.1016/j.ydbio.2017.09.034

Terreros-Roncal, J., Moreno-Jiménez, E. P., Flor-García, M., Rodríguez-Moreno, C. B., Trinchero, M. F., Cafini, F., et al. (2021). Impact of neurodegenerative diseases on human adult hippocampal neurogenesis. *Science* 374, 1106–1113. doi: 10.1126/science.abl5163

Than-Trong, E., and Bally-Cuif, L. (2015). Radial glia and neural progenitors in the adult zebrafish central nervous system. *Glia* 63, 1406–1428. doi: 10.1002/glia.22856

Than-Trong, E., Ortica-Gatti, S., Mella, S., Nepal, C., Alunni, A., and Bally-Cuif, L. (2018). Neural stem cell quiescence and stemness are molecularly distinct outputs of the Notch3 signalling cascade in the vertebrate adult brain. *Development* 145:dev161034. doi: 10.1242/dev.161034

Thummel, R., Kassen, S. C., Montgomery, J. E., Enright, J. M., and Hyde, D. R. R. (2008). Inhibition of Müller glial cell division blocks regeneration of the light-damaged zebrafish retina. *Dev. Neurobiol.* 68, 392–408. doi: 10.1002/dneu.20596

Urbán, N., Blomfield, I. M., and Guillemot, F. (2019). Quiescence of Adult Mammalian Neural Stem Cells: A Highly Regulated Rest. *Neuron* 104, 834–848. doi: 10.1016/j.neuron.2019.09.026

Urbán, N., van den Berg, D. L. C., Forget, A., Andersen, J., Demmers, J. A. A., Hunt, C., et al. (2016). Return to Quiescence of mouse neural stem cells by degradation of a pro-activation protein. *Science* 353, 292–295. doi: 10.1126/science.aaf4802

Ventura, T., Stewart, M. J., Chandler, J. C., Rotgans, B., Elizur, A., Hewitt, A. W., et al. (2019). Molecular aspects of eye development and regeneration in the Australian redclaw crayfish. *Aquac. Fish.* 4, 27–36. doi: 10.1016/j.aaf.2018.04.001

Verkhatsky, A., Ho, M. S., and Parpura, V. (2019). Evolution of neuroglia. *Adv. Exp. Med. Biol.* 1175, 15–44. doi: 10.1007/978-981-13-9913-8_2

Voigt, T. (1989). Development of glial cells in the cerebral wall of ferrets: Direct tracing of their transformation from radial glia into astrocytes. *J. Comp. Neurol.* 289, 74–88. doi: 10.1002/cne.902890106

Wahane, S., Halawani, D., Zhou, X., and Zou, H. X. (2019). Epigenetic regulation of axon regeneration and glial activation in injury responses. *Front. Genet.* 10:640. doi: 10.3389/fgene.2019.00640

Walder, S., Zhang, F., and Ferretti, P. (2003). Up-regulation of neural stem cell markers suggests the occurrence of dedifferentiation in regenerating spinal cord. *Dev. Genes Evol.* 213, 625–630. doi: 10.1007/s00427-003-0364-2

Walker, S. E., and Echeverri, K. (2022). Spinal cord regeneration - the origins of progenitor cells for functional rebuilding. *Curr. Opin. Genet. Dev.* 24:101917. doi: 10.1016/j.gde.2022.101917

Wei, X., Fu, S., Li, H., and Gu, Y. (2022). Single-cell Stereo-seq reveals induced progenitor cells involved in axolotl brain regeneration. *Science* 377:eab9444. doi: 10.1126/science.abp9444

Yao, Y., and Wang, C. (2020). Dedifferentiation: Inspiration for devising engineering strategies for regenerative medicine. *NPJ Regen. Med.* 5:14. doi: 10.1038/s41536-020-00099-8

Zamboni, M., Llorens-Bobadilla, E., Magnusson, J. P., and Frisén, J. A. (2020). Widespread Neurogenic Potential of Neocortical Astrocytes Is Induced by Injury. *Cell Stem Cell* 27, 605–617.e5. doi: 10.1016/j.stem.2020.7.006

Zambusi, A., and Ninkovic, J. (2020). Regeneration of the central nervous system-principles from brain regeneration in adult zebrafish. *World J. Stem Cells* 12, 8–24. doi: 10.4252/wjsc.v12.i1.8



OPEN ACCESS

EDITED BY

Juan Rafael Riesgo-Escovar,
Universidad Nacional Autónoma
de México, Mexico

REVIEWED BY

Balazs Varga,
University of Cambridge,
United Kingdom
Alfredo Varela-Echavarría,
National Autonomous University
of Mexico, Mexico

*CORRESPONDENCE

Luis Covarrubias
luis.covarrubias@ibt.unam.mx

†PRESENT ADDRESSES

Dulce-María Arzate and
Edwards Antonio-Cabrera,
Instituto Cajal-Consejo Superior
de Investigaciones Científicas (CSIC),
Madrid, Spain
Gilda Guerrero-Flores,
Laboratorio Nacional de Recursos
Genómicos,
Instituto de Investigaciones
Biomédicas, UNAM, Ciudad de México,
Mexico

‡Deceased

SPECIALTY SECTION

This article was submitted to
Neurodevelopment,
a section of the journal
Frontiers in Neuroscience

RECEIVED 24 May 2022

ACCEPTED 18 November 2022

PUBLISHED 14 December 2022

CITATION

Arzate D-M, Valencia C, Dimas M-A,
Antonio-Cabrera E,
Domínguez-Salazar E,
Guerrero-Flores G,
Gutiérrez-Mariscal M and
Covarrubias L (2022) *Dll1*
haploinsufficiency causes brain
abnormalities with functional
relevance.
Front. Neurosci. 16:951418.
doi: 10.3389/fnins.2022.951418

Dll1 haploinsufficiency causes brain abnormalities with functional relevance

Dulce-María Arzate^{1†}, Concepción Valencia¹,
Marco-Antonio Dimas¹, Edwards Antonio-Cabrera^{2†},
Emilio Domínguez-Salazar^{2‡}, Gilda Guerrero-Flores^{1†},
Mariana Gutiérrez-Mariscal¹ and Luis Covarrubias^{1*}

¹Instituto de Biotecnología, Universidad Nacional Autónoma de México, Cuernavaca, Mexico,

²Departamento de Biología de la Reproducción, Universidad Autónoma Metropolitana Unidad Iztapalapa, Ciudad de México, Mexico

Introduction: The Notch pathway is fundamental for the generation of neurons during development. We previously reported that adult mice heterozygous for the null allele of the gene encoding the Delta-like ligand 1 for Notch (*Dll1*^{lacZ}) have a reduced neuronal density in the substantia nigra pars compacta. The aim of the present work was to evaluate whether this alteration extends to other brain structures and the behavioral consequences of affected subjects.

Methods: Brains of *Dll1*^{+/lacZ} embryos and mice at different ages were phenotypically compared against their wild type (WT) counterpart. Afterwards, brain histological analyses were performed followed by determinations of neural cell markers in tissue slices. Neurological deficits were diagnosed by applying different behavioral tests to *Dll1*^{+/lacZ} and WT mice.

Results: Brain weight and size of *Dll1*^{+/lacZ} mice was significantly decreased compared with WT littermates (i.e., microcephaly), a phenotype detected early after birth. Interestingly, enlarged ventricles (i.e., hydrocephalus) was a common characteristic of brains of *Dll1* haploinsufficient mice since early ages. At the cell level, general cell density and number of neurons in several brain regions, including the cortex and hippocampus, of *Dll1*^{+/lacZ} mice were reduced as compared with those regions of WT mice. Also, fewer neural stem cells were particularly found in the adult dentate gyrus of *Dll1*^{+/lacZ} mice but not in the subventricular zone. High myelination levels detected at early postnatal ages (P7–P24) were an additional penetrant phenotype in *Dll1*^{+/lacZ} mice, observation that was consistent with premature oligodendrocyte differentiation. After applying a set of behavioral tests, mild neurological alterations were detected that caused changes in motor behaviors and a deficit in object categorization.

Discussion: Our observations suggest that *Dll1* haploinsufficiency limits Notch signaling during brain development which, on one hand, leads to reduced brain cell density and causes microcephaly and hydrocephalus phenotypes and, on the other, alters the myelination process after birth. The severity of these defects could reach levels that affect normal brain function. Therefore, *Dll1* haploinsufficiency is a risk factor that predisposes the brain to develop abnormalities with functional consequences.

KEYWORDS

notch signaling, neuronal density, microcephaly, hydrocephalus, myelination

Highlights

- *Dll1* haploinsufficient mice (*Dll1*^{+/lacZ}) develop microcephaly and hydrocephalus neuropathologies
- *Dll1*^{+/lacZ} mice showed a reduced neuronal density
- *Dll1*^{+/lacZ} mice have a reduced NSC pool in the hippocampus
- *Dll1*^{+/lacZ} mice showed an altered myelination pattern
- *Dll1*^{+/lacZ} mice showed neurological deficits
- *Dll1* haploinsufficiency is a risk factor for congenital brain malfunctions

Introduction

The Notch pathway is highly conserved and fundamental for the generation of new neurons and their specification during development (Pierfelice et al., 2011). In mammals, Notch is a family of transmembrane receptors activated by transmembrane ligands such as Delta-like (DLL1, DLL3, and DLL4) and Jagged (JAG1 and JAG2) family members. After its activation, the Notch intracellular domain (NICD) is released and translocated to the nucleus, where it binds to RBPjk and induces the expression of genes such as members of the *Hes* and *Hey* gene families (Louvi and Artavanis-Tsakonas, 2006). The blockade of this pathway leads to neural precursor cells (NPCs) exhaustion by promoting their early differentiation, which results in a decrease in the number of neurons (Grandbarbe et al., 2003; Trujillo-Paredes et al., 2016). In the glial lineages, Notch signaling promotes astrocytic differentiation (Freeman, 2010) or oligodendrocyte precursor cell proliferation (Wang et al., 1998). Although the requirement of a specific Notch ligand is associated with a particular function, Delta-like canonical Notch ligand 1 (DLL1) appears to be the most widely distributed and more relevant both during development and in the adult (Beckers et al., 1999; Siebel and Lendahl, 2017).

We previously reported that mouse embryos homozygous for a *Dll1* null mutation (*Dll1*^{lacZ/lacZ}) show premature

dopaminergic differentiation in the midbrain, which is accompanied by a reduction in NPCs without altering their specification (Trujillo-Paredes et al., 2016). This phenomenon appears to be the main cause of the fewer dopaminergic neurons present in the substantia nigra pars compacta of adult mice heterozygous for the *Dll1*^{lacZ} null allele (Trujillo-Paredes et al., 2016). Since *Dll1*^{lacZ/lacZ} mice die few days after neurogenesis initiation (i.e., E11.5-E12.5; Hrabe de Angelis et al., 1997; Trujillo-Paredes et al., 2016), likely due to a disruption in vasculature development, detailed analysis of the role of DLL1 in the control of differentiation by Notch within different neuronal lineages is not possible.

Congenital anomalies can result from gene-environment interactions that modify the penetrance of defective alleles (Nishimura and Kurosawa, 2022). In particular, it is apparent that genes encoding Notch signaling components are prompt to environmental influences. In humans, members of families carrying putative mutant alleles for NOTCH1, NOTCH2, JAG1, DLL3, MESP2, LFNG, and HES7 show congenital anomalies of the heart and the vertebrae (Sparrow et al., 2012). Evidence of environmental influence has been demonstrated by showing that *Hes7* haploinsufficient mouse embryos exposed to hypoxia at certain developmental stage increases the incidence of scoliosis, a typical abnormality associated with Notch signaling deficiency (Sparrow et al., 2012). Since Notch signaling is key for the correct development of the brain, it is predicted that congenital brain anomalies develop under reduced Notch signaling.

Considering our previous observations (Trujillo-Paredes et al., 2016), the aim of the present work was to extend the analysis of brain abnormalities in *Dll1* haploinsufficient adult mice to underscore the possible congenital neurological dysfunctions that may emerge under reduced Notch signaling. The present work reveals distinct brain abnormalities (i.e., microcephaly, hydrocephalus, altered myelination) that might be the cause of brain function and mouse behavior alterations.

Results

Anatomical and histological evaluation

Dll1^{+/lacZ} embryos were largely normal, nonetheless, mild brain abnormalities were observed. These abnormalities could be related to signs of premature neurogenesis (i.e., more neurons and less NPCs), as seen in the mesencephalon of *Dll1*^{+/lacZ} embryos at E11.5 (Figure 1A; see also Trujillo-Paredes et al., 2016), whereas others might be due to a developmental asynchrony (i.e., altered progression from NPCs toward neurons), as it is apparent in the developing cortex of most *Dll1* haploinsufficient embryos compared with their WT littermates (Figures 1B,C). Allele segregation analysis of progeny from backcrosses suggests *Dll1*^{lacZ} mendelian inheritance and low embryo lethality ($46.2 \pm 3.6\%$ *Dll1*^{+/lacZ} born mice, $n = 213$). Interestingly, *Dll1*^{+/lacZ} newborn mice were smaller than age-matched WT mice, with a reduced total body and brain weight (Figures 1D,E). Without considering rare cases (less than 1 among 500 mice) in which *Dll1*^{+/lacZ} young mice (i.e., before 2 months of age) were sacrificed due to a spontaneous very high hyperactivity, most pups born carrying the *Dll1*^{lacZ} allele survived to adulthood.

Brains of adult *Dll1*^{+/lacZ} mice were smaller compared with brains of WT mice of the same age and strain (Figure 2A). This was consistent with measurements done on slices of brains of aged mice (Figure 2B). In agreement with a previous report (Rubio-Aliaga et al., 2009), a decline in body weight gain as aging progress was noted for *Dll1*^{+/lacZ} mice in comparison with WT mice (Figure 2C), but a significant difference was not noted in mouse size, as estimated by X-ray skeletal analysis (Figure 2D). Therefore, although the specific reduction in brain size of *Dll1*^{+/lacZ} mice was not apparent in newborn mice due to a comparative decrease in body weight (Figure 2C; see also Figures 1D,E), this phenotype became evident as mice aged (Figure 2E).

MRI analysis performed in adult brains confirmed the smaller size of the brain of *Dll1*^{+/lacZ} mice; total brain volume of *Dll1*^{+/lacZ} mice was about 15% less than that of WT mice (Figures 3A,C). Notably, the reduced brain volume of *Dll1*^{+/lacZ} mice included a larger ventricular volume in comparison with that present in brains of WT mice (Figures 3B,D, 5D,E). Suggesting a developmental origin, this latter characteristic was a penetrant phenotype noted from a few days after birth in brains of mice carrying the *Dll1*^{lacZ} null allele and, interestingly, the ventricular volume increased as mice reached adulthood (Figure 3E).

Cell density analysis

In addition to the apparent reduction in the size of some structures (e.g., dentate gyrus, substantia nigra pars

compacta) and in the thickness of cortex layers, brains of *Dll1*^{+/lacZ} mice also showed a more scattered distribution of cells in comparison with brains of WT mice (Figures 4A–C). The differences in cell density were not homogeneous, finding only trends to reduced cell density in some regions (e.g., striatum, substantia nigra pars reticulata) of brains of adult *Dll1*^{+/lacZ} mice in comparison with brains of WT mice (data not shown). Notably in the hippocampus, in addition to the apparent smaller size of the dentate gyrus (DG), lower cell density was found in the DG and the CA3sp areas and, in the cortex, the thinner layers correlated with a sustained reduction in cell density from early postnatal ages (Figures 4D,E).

As previously reported for the substantia nigra pars compacta, in which we found a reduction in the number of TH⁺ neurons (Trujillo-Paredes et al., 2016), a significant reduction in the percentage of NEUN⁺ cells in brains of *Dll1*^{+/lacZ} mice in comparison with those of WT mice was found in the cortex (Figures 4F,F',G), the striatum (Figures 4H,H',I) and the substantia nigra pars reticulata (Figures 4J,J',K). Interestingly, the reduction in NEUN⁺ cells observed in these brain areas of *Dll1*^{+/lacZ} mice correlated with a corresponding increase in the percentage of GFAP⁺ cells (Figures 4G,I,K). These data suggest, not only a tendency to a reduction in brain cell density in *Dll1*^{+/lacZ} mice that correlates with a smaller brain size, but also a diminished proportion of neurons in the evaluated areas.

As Notch signaling participates in the generation of new neurons from two well-recognized neurogenic niches, the number of GFAP and SOX2 (a neural stem cell, NSC, marker) positive cells were determined in the DG of the hippocampus and the subventricular zone (SVZ). In agreement with a specific reduction in NSCs in the dentate gyrus, a lower percentage of GFAP⁺ cells (Figures 5A,F) and SOX2⁺ cells (Figures 5B,C,E,G) was found in the brain of *Dll1*^{+/lacZ} mice in comparison with that of WT mice, that was reflected in a reduction in the percentage of NEUN⁺ cells (Figures 5A,F). It was also found that there were fewer DCX⁺ neuroblasts in this region in association with *Dll1* haploinsufficiency (Figures 5C,G), but a significant difference was not found in the DCX⁺/SOX2⁺ cell ratio (Figure 5H), suggesting that adult neurogenesis is similarly active but limited by the number of NSCs present (see Discussion). In the SVZ of *Dll1*^{+/lacZ} animals in comparison with the WT counterpart, a significant reduction in the number of cells was evident (125.86 ± 7.0 vs. 227.33 ± 8.97 total cells within 20 μ m from the ventricle/slide, $P < 0.001$; see insets in Figure 5E), which was accompanied by a significant increase in the proportion of GFAP⁺ cells (Figure 5D,I), but a significant difference was not found in the proportion of SOX2⁺ cells (Figures 5E,I).

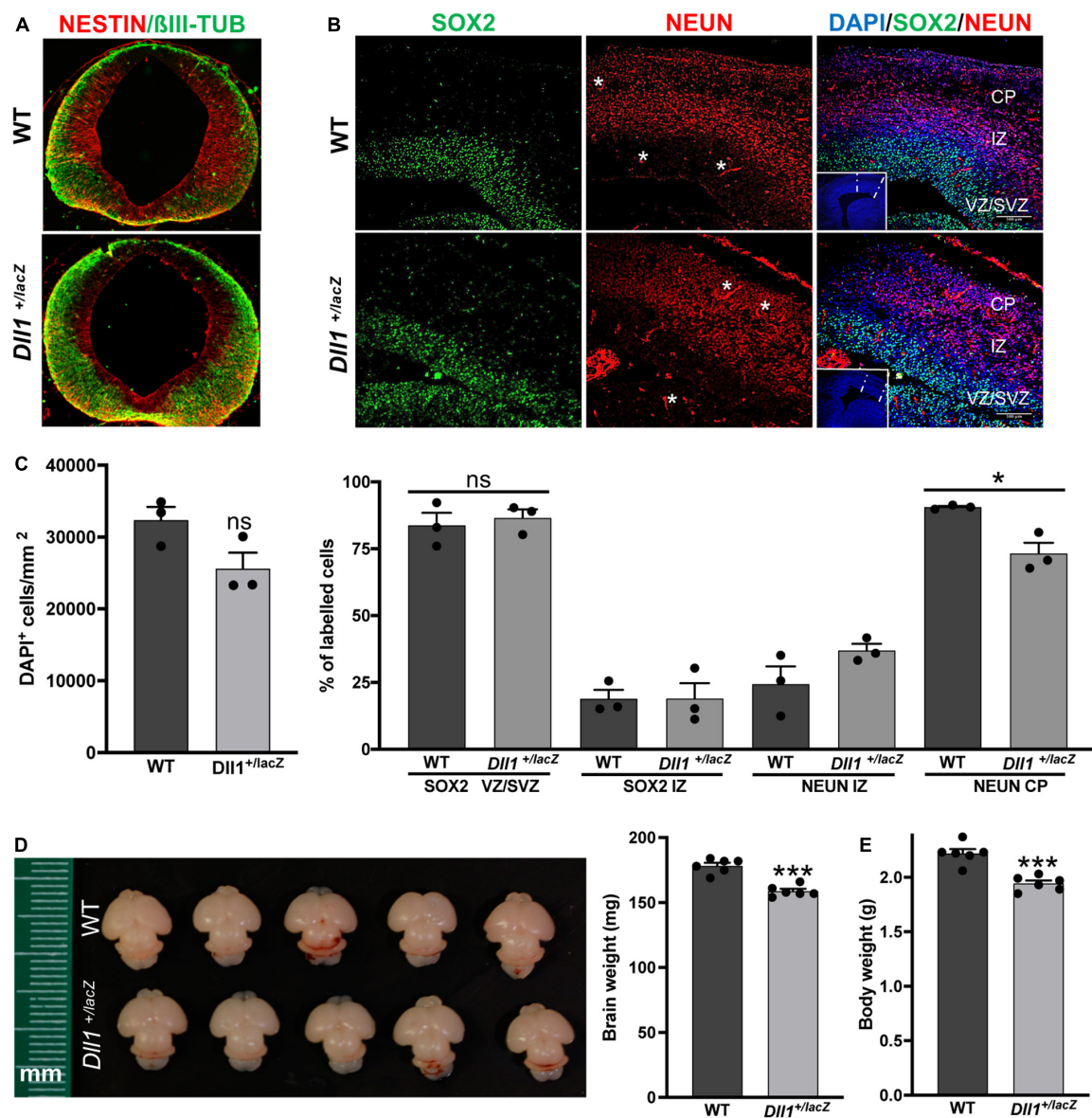


FIGURE 1

Dll1 haploinsufficiency causes abnormalities in embryonic and neonatal brains. (A) Immunolabelling against NESTIN and β III-TUBULIN in coronal mesencephalon sections of E11.5 WT and *Dll1*^{+/lacZ} embryos. A more abundant amount of β III-TUBULIN and a reduced amount of NESTIN was a recurrent characteristic found in samples from *Dll1*^{+/lacZ} embryos when compared with WT embryos derived from the same pregnant female. (B) SOX2, NEUN (nuclear staining) and DAPI staining images in coronal telencephalic sections of E15.5 WT and *Dll1*^{+/lacZ} embryos; insets are low magnification images of the telencephalic sections under analysis (CP, cortical plate; IZ, intermediate zone; VZ, ventricular zone; SVZ, subventricular zone; asterisks, autofluorescence from blood vessels; scale bar, 100 μ m). (C) Quantification of cell density (DAPI⁺ cells/mm²), and determination of the proportion of SOX2⁺ progenitors and NEUN⁺ neurons in samples as those shown in B (* P < 0.05; number of telencephalons analyzed = 3). Note that *Dll1* haploinsufficiency did not change the number of SOX2⁺ cells or neurons in the developing cortex, but their distribution was altered, resulting in a reduced number of neurons in the CP of samples from *Dll1*^{+/lacZ} embryos. (D) Representative brains of WT and *Dll1*^{+/lacZ} mice at postnatal day 3 (P3). (E) Brain and body weight of WT and *Dll1*^{+/lacZ} mice at P3 (*** P < 0.001; n = 6 for each genotype). From these observations, it is apparent that *Dll1*^{+/lacZ} mice are born with a brain smaller than that of their WT siblings.

Myelination analysis

In contrast with WT mice, *Dll1*^{+/lacZ} mice showed increased levels of myelinated axons in most brain structures (e.g., corpus callosum, cortex, caudate putamen), from postnatal age P7 and

up to P24, as assessed by Black-Gold II staining (Figures 6A,D) and detection of myelin basic protein (Figures 6B,E). This difference in myelination levels, however, was not detected in most 2-3-months-old adult mice (data not shown). Actually, only one among 5 brains of 2-3-months-old *Dll1*^{+/lacZ} mice

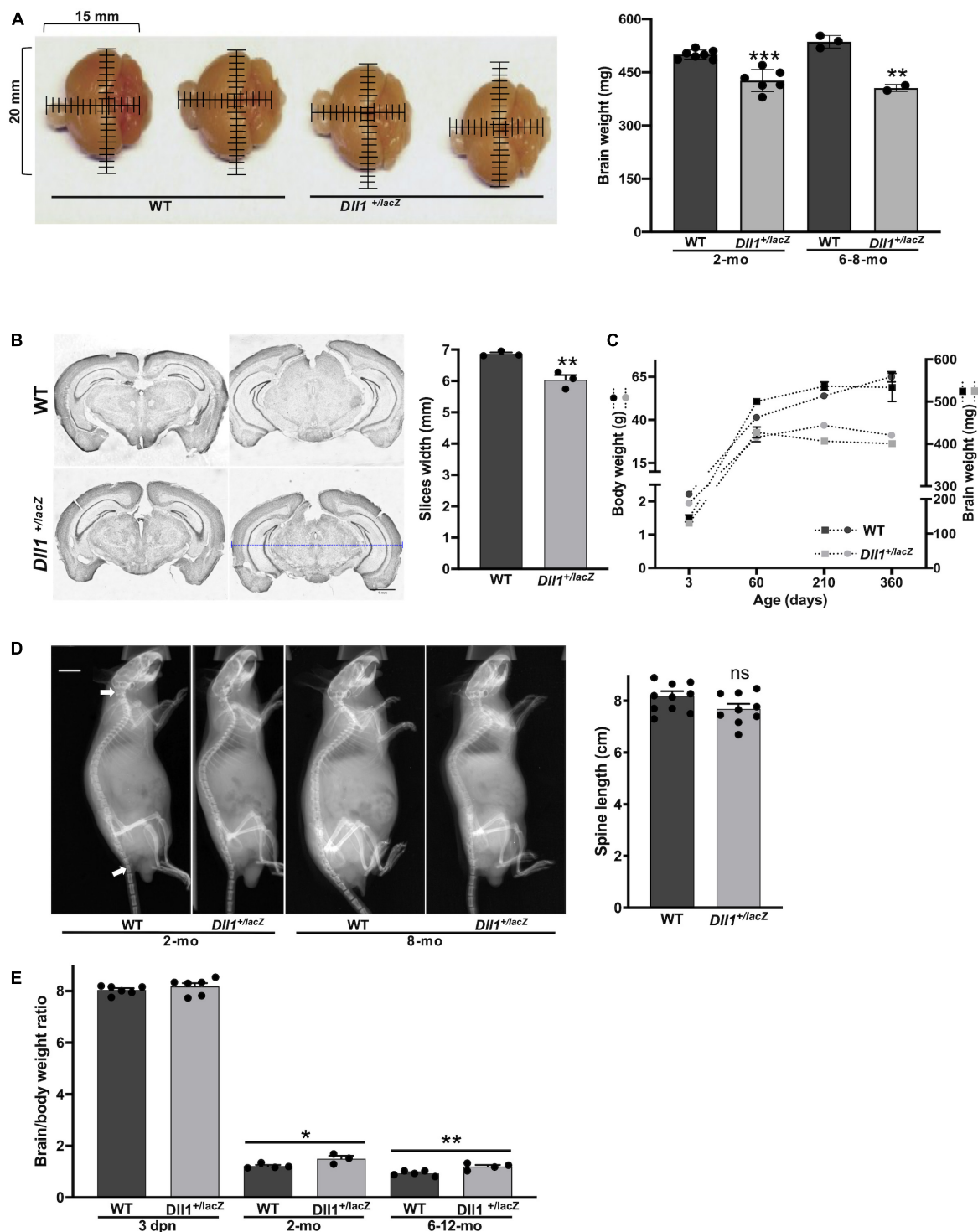


FIGURE 2

Dll1^{+/-lacZ} mice have smaller brains than WT mice. (A) Brains of WT and *Dll1*^{+/-lacZ} adult mice. Images allow to appreciate the smaller brain size of *Dll1*^{+/-lacZ} mice in comparison with that of WT mice (2 months of age; mm, millimeters), which is confirmed by comparing the weight of brains in graph (WT, *n* = 10, and *Dll1*^{+/-lacZ}, *n* = 8, of 2-months-old and 6-8-months-old mice; ****P* < 0.001). (B) Representative coronal brain slices from WT and *Dll1*^{+/-lacZ} adult mice after Nissl staining and the corresponding average width of fifteen rostrocaudal matched slices per subject (*n* = 3, ***p* < 0.01). The blue dashed line denotes the width measurement (scale bar, 1 mm). (C) Evolution of body (left) and brain (right) weight of WT and *Dll1*^{+/-lacZ} mice along aging. (D) Spine length. Spine length was determined from X-ray skeletal images (left); arrows indicate the references used for measurements (WT, *n* = 11, and *Dll1*^{+/-lacZ}, *n* = 9; ns, no significant). (E) Brain to body weight ratio of WT and *Dll1*^{+/-lacZ} animals (**P* < 0.05 and ***P* < 0.01). All data together support that microcephaly is a phenotype of mice with reduced DLL1 levels.

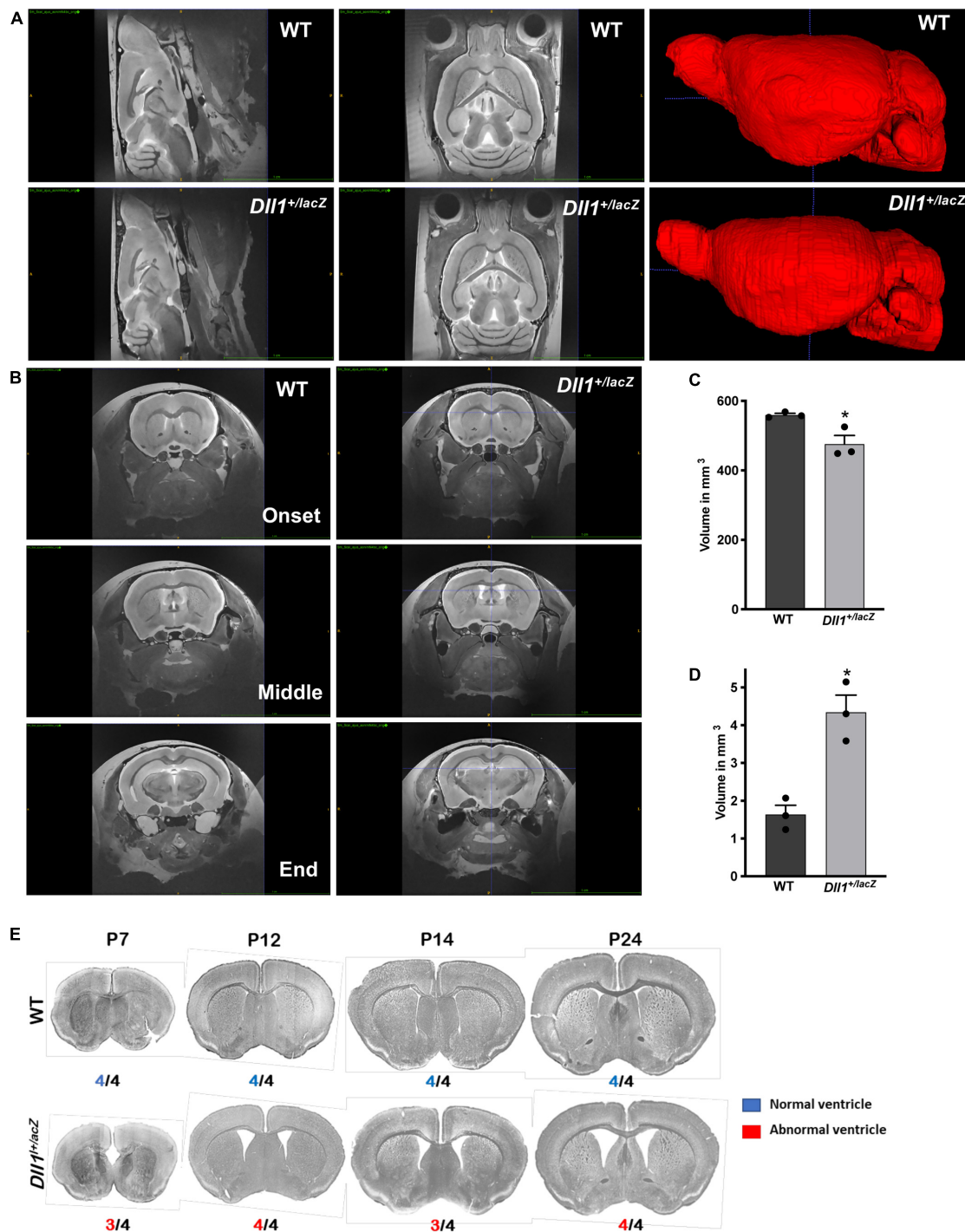


FIGURE 3

Increased lateral ventricle volume in brains of *DII1*^{+/lacZ} mice. The volumes of whole brain and lateral ventricles were determined by MRI analysis. **(A)** Sagittal and dorsoventral views of representative brains of WT and *DII1*^{+/lacZ} mice (4–5 months of age). On the right, 3D reconstructions after a manual segmentation of brains are shown. **(B)** Coronal views of brains of WT and *DII1*^{+/lacZ} mice showing the initial, the middle and the final position along the rostro-caudal axis used to determine the lateral ventricle volume. **(C,D)** Total **(C)** and lateral ventricle **(D)** volume of brains of WT and *DII1*^{+/lacZ} mice ($n = 3$ for both genotypes; Student t -Test: $*P < 0.05$). Note that, because the ventricular volume is included in the determinations of total brain volume, the microcephaly phenotype estimated from the total volume is an underestimation of the actual reduction in brain tissue of *DII1*^{+/lacZ} mice. **(E)** Incidence of enlarged ventricles in *DII1*^{+/lacZ} mice. Ventricular size was estimated from coronal slices of brains of WT and *DII1*^{+/lacZ} mice at different postnatal ages (P7 to P24); incidence of the phenotype shown is indicated below each image. Note that the high incidence of enlarged ventricles was observed from a very early age after birth (P7) and remained up to reaching adulthood (after P24).

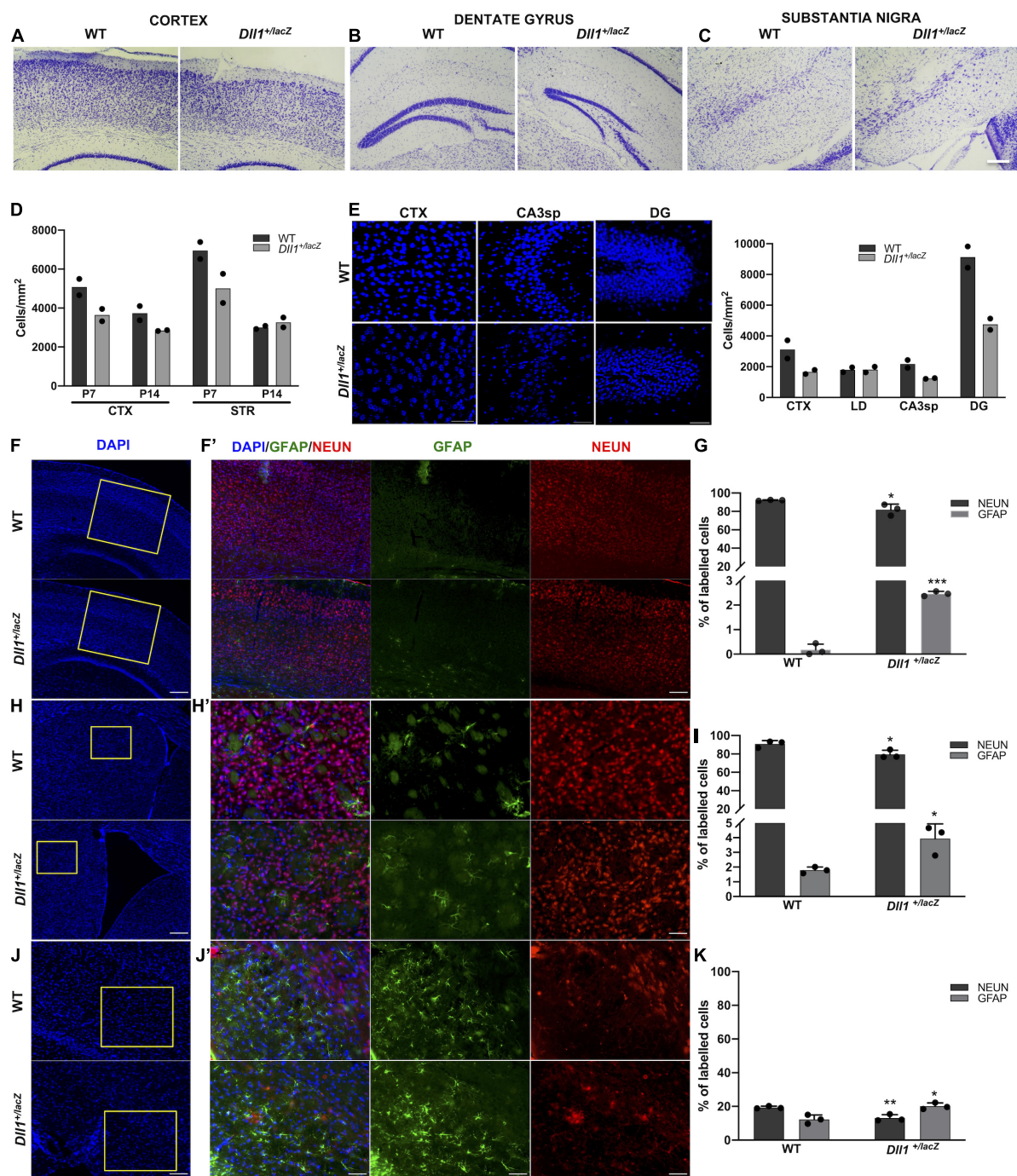


FIGURE 4

Adult brains of *Dll1*^{+/lacZ} mice have an altered density of neurons and astrocytes. (A–C) Representative images of the cortex, the dentate gyrus and the substantia nigra from brain slices stained with cresyl violet (Nissl staining; scale bar, 100 μ m). (D) Cell density quantification in selected brain areas of postnatal mice (P7, P14). (E) Representative images of DAPI stained samples showing cell density in selected brain regions (CTX, cortex; STR, striatum; LD, lateral dorsal nucleus of thalamus; CA3sp, CA3 pyramidal layer; DG, dentate gyrus) of 3-months-old mice; the corresponding quantifications are shown in the graph. Observe the decreased cell density in samples from *Dll1*^{+/lacZ} mice in comparison with those from WT mice. (F,H,J) Panoramic views (nuclei counterstained with DAPI; scale bar, 200 μ m) and the corresponding insets with GFAP⁺ and NEUN⁺ cells in the cortex (F,F'; scale bar 200 μ m and 50 μ m, respectively), the striatum (H,H'; scale bar 200 μ m and 50 μ m, respectively), and the substantia nigra pars reticulata (J,J'; scale bar, 100 μ m and 50 μ m, respectively) of *Dll1*^{+/lacZ} mice and their WT siblings are shown. Percentage of GFAP⁺ and NEUN⁺ cells, calculated from total DAPI⁺ cells in those regions, are shown in graphs (G,I,K). Observe the reduction in the percentage of neurons and the increase in the proportion of glial cells in all regions shown ($n = 3$; * $P < 0.05$, ** $P < 0.01$, *** $P < 0.001$).

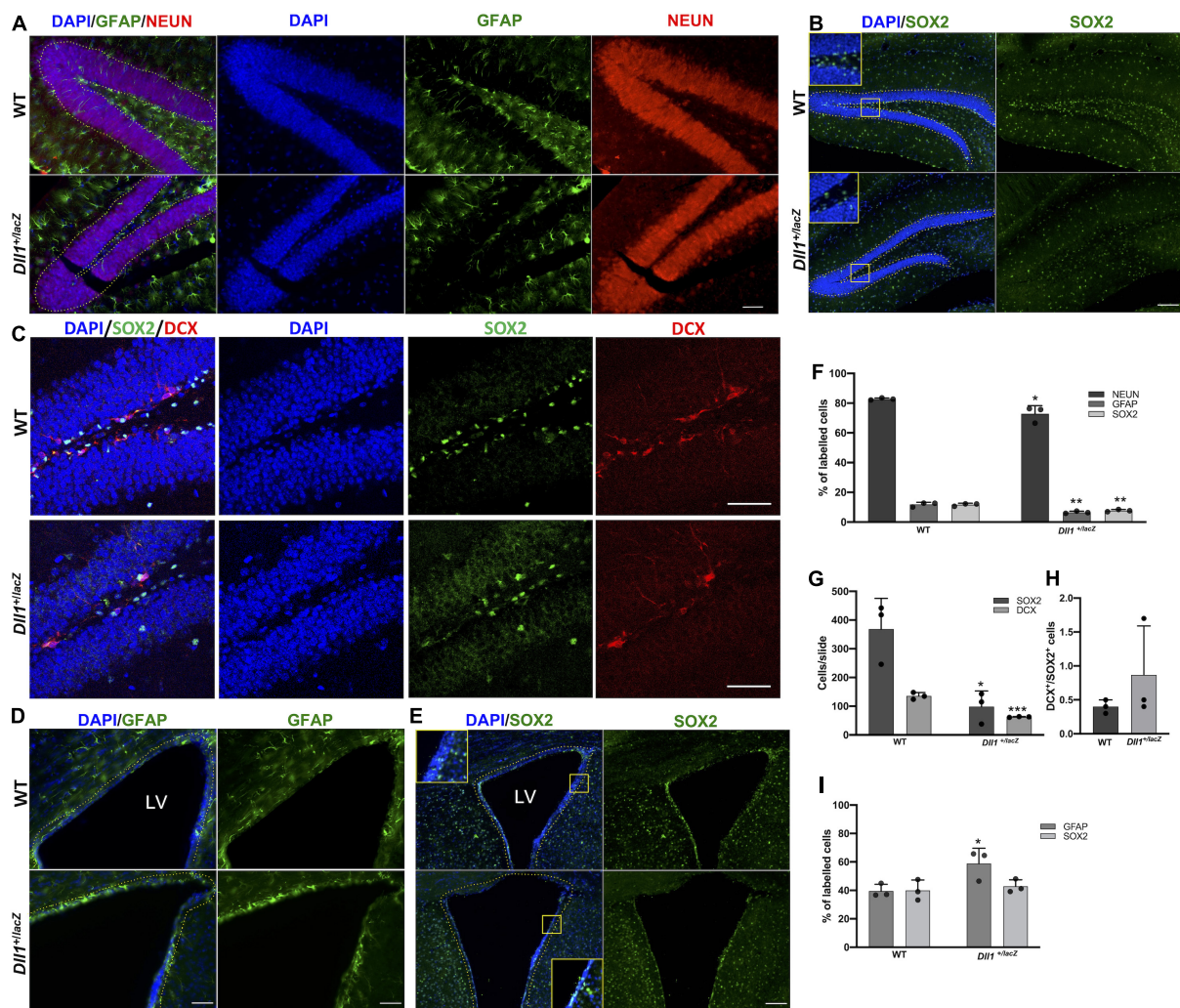


FIGURE 5

Neurogenic niches in the *Dll1*^{+/-lacZ} mice have a reduced number of cells, including precursor cells. (A–E) Representative images showing GFAP⁺ and NEUN⁺ cells (A; scale bar, 50 μ m), SOX2⁺ cells (B,C; scale bar, 100 μ m), and DCX⁺ cells (C; scale bar, 50 μ m) in the dentate gyrus; and GFAP⁺ and SOX2⁺ cells (E; scale bar, 100 μ m) in the SVZ (LV, lateral ventricle). Quantifications of GFAP⁺, NEUN⁺, DCX⁺ and SOX2⁺ cells are shown in graphs (F,G,I; $n = 3$; * $P < 0.05$, ** $P < 0.005$, *** $P < 0.001$). DCX⁺/SOX2⁺ cell ratio in the DG is also shown (H). Only cells comprising the subgranular zone-granular cell layer or the cells lining the third ventricle were taken into account (dashed lines).

showed reduced Black-Gold staining levels (Figure 6C) and myelin basic protein amount (data not shown) in distinct regions in comparison with 7 brains of WT mice. In contrast with the myelination pattern, fewer cells positive for NG2, a marker of oligodendrocyte precursor cells (OPCs), were found in different brain regions (e.g., corpus callosum, cortex, subventricular zone) of *Dll1*^{+/-lacZ} mice than in those of WT mice from P7 and to P14 (Figure 6F). Specifically, in the subventricular zone, a neurogenic region that produces OPCs that migrate to different regions throughout life (Menn et al., 2006), a significant reduction in the number of NG2⁺ cells was observed (Figure 6G). By P24 no difference was noted in this region but, interestingly, in young adults (2-months-old mice), increased number of NG2⁺ cells was detected in the

subventricular zone of WT mice but not in that of *Dll1*^{+/-lacZ} mice, that later (in 3-months-old mice) decreased to equivalent levels for mice of both genotypes (Figures 6F,G). These observations are consistent with premature oligodendrocyte differentiation that leads to fewer oligodendrocyte precursors early in life and, later, to alterations that might impact the myelination dynamics as aging progresses.

Neurological deficit evaluations

In order to determine general behavioral alterations in *Dll1* haploinsufficient mice, a set of neurological tests were performed (see Materials and methods; Tables 1, 2).

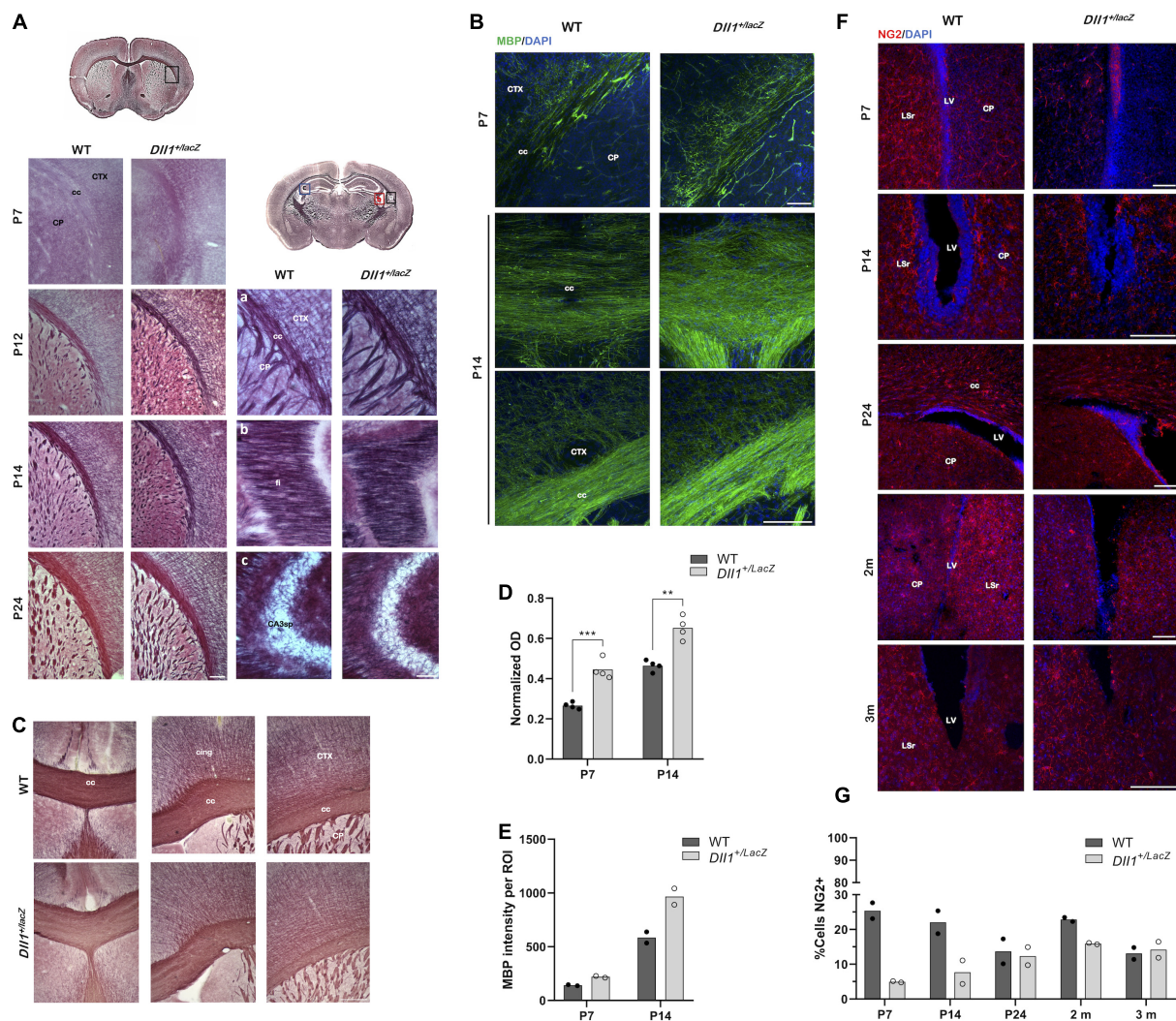


FIGURE 6

Myelination dynamics is altered in *Dll1*^{+/lacZ} mice. (A) Areas (insets in drawings) of brain coronal slices from WT and *Dll1*^{+/lacZ} mice at different postnatal ages (P7, P12, P14, P24) stained with Black-Gold II to reveal myelin levels (cc, corpus callosum; CTX, cortex; CP, caudo-putamen; fi, fimbria; CA3sp, pyramidal layer; scale bar, 100 μ m). (B) Brain coronal slices, including similar areas as in A, from WT and *Dll1*^{+/lacZ} mice at P7 and P14 stained for myelin basic protein (scale bar, 500 μ m). Note that stainings were stronger in samples from *Dll1*^{+/lacZ} mice than in those from WT mice. (C) Myelination levels in adult WT and *Dll1*^{+/lacZ} mice. Images show Black-Gold II stained structures in equivalent brain slices of an anterior brain region of 2-months-old mice (cing, cingulum scale bar, 500 μ m). Pictures are representative images from brain sections of a WT mouse, out of 7 analyzed, showing normal myelination levels (top panels) in comparison with images from sections of 1 brain found, out of 6 analyzed, of a *Dll1*^{+/lacZ} mouse showing reduced myelination levels (bottom panels). (D) Quantification of normalized optical density (OD) of corpus callosum in images of samples stained with Black-Gold II ($n = 4$; $**P < 0.01$, $***P < 0.001$). (E) Immunofluorescence intensity quantification of myelin basic protein in the corpus callosum of brains of mice at the postnatal ages indicated ($n = 2$). (F) Detection of NG2⁺ cells in areas of brain coronal slices from WT and *Dll1*^{+/lacZ} mice at different postnatal ages (P7, P14, P24) and adult mice (2–3 months of age). Representative images are shown (LV, lateral ventricle; LSr, lateral septal nucleus rostral; scale bar, 100 μ m). (G) Determinations of the percentage of NG2⁺ cells in the SVZ at different postnatal ages (P7, P14, P24) and of adult (2–3 months-old) mice. Note the marked increase in NG2⁺ cells in 2-months-old WT mice.

A specific deficit was detected in hypomobility, piloerection and absence of equilibrium tests among young *Dll1*^{+/lacZ} male mice, and taking all neurological deficit tests together, young but not aged *Dll1*^{+/lacZ} mice showed a significant higher deficit score than WT male mice (Table 1). Male sexual behavior was generally normal (e.g., mounting and ejaculation per session), though it was noted that intromission

in the first mating session was more frequent for young *Dll1*^{+/lacZ} mice than for WT mice (43% vs. 20%, respectively) and reached over 50% by the second and third sessions (Table 2).

Alterations in locomotor activity were assessed in more detail. Using a laser-based detector of locomotor activity (see Materials and methods; Figure 7A) the accumulative

TABLE 1 Neurological deficit evaluation.

Parameters	Young WT		Young <i>Dll1</i> ^{+/lacZ}		Aged WT		Aged <i>Dll1</i> ^{+/lacZ}	
Phase 1		<i>n</i>		<i>n</i>		<i>n</i>		<i>n</i>
Hypomobility	1.3 ± 0.1	11/11	1.7 ± 0.1*	15/15	2.0 ± 0.0	3/3	1.0 ± 0.0	3/3
Lateralized posture	0.0 ± 0.0	0/11	0.0 ± 0.0	0/15	0.0 ± 0.0	0/3	0.0 ± 0.0	0/3
Flattened posture	0.0 ± 0.0	0/11	0.0 ± 0.0	0/15	0.0 ± 0.0	0/3	0.0 ± 0.0	0/3
Hunched back	0.0 ± 0.0	0/11	0.0 ± 0.0	0/15	0.0 ± 0.0	0/3	0.0 ± 0.0	0/3
Piloerection	0.3 ± 0.1	3/11	0.8 ± 0.1*	12/15°	1.0 ± 0.0	3/3	0.7 ± 0.3	2/3
Ataxic gait	0.0 ± 0.0	0/11	0.0 ± 0.0	0/15	0.0 ± 0.0	0/3	0.0 ± 0.0	0/3
Circling	0.0 ± 0.0	0/11	0.0 ± 0.0	0/15	0.0 ± 0.0	0/3	0.0 ± 0.0	0/3
Tremors	0.2 ± 0.1	2/11	0.2 ± 0.1	3/15	0.3 ± 0.3	1/3	0.3 ± 0.3	1/3
Twitches	0.0 ± 0.0	0/11	0.1 ± 0.1	1/15	0.0 ± 0.0	0/3	0.0 ± 0.0	0/3
Convulsions	0.0 ± 0.0	0/11	0.0 ± 0.0	0/15	0.0 ± 0.0	0/3	0.0 ± 0.0	0/3
Respiratory distress	0.1 ± 0.1	1/11	0.0 ± 0.0	0/15	0.0 ± 0.0	0/3	0.3 ± 0.3	1/3
Phase 2								
Passivity	0.5 ± 0.2	5/11	0.5 ± 0.1	8/15	1.0 ± 0.0	3/3	0.7 ± 0.3	2/3
Hyperreactivity	0.0 ± 0.0	0/11	0.1 ± 0.1	2/15	0.0 ± 0.0	0/3	0.0 ± 0.0	0/3
Irritability	0.0 ± 0.0	0/11	0.1 ± 0.1	2/15	0.0 ± 0.0	0/3	0.0 ± 0.0	0/3
Ptosis	0.0 ± 0.0	0/11	0.0 ± 0.0	0/15	0.3 ± 0.3	1/3	0.0 ± 0.0	0/3
Urination	0.5 ± 0.2	5/11	0.1 ± 0.1	2/15	0.3 ± 0.3	1/3	0.0 ± 0.0	0/3
Decreased body tone	0.1 ± 0.1	1/11	0.3 ± 0.1	5/15	0.3 ± 0.3	1/3	0.3 ± 0.3	1/3
Forelimb flexion	0.1 ± 0.1	1/11	0.0 ± 0.0	0/15	0.0 ± 0.0	0/3	0.0 ± 0.0	0/3
Decreased muscle strength	0.1 ± 0.1	1/11	0.1 ± 0.1	1/15	0.7 ± 0.3	2/3	0.0 ± 0.0	0/3
Body rotation	1.2 ± 0.1	11/11	0.2 ± 0.1*	3/15°	0.3 ± 0.3	1/3	0.0 ± 0.0	0/3
Motor incoordination	1.2 ± 0.1	11/11	1.5 ± 0.1	15/15	1.7 ± 0.3	3/3	2.3 ± 0.7	3/3
Absence of equilibrium	1.2 ± 0.1	11/11	1.8 ± 0.2*	15/15	2.0 ± 0.0	3/3	2.0 ± 0.6	3/3
Hypoalgesia	0.3 ± 0.1	3/11	0.6 ± 0.1	9/15	0.0 ± 0.0	0/3	0.3 ± 0.3	1/3
Hyperalgesia	0.0 ± 0.0	0/11	0.0 ± 0.0	0/15	0.0 ± 0.0	0/3	0.0 ± 0.0	0/3
Phase 3								
Vibrissae sensitivity	0.0 ± 0.0	0/11	0.0 ± 0.0	0/15	0.0 ± 0.0	0/3	0.0 ± 0.0	0/3
Touch sensitivity	0.0 ± 0.0	0/11	0.0 ± 0.0	0/15	0.0 ± 0.0	0/3	0.0 ± 0.0	0/3
Visual sensitivity	0.0 ± 0.0	0/11	0.0 ± 0.0	0/15	0.0 ± 0.0	0/3	0.0 ± 0.0	0/3
Olfactory sensitivity	1.6 ± 0.2	11/11	1.7 ± 0.2	15/15	1.3 ± 0.3	3/3	2.0 ± 0.5	3/3
Global score	7.5 ± 0.8		9.9 ± 0.6*		11.3 ± 1.2		10.0 ± 1.2	

Student-*t* test. *Different to Young WT group: *p* < 0.05. Fisher Exact test. Different to Young WT group: *p* < 0.05.

ambulatory movements of mice after habituation were recorded along the natural activity period (i.e., 12 h of darkness). Although it was only apparent at young adult age that *Dll1*^{+/lacZ} mice moved less (i.e., fewer beam breaks) than WT mice, aged mice showed a significant difference in this test (Figure 7A), more evident within the inner zone (Figure 7A). In a different test, ambulatory movements of young adults in an unexplored area were determined using a video-based detector within a 5 min time limit (Figure 7B). Interestingly, in this latter test, *Dll1*^{+/lacZ} mice moved a longer distance than WT mice, activity that occurred mostly in the outer zone (Figure 7B). As time in the outer versus the inner zone was not significantly different (data not shown), this behavior cannot be considered a sign of increased anxiety. Accordingly, in the elevated plus maze test, despite that all mice stayed most of the time

in the closed arm, *Dll1*^{+/lacZ} mice spent more time in the open arm than WT mice soon after exposure to a novel environment (Figure 7C). Therefore, it is apparent that *Dll1* haploinsufficient mice move less in the long term but, in the short term, a hyperactive-like behavior is uncovered under certain circumstances (e.g., soon after exposed to a novel environment). In agreement with this conclusion, a previous study reports hyperactivity in *Dll1* haploinsufficient mice under a different genetic background than the one of mice used here (Rubio-Aliaga et al., 2009).

The neuromuscular function was evaluated by performing equilibrium and gripping tests (Figure 8). No major differences in performance by *Dll1*^{+/lacZ} and WT mice was observed in the rotarod test (Figure 8A). In addition, performance differences in the equilibrium bar test were not found (Figure 8B). However,

TABLE 2 Temporal (seconds) and numeric parameters of the copulatory behavior in young and aged WT and *Dll1*^{+/lacZ} male mice (ML, mounting latency; IL, intromission latency; EL, ejaculation latency; NM, number of mounts; NI, number of intromissions).

		Sessions					
	Group	1	n	2	N	3	n
ML	Young WT	1700.7 ± 218.9	7/10	944.4 ± 179.7	8/10	790.4 ± 163.2	9/10
	Young <i>Dll1</i> ^{+/lacZ}	1054.3 ± 75.0	8/14	1294.2 ± 181.1	11/13	1026.3 ± 196.4	10/10
	Aged WT	1871.0	1/3	1741.0 ± 59.0	2/3	—	0/3
	Aged <i>Dll1</i> ^{+/lacZ}	2329.0	1/3	—	0/3	—	0/3
IL	Young WT	1785.0 ± 315.0	2/10	1058.7 ± 166.4	8/10	863.0 ± 171.7	9/10
	Young <i>Dll1</i> ^{+/lacZ}	1345.0 ± 196.7	6/14	1522.6 ± 249.2	7/13	1164.6 ± 243.8	9/13
	Aged WT	—	0/3	—	0/3	—	0/3
	Aged <i>Dll1</i> ^{+/lacZ}	2329.0	1/3	—	0/3	—	0/3
EL	Young WT	—	0/10	—	0/10	2370.0	1/10
	Young <i>Dll1</i> ^{+/lacZ}	—	0/14	—	0/13	1759.0 ± 72.0	2/13
	Aged WT	—	0/3	—	0/3	—	0/3
	Aged <i>Dll1</i> ^{+/lacZ}	—	0/3	—	0/3	—	0/3
NM	Young WT	4.6 ± 1.6	7/10	11.1 ± 1.8	8/10	7.8 ± 1.8	9/10
	Young <i>Dll1</i> ^{+/lacZ}	8.1 ± 1.3	8/14	7.3 ± 1.3	11/13	10.7 ± 3.0	10/13
	Aged WT	3.0	1/3	2.0	2/3	—	0/3
	Old <i>Dll1</i> ^{+/lacZ}	2.0	1/3	—	0/3	—	0/3
NI	Young WT	6.0 ± 3.0	2/10	16.1 ± 4.0	8/10	12.4 ± 2.7	9/10
	Young <i>Dll1</i> ^{+/lacZ}	4.8 ± 1.4	6/14	7.9 ± 1.6	7/13	9.1 ± 2.7	9/13
	Aged WT	—	0/3	—	0/3	—	0/3
	Aged <i>Dll1</i> ^{+/lacZ}	—	1/3	—	0/3	—	0/3

it was noted that most *Dll1*^{+/lacZ} mice did not wrap their tail on bar and traveled a longer distance than WT mice (Figure 8B), possibly reflecting a neurological deficit, but it cannot be discarded that it is due to tail vertebra abnormalities, frequent in *Dll1* haploinsufficient mice (Rubio-Aliaga et al., 2009). In contrast, the hanging time of *Dll1*^{+/lacZ} mice was significantly shorter than the time WT mice remained suspended (in 5-months-old mice but only apparent in 3- and 10-months-old mice; Figure 8C). Therefore, these tests did not reveal motor coordination abnormalities, but gripping strength appeared reduced in *Dll1* haploinsufficient mice.

A deficit in object recognition was a highly penetrant phenotype due to *Dll1* haploinsufficiency. As expected, WT mice spent a longer time exploring a novel object than the familiar one but, in contrast, *Dll1*^{+/lacZ} mice spent the same time exploring both objects (Figure 9A). These observations are in agreement with a deficit in the ability to identify objects (i.e., deficit in recognition memory). As estimated from comparing the immobility time of mice in the tail suspension test (data not shown), no depressive behavior was detected due to *Dll1* haploinsufficiency, but the apparent shorter exploration time devoted to objects by *Dll1*^{+/lacZ} mice in comparison with WT mice (Figure 9B) suggests a cognitive disability (e.g., inability to categorize objects).

Materials and methods

Animals

All experiments were performed under the ethical guidelines of the Instituto de Biotecnología, UNAM and of the Universidad Autónoma Metropolitana-Unidad Iztapalapa. In the mice studied, the *Dll1*^{lacZ} allele is under the outbred genetic background of the CD1 strain. Mice were genotyped by staining for LacZ and/or by an allele-specific PCR. Backcrosses were performed in order to maintain the genetic variability of the CD1 strain, that is, matings between brothers and sisters or parents were avoided, and non-related WT CD1 mice were introduced after 3-4 matings. Generally, male mice were studied, and for comparisons, divided into groups by age. The animals were housed in a room with a light-dark cycle of 12-12h and controlled temperature of 21 ± 1°C. The water and food were provided *ad libitum*. Mice were sacrificed by cervical dislocation or by an intraperitoneal injection of a pentobarbital overdose (200 mg/Kg pentobarbital/mouse or 20 µl/g 2.5% avertin). When required, a perfusion was intracardially performed, first with 30 ml of phosphate buffer saline (PBS 0.1M) at 100 ml/h, and then with 30 ml of 4% paraformaldehyde (PFA) at the same rate. Specifically for MRI acquisitions, six young WT and *Dll1*^{+/lacZ} mice

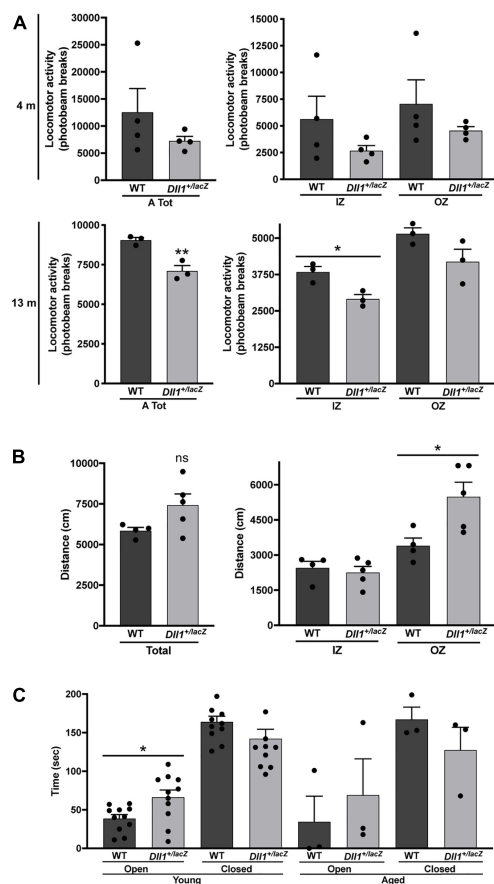


FIGURE 7

Dll1 haploinsufficiency leads to locomotor behavioral alterations. (A) Mean locomotor (ambulatory) activity recorded as total (left graph) or inner (IZ) and outer (OZ) zone (right graph) photobeam breaks for 12 dark hours (see Materials and Methods) of WT and *Dll1*^{+/-lacZ} mice; young (4 months-old; $n = 4$ of each genotype) and aged (13 months-old; $n = 3$ of each genotype) mice were analyzed (** $P < 0.01$; * $P < 0.05$). (B) Total distance traveled (left graph) and distance traveled in the IZ or OZ (right graph) by young WT ($n = 4$) and *Dll1*^{+/-lacZ} ($n = 5$) mice (* $P < 0.05$). Note that, although contrasting differences between *Dll1*^{+/-lacZ} and WT mice were observed in the locomotor activity tests performed, likely, each test was revealing a distinct behavioral deficit. (C) Time spent in the open or closed arms of the elevated plus maze by WT ($n = 11$) or *Dll1*^{+/-lacZ} ($n = 11$) mice of 4–5 months of age (young) and WT ($n = 3$) or *Dll1*^{+/-lacZ} ($n = 3$) mice of 14–16 months of age (aged) (* $p < 0.05$).

were used and the PFA solution was supplemented with gadolinium (2 mM, Gadovis kindly provided by Prof. Andres Morón, Centro Nacional de Imagenología e Instrumentación Médica, Universidad Autónoma Metropolitana). The heads were removed along with the skin, lower jaw, ears, and the cartilaginous nose tip. The skull was then stored in PBS 0.1M containing sodium azide (0.02%) and gadolinium (2 mM) at 15°C for, at least, four days and not longer than 2.5 months post-perfusion before MRI acquisition (see below).

Anatomical and histological evaluations

Brains of animals were analyzed at different ages. Brains were collected and cryopreserved before obtaining 10–50 μ m slices, which were preserved at -70°C until use. Brains of E11.5–E15.5 embryos were fixed for 2 h at 4°C in 4% PFA in PBS, washed with PBS, dehydrated with 30% sucrose and sectioned (10 μ m slices) after freezing (Leica cryostat CM 1850, Wetzlar, Germany). P7–P24 and adult mice were perfused intracardially, first with PBS, followed by 4% PFA. Brains were removed and placed in 4% PFA for 24 h. Subsequently, the tissues were cryopreserved by immersion in 30% sucrose for at least 48 h; 50 μ m (early postnatal ages) or 30 μ m (adult) slices were obtained. Nissl and DAPI staining was used to evaluate cell distribution in tissue slices. Immunostaining for embryonic brain and adult brain sections was performed as previously described in Guerrero-Flores et al. (2017) and in Arzate et al. (2019), respectively. For cell density quantifications, only cells comprised within the region under evaluation were taken into account. Primary antibodies used were: anti-Nestin (Millipore, MAB353), anti-SOX2 (Santa Cruz, sc-17320), anti-NEUN (Chemicon, MAB377), anti-GFAP (DAKO, Z0334), anti-DCX (Santa Cruz, sc-8067), anti-MBP (Covance, SMI-99) and anti-NG2 (Millipore, AB5320). Secondary antibodies used were Alexa 488- and Alexa 595-conjugate anti-mouse, anti-goat or anti-rabbit antibodies (Invitrogen). After single or double staining, sections were mounted and analyzed using a Zeiss Apotome microscope (Zeiss, Oberkochen, Germany) and a confocal microscope Olympus FV1000 (Olympus, Tokyo, Japan).

Myelination analysis

Brain frozen sections (50 μ m thick) mounted on slide were stained using the Black-Gold II Myelin Staining Kit (Histo-Chem Inc., #2BGII). Briefly, samples were incubated with the Black-Gold II solution for up to 15 min at 65°C , washed twice with water, incubated with 1% sodium thiosulfate solution for 3 min at 65°C , and washed three times with water before dehydration and mounting. Myelination levels were quantified by determining the mean optical intensity of a delimited area (region of interest, ROI; i.e., corpus callosum) in grayscale images (8 bits) of stained sections using the FIJI Image J. software. The normalized optical density values were calculated by subtracting the mean optical intensity of the ROI from the intensity detected in the background of each image and then divided by the same factor. Fluorescence intensity after MBP immunofluorescence was also quantified using the FIJI Image J. software applied on confocal images. In this case the ROI in images was delimited (corpus callosum) and the intensity

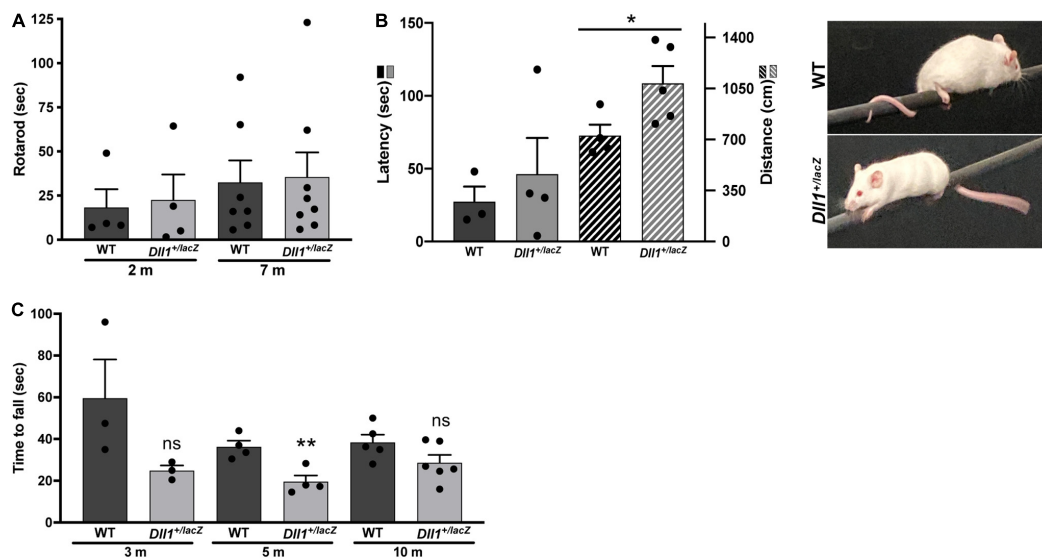


FIGURE 8

Differences in motor activity and strength performance due to *Dll1* haploinsufficiency. WT and *Dll1*^{+/lacZ} mice were tested for motor functions. (A) Rotarod test. Two- ($n = 4$ of each genotype) and 7-months-old ($n = 7$, WT and $n = 8$, *Dll1*^{+/lacZ}) mice were used. Due to the high variability of this test, no difference between WT and *Dll1*^{+/lacZ} mice was observed. (B) Balance beam test. WT ($n = 3$) and *Dll1*^{+/lacZ} ($n = 4$) young mice were used; note that, although there was no significant difference in the time to fall from the bar, *Dll1*^{+/lacZ} mice traveled a longer distance on the bar than WT mice ($*P < 0.05$). Images show how mice used its tail to stay on the bar. (C) Inverted grid test. Mice at 3 different ages were tested: 3 months-old (WT, $n = 3$; *Dll1*^{+/lacZ}, $n = 3$), 5 months-old (WT, $n = 4$; *Dll1*^{+/lacZ}, $n = 4$), and 10 months-old (WT, $n = 5$; *Dll1*^{+/lacZ}, $n = 6$). Generally, a decreased motor strength was detected in *Dll1*^{+/lacZ} mice, though significance was limited ($**P < 0.01$).

calculated by subtracting the background intensity from the mean intensity in the ROI.

X-ray and magnetic resonance image analysis

Young and adult WT and *Dll1*^{+/lacZ} mice were anesthetized and X-ray images captured using the *In vivo* Xtreme instrument (Bruker, Billerica, Massachusetts). The mice spine length was estimated based on X-ray images considering the distance from neck to tail base, (WT, $n = 11$; *Dll1*^{+/lacZ}, $n = 9$). MRI acquisition was conducted with a Bruker Pharmascan 70/16US, 7 Tesla magnetic resonance scanner (Bruker, Ettlingen, Germany). An anatomical scan was obtained using a spin-echo rapid acquisition with refocused echoes (Turbo-RARE) sequence with the following parameters: TR = 400 ms, TE = 21.3 ms, matrix dimensions = 396×396 , 396 slices, slice thickness = 0.040 mm, no gap, resulting in isometric voxels $0.040 \times 0.040 \times 0.040 \text{ mm}^3$ in size. The volume of the whole brain and lateral ventricles were determined manually drawing regions of interest (ROIs) using the segmentation function of ITK-SNAP software (Yushkevich et al., 2006). For LV measurements, we considered the volume from the anterior truncated part of the corpus callosum named the genu (onset in Figure 3B) to the splenium (end in Figure 3B).

Behavioral evaluations

General neurological deficit evaluation

The neurological deficit evaluation was performed in a lighted room. We followed the protocols validated by Rodriguez et al. (2005) and Irwin (1968). In the first stage, the examiner recorded the presence or absence of a lateralized posture, flattened posture, hunched back, piloerection, ataxic gait, circling, tremors, twitches, convulsions, respiratory distress, and the degree of hypomobility (1 slight, 2 moderate, 3 severe). In the second stage with manipulation, the examiner recorded the passivity, hyperreactivity, irritability, ptosis, urination, decreased body tone, forelimb flexion, decreased muscle strength, body rotation, motor incoordination, absence of equilibrium, hypoalgesia, and hyperalgesia. Table 1 shows the average score determined for the number of mice indicated at two ages (young and aged).

Sexual behavior test

The male sexual behavior test was performed 2 h after the onset of darkness and under dim red light. Inside of the home-cage of each male mouse, a receptive female of the same strain (20–30 g) was introduced and allowed mating for 45 min or until ejaculation. The female mice were brought into estrous by hormone treatment. Specifically, mice were ovariectomized (GDX) and subcutaneously injected with 20 μg of estradiol benzoate (EB) and 500 μg of

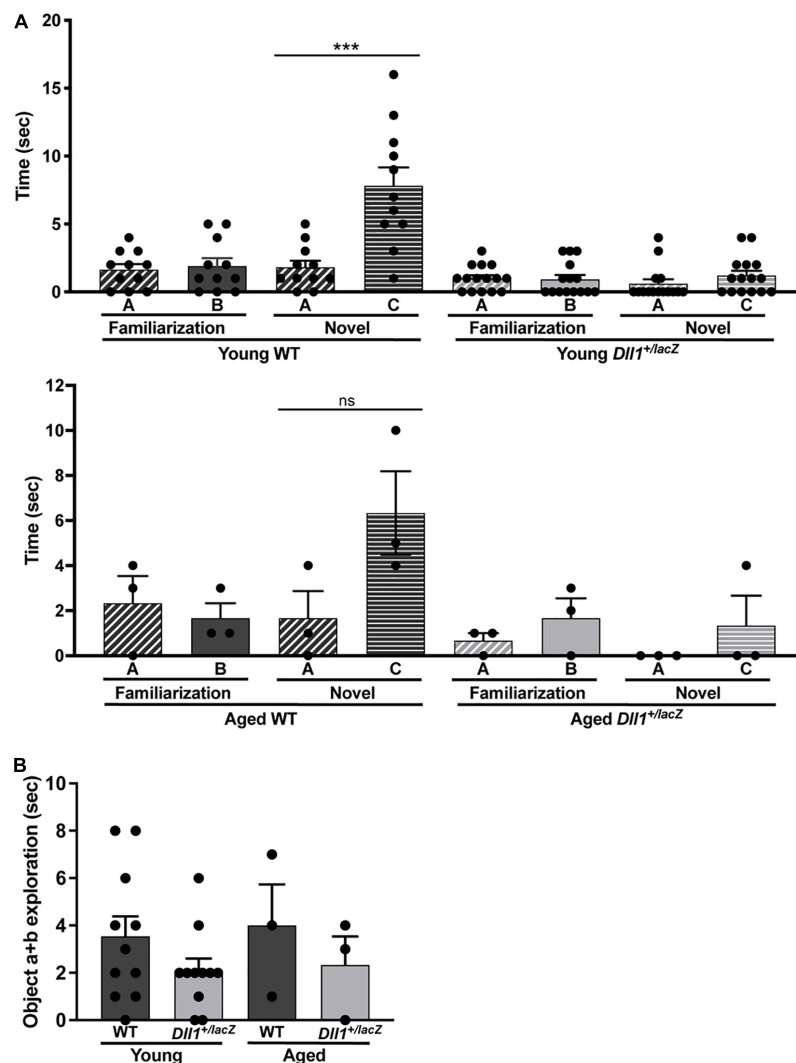


FIGURE 9

Dll1^{+/lacZ} male mice have a deficit in the ability to categorize objects. Young WT ($n = 11$) and *Dll1*^{+/lacZ} ($n = 11$) or aged WT ($n = 3$) and *Dll1*^{+/lacZ} ($n = 3$) male mice were used for the test. The time mice spent with A or B objects during the familiarization session and the time spent exploring A or C objects in the novel session were evaluated (A). Additionally, we show the time spent by mice exploring any object during the familiarization session (B). Note that, in the novel session, *Dll1*^{+/lacZ} mice did not show the typical increase in time spent exploring the novel object ($***p < 0.05$ for young mice; ns, no statistically significant). In addition to the impairment in novel object recognition, *Dll1*^{+/lacZ} mice also showed an apparent reduction in total time devoted to object exploration (ns, no statistically significant).

progesterone (P) 48 and 6 h, respectively, before each mating test. All male mice were evaluated in three mating sessions, each separated by at least 48 h. The number of male mice that mounted, intromitted or ejaculated is shown in Table 2, as well as, the latency of mount (LM; time from introduction of the male into the test cage until the first mount with pelvic thrusting), latency of intromission (LI; time for the first intromission behavior pattern), latency of ejaculation (LE; time from the first intromission behavior pattern until the first ejaculation behavior pattern), the number of mounts (NM) and the number of intromissions (NI) until ejaculation.

Locomotor activity tests

(a) Photobeam breaks Open Field test. Locomotor activity was tracked with the Photobeam Activity System-Home Cage (PAS-HC, 4 × 8 photobeam configuration; SD Instruments). Each mouse was habituated by placing the cage on the chamber for 4 h one day before the test. The test was run with one mouse per chamber for 24 h and photobeam breaks registered at 30 min intervals. Only movements during the dark phase were considered (20–48 intervals). (b) Video-tracking in an open field test. In a lighted room, animals were placed on the center of a 60 × 60 cm dark arena. Movements were recorded for 5 min using the SMART 2.0 software (PanLab, S.L.U. Barcelona,

Spain); outer and inner zones were pre-defined. The software analyzes the trajectory of the animal and measures the time spent and the distance traveled in each defined zone.

Rotarod test

The Rotarod 755 unit was used (IITC Life Science, San Diego, CA, USA). Mice were habituated to the unit without movement for 1 min before running every trial, and trained by performing 2 sessions per day for 3 days at 4–20 rpm rate. The test included 5 consecutive determinations, one per day at the same daytime (in a lighted room). In the testing trials, the animals were placed at an initial speed of 10 rpm, and then rod speed gradually increased to 45 rpm over 180 s. Time and speed were registered until animal falls.

Inverted grid test

In a lighted room, mice were placed one by one on a grid (i.e., a cage lid), and after 5 s, the grid was inverted and held at 35 cm over a mouse cage with enough mouse bedding. The average time to fall (max 5 min) was recorded in 3 trials per session and 3 sessions along 3 consecutive days.

Elevated plus maze test

The elevated plus maze test was performed in a dark room with the elevated plus maze illuminated. The male mice were placed in the core of the elevated plus maze and were allowed to freely explore the arms for 5 min. The time that mice spent in the open or closed arm was registered.

Tail suspension test

The tail suspension test was performed 2 h after onset of darkness and under dim red light. Each mouse was suspended 40 cm up the floor by the tail with a masking tape. The immobility time was recorded in a 5 min session.

Object recognition test

The object recognition test (Walf et al., 2008; Leger et al., 2013) was performed in a lighted room. First, male mice were habituated to the open field box (60 × 40 × 40 cm) for 5 min once a day for 3 days. After the habituation sessions, each mouse was free to explore the two objects, different in form and texture, during 3 min (familiarization session). The time that each mouse spent exploring the objects was registered. Thirty minutes later, one object was replaced for a different one and the time that mice spent exploring this novel object vs. the familiar object (A vs. C) was registered (novel session).

Balance beam test

Each mouse, WT or *Dll1*^{+/-lacZ}, was individually placed at one end of a bar (1.0 m long, 1.0 cm in diameter, suspended at 60 cm height) and allowed to move along it for 2 min. Latency (time before first fall), number of falls and distance traveled were recorded using the SMART 2.5

software (PanLab, S.L.U. Barcelona, Spain). Two independent experiments were performed.

Statistics

For statistical analysis, a two-tailed Student *t* test or One-Way ANOVA were employed for comparison between genotype conditions, except for data that did not pass a normality (Shapiro-Wilk) and the equal variance tests, in which case, the Rank sum Test followed by the Dunn's method for multiple comparisons were employed. The data of copulatory parameters between test sessions were analyzed using the Analysis of Variance on Rank (Kruskal Wallis) followed by Dunn's method for multiple comparisons. The percentage of male mice that displayed mounts, intromissions, and ejaculations in each sexual behavior test were analyzed using a Chi-square test. All values are represented as mean ± SEM. A *P* value less than 0.05 was considered significant.

Discussion

Notch signaling participates in the differentiation of many cell types. Thus, a profound reduction in Notch signaling during development would be generally lethal, though in some instances, likely due to a transient Notch signaling depletion, animals survive but still display abnormalities in organs or structures (e.g., vertebrae, heart; Siebel and Lendahl, 2017). Mild reduction in Notch signaling apparently does not cause a major alteration in most tissues and organs, but the brain is expected to be more prone to morphological alterations with functional consequences. The observations of the present study are consistent with a major and non-redundant role of *DLL1* in the regulation of Notch signaling during brain development, participating in the control of both neurogenesis and oligodendrogenesis. Therefore, *Dll1* haploinsufficiency in mice could be a useful genetic condition to determine non-life threatening abnormalities associated with Notch signaling that might influence brain function. The present study was not designed to identify the specific circuits affected by the shortage in Notch signaling but, rather, to uncover brain abnormalities that could cause neurological anomalies. We recognize that, perhaps due to the relatively small number of animals used for the determinations, a statistical difference was not observed in some instances. The recurrence of neurological anomalies, however, is evidence of the broad influence of Notch signaling in brain development and function and coincident with the expected incidence of a congenital disorder. Therefore, without referring to a specific brain function, *Dll1* haploinsufficiency can be considered a risk factor for congenital brain malfunctions.

Dll1 haploinsufficiency alters brain development

The brain alterations observed likely have a developmental origin. It is well known that reducing Notch signaling causes premature differentiation of stem cells within different lineages (Koch et al., 2013). In particular, reduction in Notch signaling causes neuronal differentiation of NPCs that, in some instances, is accompanied by an increase in astrocytes (Louvi and Artavanis-Tsakonas, 2006). The key role of Notch signaling in cell differentiation is the expansion of the stem cell population, upon which the number of cellular derivatives depends. Therefore, premature neuronal differentiation could cause an exhaustion of stem cells with the consequential reduction in the total number of neurons produced (Chapouton et al., 2010; Imayoshi et al., 2010; Trujillo-Paredes et al., 2016). Generally, signaling by Notch receptors depends on its recognized ligands, among which DLL1 is the most widely active. Considering that most neurons are produced before birth, *Dll1* haploinsufficiency could cause a mild premature neuronal differentiation in the embryo and, consequently, the reduction in the number of neurons observed in the adult brain. In agreement with a broad influence of DLL1 in the determination of neuronal density in the brain, mild microcephaly was a penetrant phenotype detected early after birth in *Dll1*^{+/lacZ} mice. Nonetheless, variations in the level of influence within different brain regions could be due to the participation of other Notch ligands or a compensation by additional factors in the niche controlling stem cell proliferation and maintenance (Fuchs and Blau, 2020).

Despite that Notch signaling in the adult brain neurogenic niches has a similar role in neuronal differentiation as during development (Imayoshi and Kageyama, 2011), the presence of other ligands should be considered to estimate how a decrease in DLL1 can affect brain functionality. For instance, in the subventricular zone, a recent report shows that *Jag1* neural-specific haploinsufficiency reduces the expansion of progenitor cells, which limits the production of migrating neuroblasts and olfactory bulb interneurons (Blackwood et al., 2020). In the adult hippocampus, *Jag1* seems to be also the major Notch ligand controlling NSC maintenance and neurogenesis (Lavado and Oliver, 2014), and although *Dll1* is also expressed in this brain region, this appears to occur in mature neurons (Breunig et al., 2007). Therefore, any neurological dysfunction that relates to the production of new neurons in the postnatal dentate gyrus of *Dll1* haploinsufficient mice (e.g., memory acquisition; see below) could be a consequence of a misregulated developmental process (e.g., the one that caused a reduction in the number of SOX2⁺ cells).

Oligodendrocyte differentiation and myelination are processes occurring early after birth (Nishiyama et al., 2021). In agreement with premature OPC differentiation due to a reduced amount of DLL1, increased levels of myelination with the consequent reduction in OPCs were observed in brains of *Dll1*^{+/lacZ} mice during the early myelination waves. This

pattern is similar to the one observed in brains of *Notch1* haploinsufficient mice (Givogri et al., 2002), suggesting that DLL1 is the main ligand interacting with NOTCH1 to control, at least, the initial waves of OPC differentiation and myelination. Interestingly, although alterations in myelination levels were not frequent in adult *Dll1*^{+/lacZ} mice, the absence of the transient increase in OPCs originated from the subventricular zone of juvenile WT mice suggests that myelin replacement dynamics and maintenance could be determined by Notch signaling and cause neurological alterations (see below).

Hydrocephalus is a congenital condition which origin is not completely understood. Generally, it is assumed that hydrocephalus originates from a disruption of the mechanisms that regulate the cerebrospinal fluid (CSF) homeostasis, including fluid production, absorption and circulation (Tully and Dobyns, 2014; McKnight et al., 2020). However, a recent report points to the possibility that altered developmental neurogenesis could cause hydrocephalus. Specifically, it has been found that mutations in *TRIM71* are frequent in congenital hydrocephalus patients (Duy et al., 2022). Interestingly, *Trim71* deficiency in mice causes premature neural differentiation and the development of small brains with fewer neurons than in WT brains (Duy et al., 2022), in close correlation with the observations in *Dll1* haploinsufficient mice. Detailed determinations in brain ventricles of *Trim71* deficient mice suggest a biomechanical disruption due to deficient neurogenesis as the initial origin of hydrocephalus (Duy et al., 2022). That is, scattered cell distribution, observed in brains of *Trim71* deficient and *Dll1* haploinsufficient mice, could reduce tissue stiffness to a point that is not sufficient to support the pressure from the CSF, causing dilation as ventricles adjust to a greater volume. Therefore, mild microcephaly resulting from deficient neurogenesis due to reduced DLL1 levels is a condition that favors hydrocephalus development.

Attenuation of neurogenesis/oligodendrogenesis as a cause of neurological deficits

The genetic contribution to the morphological and behavioral phenotypes caused by *Dll1* haploinsufficiency cannot be discarded, but the fact that mice carrying the null *Dll1*^{lacZ} allele are maintained as an outbred strain makes unlikely that a specific gene interaction is the cause of phenotypes observed. Rather, we propose that the display and penetrance of phenotypes observed could receive strong influence of environmental factors. Particularly relevant in this regard is hypoxia which is known to interact with Notch signaling (Landor and Lendahl, 2017) and has been shown to be determinant in scoliosis penetrance in association with reduced Notch signaling (Sparrow et al., 2012). Interestingly, the lack of Hif1a in brain results in alterations similar to the ones determined in the present study, such as reduced neurogenesis

and hydrocephalus (Tomita et al., 2003). Therefore, reduced Notch signaling should behave as a sensitive condition to cause congenital brain abnormalities (e.g., microcephaly, hydrocephalus) due to environmental factors with possible impairment of relevant brain functions.

Although aging has not been studied in detail under *Dll1* haploinsufficiency, *Dll1*^{+/lacZ} mice have relatively high survival up to late adult life (i.e., 14 months of age) without evident neurological deficits within the adapted life in the animal facility. However, as shown here, specific tests revealed neurological deficits, some more penetrant than others, that might be part of the expected behavioral/psychiatric anomalies associated with microcephaly and/or hydrocephalus in humans (Tully and Dobyns, 2014; McKnight et al., 2020). Relevant in this regard, a recent report with human patients shows that *DLL1* haploinsufficiency correlates with intellectual disability, autism and seizures, in addition to variable prenatally detected brain malformations (Fischer-Zirnsak et al., 2019). At this point, the specific cause of neurological deficits remains obscure; for instance, the inability to categorize objects was an interesting neurological impairment detected in *Dll1* haploinsufficient mice, but that could not be directly originated from disrupting adult neurogenesis in the hippocampus. Among possible causes, a reduced number of neurons could prevent correct neuronal circuit assembly, and circuit performance efficiency could be influenced by the morphological anomalies induced by ventriculomegaly and/or poor axonal myelination as it has been previously reported (Bonetto et al., 2021). In any case, the present work suggests that brain function disabilities in humans could arise from genetic or non-genetic factors (e.g., congenital) that reduce Notch signaling, which could be anticipated from early detection of mild microcephaly/hydrocephalus brain abnormalities. As a corollary, the efforts to identify the factors that interfere with Notch signaling (e.g., hypoxia) should result in the application of certain prenatal measures that likely prevent neurological deficits and increase life quality.

The mild alterations described here could be a factor that predisposes the development of specific neurological diseases, more easily to appreciate in those characterized by neuronal degeneration. Neuronal differentiation is not developmentally synchronized but, rather, different neuronal types emerge within particular regions of the developing brain and at a specific time. Therefore, in a genetic condition that prompts reduction in neurogenesis (e.g., *Dll1* haploinsufficiency), the transient influence of environmental factors (e.g., hypoxia) at a particular time would affect the production of a set of specific neurons. The number of neurons in the adult brain, determined after NPC proliferation/differentiation, neuroblast migration and neuronal circuit integration, defines the gap of neurons that can die. Hence, animals may be predisposed to neurological alterations even if the number of specific neuronal types in the adult brain are below normal, but above the threshold at which symptoms of a particular neurodegenerative disease are

expressed or can be diagnosed. For example, fewer cholinergic neurons in the cortex or dopaminergic neurons in the substantia nigra are conditions that prompt early development of Alzheimer's or Parkinson's diseases, respectively (Spada, 2006; Oliveira et al., 2017). In a contrasting view, recently it was proposed that the function of a truncated form of Notch2, only present in humans (NOTCH2NL), is to enhance Notch signaling activation by *DLL1* (Suzuki et al., 2018), hypothetically improving neurogenesis and cortex performance. Therefore, the present work has an additional translational value: treatments that boost Notch signaling could prevent neurodegeneration and improve intellectual performance in humans.

Data availability statement

The raw data supporting the conclusions of this article will be made available by the authors, without undue reservation.

Ethics statement

The animal study was reviewed and approved by the Ethics Committee of the Instituto de Biotecnología, Universidad Nacional Autónoma de México.

Author contributions

LC led the research, designed experiments, analyzed the data, and wrote the manuscript. D-MA designed and performed the experiments, analyzed the data, and wrote the manuscript. CV, M-AD, EA-C, ED-S, GG-F, and MG-M designed and performed the experiments and analyzed the data.

Funding

This work was supported by grants IN214219 from PAPIIT-UNAM and FOINS1723 from CONACyT. D-MA, MA-D, and E-AC are recipients of CONACyT fellowships.

Acknowledgments

We appreciate the technical support of Rubén Blancas at the Instituto de Biotecnología. We also acknowledge the assistance of the LNMA facility core members (Andrés Saralegui, Verónica Rojo and Arturo Pimentel) and of the Animal Care Facility members (Graciela Cabeza Pérez, Sergio González Trujillo and Elizabeth Mata Moreno), of the Instituto de Biotecnología, UNAM. Finally, we are grateful to Juan J. Ortiz and Sarael Alcauter-Solórzano of the Laboratorio Nacional de

Imagenología por Resonancia Magnética for their unconditional support in the MRI acquisitions performed.

Conflict of interest

The authors declare that the research was conducted in the absence of any commercial or financial relationships that could be construed as a potential conflict of interest.

References

- Arzate, D. M., Guerra-Crespo, M., and Covarrubias, L. (2019). Induction of typical and atypical neurogenesis in the adult substantia nigra after mouse embryonic stem cells transplantation. *Neuroscience* 408, 308–326. doi: 10.1016/j.neuroscience.2019.03.042
- Beckers, J., Clark, A., Wunsch, K., Angelis, M. H. D., and Gossler, A. (1999). Expression of the mouse Delta1 gene during organogenesis and fetal development. *Mech. Dev.* 84, 165–168. doi: 10.1016/s0925-4773(99)00065-9
- Blackwood, C. A., Bailetti, A., Nandi, S., Gridley, T., and Hébert, J. M. (2020). Notch dosage: Jagged1 haploinsufficiency is associated with reduced neuronal division and disruption of periglomerular interneurons in mice. *Front. Cell. Dev. Biol.* 8:113. doi: 10.3389/fcell.2020.00113
- Bonetto, G., Belin, D., and Káradóttir, R. T. (2021). Myelin: A gatekeeper of activity-dependent circuit plasticity? *Science* 374:eaba6905.
- Breunig, J. J., Silbereis, J., Vaccarino, F. M., Šestan, N., and Rakic, P. (2007). Notch regulates cell fate and dendrite morphology of newborn neurons in the postnatal dentate gyrus. *Proc. Natl. Acad. Sci. U.S.A.* 104, 20558–20563. doi: 10.1073/pnas.0710156104
- Chapouton, P., Skupien, P., Hesl, B., Coolen, M., Moore, J. C., Madelaine, R., et al. (2010). Notch activity levels control the balance between quiescence and recruitment of adult neural stem cells. *J. Neurosci.* 30, 7961–7974. doi: 10.1523/jneurosci.6170-09.2010
- Duy, P. Q., Weise, S. C., Marini, C., Li, X.-J., Liang, D., Dahl, P. J., et al. (2022). Impaired neurogenesis alters brain biomechanics in a neuroprogenitor-based genetic subtype of congenital hydrocephalus. *Nat. Neurosci.* 25, 458–473. doi: 10.1038/s41593-022-01043-3
- Fischer-Zirnsak, B., Segebrecht, L., Schubach, M., Charles, P., Alderman, E., Brown, K., et al. (2019). Haploinsufficiency of the notch ligand DLL1 causes variable neurodevelopmental disorders. *Am. J. Hum. Genet.* 105, 631–639. doi: 10.1016/j.ajhg.2019.07.002
- Freeman, M. R. (2010). Specification and morphogenesis of astrocytes. *Science* 330, 774–778. doi: 10.1126/science.1190928
- Fuchs, E., and Blau, H. M. (2020). Tissue stem cells: Architects of their niches. *Cell Stem Cell* 27, 532–556. doi: 10.1016/j.stem.2020.09.011
- Givogri, M. I., Costa, R. M., Schonmann, V., Silva, A. J., Campagnoni, A. T., and Bongarzone, E. R. (2002). Central nervous system myelination in mice with deficient expression of Notch1 receptor. *J. Neurosci. Res.* 67, 309–320. doi: 10.1002/jnr.10128
- Grandbarbe, L., Bouissac, J., Rand, M., Hrabé de Angelis, M., Artavanis-Tsakonas, S., and Mohier, E. (2003). Delta-Notch signaling controls the generation of neurons/glia from neural stem cells in a stepwise process. *Development* 130, 1391–1402. doi: 10.1242/dev.00374
- Guerrero-Flores, G., Bastidas-Ponce, A., Collazo-Navarrete, O., Guerra-Crespo, M., and Covarrubias, L. (2017). Functional determination of the differentiation potential of ventral mesencephalic neural precursor cells during dopaminergic neurogenesis. *Dev. Biol.* 429, 56–70. doi: 10.1016/j.ydbio.2017.07.008
- Hrabé de Angelis, M., McIntyre, J., and Gossler, A. (1997). Maintenance of somite borders in mice requires the delta homologue Dll1. *Nature* 386, 717–721. doi: 10.1038/386717a0
- Imayoshi, I., and Kageyama, R. (2011). The role of notch signaling in adult neurogenesis. *Mol. Neurobiol.* 44, 7–12. doi: 10.1007/s12035-011-8186-0
- Imayoshi, I., Sakamoto, M., Yamaguchi, M., Mori, K., and Kageyama, R. (2010). Essential roles of notch signaling in maintenance of neural stem cells in developing and adult brains. *J. Neurosci.* 30, 3489–3498. doi: 10.1523/jneurosci.4987-09.2010
- Irwin, S. (1968). Comprehensive observational assessment: Ia. A systematic, quantitative procedure for assessing the behavioral and physiologic state of the mouse. *Psychopharmacologia* 13, 222–257. doi: 10.1007/bf00401402
- Koch, U., Lehal, R., and Radtke, F. (2013). Stem cells living with a notch. *Development* 140, 689–704. doi: 10.1242/dev.080614
- Landor, S. K.-J., and Lendahl, U. (2017). The interplay between the cellular hypoxic response and Notch signaling. *Exp. Cell Res.* 356, 146–151. doi: 10.1016/j.yexcr.2017.04.030
- Lavado, A., and Oliver, G. (2014). Jagged1 is necessary for postnatal and adult neurogenesis in the dentate gyrus. *Dev. Biol.* 388, 11–21.
- Leger, M., Quiedeville, A., Bouet, V., Haelewyn, B., Boulouard, M., Schumann-Bard, P., et al. (2013). Object recognition test in mice. *Nat. Protoc.* 8, 2531–2537. doi: 10.1038/nprot.2013.155
- Louvi, A., and Artavanis-Tsakonas, S. (2006). Notch signalling in vertebrate neural development. *Nat. Rev. Neurosci.* 7, 93–102. doi: 10.1038/nrn1847
- McKnight, I., Hart, C., Park, I.-H., and Shim, J. W. (2020). Genes causing congenital hydrocephalus: Their chromosomal characteristics of telomere proximity and DNA compositions. *Exp. Neurol.* 335:113523. doi: 10.1016/j.expneurol.2020.113523
- Menn, B., Garcia-Verdugo, J. M., Yaschine, C., Gonzalez-Perez, O., Rowitch, D., and Alvarez-Buylla, A. (2006). Origin of oligodendrocytes in the subventricular zone of the adult brain. *J. Neurosci.* 26, 7907–7918. doi: 10.1523/jneurosci.1299-06.2006
- Nishiyama, Y., and Kurosawa, K. (2022). Analysis of gene-environment interactions related to developmental disorders. *Front. Pharmacol.* 13:863664. doi: 10.3389/fphar.2022.863664
- Nishiyama, A., Shimizu, T., Sherafat, A., and Richardson, W. D. (2021). Life-long oligodendrocyte development and plasticity. *Semin. Cell Dev. Biol.* 116, 25–37. doi: 10.1016/j.semcdb.2021.02.004
- Oliveira, M. A. P., Balling, R., Smidt, M. P., and Fleming, R. M. T. (2017). Embryonic development of selectively vulnerable neurons in Parkinson's disease. *Npj Park. Dis.* 3:21. doi: 10.1038/s41531-017-0022-4
- Pierfelice, T., Alberi, L., and Gaiano, N. (2011). Notch in the vertebrate nervous system: An old dog with new tricks. *Neuron* 69, 840–855. doi: 10.1016/j.neuron.2011.02.031
- Rodriguez, R., Santiago-Mejia, J., Gomez, C., and San-Juan, E. R. (2005). A simplified procedure for the quantitative measurement of neurological deficits after forebrain ischemia in mice. *J. Neurosci. Meth.* 147, 22–28.
- Rubio-Aliaga, I., Przemeck, G. K. H., Fuchs, H., Gailus-Durner, V., Adler, T., Hans, W., et al. (2009). Dll1 Haploinsufficiency in adult mice leads to a complex phenotype affecting metabolic and immunological processes. *PLoS One* 4:e6054. doi: 10.1371/journal.pone.0006054
- Siebel, C., and Lendahl, U. (2017). Notch signaling in development, tissue homeostasis, and disease. *Physiol. Rev.* 97, 1235–1294.
- Spada, A. R. L. (2006). Neurodegeneration: A case of arrested development? *Cell* 127, 669–671. doi: 10.1016/j.cell.2006.11.010
- Sparrow, D. B., Chapman, G., Smith, A. J., Mattar, M. Z., Major, J. A., O'Reilly, V. C., et al. (2012). A mechanism for gene-environment interaction in the etiology of congenital scoliosis. *Cell* 149, 295–306. doi: 10.1016/j.cell.2012.02.054

Publisher's note

All claims expressed in this article are solely those of the authors and do not necessarily represent those of their affiliated organizations, or those of the publisher, the editors and the reviewers. Any product that may be evaluated in this article, or claim that may be made by its manufacturer, is not guaranteed or endorsed by the publisher.

Suzuki, I. K., Gacquer, D., Heurck, R. V., Kumar, D., Wojno, M., Bilheu, A., et al. (2018). Human-Specific NOTCH2NL genes expand cortical neurogenesis through delta/notch regulation. *Cell* 173, 1370.e–1384.e. doi: 10.1016/j.cell.2018.03.067

Tomita, S., Ueno, M., Sakamoto, M., Kitahama, Y., Ueki, M., Maekawa, N., et al. (2003). Defective brain development in mice lacking the Hif-1 α gene in neural cells. *Mol. Cell Biol.* 23, 6739–6749. doi: 10.1128/mcb.23.19.6739-6749.2003

Trujillo-Paredes, N., Valencia, C., Guerrero-Flores, G., Arzate, D.-M., Baizabal, J.-M., Guerra-Crespo, M., et al. (2016). Regulation of differentiation flux by Notch signalling influences the number of dopaminergic neurons in the adult brain. *Biol. Open* 5, 336–347. doi: 10.1242/bio.013383

Tully, H. M., and Dobyns, W. B. (2014). Infantile hydrocephalus: A review of epidemiology, classification and causes. *Eur. J. Med. Genet.* 57, 359–368. doi: 10.1016/j.ejmg.2014.06.002

Walf, A. A., Koonce, C. J., and Frye, C. A. (2008). Estradiol or diarylpropionitrile administration to wild type, but not estrogen receptor beta knockout, mice enhances performance in the object recognition and object placement tasks. *Neurobiol. Learn. Mem.* 89, 513–521. doi: 10.1016/j.nlm.2008.01.008

Wang, S., Sdrulla, A. D., diSibio, G., Bush, G., Nofziger, D., Hicks, C., et al. (1998). Notch receptor activation inhibits oligodendrocyte differentiation. *Neuron* 21, 63–75. doi: 10.1016/s0896-6273(00)80515-2

Yushkevich, P. A., Piven, J., Hazlett, H. C., Smith, R. G., Ho, S., Gee, J. C., et al. (2006). User-guided 3D active contour segmentation of anatomical structures: Significantly improved efficiency and reliability. *Neuroimage* 31, 1116–1128. doi: 10.1016/j.neuroimage.2006.01.015

COPYRIGHT

© 2022 Arzate, Valencia, Dimas, Antonio-Cabrera, Domínguez-Salazar, Guerrero-Flores, Gutiérrez-Mariscal and Covarrubias. This is an open-access article distributed under the terms of the [Creative Commons Attribution License \(CC BY\)](https://creativecommons.org/licenses/by/4.0/). The use, distribution or reproduction in other forums is permitted, provided the original author(s) and the copyright owner(s) are credited and that the original publication in this journal is cited, in accordance with accepted academic practice. No use, distribution or reproduction is permitted which does not comply with these terms.

Frontiers in Neuroscience

Provides a holistic understanding of brain
function from genes to behavior

Part of the most cited neuroscience journal series
which explores the brain - from the new eras
of causation and anatomical neurosciences to
neuroeconomics and neuroenergetics.

Discover the latest Research Topics

[See more →](#)

Frontiers

Avenue du Tribunal-Fédéral 34
1005 Lausanne, Switzerland
frontiersin.org

Contact us

+41 (0)21 510 17 00
frontiersin.org/about/contact

